Characterising HIV-associated *Mycobacterium tuberculosis* blood stream infection

Thesis submitted in accordance with the requirements of the University of Liverpool for the degree of Doctor in Philosophy by

David Adam Barr

Wellcome Trust Liverpool Glasgow Centre for Global Health Research

University of Liverpool

&

Institute of Infection and Global Health

University of Liverpool

&

Institute of Infectious Disease and Molecular Medicine

University of Cape Town

July 2018

Declaration

The work described is my own and has not been submitted for a degree or other award at any other institution.

Several parts of these thesis are the result of collaborative work.

- The KDHTB study, in which this work was nested, was designed by principal investigator Professor Graeme Meintjes, and run by Dr Charlotte Schutz, both of University of Cape Town.
- The individual patient data meta-analysis reported in chapter 3 was designed, conducted, and analysed in full collaboration with Dr Joseph Lewis of Liverpool School of Tropical Medicine.
- Mycobacterial cell-sorting using BioRad S3 cytometer (in chapter 4) was conducted with assistance from Dr Charles Omollo from the Molecular Mycobateriology Research Institute, University of Cape Town. Mycobacterial cell-sorting using FACS Vantage cytometer (in chapter 4) was conducted with assistance from Mr Ronnie Dreyer from Division of Immunology University of Cape Town, University of Cape Town.
- Mr Avuyonke Balfour ran the Xpert-ultra cartridges for the sub-study described in chapter 5.

Funding

This study was funded by a Wellcome Trust Clinical PhD Fellowship awarded to David Barr (Award 105165/Z/14/A).

Dedication

For Martha and Iomhar

And in memory of Martha Agnes Fieldhouse, 1918-2017

Acknowledgements

I would like to thank the following people.

The patients at Khayelitsha Hospital, who participated in research, understanding that this wouldn't help them, but might help others.

My supervisors: Gerry Davies, David Lalloo, and Graeme Meintjes. Choosing these supervisors is the best decision I've made in my research career.

Charlotte Schutz, Amy Ward, and M. K. Mpalali, whose dedication and skill made the KDHTB study, and this thesis, possible. I learnt a lot from all three. Avuyonke Balfour, Muki Shey, Anna Coussens, and Katalin Wilkinson for their support and advice in laboratory techniques.

Robert Davidson for his mentorship, which has been instrumental in my development as an infectious disease clinician and tuberculosis researcher. In addition, Rose, Alice and Mary Davidson for their support and encouragement while in Cape Town.

Gary Maartens, Andrew Kerkhoff, Joe Lewis, Derek Sloan, Liz Corbett, Bertie Squire, Sean Wasserman, Benny Patterson, Shevin Jacob, Jamilah Meghji, Andrew McCallum and most of all Douglas Wilson, for their suggestions and discussions of the ideas in this thesis. Digby Warner and Valerie Mizrahi, and many other members of the Institute of Infectious Diseases and Molecular Medicine at the University of Cape Town, for their expert advice and razor-sharp insights. My PhD examiners Saye Khoo and Martin Dedicoat for detailed engagement with and questioning of this thesis.

The staff of The Brownlee Centre, Glasgow, for excellent clinical training, and for supporting me taking time out of that training: Andrew Seaton, David Bell, Alisdair MacConnachie, Erica Peters, Emma Thomson, Ray Fox, Beth White, Neil Ritchie, Celia Jackson, Toni Ho, and Sharon Irvine.

Last, but not least, my family. Matt, who proof-read drafts (remaining errors are mine). Faisal and Sue, who have done so much extra child-care. Gee, who fought to make all the opportunities I've had possible. Nina, who carried much of the burden of work behind this thesis with great selflessness and strength. Martha and Iomhar, who ran to the door every time I got home late.

Abstract

Despite the success of antiretroviral therapy roll-out, one-million people still die with HIV-infection annually. In high-burden settings, tuberculosis remains the most common proximal cause of hospital admission and death in people living with HIV. In post-mortem series, 90% of fatal HIV-associated tuberculosis is 'disseminated'. This is a form of tuberculosis which has been poorly characterised and, despite the high associated-mortality, never been the subject of interventional trials to define optimal treatment strategies.

This thesis contends that the mode of severe HIV-associated tuberculosis is blood stream infection. First it is argued with reference to historical literature that blood stream dissemination is part of the natural history of post-primary tuberculosis infection, and that HIV-associated *M. tuberculosis* blood stream infection (MTBBSI) can be conceived of as a reversion to, and exaggerated form of this natural history. Using data from a large cohort (n=571) of HIV-infected inpatients with CD4 cell count <350 cells/mm^3 and a new TB diagnosis from Khayelitsha Hospital, South Africa (the KDHTB study), the extent and magnitude of MTBBSI is shown to be a major determinant of clinical phenotype and mortality risk. Systematic, quantitative markers of blood stream dissemination, including TB blood culture, urine-lipoarabinomannan (uLAM), and urine GeneXpert MTB/RIF testing (uXpert), can be combined into a 'disseminated TB score. KDHTB patients have high prevalence of abnormal sodium and fluid balance, metabolic acidosis associated with acute kidney injury, hyperlactataemia, infiltrative liver and splenic pathology, and anaemia. Each of these pathophysiologies in turn correlates to disseminated TB score, and to risk of death, suggesting bacterial burden and MTBBSI are central to the pathophysiology of severe HIV-associated tuberculosis.

An individual patient data meta-analysis, with 20 independent data sets comprising over 6000 patients, is used to establish the prevalence of TB blood culture positive disease amongst critically unwell HIV-infected inpatients. This shows that MTBBSI is more common than previous estimates suggest, is a strong independent association with

mortality risk, and is also associated with specific increased risk of death if empirical treatment is delayed.

The development of tools to identify and measure MTBBSI is described, including Xpert-ultra testing of blood, and the use of a novel dye, DMN-trehalose, to perform direct microscopy on patient blood samples. These techniques are used to provide the first description of the pharmacodynamics of MTBBSI, by serially quantifying blood bacilli load over the first 72-hours of standard TB therapy, in 28 patients with high predicted probability of bacteraemia. In this cohort, risk of mortality is related to several summary measures of MTBBSI dynamics in the first 72-hours of therapy, suggesting this approach can be used to define biomarkers of treatment response.

In conclusion, MTBBSI is a highly-specific diagnosis responsible for substantial mortality in hospitalised people living with HIV. Interventions with strengthened bacteriocidal activity, focussed on reducing bacterial burden, are warranted for MTBBSI. Tools developed in this thesis, including potential pharmacodynamic biomarkers, should facilitate such trials.

Table of Contents

0 Introduction 1

0.1 Background & motivation 1

0.2 Thesis 4

0.3 Overview of chapters 5

0.4 The KDHTB study 7

0.4.1 Study procedures 7

0.4.2 Setting 7

0.4.3 Cohort description 8

1 Clinical description of HIV-associated M. tuberculosis blood stream infection 11

1.1 Introduction 11

1.2 What is disseminated TB? Classifications, definitions & mechanisms. 12

1.2.1 The classification of disseminated tuberculosis 12

1.2.2 Classical descriptions of miliary tuberculosis 14

1.2.3 Mechanisms of TB bacillaemia 17

1.3 Prior descriptions of HIV-associated MTBBSI 19

1.3.1 Clinical descriptions of HIV-associated MTB BSI 20

1.3.2 Observational studies of MTBBSI which explore pathophysiology 24

1.3.3 Urine-based assays as surrogate measures of MTBBSI 26

1.4 Novel methods for describing the clinical phenotypes 28

1.4.1 Clinical variable dimension reduction: a motivating example 29

1.4.2 Covariance in TB diagnostic test results 32

1.5 Patterns of covariance in categorical clinical variables & markers of MTBBSI 35

1.5.1 Presenting symptoms 35

1.5.2 Imaging categories 38

1.6 Overall covariance in continuous clinical variables & markers of MTBBSI 41

1.6.1 A priori selection and transformation of quantitative clinical variables 41
1.6.2 Association of quantitative variables with mortality 45
1.6.3 Associations of quantitative variables with positive TB blood culture..... 48
1.6.4 Algorithmic dimension reduction in quantitative clinical variables 50
1.7 A more supervised approach to dimension reduction in continuous clinical variables 55
1.7.1 Patterns of covariance in liver enzymes 55
1.7.2 Acid-base balance and renal impairment..... 58
1.7.3 Hyponatraemia..... 64
1.7.4 Covariance in Leukocytes 67
1.7.5 Fever and globulins 72
1.7.6 Physiological sepsis response 75
1.7.7 Thrombocytopenia..... 80
1.8 Structural equation model of core variables relationship to disseminated TB and mortality..... 82
1.9 Concluding discussion 89
2 Predicting TB blood culture results 92
2.1 Introduction 92
2.2 Predictions & clinical decision rules in medicine 93
2.3 Resampling methods & model tuning 95
2.4 Published MTBBSI prediction models 96
2.5 Summary of predictive modelling strategy used in this chapter 97
2.5.1 Included data..... 97
2.5.2 Model types..... 98
2.5.3 Variable selection and dimension reduction 100
2.5.4 Total number of models assessed..... 104

2.5.5 Model training and assessment 104
2.6 Results of 45 MTBBSI predictive models 108
2.7 Combining models for a final ensemble model 108
2.8 Building an app' to make predictions accessible at bedside 110
2.9 Prospective validation sub-study 111
2.9.1 Method 111
2.9.2 Results – prediction accuracy 111
2.9.3 Results – yield from additional MFL cultures 113
2.10 Discussion 114
3 Individual Patient Data meta-analysis of TB blood culture studies 119
3.1 Introduction 119
3.1.1 Statement on collaboration 120
3.2 Methods 121
3.2.1 Meta-analysis questions 121
3.2.2 Literature search strategy and selection criteria 122
3.2.3 Procedures 122
3.2.4 Individual patient data inclusion criteria 123
3.2.5 Synthesis strategy and statistical analysis 123
3.2.6 Prevalence of positive TB blood culture analysis 123
3.2.7 Diagnostic performance of sputum Xpert and urine-LAM in TBBC+ disease 125
3.2.8 Mortality association analysis 126
3.3 Results 127
3.3.1 Identified studies and IPD description 127
3.3.2 Prevalence of TBBC+ disease 131
3.3.3 Diagnosis of TB in patients with TBBC+ 136

3.3.4 Mortality associated with TBBC+ 140
3.4 Discussion 143
3.4.1 Implications & conclusions 147
4 Counting mycobacteria in vitro 151
4.1 Introduction 151
4.2 Established methods for counting mycobacteria 152
4.2.1 Bulk or batch measures 152
4.2.2 Microscopy methods 153
4.2.3 Secondary culture methods: CFU counting, TTD, and MPN. 155
4.2.4 Molecular techniques 157
4.3 Flow cytometry & the live/dead discrimination of microbes 159
4.3.1 Technical challenges of bacterial FCM 159
4.3.2 Live/Dead discrimination of bacteria by fluorescence staining 161
4.4 Defining cell viability & death in bacteria 163
4.5 Flow cytometry of mycobacteria 164
4.6 Aims of current analysis 172
4.7 General methods 173
4.7.1 Flow cytometer 173
4.7.2 Broth culture conditions 173
4.7.3 CFU plating 173
4.7.4 Antibiotic preparations 174
4.7.5 Isolates of mycobacteria ..... **Error! Bookmark not defined.**
4.7.6 Screening fluorescent dyes for use in mycobacteria 174
4.8 Validation of thresholding and gating strategy for absolute cell counts 177
4.9 Clumping in mycobacterial cultures can be observed and measured with FCM 181

4.10 Cell-subpopulation dynamics during antimicrobial free in vitro growth of mycobacteria 187
4.11 In vitro pharmacodynamics of mycobacteria by FCM & CFU counts..... 192
4.11.1 Raw FCM data: qualitative FCM plots & clustering 193
4.11.2 Classification of FCM events by clustering..... 196
4.11.3 Time-kill curves 199
4.11.4 Modelling FCM pharmacodynamics 201
4.12 Dual SG+ population 208
4.12.1 Development of a membrane permeabilization method 209
4.12.2 Differential dual SG staining population characteristics by antimicrobial action 211
4.12.3 Imaging characteristics of the dual SG+ bacilli populations..... 213
4.13 Discussion 217
5 Pharmacodynamics of MTBBSI: development of biomarkers & a clinical study.... 222
5.1 Introduction 222
5.1.1 Rationale for developing PD biomarkers of MTBBSI..... 222
5.1.2 Chapter aims 223
5.1.3 Chapter outline 224
5.2 Identifying & quantifying mycobacteria in blood: prior literature..... 224
5.2.1 Culture 224
5.2.2 Microscopy 227
5.2.3 Nucleic acid amplification..... 227
5.3 Development of methods for identifying & quantifying bacilli in blood 230
5.3.1 Blood microscopy..... 232
5.3.2 MFL blood culture 242
5.3.3 Xpert-ultra testing of processed blood 247

5.3.4 Location of bacilli in MTBBSI 251
5.4 KDHTB sub-study to characterise clinical pharmacodynamics of MTBBSI . 255
5.4.1 Sub-study Methods 255
5.4.2 Sub-study results 258
5.5 Discussion 282
6 Conclusion 285
6.1 Main findings & call for interventional trials in MTBBSI 285
6.2 Secondary findings & future directions 288
6.3 Conclusion 290
7 References 291

Table of Figures

Figure 0-1. Post-mortem studies in HIV-associated adult inpatient deaths. 3
Figure 0-2. STROBE flow diagram for KDHTB study..... 8
Figure 1-1. Definition of disseminated TB in n=50 random sample from PubMed Disseminated & TB & HIV [Title/Abstract]..... 13
Figure 1-2. Clinical predictors associated with MTBBSI from studies in preceding table 22
Figure 1-3. Plasma hepcidin by site of positive TB microbiology, extracted from Kerkhoff *et al*. 2016. 24
Figure 1-4. Ex vivo monocyte function in HIV-associated TB, data extracted from Janssen *et al*. 2017.[142] 26
Figure 1-5. Theoretical schematic relating uLAM, uGXP and TB blood culture..... 28
Figure 1-6. Reduced dimension representation of variables in Jooste dataset using PCA 31
Figure 1-7. Urine versus sputum TB diagnostics agreement with TB blood culture status in patients with proven HIV-associated TB..... 33
Figure 1-8. MCA TB diagnostics in proven TB cases from two independent datasets 34
Figure 1-9. MCA and clustering on presenting symptoms 37
Figure 1-10. MCA and clustering on radiology findings..... 40
Figure 1-11. Univariate distributions of transformed numerical variables. 42
Figure 1-12. Matrix plot showing missing observations by patient (rows) and variable (columns). 44
Figure 1-13. Mortality hazard over 84days of follow up. 45
Figure 1-14. Variables as predictors of early versus late deaths during 84-day follow-up 47
Figure 1-15. Pairwise correlation matrix major quantitative clinical variables 50
Figure 1-16. Dendrogram by alternative hierarchical clustering method (average linkage) 51
Figure 1-17. Previous correlation matrix reduced to 2 dimensions of covariance using PCA..... 51
Figure 1-18. Mapping outcome and disseminated TB score to PCA..... 52
Figure 1-19. K-means cluster association with mortality..... 54
Figure 1-20. K-means cluster association with TB diagnostic results. 54
Figure 1-21. Transaminases relationship to MTBBSI and mortality..... 56
Figure 1-22. Adjusting AST for ALT changes its relationship to other variables 56

Figure 1-23. Correlation of individual liver enzymes with their first 3 principal components 57
Figure 1-24. Liver enzyme principal component 3 relationship with DTB score and mortality 58
Figure 1-25. Acid-base balance overview 59
Figure 1-26. Directed acyclic graph: age and acid-base balance 60
Figure 1-27. Age - adjusted pCO2 from model based on DAG in preceding figure 61
Figure 1-28. PCA of renal/acid-base variables 62
Figure 1-29. Hyponatraemia, calculated osmolarity, and urea. 65
Figure 1-30. Serial measurement of sodium and creatinine during admission. 66
Figure 1-31. Pairwise relationships in blood cells. 68
Figure 1-32. Correlation of WBC and inflammatory markers with their first 3 PCs (varimax rotation). 69
Figure 1-33. WBC principal components relationship with TB blood culture, DTBs core, and mortality outcome. 69
Figure 1-34. Correlation between total white cells, neutrophil measures, and DTB score. 70
Figure 1-35. Temperature (°C) relationship with mortality and MTBBSI 74
Figure 1-36. Albumin and globulins by outcome and MTBBSI. 74
Figure 1-37. SIRS, qSOFA, SOFA Venn diagram 75
Figure 1-38. Correlation of variables traditionally associated with sepsis with their first 3 PCs (varimax rotation). 76
Figure 1-39. 'Sepsis' variables PCs association with MTBBSI and mortality. 76
Figure 1-40. Lactate, and sepsis principal component 2, correlate with glucose and inflammation markers. 78
Figure 1-41. Regression model predicting venous glucose from independent variables lactate and age. 79
Figure 1-42. Trend in platelet count during admission in 43 patients from KDHTB cohort. 81
Figure 1-43. Covariance in core variables related to MTBBSI and mortality. 86
Figure 1-44. Structural equation model relating selected core variables to disseminated TB and mortality outcome. 87

Figure 1-45. Acute Kidney Injury SEM. 88
Figure 2-1. Sources of error in prediction schematic. 95
Figure 2-2. Consort diagram for May 2016 predictive modelling analysis. 98
Figure 2-3. Model performance measured by ROC AUC. 106
Figure 2-4. Training versus test data estimates of ROC AUC. 108
Figure 2-5. ROC curve plots for ensemble model 109
Figure 2-6. Predicted probability from ensemble model mapped to classification rule. . 110
Figure 2-7. Increasing yield from additional MFL blood cultures. 113
Figure 3-1. WHO algorithm: managing PLWHIV & suspected of having TB (seriously ill) 121
Figure 3-2. Identification of primary datasets, flowchart. 128
Figure 3-3. Proportion data missing by variable and primary dataset. 131
Figure 3-4. Predicted probability of TBBC+ by CD4 count, danger sign, and hospitalisation status. 135
Figure 3-5. Availability and results of sputum Xpert or culture, and urine-LAM in patients with TBBC+. 137
Figure 3-6. Sensitivity and diagnostic yield of sputum Xpert/culture and urine-LAM in patients with TBBC+. 138
Figure 3-7. Naive Kaplan-Meier plot showing mortality over time by TBBC status. 141
Figure 3-8. Mosaic plots of early mortality by time-to-TB-treatment in different patient strata. 142
Figure 3-9. Predicted probability of early mortality in TB patients by CD4 count, danger signs, TBBC+, and TB treatment delay. 142
Figure 3-10. Simulating Simpson's paradox in relationship between urine-LAM and death 146
Figure 4-1. Hobby et al. comparison of CFU & Ziehl-Neelsen microscopy counts in sputum during first 150 days pulmonary TB treatment 154
Figure 4-2. Continuous spectrum of live/dead cell states of bacteria. 164
Figure 4-3. Example test runs of nine different fluorescent dyes on BCG broth cultures. 175
Figure 4-4. Linearity of SYBR-gold bacilli counts across different live / heat-killed cell preparation mixes 176

Figure 4-5. Example screening experiment for optimal SSC & FSC thresholding strategy. 179
Figure 4-6. Comparison 3 thresholding strategies in heat killed and SYBR-gold stained mid-log phase BCG broth culture. 180
Figure 4-7. Changing FSC/SSC region of mycobacteria during log-phase growth. 182
Figure 4-8. Sorting populations of mycobacteria based on light scatter for downstream microscopy characterisation. 182
Figure 4-9. Effect of vortex, sonication, and needle emulsification on FCM population and CFU counts. 184
Figure 4-10. Clumps not disrupted by emulsification eventually emerge in late log-phase cultures. 185
Figure 4-11. Quantification of clumping despite emulsification over growth phases. 185
Figure 4-12. Testing Saito 'centrifuge' method for single-cell preparation 186
Figure 4-13. Schematic of final FCM method. 187
Figure 4-14. CFU and FCM defined *in vitro* growth curves of *M. bovis* BCG. 188
Figure 4-15. Optical density defined *in vitro* growth curves of *M. bovis* BCG. 188
Figure 4-16. Sub-populations as a proportion of total cell count denominator. 189
Figure 4-17. Rate of growth in broth culture correlates with proportion of cells CA+, but not proportion CFU positive. 190
Figure 4-18. Correlation between CFU and CA+ counts under normal *in vitro* growth conditions. 190
Figure 4-19. Optical density is determined by total biomass in culture, with condition dependent correlation with CFU count. 191
Figure 4-20. Sample processing for time-kill experiments. 192
Figure 4-21. Raw data FCM plots for CA+ bacilli by time & antimicrobial condition ... 194
Figure 4-22. Raw data FCM plots for heat-killed SYBR-gold stained bacilli (HK total cell count data) 195
Figure 4-23. Raw data FCM plots for SYBR-gold stained bacilli (not heat-killed prior to staining) 196
Figure 4-24. K-means clustering classification ("gating") of FCM events. 197
Figure 4-25. CA+ event clustering applied to new data 198
Figure 4-26. Time-kill curves for absolute counts. 199

Figure 4-27. Time-kill curves based on proportions. 200
Figure 4-28. CA+ count time-kill data: raw (A) & modelled (B). 202
Figure 4-29. CFU count time-kill data: raw (A) & modelled (B). 203
Figure 4-30. HK (total-cell) count time-kill data: raw (A) & modelled (B). 204
Figure 4-31. SG+ count time-kill data: raw (A) & modelled (B). 205
Figure 4-32. Sigmoid E_{max} models applied to CFU & FCM time-kill data. 207
Figure 4-33. Example of dual SG staining population. 208
Figure 4-34. Permeabilization method development, experiment 3.4. 209
Figure 4-35. Permeabilization method development, experiment 5.0 & 5.1. 210
Figure 4-36. Permeabilized BCG cells show dual SG staining under all antimicrobial conditions tested. 212
Figure 4-37. Ratio of P2 to P1 bacilli by antimicrobial condition. 214
Figure 4-38. Ratio of P1 to P2 bacilli by antimicrobial and duration of exposure. 214
Figure 4-39. Images of bacilli stained with SYBR-gold and sorted by P1 & P2. 215
Figure 4-40. Fluorescence along longitudinal axis of P2 & P1 bacilli. 216
Figure 4-41. Number of fluorescent peaks and bacilli length by P1 & P2. 216
Figure 4-42. Continuous spectrum of live/dead cell states of bacilli, as observed by CFU & fluorescent probes in FCM. 219
Figure 5-1. Two pilots & sub-study used to develop methods to identify &quantify MTBBSI. 231
Figure 5-2. Visualisation of a 13mm filter membrane sealed in a 20mm tissue culture dish secured on microscope stage using custom machined aluminium holder. 233
Figure 5-3. Centrifuge filter holder (right). 234
Figure 5-4. Centrifuge parameters to maximise recovery of bacilli in suspension. 235
Figure 5-5. Example experiment testing different detergent & enzyme conditions of blood lysis buffer. 236
Figure 5-6. Summary of iterative development of selective lysis method. 237
Figure 5-7. Initial test of DMN-tre staining of BCG spiked blood versus SYBR-gold staining. 239
Figure 5-8. DMN-tre microscopy images from pilot 2. 242
Figure 5-9. Time-to-detection in MFL for paired positive samples: direct versus cell pellet inoculation. 243

Figure 5-10. Time-to-detection in MFL for paired positive samples: blood lysate versus cell pellet inoculation. 245
Figure 5-11. Serial MFL culture results from pilot 1. 246
Figure 5-12. TTD from serial MFL culture results from pilot 1. 247
Figure 5-13. Xpert-ultra CT correlation with number of bacilli in spiked blood. 249
Figure 5-14. Blood Xpert-ultra versus MFL results from clinical pilot testing. 250
Figure 5-15. Comparing Xpert-ultra CT values based on rpoB & IS6110-IS1081 probes. 251
Figure 5-16. Polymorphprep SOP 253
Figure 5-17. Comparison Xpert-ultra CT values for different blood compartments. 254
Figure 5-18. MTBBSI detection by method, patient & timepoint. 265
Figure 5-19. MTBBSI detection across patients by method & timepoint. 266
Figure 5-20. MTBBSI quantification: distribution of maximum values by method. 267
Figure 5-21. Pairwise correlations for MTBBSI quantification methods, & urine Xpert-ultra CT. 267
Figure 5-22. TTD in MFL MTBBSI time-kill curve. 269
Figure 5-23. Log DMN-tre+ bacilli per ml MTBBSI time-kill curve 270
Figure 5-24.Blood Xpert-ultra CT value MTBBSI time-kill curve 271
Figure 5-25. Urine Xpert-ultra CT value MTBBSI time-kill curve. 272
Figure 5-26. Deriving AUC PD summary for time-kill curves 273
Figure 5-27. Correlation of clinical variables with PD summary measures. 276
Figure 5-28. Correlation of clinical variables with AUC72h log DMN-tre bacilli per ml. 277
Figure 5-29. DMN-tre microscopy of MTBBSI: single bacilli 2-4µm. 278
Figure 5-30. DMN-tre microscopy of MTBBSI: doublet bacilli 279
Figure 5-31. DMN-tre microscopy of MTBBSI: single bacilli 4-10µm 279
Figure 5-32. DMN-tre microscopy of MTBBSI: microcolonies. 280
Figure 5-33. Bacilli length on DMN-tre microscopy by sample timepoint 281

Table of Tables

Table 0-1. Basic descriptors of KDHTB cohort by TB diagnosis category. 9
Table 1-1. Principal forms of tuberculosis according to Pagel[107] 18
Table 1-2. Case series of MTBBSI from the first decade of the global HIV epidemic..... 20
Table 1-3. Cohort and case-control studies reporting clinical predictors of MTBBSI in PLWHIV 21
Table 1-4. Associations with mortality in 132 HIV-associated TB patients from Jooste dataset. 29
Table 1-5. Symptoms associated with blood culture status 36
Table 1-6. Radiology associations with TB blood culture. 39
Table 1-7. Quantitative clinical variables used in subsequent analysis. 43
Table 1-8. Univariate mortality associations 46
Table 1-9. Univariate associations with positive TB blood culture 49
Table 1-10. TB diagnostic results as predictors of cluster 2 membership. 54
Table 1-11. Predictors of metabolic acidosis 58
Table 1-12. Multivariate linear regression predicting platelets_sqrt. 80
Table 1-13. Core variables relating MTBBSI & mortality after supervised dimension reduction. 83
Table 1-14. Summary of core variable association with DTB score and mortality outcome; medians by grouping variables and test of significance. 85
Table 2-1. Full variable set considered for predictive modelling. 101
Table 2-2. List of 45 models assessed in May 2016 analysis 105
Table 2-3. Cross-validated model ROC AUCs in training data. 107
Table 2-4. Performance of predictive model in prospective sub-study. 112
Table 3-1. WHO algorithm: managing PLWHIV & suspected of having TB (seriously ill)[48] 120
Table 3-2. Identified primary datasets. 129
Table 3-3. IPD characteristics by primary dataset in 5746 patients meeting harmonised inclusion criteria for meta-analysis 130
Table 3-4. Iterative mixed-effect models for logged-odds of TBBC+. 134
Table 3-5. IPD associations with probability of no sputum obtained. 139
Table 3-6. IPD associations with probability of no uLAM obtained. 139

Table 3-7. Fixed effect associations with 30-day or inpatient mortality. 141
Table 4-1. Flow cytometry of mycobacteria: prior literature. 166
Table 4-2. Flow Cytometry defined cell populations. 181
Table 5-1. Direct comparisons of MFL & alternative culture methods for recovery of M. tuberculosis from blood. 226
Table 5-2. Selected blood PCR studies for TB diagnosis. 229
Table 5-3. Direct versus pellet MFL blood culture results from pilot 1 243
Table 5-4. Lysate versus pellet MFL blood culture results from sub-study 244
Table 5-5. Qualitative results Xpert-ultra for different blood compartments 253
Table 5-6. Patient presenting histories, summary by 12-week outcome. 258
Table 5-7. Baseline examination findings, summary by 12-week outcome. 259
Table 5-8. Imaging, sputum & uLAM findings, summary by 12-week outcome. 260
Table 5-9. Baseline blood results, summary by 12-week outcome. 261
Table 5-10. Daily rate of change in platelet count, haemoglobin, & log creatinine during admission period. 261
Table 5-11. Available samples by method. 262
Table 5-12. Pairwise comparison of method for detecting MTBBSI across all patient timepoints. 263
Table 5-13. Sensitivity & specificity of MTBBSI detection in patient for each diagnostic. 263
Table 5-14. Pharmacodynamic summary measures association with outcome. 275

0 Introduction

0.1 Background & motivation

The roll-out of antiretroviral drugs has arguably been the greatest public health initiative of our time. The headline global figures are astonishing. Over 20 million people are accessing treatment.[1] Millions of deaths have been avoided.[2] Life expectancy on antiretroviral therapy is rising, up to 60-90% of that of the general population in different settings.[3] But the pool of HIV infection continues to grow, with an estimated 37 million people living with HIV in 2016, and one million people still die with HIV infection annually.[1,4]

Any complacency is dispelled with a review of recent evidence from the front-line of the HIV epidemic. In high-burden settings, the proportion of patients initiating antiretroviral therapy when already profoundly immunosuppressed is not declining despite changes to national and international guidelines.[5-7] There is little evidence of shifting disease burden: people living with HIV still present and die from opportunistic infections.[8-10] In South African district hospitals, 10-years after the start of antiretroviral scale-up, the majority of medical inpatients are HIV-infected, and there is no evidence the proportion has yet fallen.[11] A marked burden of advanced HIV-disease and associated critical illness persists in high-prevalence settings.

A greater part of this critical illness is caused by HIV-associated tuberculosis. TB is the leading cause of admission worldwide in people living with HIV; 25% of HIV-associated in-hospital deaths are in patients diagnosed with TB.[12] The prevalence of TB in adult inpatients dying with HIV-infection is greater than 25% in most post mortem studies (pooled estimate, 40%).[13] Patients hospitalised with HIV-TB have case fatality rates in the range 10 to 50% (depending on setting case-mix, definitions and follow-up, which are highly variable between studies).[14-19]

Critically unwell, HIV-infected inpatients with advanced immunosuppression do not have typical TB presentations. Symptom screens which are well established in ambulant outpatients,[20] are unreliable in hospitalised people living with HIV.[21,22] Radiology findings are atypical and non-specific at lower CD4 counts.[23] Patients may be unable to produce sputum,[24,25] and are more likely to have sputum smear or culture negative disease with advanced HIV infection, which is in turn associated with higher risk of mortality.[26-29] Extra-pulmonary TB is also more common at lower CD4 counts and associated with mortality. [30,31] In keeping with these clinical findings, meta-analysis of post-mortem data shows that HIV-associated tuberculosis is 'disseminated' in 90% of fatal cases, and is undiagnosed ante-mortem in half of these patients.[13] The term 'disseminated' isn't defined in this systematic review, but high rates of reticulo-endothelial, intestinal, renal and hepatic involvement are reported in the best described individual studies (figure 1A).

In summary, HIV-associated tuberculosis in critically unwell inpatients is 'atypical' – often smear-negative, extra-pulmonary or disseminated. It is, however, managed with the same antimicrobial chemotherapy as other, 'typical' forms of tuberculosis: 6-month rifampicin-based regimen 2HRZE/4HR, with daily dosing, and rifampicin at ~10mg/Kg.[32] The systematic review and meta-analysis which supports standard therapy for tuberculosis in HIV co-infection found only trials which recruited pulmonary (>90% smear-positive) tuberculosis cases, with 24/27 trials specifically excluding patients who also had concomitant extra-pulmonary disease.[33] This is standard practice in TB PK/PD studies which assess treatment response by clearance of bacilli from sputum. In addition, the primary outcome for anti-tuberculosis therapy phase III trials is sterilising cure, not mortality. Consequently, while on meta-analysis there are trends towards higher mortality for HIV-infected patients in lower rifampicin exposure arms (e.g. thrice weekly versus daily dosing), no comparisons are adequately powered for death end-points.[33] There is a profound absence of evidence that standard TB therapy is adequate for critically unwell HIV-infected inpatients.

Indeed, observational data is in keeping with therapeutic failure in this patient group, with evidence of significant mortality in patients despite receipt of anti-tuberculosis therapy (figure 1B). For comparison, it is hard to think of other common infections which are managed with the same antimicrobial regimen irrespective of whether the patient has a predicted probability of death of close to zero or approaching 50%. But no interventional

trials have ever been conducted that test adequacy of current standard therapy for preventing mortality in these high-risk patients. In this regard, it could be argued that the disseminated form of tuberculosis seen in critically unwell HIV-infected inpatients is a neglected disease, an overlooked clinical problem festering despite the successes of the public-health approach to the HIV in high-burden settings. HIV wasn't historically a disease of poverty,[34] and its major route of transmission – sex – is fairly evenly distributed in society. But like other neglected diseases, dying from HIV and tuberculosis in the antiretroviral-era is disproportionately a fate of disenfranchised people.[35-38]

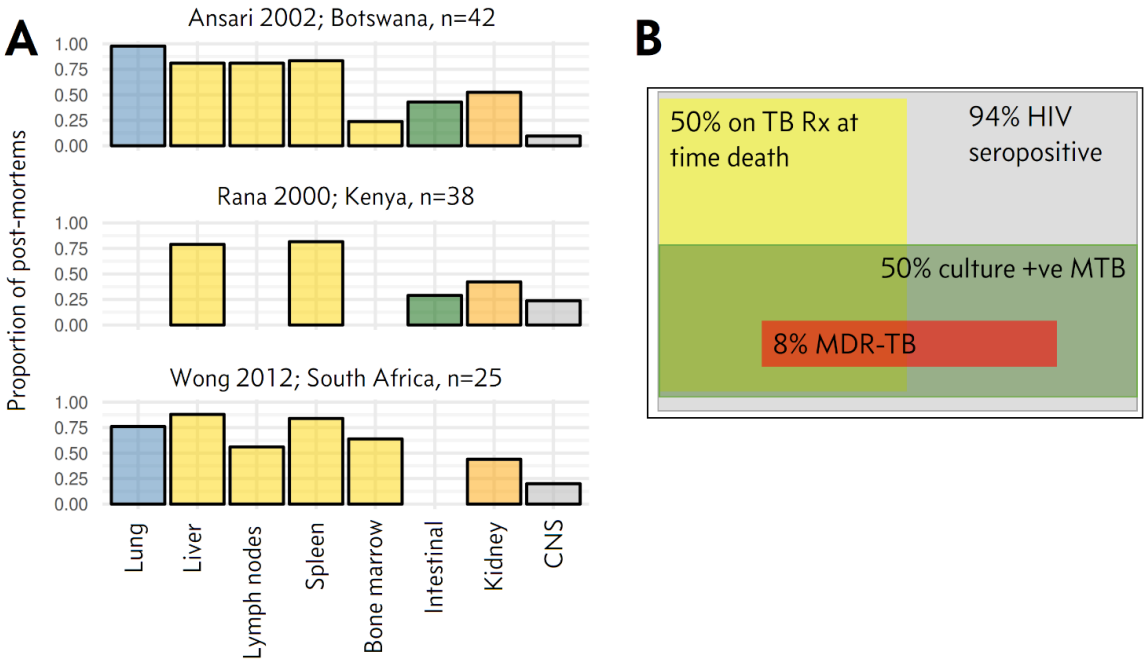

Figure 0-1. Post-mortem studies in HIV-associated adult inpatient deaths.

A. Three of the best described post-mortem studies[39-41] of patients dying with HIV-associated TB show the disseminated nature of this disease, with extensive reticulo-endothelial involvement. Categories without a bar were not assessed in the study.

B. A study from Edendale Hospital in KwaZulu-Natal performed limited post-mortem examinations on a random sample of all adult inpatient deaths, excluding only trauma and obstetric cases.[42] 94% of cadavers were HIV sero-positive, half were culture positive for *M. tuberculosis*, and half had been diagnosed with TB prior to death. The overlap between culture positive and TB diagnosed ante-mortem cases was 58%. This means that 42% had died with undiagnosed TB (a diagnostic failure), but also that a substantial number of patients died despite being on anti-tuberculosis therapy – evidence of a therapeutic failure. Median time from admission to death was only 4-days in these patients.

0.2 Thesis

The central thesis presented in this volume is that severe HIV-associated tuberculosis needs to be better characterised to develop a rational basis for future interventional trials. It is argued that 'atypical', 'smear-negative', 'extra-pulmonary' or 'disseminated' HIV-associated tuberculosis is better understood as a bacteraemic disease, fundamentally gauged by the bacilli burden and extent of blood stream infection. This specific and mechanistic clinical characterisation allows novel exposition of disease phenotype and pathophysiology, makes a case for investigating therapies with intensified bactericidal activity, and provides tools which may facilitate testing these interventions.

This thesis is *not* a case for expanding the use of blood cultures for diagnosing tuberculosis in advanced HIV-infection. TB blood culture is an expensive test of limited clinical value in low-resource settings. Even where available, the time to detection (averaging around 3 weeks) means TB blood culture has limited scope to influence management. Calls to roll-out TB blood culture were rightly dismissed by experts 20 years ago,[43] and subsequent developments in TB-diagnostics[22] make the case for blood culture even weaker now. Nonetheless, it will be shown in this thesis that, in research settings, TB blood culture is a useful tool for understanding severe HIV-associated tuberculosis. As an analogy, PET-CT scanning has been used to better characterise latent TB infection,[44] but this does not imply that TB contacts should now be sent for PET-CT. Similarly, better clinical descriptions of *M. tuberculosis* blood stream infection (MTBBSI) empower clinicians to make empirical diagnoses, just as we don't only rely on blood culture to diagnose bacterial endocarditis in a patient with myalgia, fever, and Osler's nodes, or to diagnose blood-stream embolic *S. aureus* in an intravenous drug user with sepsis and multiple peripheral lung abscesses on chest x-ray.

This is a general theme of this work, that detailed clinical description of severe HIV-associated tuberculosis – and specifically of *M. tuberculosis* blood stream infection – remains fruitful. Clinical descriptions may seem an anachronism at a time when clinical science increasingly looks to systems biology and the 'omics for inspiration. But the power of these techniques rests on them being related to real-world phenotypes: without clinical metadata, big-data is just noise. A second, related, theme in this thesis is that the dichotomy between a traditional clinical research approaches (data from observation and

description, e.g. the much-maligned case series) and 'modern' approaches (systematic, unbiased, high-resolution data, e.g. gene-expression analysis) is not as stark as it seems. Clinicians have always handled high-dimensional data, and are running causal models and classification algorithms intuitively every time they make a diagnosis. In this thesis, computationally intensive methods espoused by systems biology – such as hierarchical clustering and principle components analysis – are successfully applied to clinical data, to give a low-dimensional summary of clinical phenotypes and relate this to bacilli burden and extent of blood stream infection.

The idea that bacilli burden – or indeed extent of blood stream dissemination – are the major axis determining clinical variation in tuberculosis disease is not new, but can be dated back to the early 20th century giants of TB pathology,[45,46] or even Robert Koch.[47] Measuring and counting bacilli is a theme throughout this thesis. Novel techniques are developed and explored for quantifying mycobacteria in the lab and in blood or urine. Importantly, these methods allow systematic assessment of bacilli burden in the body and in the blood in a way which would have been unimaginable to Krause, Pagal, or Koch, but substantiates their ideas intently.

0.3 Overview of chapters

Chapter 1 reviews some of these historical ideas, reviewing the semantic classifications of disseminated and blood stream tuberculosis. It is argued that blood stream infection is a mode of tuberculosis infection, which has an exaggerated form in advanced-HIV co-infection. The clinical phenotype of advanced HIV-associated tuberculosis is then described using unprecedented detail afforded by the results of the KDHTB cohort study (detailed below), and it shown that a substantial portion of co-variance in clinical variables and death can be related to TB blood culture positivity, or the combined measure of blood culture, urine-Xpert and urine-lipoarabinomannan positivity, which are all hypothesised to be mechanistically related to total bacilli burden and blood stream dissemination.

In chapter 2 the ability to predict TB blood culture positivity from baseline clinical variables available on day of admission to hospital is shown. Using training and test data sets from the KDHTB study, a variety of machine-learning techniques are employed to

develop a final model with area under ROC curve around 0.85 for TB blood culture positivity. This is validated in a prospective cohort, which is also used to show that the additional yield associated with doing more than one TB blood culture is similar to that established for other non-mycobacterial blood stream infections. The predictive modelling developed here is used to enrich recruitment to the KDHTB sub-study presented in chapter 5.

The third chapter reports a 7000 patient individual participant data meta-analysis used to define rates of TB blood culture positivity in HIV-associated tuberculosis. The prevalence of MTBBSI has been underestimated in previous studies, and WHO danger-sign positive HIV-infected inpatients with tuberculosis and a CD4 count less than 100 cells/mm^3 are more likely than not to be TB blood culture positive if at least 2 cultures are sent prior to start of TB therapy. It is argued that patients with MTBBSI are therefore an important group in which to validate the WHO '*algorithm for managing people living with HIV and suspected of having TB (seriously ill)*'.[48] Evidence is presented to show that sputum diagnostics are unreliable rule-out tests for TB in patients with BSI, particularly if critically unwell. In addition, delay in empirical treatment is likely independently associated with mortality in MTBBSI patients.

Chapter 4 reviews some of the difficulties of quantifying mycobacteria, and describes the development of a novel flow cytometry method for absolute counting of mycobacteria in *in vitro* broth cultures. This method is used to describe sub-populations of bacilli with differential response to antimicrobials – i.e. phenotypic heterogeneity related to antimicrobial action – and supports the idea that culturability gives a limited window on pharmacodynamics of mycobacteria.

The flow cytometry method is used in the development of methods for identifying and quantifying *M. tuberculosis* in blood, described in chapter 5. A novel blood microscopy technique using mycobacterial dye 4-N,N-dimethylaminonaphthalimide-trehalose (DMN-tre), and a method for detecting TB in blood using GeneXpert-ulta cartridges, are shown to have equal or greater sensitivity compared to Myco/F lytic blood culture. All three methods are used to serially quantify MTBBSI over the first 24-hours of anti-tuberculosis treatment in 28 HIV-infected inpatients. This shows marked variation in blood bacilli burden and response to treatment between patients, and provides evidence

that this in turn is related to mortality outcome. It is argued this can be the basis of a pharmacodynamic biomarker of treatment response, to facilitate future interventional trials focussed on MTBBSI.

0.4 The KDHTB study

All the work in this thesis is based on or nested within the "Defining interventions to reduce mortality in severe HIV-associated tuberculosis" (KDH-TB) study, PI Professor Graeme Meintjes. The study is referenced continually throughout so is summarised here.

0.4.1 Study procedures

KDHTB ran from January 2014 to October 2016 and recruited HIV-infected patients newly admitted to Khayelitsha Hospital aged 18-years or more, with CD4 count less than 350 cells/mm3, and suspected of having TB (i.e. a new diagnosis). Pregnant patients and those in receipt of 3 or more doses of TB therapy within the preceding month were excluded.

Consenting patients had extensive assessment and sample collection on day of recruitment, including unselected Myco/F lytic TB blood culture (5ml blood), collection of urine for lipoarabinomannan testing and concentrated urine GeneXpert testing, and sputum (with induction attempted if non-productive or absent cough) GeneXpert and culture. Patients were managed by non-study health care team at Khayelitsha Hospital, and followed-up by study team at 4 and 12 weeks to ascertain survival (by hospital visit, or failing this telephone or hospital record or death registry review).

0.4.2 Setting

Khayelitsha is a township near Cape Town, South Africa, with an official population estimate of approximately half-a-million residents; two-thirds of households have a monthly income less than R3200 (~US$200), half of households are informal settlements, and 61% have access to piped water.[49] HIV-seroprevalence is ~34% in antenatal attendees,[50] and TB notification rate was at least 1500/100,000 in 2011.[51] Khayelitsha Hospital is a public sector district facility where patients too ill to be managed in the

community are referred from primary care clinics. It has approximately 150 inpatient medical beds but no high-dependency or intensive care unit.

0.4.3 Cohort description

For the purposes of analysis in this thesis, patients were classified as confirmed TB if they had *M. tuberculosis* identified on at least one culture sample or by GeneXpert. Patients were classified as having a clinical TB diagnosis if they had a compatible clinical picture,* were treated for TB, and no alternative diagnosis was made, or if they were urine-lipoarabinomannan positive (≥1 on Alere lateral flow assay). A STROBE flow chart showing recruitment is shown in figure 2. Basic descriptions of the cohort are shown in table 1.

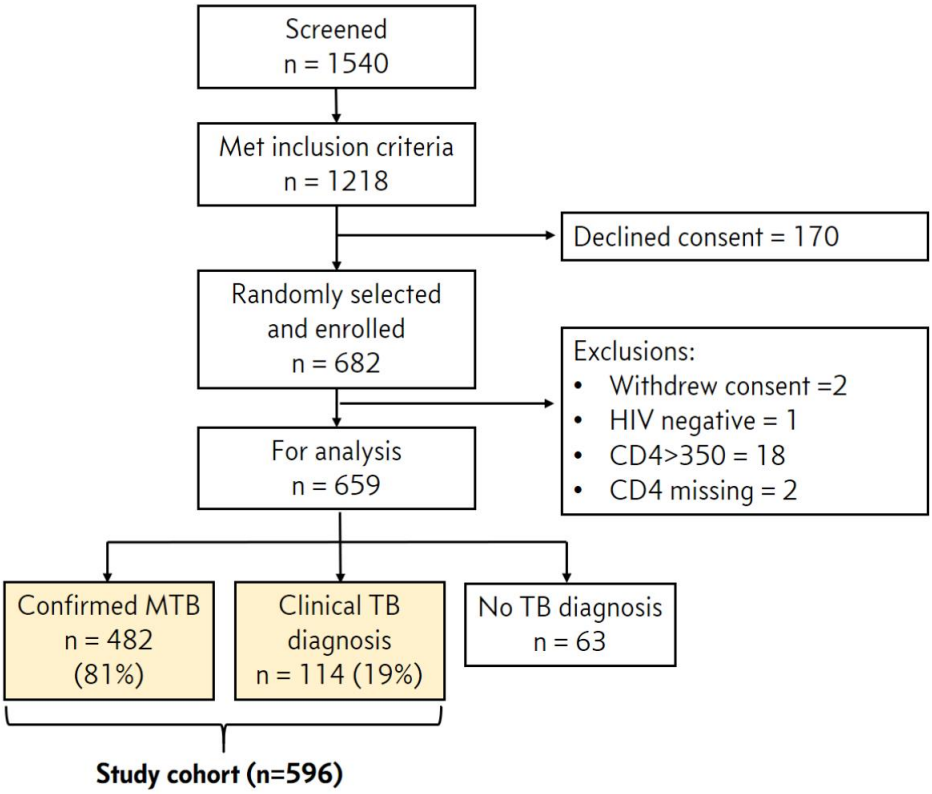

Figure 0-2. STROBE flow diagram for KDHTB study.

* Exudative or lymphocytic pleural effusion; pericardial effusion; adenopathy greater than 2cm in diameter; compatible chest x-ray findings.

Table 0-1. Basic descriptors of KDHTB cohort by TB diagnosis category.

	Clinical TB (N=114)	Proven MTB (N=482)	Total (N=596)	p value
Male	43 (37.7%)	243 (50.4%)	286 (48.0%)	0.02
Age, years	37.6 (31.0 to 43.6)	35.8 (30.8 to 43.3)	35.9 (30.9 to 43.4)	0.674
ART status				0.052
Defaulted	34 (30.1%)	111 (23.2%)	145 (24.5%)	
Naive	33 (29.2%)	198 (41.3%)	231 (39.0%)	
On ART	46 (40.7%)	170 (35.5%)	216 (36.5%)	
CD4 count, cells/mm3	97 (44 to 186)	53 (18 to 111)	59 (22 to 121)	< 0.001
Detectable plasma HIV	96 (85.0%)	414 (87.0%)	510 (86.6%)	0.68
Previous TB history				0.012
None	47 (43.9%)	270 (57.9%)	317 (55.3%)	
Previous TB	60 (56.1%)	196 (42.1%)	256 (44.7%)	
TB treatment doses prior to recruitment				0.71
0	100 (87.7%)	422 (87.6%)	522 (87.6%)	
1	9 (7.9%)	46 (9.5%)	55 (9.2%)	
2	5 (4.4%)	13 (2.7%)	18 (3.0%)	
3	0 (0.0%)	1 (0.2%)	1 (0.2%)	
Any antibiotics prescribed	111 (97.4%)	460 (95.4%)	571 (95.8%)	0.505
Ceftriaxone prescribed	104 (91.2%)	420 (87.1%)	524 (87.9%)	0.296
Serum cryptococcal antigen test				0.296
Negative	109 (95.6%)	455 (94.8%)	564 (94.9%)	
Positive	5 (4.4%)	16 (3.3%)	21 (3.5%)	
Detectable CMV viraemia				0.25
FALSE	73 (65.8%)	281 (59.3%)	354 (60.5%)	
TRUE	38 (34.2%)	193 (40.7%)	231 (39.5%)	
Sputum TB culture				< 0.001
Missing result	43	135	178	
Negative	71 (100.0%)	38 (11.0%)	109 (26.1%)	
Positive	0 (0.0%)	309 (89.0%)	309 (73.9%)	
Sputum Xpert				< 0.001
Missing result	33	96	129	
FALSE	80 (98.8%)	63 (16.3%)	143 (30.6%)	
TRUE	1 (1.2%)	323 (83.7%)	324 (69.4%)	
Urine-Xpert				< 0.001
Missing result	8	71	79	
Positive	0 (0.0%)	227 (55.2%)	227 (43.9%)	
Negative	106 (100.0%)	184 (44.8%)	290 (56.1%)	
Urine-LAM				< 0.001
Missing result	7	65	72	
Negative	55 (51.4%)	131 (31.4%)	186 (35.5%)	
Positive	52 (48.6%)	286 (68.6%)	338 (64.5%)	
TB blood culture				< 0.001
Missing result	12	12	24	
Negative	102 (100.0%)	250 (53.2%)	352 (61.5%)	
Positive	0 (0.0%)	220 (46.8%)	220 (38.5%)	
Rifampicin resistance isolate	0 (0.0%)	55 (11.4%)	55 (9.2%)	< 0.001

12-week outcome				0.315
Died	19 (16.7%)	108 (22.4%)	127 (21.3%)	
Loss to follow-up	1 (0.9%)	8 (1.7%)	9 (1.5%)	
Survived	94 (82.5%)	366 (75.9%)	460 (77.2%)	
Days to death	6 (3 to 23)	15.5 (4 to 40)	13 (4 to 35)	0.097
Improved overall by 12-weeks	71 (62.3%)	295 (61.2%)	366 (61.4%)	0.916

Median (inter-quartile range), or frequency (%) shown; P-value is from Wilcox Rank-Sum test or Fisher's exact test as appropriate.
ART = Antiretroviral therapy; CMV = cytomegalovirus; Any antibiotics prescribed = any antibiotics prescribed at time of recruitment for treatment of bacterial infection (not including anti-TB therapy); Rifampicin resistance isolate = any cultured isolate had rifampicin resistance on DST or any Xpert sample had rpoB probe result in keeping with rifampicin resistance.

1 Clinical description of HIV-associated *M. tuberculosis* blood stream infection

1.1 Introduction

"If the names are unknown, knowledge of the things also perishes."
Carl Linnaeus, *Philosophia Botanica* (1751), aphorism 210.

This chapter starts with a discussion of semantics. HIV-associated TB is often described as 'disseminated', but the term is ill-defined and used inconsistently: a vague name for a condition mostly considered non-specific. Here, it is claimed that this descriptive nihilism is unwarranted. It is argued that HIV-associated disseminated tuberculosis is essentially a spectrum, characterised by bacilli burden, and degree of ongoing, active blood stream infection. *M. tuberculosis* blood stream infection (MTBBSI) is an explicit name for this condition, and can, in fact, be considered highly specific.

To support this, some compelling classical descriptions of bacteraemic dissemination of tuberculosis are reviewed and an attempt is made to summarise these mechanistically. The contention is that *M. tuberculosis* blood-stream dissemination is pivotal in TB's natural history, and that HIV-associated MTBBSI can be conceived of as a reversion to, and exaggerated form of, the bacteraemic mode of tuberculosis infection. Modern descriptions of HIV-associated MTBBSI are also reviewed, but these are argued to be haphazard and superficial. A more comprehensive clinical description is attempted using data from the uniquely rich KDHTB dataset. Statistical data reduction techniques are employed to uncover fundamental patterns of covariance. Rather than being entirely data driven and descriptive, these findings are related to prior clinical theory and to the contemporary sepsis literature, making inferences about pathophysiology where possible.

1.2 What is disseminated TB? Classifications, definitions & mechanisms.

1.2.1 The classification of disseminated tuberculosis

The International Classification of Disease[52] lists many forms of tuberculosis: respiratory (including pleural and laryngeal); 7 types of tuberculosis of the nervous system; tuberculosis of the heart; eye; ear; endocrine glands; musculoskeletal system; genito-urinary system; lymph nodes; digestive tract or hepato-biliary system; cutaneous or mucous membrane (including, explicitly, the anal canal); the placenta; and the thymus gland. Miliary tuberculosis [sub-index term, *disseminated tuberculosis*] is noted as the "widespread dissemination of *Mycobacterium tuberculosis* via haematogenous spread" and defined as millet-like seeding on chest radiography. But there is no explicit mention of tuberculosis bacteraemia anywhere in this capacious classification.[†]

HIV-associated tuberculosis is classified separately in the ICD (IC61.3: *HIV infection clinical stage IV associated with tuberculosis*, a stub, listed without further description or associated index terms), and tuberculosis BSI could reasonably be considered ontologically subsumed here. But even international standards on HIV-associated tuberculosis are reluctant to name tuberculosis bacteraemia. Like the ICD, World Health Organisation (WHO) guidelines on HIV-associated TB do not address MTB BSI directly, but instead refer to 'disseminated TB':

> "People living with HIV with extrapulmonary TB often have disseminated disease and are at high risk of rapid clinical deterioration and death. The commonest forms include lymph node (especially in the neck or under the arms), pleural (usually one-sided pleural effusion) and disseminated TB (disease that is not limited to one site in the

[†] The spleen and bone marrow are also conspicuously absent as explicit entities in the tuberculosis section.

body). Pericardial and meningeal TB are less frequent forms of extrapulmonary TB but are more likely to result in fatal outcomes."[48]

"HIV-related extrapulmonary tuberculosis is a WHO clinical stage 4 (advanced AIDS) diagnosis, and patients with HIV-related extrapulmonary tuberculosis often have disseminated disease and are at high risk of rapid clinical deterioration and death. The accurate diagnosis of extrapulmonary tuberculosis is complex and difficult…high rates of undiagnosed disseminated tuberculosis have been consistently identified in febrile, HIV-positive inpatients…"[53]

Although the five citations given to support this last statement are all *M. tuberculosis* blood culture studies,[54-58] tuberculosis bacteraemia isn't directly mentioned in any WHO HIV-TB guideline.‡ The definition of "disseminated TB" is left vague ("not limited to one site in the body"), and – in contrast to other forms of extra-pulmonary TB – disseminated TB is described as non-specific, characterised by an absence of clinical signs, and by negative test results.

This uncertainty accurately reflects the wider literature. No consistent definition is used by studies reporting on disseminated, HIV-associated, tuberculosis (figure 1). Few commentators have directly addressed the relationship between disseminated tuberculosis and blood stream infection.

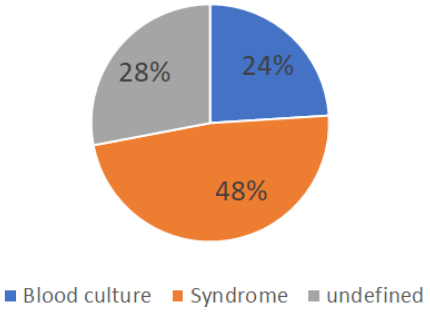

Figure 1-1. Definition of disseminated TB in n=50 random sample from PubMed Disseminated & TB & HIV [Title/Abstract]

An exception is the work of John Crump *et al.*, who consistently define disseminated tuberculosis as "isolation of *Mycobacterium tuberculosis* from blood or bone marrow, from a

‡ This apparent reticence to name TB bacteraemia is very likely partly because TB blood culture is an inappropriate diagnostic test for high-burden low-resource settings, due to its expense and limited role in clinical decision making. This point is well made in correspondence in the Lancet in 1999-2000.43. Hudson CP, Maartens G, Wood R, et al. Unrecognised mycobacterium tuberculosis (multiple letters). *Lancet* 2000; **355**(9198): 141-3. This thesis is categorically *not* arguing for greater use of blood culture in low resource settings.

liver biopsy specimen, or from specimens from ⩾2 non-contiguous organs", making MTB BSI a subset of disseminated tuberculosis.[59,60] Crump *et al*. go further, distinguishing bacteraemic from non-bacteraemic disease phenotypes in their retrospective case series (n=52, 46% HIV-infected) from Duke University Medical Centre: patients with bacteraemic disseminated tuberculosis less frequently had miliary chest x-ray (risk ratio = 0.32) but higher 30-day mortality (risk ratio = 5.6).[60] Others have specifically linked this clinical diversity to different histo-pathology determined by immune-status:

> "While tubercules form in miliary TB in the tissues, they are not present in disseminated TB: nonreactive generalized TB. The fate of host in TB bacillemia is dictated by the immune status: in case of immunocompetency, miliary TB; in case of immunocompromisation, disseminated TB. Histopathological changes are related to the degree of cellular immunodeficiency. In patients with normal CD4 lymphocyte count, classical tubercules develop. In patients with severe lymphopenia… atypical foci… unorganized granulomas, scanty giant cells… necrosis and large amounts of bacilli."[61]

The implication is that, while all miliary TB is haematogenous, not all haematogenous TB is miliary. Established descriptions of miliary TB pre-dating HIV-coinfection are worth reviewing next.

1.2.2 Classical descriptions of miliary tuberculosis

The most classical description is of uncontained primary infection (typically in children and infants) resulting in *acute* haematogenous dissemination, followed by development of 'millet-like' (1-3mm) well organised granulomas at the multitude of seeded sites.[62,63] Initially, development of chronic lung tuberculosis was thought to preclude miliary spread,[64] but by the mid-20th century substantial case and post-mortem series reported acute miliary dissemination from (presumed reactivated) chronic pulmonary and extra-pulmonary lesions in adults.[64-66] The key features in all these reports were that multiple organs – invariably including the spleen, liver, bone marrow, and often meninges and choroid – demonstrated *lesions of the same size and acute stage*, suggesting a discrete bacteraemic event, and retained ability to form organised granulomas.

A failure to form miliary granulomas after an acute haematogenous dissemination was also well recognised, under a variety of names:

- *non-reactive tuberculosis* (because of the absence of cellular reaction at foci, favoured by pathologists, who generally made the diagnosis);[67]

- *acute tuberculosis septicaemia* (classically associated with blood dyscrasias);[68-70]
- *typhoidal form* tuberculosis (described in detail by Osler: "the temperature increases, the pulse rapid and feeble, the tongue dry; delirium becomes marked and the cheeks are flushed… pulmonary symptoms may be slight… enlargement of the spleen occurs… [petechiae and] Cheyne-Stokes breathing occur towards the close");[71]
- *Yersin type* tuberculosis (Yersin recorded that rabbits injected intravenously with very large numbers of bacilli die with "septicaemic cachexy" before developing any macroscopic lesions);[72] and
- *sepsis tuberculosa acutissima*, *sepsis tuberculosis gravissima*, or Landouzy's septicaemia, which are still sometimes used to specifically describe tuberculosis associated with acute septic shock or multi-organ failure.[73-76]

Acute miliary disseminations of tuberculosis were distinguished from more chronic 'abortive dissemination'[45] of tuberculosis:

> "68 per cent of… pulmonary tuberculosis at autopsy showed extrapulmonary foci of a chronic type… [these are] ″benign generalizations″ of pulmonary forms of tuberculosis… when occasional tubercle bacilli are released, producing isolated tubercles in one or two additional sites, the disease has in a sense become generalized but is still quite distinct from acute generalized miliary tuberculosis… One must recognise, therefore, that disseminated tuberculosis infection may appear in several forms. One extreme is the acute, progressive disease… [the other] chronic, nonprogressive extrapulmonary tuberculosis lesion, which seldom, if ever, causes death."[65]

In fact, sub-acute, non-miliary, TB blood stream infection was strongly suspected by pathologists in the pre-antibiotic era, but they lacked the tools to observe this antemortem. In 244/804 post-mortems of adults dying of tuberculosis, Lewison *et al*. found TB lesions in the spleen of varying "size and chronicity", caused "in all probability, from repeated blood infection",[66] which doesn't sound very benign or non-progressive.

With the roll-out of chest radiology it was established that chronic but progressive disseminated disease was not only possible, but common, with remissions and relapses, and even recurrent miliary episodes.[77-79] This chronic course was noted to give rise to more heterogeneous pathology than was captured by the term 'miliary':

> "chronic miliary tuberculosis is a somewhat protean condition, which justifies the substitution of the name 'chronic disseminated tuberculosis'…"[80]

Subsequently, in the early-antibiotic, post-BCG era, a rapid decline in classic miliary TB in children was observed, and yet another category of disseminated TB came to the fore:

late generalised tuberculosis (LGT). This was defined as presence of miliary tubercles in multiple organs in the absence of an active primary Ghon complex.[81,82] Curiously, TB meeting this definition can be found in all prior adult post-mortem series of miliary TB that I have seen, and the new term seems to have emerged more in response to the "radical change in miliary tuberculosis epidemiology", which was now a disease of the elderly.[82,83] Physicians at the time were particularly alarmed by the fact that "cryptic"[84] miliary disease was being detected on post-mortem histology, but undetected on chest x-ray:

> "characterised by an insidious onset and progression and the absence of any reliable clinical pointers to the diagnosis… such forms of tuberculosis may even be missed on naked-eye examination of the organs at necropsy... the low rate of diagnosis in this group is disturbing."[83]

It was also clear from the post-mortem studies that some LGT was of the chronic, progressive type, where the "dissemination appeared episodic or protracted since acute lesions were admixed with tubercles showing partial or complete replacement fibrosis".[82] Choroidal lesions and meningitis appeared rare compared to classic acute miliary tuberculosis.[82-85] The insidious nature of LGT was specifically linked to waning "allergic response to the bacillus, as measured by skin tuberculin sensitivity… after the age of 50 years",[84] and "indiscriminate use of [recently discovered] cortisone therapy".[86]

How can we make sense of this shifting historical classification of disseminated TB? For a start, it's clear that classifications are made to fit the prevailing epidemiology, and biased by the available technical windows onto disease process. When only post-mortem data was available to correlate with clinical observation, disseminated TB could only be acute and fatal, or, chronic and non-progressive; the advent of chest radiology revealed this to be a biased understanding. When the case mix shifted to be dominated by elderly patients with declining cell mediated immunity and heterogeneous TB lesions, the terms "late generalised", "cryptic" and "anergic" TB were invented to emphasise a perceived departure from "classic" acute miliary presentations. If different diagnostic technologies – say, reliable blood culture, and PET-CT scans – had been available to clinicians working in the pre-antibiotic era, their classification of disseminated TB (which we have inherited) would have been different.

Further – and more speculatively – a mechanistic description of TB dissemination might help resolve some of the complexity. Specifically, how do TB bacilli end up in the blood stream?

1.2.3 Mechanisms of TB bacillaemia

I assert there are two pathophysiological processes described in the literature: (1) a sudden, stochastic event; and (2) bacillaemia as a regular event in the natural history of TB infection.

The former is clearly linked to acute miliary disease. Weigert found evidence of caseous lymph node erosion into a pulmonary blood vessel in a majority of miliary TB cases at post-mortem – the Weigert focus.[64,87] Similar cases have been made for rupture of tubercles in the vascular intima or thoracic duct, and emptying of a (pulmonary or extra-pulmonary) caseous focus into the circulation.[64,65] The sudden and stochastic nature of such dissemination events is illustrated by the rare but well described cases of miliary TB following surgical procedures or traumatic rupture[§] of latent tubercles.[88-93]

But acute miliary dissemination is an atypical process in TB's natural history. By contrast, after initial inhalation of bacilli, infection and spread via the lymphatics is an essential step in establishing infection, with a natural extension via the thoracic lymph node trunk to the subclavian vein (a "lymphatic disease with a pulmonary portal").[94] TB bacteraemia during primary infection is extensively described in animal models,[95-98] and has generally been accepted to occur in humans at least since the descriptions by Calmette.[99,100] There is even some indirect clinical evidence of an extended period of "silent bacillaemia" through post-primary infection in some patients.[101,102] In this conception, a "more general [haematogenous] distribution of infection [is] perhaps *the mode* of tuberculosis". [103]

Is such dissemination the exception or the rule? In 49 immuno-competent Mexican patients who died of causes unrelated to tuberculosis, with no history of tuberculosis disease, Barrios-Payán *et al*. identified *M. tuberculosis* DNA in lung (72%), spleen (70%), kidney (68%), and liver (66%) tissue.[104] In a post-mortem study of patients dying with

[§] "A man, aged 33, received a blow on the left testicle, followed by local and general symptoms. Eight-days later he had a rigor, and seventeen days later he died of miliary tuberculosis. Necroscopy showed that the left epididymis contained a softened caseous nodule smaller than a small cherry."88. May O. The Relation between Trauma and Tuberculosis: From the Point of View of Accident, Insurance. *Br Med J* 1928; **2**(3545): 1090-1.

HIV-associated tuberculosis, genetic distance between bacilli isolated from different body sites in the same patient do not depend on spatial proximity: TB isolated from different lungs are no more genetically related than isolates from the same lung, and even bacilli from different organs are as likely to be closely related as those from two different ling sites.[105] The authors logically conclude that "similar patterns of migration within and between organs suggest that dissemination of *M. tuberculosis* across the lungs… is no easier than dissemination across organs".[105]

This evidence implies that blood stream infection is a routine part of TB's natural history, that bacteraemia is an inevitable result of progressive primary disease, and that all tuberculosis is disseminated to a greater or lesser extent. This was certainly the view of Walter Pagel, the last great TB pathologist of the pre-antibiotic era, who called post-primary tuberculosis "haematogenous tuberculosis" (table 1).[106,107]

Table 1-1. Principal forms of tuberculosis according to Pagel[107]

Forms of tuberculosis	Description
Primary infection	"When the bacillus enters the lung a small patch of caseous broncho-pneumonia develops and later encapsulates… Before the primary focus is fully developed, a similar caseous lesion appears in one of the regional lymph nodes… The lymph nodes beyond the regional nodes first affected may become involved by lymphatic spread."
Post primary tuberculosis: haematogenous disseminated tuberculosis	"Haematogenous dissemination can be mild and benign or may cause severe and fatal illness. All intermediate stages are observed… the number of bacilli reaching the blood stream and multiplying in the tissues is the main concern."
Bronchogenic tuberculosis: lesions limited to the lungs	"Bronchogenic differs from primary tuberculosis in that the regional lymph nodes, though they may show some non-specific reactive changes… remain devoid of appreciable caseation. It differs from disseminated tuberculosis in that it is restricted to the lungs and the sputum draining channels (larynx and gut); further the lesions are asymmetrical and have a marked tendency to cavitation. As the condition progresses it is characterised by gradual destruction of the lungs by caseous and liquefying lesions produced by transmission of the bacilli along the bronchi."

All the various described classes of disseminated TB can be, tentatively, related to these two underlying processes then. Sudden releases of many bacilli into the blood stream can result in classic acute miliary tuberculosis or a non-reactive acute "typhoidal" tuberculosis septicaemia, depending on the number released and degree of hypersensitivity in the host. On the other hand, a spectrum of post-primary tuberculosis,

characterised by the "number of bacilli reaching the blood stream and multiplying in the tissues" (as a continuous process, not a discrete event) can encompass the other forms of disseminated TB. Paucibacillary extrapulmonary TB (for example, meningitis, adenitis, pleurisy – even if in "⩾2 noncontiguous" sites), "benign generalisations", "abortive dissemination" are at one end of this spectrum. Late generalised tuberculosis, "anergic TB of the elderly", and the disease often seen in post-mortem studies of HIV-associated tuberculosis, lie at the other extreme, representing failing immune containment of post-primary disease. This is a reversion to, and exaggerated form of, the bacteraemic stage of TB's natural history.

What are the implications? First, blood stream infection isn't an exotic addendum to HIV-associated disseminated TB, it's *the mode* of HIV-associated disseminated TB. The question is how much dissemination, i.e. *what is the total body bacillary burden*? And, *is the bacteraemic dissemination ongoing*? Blood culture – or other quantifications of bacilli in blood – give a direct and systematic answer to these questions. So, too, might urine based quantifications of bacilli burden and (renal) dissemination, like urine lipoarabinomannan and urine Xpert testing (discussed below). While Krause was frustrated that "native tissue reaction [is] the only visible process"[103] by which to gauge TB dissemination, we don't have to be.

Second, by accepting advanced HIV-associated disseminated TB is, fundamentally, a blood stream infection, a more explicit clinical phenotype can be demarcated. While disseminated tuberculosis is ill-defined, non-specific, and characterised by negative test results, MTB BSI is positively and mechanistically defined, homogenous and reproducible. This chapter aims to give a rigorous clinical description of MTB BSI, and show its central clinical importance in advanced HIV-associated tuberculosis, starting with a review of the previous literature.

1.3 Prior descriptions of HIV-associated MTBBSI

1.3.1 Clinical descriptions of HIV-associated MTB BSI

By the end of the 1980s there were 11 publications reporting 59 cases of tuberculosis isolated from blood culture in HIV positive patients.[108-118] These were all from high-resource, low-TB burden settings, where modern, liquid media mycobacterial blood culture techniques were starting to be adopted. Those that gave clinical descriptions reported MTB BSI to be associated with advanced immunosuppression, lymph node disease, 'atypical' presentations (i.e. limited pulmonary features), and high mortality (table 2). These descriptions were, however, far from systematic, and tuberculosis was overshadowed by *Mycobacterium avium* complex as a cause of mycobacteraemia in most of these settings.[112,113,115]

Table 1-2. Case series of MTBBSI from the first decade of the global HIV epidemic

1st Author	Year	Country	n	Clinical features reported in MTB BSI
Barnes[109]	1987	USA	6 cases	Lymphadenitis; lymphopenia; concurrent candidiasis and PCP; pulmonary symptoms, CXR and sputum microbiology of limited diagnostic value; poor prognosis
Prego[115]	1990	USA	2 cases	Liver and bone marrow involvement in both cases
Saltzman[116]	1986	USA	1 case	Anorexia, weight loss; concurrent pulmonary TB and PCP; lymphopenia
Shafer[117]	1989	USA	7 cases	Concurrent AIDS defining illness; high fever; raised alkaline phosphatase and LDH; miliary CXR; high early mortality
Bouza[110]	1988	Spain	16 cases	In 5 cases blood was the diagnostic sample; predominance of lymphatic disease; concurrent AIDS defining illnesses common; high early mortality.
Barber[108]	1990	USA	9 cases	Fever and severe weight loss; absence of pulmonary symptoms; lymphadenopathy; candidiasis; anaemia; abnormal LFTs and LDH; low CD4 counts; anergic skin tests; 4 patients had normal CXR at presentation; 2/9 cases sputum culture positive; 6 died within 7 months.
Handwerger[114]	1987	USA	5 cases	Generalised lymphadenopathy; candidiasis; chronic diarrhoea.

CXR = chest x-ray; LDH= lactate dehydrogenase; LFTs = liver function tests; PCP = *Pneumocystis carinii*

By contrast, when blood culture studies were subsequently carried out in low-resource, high-TB burden settings during the 1990s, tuberculosis was the more frequent blood pathogen.[54,55,119-123] Studies in these settings have also been – particularly in the last 20 years – increasingly systematic, with defined control groups allowing assessment of clinical features as 'predictors' of MTB BSI (table 3, figure 2). The most consistently identified predictors of MTBBSI have been low CD4 count and anaemia. Several other variables have a high 'hit rate', for example, hyponatraemia, lymphadenopathy, hypoalbuminaemia, and body mass index / mid upper arm circumference (figure 2).

Table 1-3. Cohort and case-control studies reporting clinical predictors of MTBBSI in PLWHIV

1st Author	Year published	Design	Inclusion	MTBBSI n	Algorithmic variable selection for multivariate testing
Muchemwa[124]	2016	cohort	HIV+ IP severe sepsis	n 70/201	Stepwise
Nakiyingi[125]	2015	cohort	HIV+ IP&OP suspected sm-ve TB	n 41/394	Univariate p<0.2 & stepwise
Crump[126]	2015	nested case-control	Patients who had TB blood culture performed in ACTG STRIDE study	n 18/90	Univariate p<0.1 & stepwise
Jacob[127]	2013	cohort	HIV+ IP severe sepsis	n 86/368	Stepwise
Feasey[15]	2013	cohort	HIV+ IP suspected TB	n 10/104	Univariate only presented
Crump[59]	2012	cohort	Febrile IP (157 HIV+)	n 12/403	Univariate only presented
Varma[128]	2010	cohort	HIV+ OP	n 31/2013	Univariate p<0.05 & stepwise
Lewis[57]	2002	cohort	Febrile or shock IP (285 HIV+)	n 57/344	Adjusted for a priori set demographic factors (age, sex, urban dwelling, education, AIDS diagnosis)
Lewis[57]	2002	cohort	Febrile or shock IP with TB diagnosis	n 57/116	Univariate only presented
von Gottberg[129]	2001	cohort	IP suspected TB (58 HIV+)	n 16/58	Univariate only presented
McDonald[58]	1999	cohort	Febrile IP (255 HIV+)	n 34/344	Univariate only presented

IP = Inpatient; OP = Outpatient

Studies identified from the 2375 abstracts screened for meta-analysis detailed in chapter 3. In these studies, patients with and without positive blood culture were compared within the population defined by the inclusion criteria. The two Lewis 2002 entries ([57]) are analyses from the same cohort using different inclusion criteria / control group as indicated. Associations with MTBBSI are shown in the next figure.

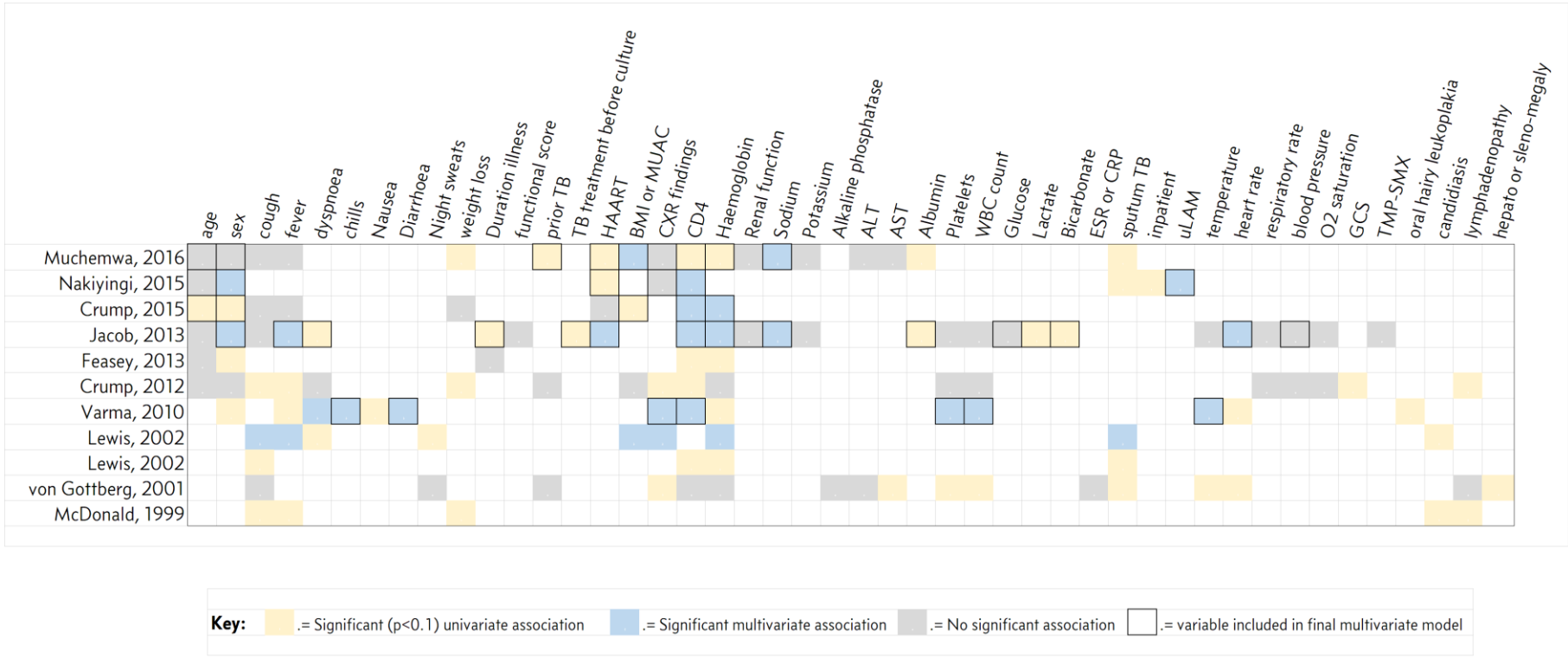

Figure 1-2. Clinical predictors associated with MTBBSI from studies in preceding table

Cells in matrix are coloured to indicate if an association was found (grey = none; yellow = univariate; blue = multivariate), with no colour (white) indicating the predictor was not assessed or not reported. In addition, predictors included in multivariate modelling are indicated by a black outline around the cell. There is substantial variation in what variables were assessed and adjusted for across studies.

There are several difficulties with interpreting these MTBBBSI clinical predictor studies:

1. Variable selection is inconsistent. Mostly, these studies are secondary analyses of datasets designed to answer other questions, so predictors are likely assessed opportunistically. While several studies emphasise variables which are 'independent' predictors, choice of variables to adjust for in multivariate models has been even more inconsistent, and generally not explicitly justified. The implicit assumption is that 'independent predictors' are 'stronger' predictors. But should we really conclude that, for example, CD4 count is not a strong predictor of MTBBSI because it becomes non-significant after adjusting for an apparently arbitrary set of co-variates?[124] Collinearity and small sample sizes increase this type II error risk.
2. Inclusion criteria, and therefore comparison groups, vary widely between studies. In studies that include substantial numbers of patients without TB in the control group, variables associated with TB generally (rather than BSI specifically) may still be strongly associated with MTBBSI. Associations could differ, or even reverse, with different inclusion criteria (Simpson's paradox[130]). For example, two of the best reported studies[124,127] recruited inpatients with severe sepsis; associations with MTBBSI within this stratum of patients may not represent the wider population of patients with HIV-associated TB. Useful metrics of clinical predictors (for example likelihood ratios) are clearly heavily dependent on the comparison group.
3. With one notable exception,[127] the studies don't report measures of predictive performance (like ROC AUC) or cross-validate their findings. Given the heavy use of automated variable selection (see table 3), overfitting is possible. This might not matter if the purpose is to assess the overall predictive performance of the (more parsimonious) model, but it likely misrepresents which individual predictors are 'important'. Is the aim a model that predicts MTBBSI in a specific population, or a model that explains clinical processes related to MTBBSI?

In sum, several seminal studies have reported clinical findings which suggest HIV-associated MTBBSI, but a systematic, substantive clinical description is yet to be advanced. Rather than relying on arbitrary or algorithmic variable selection procedures, co-variance of multiple predictors with MTBBSI could be related to "causal reasoning which relies on background

knowledge, not statistical criteria".[131] In addition to avoiding some of the above pitfalls,[132] such an approach is more likely to reflect and inform clinical reasoning.[133] The small number of previous papers which have tried to relate MTBBSI to causal processes are reviewed next.

1.3.2 Observational studies of MTBBSI which explore pathophysiology

As noted in the preceding section, anaemia has been consistently associated with MTBBSI. Hepcidin is an iron homeostasis cytokine released as part of the acute phase response, induced by type-1 interferon and IL-6 signalling and by microbial Toll-Like Receptor ligands as the mediator of a host-response restricting iron availability to invasive pathogens, with the potential to cause anaemia of chronic disease (ACD).[134,135] ACD is the major driver of anaemia in HIV-associated tuberculosis disease, with iron-deficiency playing only a minor role.[136,137] Anti-tuberculosis treatment in these patients causes resolution of elevated hepcidin levels and anaemia.[138,139] Kerkhoff *et al*. demonstrated a dose-response relationship between hepcidin concentration and anaemia severity in patients with TB and HIV infection in Cape Town, while HIV-infected patients without tuberculosis had no such relationship.[140] Median hepcidin levels were 1.8-fold higher amongst hospitalised HIV-associated TB patients who had a positive TB blood culture (figure 3), and 4-fold higher in hospitalised patients that died compared to survivors.[140]

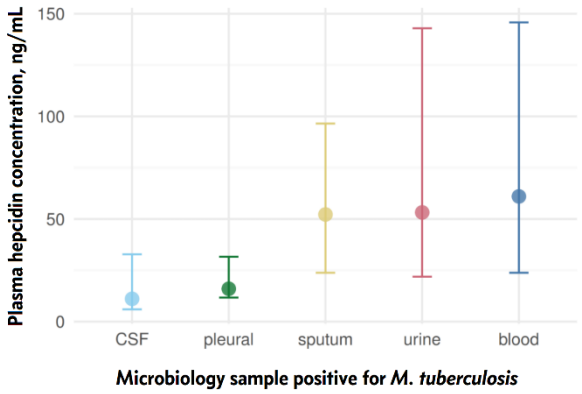

Figure 1-3. Plasma hepcidin by site of positive TB microbiology, extracted from Kerkhoff *et al*. 2016.

Median / IQR shown. Categories not mutually exclusive.

Two papers have been published from an early n=60 HIV-associated TB patient subset of the KDHTB cohort which examined haemostatic changes,[141] innate immune activation[142], and their relationship to mortality. Patients who died had higher whole-blood extracellular concentrations of pro-inflammatory (TNF-α, IL-6) and anti-inflammatory (IL-1RA) cytokines, plus higher proportion of CD16+ monocytes, but impaired monocyte activation after *ex vivo* stimulation with LPS and heat-killed pneumococcus.[142] This analysis found no difference in monocyte cytokine expression by TB blood culture status, but it is notable that the pattern of monocyte function – comparing blood culture negative to positive – mirrors the pattern of monocyte function comparing survivors to those that died. Reproduced from the manuscript, figure 4 shows the median/IQR concentrations of 7 cytokines in supernatant after monocyte stimulation with LPS or heat-killed pneumococcus. The results are arranged to show 4 HIV-TB patient groups: BC-, survived, BC+, died. Also shown is the median cytokine concentration across all the patients (dashed red line). In 12/14 cases, median values for those that died and those that were blood culture positive co-localise relative to the overall median, while those that survived and those that were blood culture negative are on the 'opposite side' of the overall median. The probability of this occurring by chance is 0.006 (i.e. the probability of 12 successes or more in 14 trials assuming BC and death are independent). The absence of 'significant' associations between blood culture status and innate-immune markers is very likely a type II error.

In the same cohort, indicators of consumptive coagulopathy, endothelial activation and tissue damage were associated with decreased survival.[141] TB blood culture status was not 'significantly' associated with most of these markers, leading to the conclusion that "mycobacteraemia… did not affect markers of coagulation, anticoagulation extracellular matrix or tissue damage" but that MTBBSI was associated with some markers of endothelial activation and fibrinolysis.[141] The data isn't presented such that the comparison can be directly made, but, subjectively, I think the distributions of most markers in blood culture positive patients are more similar to patients who died than those that survived.

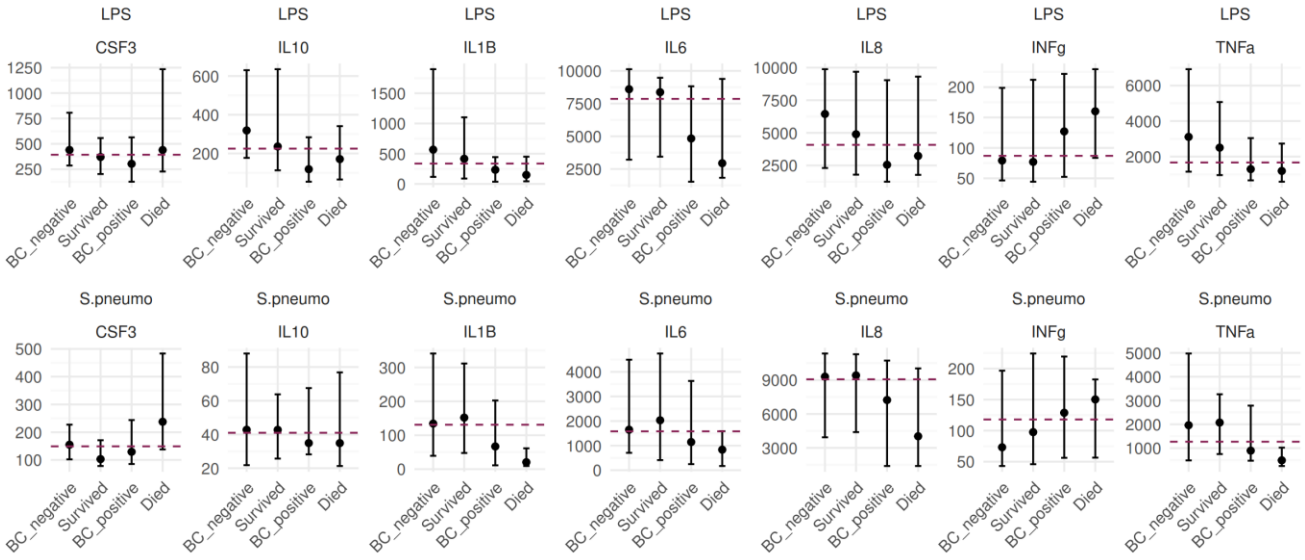

Figure 1-4. Ex vivo monocyte function in HIV-associated TB, data extracted from Janssen *et al*. 2017.[142]

Median/IQR shown by patient group. Blood culture and outcome groupings are not mutually exclusive. Monocyte stimulation with Lipopolysaccharide (LPS) or heat-killed pneumococcus (S.pneumo). The overall median across all patients is shown with dashed red line.

Confounding the under-powering in these analyses is the problem of suboptimal sensitivity of TB blood culture. Of the 60 patients analysed almost all had a single blood culture and some had anti-tuberculosis therapy initiated before time of blood culture. As shown in later chapters (2 and 3), this will have led to under-ascertainment of MTBBSI. This is a measurement error problem, adding noise to the mycobacteraemia variable, and reducing power in the analysis.[143] Potential solutions to measurement error include repeated measurement, and use of complementary or surrogate variables. The next section argues that urine-lipoarabinomannan and urine GeneXpert testing might be considered surrogate measures of MTBBSI.

1.3.3 Urine-based assays as surrogate measures of MTBBSI

In every study that has looked, a positive urine liparabinomannan (uLAM) or urine-GeneXpert (uGXP) result correlates with detection of *M. tuberculosis* by blood culture.[24,125,144]

There are two competing explanations for how LAM ends up in urine. The first is that bacilli at any site in the body release free LAM into the blood stream, and this circulating LAM is then filtered through the glomeruli into the urine. The second is that urine-LAM results from

renal tuberculosis, possibly with intact bacilli shedding into urine. Lawn and Gupta-Wright[145] summarise a case for the latter, including:

- LAM in plasma is bound to antibody[146] and lipoproteins[147], which are too large to filter through an intact glomerulus, but urine-LAM is unrelated to proteinuria and other markers of glomerular function[148];
- In a post-mortem study of adult inpatients dying with HIV infection in a Ugandan hospital,[149] 8/13 (62%) urine-LAM positive patients had histology compatible with renal TB, 6/8 with AFB detected by ZN staining. This study has significant limitations: no molecular or culture detection methods were used, and, while the urine-LAM negative control group had no evidence renal TB, this was only 3 patients.

The alternative explanation – free LAM secretion into the blood stream followed by glomerular filtration – proposes that urine-LAM detection is not caused by occurrence of renal TB, but instead represents total body bacilli load. Proponents of this explanation therefore hypothesise that LAM is present in more immunocompetent patients, but is below limit of detection for current tests.[150] Recent support for this hypothesis comes from a study where use of a novel high-affinity capture method allowed detection of LAM in urine of 46/48 HIV-*negative* Peruvian pulmonary TB patients, quantified at levels an order of magnitude less than the limit of detection of previous uLAM assays.[151] The test was positive in 1/13 hospitalised controls, and patients with abnormal urinalysis were excluded.

From a theoretical point-of-view, I don't think this debate is an obstacle to use of uLAM as a surrogate for MTBBSI. This is based on the assumption that total body bacilli burden, bacteraemic dissemination, and renal tuberculosis are all causally related, so blood culture, uLAM and uGXP are all indicators of the same underlying latent spectrum of advanced post-primary TB disease (figure 5). It is difficult to test this assumption directly with clinical data, but several lines of evidence supporting it will be presented in this chapter.

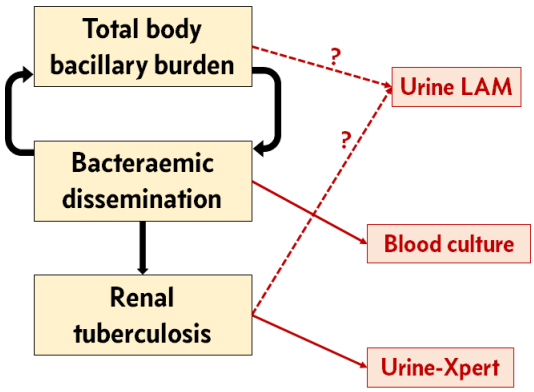

Figure 1-5. Theoretical schematic relating uLAM, uGXP and TB blood culture.

Having laid a theoretical foundation, this chapter now turns to novel data analysis.

1.4 Novel methods for describing the clinical phenotypes

The preceding sections have argued that HIV-associated disseminated TB exists on a continuum of post-primary TB disease, a continuum characterised by total body bacilli burden and blood stream infection. Blood culture, urine LAM and Xpert are systematic windows on this spectrum of HIV-associated tuberculosis. The remaining sections use this formulation to facilitate a less *ad hoc* clinical description of severe HIV-associated tuberculosis, using the KDHTB dataset.

This analysis will rely heavily on dimension reduction statistical techniques. To justify this approach, a motivating example is first presented. This shows the use of a dimension reduction technique (Principal Components Analysis) on data from a previous study of TB diagnostics in PLWHIV admitted to G. F. Jooste Hospital in Cape Town.[**]

In brief, the Jooste study[24] recruited unselected newly-admitted HIV-seropositive adults without a current TB diagnosis and systematically screened them for HIV-associated tuberculosis using

- spot and induced sputum for fluorescent microscopy, liquid culture and Xpert testing;

[**] With thanks to Dr Andrew Kerkhoff and colleagues for access to this dataset.

- Myco/F lytic blood culture;
- urine- LAM and urine-Xpert testing;

as well as collecting results of routine care investigations for tuberculosis. In total 132 patients were recruited with a subsequent new diagnosis of HIV-associated tuberculosis based on this screening; mortality outcome was ascertained at 90-days in 119 of these patients. This cohort is therefore an unbiased representation of HIV-associated tuberculosis amongst inpatients in Cape Town with systematic ascertainment of TB blood culture, uLAM and uGXP status.

1.4.1 Clinical variable dimension reduction: a motivating example

The Jooste data can be analysed for associations with 90-day mortality using a standard approach adopted by previous TB blood culture studies. An *a priori* selection of clinical variables hypothesised to be important determinants of mortality, including blood culture status, are assessed for univariate association with mortality; those with a p value below an arbitrary threshold are then carried forward to a multivariate model to see if blood culture status is an 'independent' predictor in such a model. This approach is shown in table 4.

Table 1-4. Associations with mortality in 132 HIV-associated TB patients from Jooste dataset.

	Univariate logistic regression					Multivariate logistic regression				
Variable	**OR**	**95%CI**			**p value**	**OR**	**95%CI**			**p value**
log_age	2.03	0.30	to	14.31	0.467					
Haemoglobin	**0.78**	**0.61**	**to**	**0.97**	**0.031**	1.08	0.77	to	1.56	0.655
Glomerular filtration rate	1.00	0.99	to	1.00	0.405					
Platelets	1.00	0.99	to	1.00	0.110					
Sodium	0.94	0.84	to	1.06	0.342					
log CD4 count	**0.62**	**0.42**	**to**	**0.92**	**0.017**	0.71	0.39	to	1.27	0.246
log HIV viral load	1.01	0.89	to	1.17	0.838					
log CRP	1.39	0.79	to	3.02	0.328	1.02	0.48	to	2.28	0.956
log albumin	0.30	0.05	to	1.59	0.171	0.43	0.04	to	4.61	0.476
log lymphocytes	**0.19**	**0.05**	**to**	**0.55**	**0.005**					
log monocytes	2.78	0.51	to	25.03	0.263					
log neutrophils	0.27	0.03	to	1.91	0.199					
Sputum Xpert positive	0.52	0.18	to	1.40	0.201					
uLAM grade	**1.49**	**1.15**	**to**	**1.96**	**0.003**	1.19	0.80	to	1.80	0.389
TB blood culture positive	**2.56**	**0.92**	**to**	**7.14**	**0.068**	1.34	0.30	to	5.93	0.696

OR = odds ratio; CI = confidence interval

The conclusion from this analysis would be that, although several variables, including blood culture status and uLAM, are associated with 90-day mortality in univariate analysis, none are independent predictors: all 95% confidence intervals on adjusted odds ratios comfortably cross

1. But this conclusion isn't sensible. From a technical point of view, the variables included in the multivariate logistic regression are to a greater or lesser extent collinear. This inflates the standard errors around the coefficients for each variable, a major problem for significance testing.[152] But note also that the multivariate effect sizes are also substantially reduced. This points to a more fundamental problem: all these variables are (presumably) connected in a network of causal relationships which relate fundamental disease processes to mortality. Whether adjusting one for the other is desirable depends on (a) what we think that causal structure looks like, and (b) what the purpose of the model is. If the purpose is to better 'describe' or 'explain' the clinical phenotype of high-mortality HIV-associated tuberculosis, i.e. make inferential conclusions, the modelling approach is completely dependent on our domain knowledge / prior theory.[153,154]

To illustrate, if we assume, as argued previously in this chapter, that uLAM and blood culture are both (imperfect) measures of an underlying latent variable (MTBBSI, or *HIV-associated disseminated TB bacilli burden*), then including both in the multivariate model isn't very informative. Residual variation in one after adjusting for the other isn't informative; instead we might be more interested in their co-variance as a combined measure of the underlying latent variable. The point is we need some prior beliefs about how the variables are related to make a useful inferential model.

An alternative approach to "understanding" the Jooste dataset is to reduce the dimensions of clinical variables using principal components analysis (example shown in figure 6). About half the variation in ten clinical variables selected *a priori* [haemoglobin, mean corpuscular volume (MCV), red cell distribution width (RDW), serum sodium, C-reactive protein (CRP), albumin, HIV viral load, total lymphocyte count, CD4+ cell count, and a symptom score based on number of 'TB symptoms' present (cough, haemoptysis, night sweats, fever, weight loss)] can be captured in the first two principal components (PC1, PC2). PC1 mostly captures variation in CRP, albumin and markers of anaemia – for example CRP 'loading' on PC1 was +0.7 and haemoglobin loading was -0.7 (figure 6A): a high PC1 score represents high CRP and low haemoglobin. Using our prior (theoretical) knowledge about these clinical variables (e.g. the hepcidin work described above), we can infer that the covariance captured in PC1 represents inflammation. Similarly, PC2 seems to represent immunosuppression.

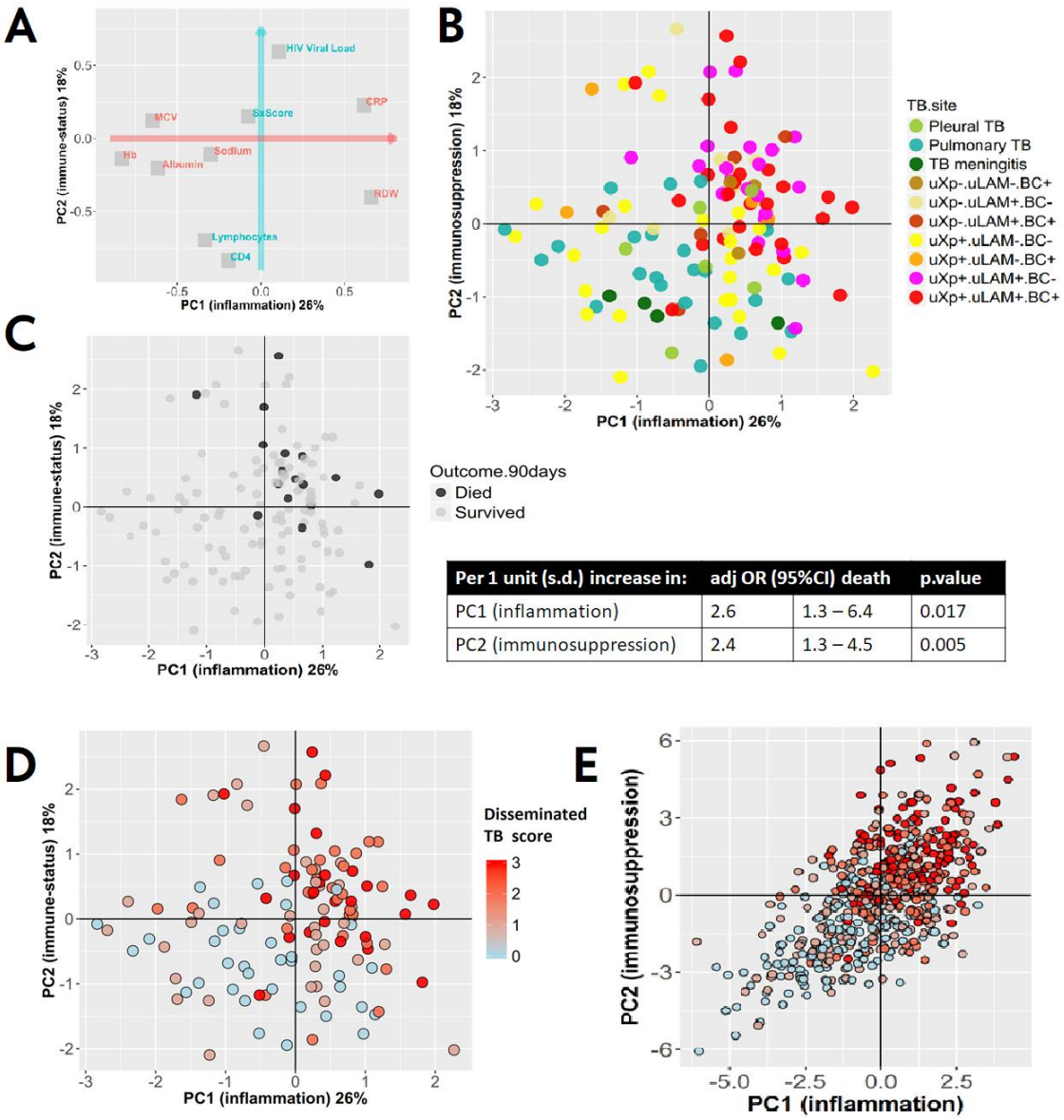

Per 1 unit (s.d.) increase in:	adj OR (95%CI) death		p.value
PC1 (inflammation)	2.6	1.3 – 6.4	0.017
PC2 (immunosuppression)	2.4	1.3 – 4.5	0.005

Figure 1-6. Reduced dimension representation of variables in Jooste dataset using PCA

PCA constructed with 10 major clinical variables. PC1 and PC2 explain 26% and 18% of variation in these variables. Loadings (correlations) of each of these variables with PCs are shown by coordinates in panel **A**. Site of TB disease groupings clustered distinctively on these dimensions (panel **B**, each point is PC1 and PC2 coordinates of an individual patient). PC1 and PC2 varied significantly overall by TB site (Kruskal-Wallis p=0.003 and p<0.001 respectively). 90-day mortality was also strongly associated with both PCs (panel **C**). More positive tests out of the three assays from set [urine-LAM, urine-Xpert, M. tuberculosis blood culture] was associated with greater inflammation and immunosuppression ("disseminated TB score", panel **D**). The loadings were used to reconstruct the same PCs in the KDHTB cohort, i.e. with PC1 and PC2 scores were calculated for KDHTB patients using the values derived from the Jooste dataset. This reproduced the same relationship with "disseminated TB score" suggesting this representation of the clinical variation has external validity.

uXp = urine-Xpert / uLAM = urine-LAM / BC = M. tuberculosis blood culture; Suffix "-" = test negative / suffix "+" = test positive; PC = principal component; adj OR = adjusted odds ratio.

When the patients' PC1 and PC2 scores are calculated and used to plot individuals in this (2-dimensional) space, several strong patterns are seen. Firstly, although TB diagnostic tests were not used to construct the PCs, the results of these tests map in a non-random way on the PCA space. Patients with positive uLAM, uGXP and/or TB blood culture are more likely to localise in the upper right quadrant (representing advanced immunosuppression and severe inflammation). By contrast, compartmentalised extra-pulmonary TB in absence of dissemination (i.e. pleural TB or TB meningitis) had significantly lower PC1 and PC2 values (figure 6B). 90-day mortality also varied by PC1 and PC2 (figure 6C); a logistic regression model containing both as independent variables showed adjusted odds ratios for mortality of 2.6 (95%CI 1.3-6.4, p=0.017) and 2.4 (95%CI 1.3-4.5, p=0.005) per one-unit (one standard deviation) increase in PC1 and PC2 respectively. If uLAM, uGXP and TB blood culture are combined in "disseminated TB score" (one point for each positive test, figure 6D), this correlates significantly with PCs (both $p<0.001$ by Spearman Rank test). This relationship is maintained when the PCs are reconstructed in the KDHTB dataset using the loadings from the Jooste analysis (figure 6E), so this is a robust representation of clinical variation in severe HIV-associated TB (contrast this with the inconsistently shown in figure 2).

I think this approach is more in keeping with clinical reasoning, where highly-dimensional data – generated by history taking, examination and investigations – is reduced, mapping individual patient findings to fit patterns, spectrums of severity, and diagnoses. The example analysis demonstrated above aims to formalises this approach and apply it to a cohort rather than an individual patient.

Dimension reduction equivalent to PCA is also possible for categorical variables, like diagnostic test results, as illustrated next.

1.4.2 Covariance in TB diagnostic test results

In the preceding sections an argument was made that uLAM, uGXP and TB blood culture are theoretically all markers of blood stream dissemination. The empirical suggestion that these tests co-vary with respect to the major dimensions of clinical variation in severe HIV-associated TB supports this argument, and will be made in more detail using the KDHTB dataset in the rest of the chapter. First, though, I want to show that correspondence between these TB test results is – by itself – in keeping with them being mechanistically related.

In patients with proven TB, the level of agreement between TB blood culture and uLAM, and between TB blood culture and uGXP is substantial; by comparison agreement between TB blood culture and sputum based diagnostics doesn't differ from chance (figure 7).

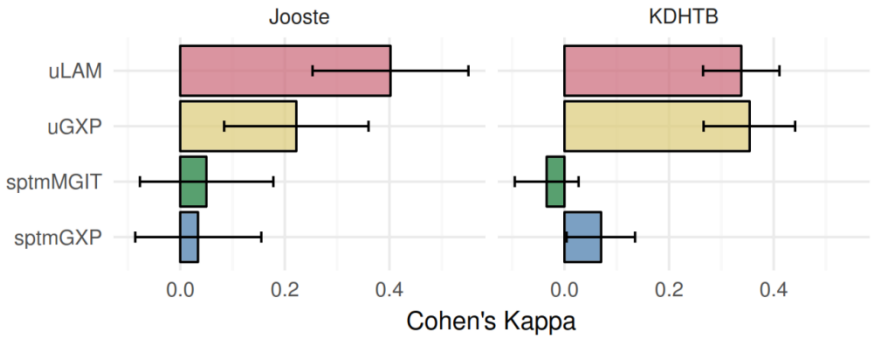

Figure 1-7. Urine versus sputum TB diagnostics agreement with TB blood culture status in patients with proven HIV-associated TB.

Cohen's Kappa for 4 diagnostic tests compared to TB blood culture are shown for patients with proven TB in Jooste dataset (left, n=129) and KDHTB dataset (right, n= 482).
uLAM = detected LAM (>0) on direct urine testing; uGXP = positive GeneXpert on concentrated urine sample; sptmMGIT = *M. tuberculosis* isolated from and sputum culture; sptmGXP = positive GeneXpert any sputum sample

These Cohen's Kappa results consider all the diagnostic tests on a single 'axis': variation in blood culture status. We might instead want to show correspondence across all 5 diagnostic tests. We could make a matrix of pairwise Cohen's Kappa results and cluster the variables in this matrix based on the Kappa results as a measure of distance. These clusters would define a lower dimensional result of the test results. Such an approach would be equivalent to Multiple Correspondence Analysis (MCA) on the set of categorical variables.[155] MCA can also be thought of as a PCA equivalent for categorical variables.[††] An MCA on the five TB diagnostic test in proven TB cases from the Jooste and KDHTB datasets is shown in figure 8.

[††] In brief, distance between categories (e.g. diarrhoea_yes, fever_no, cough_yes etc.) are derived in i-dimensional space, where i is the number of individuals in the data set. The coordinates of a category in that space are a vector length i of 1's and 0's defining if that category is present or absent in the i individuals. Distance between 2 categories is then dependent on how many individuals have co-occurrence of these categories; a category is located at the barycentre of its individuals. Rarely occurring categories are given more weight and are further from the origin of the i-dimensional space after centering – unusual categories have greater variance. In an equivalent manner to PCA, this i-dimensional space is reduced by defining orthogonal axes which capture maximum variance. Variance in a category, k, is defined as $vav(k) = \frac{1}{Pk} - 1$ where Pk is the proportion of individuals in that category; dimension 1 is the eigenvector capturing maximal covariance in the categories. The categories can be

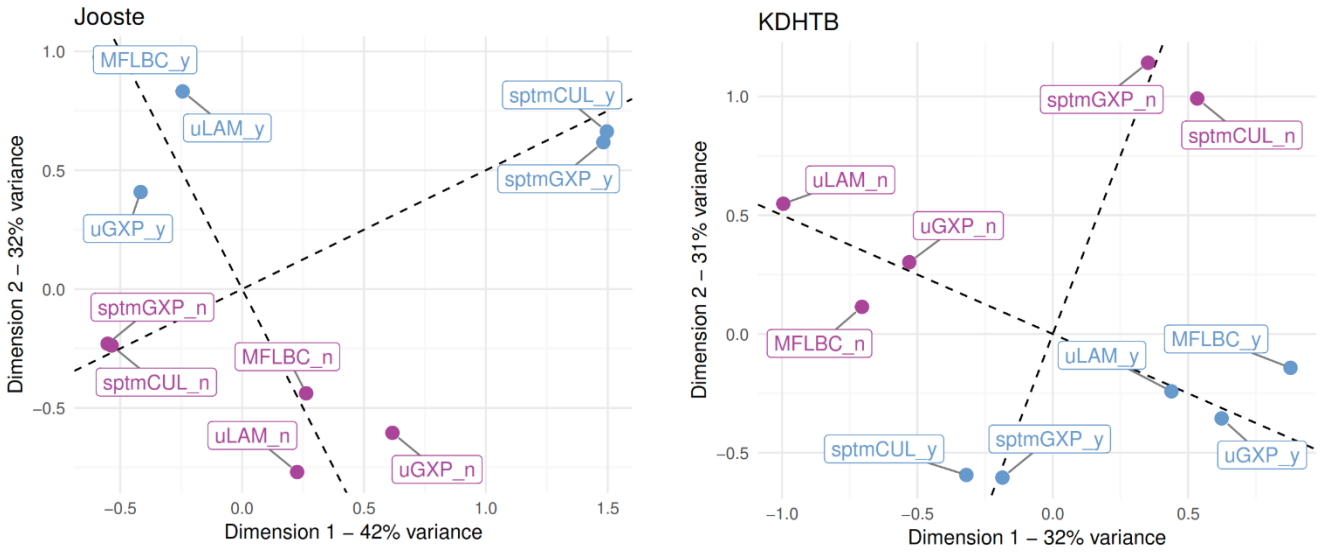

Figure 1-8. MCA TB diagnostics in proven TB cases from two independent datasets

Major patterns of co-variance in diagnostic test categories are captured on the first two dimensions of an MCA. Negative test category indicated by "_n" suffix and pink colour; positive test category indicated by "_y" suffix and blue colour. In both datasets sputum Xpert and culture show very high correspondence, but uLAM, uGXP and TB blood culture (MFLBC) also show similarly high correspondence. In addition, the two sets of diagnostic tests (sputum Xpert and culture; urine Xpert, LAM and TB blood culture) are shown to be essentially orthogonal – the manually added dashed lines are at right angles to help the reader visualise this. This relationship replicates in both independent datasets.

This shows that uLAM, uGXP and TB blood culture are highly co-variant in "TB diagnostic test space", in keeping with these tests being mechanistically related. This offers some empirical support for combining these variables to represent a single axis of variation in HIV-associated TB patients, and this insight is used extensively in the subsequent analysis.

While the Jooste study was an assessment of rapid diagnostics; the KDHTB study was specifically designed to describe severe HIV-associated tuberculosis, so presents a much richer clinical dataset. The rest of this chapter explores covariance in clinical variables in the KDHTB dataset, where possible using established clinical reasoning to 'supervise' dimension reduction and make inferences.

represented on this space. For example, two categories which frequently occur, and frequently occur together (in the same individuals), will be close to each other and close to the origin; two categories which are infrequent, and rarely occur together will be located far from the origin and far from each other, and so forth. The MCA thus gives a low-dimension summary of correspondence of multiple-categories.

1.5 Patterns of covariance in categorical clinical variables & markers of MTBBSI

Patterns of covariation of categorical variables (symptoms, signs, radiology findings) with both TB blood culture status and the "disseminated TB score" are shown in the following sections. In each case, patients with a *confirmed or clinical diagnosis* of HIV-associated TB from the KDHTB study are included in the analysis (referred to as KDHTB patients from here on); this means the comparison is between HIV-associated TB inpatients with or without MTBBSI.

Two analyses are made. First, the univariate associations are characterised with proportions, Fisher exact test of those proportions, and summarised with the likelihood ratio for having a positive blood culture. Next, multivariate patterns are considered. Rather than adjusting one categorical variable for another, an attempt is made to demonstrate major patterns of covariance in the variables, and see if "disseminated TB score" [total positive tests out of TB blood culture, uLAM, uGXP] relates to those patterns. This is achieved using MCA (the same technique as described above). In addition to summarising major dimensions of co-variation between categories, 'supplementary' variables which were not used to construct the MCA can be 'projected' on the MCA space.[155] This shows the strength of the relationship with the MCA dimensions (larger coordinates mean higher correlation of the supplementary variable with the MCA dimension – i.e. better representation, or more correspondence, with the MCA categories); the direction of the projection also indicates what categories the supplementary variable corresponds well to. In the subsequent analyses disseminated TB score is used as the supplementary variable, to answer the question are there multivariate patterns of categorical variables to which MTBBSI relates?

To reiterate, the aim is to see how MTBBSI relates to patterns of categorical variables, rather than individual symptoms or signs, to better capture and formalise the approach clinicians take to "multivariate data".

1.5.1 Presenting symptoms

499 HIV-associated TB patients from the KDHTB dataset had complete data on 7 symptom variables; association with TB blood culture is shown in table 5. Symptoms were recorded from direct questioning (not necessarily volunteered). Most symptoms showed no ability to

discriminate bacteraemic from non-bacteraemic TB. Although not 'significant', gastro-intestinal symptoms were associated with positive likelihood ratios.

Table 1-5. Symptoms associated with blood culture status

	BC negative (N=305)	BC positive (N=194)	Total (N=499)	p value	LR+
Cough	208 (68.2%)	138 (71.1%)	346 (69.3%)	0.552	**1.04**
Loss of appetite	192 (63.0%)	137 (70.6%)	329 (65.9%)	0.096	**1.12**
Loss of weight	271 (88.9%)	178 (91.8%)	449 (90.0%)	0.369	**1.03**
Night sweats	167 (54.8%)	109 (56.2%)	276 (55.3%)	0.825	**1.03**
Nausea or vomiting	70 (23.0%)	54 (27.8%)	124 (24.8%)	0.261	**1.21**
Diarrhoea	102 (33.4%)	75 (38.7%)	177 (35.5%)	0.275	**1.16**
Headache	67 (22.0%)	24 (12.4%)	91 (18.2%)	0.010	**0.56**

BC = Myco/F lytic TB blood culture; LR+ = positive likelihood ratio; p value from Fisher's exact test.

The MCA analysis (figure 7) suggests:

- The major dimension of variation in symptoms (dimension 1) is simply presence or absence of symptoms – broadly, some patients report multiple symptoms and others report few – and that this, in itself, has very little bearing on whether a patient has MTBBSI (here defined by disseminated TB score, which correlates poorly with dimension 1).
- Presence of diarrhoea, and nausea or vomiting, show some correspondence with each other, but less so with other symptoms.
- When patients are clustered based on their MCA dimensions (figure 7B), this clustering does predict DTB-score. This implies that, although individual symptoms are not strongly related to MTBBSI, there are patterns of covariation – constellations of symptoms – which are more specific to MTBBSI.

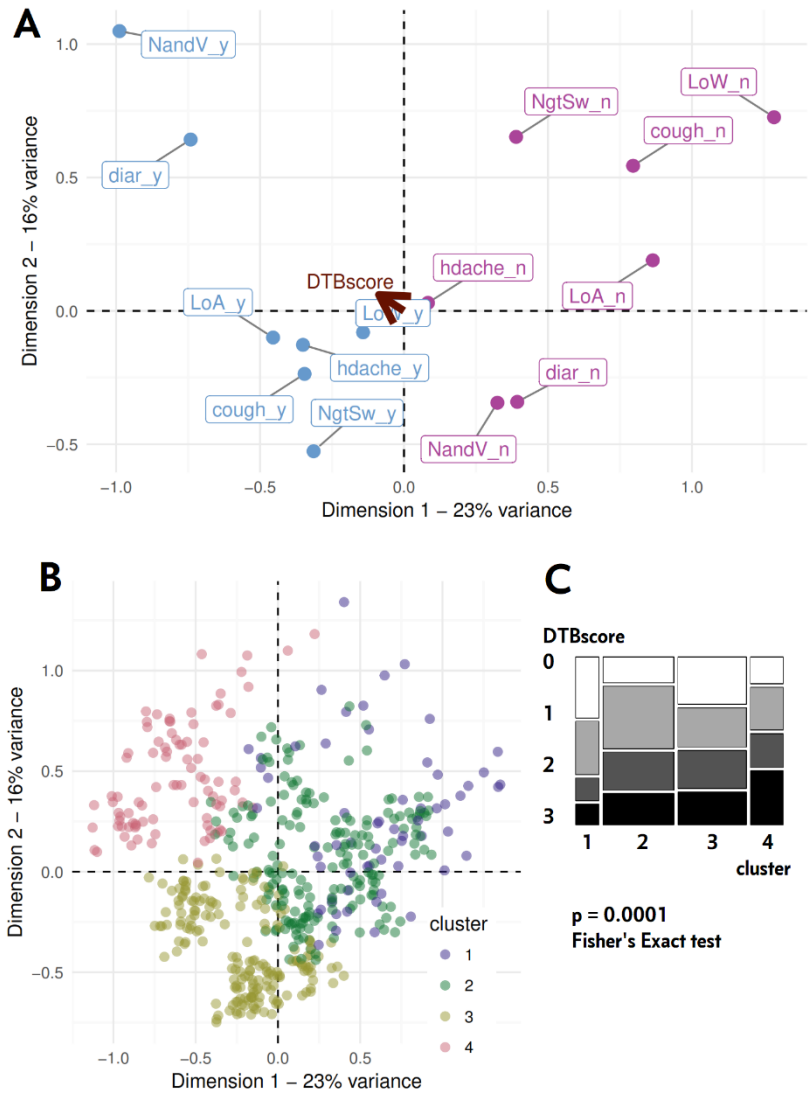

Figure 1-9. MCA and clustering on presenting symptoms

A. Major patterns of co-variance in recorded symptoms are captured on the first two dimensions of an MCA. Absence of symptom category indicated by "_n" suffix and pink colour; presence of symptom category indicated by "_y" suffix and blue colour. Projection of disseminated TB score (DTBscore, total of tests positive from TB blood culture, uLAM, uGXP) on this MCA space is shown with red arrow, coordinates of which indicate correlation with the dimensions. NandV = nausea and vomiting; diar = diarrhoea; LoA = loss of appetite; LoW = loss of weight; hdache = headache; NgtSw = drenching night sweats. **B.** The first 3 dimensions of the symptoms MCA were used categorise patients into 4 clusters using K-means clustering. The number of clusters was selected algorithmically by comparing the quality of the clustering solution for different numbers of clusters using NbClust package in R. Unlike individual symptoms, cluster was significantly associated with DTBscore (mosaic plot **C.**).

1.5.2 Imaging categories

470 (98%) patients had chest x-ray results and 278 (58%) had an abdominal ultrasound scan recorded during their admission. Several individual variables were significantly associated with positive blood culture: adenopathy (mediastinal or abdominal) and splenic micro-abscesses (table 6). Use of the word 'miliary' in free text descriptions of chest radiology was also associated with a positive blood culture, although only weakly, and the majority (41/190, 78%) of blood culture positive patients did not have a miliary x-ray by this measure. A miliary chest x-ray was also weakly associated with splenic micro-abscesses (OR 2.1; 95%CI 0.95 to 5.3). Infiltrate in all 5 lobes was associated with positive blood culture (also weakly), while pleural effusion or fibrotic changes reduced likelihood of positive blood culture (table 6).

An MCA including all systematically recorded radiology findings in patients that had both chest x-ray and abdominal ultrasound is shown in figure 10. Diffuse pulmonary pathology involving all 5 lobes, mediastinal adenopathy, splenic micro-abscesses and abdominal adenopathy broadly co-localise (lower left quadrant). Patients with pleural effusion are much less likely to have these pathologies noted (in keeping with more localised pauci-bacillary disease of the pleura). Ascities is probably associated with other abdominal disease, but not with more diffuse disease represented by chest x-ray findings. In sum, localised extra-pulmonary or pulmonary disease can be distinguished from a more disseminated phenotype. As would be expected, DTB score correlates with the more diffuse phenotype. The major axis of variation is not pulmonary versus extra-pulmonary, but whether blood stream dissemination is active or contained.

Table 1-6. Radiology associations with TB blood culture.

Chest X-ray finding	BC negative (N=280)	BC positive (N=190)	Total (N=470)	p value	LR+
Pleural effusion	103 (36.8%)	52 (27.4%)	155 (33.0%)	0.042	0.74
Increased cardio-thoracic ratio	60 (21.4%)	46 (24.2%)	106 (22.6%)	0.551	1.13
Mediastinal adenopathy	110 (39.3%)	105 (55.3%)	215 (45.7%)	< 0.001	1.41
Nodular*	169 (60.4%)	104 (54.7%)	273 (58.1%)	0.264	0.91
Miliary*	37 (13.2%)	41 (21.6%)	78 (16.6%)	0.023	1.64
Cavitation*	31 (11.1%)	16 (8.4%)	47 (10.0%)	0.433	0.76
Reticular*	24 (8.6%)	26 (13.7%)	50 (10.6%)	0.107	1.59
Fibrotic*	26 (9.3%)	6 (3.2%)	32 (6.8%)	0.016	0.34
Consolidation*	43 (15.4%)	22 (11.6%)	65 (13.8%)	0.304	0.75
Infiltrate in all 5 lobes	99 (35.4%)	86 (45.3%)	185 (39.4%)	0.039	1.28
Abdominal ultrasound finding	**BC negative (N=147)**	**BC positive (N=131)**	**Total (N=278)**	**p value**	**LR+**
Abdominal adenopathy	72 (49.0%)	84 (64.1%)	156 (56.1%)	0.016	1.31
Splenic micro-abscesses	77 (52.4%)	96 (73.3%)	173 (62.2%)	< 0.001	1.39
Ascities	45 (30.6%)	34 (26.0%)	79 (28.4%)	0.468	0.85
Pericardial effusion*	30 (20.4%)	31 (23.7%)	61 (21.9%)	0.610	1.16
Kidney abnormality*	19 (12.9%)	21 (16.0%)	40 (14.4%)	0.572	1.24
Liver enlarged and/or echo-bright*	32 (21.8%)	29 (22.1%)	61 (21.9%)	1.000	1.01

BC = Myco/F lytic TB blood culture; LR+ = positive likelihood ratio; p value Fisher's exact test.
* These variables were extracted by word search of free text variables so were not collected systematically.

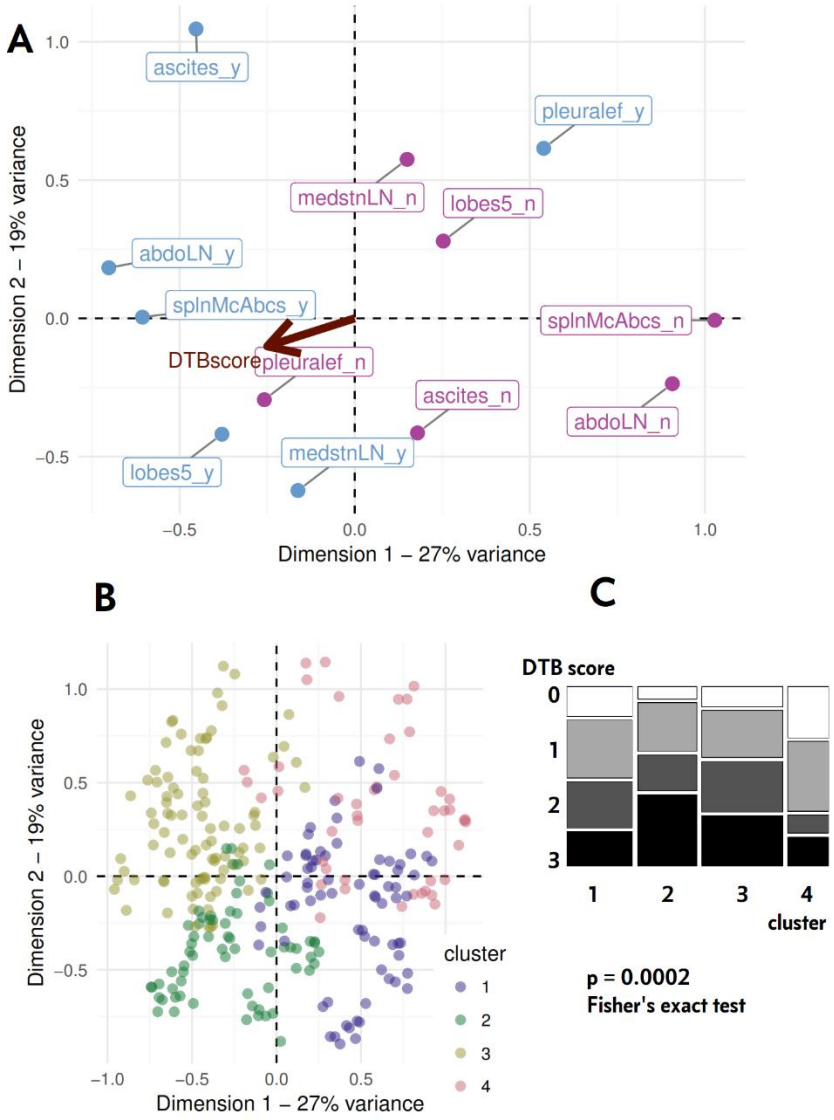

Figure 1-10. MCA and clustering on radiology findings

A. For 275 patients with chest x-ray and abdominal ultrasound results, major patterns of co-variance in radiology findings are shown on the first two dimensions of an MCA. Absence of finding indicated by "_n" suffix and pink colour; presence of finding by "_y" suffix and blue colour. Projection of disseminated TB score is shown with red arrow, coordinates of which indicate correlation with the dimensions. Pleuralef = pleural effusion; medstnLN = mediastinal adenopathy; abdoLN = abdominal adenopathy; splnMcAbcs = splenic micro-abscesses; lobes5 = infiltrate on all 5 lung lobes.
B. The first 3 dimensions of the symptoms MCA were used categorise patients into 4 clusters using K-means clustering. The number of clusters was selected algorithmically by comparing the quality of the clustering solution for different numbers of clusters using NbClust package in R. Cluster was significantly associated with DTBscore (mosaic plot **C.**).

1.6 Overall covariance in continuous clinical variables & markers of MTBBSI

1.6.1 *A priori* selection and transformation of quantitative clinical variables

46 clinical variables were selected *a priori*. Attempted transformation to univariate normal using power transformations – log and power -1, -0.5, and 0.5 (reciprocal, reciprocal square-root, and square root transformations respectively) – was assessed. Some variables could not be transformed to normal because of severe range restriction problems (eg O2 saturation), including limit of detection floors (time to positivity and cycle threshold values), because they are count data with a high proportion of zero values (e.g. CMV viral load), or because they are pseudo-numeric data (ECOG score, GCS, uLAM). Adequacy of conversions were assessed by QQplots (not shown) and density plots (figure 11). Final representations of quantitative variables are listed in table 7.

Missing observations other than time to positivity of cultures and cycle thresholds from GeneXpert tests (figure 12) were imputed using Gibb's sampling to minimise bias from data missing non-randomly (Multivariate Imputation by Chained Equations package in R).

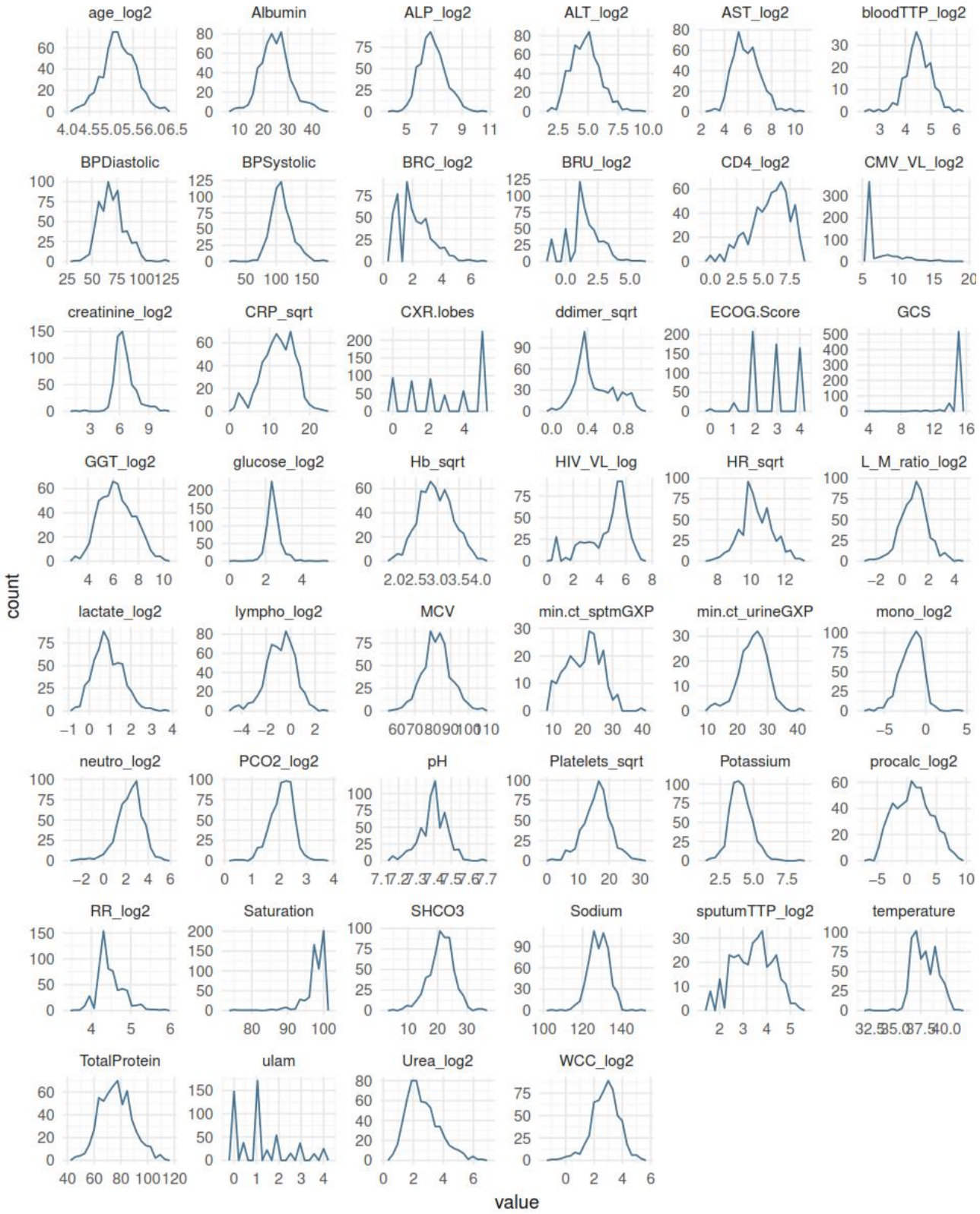

Figure 1-11. Univariate distributions of transformed numerical variables.

Table 1-7. Quantitative clinical variables used in subsequent analysis.

Variable	Description
age_log2	Age in years on log2 scale
ECOG.Score	Eastern Cooperative Oncology Group (ECOG) performance score
HR_sqrt	Hear rate per minute ^0.5 power transformed
BPSystolic	Systolic blood pressure mm/Hg
BPDiastolic	Diastolic blood pressure mm/Hg
Temperature	Composite variable: highest temperature recorded by study team (at recruitment) or in patient notes, oC
Saturation	Pulse oximeter reading at tme recruitment, %
GCS	Glasgow Coma Scale at time of recruitment
RR_log2	Composite variable: Respiratory rate recorded at time of recruitment by study team or Emergency Department at tie of admission (higher value used); on log2 scale
CD4_log2	CD4+ lymphocyte count cells/mm3 on log2 scale
glucose_log2	Venous glucose mmol/L on log2 scale
Sodium	Serum sodium mmol/L
Potassium	Serum potassium mmol/L
pH	Venous pH
SHCO3	Venous bicarbonate mmol/L
creatinine_log2	Serum creatinine mmol/L on log2 scale
Urea_log2	Serum Urea mmol/L on log2 scale
PCO2_log2	Venous PCO2 mm Hg on log2 scale
procalc_log2	Serum ProCalcitonin ng/ml on log2 scale
lactate_log2	Venous lactate mmol/L on log2 scale
CRP_sqrt	Serum C-reactive protein mmol/L
TotalProtein	Total serum protein g/L
Albumin	Serum albumin g/L
AST_log2	Serum transaminase IU/L on log2 scale
ALT_log2	Serum transaminase IU/L on log2 scale
AST_ALT_ratio	Ratio of AST to ALT on log2 scale
GGT_log2	Serum gamma-glutamyl transferase IU/L on log2 scale
ALP_log2	Serum alkaline phosphatase IU/L on log2 scale
BRC_log2	Serum conjugated bilrubin IU/L on log2 scale
BRU_log2	Serum unconjugated bilrubin IU/L (derived from total minus conjugated) on log2 scale
CXR.lobes	Number of lobes with infiltrate on ches x-ray
Hb_sqrt	Venous haemoglobin g/dL
MCV	Mean corpuscular volume fL
Platelets_sqrt	Platelet count x 10^9 /L
ddimer_sqrt	Serum D-dimer. Variable was recorded on 2 different systems, so values normalised to lie between 1 and 0 by subtracting the minimum value and dividing by the difference between the maximum and minimum value.
WCC_log2	count x 10^9 /L on log2 scale
neutro_log2	count x 10^9 /L on log2 scale
lympho_log2	count x 10^9 /L on log2 scale
mono_log2	count x 10^9 /L on log2 scale
L_M_ratio_log2	Ratio of lymphocte to monocyte count

HIV_VL_log	Serum HIV viral load in copies per ml log scale
ulam	Mean urine - lipoarabinomannan measure on Alere lateral flow test on direct urine sample by two independent readers
sputumTTP_log2	Time to positive culture of sputum in MGIT BACTEC system. If more than one sputum result was available this is mean value.
bloodTTP_log2	Time to positive culture of blood in Myco/F lytic BACTEC system. If more than one result was available this is mean value.
CMV_VL_log2	Serum CMV viral load in copies per ml log2 scale
min.ct_sptmGXP	Minimum cycle threshold value across M.tb probes for sputum sample
min.ct_urineGXP	Minimum cycle threshold value across M.tb probes for concentrated urine sample

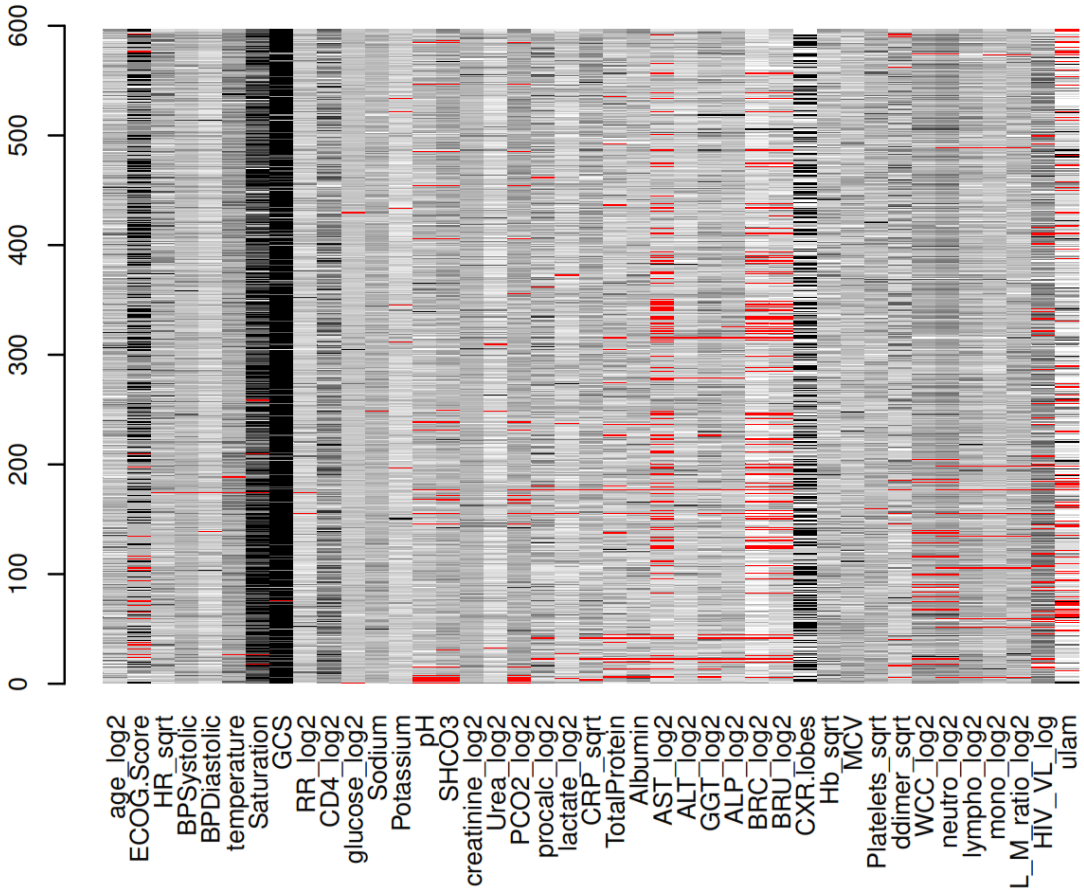

Figure 1-12. Matrix plot showing missing observations by patient (rows) and variable (columns).

Higher values in distribution of column are darker greyscale. Missing observations are in red. These missing observations were imputed for subsequent analysis.

1.6.2 Association of quantitative variables with mortality

Before looking at covariance in these variables, their individual associations with mortality are shown. Follow-up in KDHTB formally ended at 12-weeks. Over this period, mortality hazard varied substantially, with half of the deaths occurring before day 14 (figure 13). Associations with mortality varied between early (before day 14 follow-up) and later (death between day 14 and day 84 follow-up) – table 8, figure 14. Variables related to early and late deaths include those reporting tissue damage or organ dysfunction (liver tests, creatinine, D-dimer, platelets, haemoglobin) and CD4 count. Variables with marked association with early but not late deaths include acute inflammation markers (CRP, pro-calcitonin, monocytes), functional status (ECOG and GCS), age and hyponatraemia. The latter must represent more proximal acute processes related to mortality, while the former have acute and longer, sub-acute, causal 'reach'. There is a mortality cost associated with tissue damage which, even in the context of short-term survival, can affect later mortality.

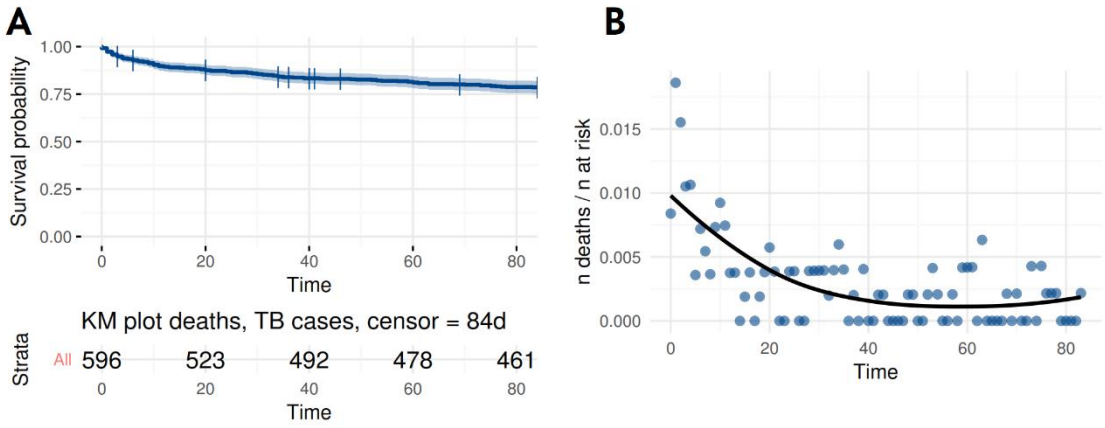

Figure 1-13. Mortality hazard over 84days of follow up.

Kaplan-Meier plot (**A.**) and daily death rate over time (**B.**)

Table 1-8. Univariate mortality associations

	Earlier death (N=65)		Later death (N=73)		Survived (N=458)		p value
	Median	IQR	Median	IQR	Median	IQR	
age_log2	5.38	5.13, 5.57	5.28	4.94, 5.52	5.14	4.92, 5.39	< 0.001
ECOG.Score	4	3.00, 4.00	3	2.00, 4.00	3	2.00, 3.00	< 0.001
HR_sqrt	10.39	9.90, 11.09	10.25	9.90, 10.95	10.2	9.71, 10.94	0.141
BPSystolic	111	97.00, 128.00	104	97.00, 116.00	108	97.00, 118.00	0.176
temperature	37.4	36.80, 38.30	38.1	37.00, 39.00	37.8	37.00, 38.90	0.028
Saturation	98	96.00, 100.00	98	97.00, 100.00	99	97.00, 100.00	0.052
GCS	15	14.00, 15.00	15	15.00, 15.00	15	15.00, 15.00	< 0.001
RR_log2	4.46	4.17, 4.58	4.32	4.32, 4.58	4.46	4.32, 4.70	0.151
CD4_log2	5.17	4.00, 6.54	5.36	4.00, 6.48	6.04	4.60, 7.11	0.001
glucose_log2	2.43	2.32, 2.72	2.43	2.32, 2.70	2.38	2.23, 2.58	0.029
Sodium	127	123.00, 130.00	129	126.00, 131.00	129	125.00, 132.00	0.037
Potassium	4	3.60, 4.70	4	3.60, 4.60	4	3.50, 4.50	0.218
SHCO3	19.5	16.10, 23.60	20.5	16.70, 23.10	21.8	19.20, 24.17	< 0.001
creatinine_log2	6.66	5.88, 7.61	6.66	5.98, 7.51	6.27	5.88, 6.72	0.001
PCO2_log2	2	1.68, 2.41	2	1.68, 2.29	2.17	1.89, 2.41	0.001
procalc_log2	3.27	1.38, 5.75	1.84	-0.27, 4.12	0.72	-1.84, 2.57	< 0.001
lactate_log2	1.26	0.68, 1.68	0.93	0.58, 1.49	0.77	0.38, 1.26	< 0.001
CRP_sqrt	14.71	12.01, 16.43	12.72	9.49, 15.05	12.13	9.29, 15.01	< 0.001
TotalProtein	73	62.00, 80.00	73	66.00, 80.00	76	69.00, 85.00	< 0.001
Albumin	21	16.00, 25.00	23	20.00, 28.00	25	22.00, 29.00	< 0.001
AST_log2	5.98	5.17, 6.86	6.02	5.13, 6.55	5.73	5.04, 6.66	0.353
ALT_log2	4.64	3.91, 5.29	4.58	3.91, 5.43	4.81	4.00, 5.58	0.481
GGT_log2	6.07	5.49, 7.33	6.52	5.29, 7.75	6.17	5.22, 7.12	0.202
ALP_log2	6.98	6.57, 7.69	7.12	6.43, 7.73	6.72	6.25, 7.36	0.001
BRC_log2	2.32	1.00, 3.32	2.58	1.58, 3.17	2	1.00, 2.58	0.004
CXR.lobes	5	2.00, 5.00	3	1.00, 5.00	3	1.00, 5.00	0.004
Hb_sqrt	2.81	2.59, 3.16	2.85	2.59, 3.16	2.98	2.72, 3.25	0.012
MCV	80.1	76.60, 86.30	83.3	78.00, 86.70	82.35	77.50, 87.18	0.755
Platelets_sqrt	15.17	11.18, 17.46	15.43	12.21, 18.14	16.52	13.83, 19.02	< 0.001
ddimer_sqrt	0.51	0.34, 0.70	0.51	0.37, 0.69	0.39	0.33, 0.59	0.002
WCC_log2	2.79	2.00, 3.38	2.86	2.22, 3.43	2.85	2.21, 3.37	0.581
neutro_log2	2.43	1.50, 3.13	2.43	1.68, 3.15	2.45	1.69, 3.08	0.958
lympho_log2	-1.4	-2.12, -0.92	-1.09	-1.60, -0.38	-0.52	-1.46, 0.12	< 0.001
mono_log2	-2.4	-3.32, -1.79	-1.69	-2.94, -0.94	-1.43	-2.47, -0.71	< 0.001
L_M_ratio_log2	1.1	0.33, 1.69	0.93	0.06, 1.51	0.94	0.31, 1.54	0.313
HIV_VL_log	5.2	3.61, 5.69	5.17	3.55, 5.77	5.11	3.73, 5.69	0.97
CMV_VL_log2	5.61	5.61, 8.75	6.14	5.61, 9.46	5.61	5.61, 8.43	0.06

Earlier deaths occurred before day 14, later deaths on or after day 14 (approximate median survival time in those that died before day 84 follow-up). IQR = interquartile range; variables are defined in table 7; p-values from Kruskal Wallis test across 3 groups.

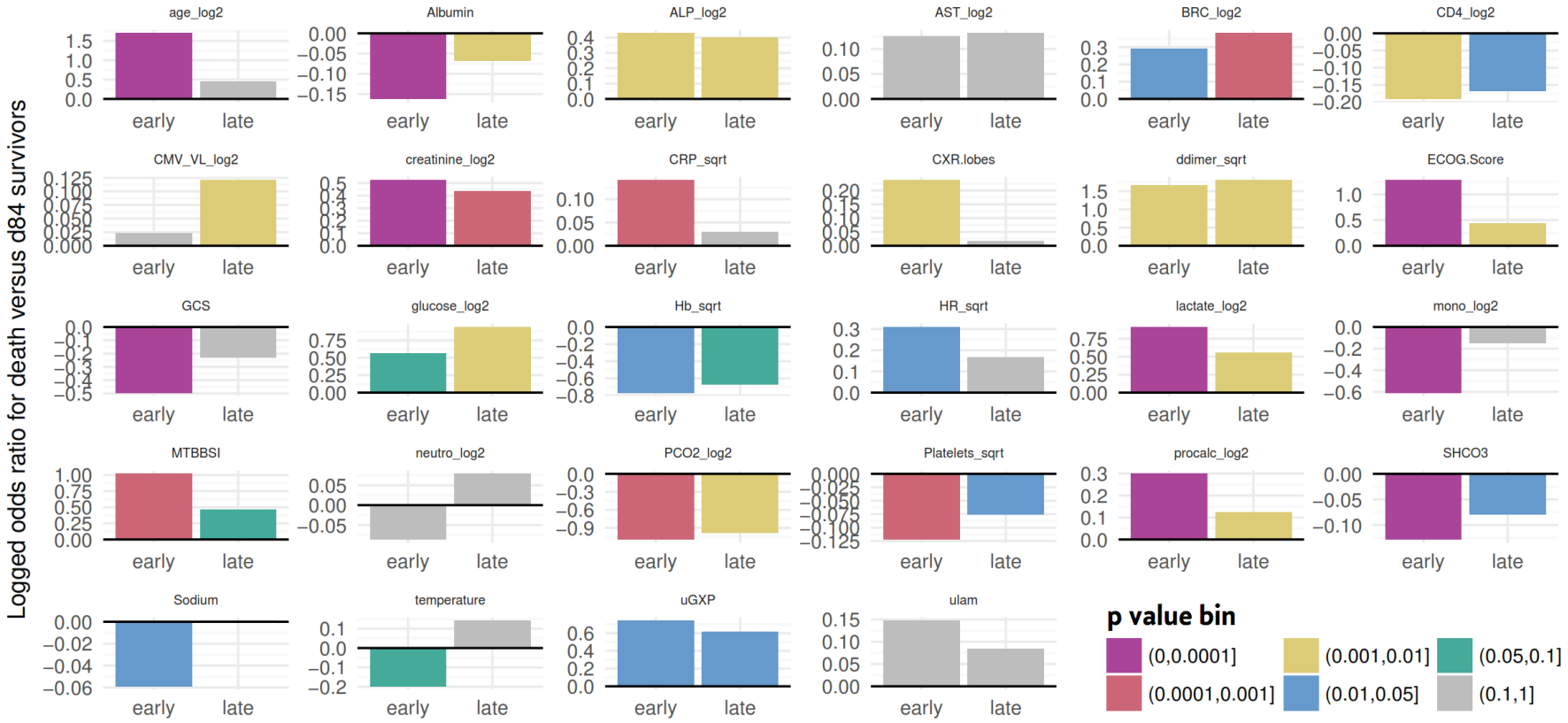

Figure 1-14. Variables as predictors of early versus late deaths during 84-day follow-up

y-axes show logged odds ratio for death (early, <14days; late≥14days) compared to those that survived to day 84. No effect is therefore y=0 [log(OR of 1) = 0] and larger effect is further from 0; 0 is indicated with back horizontal line. Significance test based on univariate logistic regression is indicated by colour (see key at bottom right for p-value bin).

1.6.3 Associations of quantitative variables with positive TB blood culture

Of the 25 variables in table 8 which were associated with mortality outcome, 23 are also associated with positive blood culture (table 9). Variables significantly associated with TB blood culture but not with mortality include some of the liver enzymes, MCV and HIV viral load. Age and O2 saturation are associated with mortality but not blood culture status.

Table 1-9. Univariate associations with positive TB blood culture

	TB blood culture negative (N=352)		TB blood culture positive (N=220)		Total (N=572)		p value
	Median	IQR	Median	IQR	Median	IQR	
age_log2	5.2	5.0, 5.5	5.2	4.9, 5.4	5.2	4.9, 5.4	0.509
ECOG.Score	3	2.0, 3.0	3	2.0, 4.0	3	2.0, 4.0	< 0.001
HR_sqrt	10.1	9.6, 10.8	10.5	9.9, 11.1	10.2	9.8, 11.0	< 0.001
BPSystolic	107	97.0, 118.0	109.5	97.8, 119.0	108	97.0, 118.0	0.437
Temperature	37.5	36.9, 38.6	38.2	37.1, 39.0	37.8	37.0, 38.9	< 0.001
Saturation	99	97.0, 100.0	98	97.0, 100.0	99	97.0, 100.0	0.746
GCS	15	15.0, 15.0	15	15.0, 15.0	15	15.0, 15.0	0.001
RR_log2	4.5	4.3, 4.6	4.5	4.3, 4.7	4.5	4.3, 4.7	0.24
CD4_log2	6.5	5.2, 7.3	4.9	3.3, 5.9	5.8	4.5, 6.9	< 0.001
glucose_log2	2.4	2.2, 2.6	2.4	2.3, 2.7	2.4	2.2, 2.6	< 0.001
Sodium	129	126.0, 132.0	127	124.0, 130.2	129	125.0, 131.2	< 0.001
Potassium	4	3.5, 4.5	4	3.4, 4.6	4	3.5, 4.6	0.748
SHCO3	22.5	19.7, 24.5	20.4	17.2, 23.0	21.5	18.7, 24.0	< 0.001
creatinine_log2	6.2	5.9, 6.6	6.6	6.1, 7.4	6.3	5.9, 7.0	< 0.001
PCO2_log2	2.2	2.0, 2.4	2	1.7, 2.2	2.1	1.8, 2.4	< 0.001
procalc_log2	-0.2	-2.3, 2.1	2.5	1.1, 4.5	1.2	-1.3, 3.3	< 0.001
lactate_log2	0.8	0.4, 1.2	1	0.6, 1.6	0.8	0.4, 1.4	< 0.001
CRP_sqrt	11.5	8.6, 14.6	13.9	11.6, 15.9	12.5	9.5, 15.2	< 0.001
TotalProtein	78	69.0, 86.0	72	65.0, 80.0	75.5	67.0, 84.0	< 0.001
Albumin	25.5	22.0, 30.0	23	20.0, 27.0	25	21.0, 29.0	< 0.001
AST_log2	5.6	4.9, 6.3	6.3	5.6, 7.1	5.8	5.1, 6.7	< 0.001
ALT_log2	4.6	3.9, 5.4	5	4.3, 5.8	4.8	4.0, 5.6	< 0.001
GGT_log2	6.1	5.2, 7.0	6.4	5.7, 7.5	6.2	5.3, 7.3	< 0.001
ALP_log2	6.8	6.3, 7.4	7	6.3, 7.6	6.8	6.3, 7.5	0.01
BRC_log2	1.6	1.0, 2.6	2.6	1.6, 3.0	2	1.6, 2.8	< 0.001
CXR.lobes	3	1.0, 5.0	4	1.0, 5.0	3	1.0, 5.0	0.068
Hb_sqrt	3	2.8, 3.3	2.8	2.6, 3.1	2.9	2.7, 3.2	< 0.001
MCV	82.5	77.7, 87.5	81.5	76.1, 85.8	82.3	77.3, 86.9	0.018
Platelets_sqrt	17	14.3, 19.4	15.1	11.6, 17.1	16.2	13.3, 18.5	< 0.001
ddimer_sqrt	0.4	0.3, 0.5	0.5	0.4, 0.7	0.4	0.3, 0.6	< 0.001
WCC_log2	2.8	2.2, 3.4	2.9	2.1, 3.3	2.8	2.2, 3.4	0.857
neutro_log2	2.4	1.6, 3.1	2.6	1.7, 3.1	2.4	1.7, 3.1	0.104
lympho_log2	-0.4	-1.2, 0.3	-1.4	-2.0, -0.7	-0.8	-1.6, -0.0	< 0.001
mono_log2	-1.4	-2.2, -0.7	-2.3	-3.2, -1.2	-1.6	-2.6, -0.8	< 0.001
L_M_ratio_log2	1	0.4, 1.5	0.9	0.2, 1.6	1	0.3, 1.5	0.337
HIV_VL_log	4.9	3.3, 5.5	5.5	4.6, 6.0	5.1	3.7, 5.7	< 0.001
CMV_VL_log2	5.6	5.6, 8.2	5.6	5.6, 8.8	5.6	5.6, 8.6	0.008

IQR = interquartile range; variables are defined in table 7; p-values from Wilcox rank test across 2 groups.

1.6.4 Algorithmic dimension reduction in quantitative clinical variables

A correlation matrix of the transformed quantitative clinical variables is shown in figure 15. Variables are ordered by a complete-linkage hierarchical clustering algorithm. An alternative clustering of variables is shown in figure 16 showing that the clustering is robust to algorithm used. Substantial multi-collinearity exists for almost all variables.

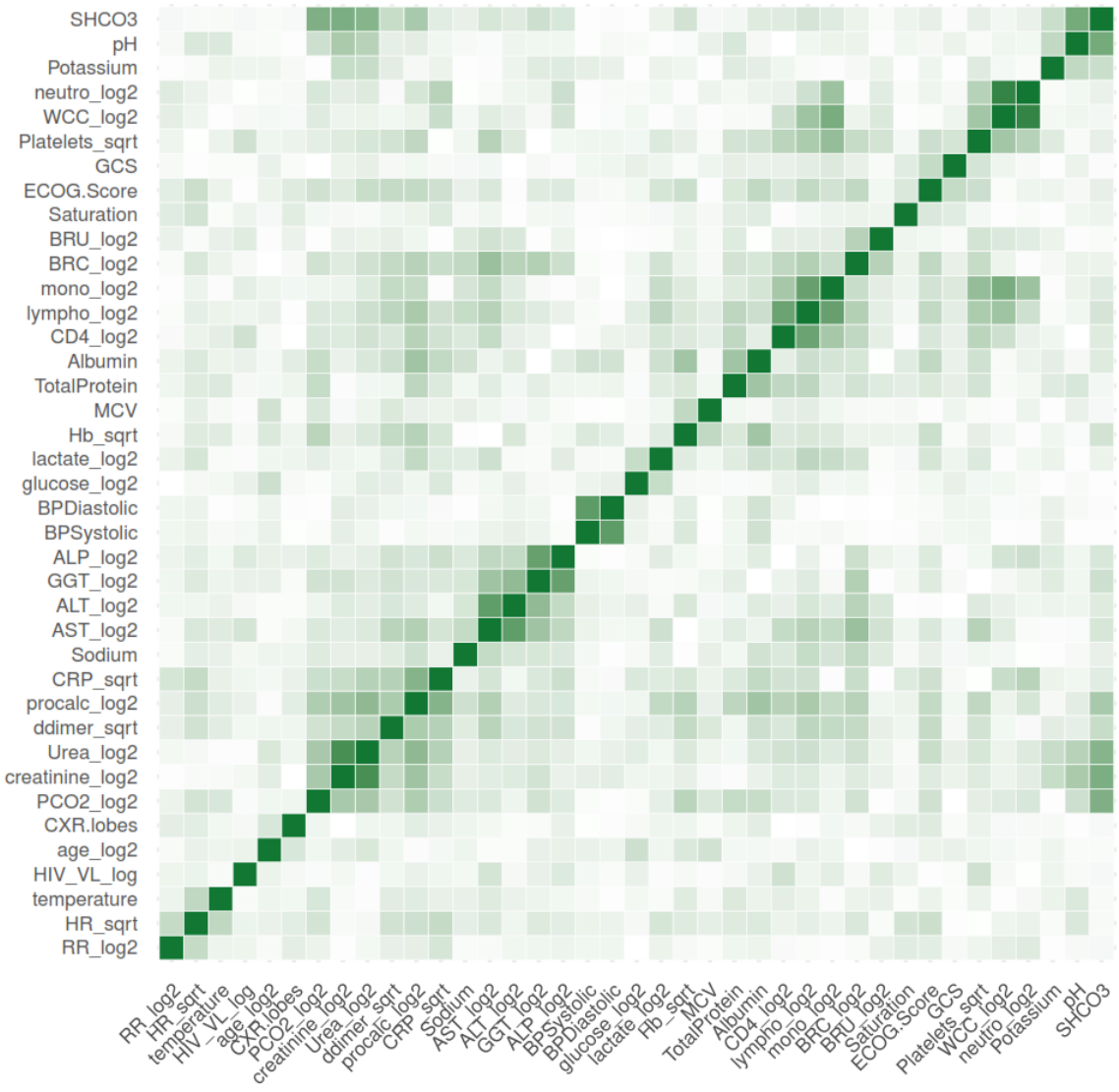

Figure 1-15. Pairwise correlation matrix major quantitative clinical variables

Absolute values of pairwise Pearson's r correlation coefficients are indicated by darker green colour and were used to define distance between variables. Variables are ordered based on a hierarchical clustering algorithm (complete linkage used to define distance between clusters).

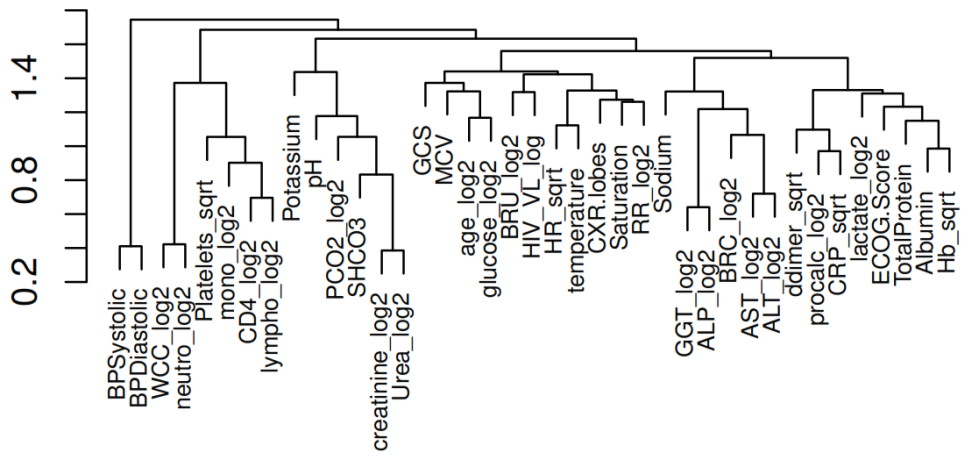

Figure 1-16. Dendrogram by alternative hierarchical clustering method (average linkage)

The 39 dimensions of the correlation matrix can be radically reduced using PCA. The first two dimension of this PCA (figure 17) are similar to those developed for the Jooste dataset (figure 6) but show that many of the other variables now considered also load on the first two principal components.

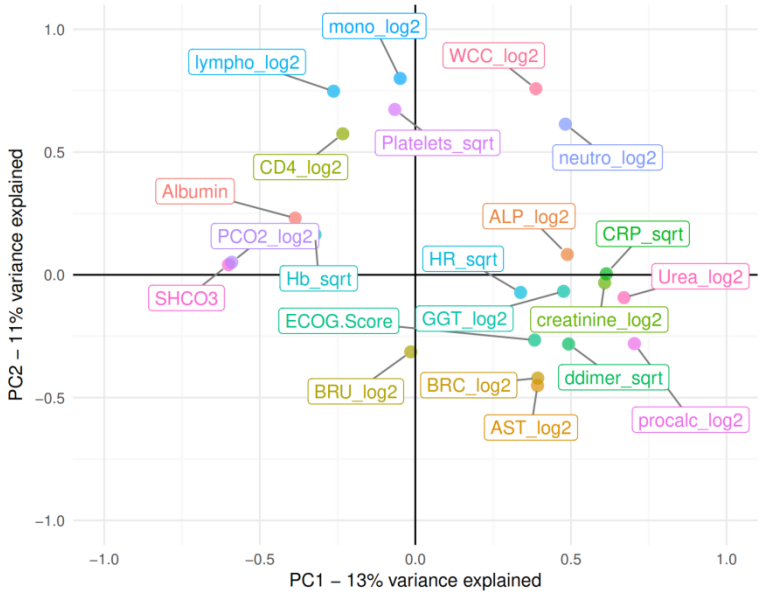

Figure 1-17. Previous correlation matrix reduced to 2 dimensions of covariance using PCA.

PCA performed on 39 variable correlation matrix shown in previous figure (using raw not absolute correlation coefficient values) with varimax rotation. Variables which 'load' on the first 2 dimension with correlation coefficient > 0.4 are shown.

Cumulatively, 24% of variance in the quantitative clinical variables is captured by the first two PCs (a substantial amount given the number of recorded variables – a quarter of the variance in 39 variables is 'explained' by just two axes). More importantly, although not used in their construction, PC1 and PC2 have a strong relationship to both mortality (figure 18 A & B) and dissemination of TB observed by diagnostic tests (figure 18 C & D). A one standard deviation increase in PC1 increases odds of death before 84 days more than 2-fold (OR 2.1; 95%CI 1.7 to 2.7; p=5.6e-11), and increase in PC2 by one standard deviation decreases odds of death by 40% (OR 0.6; 95%CI 0.5 to 0.7; p=2.4e-6).

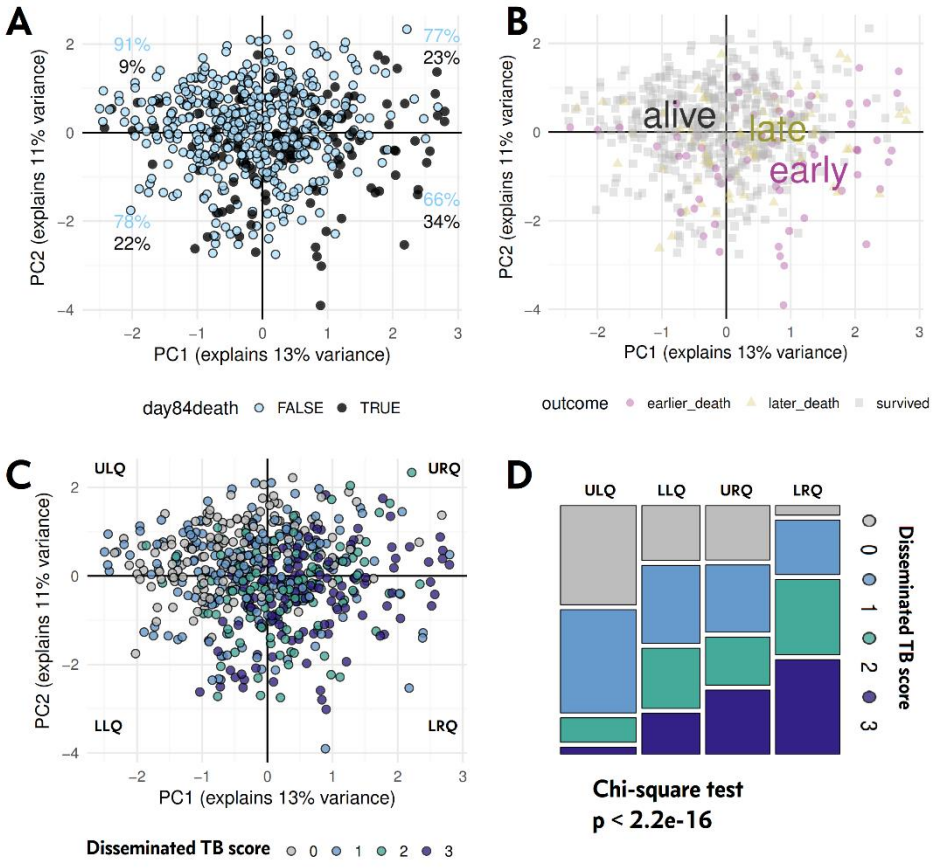

Figure 1-18. Mapping outcome and disseminated TB score to PCA

PCA performed on 39 variable correlation matrix shown in previous figure. Patients are plotted by their coordinates in PCA space based on first two components. **A.** Data points coloured by day 84 mortality outcome, with percentages of patients who died (solid black circle, black text) and survived (light blue fill circles, light blue text) by quadrant. **B**. Data points coloured by early death (before 14 days follow up, magenta), later death (between day 14 and 84, yellow-green) or survived to end of study (grey). Barycentre (centre of gravity) for each grouping shown by coloured text position. **C.** Data points coloured by disseminated TB score value. **D**. Proportions of patients by disseminated TB score and PCA

quadrant are highly dependent as shown in mosaic plot with Chi-squared testing of the equivalent frequency table. ULQ = upper left quadrant; LRQ = lower right quadrant etc.

The patients can be more formally clustered in the 39-dimensional space defined by the quantitative clinical variables using K-means clustering. This approach is complementary to PCA but allows an unsupervised classification of patients based on their similarity on all variables, rather than arbitrary cut-offs like the quadrants of the two-dimensional PCA space used in figure 18. The optimal number of clusters can be empirically derived using a variety of metrics mostly based on the magnitude of reduction in sum-of-squares versus a penalty for increasing number of clusters.[156] Using this approach for the 39 variable dataset, i.e. variables other than outcome and TB diagnostics, most metrics indicate 2 clusters are optimal. Again, this radically parsimonious representation of co-variance in clinical variables captures substantial variation in mortality outcome (figure 19) and TB diagnostic test results (figure 20, table 10).

In short, covariance in the large number of clinical variables measured by the KDHTB study provides a more compelling summary of this cohort (rather than considering individual variables as "independent predictors"), not least because it successfully separates signal from noise. When dimensions of the quantitative clinical variables are reduced by PCA or direct unsupervised clustering of patients, they are overwhelmingly related to blood stream dissemination of tuberculosis (measured by blood culture, uGXP and uLAM) and to mortality outcome. This is in keeping with a single major axis of clinical variation in these patients (rather than many different 'types' of HIV-associated TB).

This unsupervised analysis shows that substantial meaningful clinical variation is captured by the KDHTB study. Next, I want to flesh out the description of this clinical variation in a more theory-driven way, i.e. relating the variation to prior clinical domain knowledge.

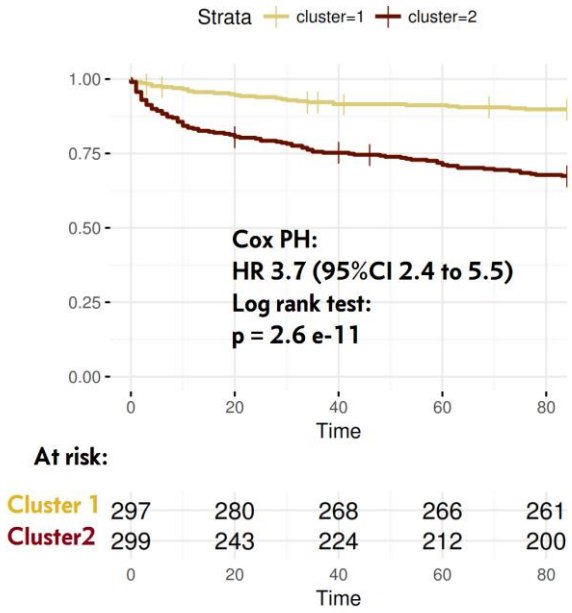

Figure 1-19. K-means cluster association with mortality.

Patients allocated to 2 clusters based on K-means algorithm which determines cluster membership that minimises sum-of-squares 'error' across all included variables (39 in this case). Cluster 2 is associated with substantially higher mortality risk.

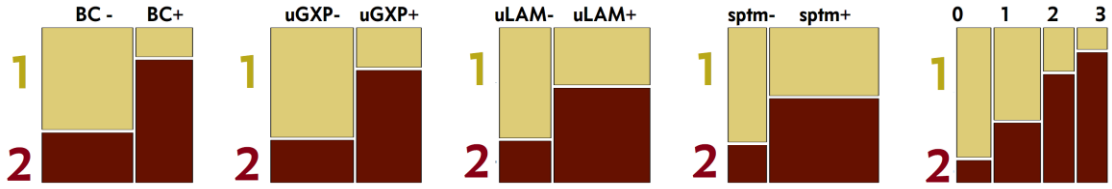

Figure 1-20. K-means cluster association with TB diagnostic results.

Although not used to construct clustering, dependence of cluster by TB diagnostic test (mosaic plot 1 to 4) and DTB score (5th plot) is seen. Positive TB blood culture (BC+) was the TB diagnostic most associated with membership of cluster 2, the high mortality cluster. DTB score has higher predictive accuracy of cluster membership than any individual test.

Table 1-10. TB diagnostic results as predictors of cluster 2 membership.

	OR	95%CI	p value	pseudoR2
DTB score (per 1-point increase)	3.39	2.77 to 4.21	1.00e-30	0.35
TB blood culture positive	8.62	5.81 to 13.03	1.10e-25	0.27
uGXP positive	7.35	4.99 to 10.95	2.10e-23	0.26
uLAM positive	4.39	3.06 to 6.38	3.00e-15	0.14
Sputum culture positive	3.76	2.33 to 6.23	1.10e-07	0.10

OR = odds ratio; 95%CI = 95% confidence interval; pseudoR2 = Nagelkerke's pseudo-R-squared measure for binary outcome models (0 if model is no better at predicting outcome than the intercept; 1 if predicts all outcomes correctly).

1.7 A MORE SUPERVISED APPROACH TO DIMENSION REDUCTION IN CONTINUOUS CLINICAL VARIABLES

In figure 15 liver enzymes were seen to be highly collinear and clustered together in figure 16. To say that liver function tests (LFTs) tend to covary is somewhat trivial from a clinical perspective; when assessing LFTs clinicians are interested in patterns of abnormalities based on prior theoretical understandings of how these patterns relate to pathology. The same is true of several other subsets of these variables. We can use 'clinical theory' – i.e. prior domain knowledge – to inform dimension reduction on these subsets of variables, and better explore their relationship to mortality and MTBBSI. Several examples are given, starting with covariance in LFTs.

1.7.1 Patterns of covariance in liver enzymes

A raised ALT is regarded is more sensitive and specific to hepaocellular injury than disturbance in AST.[157] By extension, elevated AST:ALT ratio is associated with extra-hepatic pathologies: myositis, haemolysis, critical ischaemia, tumour lysis syndrome, DIC, haemophagocytic syndrome;[158-162] and, importantly, disseminated/systemic infections (disseminated histoplasmosis, late leptospirosis, severe Rickettsia infections, Ebola virus disease and virtually all other viral haemorrhagic fevers)[163-167] in which it generally carries prognostic significance.

As shown in table 8 and 9 above, in the current cohort both AST and ALT are associated with blood culture positive TB but neither is significantly associated with mortality. Residual variation in AST after adjusting for ALT is also associated with TB blood culture, but ALT adjusted for AST is not (figure 21 A & B). Interestingly, elevated residual variation in AST after adjustment for ALT is strongly associated with mortality, while elevated adjusted ALT is (weakly) associated with lower mortality (figure 21 C & D). AST seems to be a measure of some process independent of hepatitis related to both dissemination of TB and mortality. Unlike unadjusted ALT, residual variation in AST after adjusting for ALT correlates with major markers of systemic inflammation (figure 22), and it seems most likely that this relates to

tissue damage (specifically, mitochondrial damage in organs with high mitochondrial AST such as the reticuloendothelial system)[168].

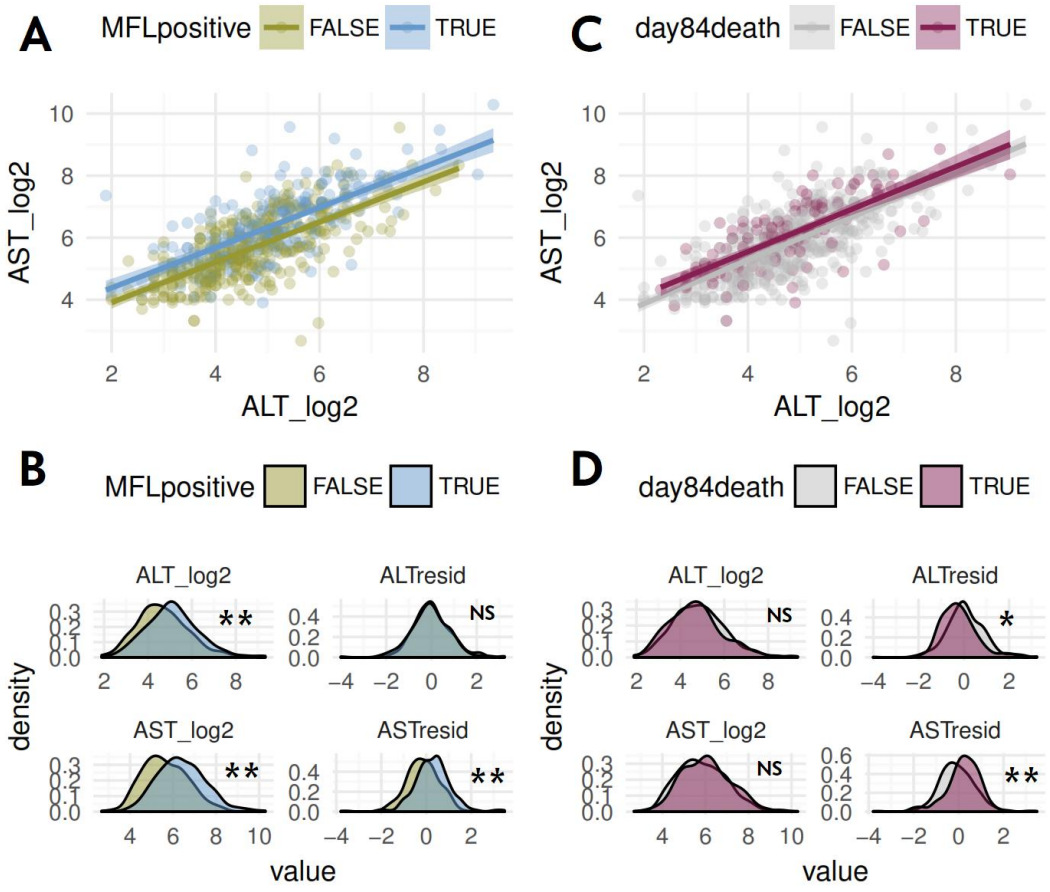

Figure 1-21. Transaminases relationship to MTBBSI and mortality

A. Scatterplot ALT versus AST (both on log2 scale) by positive TB blood culture (MFLpositive) category. **B.** Distribution density plots of ALT, ALT after adjusting for AST (ALTresid), AST, and AST after adjusting for ALT (ASTresid); disaggregated by TB blood culture. **C.** Scatterplot ALT versus AST (both on log2 scale) by day 84 mortality outcome. **D**. Distribution density plots of ALT, ALT after adjusting for AST (ALTresid), AST, and AST after adjusting for ALT (ASTresid); disaggregated by TB blood culture. ** = p<0.0001; * p < 0.01; NS = p>0.05 all by t-test.

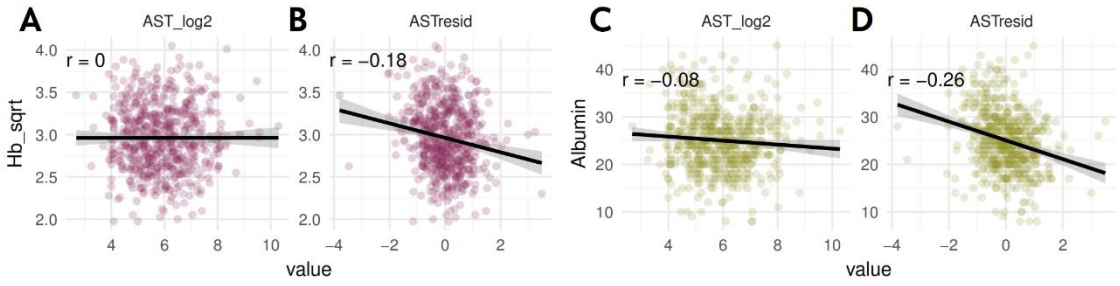

Figure 1-22. Adjusting AST for ALT changes its relationship to other variables

Classically, liver enzymes are grouped by site of predominant pathology, with hepatocellular damage associated with the transaminases and cholestasis associated with the bile canalicular enzymes (alkaline phosphatase and gamma-glutamyl transferase – ALP and GGT), while raised bilirubin can be caused by pathology at either site, or be 'pre-hepatic' from red blood cell lysis where it is then predominantly unconjugated.[157] A PCA representation of LFT covariance in the current cohort follows this classification well, with ALT and AST loading PC1; (predominantly unconjugated) bilirubin and to a lesser extent AST load on PC2; ALP, GGT and to a lesser degree conjugated bilirubin load on PC3 (figure 23). We can tentatively label these PCs hepatitic, extra-hepatic, and canalicular respectively. All three are associated with disseminated TB score (PC1, hepatitis, Rho = 0.23, p=2.4e-08; PC2, extra-hepatic, Rho=0.13, p=0.001; PC3, canalicular, Rho=0.16, p=5.7e-05), but it is the canalicular component that has the strongest relationship with mortality (figure 24). ALP and GGT rises are regarded as most typical of "infiltrative" hepatic tuberculosis,[169] irrespective of CD4 count.[170] In this cohort, ALT has significant *positive* correlation with CD4 count after adjusting for AST (Pearson's r = 0.12, p=0.004) so it may be that a hepatitic response to liver TB is immune-mediated (e.g. type IV hypersensitivity).

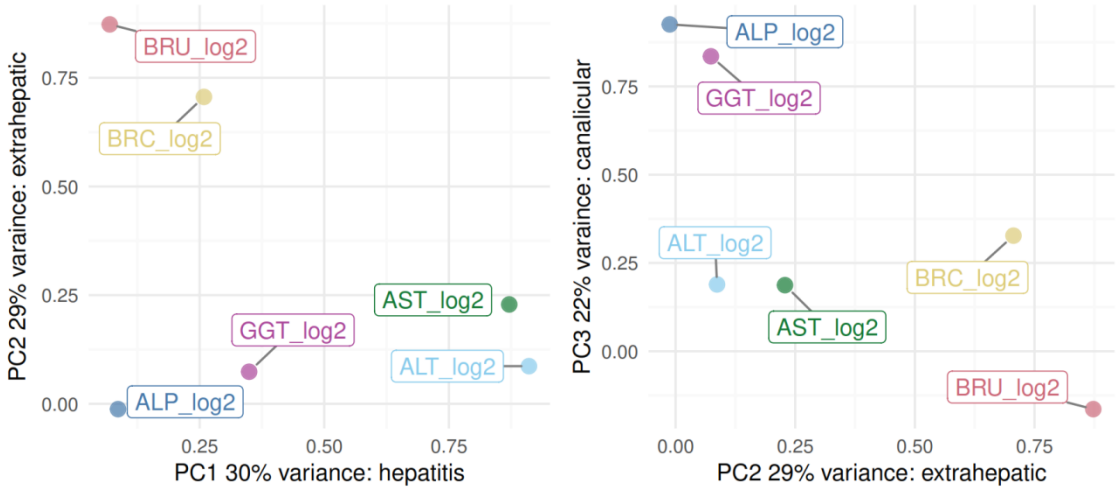

Figure 1-23. Correlation of individual liver enzymes with their first 3 principal components

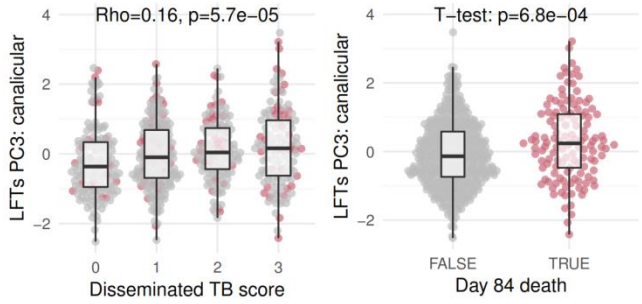

Figure 1-24. Liver enzyme principal component 3 relationship with DTB score and mortality

Patients who died shown with pink dots, survivors in grey.

1.7.2 Acid-base balance and renal impairment

Most HIV-associated TB patients in the KDHTB dataset have a metabolic acidosis (figure 25 A & B): 330/596 (55%) venous bicarbonate < 22mmol/L, of which 114/330 (35%) are decompensated with pH < 7.35. Raised venous lactate was also common (221/596, 37%, venous lactate > 2.2mmol/L), but unrelated to venous pH (raised lactate: OR for pH<7.35 = 0.98, 95%CI 0.64 to 1.50; OR for bicarbonate < 22 = 1.35, 95%CI 0.96 to 1.95; figure 25 C). Metabolic acidosis was also largely independent of levels of buffers like haemoglobin (figure 25 E). By contrast, renal dysfunction explained about 35% of variation in venous bicarbonate (figure 25 D and table 11), suggesting that renal dysfunction (+/- gastro-intestinal loss of bicarbonate, which was unobserved) was the major driver of metabolic acidosis in this cohort. In addition, DTB score was negatively correlated with venous bicarbonate (Rho = -0.19, p=2.6e-06, figure 25 F).

Table 1-11. Predictors of metabolic acidosis

Sequential addition of predictors to model predicting SHCO3: Predictor variable added	Adjusted R2	LRT p value
creatinine_log2	0.344	--
urea_log2	0.353	0.00170
lactate_log2	0.364	0.00079
Hb_sqrt	0.375	0.00076
Potassium	0.385	0.00109

Variables in first column were sequentially added to a linear model predicting venous bicarbonate. Each (nested) model was compared for improved data fit to the previous model using Likelihood ratio test (LRT)

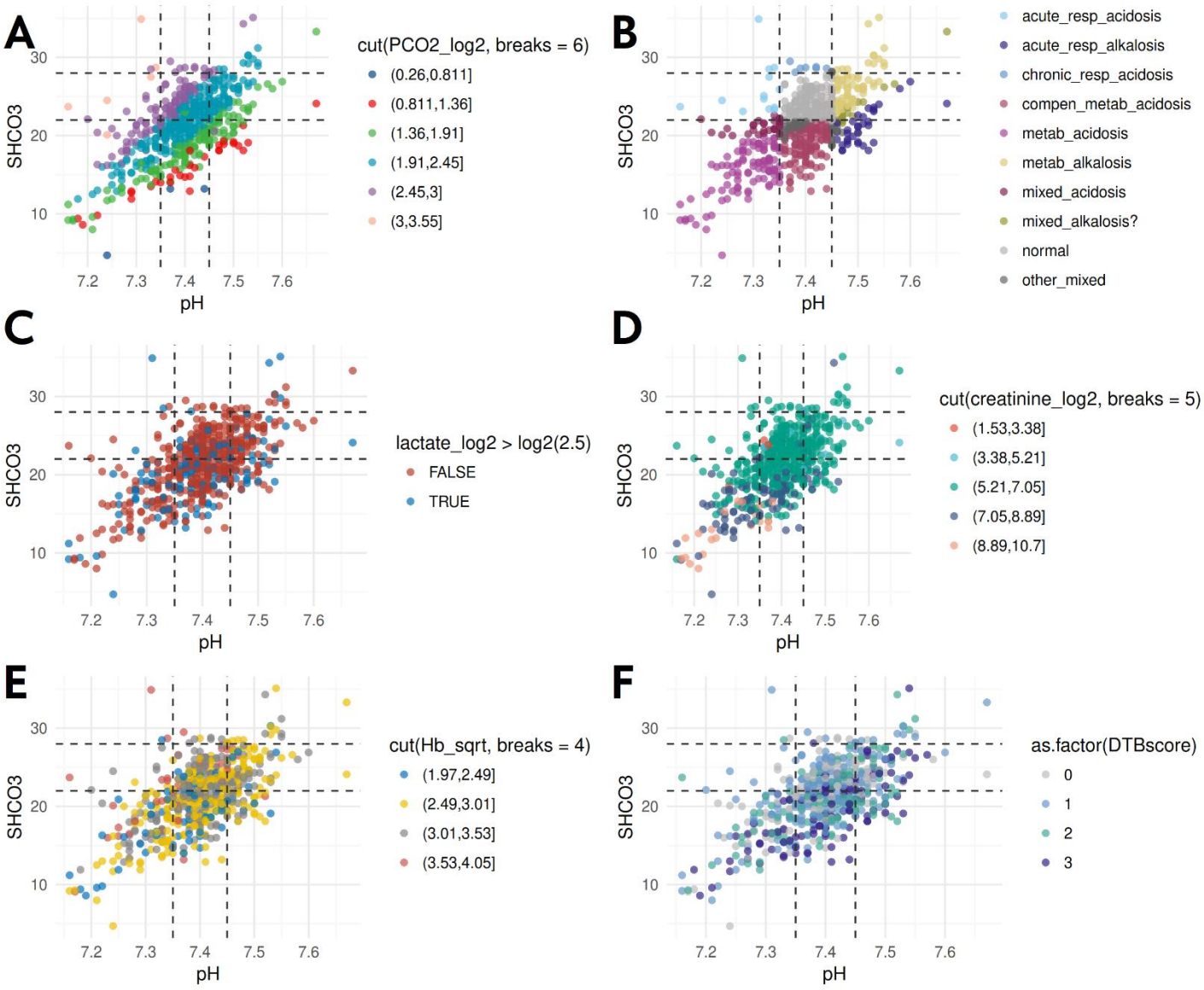

Figure 1-25. Acid-base balance overview

A. Davenport diagram showing venous pH by bicarbonate level for each patient coloured by pCO2 (distribution divided into 6 equal width intervals). **B.** Acid-base status of each patient is categorised by Boolean operators on pH, bicarbonate and pCO2. **C.** Patient data points coloured by venous lactate (>2.5mmol/L = blue; ≤2.5mmol/L = red). **D.** Patient data points coloured by creatinine (distribution divided into 5 equal width intervals). **E.** Patient data points coloured by haemoglobin (distribution divided into 4 equal width intervals). **F.** Patient data points coloured by DTB score.

Because acid-base balance is a completely understood homeostatic system, it provides a good example to test the specific hypothesis that limited physiological reserves are the mechanism by which increased age is associated with mortality in KDHTB. In summary, pH is determined by magnitude of metabolic acidosis (sHCO3) plus degree of respiratory compensation (pCO2) and secondary buffers. Upstream disease processes (D in figure 26) determine renal and lactate sources of the acidosis. There is correlation between renal dysfunction and age. We can hypothesise that age is a determinant of adequacy of respiratory compensation in metabolic acidosis (supported by the correlation between age and pCO2 in the correlation matrix presented earlier).

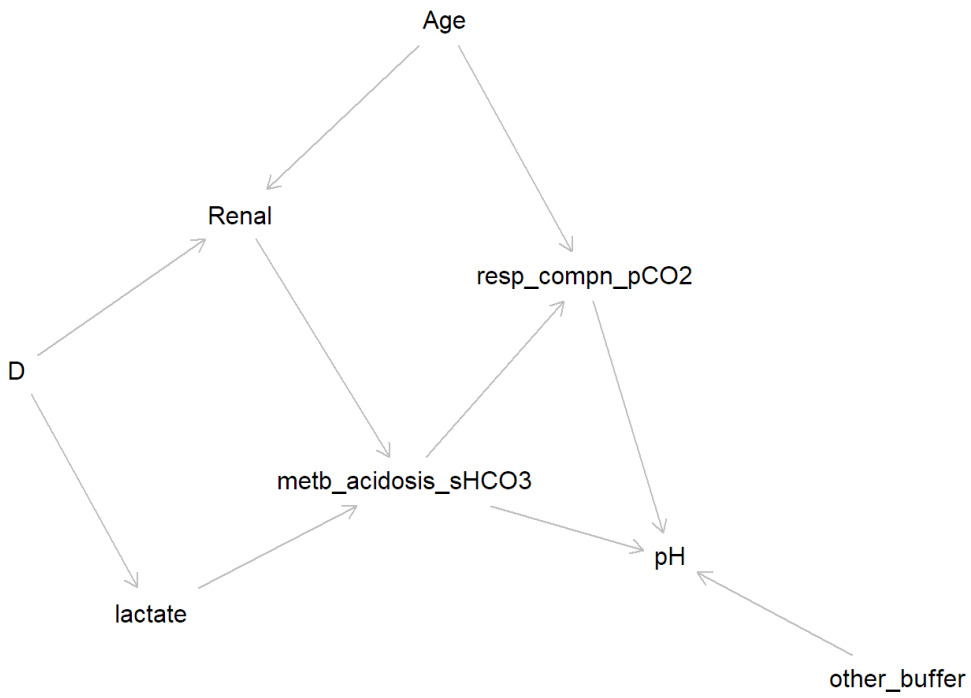

Figure 1-26. Directed acyclic graph: age and acid-base balance

This implies that, after adjusting for relevant confounders presented in figure 26 (markers of renal function and metabolic acidosis, i.e. creatinine, urea, and bicarbonate) age should 'explain' some residual variation in pCO2. In other words, for a given level of metabolic acidosis, is age associated with an 'inappropriately' high pCO2? In a linear model testing this hypothesis, age was indeed associated with a higher pCO2 (p=0.02, figure 27). Although the

effect size was small (increasing age from 18 to 36 years, with all other variables held constant at their mean value, was on average associated with a 0.2mmHg increase in pCO2) this is only one example of potential physiological reserve limitation associated with increasing age.

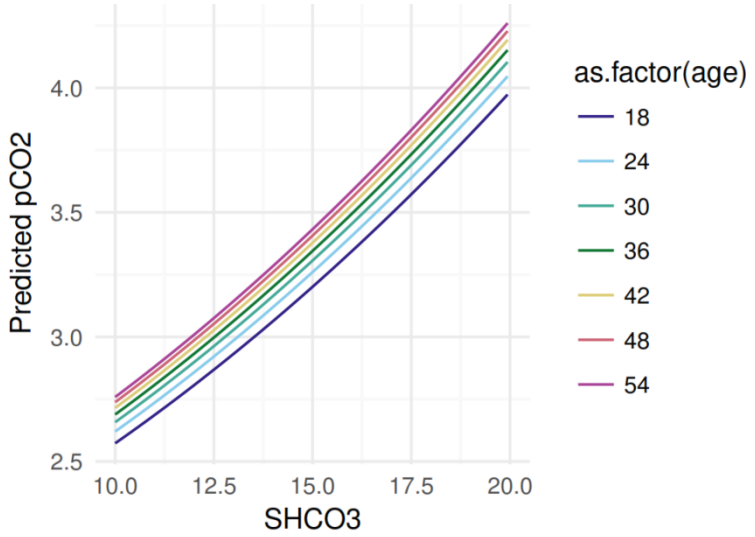

Figure 1-27. Age - adjusted pCO2 from model based on DAG in preceding figure.

A linear model of form *PCO2_log2 ~ SHCO3 + age_log2+ creatinine_log2 + Urea_log2* was fitted to the KDHTB data. SHCO3 is the major driver of pCO2 in this cohort because it is dominated by metabolic acidosis secondary to renal dysfunction. After adjusting for renal dysfunction and bicarbonate, age was associated with significantly higher pCO2 (p=0.02). Predicted pCO2 values from the model are shown for a range of SHCO3 values and 7 ages at 6- year intervals.

A PCA on acid-base and renal variables gives an intuitive representation of these variables on just 2 dimensions (figure 28). PC1 captures metabolic acidosis related to renal dysfunction (figure 28 A). PC2 captures about half of the remaining variance in acid-base status, including variation in pCO2 which is not directly correlated with renal driven metabolic acidosis – for example separating respiratory acidosis and alkalosis, and degree of respiratory compensation for metabolic acidosis.‡‡ The 2-dimensional PCA therefore replicates the standard clustering of patients based on the Davenport diagram (figure 28 B). And, in this cohort, it is PC1 that relates strongly to disseminated TB (figure 28 C) and mortality (figure 28 D). This puts renal

‡‡ Note that potassium is surprisingly strongly related to PC2; hyperkalaemia is uncommon in this cohort (11% have K+ >5.0), while one in four patients had hypokalaemia. The variance in potassium captured on PC2 may (in part) be related to respiratory alkalosis – patients with acute respiratory alkalosis do have a mean potassium 0.5mmol/L lower than the overall cohort. There isn't much evidence here of a metabolic acidosis caused by gastro-intestinal bicarb loss associated with hypokalaemia, but it could be masked by associated pre-renal acute kidney injury.

dysfunction centre-stage in the pathophysiology of advanced HIV-associated TB at least in this cohort.

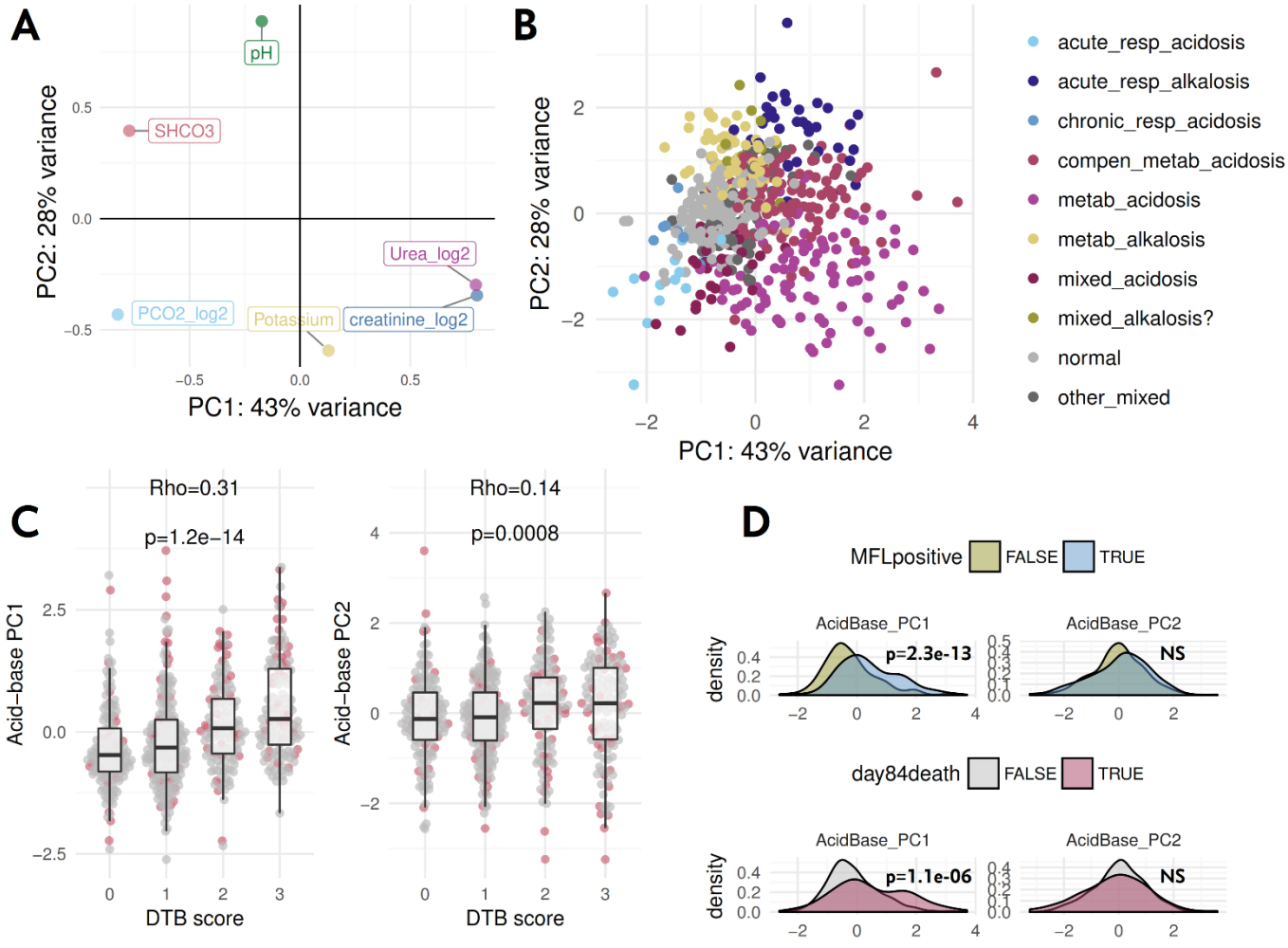

Figure 1-28. PCA of renal/acid-base variables.

A. Correlation of renal and acid-base variables with their first two principal components. **B.** Patients plotted in 2-dimension PCA space coloured by standard acid-base clustering. The colour scheme is the same as figure 25B for comparison. **C.** DTB score correlation with the first two acid-base principal components (patients who died by day 84 are coloured pink in these plots, survivors in grey). **D.** Density distributions of acid-base PCs disaggregated by TB blood culture status (MFLpositive TRUE = positive TB blood culture) and by day 84 death outcome. P-values from t-tests; NS= non-significant (both p>0.2).

What, in turn, is driving this acute kidney injury (AKI)? Historically, infection-associated AKI was described as resulting from systemic hypotension, renal vasoconstriction, and ischaemia-reperfusion damage.[171,172] AKI is unrelated to blood pressure in the present cohort (metab_pc1

correlation with systolic blood pressure = 0.03, 95%CI -0.05 to 0.11, p=0.4). This is in keeping with the growing evidence that sepsis-AKI most often occurs in the absence of overt hypo-perfusion. For example, AKI is commonly un-associated with haemodynamic instability in patients with pneumonia,[173] and animal-models of sepsis show AKI in the context of *increased* renal blood flow.[174] Consequently, focus has shifted to other mechanisms, of which a large number have been found:[175]

- direct effects of DAMPs and PAMPs on renal tubular cells causing microcirculatory flow changes (presumably of particular importance in BSI);
- endothelial activation, coagulation abnormalities, causing tissue damage;
- mitochondrial damage and/or adaptation in the face of reduced energy availability (as sources of ATP are redirected to inflammatory responses);
- circulating microparticles (intact vesicles of plasma membrane resulting from apoptosis, increased production in inflammation).

These mechanisms are "inflammation" and clearly inter-related and potentially concurrent. In the KDHTB cohort, AKI correlates strongly with markers of systemic inflammation (for example, metab_pc1 correlation with pro-calcitonin = 0.51, 95%CI 0.45 to 0.57, p<2.2e-16). An important point, though, is that the kidneys are not just passive subjects of inflammation, and all elevations in creatinine are not strictly pathological. The renal response to reduced extracellular fluid volume[§§] is to conserve water and sodium at the expense of (transient) decrease in filtration: elevated creatinine in this context has been referred to as "functional pre-renal AKI or even acute renal success".[176] The transcript signature associated with this response (osmoregulation and metabolic pathways) is completely distinct from that seen in ischaemic injury (inflammation, cell death).[177] Some authors have conceptualised sepsis-AKI as a 'second-hit' phenomenon where the protective mechanisms of functional AKI are overwhelmed by non-resolving inflammation.[176] Importantly, it should be possible to separate AKI caused by the protective response to reduced ECFV and intrinsic nephron damage using urine biomarkers.[178]

[§§] ECFV in KDHTB is discussed more in the section on hyponatraemia.

1.7.3 Hyponatraemia

Nine in ten TB patients in KDHTB have serum sodium < 135 mmol/L. Hyponatraemia is associated with a long list of infections, almost invariably as a marker of disease severity and mortality.[179-185] This ubiquity masks an assortment of underlying disease processes, from diarrhoea to syndrome of inappropriate anti-diuretic hormone secretion (SIADH),[186] so the meaning of hyponatraemia will differ between one infection and another and one patient population and another.

The volume of literature discussing hyponatraemia in HIV [187-194] suggests it is commonly multifactorial. By contrast, reference textbooks unequivocally link hyponatraemia of TB to SIADH.[165,195] Hill *et al.*'s classic study of 20 hyponatraemic HIV negative pulmonary TB patients demonstrated detectable ADH in blood, with some response to water loading, which they attributed to down regulation of osmoregulation by active TB ("reset osmostat", essentially, a subtype of SIADH).[196] The mechanism remains unknown, but the phenomenon is probably not completely TB specific.[184] More generally, IL-6, nausea & vomiting, and physiological stress (such as hypoglycaemia) are stimulants of ADH release (independent of serum osmolarity).[186]

Other hyponatraemia mechanisms potentially relevant to KDHTB patients include gastro-intestinal losses (associated with *appropriate* ADH secretion if low extracellular circulating volume, ECFV), or adrenal insufficiency.[***] Two small South African studies have looked for adrenal insufficiency in hospitalised TB patients. Venter *et al.*[197] measured cortisol in 20 inpatients with TB, randomised to rifampicin versus fluroquinolone based TB treatment. 18 patients were known HIV co-infected; 7 of these patients had hyponatraemia, none had adrenal insufficiency, all 7 had "features of SIADH", although volume status wasn't specifically commented on and mean urine sodium was only 31 mmol/L. Kaplan *et al.*[198] determined cortisol response to ACTH in 40 pulmonary TB inpatients (18 HIV co-infected). None of the 4/40 patients with hyponatraemia had adrenal insufficiency, or clinical evidence of volume depletion, but all 4 had "features of SIADH". This included low serum osmolarity (261 - 279 mOsm/Kg) and relatively high urine osmolarity (642 - 861 mOsm/Kg), although no

[***] Rates of TB meningitis were low so intra-cranial causes of hyponatraemia are unlikely. Few patients have markedly raised blood glucose suggestive of pseudo-hyponatraemia.

"inappropriate natriuresis" was noted. In both studies, patients were all sputum smear positive with mean CD4 count around 190 cells/ml, so MTBBSI was unlikely.

Following the method of both the Venter and the Kaplan studies mentioned above, serum osmolarity for the KDHTB cohort can be calculated using *2*(sodium + potassium) + urea + glucose*. Based on this, a large proportion of hyponatraemic patients appear to have normal or raised serum osmolarity (> 280, to the right of the vertical axis figure 29 A) but this is spurious, due to raised urea levels – indicated by green, yellow and red points in figure 29A (serum urea does not signal osmoreceptors in the posterior pituitary to effect ADH release[199]). In sum, the Venter and Kaplan studies could show (or assume) euvolaemia in their HIV-associated TB patients, and conclude that hypotonic hyponatraemia was due to SIADH, but such an assumption isn't valid here.

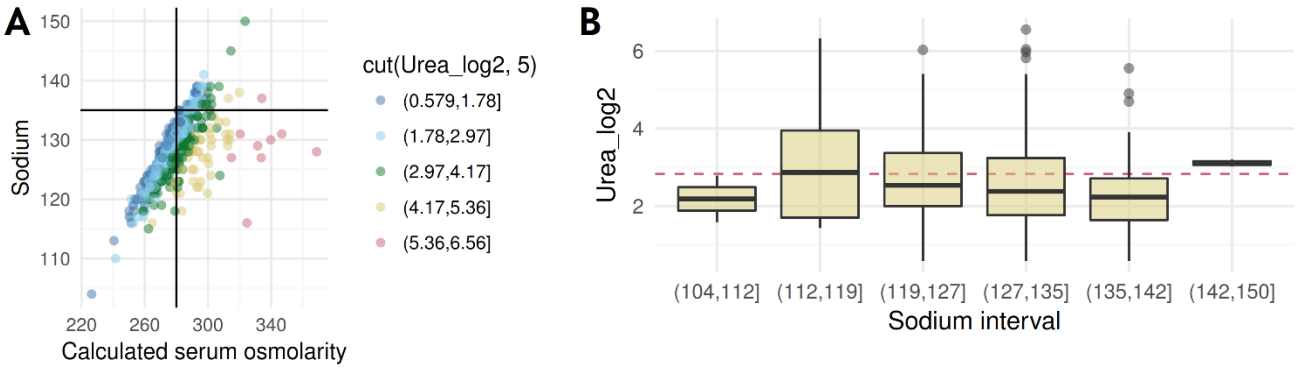

Figure 1-29. Hyponatraemia, calculated osmolarity, and urea.

A. Calculated osmolarity versus sodium. Data points are coloured by urea level (distribution divided into 5 equal width intervals). Vertical line is upper limit of normal for serum osmolarity; horizontal line is lower limit of normal for serum sodium. **B**. Boxplot urea distribution by sodium interval (median, IQR, range, outliers indicated by line, box, whiskers and dots respectively). Upper limit of normal for urea shown with dashed red line [log2(7.1) = 2.82].

Indeed, although the relationship isn't entirely linear (figure 29B), overall urea_log2 has significant negative correlation with sodium (r = -0.11, p=0.008), as does creatinine_log2 (r = -0.11, p=0.009). This *might* be in keeping with hyponatraemia due to sodium and water loss, with reduced extracellular circulating fluid volume (ECFV), and reduced glomerular filtration. This interpretation is complicated by the fact that urea and creatinine have a weak relationship with fluid volume status (being confounded by multiple factors like underlying renal function, muscle mass etc.), and secondly, because correlation between hyponatraemia and renal function could also be because they are both related to some other underlying variable (e.g.

inflammation, TB dissemination). Temporal trends in renal markers and sodium after admission help test this association. In a random subset of 50 KDHTB patients, any serial electrolyte results found on the laboratory system sent as part of their routine care were extracted; 39/50 had ≥2 measures of creatinine and 34/50 had ≥2 measures of sodium available, allowing trends to be plotted (figure 30 A & B). In addition, Emergency department records were reviewed showing that intra-venous normal saline was prescribed on admission in all patients. 32/40 patients had an increasing sodium trend (positive gradient), and 30/39 had a decreasing creatinine trend (negative gradient) observed during their admission. Further, magnitude of sodium and creatinine gradients were strongly correlated (figure 30 C). Potassium levels also fell in parallel, in keeping with return of GFR but lingering tubule dysfunction (data not shown). Despite the risk of bias associated with non-systematic ascertainment of serial measures, this is evidence that these patients' hyponatraemia was (substantially) due to sodium / ECFV depletion. By the same token, full resolution of hyponatraemia was *observed* in only 2 patients, and a substantial minority had worsening hyponatraemia after IV fluids, so it is very plausible that multiple mechanisms of hyponatraemia are present both within and between patients.

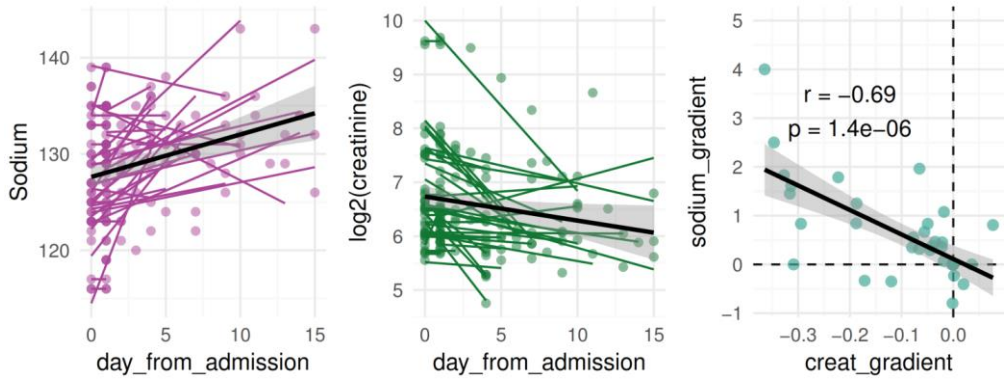

Figure 1-30. Serial measurement of sodium and creatinine during admission.

50 KDHTB patients selected at random had electrolyte results from blood tests carried out as part of their routine care (non-study samples) extracted from the National Health Laboratory Service results portal. 39 had ≥2 measures of creatinine and sodium during admission. Trends in both these electrolytes are shown (left and middle plot; coloured trend lines are lines of best fit by patient, overall line of best fit ignoring dependence by patient is shown in black with 95%CI). The gradients of these trend lines were extracted (lmList() function of lme4 package in R) and pairwise correlation between sodium and creatine gradients assessed (right plot).

1.7.4 Covariance in Leukocytes

White cells are highly collinear; total white cell count correlates to a greater or lesser extent with all subsets but is mostly related to absolute neutrophil count; lymphocyte count correlates strongly with CD4 subset and with monocytes; platelets correlate with total white cell count and monocytes; percentage neutrophil count is only moderately related to absolute neutrophil count, and has different covariance pattern with other cells (figure 31).

It is well established that HIV infection progressively diminishes CD4+ lymphocytes and monocytes,[200,201] as well as platelet and neutrophil counts.[202,203] Lymphocytopenia is also classically associated with specific infections including influenza, dengue, malaria and tuberculosis,[204] but is more commonly a general response to stress and inflammation (e.g. bacterial sepsis) in hospitalised patients.[205] Intercurrent infections cause reversible drops in total and CD4+ lymphocyte counts in HIV infected patients including tuberculosis.[206] Neutrophilia is the hallmark response to acute inflammation caused by infections (classically, more marked in pneumococci, staphylococci and clostridia infections) and/or tissue damage.[†††] In sum, variation in white blood cells (WBCs) in the KDHTB cohort will represent the net effects of at least two different (and interacting) processes: immunosuppression and inflammation.

Can these be disaggregated? Covariance of WBCs with strong markers of acute inflammatory response (CRP and procalcitonin) can be assessed, again using PCA (figure 32). The first two PCs separate variance in WBCs into axes which seem to correspond well to immune status (PC1, strong positive correlation with CD4 count, total lymphocytes, monocytes, and weak negative correlation with pro-calcitonin/CRP), and inflammation (PC2 strong positive correlation with pro-calcitonin/CRP, moderate correlation with higher neutrophils, and weak correlation with lower agranulocyte counts). In turn, WBC PC1 and PC2 both relate strongly to MTBBSI and mortality outcomes exactly as we would expect (figure 33).

[†††] The role of neutrophils in TB is discussed below.

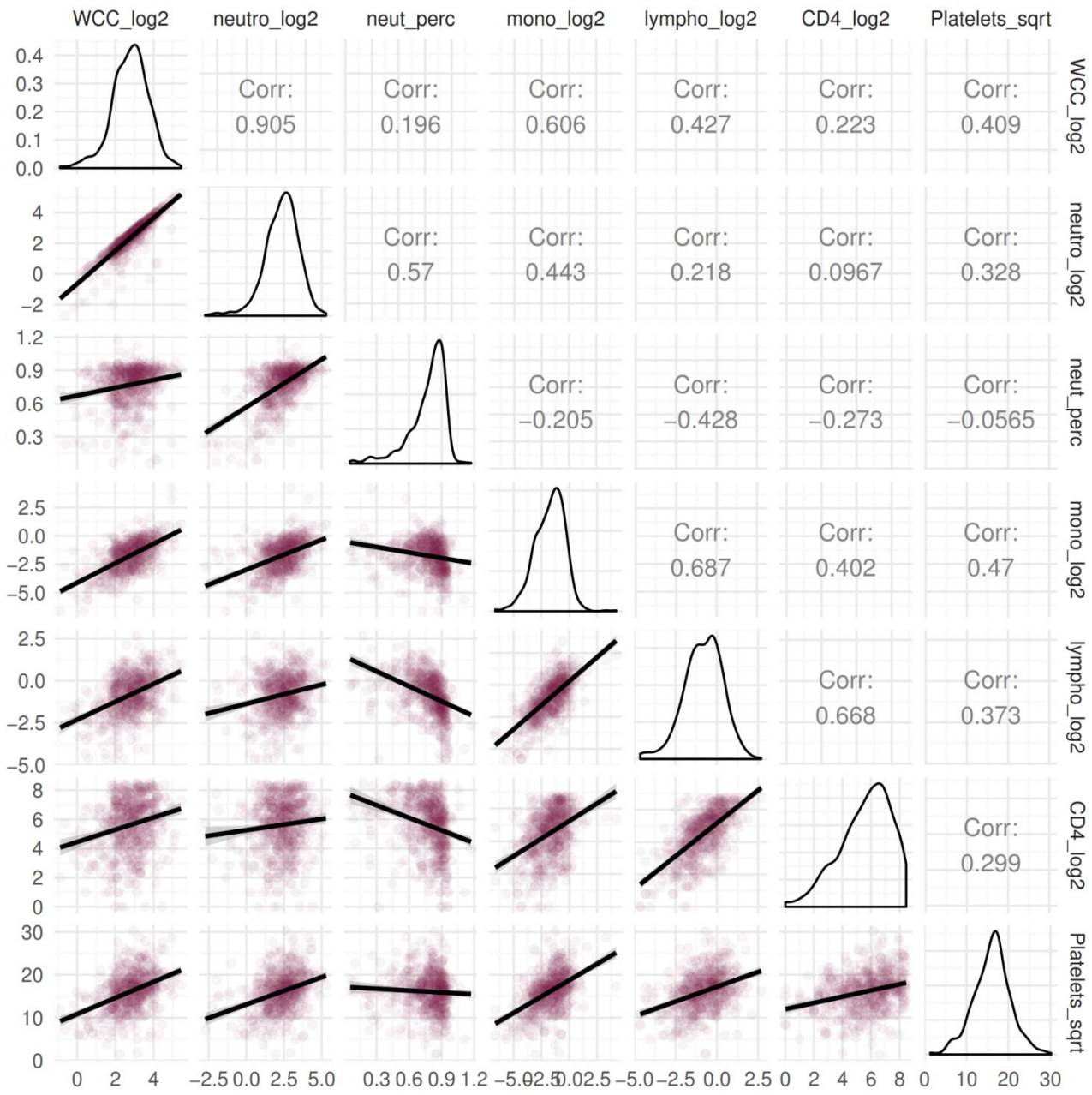

Figure 1-31. Pairwise relationships in blood cells.

Corr = Pearson's correlation coefficient; neut_perc = percentage neutrophils (absolute neutrophil count on original scale divided by total white cell count on original scale); other variables as defined in table 7. Univariate densirt distributions shown on diagonal. Bivariate distributions with line of best fit below diagonal.

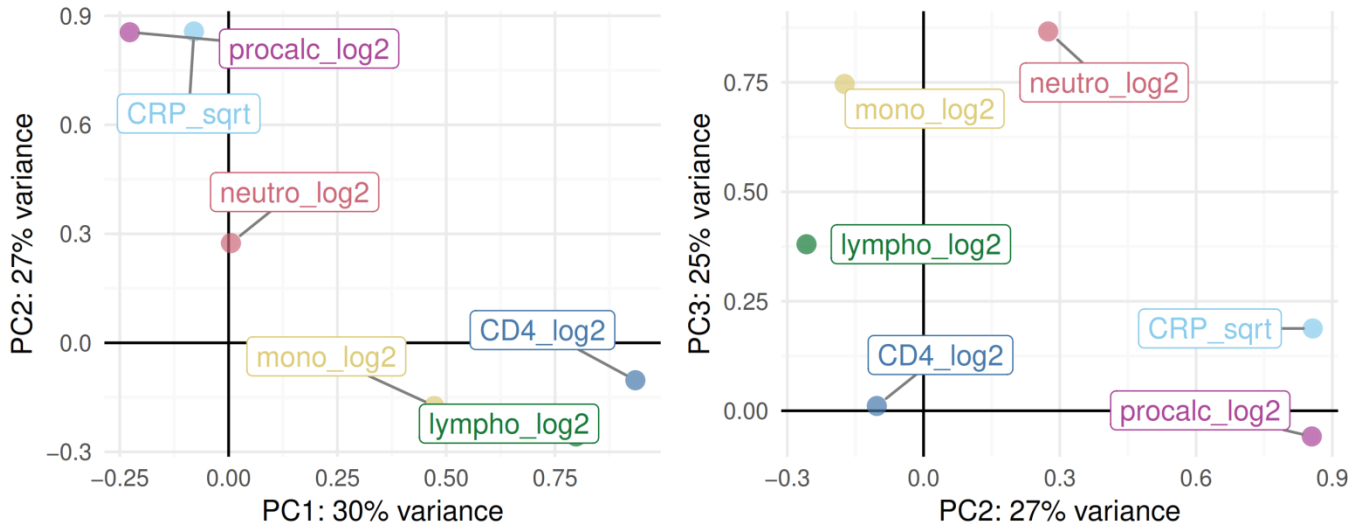

Figure 1-32. Correlation of WBC and inflammatory markers with their first 3 PCs (varimax rotation).

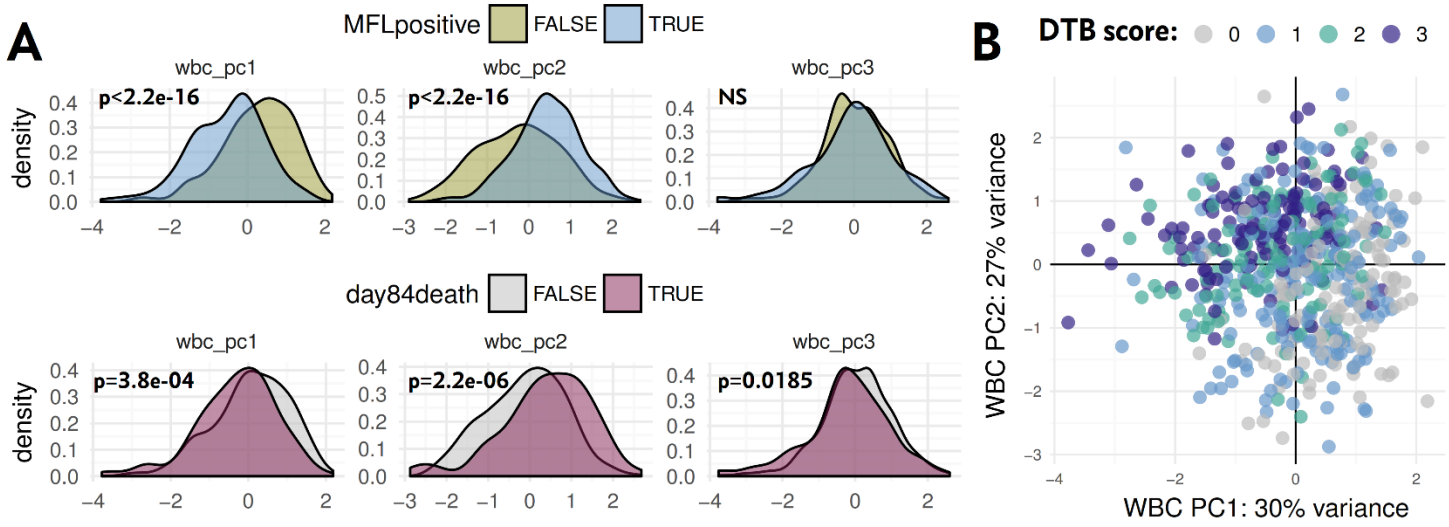

Figure 1-33. WBC principal components relationship with TB blood culture, DTBs core, and mortality outcome.

A. Density distributions of the first 3 WBC principal components disaggregated by TB blood culture status (MFLpositive, top) and day 84 outcome status (day84death, bottom). P values are from t-tests, NS = non-significant (p>0.1). **B**. Individual data points are patients plotted by their coordinates on the first two WBC principal components, coloured by DTB score.

The third WBC principal component – positively correlated with neutrophils and to a lesser extent lymphocytes and monocytes – is harder to interpret. Based on a Scree plot (eigen values of the components versus number of components, not shown) the third component probably contains signal rather than noise.[207] WBC PC3 is highly correlated with total white cell count (r = 0.86; 95%CI 0.84 to 0.86, p<2.2e-16). It has no correlation with TB blood culture status (figure 33 A) or DTB score (r = 0.00, 95%CI -0.07 to 0.09, p=0.45), but does have some relationship to mortality outcome such that a higher value is weakly associated with survival (figure 33 A). This means higher neutrophils are associated with *lower* mortality on PC3, but associated with *higher* mortality on PC1. Neutrophil variance which is collinear with inflammatory markers is harmful (and closely related to MTBBSI), but neutrophil variance correlating with total white cell count is protective (and independent of MTBBSI). This relationship can also be seen on the original variables, where percentage neutrophils are (tautologically) related to total white cell count and absolute neutrophil count; percentage neutrophils are moderately correlated with DTB score; and DTB score has no relationship to total white cell count at all (figure 34) – a good example of noncommutative pairwise correlations: neutrophils are being influenced by (at least) two completely independent processes.

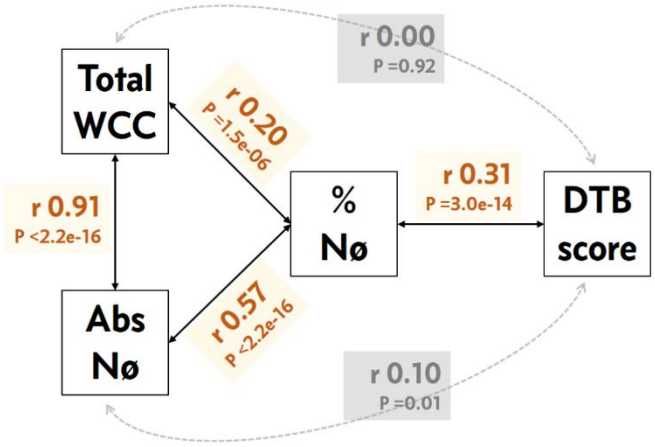

Figure 1-34. Correlation between total white cells, neutrophil measures, and DTB score.

R = Pearson's. Nø = neutrophil; % percentage; abs = absolute count; WCC = white cell count.

The role of neutrophils in tuberculosis pathology is not straight forward. Many potentially myco-bactericidal mechanisms have been found *in vitro* for neutrophils (e.g. NETs, cytokine signalling, cathcidin production) and their role in containing some stages of TB infection are thought to be important but incompletely understood.[208] In a study of household contacts of

smear-positive pulmonary TB patients, risk of TB infection (positive IGRA) was inversely proportional to peripheral blood neutrophil count.[209] Of note, in that study 95% of contacts had a neutrophil count within the normal range, but counts were higher than in healthy controls. Animal knock-out models focused on established TB disease (as opposed to early innate response to new infection) are spectacularly inconsistent.[210]

In clinical studies of established disease, neutrophilia has often been associated with adverse outcomes (slow bacillary clearance,[211,212] treatment failure,[213] and death[214-217]) , though not consistently so.[218,219] There is evidence of neutrophil count correlation with sputum bacilli load.[220] Clearly, these findings relate neutrophils to severe disease, but can't determine if they are a benefit, a liability, or a neutral marker in such disease. Studies from the pre-antibiotic era had an opportunity to observe the natural history of neutrophils in TB disease in a way not possible now. Peripheral blood neutrophilia was though to relate to abscess formation or cavitation in tubercles, but was also a non-specific marker of inflammation ("tuberculosis complications and superimposed infections influence the picture to a great extent… at times there is marked disagreement between the leukocytic picture and the impression gained from clinical observation").[45] In longitudinal follow-up of 107 patients with detailed blood examination during the 1930s, Houghton weighted neutrophil lobe count (left-shift in modern parlance, i.e. peripheral neutrophil maturity) more than absolute count as an indicator of poor prognosis.[221‡‡‡] The same finding was published in *Frontiers in Immunology* last year: using a variety of multivariate and clustering approaches data from 50 HIV-seronegative pulmonary TB patients, disease severity (pulmonary destruction, bacilli load, radiological extent of TB disease, and other clinical indices) was most closely related to band neutrophils (as compared to absolute counts, other WBC subsets, or Th1 signalling).[222]

Neutrophils are convincingly associated with TB-IRIS pathophysiology, specifically, an activated, early-cell-death, and impaired ability to kill *M. tuberculosis ex vivo* neutrophil phenotype.[223] Importantly, dynamics of neutrophil *activation markers* and tissue-destruction effectors (like neutrophil elastase) are more predictive of TB-IRIS than neutrophil *count* dynamics (distribution of neutrophil count 2 weeks after HAART initiation may not be very different between IRIS and non-IRIS patients).[224]

‡‡‡ "Houghton's Index – which included lobe counts, lymphocytes, monocytes and ESR – was in fact his heuristic attempt at dimension reduction to principal components, to separate signal from noise: "*It is certainly necessary, in view of the fluctuations which occur in the component figures of haemograms, to have a method of summarizing the information derived from each source.*" (ibid).

Finally, while the immunology literature tends to treat neutrophil count as a linear variable, it shouldn't be overlooked that severe neutropenia is a rare but grave finding in tuberculosis.[68,216]

In short, neutrophils can mediate tissue damage, with neutrophilia signalling inflammation and severe disease, but neutrophils could also have an advantageous, bactericidal role.[210] The dual covariance of neutrophils – with adverse and protective components – is, then, well in keeping with previous literature. Further, thinking about neutrophils as representing 2 orthogonal axes of covariance could help better characterise their role in TB pathophysiology in future studies.[§§§]

1.7.5 Fever and globulins

These variables are discussed together here because they are both instructive examples of Simpson's paradox in the KDHTB data set. Higher temperature is associated with MTBBSI (both TB blood culture positivity (t-test p = 1.6e-06) and DTB score (Rho = 0.20, p = 6.5e-07)) so might be expected to be a marker of adverse outcome. This would certainly be the case if the comparator group was (apyrexial) CD4 matched controls without tuberculosis, for example. But, in fact, higher temperature is weakly associated with *decreased* risk of death in KDHTB, specifically early mortality (figure 35 A). With earlier death as the outcome variable (so later death and survivors are the comparator group) a one-degree centigrade rise in temperature has odds ratio 0.80 (95%CI 0.64 to 1.00, p = 0.05). Adjusting for TB blood culture status reduces this OR to 0.72 (95%CI 0.57 to 0.90, p = 0.006). The mechanistic explanation consistent with this finding is that a blunted febrile response in MTBBSI is pathological (figure 35 B).

Hyperglobulinaemia is strongly associated with tuberculosis infection, classically indexed by an abnormally low albumin/globulin (A/G) ratio, which has been related to severity of disease and prognosis.[219,225-227] A/G ratio is a predictor of all-cause mortality in broadly defined cohorts (but in particular for pulmonary and malignancy diagnoses).[228,229] While HIV infection is associated with polyclonal gammaglobulinaemia, HIV-associated TB results in a more deranged A/G ratio than HIV alone.[169,230] Although rises in α2-globulin are perhaps "most consistent", higher levels of all globulin subsets (α1, α2, β, and γ) are seen in active TB.[226] This makes sense, as TB infection can be associated with amyloid[231] (a major α1 globulin), haptoglobin[232-234] (a major α2 globulin), complement[235] (the major β2 globulin), and specific IgGs.[236,237] Even the acute phase reactants in this list (like haptoglobin) may have a special

[§§§] For example, neutrophil transcriptomic signatures may be better related to clinical data using this approach.

association with tuberculosis, distinct from other infections.[234] Rises in all these classes, and a fall in A/G ratio despite albumin and globulins being in the "normal range", can be seen (in the absence of manifest systemic inflammation) after BCG immunisation.[238] Globulins are a major determinant of ESR; ESR is often 'disproportionately' raised in tuberculosis (one of the classic causes of ESR > 100), with distinct dynamics compared to CRP.[239,240] In sum, hyperglobulinaemia in tuberculosis isn't simply another non-specific marker of inflammation, but encompasses multiple relatively specific host-responses to TB, some of which are likely to be adaptive rather than pathological.

In keeping with above, and without exception, every patient in the KDHTB cohort has an abnormally high globulin level, and an abnormally low albumin-globulin ratio < 0.8 (figure 36 A). However, within this group of TB patients, those with more disseminated disease tend to have a paradoxically *lower* globulin level (figure 36 A & B). While albumin correlates most strongly with inflammatory markers, globulins positively correlate with lymphocyte count (and even more with WBC principal component 1, i.e. variation in mononuclear leukocytes relating to immune status rather than inflammation) – figure 36 C & D.

This is in keeping with globulin variation representing a host-response axis independent of systemic inflammation, with apparent decompensation in severe, disseminated, disease. However, curiously, only albumin and not globulin level is related to mortality (figure 36 B) so the mechanistic importance is unclear. Serum protein electrophoresis +/- longitudinal measurement might help unpick this finding. Irrespective, an important takeaway message is that pathophysiology can show non-linear relationships, with deviation from normal in mild-moderate disease, but distributions closer to the normal range when infection is severe / decompensated. The apparent relationship of such a variable to mortality will depend heavily on inclusion criteria / selection of controls. These globulin findings resonate with patterns seen in some coagulation factors (another major class of plasma proteins) in a subset of the KDHTB cohort.[141] ****

**** U-shaped patterns are seen in fibrinogen, factor IX, XI, V, II comparing HIV-infected outpatient controls, hospitalised survivors, and non-survivors.

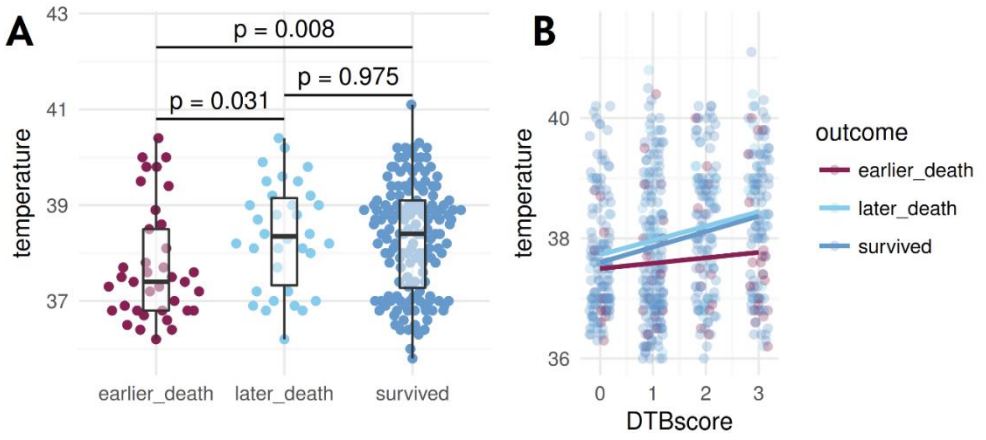

Figure 1-35. Temperature (°C) relationship with mortality and MTBBSI

A. Temperature distribution by outcome with overlaid box-plots (median, IQR, range, outliers indicated by line, box, whiskers and dots respectively). **B.** Temperature distribution by DTB score, with line of best fit by outcome status. Earlier death = death before day 14 follow-up; later death = death between days 14 and 84; survived = survived to end follow-up.

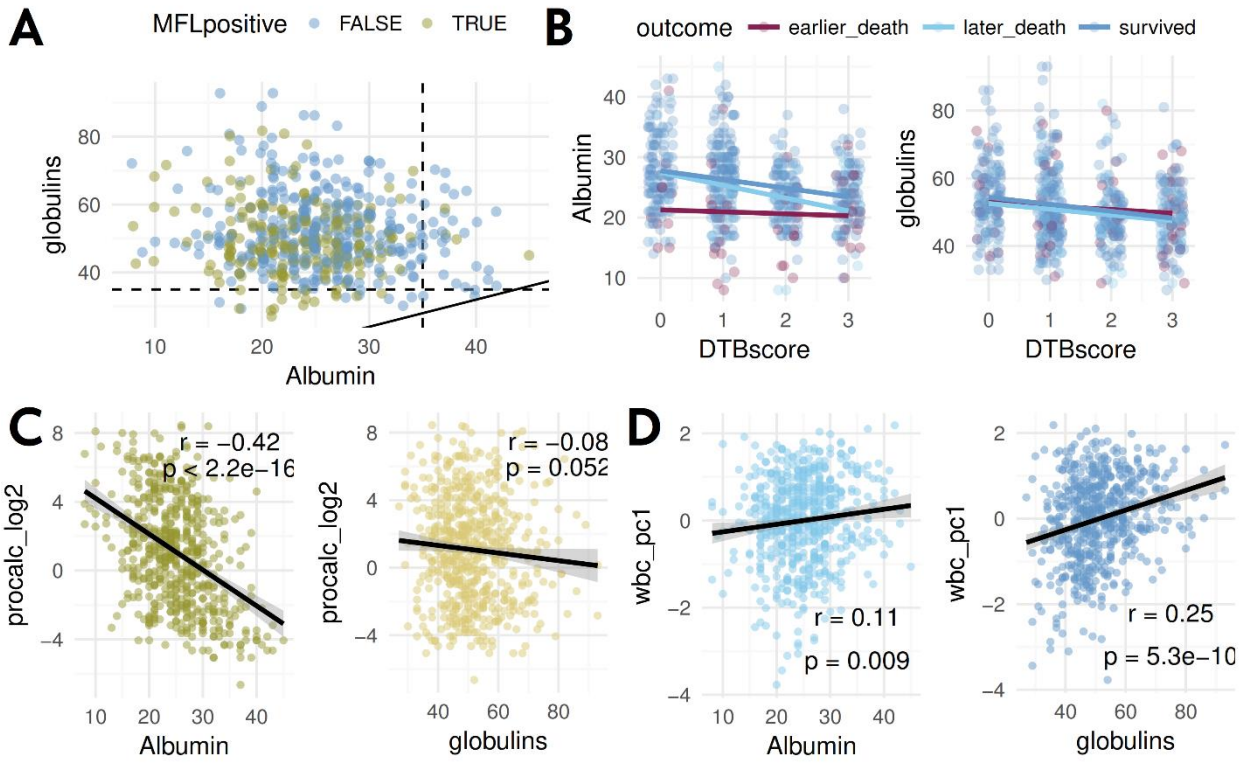

Figure 1-36. Albumin and globulins by outcome and MTBBSI.

A. Albumin versus globulin scatter plot with patient data points coloured by TB blood culture status (MFLpositive = positive TB blood culture). Lower limit of normal for albumin (35g/L) and upper limit of normal for globulins (35g/L) indicated by vertical and horizontal dashed lines respectively. The solid black line indicates albumin globulin ratio of 0.8 – all patients are to the left of this line i.e. ratio < 0.8. **B**. Albumin and globulin distributions by DTB score, with line of best fit by outcome status. Earlier death = death before day 14 follow-up; later death = death between days 14 and 84; survived = survived to end follow-up. C. Albumin and globulins linear relationship to procalcitonin. D. Albumin and globulins linear relationship to WBC principal component 1 (detailed in figure 33).

1.7.6 Physiological sepsis response

494/596 (83%) patients had ≥2 SIRS criteria,[241] 114/596 (19%) had ≥1 qSOFA criteria,[242,243] and 196/596 (33%) had SOFA[242,243] score ≥2 (when calculated without PaO2/FiO2 variable - which was not part of KDHTB protocol - and without data on inotropes/vasopressors, which were rarely used in this setting). Agreement between these "sepsis scores" is only marginally better than chance (figure 37). However, SIRS criteria were proposed to identify "sepsis syndrome" (a now defunct term), whereas qSOFA and SOFA are intended to identify organ dysfunction in high mortality risk patients. The lack of agreement between qSOFA and SOFA is largely the result of only the later including renal dysfunction, which is the most common observed organ dysfunction in this cohort.

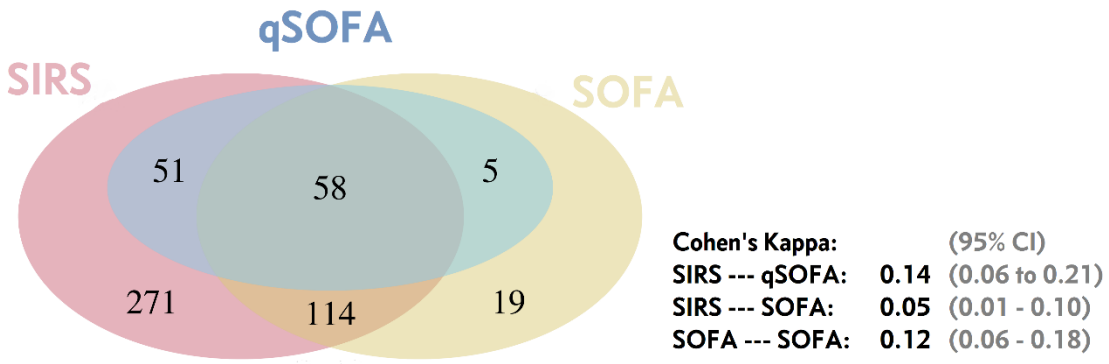

Figure 1-37. SIRS, qSOFA, SOFA Venn diagram

Numbers indicate those with 'positive' scores (e.g. 58 are positive on all three Sepsis scores).

Both SOFA and qSOFA score patients on mean arterial pressure (MAP, calculated here as [2*diastolic blood pressure + systolic pressure)/3]). 102/596 patients have MAP<70mmHg in this cohort, but as seen in table 8, blood pressure has no relationship with mortality. Systolic and diastolic pressure cluster remotely from all other clinical variables (figure 15 & 16); in particular they have no correlation with lactate (r = -0.03; 95%CI -0.12 to 0.05; p=0.378). Again, covariance in physiological sepsis variables (MAP, lactate, heart rate, respiratory rate and temperature) can be parsimoniously represented with PCA (figure 39).

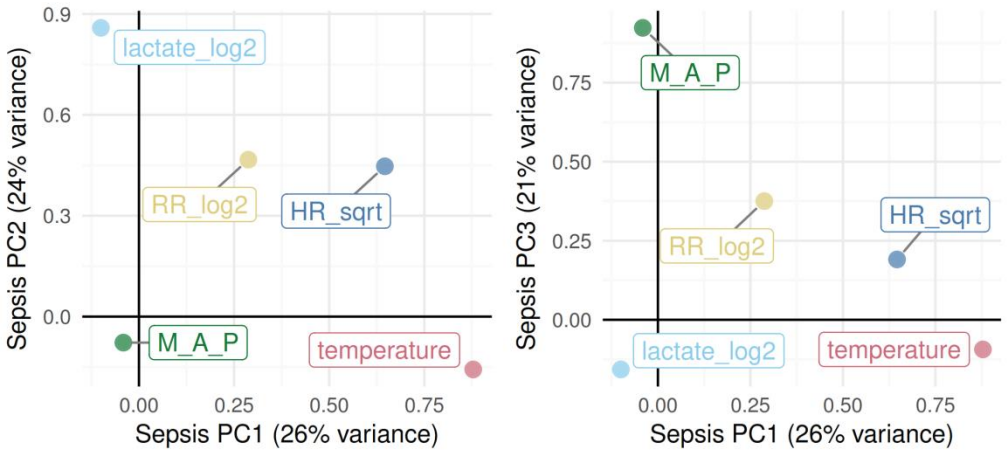

Figure 1-38. Correlation of variables traditionally associated with sepsis with their first 3 PCs (varimax rotation).

M_A_P = mean arterial pressure.

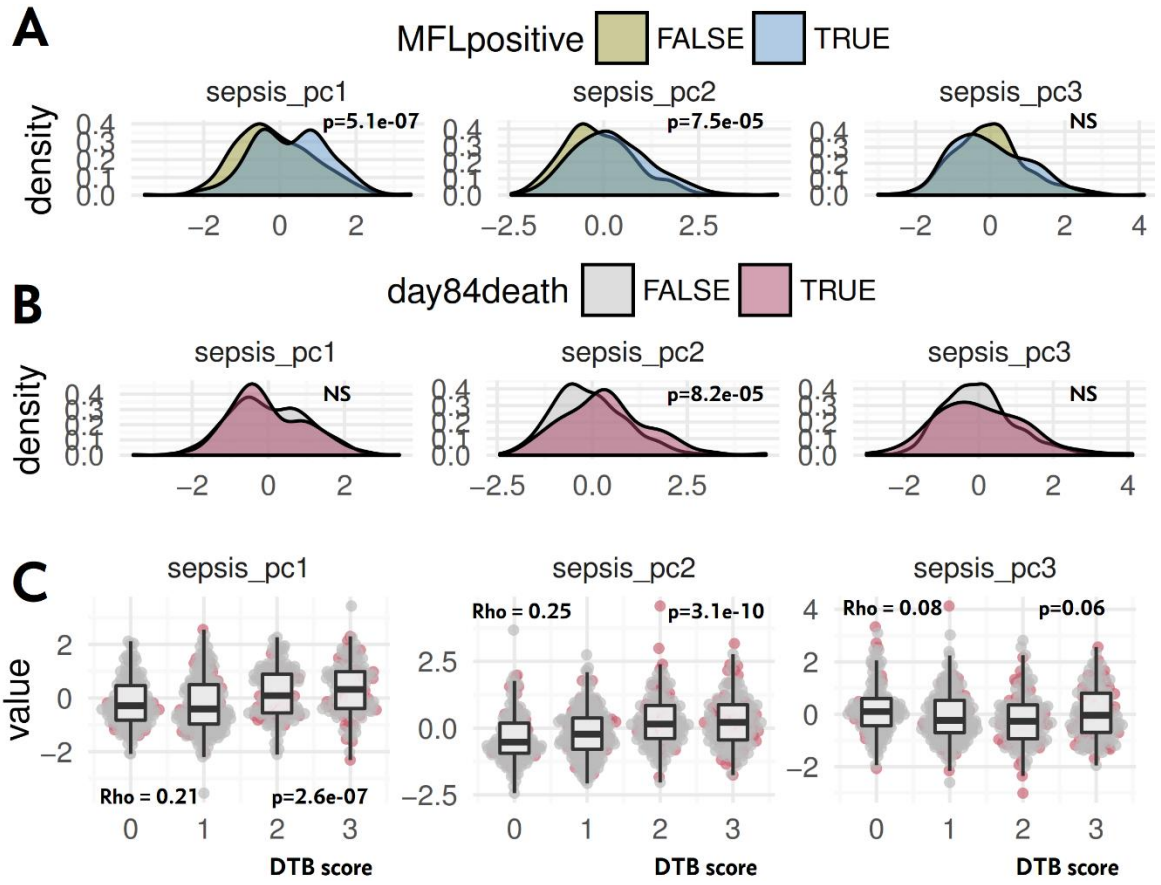

Figure 1-39. 'Sepsis' variables PCs association with MTBBSI and mortality.

A. Density distributions of the first 3 'sepsis' PCs disaggregated by TB blood culture status (MFLpositive), **B**. day 84 outcome status, and **C**. DTB score. P values in A&B are from t-tests, NS = non-significant (p>0.1).

This shows 3 major axes of variation, with temperature (PC1), lactate (PC2) and MAP (PC3) being largely independent. Respiratory and heart rate have some covariance with all three components, but note that weak correlation between these variables and PC3 (ie MAP) is *positive* – there is no tachycardia /hypotension signal here. As would be expected from the univariate analyses, PC3 has no detectable relationship to MTBBSI or mortality (figure 39 B & C). PC2 – a febrile response capturing temperature, with associated raised heart and respiratory rate – is related to MTBBSI but not to higher mortality (reiterating the analysis in the preceding section on fever). By contrast, PC2 – raised lactate with associated raised heart and respiratory rate – is firmly related to MTBBSI and mortality.

In short, there is no evidence that traditionally defined septic shock is an important feature in the KDHTB study, while raised venous lactate – independent of any strong indication of haemodynamic compromise – is strongly related to MTBBSI and mortality. It is possible that blood pressure was an insensitive measure of tissue hypo-perfusion in this cohort, or that frank hypotension only developed after recruitment in patients that died. However, irrespective of the time cut-off used to define early death, MAP remains unrelated to mortality (data not shown), and it is hard to square the complete absence of a signal at time of acute admission with a causal relationship between hypotension and adverse outcome, particularly when lactic acidosis was already manifest in so many patients. Rather, it suggests at a minimum, that lactate and hypotension are largely on different causal pathways in this cohort.

In recent years a range of data has called into question the traditional model of hyperlactataemia representing anaerobic respiration in hypoxic, hypoperfused tissues ("oxygen debt"). Endotoxin induces hyperlactataemia in healthy volunteers, with associated increased resting energy expenditure, and glucose and lactate production, in the absence of tissue hypoxia.[244] Muscle and other tissue biopsies in patients with sepsis show supernormal tissue PO2, with highest levels seen in patients with more severe sepsis.[245,246] Based on these and other findings, alternative or additional sources of hyperlactataemia in sepsis have been proposed, including *accelerated aerobic glycolysis* from sepsis-induced inflammation. The theory is that increased energy demand from inflammation exceeds the oxidative phosphorylation capacity of mitochondria, with consequent build-up of pyruvate, which drives lactate production by mass-effect.[247] This metabolic effect is likely to be predominantly in cells of the immune system, which are highly energy dependent when activated: for example, M1 (but not M2) macrophages increase glucose consumption and release lactate.[248] This metabolic shift

seems to be necessary for subsequent inflammatory cytokine response – an upstream metabolic step in the biochemistry of inflammation, not a downstream metabolic consequence of inflammation.[249] In turn, at least in cell cultures, pro-inflammatory cytokines induce glucose uptake and glycolysis, but *not* oxidation of glucose by the Kreb's cycle.[250] In severe sepsis, isotope dilution studies show increased turnover of glucose and lactate.[247] In short, aerobic glycolysis is an inefficient but rapid (and adaptive) means to meet exceptional need for ATP in inflammatory immune cells.[251]

Further, recent data links this metabolic shift directly to the host-response to *M. tuberculosis*. Human alveolar and monocyte derived macrophages switch from oxidative phosphorylation to aerobic glycolysis when infected *ex vivo* with *M. tuberculosis*, increasing lactate production; inhibition of this shift decreases IL-1β and increases IL-10 production, and impairs killing of bacilli.[252] This finding has been corroborated *in vivo*: glycolysis pathway gene expression is upregulated in human tuberculin skin test challenge model experiments, and in clinical samples from sites of TB disease.[253]

The KDHTB results support upregulated aerobic glycolysis from sepsis-induced inflammation as the main driver of hyperlactataemia in severe HIV-associated tuberculosis. In addition to the absent association with MAP, lactate (and sepsis PC2) positively correlate with markers of inflammation and with glucose (figure 40).

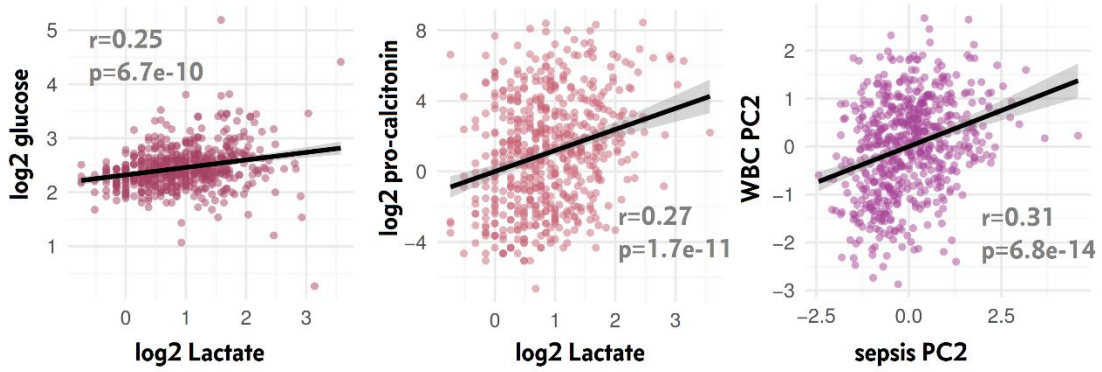

Figure 1-40. Lactate, and sepsis principal component 2, correlate with glucose and inflammation markers.

Sepsis PC2 is a composite variable mostly representing lactate, but also some covariance of respiratory and heart rate. WBC PC2 is a composite variable combining several markers of inflammation. Black lines show linear model with 95%CI in shaded area.

Given that age is not strongly related to lactate (or inflammation) – see figure 15 – what is the relationship between age, lactate and glucose? The effect of age on glucose can be shown to be largely mediated via an interaction effect on the relationship between lactate and glucose – in a linear regression model the main effect of age is non-significant, but the interaction effect with lactate is strongly related to glucose, i.e. a cross-over effect (figure 41). The parsimonious explanation is: inflammation / stress response induces metabolic shift to gluconeogenesis / oxidative glycolysis, causing increased lactate and glucose production. The extent to which increased glucose production results in venous hyperglycaemia then depends on degree of insulin resistance. Glucose tolerance / insulin sensitivity – in addition to being worsened by sepsis[254,255] – is inversely and *linearly* related to age across the range 18 to 80 years, independent of BMI and VO_2 max: 40-year olds have more insulin resistance than 30-year olds.[256,257]

A

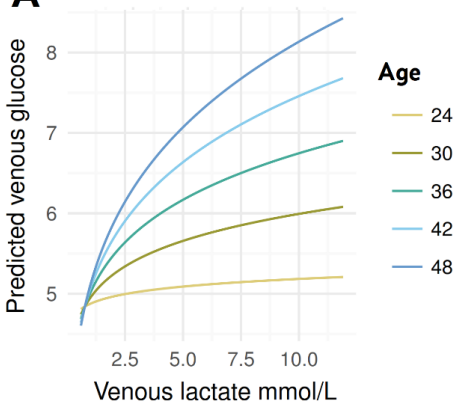

B

Parameter	Estimate	95%CI	p-value
Log2 lactate	-0.78	-1.34 to -0.18	0.011
Log2 age in years	0.07	-0.06 to 0.20	0.321
Interaction term: log2(age)*log2(lactate)	0.18	0.06 to 0.29	0.003
Model fit:	Adjusted R2 = 0.12 F-statistic 26.7 on 592 DF, p=3.3e-16		

Figure 1-41. Regression model predicting venous glucose from independent variables lactate and age.

The model form is $log2(glucose) = intercept + \beta_1 * log2(lactate) + \beta_2 * log2(age) + \beta_3 * log2(lactate) * log2(age) + \varepsilon$. Predicted values for glucose are shown across the empirical range of lactate and for 5 representative ages, converted to original scale for ease of interpretation (**A**). β estimates and their precision, with indices of model fit are shown in **B**. Addition of inflammatory markers (e.g. WBC PC2) to the model did not improve fit (p0.158 by nested model Likelihood Ratio Test), and residuals from the model (unexplained variance in glucose, ε) were not strongly related with any other variables in the dataset.

1.7.7 Thrombocytopenia

Platelet count is a complex variable, related to multiple pathogenesis mechanisms in both HIV and tuberculosis.[258] For example, in PLWHIV suffering from immune thrombocytopenia (ITP), a high proportion may additionally have a low immature platelet fraction, suggesting inappropriately suppressed megakaryocyte activity.[259] Tuberculosis is classically associated with a reactive thrombocytosis, reduced platelet survival time, and increased platelet clumping.[260] TB thrombocytosis correlates with ESR,[260] and bacilli burden in sputum[261] and within granulomas.[262] Conversely, thrombocytopenia can result from ITP caused by tuberculosis,[69,263] pancytopenia associated with bone marrow TB,[264] adverse reaction to rifampicin,[265] and disseminated intravascular coagulation,[266] especially in HIV-associated TB.[267] In the KDTH dataset, platelet count is higher with more preserved immune-status (r = 0.27, p=1.1e-11, for WBC PC1), lower with advanced inflammation (r = -0.14, p=2.5e-04, for WBC PC 2), and correlates with total white cell count independently of CD4 count (r = 0.42, p<2.2e-16, for WBC PC3). Since all these axes are largely independent, platelet count should be considered a net effect of multiple concomitant processes. HIV viral load also relates to platelet count independently of CD4 count (table 12).

Table 1-12. Multivariate linear regression predicting platelets_sqrt.

Variable	Estimate	95%CI	p-value
WBC PC1, per 1 s.d. (immune-status composite)	1.06	0.76 to 1.36	1.2e-11
WBC PC2, per 1 s.d. (inflammation composite)	-0.63	-0.93 to -0.34	2.8e-05
WBC PC3, per 1 s.d. (total white cell count surrogate)	1.84	1.55 to 2.14	<2e-16
HIV viral load, per log	-0.47	-0.66 to -0.27	2.9e-06
Model fit:	F-statistic: 63.32 on 4 & 591 DF, p < 2.2e-16 Adjusted R2 = 0.30		

Model form: √platelets = WBC_PC1 + WBC_PC2 + WBC_PC3 + log(HIV viral load), so estimates relate to a one unit increase in platelets after 0.5 power transformation.
s.d. = standard deviation.

This complicates interpretation of the association between MTBBSI and thrombocytopenia (Rho = -0.28, p= 7.7e-12, for DTB score) – is it causal, or from confounding by worse immune status? To help attribute causality, any serial measures of platelets during admission (performed as part of routine care, i.e. non-systematically) were extracted for 50 patients

selected at random from the KDHTB cohort.[††††] 12/50 had platelet count < 150 on day of study recruitment; 43/50 had platelet counts from more than one time-point. 30/43 had an average downward trend in platelet count during admission (based on line of best fit), and probability and magnitude of a downward trend was correlated with MTBBSI (figure 42). Again with a caveat from non-systematic ascertainment of serial measures, this supports a mechanistic link between MTBBSI and thrombocytopenia, within the complex causal web determining net platelet count.

We can hypothesise that the covariance of platelets with d-dimer might capture underlying pathophysiology relating to disseminated intravascular coagulation. A single principal component PCA (varimax rotation) captures 60% of variation in both variables. In turn this PC is associated with day 84 death (mean value in survivors = 0.11; mean value in those that died -0.40; p = 8.6e-07 by t-test) and with DTB score (Rho -0.39; p<2.2e-16).

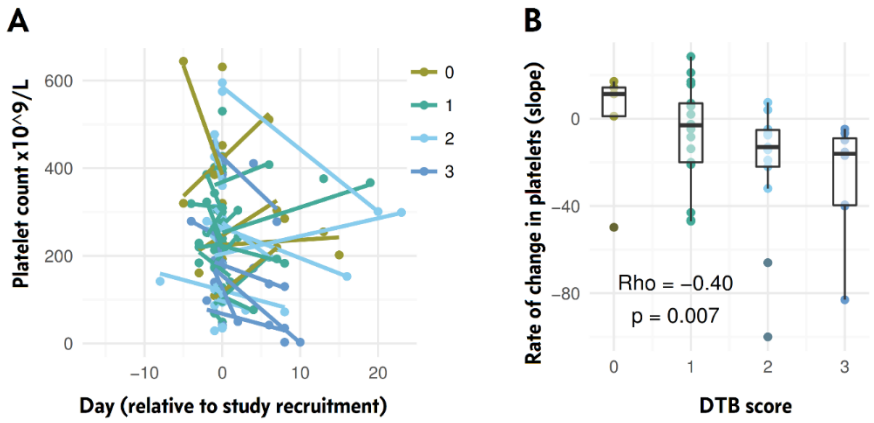

Figure 1-42. Trend in platelet count during admission in 43 patients from KDHTB cohort.

A. Line of best fit showing average trend in platelet count for patients with more than one full blood count performed during admission when study recruitment took place. Each line represents a single patient, and colour indicates DTB count of this patient on day 0 (day of recruitment). **B**. Gradient (slope) of line of best fit is extracted (using lmList() function in lme4 package of R) and plotted against DTB score. Overlaid boxplots show median, IQR, range, indicated by line, box, whiskers respectively).

[††††] The same 50 patients referred to in the serial sodium measure analysis above.

1.8 Structural equation model of core variables relationship to disseminated TB and mortality.

After the preceding supervised dimension reduction, there is a core set of (mostly constructed) variables which relate to both MTBBSI and mortality. A reminder of these variables and their proposed description is given in table 14. Covariance in these variables is shown in figure 43; a summary of their relationship to mortality and DTB score is shown in table 15.

A hypothesised structural relationship underlying these covariances is shown in figure 44. This structural equation model (SEM) attempts to reproduce the covariance matrix in figure 43A and table 15, i.e. to provide a simple explanation of the phenomena consistent with these observations. It models disseminated TB (DTB) as an unobserved latent variable which in turn determines variation in the observed ('manifest') variables TB blood culture (MFL), uGXP and uLAM – i.e. that these markers are conditionally independent given the latent variable DTB. This deals with the measurement error related to each of these manifest variables: i.e. the correlation between manifest variables is assumed to be an under-estimate of the true correlation between the latent variable and other variables in the model.

What does the SEM show? It implies that the effect of immunosuppression (wbc_pc1) on mortality in KDHTB is mediated through DTB, which in turn mediates its effects through physiological effects (sepsis_pc2 – hyperlactataemia), inflammation (wbc_pc2), and metabolic disturbance associated with renal dysfunction (metab_pc1). This is shown by the lack of significant direct effects of these upstream variables (arrows not passing through the mediating variables). Age and wbc_pc3 (the WBC PC dominated by total white cell count) by contrast have direct effects, independent of these other variables. Substantial collinearity remains between the mediating variables (sepsis_pc2, wbc_pc2, metab_pc1) suggesting they are not truly independent mechanisms.

A variety of metrics of model fit suggest this SEM is reasonably consistent with the data.[‡‡‡‡] But this model also has a number of profound limitations. Firstly, the choice of mediating variables is fairly arbitrary; replacing them with other markers (for example, haemoglobin, D-dimer-platelets covariance, albumin) makes very little difference to the model fit. Combining all these mediators inflates the standard errors in the regression rendering most non-significant. We don't really know enough about the pathways connecting these mediators to each other, and don't have unique enough assays of the pathophysiology they represent, to resolve this further. At some level, all this model says is that sick patients have worse outcomes. Secondly, the SEM assumes a static system (e.g. without feedback loops); this is theoretically implausible. Third, although the individual pathways are found to be highly significant (i.e. the z-scores of individual parameters are strong), when the total variance in mortality explained is estimated by adding up the products of all the partial correlations on each pathway, the total is only ~24%.[§§§§] In sum, there are several important associations summarised in this model, but we are far from a complete understanding of the pathophysiology of HIV-associated MTBBSI.

Table 1-13. Core variables relating MTBBSI & mortality after supervised dimension reduction.

Variable	Description
wbc_pc1	Immune status. Greater immunosuppression = lower value.
wbc_pc2	Inflammation. Greater inflammation = higher value.
wbc_pc3	Covariance in WBC relating to total white cell count, independent of immunosuppression and inflammation.
LFTs_canalicular	Predominantly gamma-GT and alkaline phosphatase elevation in abnormal LFTs
metab_PC1	Metabolic acidosis predominantly associated with worse renal function
sepsis_pc2	Predominantly variance relating to hyperlactataemia
ddm_plt_pc	Covariance in platelet count and D-dimer
Sodium	Serum sodium on original measured scale
glucose_log2	Log2 transformed venous glucose
Albumin	Serum albumin as measured on original scale
Hb_sqrt	power 0.5 transformed haemoglobin level
age_log2	Log2 transformed age in years

[‡‡‡‡] There are over 60 metrics of SEM fit available in lavaan package alone, and no consensus in the literature about which to use. As an example, Goodness of Fit index (GFI) compares the model of interest to a model which allows all included variables to covary (no *a priori* structure), and therefore gives some indication of how much covariance is explained by the structure. GFI ranges between 0 and 1, with higher values indicating better fit. GFI for the model described here is 0.96.

[§§§§] For comparison, this is similar to pseudo-R2 values for logistic regression model using all the core variables and DTB score as predictors of day 84 death.

As another example, a SEM of acute kidney injury is presented in figure 45. The hypothesis that MTBBSI effect on AKI is mediated via more than one causal pathway is consistent with the covariance structure of the data. Several other variables independently relate to AKI, including age and sodium. Mean arterial pressure has a weak association with AKI, but the direction of partial correlation is positive, again emphasising that hypotension is not a major driver of AKI in this cohort. This model would likely be substantially improved by variables specific to ECFV and cytotoxic renal cell injury (such as urine biomarkers).

Table 1-14. Summary of core variable association with DTB score and mortality outcome; medians by grouping variables and test of significance.

	DTB score					Day 84 death			Death early v later v survived			
	0 (N=144)	1 (N=196)	2 (N=129)	3 (N=127)	p value	No (N=469)	Yes (N=127)	p value	early (N=65)	later (N=73)	survived (N=458)	p value
wbc_pc1	0.66	0.19	-0.29	-0.46	< 0.001	0.14	-0.22	< 0.001	-0.23	-0.17	0.17	< 0.001
wbc_pc2	-0.42	-0.18	0.21	0.54	< 0.001	-0.04	0.51	< 0.001	0.9	0.21	-0.05	< 0.001
wbc_pc3	-0.04	0.06	-0.06	0.08	0.871	0.08	-0.19	0.009	-0.31	-0.04	0.08	< 0.001
LFTs_canalicular	-0.36	-0.1	0.04	0.16	< 0.001	-0.14	0.24	< 0.001	0.25	0.28	-0.16	< 0.001
metab_PC1	-0.48	-0.32	0.07	0.26	< 0.001	-0.24	0.22	< 0.001	0.21	0.26	-0.25	< 0.001
sepsis_pc2	-0.52	-0.22	0.15	0.22	< 0.001	-0.21	0.32	< 0.001	0.43	0.03	-0.2	< 0.001
ddm_plt_pc	0.5	0.37	-0.22	-0.48	< 0.001	0.21	-0.43	< 0.001	-0.24	-0.42	0.22	< 0.001
Sodium	130	129	127	128	< 0.001	129	128	0.124	127	129	129	0.062
glucose_log2	2.35	2.35	2.43	2.43	0.003	2.38	2.46	0.006	2.43	2.43	2.38	0.013
Albumin	27	26	23	23	< 0.001	25	22	< 0.001	21	23	25	< 0.001
Hb_sqrt	3.1	2.98	2.85	2.81	< 0.001	2.97	2.83	0.007	2.81	2.85	2.98	0.021
age_log2	5.25	5.14	5.18	5.14	0.099	5.14	5.31	< 0.001	5.38	5.28	5.14	< 0.001

Values are median for grouping level. Variables are described in previous sections and briefly again in table 14. P-values are from Kruskal-Wallis test across categories shown.

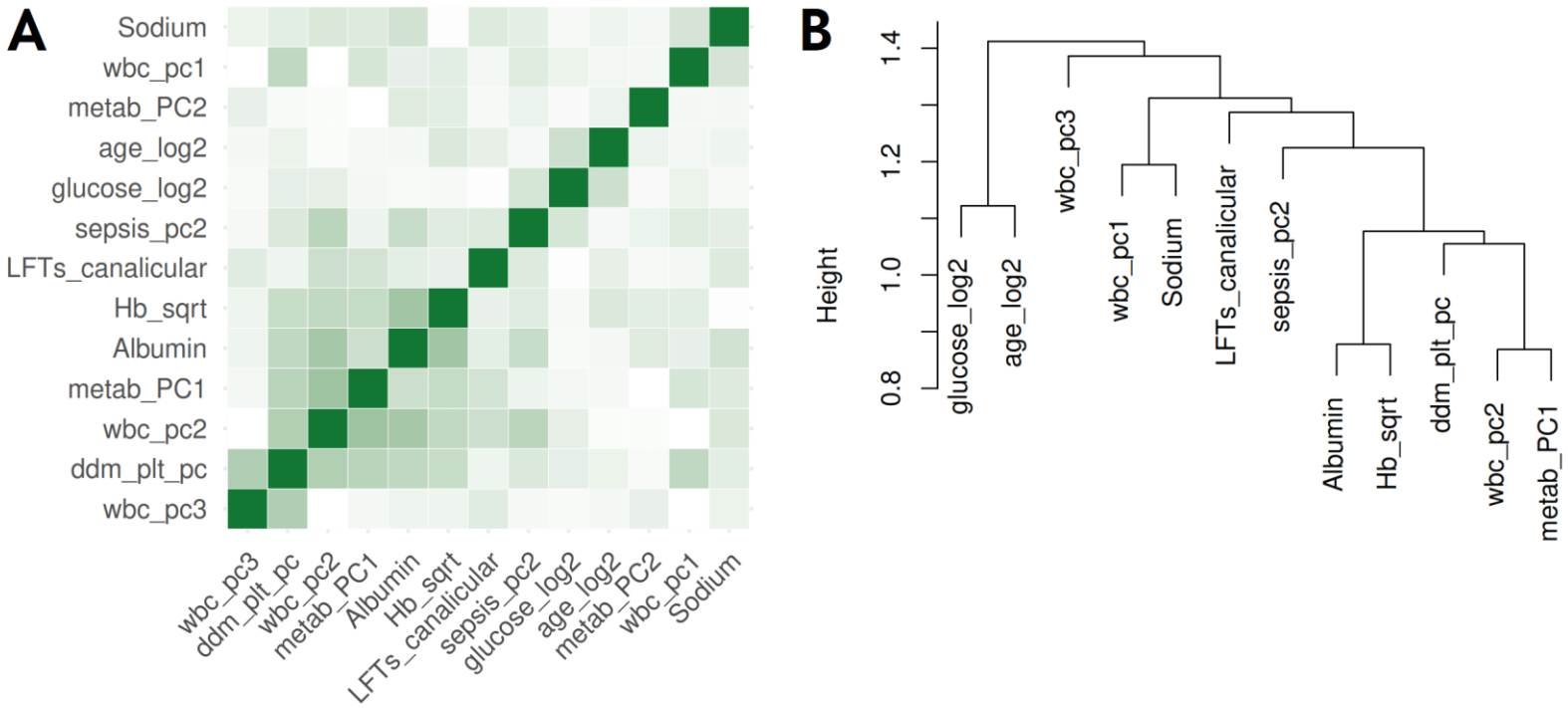

Figure 1-43. Covariance in core variables related to MTBBSI and mortality.

A. Correlation matrix in 13 core variables known to relate to mortality and MTBBSI. These variables are mostly constructed from supervised or semi-supervised dimension reduction described in preceding sections, and a brief description of each is given in table 14. Depth of green colour indicates magnitude of absolute value of Pearson's correlation coefficient. Variables are ordered based on a hierarchical clustering algorithm (complete linkage used to define distance between clusters). **B**. A complimentary clustering of the variables using average linking to test stability of the clustering solution to method.

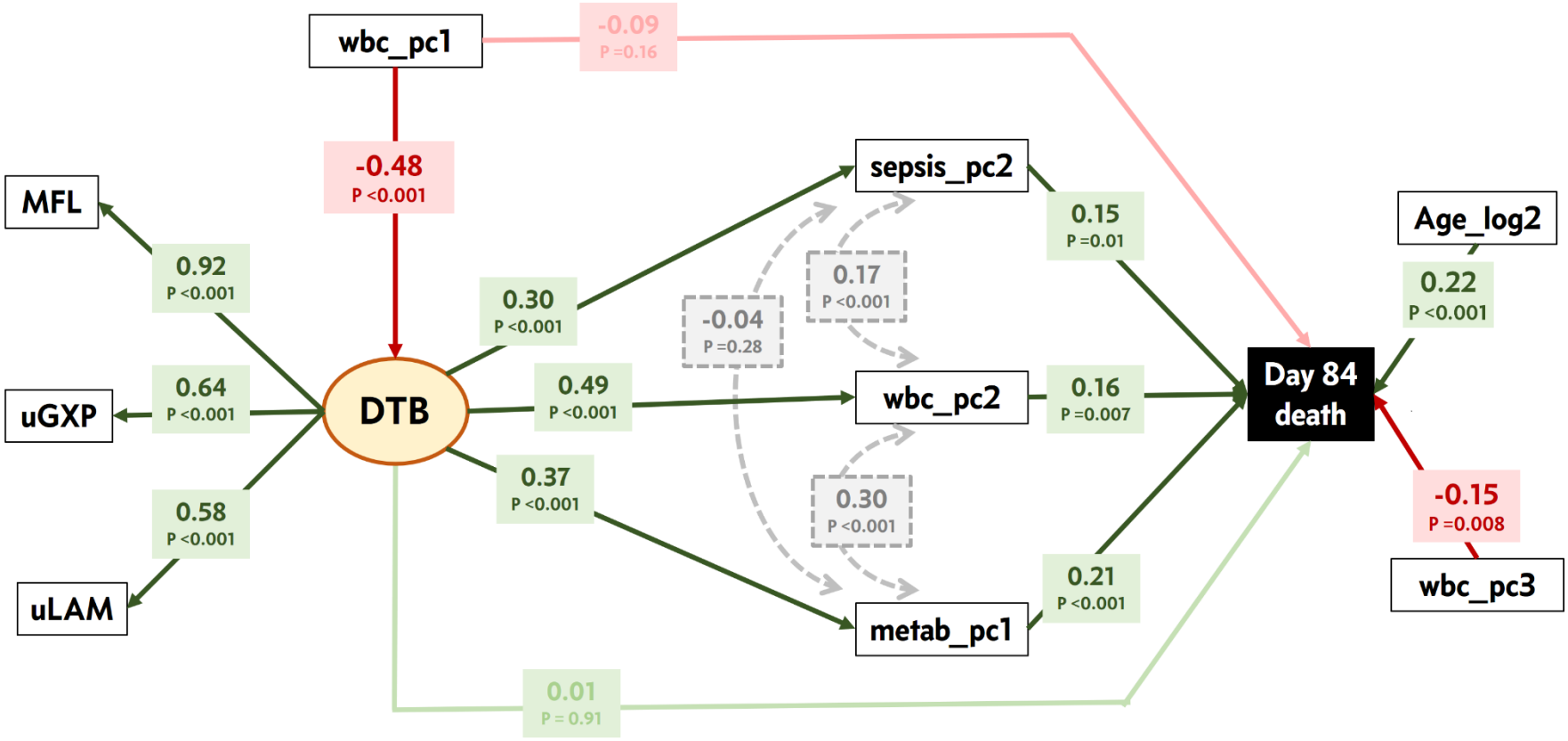

Figure 1-44. Structural equation model relating selected core variables to disseminated TB and mortality outcome.

The model was generated in lavaan package of R. DTB is modelled as a latent, unobserved, variable which causes observed variance in TB blood culture positivity (MFL), uGXP and uLAM value. Single headed arrows represent regressions; double ended curved arrows represent covariance out with the regression structure. Numbers in red/green boxes on arrow represent partial correlations – i.e. strength and direction of linear relationship between two variables after controlling for the effects of other variables in the regression structure – equivalent to a standardised regression coefficient. For example, residual variation in sepsis_pc2 after adjusting for wbc_pc1, wbc_pc2, wbc_pc3, metab_pc1, Age_log2, and DTB, has correlation coefficient 0.15 with day 84 death. Because death is a binary variable, these correlation coefficients are not Pearson's r (they are Maximum Likelihood estimates of correlations to normal distribution modelled to underlie the binary variable) but can be interpreted in the same way. Therefore, variance in death outcome explained by an individual variable in the model can be calculated by the product of all the coefficients in every path linking it to the outcome (including covariance arrows). Total variance explained is 24%.

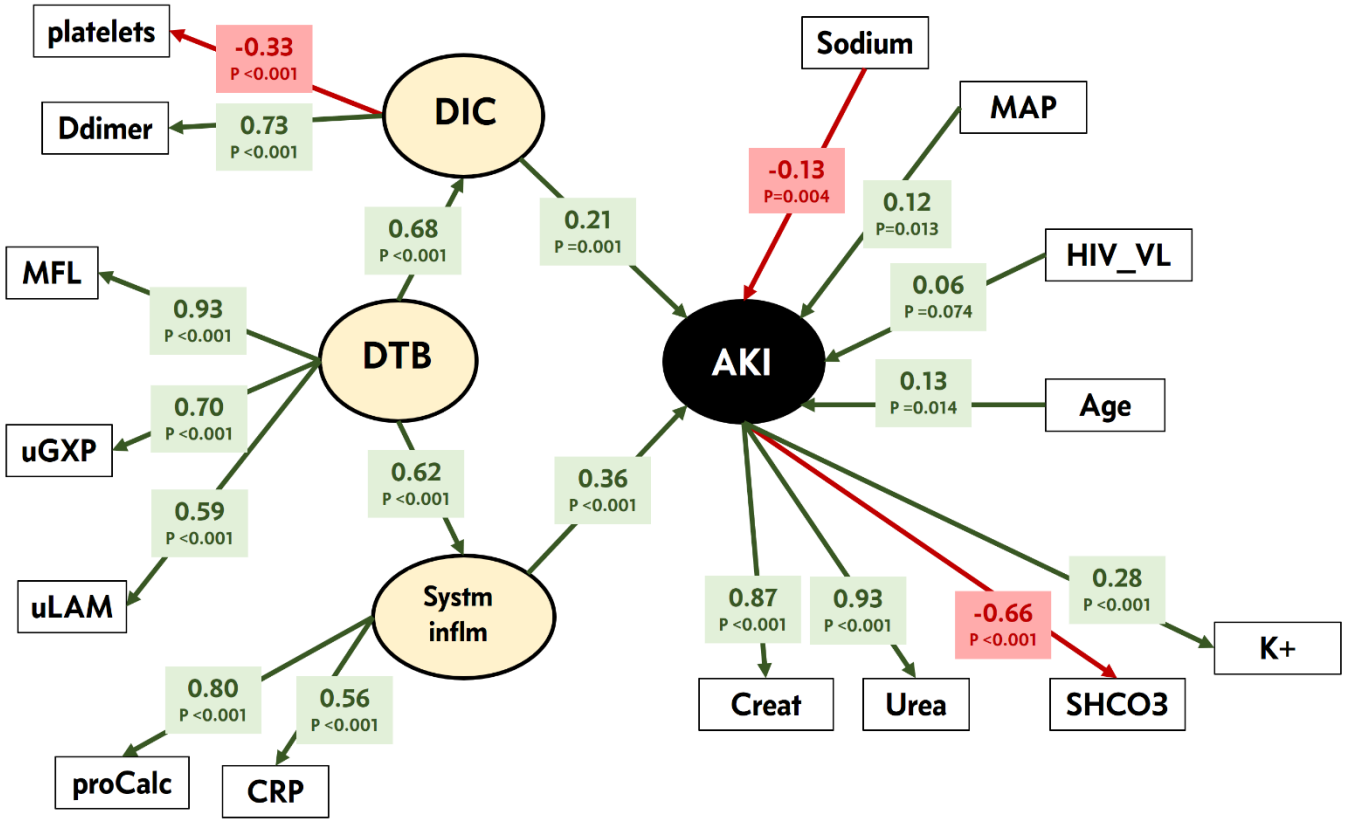

Figure 1-45. Acute Kidney Injury SEM.

DIC = latent variable represented by variance in manifest variables Ddimer and platelet count. DTB = latent variable represented by manifest variables MFL (TB blood culture), uLAM and uGXP. Systm inflm = latent variable represented by manifest variables procalcitonin and CRP. AKI = latent variable represented by manifest variables creatinine, urea, bicarbonate and potassium. HIV_VL = HIV viral load; MAP = mean arterial pressure. Overall SEMM fit is reasonable (GFI = 0.94) and 40% of variation in AK is explained by the regression pathways, indicated by partial correlations (standardised regression coefficients) in boxes.

1.9 Concluding discussion

This chapter began by showing that 'disseminated TB' is regarded as a vague diagnosis, while MTBBSI is largely ignored by HIV-associated TB guidelines and normative international classifications of tuberculosis. A different conceptualisation was offered. Active, ongoing blood stream and lymphatic dissemination is in fact the *mode* of severe HIV-associated TB. So-called "disseminated TB" in HIV is fundamentally a BSI; semantically, I would argue MTBBSI is a better description than disseminated TB, because all tuberculosis is disseminated to a greater-or-lesser extent. Blood culture is just one window on this process, but is bolstered by novel rapid diagnostics (uGXP and uLAM) to give a more complete picture of MTBBSI.

MTBBSI is not clinically vague. Gastro-intestinal symptoms combined with 'classic' TB presenting complaints, inability to walk unaided (high ECOG score), diffuse adenopathy, generalised infiltrate on chest x-ray, and splenic microabscesses all have positive likelihood ratios, while localised serositis and fibrotic changes have negative likelihood ratios for MTBBSI versus non-BSI HIV-associated TB. Immunosuppression, hyponatraemia, thrombocytopenia, anaemia, hyperlactataemia, acute kidney injury with metabolic acidosis, 'infiltrative' LFT derangement, disproportionate rise in AST, and systemic inflammation all correlate strongly with MTBBSI, but classical septic shock (hypotension, hyperpyrexia) does not. These signs suggest MTBBSI is pathophysiologically distinct, and that the term has convergent and discriminant validity. It also makes it a well-defined target for interventional trials.

All these features can be related to (semi) quantitative measures of MTBBSI (blood culture positivity and DTB score), which in turn can be related to immunosuppression, suggesting a single major axis of clinical variation in these patients. Many of the features may be adaptive (for example, pre-renal acute kidney injury, hyperlactatemia as a bioenergetic response, or anaemia if hepcidin is protective in the context of a massive and largely extracellular bacilli burden) in the face of non-resolving infection. The strong independent effect of age on

mortality may in fact be an interaction with this axis: less physiological reserve to accommodate the host-response to severe disease.

This might imply that the most obvious place to target interventions is on faster bacilli-killing and restoration of adaptive immunity, because downstream (host-response) effects of these abnormalities are complex and incompletely understood. For example, what fluid resuscitation should be recommended for these patients? Although AKI and hyperlactaemia are prevalent, hypotension is not. Sodium and water status is far from normal. But what effect would rapid fluid resuscitation have in patients who have sub-acute ECFV depletion? What if there is concurrent SIADH? Consumptive coagulopathy may be present in many of these patients – what effect would fluid dilution of clotting factors have? A recent RCT testing a 'bundle of care' intervention, including aggressive fluid resuscitation, in adult inpatients with hypotensive sepsis from Lusaka reported a 22% absolute increase in 28-day mortality in the intervention arm.[268] The trial population was predominantly patients with HIV-associated MTBBSI (21% TB blood culture positive, 11% other bacterial pathogen on blood culture; 90% HIV prevalence, median CD4 66 cells/ml, 63% clinical diagnosis of tuberculosis), median creatinine above normal range and near universal anaemia. The current analysis suggests several pathways by which fluid boluses could cause harm and suggests that any fluid administration should be cautious and individualised. Better characterisation is indicated before further interventional trials.

Sepsis is currently defined as organ dysfunction caused by an "aberrant or dysregulated host-response" to infection.[243] I would argue that to the extent that host-responses such as inflammation are proportionate to infection burden (like DTB score) it is anomalous to see them as aberrant or dysregulated. In this cohort, bacilli burden (as far as we can accurately measure it) doesn't explain *all* variance in, for example, inflammation (as measured by markers like pro-calcitonin), but the covariance is substantial, and improved by measurement error minimising techniques like PCA and SEM. A constructive takeaway conclusion would be that measures of pathogen burden could improve interpretability of sepsis studies more widely than MTBBSI.

Detection and quantification of mycobacteria are a major theme of the rest of this thesis, starting with prediction of TB blood culture status using 'baseline' clinical variables in the next chapter.

2 Predicting TB blood culture results

2.1 Introduction

The previous chapter described multiple clinical variables associated with MTBBSI, and made the inference that MTBBSI defined the major underlying axes of variation in severe HIV-associated tuberculosis. In short, plotting KDHTB patients on a spectrum of MTBBSI – represented by a 'disseminated TB score' – could *explain* a large amount of variation in clinical variables such as inflammation markers and mortality outcome. Such explanations are a way to grapple with complexity; a useful framework to generate, attach, and test knowledge.[269] But often of more interest in the real world is the use of data to *predict* future events. If it is true that MTBBSI is strongly related to clinical variance in HIV-associated TB patients, and – as argued previously – MTBBSI is ripe for positive empirical diagnosis, then it should be possible to predict which patients have MTBBSI using surrogate clinical variables. The prediction approach is complimentary, but different, to the preceding analysis. Inferences require prior theory about causal structure; predictions can be completely agnostic about mechanism.

This chapter is about development and validation of algorithms to predict TB blood culture status using clinical variables available on day of admission to hospital. Data from the first half of the KDHTB study were subjected to a variety of machine learning methods, and selected models were wrapped into a web-based 'app' for use at patients' bedside via smart 'phone. This allowed prospective validations to be carried out during the second half of KDHTB recruitment.

In addition to showing that MTBBSI (here defined as blood culture positivity) can be accurately predicted in hospitalised PLWHIV using basic clinical observations, this work had the practical application of enriching recruitment to sub-studies described here and in subsequent chapters.

2.2 Predictions & clinical decision rules in medicine

Prediction is central to clinical practice. Diagnosis, prognosis, and treatment decisions are all predictions. Use of algorithms to support practice is as old as clinical medicine, but the last 50 years has seen the rise of "clinical decision rules" (CDRs, also called clinical prediction rules, risk scores etc.).[270] Over time the methods used in development of CDRs has evolved. Early examples relied on expert opinion (e.g. SIRS criteria,[271] Glasgow Coma Scale[272], APACHE-II[273]) or combinations of risk-factors identified through strength of univariate associations (e.g. the Glasgow-Imrie Pancreatitis score[274]).

Two decades ago multivariate logistic regression became the norm for developing CDRs, archetypal examples including the Framingham cardiovascular risk calculator,[275] CURB-65 score for pneumonia,[276] FRAX osteoporotic fracture risk score,[277] and the Model for End-Stage Liver Disease[278]. To avoid the requirement for clinicians doing matrix algebra at the bedside, multivariate models are represented by normographs, converted to scores (variable reference ranges are categorised and category midpoints mapped to a points score based on non-arbitrary weights derived from the regression model parameters[279]), or accessed via the web.

More recently, a plethora of computationally intensive methods have been brought to CDR development – such as decision trees and neural networks.[280,281] Rather than resting on sophisticated 'parametric' statistical theory, these 'machine learning' methods use the brute-force of iteration made possible by the greater availability of high-speed computer processing. Typically, these 'black-box' methods don't offer easy summaries of how variables are being translated into predictions – there is no normograph or score to tot-up, so they can only be used with access to a computer (e.g. online). Despite an explosion of publications

reporting machine learning in medicine, it is still hard to find any examples that have been broadly applied in routine practice.

It is often stated that multivariate approaches are an advance on expert opinion or univariate methods, because, in the former, dependence between predictors is accounted for, and weighting for scores is non-arbitrary.[282] Similarly, the purported advantage of iterative models over logistic regression is they can include complex, non-linear relationships between variables.[281,282] This somewhat misses the point. Consider, for example, that scores based on expert opinion can – and do – include non-linearity (for instance, abnormally high or low temperature and white cell count score in SIRS criteria). Fundamentally, all that matters is predictive accuracy.

It is useful to think of predictive accuracy in terms of bias versus variance trade-off.[283-285] Any model can be made more complicated. Variance error is the extent to which the parameters of a model would change if we estimated them with a different data set.[283] Bias error is the extent to which the form of the model fails to capture the complexity of real life.[283] In general, a more flexible model will reduce bias but increase variance.[284,285] For example, fitting a linear function to a non-linear relationship will cause bias in predictions, but the slope and intercept of the model are unlikely to vary if re-estimated with a different data set. By contrast, if the 'real' relationship is substantively linear, a more flexible non-linear model is likely to be *overfitted*; its parameters would vary if re-estimated with another data set containing randomly different noise. Increasing model flexibility will have diminishing returns for reducing bias, while decreasing model flexibility will have diminishing returns for reducing variance. The optimal trade-off in appeasing these two error sources depends on what the true relationship between variables is in the real world (which we don't know), and on the quality and quantity of data available to the modelling exercise (a small number of noisy observations equates to greater variance so a less flexible model will perform better, even if this model is highly biased).

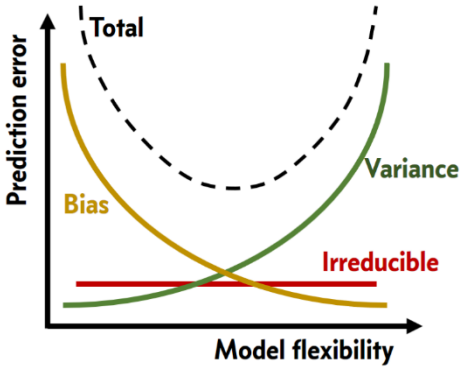

Figure 2-1. Sources of error in prediction schematic.

Total error is the sum of severally logically distinct errors. Variance – bias trade-off is described in main text. Irreducible error is unmeasured or unmeasurable factors which impact on outcome.

While novel modelling techniques allow examination of a much wider range of variance-bias trade-off points, the real power of machine learning comes from better ability to observe where that trade-off is best and 'tune' models using 'training' data to this optimum. Historical CDR development has relied on validation in new cohorts, which is expensive and inefficient: it requires a lot of data. The more data that is "spent" on validation cohorts, the less available for model development. Recall that small samples, with less power to distinguish signal from noise i.e. more variance, will select for a less flexible model, pushing the optimal trade-off towards more bias. Over-reliance on validation sets, at the expense of the sample size of the derivation cohort, might therefore increase bias.[283,286]

Resampling methods can make much more efficient use of data available at time of model development, and are the engine that runs most machine learning approaches.

2.3 Resampling methods & model tuning

Re-fitting a model from repeated subsets of available data (resampling) can generate information about the model. Resampling gives an estimate (and confidence interval) for out-of-sample model performance. In addition, the effect

of increasing or decreasing model complexity can be assessed (model 'tuning' and selection) to optimise variance-bias trade-off. [283,285,286]

k-fold cross validation is the resampling method used in the analysis described in this chapter. Observations in the dataset are divided into *k* subsets (folds) with approximately equal numbers of patients. Each fold is treated as the validation set in *k* repeated fittings of a model, giving *k* estimates of model predictive error, for which the mean and standard deviation can be calculated. [287]

The degree of flexibility in any model can be controlled, often by adjusting a single parameter. An example for linear regression would be increasing the number of function terms, from a simple linear regression to a polynomial regression. By comparing the k-fold cross-validation estimate of model performance across a range of values of this parameter (e.g. different degrees of polynomial in a linear regression) the optimal model flexibility can be learned, and the model flexibility parameter 'tuned'.[288]

2.4 Published MTBBSI prediction models

In the previous chapter associations with TB blood culture status from previous studies were reviewed. Several of these studies refer to prediction of MTBBSI in reported study objectives.

Patients recruited to the Zambian Simplified Severe Sepsis Protocol (SSSP) trials 1 & 2 had routine TB blood culture performed as part of these trials.[268,289] Muchemwa *et al*. present an analysis of 201 patients from these trials who were HIV-infected, examining predictors of a positive TB blood culture.[124] Variables collected as part of the original trials were assessed for univariate association, those with $p<0.2$ were then entered into a multivariate logistic regression, and stepwise deselected. Odds ratios from a final model are presented, but no measure of predictive performance is reported, and no validation of results is shown.

This is true of the other 'predictor' studies as well,[57,125,126] with one exception. Jacob et al. developed a clinical score for prediction of *M. tuberculosis* bacteraemia in an n=368 cohort of HIV-infected adult in-patients with severe sepsis recruited

in Uganda.[127] Variables were chosen by univariate association at p<0.2 with positive TB blood culture, and further deselected in a backwards stepwise logistic regression model. Unlike the other studies, area under the receiver operating curve (ROC AUC) was reported for the final model. In addition, a prediction score was derived using the Framingham method.[279] The ROC AUC value was determined using 10 iterations of 10-fold cross validation (AUC = 0.82, range 0.61 to 0.91 in the resamples), although it does not appear that cross-validation was used to tune the logistic regression model. Variables included in the final model were sex, heart rate, CD4 count, current HAART use, fever symptom as chief complaint, haemoglobin, and sodium. This represents the best previous literature on MTBBSI prediction so was used to inform some of the current analysis as described below. The performance of the Jacob score was assessed in both the whole KDHTB cohort (i.e. including patients who were suspected of having TB but did not have a final diagnosis of TB) and the Jooste rapid TB diagnostics study (all HIV-infected patients admitted to medical wards irrespective of suspected or final diagnosis). The Jacob score had ROC AUC 0.76 (bootstrapped 95% CI 0.72 to 0.79) and 0.78 (bootstrapped 95% CI 0.70 to 0.86) in KDHTB and Jooste data, respectively.

2.5 Summary of predictive modelling strategy used in this chapter

2.5.1 Included data

Initial predictive modelling was performed in May 2016 when 348 patients had been recruited to KDHTB and captured on the study data base. Patients were included in the analysis if they met KDHTB inclusion criteria (CD4 count < 350 cells/mm^3) and if they had a valid baseline Myco/F lytic (MFL) tuberculosis blood culture result (defined as a positive or negative MFL on day of recruitment +/- 1 day, excluding contaminated samples). Patients who had a negative baseline MFL but were TB blood culture positive at another time point were excluded. 75% of the available data was selected for a training set by random stratified allocation so that an equal proportion of patients were MFL positive in training and test sets.

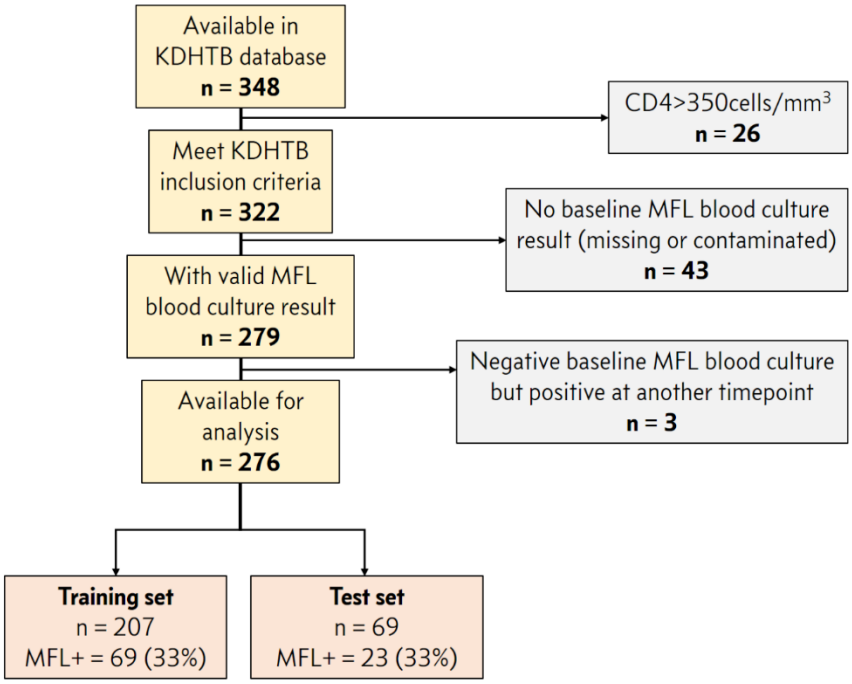

Figure 2-2. Consort diagram for May 2016 predictive modelling analysis.

MFL = Myco/F lytic TB blood culture.

2.5.2 Model types

Five model types were used, briefly described below.

2.5.2.1 Logistic regression

Generalised linear models based on the binomial probability distribution were constructed using the glm() function in R. *Method summary*: the conditional mean of the log odds ratio of the bacteraemia outcome (logit) is modelled as a linear function of the predictor variables weighted by parameters derived from maximum likelihood estimation.

2.5.2.2 Decision tree

Decision tree models were constructed using the recursive partitioning (rpart) package in R. *Method summary*: the rpart algorithm searches for a predictor variable which splits the individuals of the data set into two groups such that the homogenity (purity) of the outcome in the two groups is maximised. This is serially repeated in the 'daughter' groups until purity is not increased by further splits, or a maximum number of branches has been reached. To avoid over-fitting a 'complexity parameter', *cp*, is specified which penalises larger trees; *cp* can be optimised ('tuned') using cross-validation.

2.5.2.3 Random forest

Random forest models were produced using the randomForest package in R. *Method summary*: For a data set with N individuals (rows) and V predictor variables, a large number, K, of decision tree models are constructed as follows. To create tree k, a random sample of $n < N$ individuals is made (with replacement), with approximately 1/3 individuals held in reserve. At each node of tree k, $v < V$ predictors are randomly chosen for consideration as potential splitting variables. Predictions for new cases can be made by applying all K decision trees to the new case and counting the predicted outcomes ('votes') across all the trees. In addition, the accuracy of each tree is tracked by running the reserved cases down each decision tree to give an estimate of 'out-of-sample' error rate. The main parameter affecting random forest flexibility is the size of v, which can be 'tuned' using cross-validation.

2.5.2.4 Boosted tree

Boosted tree models were made using the gbm package in R. *Method summary*: Similar to random forest models, the boosted tree algorithm builds multiple decision trees and combines their predictions. However, unlike in the random forest method, each new tree is constructed using information from the previously constructed trees and is weighted to return more accurate predictions for cases misclassified in the previous trees. A modified version of the data set is used for each new tree. This is equivalent to running a new model to 'explain' the residuals from the previous model. The amount of 'explanation' that the new model is permitted to provide is an adjustable parameter (*lamda*, the 'shrinkage' or 'learning rate'). Other parameters include number of branches per tree, total number of trees, and maximum number of observations in each node of the tree; all can be optimised through cross validation.

2.5.2.5 Support vector machine

SVM models were implemented in R using the svmLinear2 function of the e1071 package. *Method summary*: For V predictor variables, individuals are located in $(V-1)$-dimensional space. The SVM algorithm finds the optimal separating hyperplane between the two classes by maximizing the margin between the classes' closest points using quadratic algebra. A cost parameter for misclassifying an individual, and a flexibility parameter determining the 'smoothing' in the hyperplane can be tuned using cross validation to reduce over-fitting.

2.5.3 Variable selection and dimension reduction

Feature selection for predictive modelling can, at one extreme, be completely based on domain knowledge (for example in development of CDRs based on expert opinion) or completely data driven and automated (such as in gene selection in microarray data)[290] or somewhere in between (such as the univariate testing of *a priori* variables and inclusion in final model based on an arbitrary p-value cut-off).

Selection of variables is important not just because it makes analysis more manageable and interpretable. Having a large number of variables reduces the effective sample size – as variables (or dimensions) are added the density of observations decreases quadratically in the space defined by those variables, increasing risk of overfitting and adversely shifting the dynamics of variance-bias trade-off (called "the curse of dimensionality").[291] In the machine learning literature, a distinction is made between *relevant* predictors (which are strongly associated with the outcome, but may be redundant when included with other variables) and *useful* predictors (which add predictive value despite a weaker univariate association, because they capture non-redundant information). The implication is that selecting only the most relevant variables may be suboptimal.[292] Consequently a number of alternative approaches to variable selection have been developed, several of which are adopted here.

All variables collected as part of the KDHTB study which were potentially available during the first 24 hours of admission were considered for use in the analysis. This included all clinical variables associated with TB blood culture status in previous literature. Variables with more than 20% missing observations (Body Mass Index) were excluded. Low information variables – those that showed near zero variation across the cohort, e.g. a categorical variable where nearly all observations were in one category – were identified using the nearZeroVar function of the Caret package in R and excluded (presence of central nervous system tuberculoma). This left 50 variables in the 'full variable set' (table 1). Variables were log transformed if this resulted in a more normal distribution (assessed with histograms and QQ plots).

Table 2-1. Full variable set considered for predictive modelling.

Variable	Description
Sex	
Age	
PreviousTB	History of previous (not current) TB diagnosis
Cough	Reported symptom present in study recruitment questionnaire
LossOfAppetite	Reported symptom present in study recruitment questionnaire
LossOfWeight	Reported symptom present in study recruitment questionnaire
DrenchingNightSweats	Reported symptom present in study recruitment questionnaire
Nausea.and.vomiting	Reported symptom present in study recruitment questionnaire
Diarrhea	Reported symptom present in study recruitment questionnaire
Headache	Reported symptom present in study recruitment questionnaire
BMI	Body mass index
BPSystolic	Systolic blood pressure
ECOG.Score	Eastern Cooperative Oncology Group functional performance score
GCS	Glasgow Coma Scale
BPDiastolic	Diastolic blood pressure
TempDegreesC	Recorded temperature
RR	Respiratory rate
HR	Heart rate
Lactate	Venous lactate
pH	Venous pH
SHCO3	Venous bicarbonate
BE	Venous base excess
Glucose	Venous glucose
Albumin	Serum albumin
AST	Serum aspartate transaminase
Sodium	Serum sodium
Potassium	Serum potassium
Haemoglobin	
MCV	Mean corpuscular volume
WhiteCellCount	Peripheral white cell count
Platelets	Platelet count
CD4Count	CD4 lymphocyte count
ART	Antiretroviral status (current, previous, naïve)
Any.signs.of.Tuberculosis..CXR	Chest X-ray finding as prospectively recorded on KDHTB recruitment proforma
Pulmonary.infiltrate	Chest X-ray finding as prospectively recorded on KDHTB recruitment proforma
Pleural.effusion	Chest X-ray finding as prospectively recorded on KDHTB recruitment proforma
Mediastinal.lymphnodes	Chest X-ray finding as prospectively recorded on KDHTB recruitment proforma

miliary	Chest X-ray finding mentioned in free text on KDHTB recruitment proforma
cavitary	Chest X-ray finding mentioned in free text on KDHTB recruitment proforma
nodular	Chest X-ray finding mentioned in free text on KDHTB recruitment proforma
CXR.sites	Number of lobes showing infiltrate on chest x-ray (prospectively recorded), range 0 – 5.
Tuberculoma	Central nervous system tuberculoma diagnosed
Pericardial	Pericardial effusion on chest x-ray or other imaging
Peripheral_LN	Peripheral adenopathy
Abdominal_LN	Abdominal adenopathy (on ultrasound scan)
Hepatic	Hepatic TB diagnosed
Splenic	Splenic TB diagnosed
TBM	TB meningitis diagnosed
Creatinine	Serum creatinine
Splenic.microabscesses	Splenic microabscesses reported on ultrasound

Then 4 further variable subsets were defined *a priori* as follows.

- **Prior Literature set**. All the variables from the full set which have previously been found to be significantly associated with MTB bacteraemia from literature review (reviewed in previous chapter): *fever, logCD4, Haemoglobin, Sex, lymphadenopathy (defined as peripheral OR mediastinal OR abdominal), Cough, current HAART, Diarrhoea, Heart Rate, log Respiratory Rate, Sodium, Loss of weight*.
- **Jacob et al. set**: Variables from full set which were used in the model published by Jacob et al.: *fever, log CD4, Haemoglobin, Sex, current HAART, Heart Rate, Sodium*.
- **Univariate associations set**: All variables from full set which were found to have significant associations with MTB bacteraemia at the alpha=0.05 level on univariate testing in the training set: *PreviousTB, Heart Rate, SHCO3, Albumin, Sodium, Haemoglobin, Platelets, Pleural Effusion, Mediastinal LN, miliary disease on CXR, Peripheral LN, Abdominal LN, Splenic TB diagnosis, Splenic microabscesses, log CD4, log Creatinine, log AST, fever*.
- **Supervised dimension reduction set**: Based on exploratory PCA and MCA analysis on the training set several new variables were created intended to capture variation relating to independent processes. These variables are combinations of primary variables:
    - *Immunosupression* = log(CD4count)
    - *AdvancedTB1* = 0.3∗(Haemoglobin) + 0.1∗(Albumin) − 6
    - *AdvancedTB2* =Sodium
    - *Septic1* =0.03∗(HR) + 2∗(ln(RR)) − 0.005∗(ln(lactate)) + 0.7∗(fever) − 0.5∗(SHCO3) − 10

    - *Disseminated1* = 0.05 + 1.3∗(spleen) + 1.1∗(microabscess) – 0.13∗(no.USS.done) + 1.3∗(AbdoLN) + 0.9∗(liverTB)
    - *Disseminated2* = 0.5+1.7∗(miliaryCXR) + 3.5∗(periphLN) – 0.003∗(Platelets)
- **LASSO variable set**. LASSO (Least Absolute Shrinkage and Selection Operator) fits a regression model using an adapted least squares function which forces some of the β coefficients to be zero, thus removing some predictor variables from the model. It can therefore be used as a variable selection procedure similar to stepwise regression. LASSO was applied to the full variable set using the glmnet package in R; this defined a variable sub-set with good multivariate predictive performance (BPSystolic, HR, SHCO3, Albumin, Sodium, MCV, Platelets, logCD4, Splenic.microabscesses, Haemoglobin, bacteraemia).

In addition to these variable reduction methods applied prior to modelling, unsupervised PCA pre-processing of the full variable set and the univariate association set were applied in iterations of each model. This means that, instead of entry of primary variables into the model, principal components of these variables are used as predictor variables. This has the advantage of potentially separating signal from noise, since lower Eigen value components are more likely to represent random error, while the first few principal components capture major covariance which has unlikely to have occurred by chance. In addition, because the components are orthogonal, they will not be redundant. The number of components to include is a complexity or tuning parameter which can be optimised by cross-validation.

Finally, model-type specific variable selection procedures were used:

- **Stepwise logistic regression.** Forward stepwise regression with variable inclusion based on Akaike information criterion carried out with the glmStepAIC function of the MASS package in R, using the full and the univariate association variable sets as starting points.
- **Random forest variable importance.** The RF method generates a measure of importance for variable v by comparing the out-of-sample accuracy of all trees with and without v included. Using this index, random forest models can be re-run using only variables above an arbitrary variable importance level.
- **Boosted tree variable importance.** A variable importance measure can be obtained from the boosted-tree method by tabulating the reduction in classification error attributed to each variable at each tree split and summing over each boosting iteration. Using this index, the boosted tree model can be re-run using only variables above an arbitrary variable importance level.

- **SVM variable importance.** No built-in importance score is available for SVM classification models; instead the area under the ROC curve for each variable can be used.

2.5.4 Total number of models assessed

Total number of models assessed is therefore 45:

- Six variable subsets (full, prior literature, Jacob *et al*., univariate association, supervised dimension reduction, and LASSO set) in 5 models = **30**; plus
- Full set and univariate association set with PCA pre-processing applied in 5 models = **10**; plus
- Five models re-run with variables of most importance in the previous iteration of that model = **5**.

Models are named for convenience (table 2).

2.5.5 Model training and assessment

All models were built using the training data, with 5 iterations of 10-fold cross-validation to optimise model parameters and assess out-of-sample model performance. The metric used to define model performance was ROC AUC; i.e. cross-validation was used to tune model complexity parameters to maximise estimated out-of-sample ROC AUC. This was carried-out with the train() wrapper function in the caret package (Classification And REgression Training) in R.

Final models' predictions in the test set were then assessed, also with ROC AUC (figure 3).

Table 2-2. List of 45 models assessed in May 2016 analysis

Model	Type	Variable selection
boost.comp	Boosted tree	Supervised dimension reduction composite variables
boost.full	Boosted tree	Full set
boost.jacob	Boosted tree	Jacob et. al set
boost.lasso	Boosted tree	LASSO set
boost.prLit	Boosted tree	Prior literature set
boost.univar	Boosted tree	Univariate association set
CART.comp	Decision tree	Supervised dimension reduction composite variables
CART.full	Decision tree	Full set
CART.jacob	Decision tree	Jacob et. al set
CART.lasso	Decision tree	LASSO set
CART.prLit	Decision tree	Prior literature set
CART.univar	Decision tree	Univariate association set
Logit.comp	Logistic regression	Supervised dimension reduction composite variables
Logit.full	Logistic regression	Full set
Logit.jacob	Logistic regression	Jacob et. al set
Logit.lasso	Logistic regression	LASSO set
Logit.prLit	Logistic regression	Prior literature set
Logit.univar	Logistic regression	Univariate association set
pcaboost.full	Boosted tree	Full set + PCA pre-processing
pcaboost.univar	Boosted tree	Univariate association set + PCA pre-processing
pcaCART.full	Decision tree	Full set + PCA pre-processing
pcaCART.univar	Decision tree	Univariate association set + PCA pre-processing
pcaLogit.full	Logistic regression	Full set + PCA pre-processing
pcaLogit.univar	Logistic regression	Univariate association set + PCA pre-processing
pcaRF.full	Random Forest	Full set + PCA pre-processing
pcaRF.univar	Random Forest	Univariate association set + PCA pre-processing
pcasvm.full	Support Vector Machine	Full set + PCA pre-processing
pcasvm.univar	Support Vector Machine	Univariate association set + PCA pre-processing
RF.comp	Random Forest	Supervised dimension reduction composite variables
RF.full	Random Forest	Full set
RF.jacob	Random Forest	Jacob et. al set
RF.lasso	Random Forest	LASSO set
RF.prLit	Random Forest	Prior literature set
RF.univar	Random Forest	Univariate association set
stepLogit.full	Logistic regression	Full set + stepwise selection in model
stepLogit.univar	Logistic regression	Univariate set + stepwise selection in model
svm.comp	Support Vector Machine	Supervised dimension reduction composite variables
svm.full	Support Vector Machine	Full set
svm.jacob	Support Vector Machine	Jacob et. al set
svm.lasso	Support Vector Machine	LASSO set
svm.prLit	Support Vector Machine	Prior literature set
svm.univar	Support Vector Machine	Univariate association set
vi.boost.full	Boosted tree	Full set + model specific variable importance in model
vi.RF.full	Random Forest	Full set + model specific variable importance in model
vi.svm.full	Support Vector Machine	Full set + univariate ROC AUC

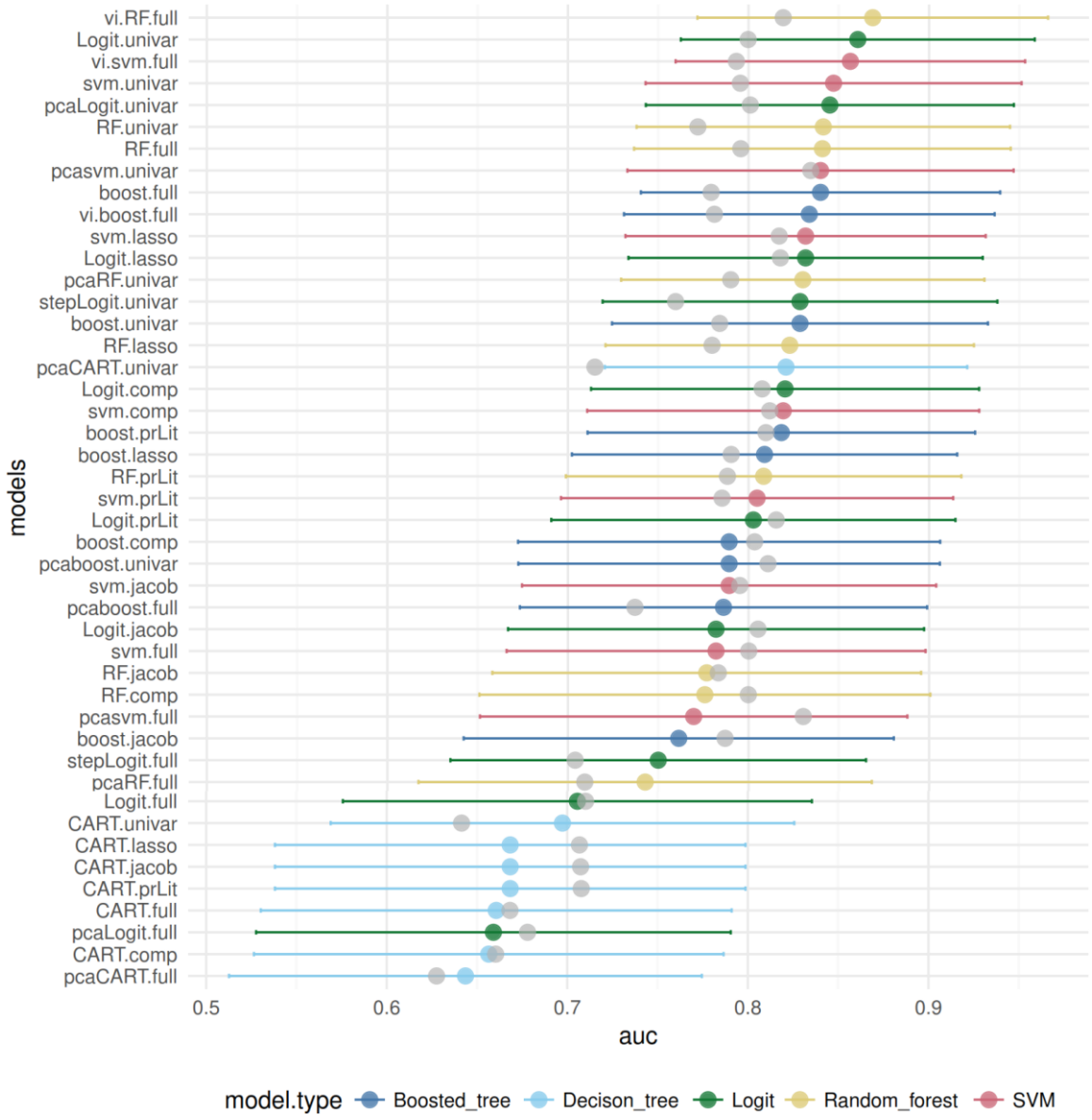

Figure 2-3. Model performance measured by ROC AUC.

For each of the 45 models the cross-validated AUC within the training data is shown with a grey point, and the AUC with 95% confidence interval for the test data is shown with coloured point and line range respectively.

Table 2-3. Cross-validated model ROC AUCs in training data.

Model	Mean	SD	IQR
pcasvm.univar	0.831	0.10	0.760, 0.889
svm.full	0.821	0.13	0.753, 0.905
svm.lasso	0.817	0.10	0.766, 0.891
pcaLogit.univar	0.815	0.12	0.760, 0.894
Logit.lasso	0.815	0.09	0.758, 0.877
boost.prLit	0.808	0.09	0.750, 0.864
Logit.comp	0.807	0.11	0.758, 0.890
svm.comp	0.805	0.11	0.744, 0.894
boost.jacob	0.804	0.09	0.750, 0.870
boost.comp	0.804	0.11	0.750, 0.886
Logit.prLit	0.802	0.10	0.748, 0.876
Logit.univar	0.801	0.13	0.737, 0.889
RF.comp	0.801	0.12	0.727, 0.890
vi.RF.full	0.800	0.13	0.690, 0.875
RF.prLit	0.799	0.11	0.717, 0.883
svm.jacob	0.799	0.09	0.734, 0.874
vi.svm.full	0.799	0.14	0.714, 0.905
svm.prLit	0.798	0.10	0.744, 0.867
pcasvm.full	0.795	0.16	0.710, 0.905
Logit.jacob	0.795	0.10	0.720, 0.868
svm.univar	0.791	0.13	0.720, 0.889
pcaboost.univar	0.791	0.16	0.713, 0.917
vi.boost.full	0.789	0.14	0.715, 0.875
RF.univar	0.788	0.13	0.734, 0.862
RF.full	0.784	0.17	0.672, 0.905
boost.lasso	0.777	0.11	0.716, 0.836
pcaRF.univar	0.776	0.13	0.678, 0.900
boost.univar	0.775	0.14	0.656, 0.875
RF.lasso	0.773	0.14	0.691, 0.879
RF.jacob	0.768	0.11	0.699, 0.852
boost.full	0.767	0.16	0.667, 0.905
pcaRF.full	0.767	0.18	0.670, 0.926
stepLogit.univar	0.752	0.14	0.669, 0.824
Logit.full	0.731	0.18	0.640, 0.881
pcaboost.full	0.723	0.19	0.629, 0.857
CART.jacob	0.721	0.12	0.640, 0.797
pcaCART.univar	0.714	0.15	0.613, 0.819
CART.prLit	0.700	0.12	0.638, 0.750
CART.lasso	0.691	0.12	0.628, 0.758
pcaLogit.full	0.689	0.18	0.595, 0.833
CART.full	0.681	0.15	0.591, 0.778
stepLogit.full	0.674	0.13	0.586, 0.750
CART.univar	0.659	0.16	0.566, 0.796
CART.comp	0.659	0.12	0.570, 0.773
pcaCART.full	0.640	0.18	0.500, 0.766

2.6 Results of 45 MTBBSI predictive models

Cross-validated training data ROC AUCs are shown in figure 3 and table 3; test set ROC AUCs are shown in figure 3. The best performing were generally Random Forest and Support Vector Machine models. Decision tree models were substantially worse than other models. Performance of logistic regression models was very dependent on variable selection method. Overall, ROC AUCs greater than 0.8 appeared achievable. Note also that the cross-validated estimates of model performance using training data are all within the 95% confidence interval for the ROC AUC from the test data. The difference in AUC by the two methods is approximately normally distributed around zero, and less than 0.05 in 35/45 cases (figure 4).

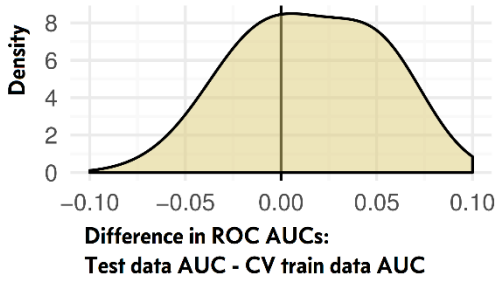

Figure 2-4. Training versus test data estimates of ROC AUC.

CV = cross validated.

2.7 Combining models for a final ensemble model

Imprecision in AUC estimates mean it isn't possible to confidently say which model is best in figure 3. Some of the models are more practical than others due to lower numbers of variables included. Several of the higher AUC models use the same or similar variable sets – all these models can therefore be run without the extra difficulty of entering more observations. Based on this, 6 models [RF.lasso,

RF.univar, Logit.lasso, Logit.univar, SVM.lasso, SVM.univar] were combined by simply averaging their predicted probabilities to give a single ensemble model. The AUC of this ensemble model was marginally higher than any of the 6 models used to construct it, though not significantly so ($p > 0.3$ for all correlated pairwise comparisons by DeLong method). Nonetheless it provides a practical way of reducing the predictions to a single value so was accepted.

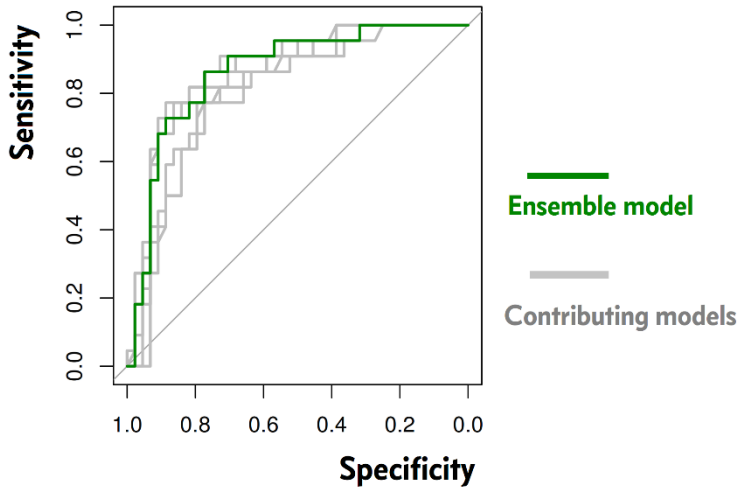

Figure 2-5. ROC curve plots for ensemble model

Curves for the 6 models used to construct the ensemble model are shown in grey for comparison. AUC for ensemble model is 0.863.

Using this final model, a predicted probability cut-off can be selected to classify new patients. The 'yield' – i.e. positive and negative predictive value – depends on the model ROC AUC but also on the prior probabilities of TB bacteraemia in the cohort the model is applied to. In the test data, 25% of patients have an ensemble model predicted probability greater than 0.56 (figure 6A); 80% of these patients had a positive blood culture (figure 6B).

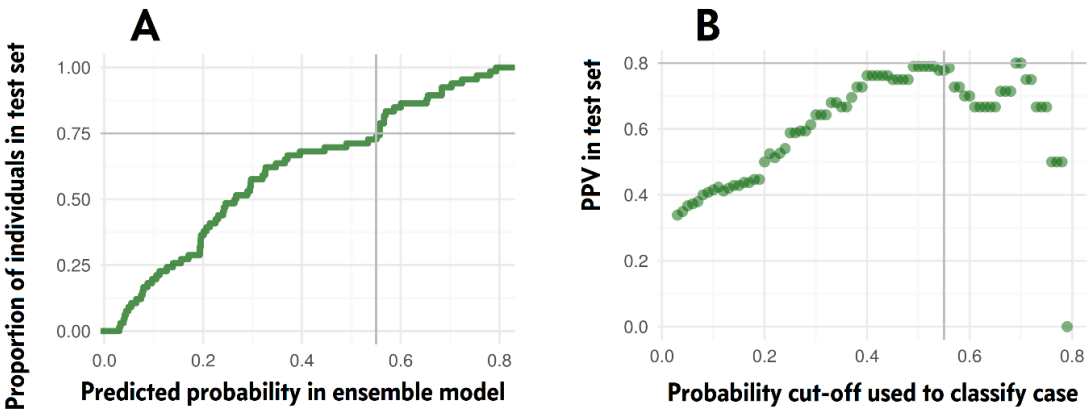

Figure 2-6. Predicted probability from ensemble model mapped to classification rule.

One-in-four KDHTB patients had predicted probability of MTBBSI above the 0.56 cut-off (**A**). Positive predictive value (PPV) of the model predicted probability steadily increased up to 0.56 cut-off, becoming unstable after this due to lower numbers of patients in the validation cohort (**B**). Note selecting all patients above a predicted probability of 0.56 can have a positive predictive value of much greater than 0.56 (in this case 0.8) because the probability distribution above 0.56 is on average higher than 0.56 – the PPV therefore depends on the distribution of predicted probabilities in a given cohort (in other words, post-test probability depends on pre-test probability).

2.8 Building an app' to make predictions accessible at bedside

The complexity of the ensemble model precludes derivation of a prediction score or normogram. Instead the model was built into an application (app) using the shiny package in RStudio. This app was uploaded to shared servers operated by RStudio via the shinyapps.io platform, so that it was accessible via the web (for example on a smart phone). At the user interface (URL https://davidadambarr.shinyapps.io/KDH_MTB_bacteraemia/) observed values for the variables [Systolic blood pressure, diastolic blood pressure, heart rate, bicarbonate, albumin, sodium, MCV, platelets, haemoglobin, CD4 count, creatinine, AST, presence of splenic micro-abscesses (no, yes, or no ultrasound performed), history of previous TB, pleural effusion, mediastinal adenopathy, peripheral adenopathy, and fever] can be input and a predicted probability of positive TB blood culture is output.

2.9 Prospective validation sub-study

2.9.1 Method

To test the predictive modelling, prospective validation was performed during the ongoing recruitment to KDHTB. Between 21 June 2016 and 18 August 2016 all patients recruited to KDHTB were additionally screened using the app. If a predicted probability of positive MFL was greater than 0.56, no anti-tuberculosis therapy had been taken in the last 4 weeks, and consent was given, patients were recruited to a sub-study. This sub-study aimed to:

1. Assess the predictive performance of the model and cut-off value when used prospectively to classify patients as having MTBBSI.
2. Estimate the increased yield from more than one MFL culture for diagnosing MTBBSI.

To this end, recruited patients had two MFL blood cultures performed at up to four time-points, for a total of up to eight samples. Time points were:

- Before commencing anti-tuberculosis therapy (0 hours);
- Within 12 hours of first dose anti-tuberculosis therapy (4-12 hours);
- Prior to second dose anti-tuberculosis therapy (24 hours); and
- Prior to third dose anti-tuberculosis therapy (48 hours).

One 3-5ml sample from each time-point pair was inoculated directly to a Myco/F lytic Bactec (BD, Sparks, MD) bottle. To minimise antimicrobial carry-over from plasma in the second sample from each time-point pair, 5 ml of blood was collected in a sterile sodium heparin tube and immediately centrifuged for 25 min at 3,000 × *g*, and the resulting cell pellet (red cells and buffy coat) inoculated into a Myco/F Lytic bottle. Both MFL bottles were then transported to the NHLS TB laboratory in Groote Schuur Hospital, Cape Town, for incubation the same day, where any subsequent growth was confirmed by secondary Löwenstein–Jensen slope culture, auramine acid-fast microscopy, and PCR/line probe assay.

2.9.2 Results – prediction accuracy

During the sub-study period, 46 patients were recruited to the main KDHTB study. A final microbiologically proven diagnosis of TB was made in 42/46 (91%) and 19/46 (41%) were MFL TB blood culture positive. This is higher than the overall KDHTB cohort (73% and 33% respectively for patients meeting inclusion criteria in the whole n=659 cohort), so prior probabilities were slightly higher than in the model development data.

Based on the app predicted probabilities, 16/46 (35%) patients were recruited to the sub-study – again slightly higher than the 25% anticipated in model development. Of these patients, 9/16 were positive on first MFL blood culture, while 14/16 had at least one positive out of any of the samples sent, giving positive predictive values of 0.56 or 0.88 for first or any blood culture respectively (table 4).

Table 2-4. Performance of predictive model in prospective sub-study.

Predicting result of first TB blood culture			
	1st MFL +	**1st MFL -**	Total
Predicted positive (recruited)	9	7	16
Predicted negative (not recruited)	5	25	30
Total	14	32	46
Point estimates and 95% confidence intervals			
Apparent prevalence	0.35	0.21 to 0.50	
True prevalence	0.3	0.18 to 0.46	
Sensitivity	0.64	0.35 to 0.87	
Specificity	0.78	0.60 to 0.91	
Positive Predictive Value	0.56	0.30 to 0.80	
Negative predictive Value	0.83	0.65 to 0.94	
Positive Likelihood Ratio	2.94	1.37 to 6.30	
Negative Likelihood Ratio	0.46	0.22 to 0.95	
Predicting positive result from any TB blood culture			
	Any MFL +	**All MFL -**	Total
Predicted positive (recruited)	14	2	16
Predicted negative (not recruited)	5	25	30
Total	19	27	46
Point estimates and 95% confidence intervals			
Apparent prevalence	0.35	0.21 to 0.50	
True prevalence	0.41	0.27 to 0.57	
Sensitivity	0.74	0.49 to 0.91	
Specificity	0.93	0.76 to 0.99	
Positive Predictive Value	0.88	0.62 to 0.98	
Negative predictive Value	0.83	0.65 to 0.94	
Positive Likelihood Ratio	9.95	2.55 to 38.7	
Negative Likelihood Ratio	0.28	0.13 to 0.61	

2.9.3 Results – yield from additional MFL cultures

In total, 111 MFL results were available from the 16 patients, with 17 results missing (3 contaminated, 4 missing due to patient declined further venesection, 10 missing due to patient transfer or discharge precluding venesection). Of these, 34/111 (30.6%) were positive for *M. tuberculosis*. Pelleted samples were more likely to result in the recovery of *M. tuberculosis* (20/55 [36%]) than directly inoculated samples (14/56 [25%]), but the difference may have been due to chance (OR 1.7, 95% CI 0.7 to 4.2, p = 0.22 by Fisher's exact test).

Nine patients were diagnosed with TB bacteraemia on the first blood culture, while 12 were positive if the first two cultures (i.e. both cultures from the first time-point pair) are considered (figure 7). This implies that only 2/3 of prevalent TB bacteraemia is diagnosed on a single blood culture.

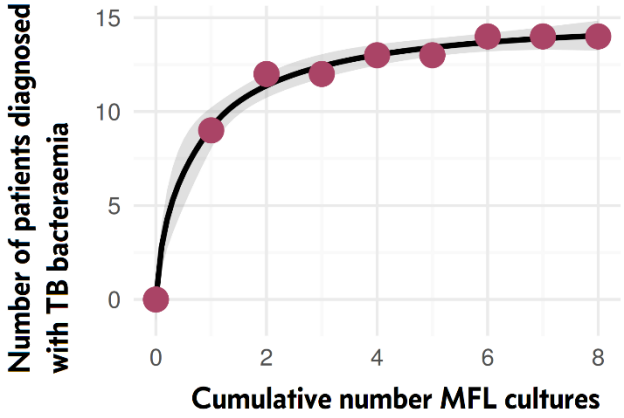

Figure 2-7. Increasing yield from additional MFL blood cultures.

This finding was further corroborated using data from the overall KDHTB cohort and data from the Jooste rapid TB diagnostics study.***** In both these studies a single MFL blood culture was performed as part of the study protocol. In addition, because recruited patients were managed by non-study clinicians, who had access to mycobacterial blood culture investigations through the National Health Laboratory Service (NHLS), a subset of patients in both cohorts had

***** This study was described briefly in the previous chapter. Again, I acknowledge Dr Andrew Kerkhoff for making this data available for the current analysis.

further MFL blood cultures if requested by their admitting medical team. Local guidelines recommend TB blood culture if CD4 count is less than 100 cells/mm^3 in a patient with TB symptoms where there is difficulty obtaining sputum samples for TB testing or the sputum Xpert MTB/RIF assay is negative, and cultures are generally sent before the start of anti-TB therapy. By interrogating the NHLS electronic records system, the results of these additional MFL blood cultures were collected.

A second (non-study) MFL result was found for 59 Jooste study patients and 169 KDHTB patients, giving a total sample size of 228 for analysis. Of these patients, 99/228 (43%) had at least one blood culture positive for *M. tuberculosis* (20/59 in JHTB and 79/169 in KHTB). Overall, 72/99 (0.73; 95% confidence interval [CI], 0.64 to 0.82) of *M. tuberculosis* bacteraemia was identified on the first culture, while 27/99 (0.27; 95% CI, 0.18 to 0.36) had a negative first culture but grew *M. tuberculosis* on the second. This is a near identical result to the prospective sub-study, where 0.75 of patients diagnosed on 2 cultures were identified on the first of the pair.

2.10 Discussion

Using a variety of modelling techniques, a positive TB blood culture can be predicted in hospitalised PLWHIV suspected of having tuberculosis, using only baseline clinical data available in the first 24 hours of admission. The accuracy of this prediction, in the Khayelitsha Hospital setting, is above 0.8 for both negative and positive predictive value. This conclusion is supported by cross-validation, test set performance, and prospective validation.

Is predicting TB blood culture status worthwhile? One short answer is yes, because blood cultures normally take several weeks to flag positive (the median is 22 days in the KDHTB cohort). Another short answer is no, because this does not change management: the real goal is to predict a TB diagnosis and risk of death without empiric treatment, and knowing that TB is bacteraemic is superfluous.

The longer answers are, however, more cogent. First, being able to predict this marker of MTBBSI facilitates research investigation. This was clearly demonstrated in the current chapter, where the predictive modelling was used to

enrich recruitment to a sub-study and show the yield of additional blood cultures for diagnosing prevalent MTBBSI. To have performed this analysis in the KDHTB cohort without predictive modelling (while achieving the same study power) would have required around 200 extra blood cultures to be performed (to recruit 14 MFL+ patients at the baseline KDHTB rate of 0.33 would require 14/0.33 ~ 42 patients; 42 * 8 = 336 MFL bottles as compared to 16*8 = 128 bottles). The predictive modelling to enrich recruitment approach was also employed in another sub-study described in chapter 5.

Second, while currently management is the same for BSI versus non-BSI tuberculosis, this is – as discussed in the thesis introduction – because there is an absence of evidence to the contrary, not because there is evidence that this is best practice. Being able to predict the presence of MTBBSI would make a focussed trial feasible. Consider that other (non-tuberculosis) BSI intervention trials must either recruit after a delay (for example, most patients in the ARREST trial of *S. aureus* BSI had >60 hours of antimicrobial therapy before randomisation),[293] or recruit based on empiric treatment and testing the intervention in a heterogeneous patient population including different infections and even non-infectious conditions.[294,295] Both these approaches could reduce power; recruiting patients at start of therapy with a >80% PPV of the target diagnosis is likely to make trial designs more efficient and affordable.

Thirdly, and more speculatively, being able to predict the presence of MTBBSI might influence empiric management of inpatients with advanced HIV infection, or at least influence prior probability and predictive value of rapid diagnostic tests. Empiric treatment of TB in high HIV-burden, low-resource settings is common,[296] but little is known about the basis on which clinicians make treatment decisions.[297] Utility theory – where treatment decisions are modelled as a risk/benefit calculation – explains some clinician behaviour,[298] but is an oversimplification. Perceived prior probability influences the sensitivity and specificity (rather than just the predictive values) with which clinicians interpret signs. For example the presence of a red dot on an x-ray, indicating that a radiographer thought there was high probability of an abnormality, increases doctors' sensitivity, and decreases specificity, for identifying abnormalities on that x-ray, without changing diagnostic odds ratios – in effect shifting the clinicians' interpretation along an implicit ROC curve.[299] A predicted probability

of MTBBSI generated from laboratory results, and flagged on the webpage portal where those laboratory results are reviewed, could similarly influence clinicians' diagnostic behaviour. More qualitatively, "mental representations" of diseases, or "illness scripts", provide the basis for diagnostic reasoning.[300] An empiric diagnosis of MTBBSI might be more compelling and urgent than "smear-negative tuberculosis".

The only validated prior attempt to predict TB blood culture status is the clinical prediction score by Jacob *et al*. discussed earlier in this chapter.[127] This score was developed in a cohort of HIV-infected inpatients with severe sepsis, and had ROC AUC 0.82 estimated through k-fold cross-validation in the same dataset the score was developed from. It is tempting to compare this performance with that seen for the best models in the current analysis. In theory, because models' variance-bias trade-off was optimised using machine learning techniques, the current models may be expected to perform better than the more traditional approach used by Jacob *et al*. However, a direct comparison isn't prudent since the study populations are different, potentially leading to spectrum (i.e. case-mix) bias.

That the prospective sub-study accurately predicted patients' blood culture status is a major strength of this analysis. Correct classification of future events requires extra assumptions – that there are no temporal biases, and that the probability cut-off remains optimal for classification – making this a more robust test of the ensemble model.[301] However, in retrospect I think there are also some weaknesses.

First, reserving a test set from the original data added little to the results. In fact, choice of models to take forward to the ensemble approach was, I think, overly influenced by test set performance. Using all the original data to train models and selecting based on cross-validated performance within this training data would have been more efficient and probably less biased (for reasons outlined in section 2.2 above).

Second, algorithmic variable selection prior to modelling – i.e. the univariate associations and LASSO selection – were performed outside of the cross-validation procedure. While this approach is quite standard in clinical research it poses a high risk of over-fitting.

Finally, the point estimates of model performance in the prospective sub-study (table 4) are, arguably, over optimistic. Patients predicted to be blood culture negative were not recruited for serial blood cultures, so mostly had only a single MFL sent (5/30 had two, the second sent by non-study clinicians). We now know that this will have underestimated the true rate of TB bacteraemia in these patients, thus inflating negative predictive value of the model. Nonetheless, the use of different procedures in those predicted to be positive versus negative (8 versus 1 blood culture) is a weakness of the comparison. Relatedly, the KDHTB training data included patients who may have received up to 2 days of antimicrobial therapy prior to MFL blood culture, adding noise (false negatives) to the dependent variable. Excluding such patients would, however, have substantially reduced sample size.

This highlights a broader point. Measurement error in the dependent (outcome) variable equates to irreducible error – the red line in figure 1 – putting a ceiling on the accuracy gain from optimising variance-bias trade-off. The current analysis is the first reported attempt to assess this measurement error. Previous studies have compared yield from different TB blood culture methods, but not the yield from additional cultures.[15,112,302-307] One previous study randomized patients to 6 blood cultures at a single time-point or 3 blood cultures at 2 time-points (i.e. the same total number of cultures) and found no difference in the recoveries of *M. tuberculosis* between these arms.[308] The finding that a single blood culture will identify only 2/3 of culturable bacteraemia is therefore novel. It is also unsurprising given the established evidence for non-mycobacterial BSI, where a single 10-ml blood culture will detect 73% and four samples will detect 90 to 95% of patients with documented bacteraemia.[309,310]

The implication of this finding is that the prevalence of MTBBSI has been systematically underestimated. Almost every prior cohort study examining prevalence and associations of MTBBSI has been based on a single blood culture. What would the estimated prevalence of MTBBSI have been in these studies if factors like number of blood cultures performed had been accounted for? This question is answered in the next chapter which reports an individual patient data meta-analysis of TB blood culture studies.

3 Individual Patient Data meta-analysis of TB blood culture studies

3.1 Introduction

In the previous chapters it was claimed that MTBBSI is a central feature of severe HIV-associated tuberculosis, and likely causally related to mortality in this patient group. The specificity of MTBBSI was contrasted with the vague recommendations on 'disseminated TB' found in WHO guidelines on management of PLWHIV suspected of having tuberculosis.

Several objections to these points could be made. First, the reported prevalence of MTBBSI in high burden settings is not consistently high, and there is marked heterogeneity in reported rates of positive blood cultures in HIV-positive adults.[311] If MTBBSI is rare in some settings, how can it be of universal importance? Second, while some studies link bacteraemia to high risk of death in HIV-associated TB,[15,59,127] others find no significant independent association.[125,126,141] Might MTBBSI be simply an incidental feature of advanced immunosuppression? Third, while WHO guidelines on HIV-associated TB do not address MTB BSI directly,[48,53] an algorithm is given for managing 'seriously ill' people living with HIV and suspected of having TB (figure 1 & table 1). Isn't this algorithm sufficient for managing patients with MTBBSI?

The analysis in this chapter uses individual patient data from 20 published and unpublished data sets to try to resolve these questions. First, it is shown that heterogeneity in reported rates of TB blood culture positivity (TBBC+) might be explained by differences in inclusion criteria, and individual level variation in clinical factors such as CD4 count, which are difficult to adjust for in aggregate meta-analysis. Failure to account for technical factors such as number and timing of blood cultures in relation to start of anti-TB treatment has underestimated

TBBC+ prevalence in some cohorts. Further, the WHO danger signs (table 1 and figure 1) positively select for inpatients with TBBC+.

Second, rapid diagnostics – including sputum Xpert – have unreliable sensitivity to diagnose unwell patients with HIV-associated TBBC+ disease.

Finally, bacteraemia is shown to be a robust predictor of mortality, independent of other factors like CD4 count. In addition, waiting 3-5 days to see if danger-sign positive patients improve before starting presumptive therapy (figure 1) is probably associated with increased mortality risk in TBBC+ patients.

3.1.1 Statement on collaboration

The work presented in this chapter is the result of a collaboration with Dr Joseph M. Lewis (JML) of the Liverpool School of Tropical Medicine. The conception of the study and analysis presented are the result of equal contributions from myself and Dr Lewis.

Table 3-1. WHO algorithm: managing PLWHIV & suspected of having TB (seriously ill)[48]

Summary points	
1	TB suspected if cough, fever, night sweats, or weight loss present.
2	*Seriously ill* defined as presence of any **danger signs**: respiratory rate > 30 per minute, temperature > 39°C, heart rate > 120 beats per minute, and inability to walk unaided.
3	Hospital admission and parenteral antibiotics for bacterial infections in all cases.
4	Xpert MTB/RIF on sputum and extra-pulmonary samples if extrapulmonary TB is suspected.
5	If Xpert MTB/RIF negative or not available, and *no clinical improvement after 3-5 days*, start presumptive TB therapy.
6	In addition, urine lateral flow lipoarabinomannan (uLAM) "may be used… regardless of CD4 count".

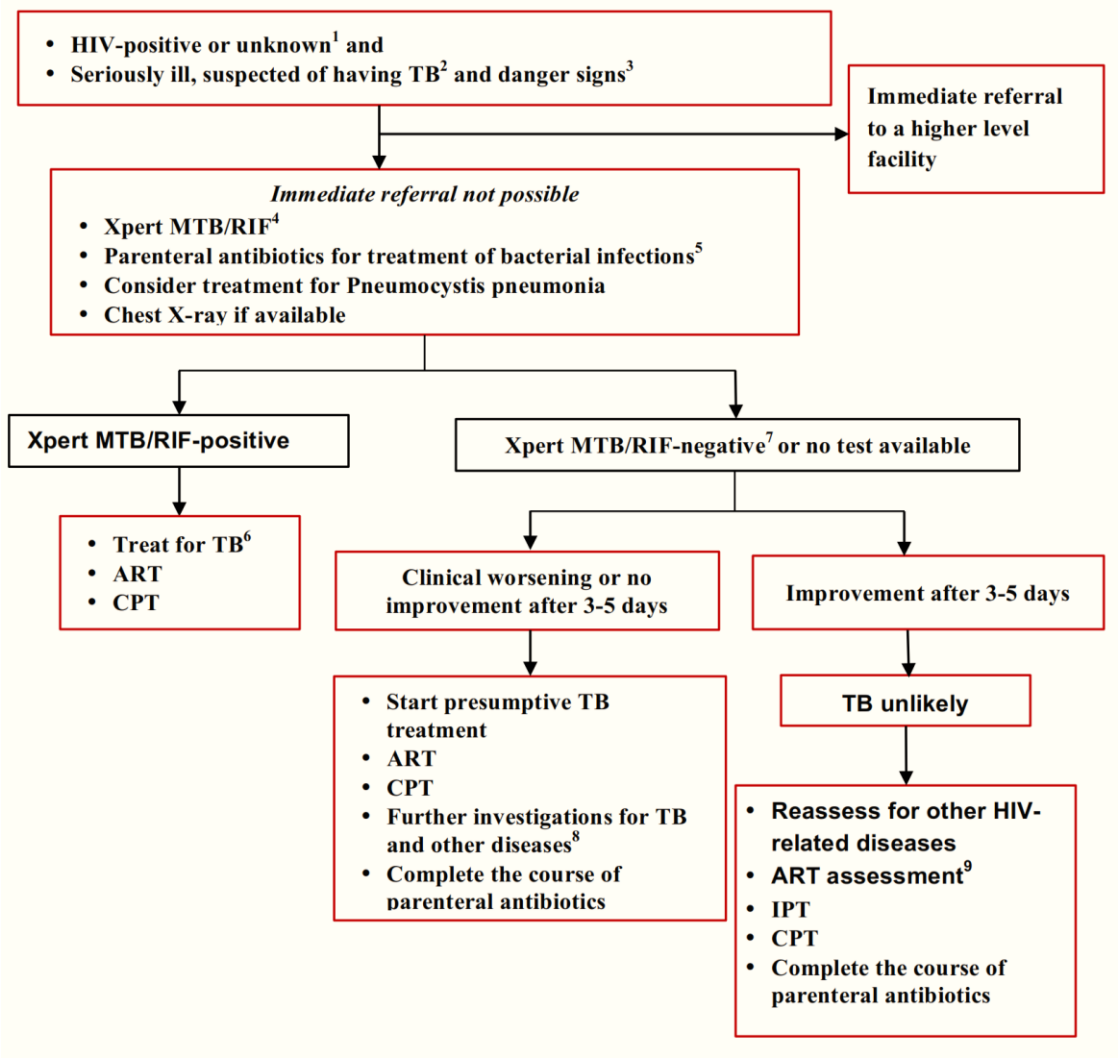

Figure 3-1. WHO algorithm: managing PLWHIV & suspected of having TB (seriously ill)

Reproduced directly from WHO 2016.[48]

3.2 Methods

3.2.1 Meta-analysis questions

1. What is the prevalence of TB blood culture positive disease amongst adult inpatients with HIV-associated TB and, in particular, those who are seriously unwell (having at least one WHO 'danger sign')?
2. What is the sensitivity and diagnostic yield of sputum Xpert MTB/RIF, and urine LAM, for diagnosing TB in patients with positive TB blood culture?

3. What is the independent mortality hazard associated with having a positive TB blood culture, compared to blood culture negative HIV-associated TB, and what proportion of TBBC+ deaths occur within 3-5 days of presentation?
4. Is there evidence of increased mortality risk from delaying treatment by 3-5 days in patients with a positive TB blood culture?

3.2.2 Literature search strategy and selection criteria

A search was conducted for prospective cross-sectional, cohort, or interventional studies where routine (non-selective) blood culture for mycobacteria was performed in a study-defined population including people living with HIV aged 13-years or more. Studies which didn't collect CD4 cell count results were excluded.

PubMed and Scopus were searched without language or publication period limits using [(*Blood stream infection* OR *BSI* OR *bacter?emia* OR *septic?emia*) AND (*tuberculosis* OR *TB*)] OR [*mycobacter?emia*]. Reference lists of identified articles and of review articles were also examined for relevant studies. Researchers known to have an interest in HIV associated tuberculosis were contacted in attempt to identify unpublished cohorts.

Abstracts were reviewed independently by JML and DAB and, if potentially eligible according to either reviewer, full texts were obtained. Full texts were reviewed independently by JML and DAB with disagreements resolved by consensus or after clarification of method details with primary authors.

3.2.3 Procedures

A meta-analysis protocol was registered on the PROSPERO database (https://www.crd.york.ac.uk/prospero/display_record.php?RecordID=50022). Original investigators of identified studies were contacted and asked to provide primary data, and provide clarification and meta-data in the event of discrepancies or unclear data coding. Individual patient observations of *a priori* specified variables were extracted from the primary datasets and resolved to a standardised format using reproducible R scripts. Patients with more than three missing observations of danger signs were deemed to be missing the composite variable "presence of danger signs".

3.2.4 Individual patient data inclusion criteria

Harmonised inclusion criteria were applied to the individual patient data (IPD). Patients from the selected studies were included in the meta-analysis if they were aged >13 years, had confirmed HIV-infection, an available CD4 count, at least one valid TB blood culture result (excluding patents with missing data for the index test, for example due lost or contaminated samples), and had at least one WHO TB screening symptom present. All included patients therefore met WHO definitions for PLWHIV and were suspected of having TB, i.e. the target population for the WHO management algorithms.[48]

3.2.5 Synthesis strategy and statistical analysis

Primary studies were classified by inclusion criteria (into categories: all HIV-infected patients; febrile HIV-infected patients; HIV-infected patients with suspected TB; HIV-infected patients with sepsis syndrome[†††††]) and by hospitalisation (inpatient; outpatient).

3.2.6 Prevalence of positive TB blood culture analysis

The starting point for this analysis was patients meeting the harmonised inclusion criteria, i.e. the target population for the WHO algorithms for managing PLWHIV and suspected of having TB.[48]

Prevalence of TBBC+ was assessed using mixed-effects logistic regression (*glmer()* function in R package *lme4*)[312] with random effects by primary study to account for random variation between studies, and fixed-effects to account for hypothesised systematic variation by *a priori* specified variables. These effects were added iteratively to the model in the following order:

- Random intercept by primary study (null model).
- Fixed effect of CD4 count.
- Random effect of CD4 count by primary study (random slope).
- Fixed effect of presence of the WHO danger signs.
- Fixed effect by admission status (outpatient versus inpatient).
- Fixed effect of already on TB treatment at time of blood culture (>1 dose prior to venesection).
- Fixed effect of number of blood samples taken for TB culture.

[†††††] Sepsis syndrome defined as per original study definitions, which in all cases were based on Sepsis-2 criteria.

- Fixed effect of final TB diagnosis. Respective original study case definitions were used to classify patients as having a final TB diagnosis. Addition of this variable to the model allows estimation of TBBC+ prevalence in patients with HIV-associated TB, rather than those suspected of having TB.

Continuous variables were standardised to have mean 0 and standard deviation 1. Each iterative model was compared to (i) a null model containing only a random effect by study on the intercept, and (ii) the preceding iteration model. Where incomplete data was available for the added variable, the comparison models were rebuilt using the same, reduced, dataset, such that the models were nested. This allowed assessment of each iterative model with the following statistics:

- **LRT_{null}**: Likelihood-Ratio test p-value testing the hypothesis that the new model has no better fit than the null model.
- **$LRT_{preceding}$**: Likelihood-Ratio test p-value testing the hypothesis that the new model has no better fit than the previous iteration model, i.e. that the added variable has not improved fit more than would be expected by chance alone.
- ***T^2***: Measures variance in the random effects, i.e. it describes variance arising from systematic differences between the primary studies, after adjustment for fixed effect cofactors have been adjusted for.[313,314]
- **Variance Partition Co-efficient (VPC)**: Measures proportion of residual individual variation arising from systematic differences between primary studies after adjusting for fixed effect cofactors in the model. The 'latent variable' method was used, which assumes that the binary outcome results from a dichotomised underlying (latent) continuous variable, which follows a logistic probability distribution.[313,315]
- **$R^2_{marginal}$**: Measures proportion of total variance explained by fixed-effects. Calculated using *r.squaredGLMM()* function of R package *MuMIn*.[313,316-319]
- **$R^2_{conditional}$**: Measures variance explained by the complete model – i.e. by fixed and random effects. Calculated using *r.squaredGLMM()* function of R package *MuMIn*.[313,316-319]
- **ROC AUC**: Area under the receiver operating characteristic curve capturing the within-sample prediction accuracy of the complete model (fixed and random effects). Calculated using the model predicted probabilities compared to the observed outcome.

- **ΔAUC**: Measures the importance of clustering by primary study after adjusting for fixed effect variables. A model containing only fixed-effects variables (no random effect by primary study), and a mixed-effect model containing the same as fixed-effects plus random effects by primary study, are made, and the difference in ROC-curve AUC between these two models is calculated.[313]

As fixed-effect variables are iteratively added to the model, if they 'explain' heterogeneity between primary study estimates, T^2, VPC, and ΔAUC will decrease; while $R^2_{marginal}$, $R^2_{conditional}$, and ROC AUC will increase.

Having established model fit using the above statistics, estimated prevalence of TBBC+ in specific patient populations was defined using predicted probability of positive MTB blood culture for given levels of the relevant fixed-effects in the final models. Estimates of predicted probability of TBBC+ from the final models were generated both for each primary study included in the model, and an aggregate 'grand mean' predicted probability across all studies. These were presented in forest plots. To capture uncertainty in these estimates boot-strapping and simulation methods were used. A 95% confidence interval for the predicted probability of TBBC+ in each primary study was generated using repeated estimates of the random- and fixed-effects parameters across 100 parametric bootstrap-resampled versions of the dataset, stratified by primary study. A 95% confidence interval for the predicted probability 'grand mean' – the range within the mean predicted probability is expected to lie if we continue to add new studies – was generated by stratified bootstrap of the fixed-effect parameters. Finally, a 95% prediction interval for the grand mean – the range within which the mean for a new, unobserved, study is expected to lie – was estimated by 100 bootstrapping simulations based on the probability distributions in the fitted models.[320] The *boot()* function in R package *boot*[321] was used for the bootstrapped confidence intervals, and *bootMer()* in the R package *lme4*[312] for the simulated prediction interval.

3.2.7 Diagnostic performance of sputum Xpert and urine-LAM in TBBC+ disease

Studies which collected IPD on sputum Xpert and urinary-LAM were included in this analysis; diagnostic tests actively carried out as part of the original study

protocol, or passively recorded from routine care were accepted. Sputum MTB culture results were accepted as a surrogate of sputum Xpert results if Xpert was not performed. Information on use of sputum induction was collected where available.

To assess diagnostic performance of the index test (sputum Xpert or urine-LAM) against the reference test (TB blood culture) two measures were applied:

1. **Sensitivity of index test**. A bivariate meta-analysis *excluding patients who had no recorded result for the index test* was performed, and sensitivity estimates extracted. For sputum, heterogeneity by primary study was investigated using study level covariates in meta-regression. This analysis gives summary estimates of the test characteristics but ignores participants for whom sputum or urine was unavailable
2. **Diagnostic yield of index test**. 'Diagnostic yield' was assessed by two-stage meta-analysis of *the proportion of TBBC+ patients who were identified as having TB using the index test*; this proportion was assumed to follow a binomial distribution, with a normally distributed random effect by primary study. Diagnostic yield considers the real-world performance of the test, as it includes patients for whom a sample could not be obtained.[322] Heterogeneity in diagnostic yield by primary study was also investigated using study level co-variate meta-regression.

3.2.8 Mortality association analysis

This analysis was restricted to patients with a TB diagnosis, as per the respective original study case definitions. A naïve, aggregated Kaplan-Meier plot (ignoring dependence by primary study) was used to visualise mortality stratified by TB blood culture status amongst patients with HIV-associated TB. A mixed-effects logistic regression model was developed to quantify the independent odds ratio of positive TB blood culture for death by day 30 or inpatient death, using the *glmer()* function in R package *lme4*.[312] A random intercept by primary study, and fixed-effects for age, sex, CD4 count, presence of WHO danger signs, and positive TB blood culture (TBBC+) were specified *a priori*. Patients with missing observations on these variables were excluded. Confidence intervals on coefficients were calculated from 1000 bootstrap replicates.

In addition to this core mortality analysis, two other exploratory analyses were performed. First, to assess the effect of urine-LAM positivity on mortality, the

TBBC+ result was replaced with urine-LAM result as an independent variable in the above mixed-effects logistic regression model.

Second, an association between delaying TB treatment by 3-5 days – as recommended in the WHO algorithm when sputum Xpert is non-diagnostic (table 1, figure 1) – and mortality in patients with TBBC+ was examined. The hypothesis was that any mortality association of treatment delay would be more pronounced in patients with bacteraemic infection. Therefore the *a priori* variable of interest was an interaction term between TBBC+ and treatment delay. Treatment delay was defined as a greater than 4-day time difference between blood culture being taken and anti-TB treatment being started. Patients without a final TB diagnosis, those with incomplete observations, and patients starting anti-TB treatment more than 24-hours before blood culture was taken, were excluded from this analysis. Outcome was again 30-day death or non-survival to discharge (the most complete outcome variables across primary datasets).

3.3 Results

3.3.1 Identified studies and IPD description

The literature database search strategy identified 18 primary studies reporting on 19 datasets for inclusion. An additional 4 datasets were identified from other sources. Responses were obtained from all primary study authors; IPD had been lost for 2 datasets, and 1 further dataset was not received. The remaining 20/23 datasets were contributed to the meta-analysis, representing 96.1% of the IPD identified for potential inclusion (figure 2). All received datasets were from studies published since the year 2000, all studies for which IPD was not received predated the HAART era. Of the received datasets, 16/20 were from sub Saharan Africa; 12/20 had recruited patients suspected of having TB; 15/20 had recruited exclusively inpatients, 2/20 exclusively outpatients, and 3/20 a mix (table 2).

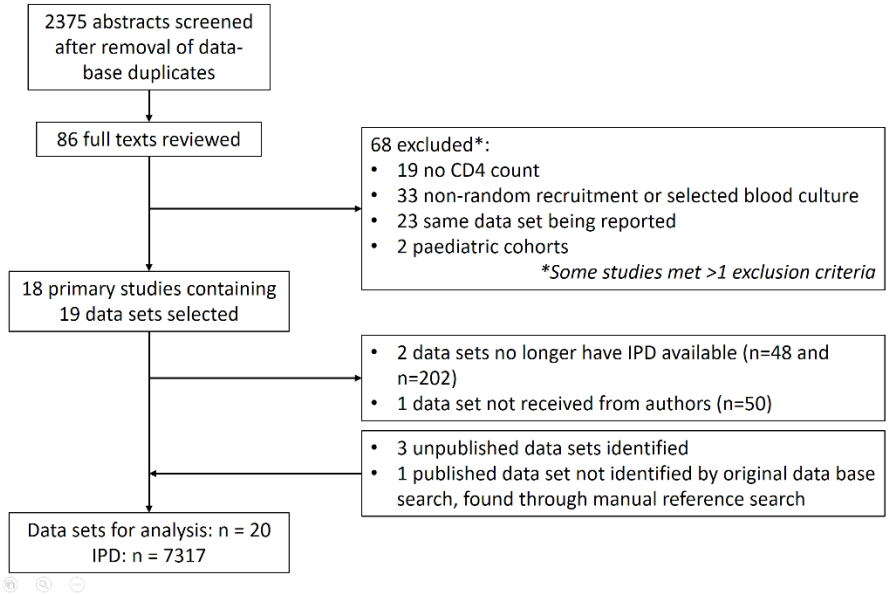

Figure 3-2. Identification of primary datasets, flowchart.

Application of the harmonised IPD level inclusion criteria left 5746 patients available for subsequent analyses. Characteristics of these patients are shown in table 2. Proportion of missing variables by study (which limits available data in subsequent analyses on a case-by-case basis) is shown in figure 3.

Table 3-2. Identified primary datasets.

Dataset ID	Source	Data	Site	Design	Dates	Primary study population category	MTB blood culture positive *	n IPD available	n meet inclusion
Brazil_2004[323]	DS	Received	3o care hosp	cohort	2001 -02	Spct TB IP	29.5%	53	44
Brazil_1997[324]	DS	Not received	3 specialist ID centres	cohort	1992-94	Spct TB	38.0%	NA	NA
SE.Asia_2010[128]	DS	Received	VCT OPCs	cohort	2006-08	OP	1.8%	2009	1338
India_2008[325]	DS	Received	3o care hosp	cohort	2005-06	Spct TB IP	30.8%	52	36
Ivory Coast_1993[326]	DS	No IPD	3o care hosp	cohort	1991	Febrile IP?	4.0%	NA	NA
Kenya_1995[120]	DS	No IPD	?3o care hosp	cohort	1992	Spct TB IP	22.9%	NA	NA
Malawi_2012[327]	DS	Received	OP clinics	cohort	2010	Spct TB OP	2.3%	469	411
Malawi_2013[15]	DS	Received	2o care hosp	cohort	NA	Febrile IP	8.7%	104	90
South Africa_2015[24]	DS	Received	2o care hosp	cohort	2012-13	IP	9.6%	427	338
South Africa_2009[144]	DS	Received	3o and 2o care hosps	nested cohort	NA	Spct TB IP	8.6%	498	264
South Africa_2001[129]	DS	Received	3o care hosp	cohort	1998	Spct TB IP	22.5%	45	44
South Africa_2018[328]	PC	Received	2o care hosp	cohort	2014-17	Spct TB IP	NA	679	614
South Africa_2017[21]	PC	Received	2o care hosps	cohort	2011-14	Spct TB IP	23.6%	484	444
South Africa_2006[329]	RS	Received	2o care hosp	cohort	2002	Spct TB IP & OP	24.5%	147	141
South Africa_2014[330]	DS	Received	2o care hosps + OPCs	cohort	2011	Spct TB IP & OP	9.5%	513	483
Uganda_2014[330]	DS	Received	2o care hosps + OPCs	cohort	2011	Spct TB IP & OP	15.6%	524	479
Tanzania_2012[59]	DS	Received	3o care hosps	cohort	2006-10	Febrile IP / spct TB IP	5.70%	411	145
Tanzania_2011[308]	DS	Received	2o care hosps	RCT	2007-08	Spct TB IP	15.9%	258	226
Vietnam_2004[331]	DS	Received	3o care hosp	cohort	2000	IP	12.3%	100	61
Uganda_2009[332]	DS	Received	3o care hosps	cohort	2006	Sepsis IP	22.1%	150	98
Uganda_2013[127]	DS	Received	3o care hosps	nested cohort	2008-09	Sepsis IP	23.4%	427	315
Zambia_2014[289]	DS	Received	3o care hosp	RCT	2012	Sepsis IP	37.8%	88	58
Zambia_2017[268]	PC	Received	3o care hosp	RCT	2012-13	Sepsis IP	20.6%	187	117

DS = database search; PC = personal contact; RS = manual reference search; hosp = hospital; VCT = Voluntary Counselling and Testing; OPC = outpatient clinic; 1o = primary; 2o = secondary; 3o = tertiary; OP = outpatient; IP = inpatient; NA = not available; spct = suspected; ? = unclear from publication (and no IPD or meta-data received)
*Disaggregated HIV-positive sample if available.

Table 3-3. IPD characteristics by primary dataset in 5746 patients meeting harmonised inclusion criteria for meta-analysis.

Primary dataset	Female	Median age (IQR)	Inpatient	Median CD4 (IQR)	Danger sign present	Final TB diagnosis rate[$]	MTB blood culture positive	Sputum positive	uLAM positive	Early mortality*
Brazil_2004	32%	34 (9)	100%	45 (80)	--	50%	30%	--	--	--
India_2008	10%	32 (10)	0%	230 (92)	--	50%	33%	33%	--	--
Malawi_2012	61%	35 (12)	0%	129 (172)	--	11%	3%	11%	--	6%
Malawi_2013	31%	36 (13)	100%	94 (184)	81%	42%	10%	46%	--	9%
S.E.Asia_2010	48%	32 (11)	3%	216 (304)	7%	25%	2%	17%	--	--
SouthAfrica_2001	41%	36 (12)	100%	68 (98)	42%	59%	34%	64%	--	9%[#]
SouthAfrica_2006	65%	32 (12)	25%	107 (182)	17%	89%	23%	64%	--	7%
SouthAfrica_2009	70%	35 (13)	100%	82 (155)	89%	61%	13%	34%	35%	11%[#]
SouthAfrica_2014	63%	35 (13)	42%	154 (160)	0%	42%	10%	36%	11%	2%
SouthAfrica_2015	59%	35 (13)	100%	132 (225)	--	36%	12%	26%	16%	8%
SouthAfrica_2017	66%	36 (12)	100%	88 (175)	100%	54%	25%	48%	40%	8%
SouthAfrica_2018	51%	36 (13)	100%	60 (113)	45%	86%	34%	62%	24%	14%
Tanzania_2011	65%	36 (12)	100%	74 (191)	12%	27%	15%	16%	--	40%
Tanzania_2012	65%	39 (15)	100%	110 (199)	53%	8%	8%	--	--	17%
Vietnam_2004	16%	30 (15)	100%	20 (89)	51%	49%	13%	50%	--	38%[#]
Uganda_2009	66%	34 (15)	100%	34 (94)	96%	--[£]	13%	--	--	38%
Uganda_2013	53%	35 (13)	100%	49 (118)	97%	--[£]	24%	--	--	32%
Uganda_2014	64%	32 (11)	71%	97 (266)	0%	42%	11%	35%	14%	4%
Zambia_2014	57%	34 (12)	100%	49 (83)	93%	--[£]	47%	--	50%	62%
Zambia_2017	45%	34 (13)	100%	60 (120)	85%	--[£]	30%	--	28%	53%

[$] Number of patients with final TB diagnosis as per original study definitions divided by number with non-missing observation of this variable. Four data sets had high proportions of missing observation of final TB diagnosis and are redacted for this summary estimate (marked with [£]).

Diagnostic test percentages are number positive for this test divided by number of patients who had a valid test result in the whole cohort (not sensitivity or yield within those that had a final TB diagnosis).

Note that final Tb diagnosis and diagnostic test percentages are using different denominators so having a higher percentage test positive than diagnosis positive is not contradictory.

* Early mortality defined as death by day 30 or inpatient death if primary study follow-up was less than 30 days or only inpatient death was ascertained (these studies marked with [#]).

IQR = Magnitude of inter quartile range; uLAM = urine-LAM

	Primary dataset:																			
	Brazil_2004	*India_2008*	*Malawi_2012*	*Malawi_2013*	*S.E.Asia_2010*	*SouthAfrica_2001*	*SouthAfrica_2006*	*SouthAfrica_2009*	*SouthAfrica_2014*	*SouthAfrica_2015*	*SouthAfrica_2017*	*SouthAfrica_2018*	*Tanzania_2011*	*Tanzania_2012*	*Thailand_2004*	*Uganda_2009*	*Uganda_2013*	*Uganda_2014*	*Zambia_2014*	*Zambia_2017*
Sex	0	0.17	0	0	0	0	0	0	0	0	0	0	0	0	0	0	0	0	0	0
Age	0	0.17	0.01	0	0	0	0	0	0	0	0	0	0	0	0	0	0	0.04	0	0
Danger signs	1	1	1	0	0	0.02	0	0	0	1	0	0	0	0	0	0	0	0	0	0
Sputum result	1	0.17	0.07	0.12	0.01	0	0.1	0.22	0.01	0.59	0	0.18	0.15	1	0.28	1	1	0.04	1	1
ULAM result	1	1	1	1	1	1	1	0	0	0.02	0.33	0.12	1	1	1	1	1	0	0.79	0.73
Final TB diagnosis	0	0	0	0	0	0	0	0	0	0	0	0	0	0	0	0.87	0.36	0	0.62	0.56
Start date TB therapy	1	1	0.75	0.63	1	1	0.01	0.45	0.7	1	0.36	0.11	1	1	0	1	1	0.72	0.71	0.56
TB treatment prior to blood culture	0	0	0	0	0	0	0	0.45	0	0	0	0	1	0	0	0.01	0.03	0	0.71	0.56
Early death*	1	1	0.06	0.1	1	0	0.13	0.06	0.05	0	0	0.01	0.56	0.01	0.18	0	0	0.03	0	0
Follow up censor date	1	1	0.06	0.01	1	0.64	0.04	0.02	0	0.01	0	0	0.55	0.01	0	0	0	0	0	0

Figure 3-3. Proportion data missing by variable and primary dataset.

* Early mortality defined as death by day 30 or inpatient death if primary study follow-up was less than 30 days.

3.3.2 Prevalence of TBBC+ disease

Compared to the prevalence reported in the original publications (table 1; mean proportion 0.171, coefficient of variation 59.1%), the proportion of patients with positive TB blood culture (TBBC+) after application of harmonised IPD inclusion criteria was higher, but no less heterogeneous (table 3; mean proportion 0.195, coefficient of variation 62.4%).

Heterogeneity in probability of TBBC+ between primary datasets was investigated using a logistic regression model containing random-effects by primary dataset. The following hypothesised explanatory variables were added as fixed-effects to this null model:

- CD4 count
- Presence of WHO danger signs
- Hospitalisation (inpatient or outpatient)

- Whether anti-TB treatment was given before blood culture taken
- Total number of blood cultures performed
- If final diagnosis was TB or if an alternative diagnosis was made

Each of these improved model fit ($p<0.001$ by Likelihood-Ratio test comparison to preceding model, table 4), and explained variance attributable to fixed-effects ($R^2_{marginal}$ 0.66 for model containing all, table 4), increasing total variance explained by the full model ($R^2_{conditional}$ 0.19 in null model, 0.72 in the final iteration model, table 4). Within-sample predictive accuracy also increased with the addition of each fixed-effect variable (ROC AUC 0.75 in null model, 0.91 in final iteration model, table 4), with reciprocal decline in importance of clustering by primary dataset for predictive accuracy (ΔAUC 0.02 in final iteration model, table 4).

The final iteration model (model 7, table 4) was used to estimate predicted probability of TBBC+ in patients with a diagnosis of HIV-associated TB made by the study. Estimates for patients suspected of having TB were taken from the previous iteration, which did not include final TB diagnosis as a variable (model 6, table 4). Estimates were generated for patient populations defined by specific levels of CD4 count, hospitalisation status, and presence of danger signs. In all estimates, it was assumed that 2 blood cultures were taken prior to anti-TB therapy.‡‡‡‡‡

In all models, inpatients with danger signs had highest mean predicted probability of TBBC+, with probability rising rapidly at CD4 counts less than 100 cells/μL (figure 4A & B).

Mean predicted probability and uncertainty estimates were generated for a hypothetical population of seriously unwell (danger sign positive) inpatients with CD4 count 50 cells/μL (figure 4C & D). Uncertainty in the location of this mean was captured with boot-strapped 95% confidence intervals, estimating uncertainty for the aggregate predicted probability (or in an 'average' dataset with random-effects of zero). The random-effects, or residual heterogeneity between datasets, was used to simulate a 95% prediction interval. Assuming the datasets in this

‡‡‡‡‡ Across all studies, 457/5746 (8%) patients actually had more than 1 blood culture. Using data from these patients the effect of having 2 cultures versus 1 is being estimated and applied to the whole data set.

meta-analysis are a random sample of different settings, the prediction interval captures the expected probability of TBBC+ in 95% of settings (or where the mean probability would lie 95% of the time in a new, unobserved, dataset).

Predicted probability of TBBC+ for danger sign positive inpatients with CD4 count 50 cells/μL and *suspected TB* was 0.31 (95% confidence interval for overall mean, 0.27 to 0.42; 95% prediction interval for an unobserved dataset 0.13 to 0.66; figure 4C). For danger sign positive inpatients with CD4 count 50 cells/μL and HIV-associated TB, the predicted probability of blood stream infection was 0.58 (95% confidence interval, 0.50 to 0.68; 95% prediction interval, 0.29 to 0.85; figure 4D).

Table 3-4. Iterative mixed-effect models for logged-odds of TBBC+.

Iteration		N obs[ı]	N datasets[ı]	LRT *null* p value	LRT *preceding* p value	T^2	VPC	R^2 *marginal*	R^2 *conditional*	ROC AUC	ΔAUC
Model 0	Null model (RE by primary dataset)	5746	20	NA	NA	0.79	0.194	0	0.194	0.752	NA
Model 1	Null model + CD4 count[#] FE	5746	20	1.26E-67	1.26E-67	0.81	0.198	0.113	0.289	0.804	0.071
Model 2	Model 1 + CD4 count[#] RE by primary study	5746	20	2.71E-71	6.77E-07	0.76	0.188	0.089	0.278	0.814	0.081
Model 3	Model 2 + presence of danger signs FE	4916	16	5.15E-71	7.57E-06	0.538	0.141	0.13	0.274	0.816	0.059
Model 4	Model 3 + hospitalisation (inpatient v outpatient) FE	4916	16	2.42E-78	5.14E-10	0.404	0.109	0.257	0.363	0.821	0.041
Model 5	Model 4 + TB treatment prior* to blood culture FE	4453	15	6.70E-82	9.84E-07	0.422	0.114	0.283	0.386	0.837	0.035
Model 6	Model 5 + number of blood cultures performed FE	4453	15	1.75E-83	0.00062	0.433	0.116	0.288	0.392	0.839	0.032
Model 7	Model 6 + final diagnosis was TB[$] FE	4223	15	1.93E-190	4.06E-113	0.399	0.108	0.66	0.716	0.913	0.02

RE = Random-effect; FE = Fixed-effect
LRTnull = p-value testing the hypothesis that the new model has no better fit than the null model.
LRTpreceding = p-value testing the hypothesis that the new model has no better fit than the previous iteration model.
T2 = Variance in random effects; describes magnitude of systematic differences between the primary datasets, after adjustment for fixed-effects in model.[313,314]
VPC = Variance Partition Co-efficient; proportion of residual individual variation arising from random effects. [313,315]
R2marginal = Measures proportion of total variance explained by fixed-effects.[313,316-319]
R2conditional = Measures variance explained by the complete model.[313,316-319]
ROC AUC = Area under the receiver operating characteristic curve for within-sample prediction by the complete model (fixed and random effects).
ΔAUC = Measures the difference in ROC AUC if model includes random effects (compared to fixed-effects only model).[313]
CD4 count log converted and standardised to have mean 0 and standard deviation 1.
* Defined as any dose of anti-TB treatment more than 24 hours prior to blood culture being taken
$ As per primary study case definitions.
[ı] Describes data available for this iteration, after missing observations on added variable are excluded. At each iteration, Null and preceding model were re-built with this reduced dataset, and these nested models used for LRT comparisons.

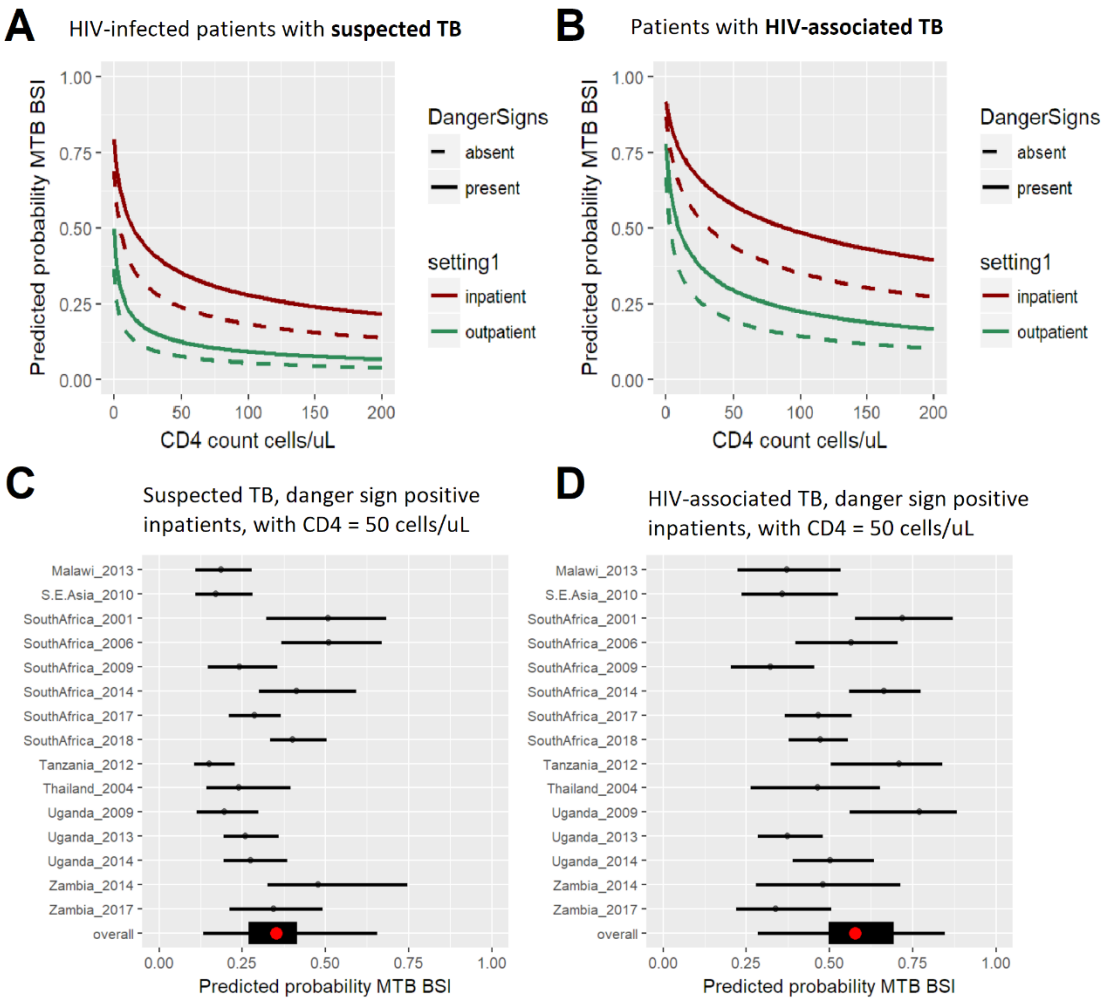

Figure 3-4. Predicted probability of TBBC+ by CD4 count, danger sign, and hospitalisation status.

Predicted probabilities from the mixed-effects models 6 and 7 (described in table 4) were used to estimate prevalence of positive TBBC in patients with suspected TB, and those with a final TB diagnosis, respectively. For all predictions, 'TB treatment prior to blood culture' was set to *nil*, and 'number of blood cultures' set at 2. The mean population predictions (zero random-effects) are shown for CD4 count 0 to 200 cells/μL, danger sign and hospitalisation status in **A** & **B**.

Estimates accounting for random-effects by primary dataset are shown in forest plots **C** & **D** *for inpatients with danger signs and a CD4 count of 50 cells/μL*. Fixed-effects parameters were re-estimated in 1000 bootstrap replicates (stratified by primary dataset) and used to generate a 95% confidence interval around the overall population mean predicted probability (black box around red dot). Fixed *and* dataset specific random-effects were similarly re-estimated for 95% confidence intervals around each dataset prediction. The distribution of random effects around the overall population mean was also re-estimated by bootstrap resampling, and used to simulate a 95% 'prediction interval' within which the mean predicted probability of TBBC+ in a new, unobserved or random, dataset is expected to lie (whiskers around 'overall' box).

3.3.3 Diagnosis of TB in patients with TBBC+

Fifteen primary studies had available sputum Xpert or culture data, which included 5750 patients with 410 TBBC+. Eight studies had sputum induction available as part of the study protocol. Urine-LAM was available in 8 studies, totalling 2797 patients with 554 TBBC+. Patients with available urine-LAM data were predominantly recruited in South Africa (79%). Availability and results of index tests in patients with TBBC+ varied substantially by primary dataset (figure 5).

Diagnostic utility of sputum Xpert/culture and urine-LAM were assessed in patients with a positive TB blood culture. Sensitivity of index tests was defined as number of patients with a positive result divided by number of patients with an available result. Diagnostic yield was defined as number of patients with a positive result divided by total number of patients (including those with an unavailable test result, e.g. unable to produce sputum).

For sputum, the combined estimate of sensitivity from a bivariate random-effects model was 0.83 (95%CI 0.76 to 0.88), with significant heterogeneity between datasets (I^2 45%, 95%CI 0 – 70%; test for heterogeneity on Cochrane's Q, p=0.0336; Figure 5A). Addition of study level co-variates – including median number of sputa obtained, availability of sputum induction, proportion of patients with danger signs – did not improve model fit (data not shown). Because of substantial variation in sputum availability, diagnostic yield of sputum showed even greater heterogeneity between datasets (mean 0.69, 95%CI 0.55 to 0.83; figure 5B).

Compared to sputum, urine-LAM had lower overall sensitivity in TBBC+ patients (0.70, 95%CI 0.58 to 0.80 in bivariate mixed-effects model), and comparable heterogeneity between datasets (I^2 79%, 95%CI 59 – 89%; test for heterogeneity on Cochrane's Q, p<0.001; Figure 5C). Diagnostic yield was similar to sputum, also with substantial heterogeneity driven by sample availability, rather than sensitivity of the test (mean 0.51, 95%CI 0.31 to 0.71, figure 5D).

A *post-hoc* exploration of individual patient factors associated with missing index test results was performed. Inability to walk unaided, reduced consciousness, severe sepsis, presence of danger signs, TBBC+, lactic acidosis, and early mortality were all associated with both no sputum, and with no urine, being obtained (tables 5 & 6).

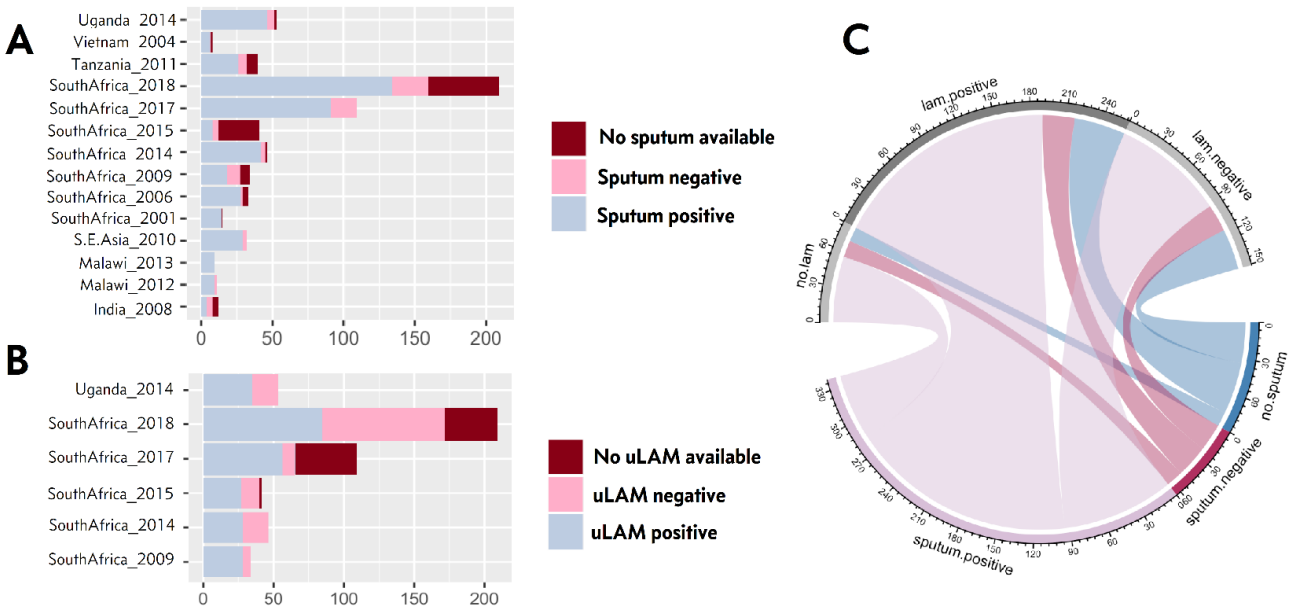

Figure 3-5. Availability and results of sputum Xpert or culture, and urine-LAM in patients with TBBC+.

Sputum results and urine-LAM are summarized by primary dataset (**A** & **B** respectively). **C**. Aggregate results of both index tests for datasets shown in B. This is a graphical representation of a contingency table. Marginal frequencies of the individual categories (sputum positive, sputum negative, no sputum available; uLAM positive, uLAM negative, no uLAM available) are shown by size of the radial segment. Cross-tabulations are shown by 'chords' connecting these segments; for example, the red chords show the number of sputum negative patients who were uLAM positive, uLAM negative, or had no uLAM available.

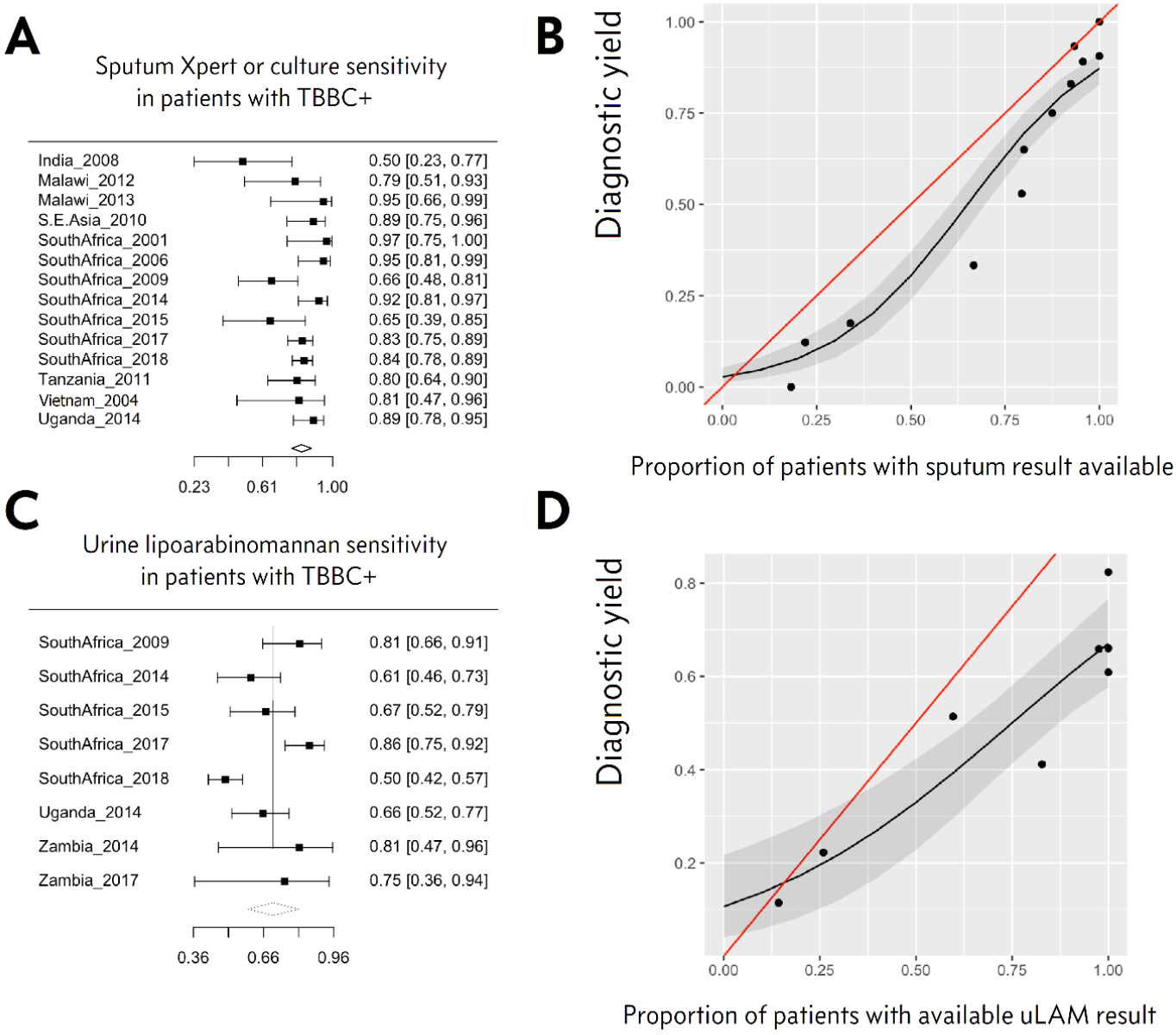

Figure 3-6. Sensitivity and diagnostic yield of sputum Xpert/culture and urine-LAM in patients with TBBC+.

A & **C**: forest plots of sensitivity (non-available tests excluded from denominator) of sputum testing and urine-LAM testing in patients with TBBC+. Where a sputum Xpert result was not available, sputum culture result was accepted as a surrogate. **B** & **D**: diagnostic yield – which accounts for non-diagnosis when test result is unavailable – of sputum testing and urine-LAM testing in patients with TBBC+, versus test availability. Red diagonal identity line represents maximum possible yield for given test availability (diagnostic yield = proportion with test sent who were positive). Each dot represents a dataset. Black curve shows predicted diagnostic yield for given proportion with test available, from a mixed-effects model with random effect by study and fixed effect of proportion of available test, with shaded 95% confidence interval generated from 1000-bootstrap replicates.

Table 3-5. IPD associations with probability of no sputum obtained.

	N	Unadjusted					N	Adjusted for clustering by dataset				
	obs	OR	95%CI			pvalue	datasets	OR	95%CI			p-value
Walks unaided	1859	0.41	0.29	to	0.57	0.00000	9	0.52	0.35	to	0.77	0.00100
Encephalopathic	977	2.63	1.67	to	4.09	0.00002	5	4.17	2.53	to	6.88	0.00000
Sepsis	1483	1.03	0.73	to	1.45	0.87107	10	0.91	0.62	to	1.35	0.65118
Severe sepsis	1350	1.23	0.84	to	1.78	0.27693	7	1.68	1.12	to	2.53	0.01266
Danger signs	1945	1.96	1.43	to	2.68	0.00003	11	1.62	1.11	to	2.37	0.01212
TBBC+	2131	1.82	1.39	to	2.38	0.00001	14	1.69	1.25	to	2.31	0.00080
Early mortality	1687	2.74	1.90	to	3.91	0.00000	12	2.71	1.78	to	4.11	0.00000
log CD4 count	2131	0.87	0.79	to	0.96	0.00663	14	0.93	0.83	to	1.04	0.20357
Age, per 10 years	2124	1.04	0.90	to	1.20	0.57781	14	1.04	0.88	to	1.22	0.65606
Tachypnoeic	1742	0.95	0.57	to	1.51	0.83815	9	1.44	0.82	to	2.53	0.20939
Pulse, per 10bpm	1318	1.01	0.94	to	1.09	0.75512	6	1.03	0.95	to	1.12	0.44950
Hypotensive	1017	0.76	0.50	to	1.14	0.19013	6	0.70	0.46	to	1.06	0.09467
log blood lactate	528	2.11	1.34	to	3.35	0.00133	1	-		-		-

Table 3-6. IPD associations with probability of no uLAM obtained.

	N	Unadjusted					n	Adjusted for clustering by dataset				
	obs	OR	95%CI			pvalue	datasets	OR	95%CI			ɔpvalue
Walks unaided	1334	0.20	0.14	to	0.29	0.00000	7	0.39	0.25	to	0.60	0.00002
Encephalopathic	949	4.17	2.79	to	6.22	0.00000	5	2.63	1.63	to	4.25	0.00007
Sepsis	950	1.63	1.05	to	2.63	0.03708	5	0.89	0.53	to	1.49	0.65336
Severe sepsis	950	3.51	2.44	to	5.10	0.00000	5	1.87	1.15	to	3.03	0.01195
Danger signs	1350	5.64	3.73	to	8.80	0.00000	7	2.38	1.43	to	3.96	0.00087
TBBC+	1473	1.76	1.24	to	2.47	0.00135	8	2.18	1.44	to	3.31	0.00026
Early mortality	1449	5.22	3.54	to	7.66	0.00000	8	2.18	1.33	to	3.58	0.00203
log CD4 count	1473	0.86	0.76	to	0.98	0.02158	8	0.88	0.75	to	1.03	0.11321
Age, per 10 years	1468	1.15	0.96	to	1.37	0.12704	8	1.09	0.88	to	1.33	0.43182
Tachypnoeic	1346	3.67	2.53	to	5.31	0.00000	7	1.47	0.85	to	2.53	0.16406
Pulse, per 10bpm	947	1.16	1.08	to	1.26	0.00014	5	1.14	1.03	to	1.27	0.01157
Hypotensive	945	1.94	1.35	to	2.78	0.00029	5	0.72	0.44	to	1.18	0.19769
log blood lactate	576	3.60	2.44	to	5.40	0.00000	2	1.93	1.20	to	3.09	0.00627

Encephalopathic = GCS<15 or AVPU < 4; sepsis & severe sepsis by Sepsis-2 definitions; early mortality = death in hospital or by 30-days follow-up; tachypnoeic = respiratory rate > 30 per minute; hypotensive = systolic BP < 100 mmHg.
Unadjusted estimates from univariate logistic regression; adjusted estimates are fixed-effects from mixed-effects logistic regression including random-intercept by primary dataset. OR = odds ratio of no available index test (sputum or urine); 95%CI estimated from fixed-effect standard errors (* +/- 1.96).

3.3.4 Mortality associated with TBBC+

Including only patients with a final TB diagnosis, and excluding those with missing observations on pre-specified variables, 2454 patients' IPD was available for mortality analysis. TBBC+ compared to blood-culture negative TB had a strong unadjusted hazard of mortality, which was most pronounced in the first 30 days of follow up (figure 6). Across all datasets, 10% (55/539) of patients with TBBC+ had died by day 5.

This association was adjusted for pre-specified dependent variables (age, sex, presence of WHO danger signs, CD4 count), and clustering by primary dataset, using mixed-effects logistic regression modelling. All variables were independently significant at $p<0.05$ except sex (table 7), and TBBC+ had the strongest association with OR 2.54 (95% 1.85 to 3.48).

On univariate, testing urine-LAM positivity was associated with death (OR 2.15, 95%CI 1.55 to 2.98, p=4.4e-06). This effect varied substantially by study, but a fixed effect of urine-LAM remains after accounting for random-effect by study (fixed-effect OR 1.67, 95%CI 1.13 to 2.46, p=0.0101). However, the effect is not independent of other variables in the model from the previous paragraph / table 7. This same model was reconstructed including only patients with available urine-LAM results. In this model, inclusion of TBBC+ significantly improved fit ($p<0.001$, comparing model with and without blood culture result by likelihood ratio test). By contrast, there was no evidence that urine-LAM improved model fit, either when included in addition to blood culture result ($p = 0.952$), or when added in place of blood culture result as a surrogate variable ($p=0.264$).

Finally, the association between time-to-TB-treatment (number of days from blood culture being taken to start of anti-TB therapy) and early mortality (dying before discharge or 30-days follow-up) was examined. In patients with TBBC+, early mortality varied in a 'U-shape': highest proportion of deaths was seen in patients with longest, or shortest, time-to-TB-treatment (figure 8). To reflect the WHO algorithm, 'treatment delay' was defined as time-to-TB-treatment greater than 4 days. Association of treatment delay with early mortality was adjusted for potential confounders in a logistic regression model (figure 9B). The strongest evidence for an

association between treatment delay and higher mortality was in patients with TBBC+, and the highest predicted probability of early death was in seriously unwell (danger sign positive) TBBC+ patients who had a delayed start to anti-TB treatment (figure 9A).

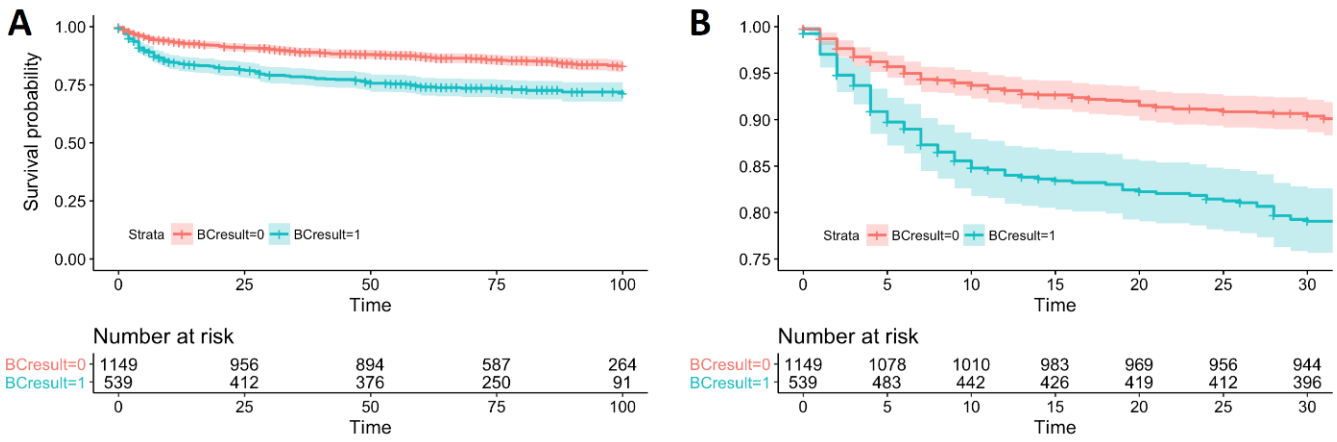

Figure 3-7. Naive Kaplan-Meier plot showing mortality over time by TBBC status.

Plots are unadjusted for dependence on primary dataset or other dependent variables. Mortality association with TBBC is maintained out to 100 days follow up (**A**), but occurs mostly in the first 30-days (**B**). Time in days since recruitment.

Table 3-7. Fixed effect associations with 30-day or inpatient mortality.

	Fixed effect OR	95%CI	p-value
Age, per 1 standard deviation increase	1.35	1.17 to 1.55	3.50E-05
Female sex	0.78	0.58 to 1.05	0.0981
Danger sign positive	1.87	1.23 to 2.84	3.20E-03
CD4 count, per 1 standard deviation increase	0.84	0.72 to 0.98	2.35E-02
TBBC+	2.54	1.85 to 3.48	7.24E-09

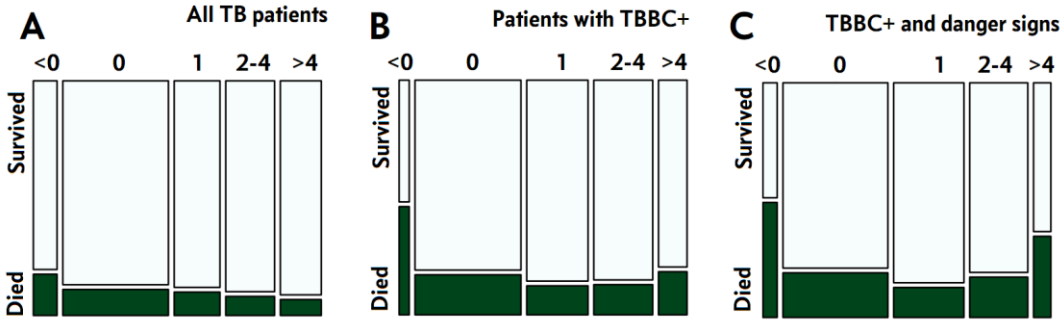

Figure 3-8. Mosaic plots of early mortality by time-to-TB-treatment in different patient strata.

Plots are proportional representations of contingency tables made from all IPD aggregated across primary datasets with available data. Time-to-TB-treatment was categorised into bins <0 (treatment started at least one day before blood culture), 0 (same day as blood culture), 2-4, or >4 days after blood culture. All patients with a final TB diagnosis (**A**), patients with a positive TB blood culture (**B**), and patients with a positive blood culture and at least one WHO danger sign recorded (**C**) are shown.

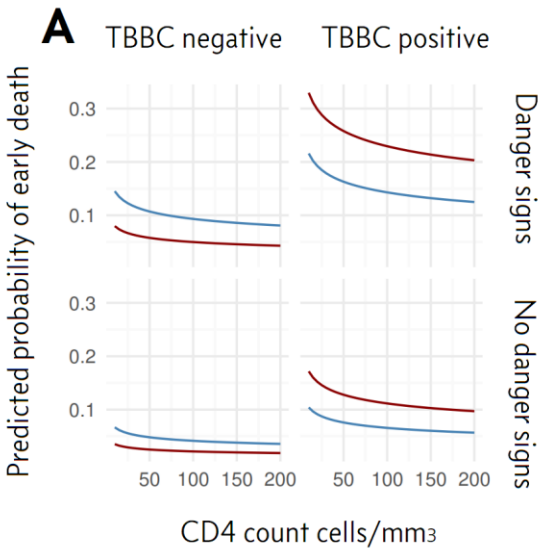

B

Variable	aOR	95%CI	p-value
Age, per 10-year increase	1.55	1.27 to 1.88	0.0002
CD4 count, per 1-log increase	0.58	0.47 to 0.72	0.0072
WHO danger sign positive	2.37	1.56 to 3.68	0.0001
TBBC+	1.62	1.03 to 2.57	0.0371
Treatment delay	0.51	0.17 to 1.22	0.1685
TBBC+ * treatment delay	3.50	1.03 to 13.0	0.0497

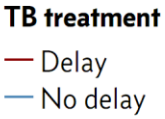

Figure 3-9. Predicted probability of early mortality in TB patients by CD4 count, danger signs, TBBC+, and TB treatment delay.

Adjusted odds ratios (**B**) for early mortality (death before discharge or before day 30 follow-up) in a logistic regression model including all patients with a final diagnosis of TB. Patients starting anti-TB treatment more than 24-hours before blood culture was taken were excluded due to concerns about confounding bias (patients who blood culture positive despite antimicrobial carry-over in plasma may have atypically high-burden or drug resistant disease). Available data did not permit inclusion of random-effects by primary dataset. An interaction term between TBBC+ and treatment delay (TBBC+ * treatment delay in B) was pre-specified. Age and log CD4 count were standardised (to have mean=0 and s.d.=1) for modelling.

3.4 Discussion

This analysis shows that blood culture positive tuberculosis is more common in HIV-infected inpatients than previously appreciated. A substantial amount of apparent heterogeneity between studies and settings can be explained by technical and clinical co-factors. Previous reports of TBBC+ prevalence are under-estimates because most studies have relied on a single blood culture, have not accounted for false negative results from antimicrobial carry-over in plasma, and have included patients with unobserved blood culture status (e.g. due to contamination) in the study denominator.

After adjusting for these co-factors, heterogeneity was reduced but not eliminated: estimated prevalence of positive TBBC amongst seriously unwell HIV-infected inpatients suspected of having TB still showed pronounced variation between primary study populations. This likely reflects differences in settings or inclusion criteria in the original studies resulting in different prior probabilities of tuberculosis. This interpretation is supported by the marked reduction in heterogeneity when only patients with a final TB diagnosis are considered.

Whatever the prior probability of TB in a given setting, presence of WHO danger signs and being unwell enough to be admitted to hospital both substantially and independently increase the posterior probability of a patient being TBBC+. In the final prevalence estimation model (model 7, table 4) adjusted fixed-effect ORs were 1.74 (95%CI 1.28 to 2.36) and 3.26 (95%CI 2.09 to 5.07), respectively, for presence of a danger sign and hospitalisation. In other words, the 'WHO algorithm for managing seriously unwell PLWHIV and suspected of having TB' is selecting for TBBC+ disease. The recommendations contained in the algorithm therefore need to be valid for patients with bacteraemic tuberculosis.

Sputum testing with Xpert is the central rapid-diagnostic step recommended in the WHO algorithm. We found a reasonable summary estimate of sensitivity for sputum testing (0.83; 95%CI 0.76 to 0.88), but with variation between datasets. Performance of sputum tests for diagnosis of TB in people living with HIV consistently show substantial unexplained heterogeneity on meta-analysis.[333-336] By limiting the case-mix

to patients with TBBC+ (lessening "spectrum-bias"[337]), heterogeneity was certainly reduced, but not eliminated. Variation in study design and conduct may have contributed to residual variance. Two studies had explicit biases – exclusion of patients unable to produce sputum despite induction,[21] and exclusion of smear-positive patients.[327] Datasets where the primary study aim was testing performance of diagnostics had highest observed sensitivity,[15,129,329,330] while cohorts recruited to define and explore mortality associations had lower sensitivity.[24,328] Arguably, the later better represent real-world conditions.

Further, use of sputum culture as a surrogate for Xpert result in this analysis will have overestimated sensitivity of rapid sputum diagnosis (sensitivity of Xpert is 0.89 overall, 0.67 in smear-negative cases, compared to culture, in meta-analysis),[335] but the newer Xpert-ultra platform (currently being rolled-out in South Africa) has improved performance (sensitivity 0.63 versus 0.43 for smear negative culture positive cases in the largest validation to date).[338]

A greater concern may be the even larger between-study differences in diagnostic yield, resulting from marked variation in sputum and urine availability. In *post-hoc* exploratory analysis, probability of obtaining sputum and urine was reduced in the sickest patients, a significant concern for the *seriously ill patient* algorithm, as reliance on these rapid diagnostics may be delaying diagnosis and treatment in patients at greatest risk of death.

An ideal rapid diagnostic test in patients with MTBBSI would be easily obtainable in critically unwell patients, and not show evidence of marked heterogeneity in diagnostic yield in different settings. This is emphasised by the finding that TBBC+ is strongly associated with early mortality (adjusted OR 2.54, 95%CI 1.85 to 3.48), with 10% of TBBC+ patients dying within 5 days of presentation in the pooled IPD.

The WHO *seriously unwell patient* algorithm recommends delaying presumptive treatment for 3-5 days when rapid tests are non-diagnostic. Evidence was presented suggesting that such a treatment delay is associated with a higher risk of mortality, specifically in TBBC+ patients. This analysis was complicated by confounding. In the unadjusted data, the highest risk of death was seen in patients with treatment delay of long or short duration. A plausible interpretation is that clinicians in these datasets were often prioritising early treatment in the most moribund patients. After adjusting

for factors like presence of TBBC+ and danger signs, the highest risk of death was in patients experiencing treatment delay. Time-to-antibiotic benchmarks are an accepted standard of care in severe bacterial and (non-tuberculosis) sepsis guidelines;[339-341] several of the cohort studies which underlie these recommendations have also shown a 'U-shaped' relationship between time-to-antibiotic and risk of death. [342-344] Studies which don't report an association between treatment delay and mortality in sepsis generally present the data in a way that such a U-shaped relationship would be obscured if present, and model the effect of treatment delay as linear. In the best-reported sepsis cohorts, a higher risk of death at shortest time-to-antibiotics is seen in the crude data, but shown to disappear in disease severity adjusted analysis, which instead affirm a mortality risk with treatment delay.[345,346] The current analysis is therefore consistent with the bacterial sepsis literature, and supports a similar emphasis on avoiding treatment delay in seriously unwell patients with HIV-associated TB. Nonetheless the confounding, and small sample size precluding modelling of random-effect by study, are weaknesses of this analysis.

While TBBC+ was strongly and independently associated with early mortality, positive urine-LAM was not. This is a surprising finding. Urine-LAM has been associated with mortality in previous studies, including several which contributed IPD to this meta-analysis. As shown here and elsewhere,[125,144] positive urine-LAM is strongly correlated with TBBC+. Even more importantly, two RCTs have shown large absolute mortality benefit from access to urine-LAM testing, specifically in patients with low CD4 count and anaemia who were very likely to have MTBBSI.[22,347]

Two factors can explain the weak association of urine-LAM with mortality in this meta-analysis. First, there was a strong association between non-availability of a urine-LAM result and death, suggesting missing-data bias reduced the mortality effect-size for urine-LAM. Secondly, heterogeneity in this effect size between primary studies was marked. Four studies have an above average mortality effect size for urine-LAM (SouthAfrica_2009, SouthAfrica_2014, SouthAfrica_2015, Uganda_2014), while the other four studies (SouthAfrica_2017, SouthAfrica_2018, Zambia_2014, Zambia_2017) have a below average effect size. These lower urine-LAM effect studies have higher mortality rates, more patients with profound CD4 count suppression, and higher rates of TBBC+ (table 3). In short, these studies recruited a *different patient stratum*. The consequence of stratifying analysis by a variable is the same as adjusting

for that variable. The effect size of urine-LAM is reduced when more urine-LAM negative, low-risk of death patients are excluded from a study: a Simpson's paradox.[130,131] This is illustrated with simulated data in figure 10. The TBBC+ mortality effect is robust to this adjustment, i.e. it is more independent of the stratification resulting from different recruitment criteria and settings.

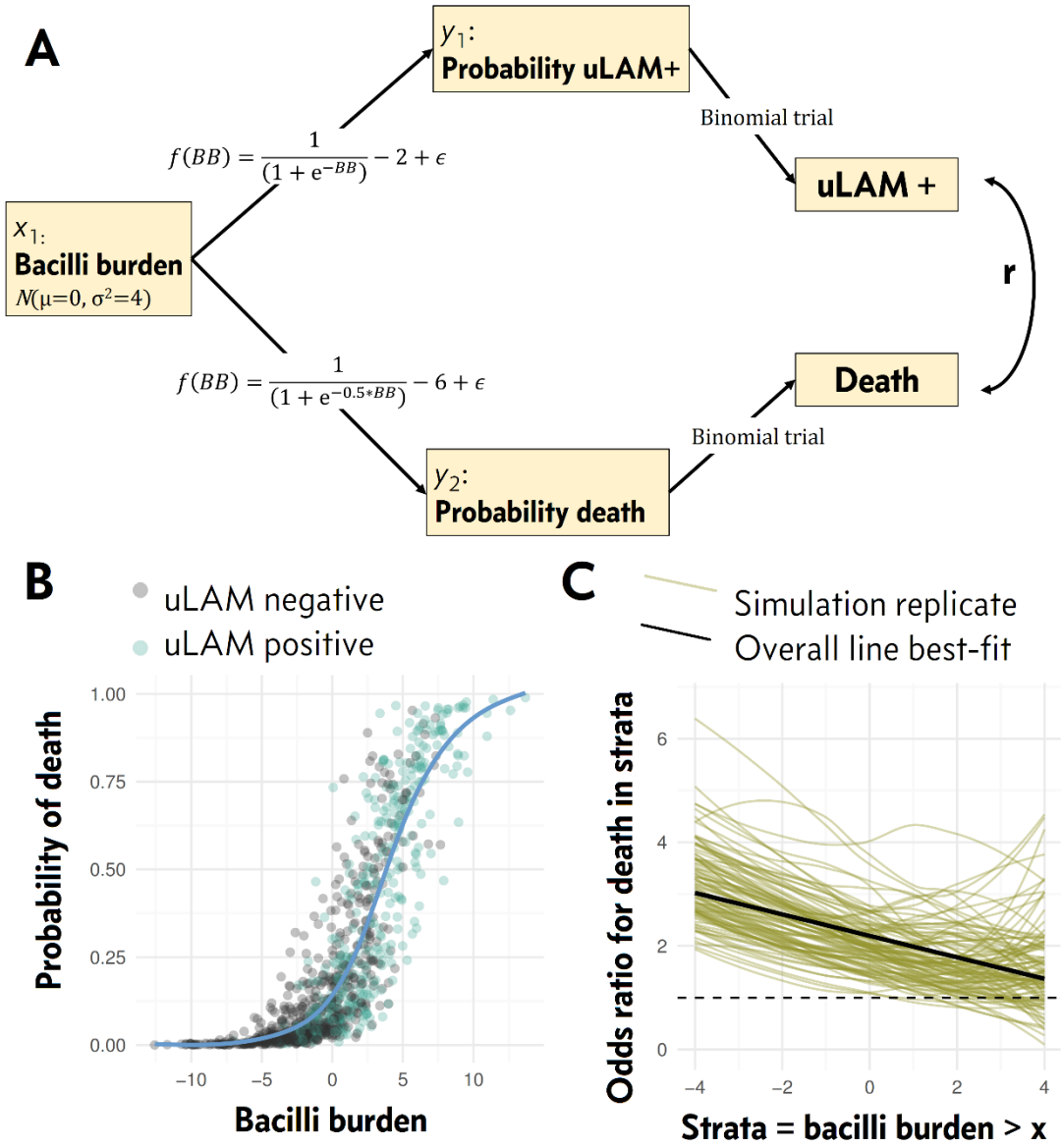

Figure 3-10. Simulating Simpson's paradox in relationship between urine-LAM and death.

A. Assumed causal structure in simulated data. Probability of urine-LAM positivity and probability of death are modelled as sigmoidal functions (plus random noise) of an underlying latent (unobserved) variable: "bacilli burden", which is itself a random normal variate amongst TB patients. A positive urine-LAM event and mortality event are in turn modelled as binomial trials of their respective probabilities. Urine-LAM positivity and mortality are therefore

correlated (r), but dependent on the underlying latent variable bacilli burden (which could be replaced by a proxy such as CD4 count or "MTBBSI" etc.). Adjusting for bacilli burden will render urine-LAM and death independent.

B. Example simulation based on the causal structure defined in A. 1000 patients were simulated with mean bacilli burden = 0, s.d. = 4, and dependent variables (urine-LAM and death) derived based on this variable. In this simulated data set there is an overall odds ratio for death from positive urine-LAM of ~ 2.5. If the data set is stratified by bacilli burden, such that only patients with more severe disease are included, with bacilli burden > 0, this reduces the odds ratio to ~1.4.

C. 100 repeated simulations of 1000-patients as per A&B were run. The mortality odds ratio for death from positive urine-LAM were recalculated for strata defined by a range of bacilli burden cut-offs in each simulation. As a higher cut-off is used, defining increasingly high bacilli burden strata, on average the odds ratio progressively falls. This is equivalent to adjusting the odds ratio by bacilli burden, by stratified analysis. The apparent effect-size of urine-LAM will depend on how inclusion criteria of a study sample across the range of patients' bacilli burden.

3.4.1 Implications & conclusions

Taken together, the above results argue that there are weaknesses in the WHO algorithm for managing seriously ill PLWHIV suspected of having TB. The algorithm selects for patients with TBBC+ disease; a significant proportion of these patients may be undiagnosed by sputum Xpert testing, and a significant proportion will die untreated if presumptive therapy is deferred for 3-5 days observation. PLWHIV with bacteraemic TB warrant specific research and guidance on diagnosis and empiric treatment.

To illustrate this point, consider the three randomised trials of presumptive TB therapy in PLWHIV reported to date.§§§§§ None of these trials have shown a mortality benefit, but all have used inclusion criteria likely to have selected against TBBC+ disease. The REMEMBER study randomised patients with CD4 count < 50 cells/mm^3 to receive HAART plus pre-emptive TB therapy, or HAART plus isoniazid preventive therapy (IPT), with identical 24-week mortality in both arms.[349] However, despite the low CD4 count, exclusion criteria included need for hospital admission (Karnofsky < 30), creatinine clearance < 30mL/min, and LFTs>2.5x upper limit of normal. In addition, participants suspected of having TB by their (non-study) clinician were

§§§§§ A fourth, the PrOMPT study was stopped early due to poor recruitment and has no useful results.348. Manabe YC, Worodria W, van Leth F, et al. Prevention of Early Mortality by Presumptive Tuberculosis Therapy Study: An Open Label, Randomized Controlled Trial. *Am J Trop Med Hyg* 2016; **95**(6): 1265-71.

excluded. As a result, only 5% of participants had haemoglobin < 8g/dL, 6% had a temperature ≥38.0°C, and 24-week mortality was only 5.2%.[349]

The TB FAST TRACK study was a cluster randomised trial in 24 antiretroviral outpatient clinics in South Africa.[350] In the intervention arm, HIV-infected patients with CD4 count < 150cells/mm^3 at high risk of TB (urine-LAM positive, haemoglobin<10g/dL, or BMI<18.5) had immediate initiation of TB treatment; medium risk patients (symptom screen positive but no high-risk criteria) had further TB investigations and review in a week; and in low-risk patients (not meeting criteria for medium or high risk) HAART was initiated immediately. Two-month TB treatment initiation rates were 62% versus 11%, and six-month mortality was 19 and 21 per 100 person-years, in the intervention and control arms respectively (adjusted mortality rate ratio 0.87, 95% CI 0.61 to 1.24). The trial has not yet been fully reported so sub-group analyses are not available, but it should be noted that only ambulant outpatients were recruited, and presence of danger signs was an exclusion criterion.

The third trial, STATIS, compared automatic TB treatment initiation in HIV-infected adults with CD4 count < 100 cells/mm^3, versus treatment based on extensive screening including chest x-ray, sputum Xpert and urine-LAM, with no difference in 24-week mortality between the arms (6.3% and 6.9% respectively).[351] Only ambulant outpatients with creatinine clearance > 50 mL/min and "no overt evidence that TB treatment should be started immediately" were included, and the final study population had relatively favourable characteristics (median haemoglobin 11.5g/dL, 95% with Karnofsky score > 80%).

Therefore, all three trials have – to a greater or lesser extent – recruited patient populations unlikely to have TBBC+ disease. No trial to date has adequately assessed for mortality benefit of empirical therapy in patients at high risk of MTBBSI.[******] Each of the three trials is also confounded by the ability of local clinicians to identify high-risk TB patients, who were excluded, or treated empirically in the control arms. The

[******] If this seems obvious, note that summaries of these trials often gloss over the highly selective inclusion criteria: "The STATIS study confirms and extends the findings of [the REMEMBER trial] that failed to demonstrate mortality-related benefits of empiric TB [therapy] among individuals with low CD4+ cell counts."352. Currier JS, Havlir DV. CROI 2018: Complications of HIV Infection and Antiretroviral Therapy. *Top Antivir Med* 2018; **26**(1): 22-9.

greater the ability of these clinicians to identify high-risk TB disease, the lower the effect size of presumptive therapy. Alternative designs would likely have been unethical, but this means these trials in fact tell us little about who should be treated empirically. The current meta-analysis suggests risk from delayed treatment would be most marked in danger sign positive TBBC+ patients. Hospitalised PLWHIV, who have danger signs and low CD4 count, and are suspected of having TB, should be treated without delay. This is particularly true if sputum is unobtainable and/or urine-LAM is not available. Patients with TBBC+ disease would be a rational pre-specified subgroup for analysis in any future empirical therapy trials. Proportion of TBBC+ patients treated as part of a presumptive therapy algorithm would also be a rational secondary outcome, more likely to be adequately powered than a hard mortality endpoint.

In contrast to the three empirical therapy trials, the STAMP study[22] recruited patients at much higher risk of TBBC+ disease: hospitalised patients with no exclusions based on danger signs, performance score or organ dysfunction. This study compared standard of care (sputum Xpert screening) to additional urine Xpert and urine-LAM testing in all HIV-infected adult inpatients in two hospitals in Southern Africa with severe burden of disease. Rates of empirical TB diagnosis were 8.3% versus 5.6%, and overall rates of inpatient TB treatment were 21% versus 14%, in the intervention and control arms respectively. Substantial absolute reductions in 56-day mortality were seen, but only in the pre-specified subgroups: CD4 count <100cells/mm3 (-7.1%, 95%CI -0.4 to -13.7%), and haemoglobin < 8g/dL (-9.0%, 95%CI -1.3 to -16.6%). These are sub-groups at increased risk of TBBC+ disease. This implies empirical treatment coupled with sputum Xpert screening misses fatal TB cases in these hospitals, and that these missed cases are predominantly in high-TBBC risk patients. The question is, are all of these cases detected by urine-LAM and urine-Xpert? Might a rapid blood diagnostic detect more cases, or detect MTBBSI cases more expediently? There have been calls for novel rapid diagnostic tests to be specifically validated in MTB BSI.[353] Chapter 5 of this thesis discusses development of novel same-day tests for identifying TB in blood.

Finally, the current meta-analysis supports the idea that, rather than being a rare event, MTBBSI is the mode of HIV-associated TB infection in hospitalised patients with severe disease. In the final prevalence estimation model (model 7, table 4)

adjusted fixed-effect OR for increasing from one to two TB blood cultures was 1.8 (95%CI 1.3 to 2.6). More than two blood cultures might increase the prevalence estimate for TBBC+ further still, but was not estimated because this would have extrapolated beyond the observed data. It was argued in chapter 1 that TBBC+ was just one window on MTBBSI. As discussed in the next chapter, culture may have limited sensitivity for detecting TB, both *in vitro* and in clinical samples. In chapter 5, the sensitivity of culture is compared to novel MTBBSI diagnostics, with the suggestion that, even with multiple cultures performed, TBBC+ patients are just a subset of patients with detectable TB in the blood stream.

4 Counting mycobacteria *in vitro*

4.1 Introduction

The idea that tuberculosis is best characterised as a continuous spectrum of infection – a spectrum chiefly established by the total number of bacilli in the body – is as old as the discovery that tuberculosis is caused by a bacillus.[47] As reviewed earlier, classical descriptions of tuberculosis held that "the number of bacilli reaching the blood stream and multiplying in the tissues is the main concern" for understanding post-primary disease.[106,107] It was further postulated in chapter 1 that HIV-associated MTBBSI was an extreme form of this haematogenous post-primary tuberculosis, and that TB blood culture, urine-LAM and urine-Xpert gave non-redundant, systematic measurements of this process. For diagnostics, clinical phenotyping, and assessing response to treatment, quantifying mycobacteria is of basic importance in clinical TB science.

Counting bacilli is also a fundamental task for basic TB research. Molecular mycobacteriology experiments, drug discovery assays, immune-cell multiplicity-of-infection protocols, and animal models in TB vaccine research, all rely on accurate, reproducible quantification of bacilli. How we count bacilli is a methodological issue underlying much of our current knowledge of tuberculosis.

Measuring mycobacteria is, however, not straightforward, in either research laboratory or clinical settings. And, while a multitude of methods have been described, direct comparisons and cross-validation between these methods are partial. In this chapter, established laboratory methods for quantifying mycobacteria are reviewed, with emphasis on inter-method comparisons and *M. tuberculosis* where data are available. The potential and technical difficulties of flow cytometry for counting and live/dead discrimination of bacteria are discussed. A novel *in vitro* method for flow cytometry

based absolute counting of mycobacteria is then described. This method is compared to gold-standards like colony forming unit (CFU) counting, exposing some major limitations of established approaches. Finally, *in vitro* antimicrobial killing of *M. bovis BCG* cultures is explored using the flow cytometry method, and it is concluded that additional pharmacodynamic information can be gleaned using this tool.

4.2 Established methods for counting mycobacteria

For convenience, methods have been grouped under the following sub-headings for review:

- bulk or batch measures;
- microscopy methods;
- secondary culture methods;
- molecular methods.

These distinctions are not absolute (e.g. several secondary culture methods could also be described as bulk or batch measures).

4.2.1 Bulk or batch measures

These are methods which quantify growth of a culture by directly or indirectly measuring cumulative mass or metabolic activity across the whole population of cells. These measures are, therefore, not count data, but are often – explicitly or implicitly – used to estimate bacterial number.

The classic bulk measure of broth cultures is *turbidity* (light scatter; assessed visually as degree of 'cloudiness') or *optical density* (attenuation of a transmitted light beam caused by absorption, reflection, scatter, and other physical processes; assessed with a nephelometer or spectrophotometer). These techniques are commonly used as methodological steps in mycobacterial research,[354-358] often to standardise an inoculum size. The assumption that optical density (OD) has a linear relationship with bacilli density is often implicit, and sometimes extrapolates from turbidity data for *E. coli* cultures (using 'McFarland standards') without further justification.[356,357] Only a few studies[359-361] have tried to empirically assess the relationship between turbidity / optical density and genuine count measures of *M. tuberculosis*, with conflicting

conclusions. Peñuelas-Urquides et al.[359] report R^2 values of 0.89 and 0.93 between CFU count and OD_{600} or McFarland units respectively. However, the figures in this paper suggest a non-linear relationship, over only 7 data points, with clear dependence of the residuals on culture growth phase – strongly suggesting the R^2 values are based on a mis-specified model. By contrast, Martin-Casabona et al.[361] show data with similar dependence of correlation between *M. tuberculosis* CFU/ml and OD on growth phase, but conclude that, overall, there is "no significant correlation" between these metrics.

Much more data is published for other mycobacterial species, but does little to resolve the confusion. For example, for *M. avium subsp. paratuberculosis* (MAP, a focus of bovine microbiology research) CFU/ml has been equated linearly to OD measures by several groups, including as follows:

- OD_{600} of 0.3 ≡ 10^9 CFU/ml;[362]
- OD_{540} of 0.65 ≡ 4 x 10^8 CFU/ml;[363]
- OD_{550} of 1.0 ≡ 2.8 x 10^6 to 10^7 CFU/ml.[364]

Note that, across studies, this would suggest that higher CFU/ml are associated with *lower* OD, which is nonsensical, beyond the conclusion that there is substantial, unexplained, between-study heterogeneity for the relationship between mycobacterial CFU and OD measures.

Alternative batch measures used for mycobacteria include those based on metabolic activity rather than cell mass. Examples include the "Alamar-Blue®" assay, in which non-fluorescent, blue oxidised resazurin is irreversibly reduced to fluorescent, pink resorufin when aerobically active cells consume available oxygen. This colour change can be detected giving a bulk-measure of cumulative metabolic activity of a broth culture. Resazurin assays are frequently used for qualitative or semi-quantitative read-outs in drug sensitivity testing of mycobacteria,[365-373] with only limited attempts to relate colorimetric values to cell counts such as CFU/ml.[371]

4.2.2 Microscopy methods

Semi-quantitative assessments of bacilli load are routinely made on clinical specimens using acid-fast staining and microscopy.[374] It is commonly asserted that the limit of detection for *M. tuberculosis* in sputum is 5000-10000 CFU/ml.[375-378] This seems to be based on a handful of small studies from the mid-20th century.[379-381] Only one of these studies reports crucial methodological details such as sputum volume processed or

number of microscopic fields examined. In that study (Hobby et al., 1973),[381] microscopy limit of detection was estimated 7.8 x 10^3 CFU/ml when 0.04 ml of sputum was examined on a $1cm^2$ area using a 97x objective. Importantly, this detailed study also reported that the ratio of microscopy bacilli count to CFU count was highly dependent on the patient that sputum was obtained from, and time on treatment: patients with extensive cavitation at baseline often had higher microscopy counts than CFU counts, and the difference increased with time on treatment (figure 1).[381]

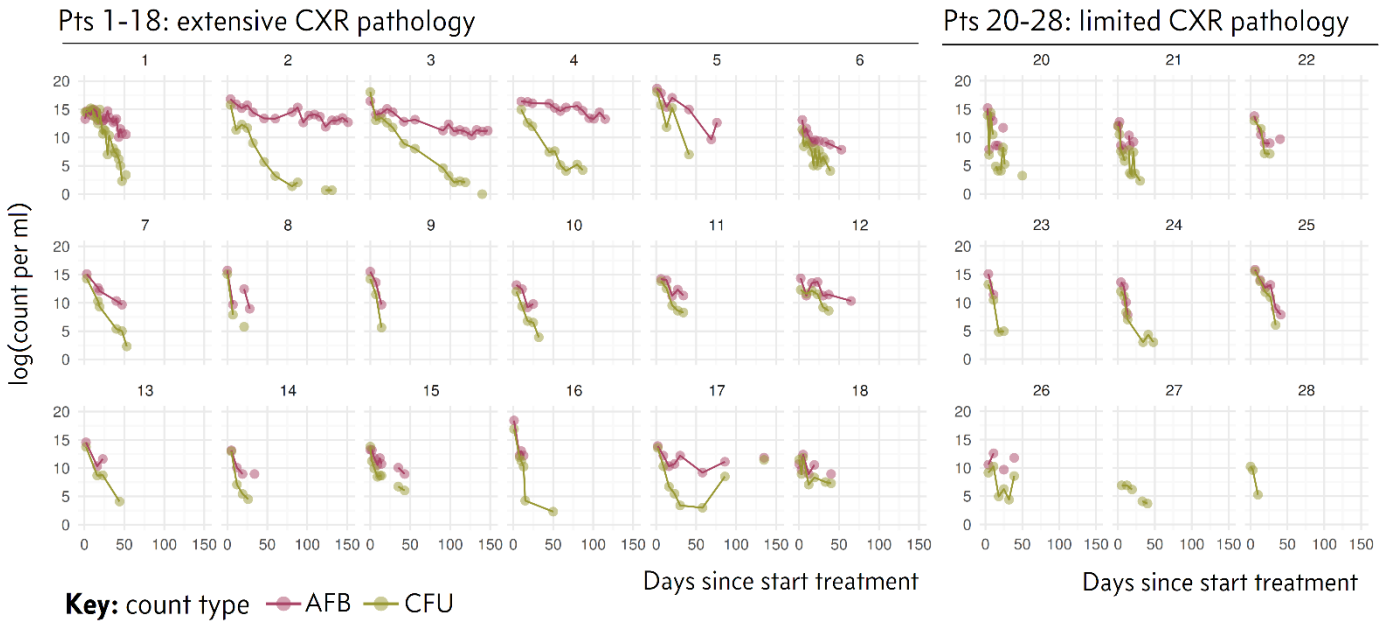

Figure 4-1. Hobby et al. comparison of CFU & Ziehl-Neelsen microscopy counts in sputum during first 150 days pulmonary TB treatment.

Raw data was extracted from the tables presented in Hobby et al. 1973[381] and plotted. Patients (pts) 1-19 had extensive chest X-ray (CXR) pathology; patients 20-28 had limited CXR pathology. AFB = microscopy.

Hobby et al. speculated that microscopy count may be more useful than CFU counting for assessing treatment effect in some patients. This line of enquiry has not been pursued. Instead development of mycobacterial microscopy has focused on improving qualitative, diagnostic sensitivity, with improvements in sample processing and use of alternative acid-fast staining techniques such as auramine-O.[382]

Quantitative microscopy of mycobacteria is seldom reported for *in vitro* samples. One protocol using acid-fast staining (Kinyoun method) and a Hausser counting chamber (haemocytometer) has been published.[383] The authors found microscopy counts and CFU counts to be the same (or within 1 standard deviation on technical replicates) for *M. bovis*, *M. marinum* and *M. smegmatis*, but found CFU counts to be over 3-times higher than microscopy counts in an *M. tuberculosis* multiplicity-of-infection assay – no explanation for this difference is suggested.[383]

Despite widespread use, standard acid-fast staining methods (auramine, Ziehl-Neelsen, Kinyoun) are surprisingly insensitive for mycobacteria. Compared to a gold standard of phase contrast microscopy, the novel fluorescent stain SYBR-gold identifies 99% of *M. tuberculosis* bacilli in log phase and non-replicating hypoxic broth cultures; transmission light microscopy with Ziehl-Neelsen stain, or fluorescence microscopy with auramine-O or auramine-rhodamine reveals only 54% to 86%, with particularly poor sensitivity for non-replicating cultures.[384] In addition, a wealth of evidence suggests that TB bacilli often lose acid-fastness; in some growth conditions, acid-fast bacilli may be the exception not the rule.[385-390]

4.2.3 Secondary culture methods: CFU counting, TTD, and MPN.

Following extensive optimisation work in the first half of the 20th century, CFU counting has remained the gold standard for mycobacteria quantification, for *in vitro* and clinical samples. CFU counting has the major advantage of giving a read-out for cells which are unequivocally alive, as proven by their ability to undergo binary fission and form colonies. However, CFU counting has notable limitations. From a practical perspective, CFU counting is slow, resource intensive, and requires extensive bio-safety level 3 (BSL3) precautions. It also has intrinsic accuracy constraints,[391] and – at least in clinical specimens – may show significant within and between lab variability.[392,393]

It is, however, possible that the major limitation of CFU counting is strategic rather than practical, and relates to the status of cells which do not grow on agar. Colony formation is unequivocal evidence of the existence of a living progenitor cell(s), *but the converse is not true*. Several lines of evidence point to the existence of a substantial viable but non-culturable (or at least 'differentially culturable') numbers of cells in a given *M. tuberculosis* population. First, clinical samples which are culture negative on

solid media can be culture positive when inoculated into parallel liquid broth cultures.[394-396] Serial dilution experiments suggest numbers of bacilli recoverable from sputum in liquid culture may be 10-fold higher than CFU counts from the same sputum.[397]

Bacilli growth is also dependent on presence of secreted enzymes, including resuscitation-promotion factors (Rpfs) and/or other molecules found in mycobacterial culture filtrate (CF).[398-400] These factors are not required for standard *in vitro* log-phase growth, but may be essential for recovery from a 'dormant' state and for survival in animal models.[400-404] Consequently, apparent numbers of viable bacilli may be up to 2 logarithms higher than CFU count, both in animal models, and *in vitro* depending on growth conditions.[405] Two groups have assessed Rpf-dependency of bacilli in patient sputum. Mukamolova *et al*. found that in 20/25 patients, 80 to 99.9% of bacilli in pre-treatment sputum were only detectable in presence of Rpf, that this dependence was lost in secondary cultures, and that the proportion increased in sputum samples obtained after start of anti-TB chemotherapy.[406] In a larger study, Chengalroyen *et al*.[407] found that 95/110 PTB patients had Rpf and/or CF dependent bacilli in spot sputums (some of which were probably from after start of treatment). In these 95 patients, the log ratio of CFU count to Rpf/CF dependent most-probable number seems to have ranged from ~0.2 to ~7.8;[††††††] this equates to 18 to 99.96% of bacilli being resuscitation dependent.

Returning to the practical limitations of CFU counting, other more convenient secondary culture methods have been developed to quantify bacilli. Several commercial liquid culture systems have been developed based on radiometric or colorimetric detection of metabolic activity (a bulk measure of bacterial growth), and are more standardised than, for example, the resazurin assay described previously. In spiking experiments, time to detection (TTD) of growth in these systems correlates with the number of CFU in the inoculum.[408] Although there may be other confounding attributes of the inoculum which influence TTD independent of bacilli number,[409,410] this correlation appears to be log-linear for clinical samples, at least over some range.[410-417]

[††††††] Reading from figure 2 in ref 407. Chengalroyen MD, Beukes GM, Gordhan BG, et al. Detection and Quantification of Differentially Culturable Tubercle Bacteria in Sputum from Patients with Tuberculosis. *Am J Respir Crit Care Med* 2016; **194**(12): 1532-40.

A second liquid culture quantification technique – most probable number (MPN) – has recently become prominent.[418] This method, used in the Rpf studies referenced above,[406,407] extrapolates results of a limiting dilution series to a bacilli count using a Poisson probability distribution. As well as greater speed, this method may have the advantage over CFU counting for detecting a greater proportion of the bacterial population – specifically bacilli which are culturable in liquid but not solid media. What proportion of "viable non-culturable" cells this represents in unknown.

4.2.4 Molecular techniques

Detection of nucleic acid has become a mainstream approach for *M. tuberculosis* diagnosis with the roll-out of the Xpert MTB/RIF platform. Xpert modules use real-time polymerase chain reactions (RT-PCR) and can therefore report cycle threshold (C_T) values which should reflect number of genomic copies in the original sample. Xpert C_T values have been shown to have log-linear correlation with CFU count in spiking experiments across range 2 to 7 $\log_{10}$ per ml.[419,420] In a multisite comparison study of clinical sputum samples, Xpert C_T correlated with AFB smear grade (Spearman's rho, -0.63), TTD in liquid culture (rho, 0.67), and CFU count (rho = -0.53).[421] All these correlations were strengthened by excluding samples with high internal control C_T values (an indication of PCR inhibition), and all were noted to vary substantially between different sites. Xpert C_T values have been largely dismissed as a measure for pharmacodynamic studies, due to comparatively low (compared to TTD and CFU counts) ratio of between-group to within-group variance when comparing groups of patients on different antimicrobial regimens in an EBA study.[422] Given how poorly CFU and TTD dynamics predict phase 3 trial end-points the logic of this is unclear to me: the real question is whether the between-group variance (whatever its magnitude) correlates with relevant clinical endpoints, and this remains untested to my knowledge. Nonetheless, one theoretical concern is that, although Xpert only processes intact bacilli, the viability of these bacilli is unknown. In qPCR systems where genomic copies are related to C_T values by an empirically derived standard curve a 10 to 100-fold excess of genomic copies is reported compared to CFU in animal or cell-culture derived bacilli.[423] The use of 16S rRNA instead of DNA for qPCR is the basis of the molecular bacterial load assay (MBLA) based on the tenet that rRNA levels will decline more rapidly with cell death.[424] Normalised against C_T values from an *in vitro M. tuberculosis* culture, the MBLA measure correlates with CFU count

in clinical samples.[425] This would imply MBLA does not 'observe' the differentially culturable bacilli described by Chengalroyen *et al*. and Mukamolova *et al*. Conversely, MBLA showed a different pharmacodynamic profile compared to CFU or TTD in a mouse model of tuberculosis, implying that it does measure a different subpopulation of bacilli.[426] In that study, MBLA predicted numbers of bacilli were *lower* than CFU count at baseline, becoming higher than CFU count after ~4 weeks of treatment. This is unsurprising given that the MBLA assay is normalised against *in vitro M. tuberculosis* cultures, and highlights that the relationship between number of bacilli and RNA production is likely to be highly non-linear and dependent on conditions. Of note, mRNA can be detected in (culture-negative) broncho-alveolar lavage samples at end of treatment in pulmonary TB patients with stable cure.[427]

C_T values may not be directly comparable across different sites / instruments, due to differences in amplification curve performance and background fluorescence. Digital PCR (dPCR) overcomes this problem by providing true count data. By running individual well PCRs in limiting dilution series, the most probable number of genome copies can be determined with reference to an essential Poisson probability distribution rather than an empirically derived reference curve. Consequently, dPCR has substantially lower between lab variance, and has been suggested as an appropriate QA reference for TB laboratories running other PCR techniques like Xpert, avoiding the uncertainties about CFU counts.[428] Number of genomic copies found by dPCR in a broth culture of *M. tuberculosis* are approximately 2-fold in excess of CFU counts, although this estimate is based on a single culture preparation without any published details of culture conditions.[428]

Of note all the above molecular methods are subject to the efficiency of nucleic acid extraction methods. Comparisons of methods in mycobacteria suggest efficiency differs by orders of magnitude, without obvious consensus as to the best method.[429-434]

In summary, CFU counting remains the gold standard for enumeration of mycobacteria. Other methods are generally normalised against this standard, but also indicate that a proportion of bacilli do not form CFU, and this proportion differs by growth conditions. Alternate methods which aim to capture viability, such as those based on oxygen consumption or RNA production, do not provide direct count data. The only alternative direct-count viability read-out method is MPN, which has been

used to show that CFU forming bacilli are a minority population of viable bacilli in sputum samples from most, but not all, patients. Counting bacilli may be fundamental to clinical and basic TB science, but there is much uncertainty about established techniques.

New methods able to give direct cell counts, with single-cell level viability assessment, and an absolute cell count 'denominator', would help resolve some of these uncertainties.

4.3 Flow cytometry & the live/dead discrimination of microbes

The potential of flow cytometry (FCM) to advance microbiology has been heralded by many, largely for two reasons. First, FCM characterises individual cells, and therefore may reveal phenotypic heterogeneity across microbial populations. Second, this single-cell analysis can occur without prior culture amplification, potentially avoiding biases introduced by this manipulation of the microbes under study. However, despite this anticipation, FCM has not yet been widely adopted in microbiology, and there are several difficulties associated with flow cytometry of prokaryotes.

4.3.1 Technical challenges of bacterial FCM

4.3.1.1 Size, sensitivity and specificity

Mammalian cells typically examined by FCM are about 1000-fold larger than typical bacterial cells,‡‡‡‡‡‡ and flow cytometer hardware parameters (such as acceptable levels of stray light, and size of sheath fluid core) are calibrated to measure eukaryotes, not prokaryotes.[435] Therefore, FCM detection of bacteria is relatively insensitive. It also means FCM signals from bacterial cells, e.g. light scatter, readily overlap with 'background' signals such as electronic noise and/or physical artefacts such as bubbles and micelles found even in 0.22µm filtered media and buffers.[436]

‡‡‡‡‡‡ Assuming *E. coli* width and height 0.5 and 2 µm and approximately cylindrical shape, gives volume, $V = \pi(0.5/2)^2*2 = 0.4\ \mu m^3$; assuming diameter 12µm and approximately spherical shape for a large human lymphocyte, gives volume, $V = 4/3\ \pi(12/2)^3 = 900\ \mu m^3$

This sensitivity and specificity problem is the primary challenge in bacterial FCM, and several strategies have been suggested to overcome it. Firstly, dual-thresholding – using two FCM signals, e.g. forward and side scatter, as a composite threshold / trigger-channel for recording events§§§§§§ – is recommended, along with extensive empirical determination of cut-off values for a specific experiment's conditions.[437,438] Second, it is preferable that a fluorescence signal from a nucleic acid stain be used as one of the dual threshold signals, instead of the two light scatter signals.[436,438] Third, given the smaller volume, surface area, protein or nucleic acid content of prokaryotes, very bright dyes are required.[438,439] Fourth, because saturation of data acquisition capacity can occur, and duration of laser excitation can increase fluorescence or decrease it through bleaching, the flow rate and cell density of the FCM sample must be optimised to the specific experiment.[435,437,438,440]

4.3.1.2 Cell clumping

Many bacteria clump during liquid culture in suspended biofilms or microcolonies,[441] a specific problem for single-cell FCM analysis, but also a general problem for any bacterial quantification method. Bacteria can also form exopolysaccharides in response to common fixation procedures which results in further agglutination.[436] Disaggregation strategies include chemical and physical processes. For mycobacteria, high concentrations of the detergent Tween80 have been used in media along with continuous agitation during culture.[442,443] Vortexing, sonication or repeated needle passage (e.g. through a micro-emulsifying needle) have also been used.[444-447]

4.3.1.3 Unpredictable response to fluorescent staining

Bacterial species have greater physiological and genomic diversity than mammalian cells, and dyes which reliably stain one bacteria may show different and unpredictable uptake or efflux. Early proponents of bacterial flow cytometry were surprised to find that DNA staining by a given dye varied between closely related species, and that chemically similar dyes gave unpredictable results within the same species.[435,448] More recently, it was shown that membrane integrity, as measured by 'cell impermeant' nucleic acid stains (described in detail below), could vary depending on growth stage of a batch culture, with this variability in turn being species dependent.[449] Therefore,

§§§§§§ The concept of thresholding is described in more detail in section 4.8 for readers unfamiliar with flow cytometry jargon.

while commercial staining kits for bacterial FCM exist, testing and calibration to specific species and experimental conditions is required.

4.3.2 Live/Dead discrimination of bacteria by fluorescence staining

For some dyes the degree to which their fluorescence associates with a cell depends on a specific structural or physiological attribute of that cell. Functional status can therefore be probed by these fluorescent stains, and this information used to define bacteria as alive or dead. Examples of functional parameters probed by these dyes are described below.

4.3.2.1 Membrane integrity

It is argued that an intact cell membrane is necessary condition for a bacterium to be considered living. An incompetent membrane can be detected when a cell exhibits fluorescence from a dye normally excluded by an intact membrane. These 'dye exclusion tests' often use a molecule which increases fluorescence when bound to an intracellular component such as nucleic acid; this improves signal to noise ratio, and can remove the need for a wash step to remove extracellular dye. Accuracy of the membrane integrity signal can be further improved with normalisation against a second concomitant dye which stains cells irrespective of membrane integrity.

This is the basis for several commercially available bacterial FCM staining kits, such as BD Biosciences' Cell Viability Kit[450] and ThermoFisher's LIVE/DEAD® BacLight™ Bacterial Viability Kit,[451] both of which use the cell impermeant red nucleic acid stain propidium iodide (PI) to detect membrane incompetence, and a secondary cell permeant green fluorescence stain (thiazole orange or SYTO-green respectively): dead bacteria are purported to have a high red to green fluorescence ratio – revealed as a discrete population on a red against green fluorescence scatter plot.

Despite the commercial kits' resounding names, there are multiple warnings in the literature against a simplistic live/dead inference based on PI staining of bacteria. As mentioned above, some species show high PI uptake during early exponential growth, and are still able to form colonies despite PI positivity during cell sorting.[449] Other conditions – including sonication – have also been found to cause temporary PI permeability.[452] *Micrococcus luteus* cultures rendered PI positive and unable to form colonies by prolonged starvation may be resuscitated under specific conditions.[453]

Even if a (PI impermeable) intact cell membrane is a necessary condition for a bacterial viability, it may not be a sufficient one, if dead cells can still have intact membranes. Bacteria inactivated by ultraviolet radiation provide a model example of cells with intact membranes which are found to be non-viable by any other measure.[454]

Further, it has been pointed out that any bacterial killing which aggressively damages nucleic acids may give a weak fluorescent signal as the dye target site is degraded along with the membrane.[455,456] Generalising this observation, the temporal mechanisms of cell death will likely influence dye exclusion tests such as PI positivity. For example, from the point of view of a dye exclusion test, bacterial killing via non-membrane targets ultimately leading to rapid lysis and disappearance of the cell would look very different to bacterial killing through progressive cell membrane damage, even when both killing mechanisms were equally effective. This implies that serial observations and absolute cell counts (i.e. a total cell denominator) could be useful for unbiased assessment of bacterial killing by fluorescent staining methods.

The secondary dye common to commercial bacterial viability staining kits, intended to stain both live and dead cells, could facilitate absolute counts. This hinges on the ability of the secondary dye to reliably penetrate intact membranes, and again this is shown to be dependent on species and conditions. Langsrud & Sundheim found that SYTO-9 reliably penetrated *Staphylococcus Aureus* but not ~30% of pseudomonas species tested, resulting in poor correlation between live/dead counts and CFU counts, but also found that the alternative dye SYTOX-green reliably penetrated all the pseudomonas species tested.[457] Again the emphasis here is that dyes behave differently in different species of bacteria.

Finally, while PI is the most common fluorescent dye for bacterial dye exclusion testing, several others exist. Predictably this adds a further dynamic to the interpretation of membrane function as a viability indicator: in head-to-head comparisons different membrane exclusion probes are taken up by different proportions of bacteria under the same controlled conditions.[458] Some authors have suggested that "the magnitude of membrane damage can be measured with the use of different [membrane integrity probe] dyes, but conclusive information in this regard is still required".[459]

4.3.2.2 Enzyme activity

Esterases with broad substrate activity are ubiquitous in the cytoplasm of bacteria.[460] Esters which are lipophilic, non-polar, and non-fluorescent, but become charged and fluorescent on hydrolysis by these bacterial 'house-keeping' esterases, can function as fluorescent probes of enzyme activity or metabolic competence. Examples of such dyes include fluorescein diacetate (FDA) and calcein-AM.

While esterase activity may correlate with concentration of ATP in microbial samples,[461] the actual hydrolysis reaction is not energy dependent, so is not a direct assessment of vitality.[462] Cells with damaged membranes may even display higher ester-dye cleavage, presumably because of better transport of the dye into the cell which still has intact enzymes.[463] Conversely, 'dormant' cells may have low esterase activity but still be culturable.[464] Therefore, interpretation of FDA or calcein-AM fluorescence probably requires a trend rather than a single time point.

4.3.2.3 Other methods

Maintenance of membrane potential, which drives ATP synthesis, active transport of ions, and homeostasis of the intracellular environment, is a requirement for cell viability. Uptake of some charged dye molecules is also dependent on membrane potential (cationic dyes can accumulate in polarised cells, anionic dyes can accumulate in depolarised cells).[437,464,465] Use of these dyes is technically challenging because outer membranes may have to be permeabilised to test the membrane potential of the inner membrane, and these dyes are fluorescent irrespective of location so may require wash steps and specific additives to define negative controls.[437,464,465] Further, the mechanism of cell death would in theory impact on the time-dependence of observed changes in membrane potential.[464]

4.4 Conceptualising cell viability & death in bacteria

It is clear from the above review that defining bacterial viability or death is not straightforward. Consequently, several authors have proposed conceptualising a continuous spectrum of cell states between alive and dead, "perhaps defining one or more pathways by which [bacilli] are eliminated [in an] experimental system or host".[466] Two examples schematics are reproduced in figure 2. The final determining

events in bacterial cell death – the "points of no return" on the different measurable dimensions of cell viability – are unknown.

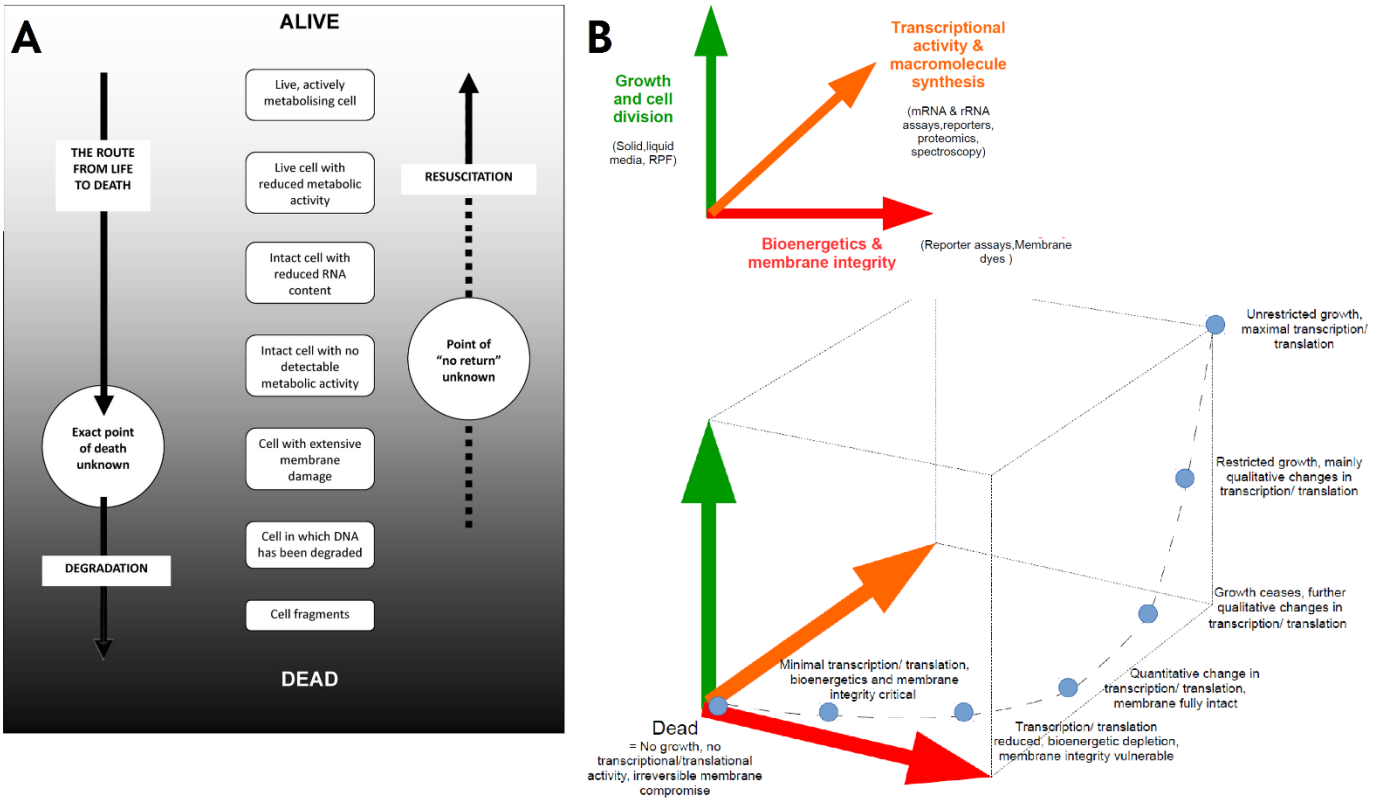

Figure 4-2. Continuous spectrum of live/dead cell states of bacteria.

A. Ability to probe more microbial cell characteristics than just CFU formation means cells can be classified into more subpopulations than just "live" and "dead". The route from live to dead can therefore be thought of to contain several steps, not all of which may occur in all cases. Reproduced from Davey 2011.[467] **B**. Probes of cell state represented on 3 axes. The lower plot shows one of many possible pathways to death for mycobacteria. Reproduced from Davies 2015.[466]

4.5 Flow cytometry of mycobacteria

Several reports of the use of flow cytometry to quantify viability of mycobacteria have been published (table 1). To summarise:

- Previously used fluorescent stains include nucleic acid binding dyes (SYTOX-green, SYTO-9, SYTO-BC, SYTO-16, SYBER-green I, propidium iodide, TO-PRO-3 iodide, auramine-O) either to probe membrane integrity or in an attempt to stain all cells; esterase substrate dyes (fluorescein diacetate, calcein-violet); and membrane potential probes (diethyloxacarbocyanine iodide, rhodamine-123).

- Few studies have reported methods or justification for how bacilli have been separated from noise, i.e. how sensitivity and specificity have been optimised. Those that do have mostly used side and forward light scatter (SSC & FSC) to set thresholds/trigger levels, voltages, and gates to define what is a bacillus, along with a variety of negative controls and positive controls (e.g. beads) to assist with gating.
- With only one exception,[444] absolute bacilli counts have not been derived from FCM, instead batch measures of fluorescence (e.g. mean fluorescence signal), qualitative results (e.g. scatter-plots), or percentages are reported. No comparisons of flow counts to CFU exist.
- Growth conditions, processing (e.g. washes and fixation), staining protocols, vary widely. In the few cases where the same stains have been used by different groups, results are contradictory; for example propidium iodide is reported to stain 0% of heat killed *M. tuberculosis* by one study,[468] and 100% by another.[469]

Table 4-1. Flow cytometry of mycobacteria: prior literature.

Ref	Myco-bacteria	Purpose of the cytometry	Stain	Incubation	Output	Permeablisation, wash, fixation etc	Flow parameters
Hendon-Dunn, 2016.[443]	H37Rv	Develop rapid FCM tool for determining antibiotic activity against M.tb	Calcein violet AM SYTOX-green	60 min at RT	%s in four populations defined by Calcein violet and SYTOX-green staining, across serial time points and concentrations of antimicrobials	After staining, 2885g 2min, resuspended in HBSS with 4% formaldehyde v/v 30min fixation time for sterility.	Unstained controls used to set SSC FSC defined gate on 'bacteria'. Voltages in SG and CV-AM channels set such that unstained events were all in the first order of log scale histogram, all samples analysed on these settings.
Hammond, 2015.[470]	*M. smegmatis, marinum, fortuitum, bovis (BCG)*	To measure the proportion of lipid body +ve cells in *in vitro* cultures	Nile red	20min at RT, with agitation	%s Nile red +ve and -ve over time points	They probably washed with 100% ethanol, and then PBS	Unknown
Gonzalez, 2012.[471]	*M. smegmatis mc2 155*	Defining growth curves	SYTO 9; PI; SYTO BC	25min RT	Unclear	None (not specifically mentioned)	FSC and SSC "used to discriminate bacteria from background"
Soejima, 2009. [469]	H37Ra	Live dead discrimination, method development	SYTO9 and PI	unknown	Unclear	Unknown	Unclear
Qin, 2008.[472]	H37Ra	Detection of *M.tb* in clinical specimens (spiked urine).	Anti-MTB conjugate fluoresecent silica nanoparticles and	1 h at 37oC for the conjugated nanoparticles, then 15min RT for the	Absolute counts are shown, but unclear how they were derived.	None	Unclear

			SYBR green I	SYBR-green			
Shapiro, 2008. [473]	*M. smegmatis*	SOP for live dead discrimination with DiOC2(3)	DiOC2(3) TO-PRO-3 iodide	5 min at RT	Qualitative plots	None	FSC and SSC as trigger signal +/- 'software gate' to exclude noise/debris. Detailed normalisation of signals to adjust for cell size.
Shi, 2007.[449]	*M. frederiksbergense*	Comparing different markers of proliferation/viability	PI; diOC6(3); Hoechst 33342	diCO6(3): 4 min at 20oC PI: 10 min at 20oC Hoechst: 45min at 20oC	% PI positive and diCO6(3) positive. Proportions with different chromosome numbers as a marker of physiological / growth state.	Various wash steps; no fixation/permeabilisation.	FSC and SSC "trigger signal for first observation point", amplification on linear or log scale dep on application. Beads and internal DAPI stained bacterial controls for alignment of FCM, max CV value 6%.
Fredricks, 2006.[474]	35 clinical *M.tb* isolates; *M bovis BCG*.	DST	unknown	unknown	Aggregate measures only (no single cell counts)	paraformaldehyde to final concentration of 1.4%	Unclear
DeCoster, 2005. [475]	*M.tb* clinical isolates	DST	FDA	37oC 30min	Ratios of mean fluoresence channel (cf controls) - summary measures, no true single cell data.	None	Unclear
Akselband, 2005. [447]	*M.tb, M. bovis (BCG), M. avium*	DST	Auramine-O	Cellswere incubated inside gel microdrops	Aggregate measures only (no single cell counts)	Washing and fixation carried out - all inside microdrops	Light scatter thresholding to exclude 'majority of unoccupied microdrops', a gate on remaining microdrop population applied before FL1 analysis. Time 0 sample used to set voltage.
Reis, 2004. [476]	*M.tb* isolates	DST	FDA	Norden method	Aggregate measures only (no single cell counts)	formaldehyde to final concentration 10% for 1 h	Unclear
Govender, 2010. [477]	13 MDR-TB	DST	SYTO16; PI	SYTO16 [10uM]	Aggregate measures only (no single cell counts)	Pellet resuspended in 250 µl Isoflow sheath fluid.	Unclear

	isolates plus H37Rv			30min; PI [20 µg/ml] for 60 min		Vortex, needle emuslification.	
Burdz, 2003. [478]	H37Ra and various respiratory tract bacteria	Live / dead discrimination, testing sputum decontamination methods	SYTO 9 and PI; SYTO BC plus microsphere standard	"as per manufacturer instructions "	Absolute counts are made, but the data presented are the 'log-kill' which is baseline log count - log count post decontamination…	Multiple wash steps.	Unclear
James, 2000. [442]	H37Rv	Characterisation of the light scatter properties of continuously cultured M.tb	None	n/a	Qualitative plots	None (not specifically mentioned)	Minimal detail
Piuri, 2009. [479]	*M. smegmatis, M.tb* MC(2)6230	DST	In house fluoromyccobacteriophages	variable	Qualitative plots	2% paraformaldehyde	Minimal detail
Norden, 1995. [480]	H37Ra	DST	FDA 250ng/mL final conc	30min at 37oC	Mean channel fluoresecnce and 'events per second' - but not validated as an absolute count	Foramlin fixation	"Initially, viable and heat-killed... differentiated from 7H9 particles by using FDA fuorescence. Live gating was performed ... during data acquisition to exclude all 7H9 particles"
Bownds, 1996. [481]	*M. avium, fortuitum, gordonae, marinum*	DST	FDA 100ng/mL final conc	30min at 37oC	See Norden 1995 method	None	See Norden 1995 method
Kirk, 1998. [482]	*M. tb* clinical isolates	DST	FDA 250ng/m	30min at 37oC	Aggregate measures only (no single cell counts)	None	"M. tuberculosis cells were detected and differentiated from non-Mtb particles by FSC and SSC… background events and

			L final conc				electronoc noise eliminated by thresholding"
Moore, 1999. [483]	*M.tb* clinical isolates	DST	None	n/a	Same as Vena 2000 / based on Norden 1995	~1% paraformaldehyde for 40 min	Based on Norden 1995
Vena, 2000. [484]	MAC	DST	None	n/a	A ratio of events per unit time for condition versus control is given, but no validation of these as absolute counts	200uL culture added to 200uL PBS + paraformaldehyde (->final conc 1%), 45minutes.	"Electronic noise and background particles in the 7H9 medium excluded... by adjusting the threshold monitor listed on the WinBryte software program... [on FSC & SSC]"
Ibrahim, 1997. [485]	MAC	Investigating growth cycle, including effects of isoniazid	SYTO16	Overnight at RT	Essentially qualitative	Pellet resuspended in ice-cold 70% ethanol through a 24-gauge needle; stored at – 20oC. Washed filtered distilled water.	Unclear
Ryan, 1995. [486]	*M. bovis, M smegmatis*	DST	Auramine -O PI	See Akselband 2005	See Akselband 2005	See Akselband 2005	See Akselband 2005
Yi, 1998. [487]	*M. tb*	Detection of *M.tb* in clinical specimens.	Fluoroscein labelled Ab	Variable	Aggregate measures only (no single cell counts)	Multiple wash steps	Unclear
Resnick, 1985. [488]	*M. smegmatis*	To detect changes in membrane potential	Rhodamine 123	60min (?at 37oC)	Aggregate measures only (no single cell counts)	Washed twice in PBS	Unclear
Scott, 2011.[444] *	*M.tb*	Enumeration as part of GXP EQA pilot study	Auromine O	None: "immediately analysed"	Absolute counts from FCM	All cultures inactivated by resuspension in PBS/GXP sample reagent mix for 2h; this then washed twice in PBS.	Used 1uM beads to initially set light scatter thresholds and amp gains. Side scatter used to threshold flow on bacilli. FL1/SSC gating to define final bacilli population for counting.

Studies identified by search PUBMED (mycobacter* AND cytometry)ALL FIELDS , plus references screen

* Flow cytometry method obtained by personal communication as not detailed in publication.
M.tb = *M. tuberculosis*. DST = Drug sensitivity testing. GXP = GeneXpert. EQA = External Quality Assurance. PI = propridium iodide. SYTO, SYTO , SYTOX are proprietry dye names. FDA = fluorescein diacetate. DiOC = diethyloxacarbocyanine iodide. RT = room temperature. FSC = forward scatter. SSC = side scatter. FL1 = fluorescence channel 1. Ab = antibody. CV = coefficient of variation. +ve = positive. -ve = negative.

Studies which have explicitly used flow cytometry to study 'viable non-culturable', or 'differentially culturable' bacilli are rare. The leading example is a study by Hendon-Dunn *et al*. which aimed to assess antibiotic effects against the whole population of *M. tuberculosis* in a broth culture rather than "just those bacteria that can grow in media post-exposure".[443]

It is worth reviewing the methodology and results of this seminal work in detail. H37Rv was grown in continuous culture using a chemostat system; the esterase substrate dye Calcein violet AM (CV-AM), and the membrane integrity probe SYTOX-green were used for flow cytometry. Signal thresholding / voltage manipulation strategy to define flow events as cells used unstained control samples to set a population gate around bacteria using FSC and SSC; voltages in the fluorescence channels were then adjusted so that histograms of unstained bacteria were contained in first order of log scale for fluorescence. Dual-staining of a variety of controls were used to define 4 functional subpopulations (P1 to P4) on CV-AM versus SYTOX-green fluorescence flow plots:

- P1: CV-AM negative / SYTOX-green negative; gate set so >95% of unstained control cells were within P1.
- P2: CV-AM positive / SYTOX-green negative; antibiotic free controls which were dual stained or CV-AM only; gate set on SYTOX-green so that all cells in antibiotic free controls were SYTOX-green negative, and so that CV-AM negative (as per P1) cells excluded.
- P3: CV-AM positive / SYTOX-green positive; events which did not fall in any of the other 3 gates.
- P4: CV-AM negative / SYTOX-green positive; heat-killed dual and SYTOX-green only stained; gate set so 100% of heat-killed cells were CV-AM negative, and so that SYTOX-green negative (as per P1) events excluded.

P2 was interpreted as "live" cells; P4 as "dead cells. P3 was interpreted as cells which were damaged but still producing esterases. P1 was not normatively interpreted. The primary outputs for the analysis were percentages of events in each population by time and antibiotic condition (i.e. time-kill curves). As per the population definitions, almost 100% of cells at time 0 in the time-kill curves were in P2. Over a 4-day time course, isoniazid at higher concentrations had profound depletion of %P2, with reciprocal rises in P3 and P4, e.g. at 8ug/ml by day 3 ~20% were P3, ~60% were P4, and only ~20%

remained in P2. Maximal effects of rifampicin in 4-day time-kill were less marked; e.g. at 8ug/ml by day 3 ~20% were P3, ~20% were P4, and ~60% remained in P2. In follow-up experiments rifampicin did show time dependent and post-antibiotic effects unobserved by the 4-day time-kill. Also of note, and not discussed in the manuscript, is that the proportion of cells in P1 was consistently higher for rifampicin than isoniazid at all time points: up to a maximum of ~20% at rifampicin 0.128 to 32 ug/ml after 24hours exposure. This seems important, because if rifampicin kills bacilli through a route without a marked SYTOX-green positive phase, this killing wouldn't be observed in P3 or P4. The absence of a total cell denominator might bias the "percentages" in the plots: what if rifampicin caused cells to disintegrate more rapidly than isoniazid? This would render proportions observed in remaining cells hard to interpret. Indeed, Hendon-Dunn *et al*. also showed that their dual stained fluorescent profiles could differentiate antimicrobials by mechanism of action. An early (day-2) peak in %P3 followed by marked peak in %P4 was characteristic of cell-wall active compounds (isoniazid and a benzothiazinone), while intracellular acting (rifampicin, kanamycin and ciprofloxacin) had less dramatic rises in P3 and P4, but more marked increases in P1. Other important findings included that the mean CV-AM fluorescence of cells grown in continuous chemostat culture depended on growth rate, and that, while parallel CFU counts in the time-kill curves showed similar trends, there was a "lack of correlation" such that "flow cytometry analysis potentially captured information about cell populations that were unable to grow under standard conditions".[443]

4.6 Aims of current analysis

1) To develop and validate a method of absolute counting of mycobacteria *in vitro* using FCM.
2) Explore use of fluorescent dyes as probes of cell function to define subpopulations of bacilli in different physiological states.
3) To compare this FCM method to CFU counts and optical density measures, both in normal broth cultures and in the presence of antimicrobials.
4) To produce antimicrobial time-kill curves using these absolute counts and compare the dynamics of subpopulations defined by the different assays.

4.7 General methods

To avoid repetition, the following methods apply to the experiments described in subsequent sections unless otherwise stated.

4.7.1 Flow cytometer

The majority of flow cytometry was carried-out on a BD Accuri C6™, a benchtop flow cytometer equipped with forward and side scatter detectors and four fluorescence detectors (FL1, 533/30 nm; FL2, 585/40 nm; FL3, > 670 nm; FL4, 675/25 nm) with fixed alignment and pre-optimised detector settings, and a non-pressurized fluidics system, and two lasers (488nm and 640nm). Data acquisition used BD Accuri C6™ software. Because the fluidics system uses a peristaltic pump mechanism, volume of sample processed can be derived directly. This volume, and the optical performance of the instrument, was regularly quality assured using fluorescent beads as per manufacturer protocol. Manual and extended cleaning cycles were performed at the beginning and end of each flow cytometry session with verification of low event rate in filtered PBS before each run.

4.7.2 Broth culture conditions

All broth was made using Middlebrook 7H9 media (211887 BD Diagnostics) and 0.22um filtered deionized water according to manufacturer instructions. This was supplemented with 10% v/v Middlebrook OADC (212240 BD Diagnostics), 0.2% v/v glycerol and 0.15% v/v Tween 80 (lab stock). All broth was autoclaved prior to supplementation, and 0.22um filtered prior to use.

Cultures were at 37^{o}C in the dark with 150-200rpm agitation in 50ml sterile polyethylene conical flasks.

4.7.3 CFU plating

Middlebrook 7H10 (262710 BD Diagnostics) agar was prepared with 0.22um filtered deionized water according to manufacturer instructions, with v/v 0.5% glycerol added before autoclave sterilisation. When cooled to 45^{o}C, v/v 10% ADC supplement was added and tri-segmented plates poured to depth 5mm.

For CFU counting, 10-fold serial dilutions of samples were prepared in 96-well plates using 0.22um filtered 0.15% v/v Tween 80 sterile PBS. Each segment of a plate was

inoculated with 50uL of serial dilutions and spread using disposable, sterile loop spreaders. These were allowed to dry in a class-2 bio-safety cabinet for up to 2 hours before being incubated upside-down in double containment with polyethylene bags and boxes. CFU counts were performed with 3-fold technical replicates and counts averaged unless otherwise stated. Colony counts between 1 and 100 per segment were accepted and averages across dilutions were made where available (after adjustment for dilution). Counts were performed on 3 occasions (14, 21, and 28 days) to allow colonies to be counted before overgrowth.

4.7.4 Antibiotic preparations

Primary stock dilutions of antibiotic powders (kindly donated by Professor Digby Warner) were made in 100% DMSO and frozen at-20^{o}C wrapped in tinfoil. Fresh working dilutions were prepared in PBS prior to each experiment, 0.22nm filtered, and stored wrapped in tin foil at 2-5^{o}C refrigeration.

4.7.5 Screening fluorescent dyes for use in mycobacteria

All fluorescent stains reported in prior literature to probe mycobacterial cell physiology and compatible with the excitation and emission ranges obtainable on the Accuri C6 instrument were tested, including:

- Fluorescein diacetate (FDA)
- Calcein-AM (in lieu of calcein-violet which has emission and excitation spectra outwith the Accuri C6 range)
- SYTOX-red
- Acridine orange
- Rhodamine 123
- Baclight membrane potential kit (DiOC2(3))

In addition, stains not previously reported for use in mycobacteria were tested, including:

- TOPRO-3 iodide
- Live/Dead Fixable far red
- SYBR-gold

SYBR-gold has not, to my knowledge, been used for flow cytometry of any cell, or for physiology probing, but was tested because of its high sensitivity for fluorescent microscopy of mycobacteria (discussed in previous section).

All dyes were tested at a range of concentrations and incubation conditions, on live and heat-killed mid-log phase BCG at different ratios. Examples of flow plots from some of these tests are shown in figure 3.

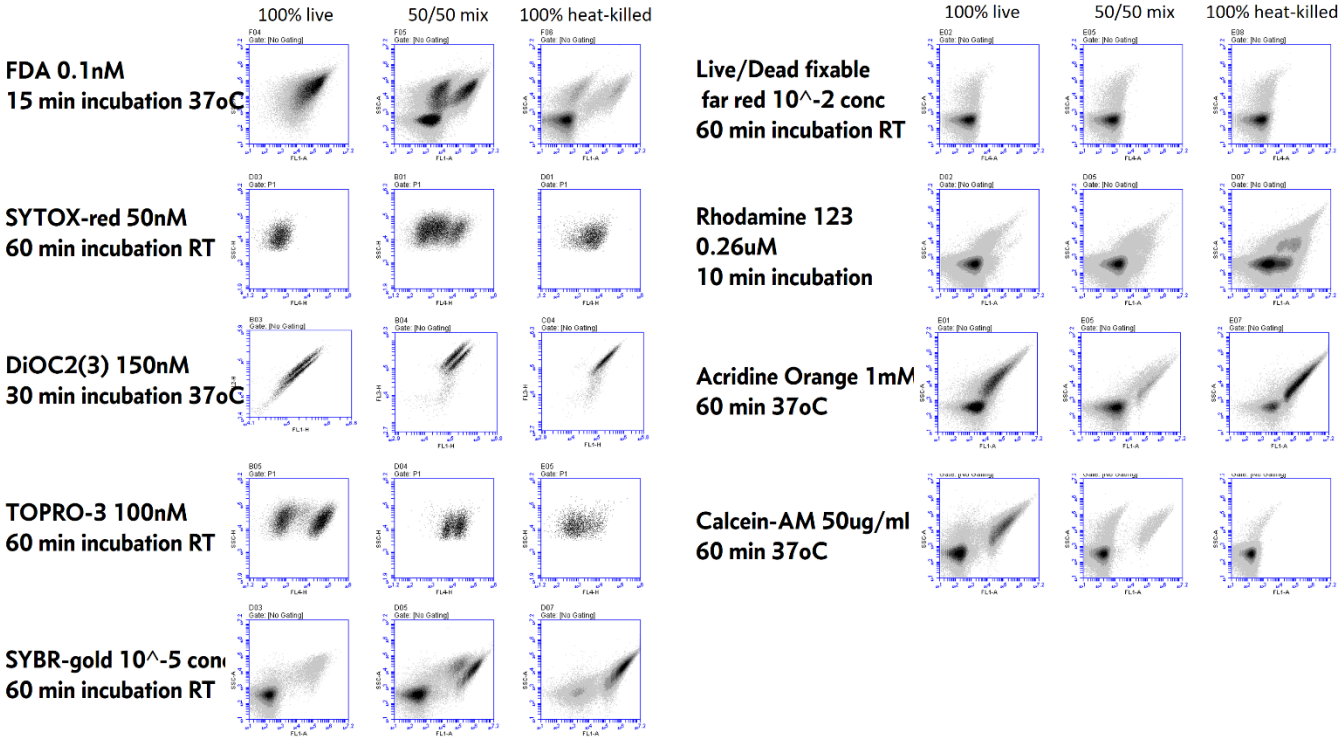

Figure 4-3. Example test runs of nine different fluorescent dyes on BCG broth cultures.

For each dye, a fluorescence versus light-scatter plot is shown for 100% live mid-log phase *M. bovis* BCG (first column), 100% heat-killed bacilli from the same culture (third column) or a 50/50 mix of the live and heat-killed (middle column). Only one specific iteration of processing conditions is shown for each (summarised in adjoining text), but a minimum of 50 different concentration/incubation parameters were tested for every dye.

Dyes which showed the most consistent performance after optimisation were calcein-AM and SYBR-gold. Of note, SYBR-gold showed extremely bright staining of cells, with mean FL1 fluorescence in heat-killed samples being approximately 1000-fold greater than unstained cell controls or stained cell-free broth controls. In addition, near perfect linearity of FCM counts across mixtures of live and heat-killed bacilli preparations were seen after SYBR-gold staining, such that, for example, SYBR-gold positive cell concentrations in 50/50 live dead mix preparations were always close to half those of 100% heat-killed samples (figure 4). Like many commercial "live/dead" discrimination dyes which are excluded from cells with intact membranes, SYBR-gold fluoresces only

when bound to intracellular nucleic acid. The results are in keeping with SYBR-gold also acting as a membrane permeability probe, but in the current work it was found to give more reproducible results than any of the commercial membrane impermeant dyes tested (and is substantially cheaper).

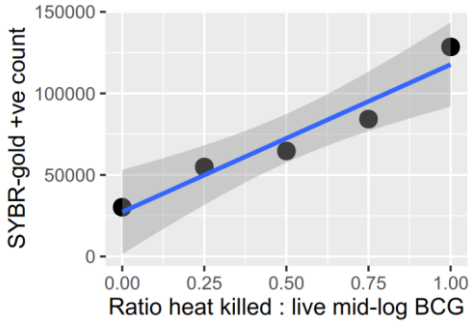

Figure 4-4. Linearity of SYBR-gold bacilli counts across different live / heat-killed cell preparation mixes.

A mid-log phase 7H9/OADC broth culture of *M. bovis* BCG was split into two samples; one was heat killed at 65oC for 12 minutes. The two samples ("live" and "heat killed") were mixed in the ratios shown before staining with SYBR-gold followed by FCM counting.

Final, optimised, SOPs for calcein-AM and SYBR-gold staining of bacilli were:

Calcein-AM

1. Fresh 50µg vials (ThermoFisher, C3100MP) reconstituted in 50µL of DMSO daily for each experiment, further diluted to 200µL with PBS for "working stock".
2. 6µL of working stock added per 100µL of sample to be stained, with pipette mixing.
3. Incubated in the dark at room temperature for 45-60 minutes before resuspension of bacilli with pipetting.
4. Fluorescence remains stable for up to 2.5 hours (in dark).

SYBR-gold

1. Propriety stock is of unknown concentration (sold already in solution, ThermoFisher, S-11494). Diluted 1000-fold in PBS, aliquoted and frozen at -20oC until use. After thawing further dilution (to 10^{-4}) in PBS.
2. 6µL of working stock added per 100µL of sample to be stained, with pipette mixing.
3. Incubated in the dark at room temperature for 45-60 minutes before resuspension of bacilli with pipetting.
4. Fluorescence remains stable for at least 24 hours (in dark).

4.8 Validation of thresholding and gating strategy for absolute cell counts

All flow cytometers measure light signals (forward or side scattered light, or light passing through a specific wavelength filter corresponding to a specific fluorescence) generated by laser excitation of particles passing through a chamber with precisely controlled fluidics. Photodetectors convert these light signals (i.e. photons) into electronic signals (i.e. electrons). The voltage and amplification (gain) applied to this conversion of photons to electrons control how the electronic signal varies as a function of the light signal, but, within a given range, a brighter light signal results in a larger electronic signal. An analogue-to-digital converter (ADC) bins this (continuous) signal into a discrete 'channel' for data recording; what range of light signal a given channel represents depends in turn on the voltage and gain applied in the detector. A "threshold" is an electronic mechanism which causes the ADC to 'ignore' signals less than a specified value. Typically, this threshold is set on FSC, with the purpose of eliminating noise (e.g. physical debris and electronic noise) from data acquisition. The aim is to exclude noise without inadvertent exclusion of 'real' events of interest (i.e. cells).

The Accuri C6 flow cytometer has a fixed dynamic range for voltage and gain, but allows thresholding on up to two signal values; these can be light scatter and/or fluorescence channels. The default threshold setting is FSC > 80,000, but any combination of two signals can be set as threshold for data acquisition by the user (for example, FSC >20,000 and SSC > 1000; or SSC>2000 and FL1>10,000 etc.).

An important principle is that setting a lower threshold does not simply increase sensitivity and decrease specificity for 'real' events: there is an absolute limit to the number of events that can be registered and recorded by the photodetector and ADC in a given time period (equivalent to a refractory period of a neuron). Therefore, setting too low a threshold overwhelms the electronics and some real events are not recorded.[438]

Optimal thresholding strategy depends on the experiment and has to be determined by trial-and-error. As mentioned previously in this chapter, thresholding is particularly

difficult and important in flow cytometry of bacteria because of the smaller size of the cells compared to eukaryotes.

For the current work, the effect of thresholding on absolute counts of mycobacteria on the Accuri C6 system was investigated extensively. Mid-log phase BCG cultures were analysed after 2-fold dilution in 0.15% v/v Tween80 PBS solution. These were compared to identical preparation of cell-free 7H9 broth as a negative control. Matrices of threshold settings were screened. In each case a gate was set around an apparent discrete population of cells on a log(SSC) by log(FSC) plot, with the gate being set to maximise difference between the BCG broth and the negative control. The (optimised) ratio of events in the negative control to the events in the BCG broth was defined as the false discovery rate. The optimal thresholding strategy was defined as the settings which maximised the absolute count in the BCG broth gate, and minimised the false discovery rate, with the anticipation that these maxima and minima would be reliably modelled from the data.

Several hundred combinations of combined FSC and SSC thresholding were assessed. In individual experiments, values which maximised counts were apparent (figure5), but false discovery rates were never less than 10%. More crucially, the apparent FSC/SSC threshold optima differed across biological replicates (i.e. new broth cultures of the same BCG isolate), with the impression that culture at different stages of growth had different FSC and SSC distributions (thus moving the optimal threshold level).

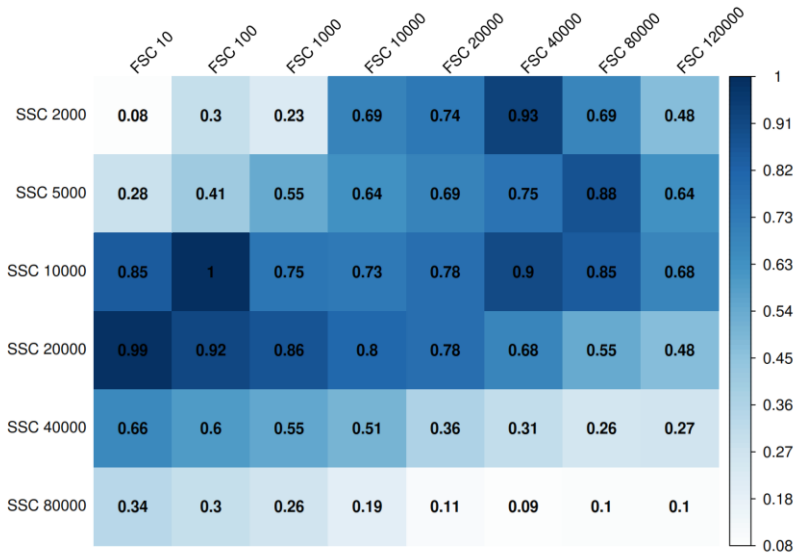

Figure 4-5. Example screening experiment for optimal SSC & FSC thresholding strategy.

A matrix of threshold values for SSC [rows, SSC > 2000; 5000; 10000; 20000; 40000; 80000] and FSC [columns, FSC > 10; 100; 1000; 10000; 20000; 40000; 80000; 120000] tested on the same mid-log broth culture of BCG (unstained). In this experiment, the maximum apparent count of bacilli was given by threshold SSC>10000, FSC>100, indicated by darkest blue/ "1". Other counts are shown as a proportion of this maximum, for example threshold SSC>2000 / FSC>40000 gave a count 93% of the maximum observed count. This shows that lower thresholds do not generally result in higher counts. The false discovery rate (events in 'cell' gate on a cell-free negative control divided by cell count in equivalent gate on BCG sample) was above 10% for all thresholding conditions in the experiment. When similar matrices were repeated using new BCG cultures (biological replicates) the specific optimal threshold values were different.

An alternative strategy of thresholding on fluorescence was assessed. Because cells stained with SYBR-gold were about 100 to 1000x brighter on FL1 than debris, choosing an optimal FL1 threshold value for these cells is straightforward. A thresholding strategy based on FL1, in heat-killed, SYBR-gold stained mid-log BCG, consistently reduced false discovery rate to <0.5%, while at the same time increasing absolute cell counts by more than a logarithm compared to thresholding on light scatter alone on the same samples (figure 6). Further, this strategy reduced the coefficient of variation between technical replicates, and gave near perfect linearity across serial dilutions of the same sample (figure 6).

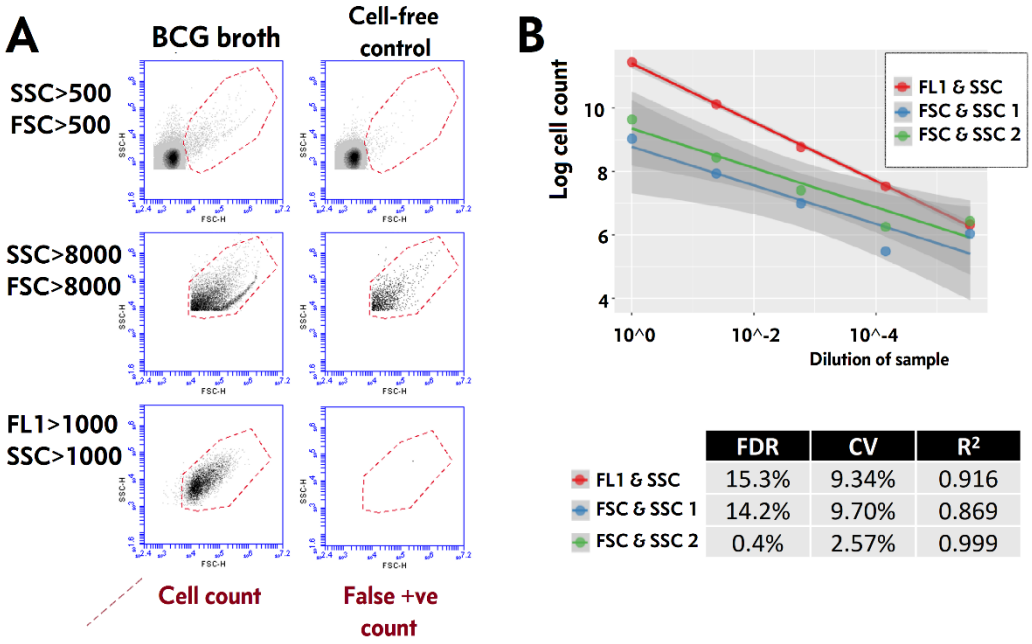

	FDR	CV	R^2
FL1 & SSC	15.3%	9.34%	0.916
FSC & SSC 1	14.2%	9.70%	0.869
FSC & SSC 2	0.4%	2.57%	0.999

Figure 4-6. Comparison 3 thresholding strategies in heat killed and SYBR-gold stained mid-log phase BCG broth culture.

A. Example FCM plots for three thresholding strategies (rows) applied to BCG broth culture (positive control, column 1) and cell free broth (cell-free negative control, column 2). Counts are extracted for the gated population (dashed red line), which is placed to maximise the count and in BCG broth and minimise the count in cell-free control. Recorded events in the low light scatter value thresholding (top row) are dominated by debris / noise, which can be seen as a dense population with low SSC and FSC values in lower left quadrant, equally apparent in the cell-free control. Higher light scatter thresholding (second row) excludes these events, but still records a substantial portion of higher SSC/FSC noise (seen in cell-free control), and the threshold level appears to bisect the 'real' cell population, i.e. losing cells from analysis. By contrast the thresholding based on fluorescence is qualitatively better, with very few false positive events in cell-free control, and a discrete cell population in BCG broth which is not artificially bisected. **B**. Greater internal consistency of the FL1/SSC thresholding strategy, with less error across serial dilutions of a BCG culture, is apparent. Quantitative evidence of improved absolute count validity includes a lower false discovery rate (FDR, defined as false positive cell count in cell-free control divided by paired cell count from broth); lower coefficient of variation (CV, calculated by standard deviation/mean from 5 technical replicates, averaged for 3 biological replicates); and higher R^2 from linear fit across serial dilution series (one biological replicate as shown in figure; $p<0.001$ for F test comparing FL1/SCC to either FSC/SSC strategy)

Thresholding based on fluorescence was therefore adopted for all subsequent experiments. This has the important implication that fluorescence negative cells could not be observed or counted. This is unusual for readers used to flow cytometry analysis of human cells, who expect to see % stain negative and % stain positive populations, typically combining one than one stain in the experiment to define multiple

subpopulations. Such an analysis will not be presented here. Instead, different preparations of the same culture are run in parallel to define subpopulations as follows:

Table 4-2. Flow Cytometry defined cell populations.

Cell Population		Description
HK	Heat-killed SYBR-gold stained total cell count denominator	Sample is processed by incubation in water-bath at 60°C for 12 minutes, followed by addition of SYBR-gold and incubation at room temperature for 10 to 60 minutes. This gives a total count of intact cells containing nucleic acid, used as a denominator for calculating proportions represented by subpopulations. Thresholding on SSC and FL1 (SYBR-gold fluorescence)
CA	Calcein-AM positive cells	Live sample stained with calcein-AM incubated in dark for 60 minutes at room temperature. This gives an esterase positive, or metabolically active, cell count, and an esterase negative cell count is derived by subtracting from the HK total cell count denominator. Thresholding on SSC and FL1 (Calcein-AM fluorescence)
SG	SYBR-gold positive cells	Live (not heat-killed) sample stained with SYBR-gold and incubated in dark for 60 minutes at room temperature. This gives a cell-membrane permeant cell count, and a membrane-impermeant cell count is derived by subtracting from the HK total cell count denominator. Thresholding on SSC and FL1 (SYBR-gold fluorescence)

This has the disadvantage of precluding observation of dual-staining characteristics, but the advantage of being able to use two FL1 / green fluorescent dyes, and, crucially, reliable absolute cell counts.

4.9 Clumping in mycobacterial cultures can be observed and measured with FCM

In all mycobacterial cultures tested (*M. bovis* BCG, *M. tuberculosis*, *M. smegmatis*), from early-log phase onwards a second population of events with higher FSC and SSC developed in flow plots (figure 7), becoming the dominant population in mid or late log phase. To investigate the nature of these distinct light-scatter populations, events gated on the two populations were sorted for downstream microscopy (figure 8 A&B). This demonstrated that the higher light-scatter population was composed of clumped cells, despite all cultures being grown in detergent (Tween 80 0.1% to 0.25%) and under agitation (150 to 200 rpm), and despite sonication prior to flow cytometry (figure 8 C).

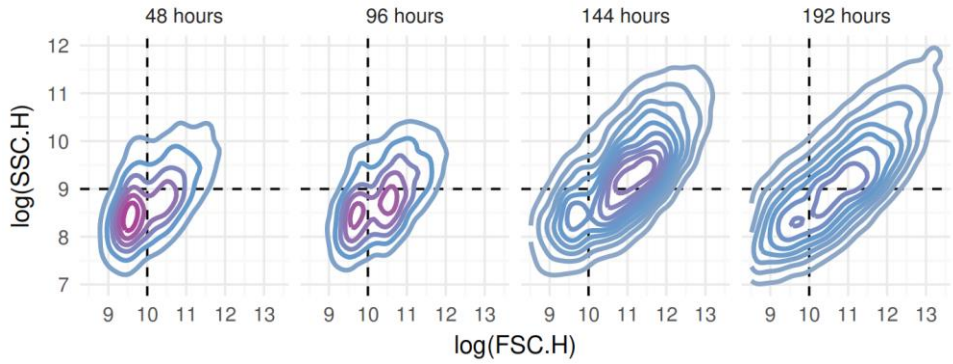

Figure 4-7. Changing FSC/SSC region of mycobacteria during log-phase growth.

2d-density plots of FSC v SSC on log scale for a culture of *M. bovis* BCG grown with v/v 0.15% Tween 80 at 180 rpm. Plots are from samples taken at 48, 96, 144, and 192 hours after culture was subbed from a log-phase starter culture into warmed broth; the samples are from early, early-mid, late-mid and late log-phase. Samples were diluted 10-fold or 100-fold (later samples) in 0.25 v/v Tween 80 PBS and sonicated for 60 seconds prior to flow cytometry. The tail of higher SSC&FSC events at 48-hours is seen to resolve into a second subpopulation by 96-hours, which continues to expand into a higher SSC&FSC region and become the predominant population by end of log-phase.

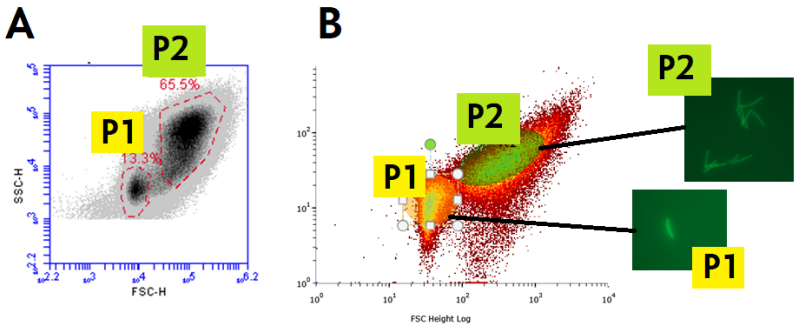

C

	Single	Doublet	Clump	Ratio clump:single
P1	28	13	4	0.14
P2	8	2	22	2.75
Unsorted	25	8	29	1.16

Fisher exact test: p = 1.3e-07

Figure 4-8. Sorting populations of mycobacteria based on light scatter for downstream microscopy characterisation.

A. Accuri C6 flow cytometry plot of mid-log phase culture of *M. smegmatis* stained with calcein-AM. Grown in v/v 0.15% Tween 80 7H9 with 150 rpm agitation and diluted 10-fold in v/v 0.15% Tween 80 PBS prior to FCM. Data acquisition with threshold SSC>1000 and FL1>1000. Two

discrete populations of cellular events are seen one with lower (P1) and one with higher (P2) light scatter values.
B. The same sample run on a Bio Rad S3 cell sorter with voltage and gain set to recreate Accuri C6 plot. P1 and P2 were sorted for downstream fluorescence microscopy.
C. P1 was majority single cells or doublets, and P2 majority clumps.

Clumping is a major determinant of total cell and CFU counts and can be limited by needle emulsification, but not vortex or sonication (figure 9). Consequently, needle emulsification increases both CFU and total FCM cell count of mycobacteria by an order of magnitude (over 2-fold in experiments performed for this thesis, figure 9B).

As noted previously, FCM shows that clumping increases to become the norm during normal *in vitro* 'planktonic' growth of mycobacteria. The ability of needle emulsification to disrupt these clumps is limited in later stage cultures such that late log-phase cultures show extensive clumping despite emulsification (figure 10). Further, average size of clumps (approximated by mean FSC value) increases progressively in late stage cultures (figure 11), eventually producing clumps visible to the naked-eye. These clumps can be broken-up by more aggressive emulsification, but this results in structures which resemble debris rather than individual cells on microscopy. *M. bovis* BCG cultures grown in v/v 0.15% Tween 80 under agitation are predominantly clumps before reaching OD_{600} of 0.5 and before broth is visibly different to cell-free broth.

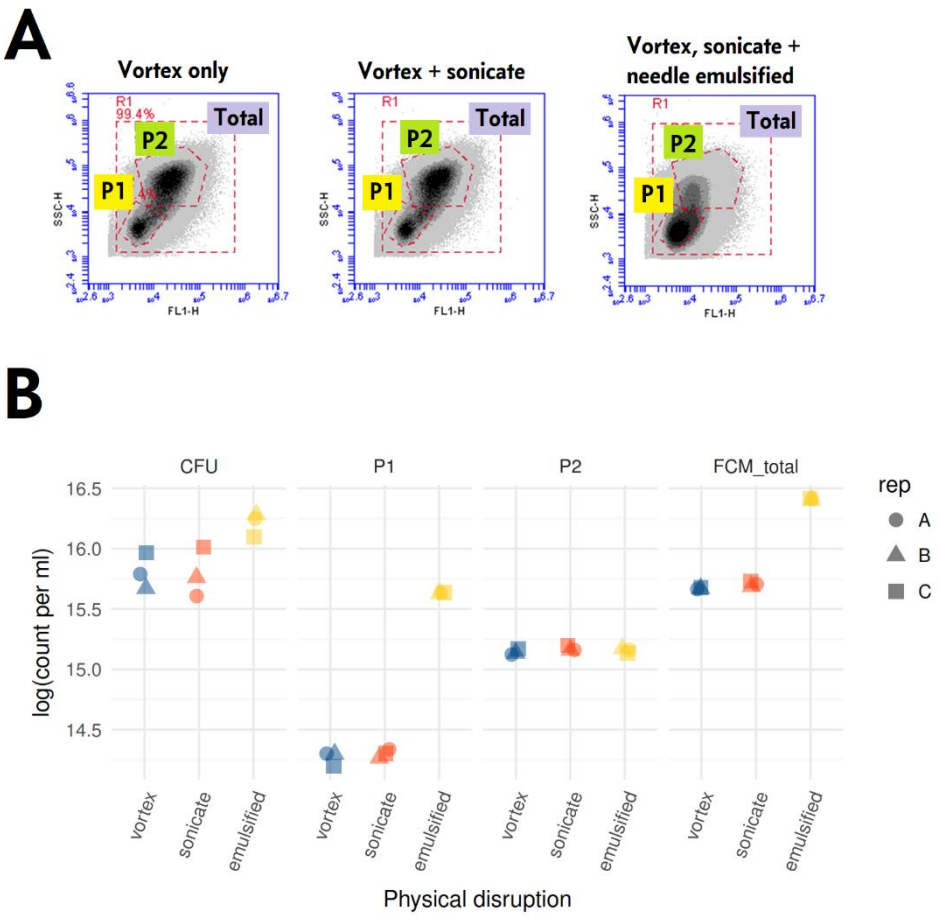

Figure 4-9. Effect of vortex, sonication, and needle emulsification on FCM population and CFU counts.

Mid-log phase culture of *M. smegmatis* grown in v/v 0.15% Tween 80 7H9 with 150 rpm agitation and diluted 10-fold in v/v 0.15% Tween 80 PBS and stained with calcein-AM prior to FCM on Accuri C6. Data acquisition with threshold SSC>1000 and FL1>1000. Samples were processed by 60 second vortex, or by 60 second vortex followed by 5-minutes sonication in water bath, or by both these methods followed by needle emulsification (12 passes through a double luer-lock ended, 25 Gauge, 4-inch, micro-emulsifying needle with a reinforcing bar (Cadence Inc.).

A. Two discrete populations differentiated by light-scatter are seen: single cells (P1) and clumps (P2). Qualitatively, it can be seen that vortex and sonication processing have not disrupted clumps, but needle emulsification (far right plot) has shifted predominant P2 (clumps) t predominant P1 (single cells).

B. Emulsification changes apparent cell counts by an order of magnitude; both CFU count and total flow cytometry count increased by half to one unit on log scale.The total P2 count doesn't change much: larger clumps are partly replaced by smaller clumps, but the single cell count rises by more than 1 logarithm, and this results in the higher CFU / total FCM cell count.

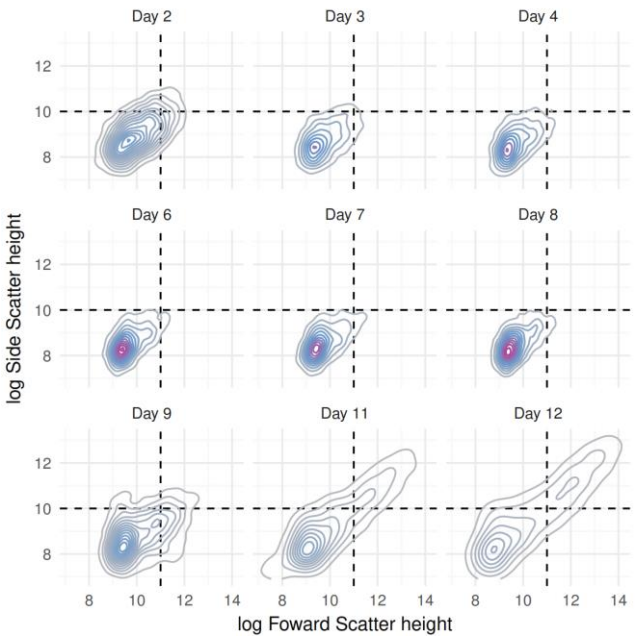

Figure 4-10. Clumps not disrupted by emulsification eventually emerge in late log-phase cultures.

M. bovis BCG culture in v/v 0.15% Tween 80 7H9 with 150 rpm agitation and diluted 10-fold in v/v 0.15% Tween 80 PBS before heat-killed and stained with SYBR-gold. Samples were needle-emulsified (12 passes through a double luer-lock ended, 25 Gauge, 4-inch, micro-emulsifying needle) prior to FCM on Accuri C6; Data acquisition with threshold SSC>1000 and FL1>1000. Timepoints are days from inoculation into warmed broth from log phase starter culture. A long-tail of clumps, extending into the upper-right quadrant of higher SSC and FSC, emerges from around day 9, when OD_{600} was around 0.3.

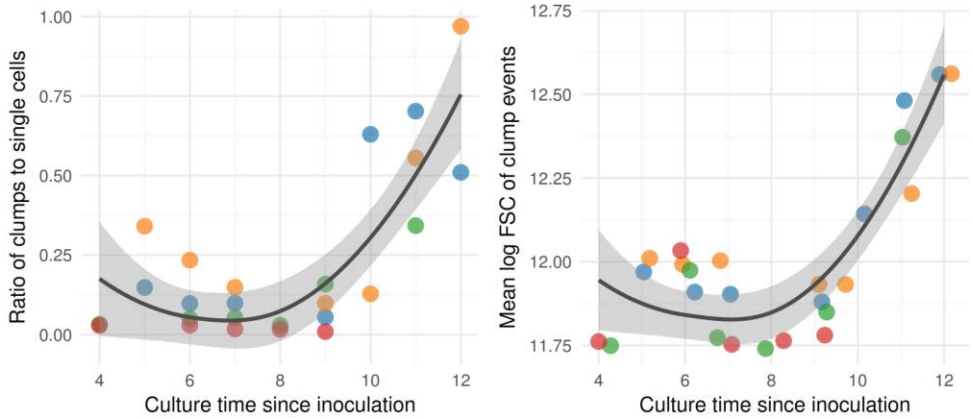

Figure 4-11. Quantification of clumping despite emulsification over growth phases.

Four replicates of the data in figure 10 (i.e. 4 different cultures of BCG processed as per figure 10) had clumps and single cells quantified by flow cytometry: clumps defined as events with SSC and FSC values greater than a manually applied cut-off (similar to axes in figure 10). Four replicates shown with different colours. The ratio of clumps to single cells is suppressed by emulsification until late log-phase (~day 8), when both the number and size (approximated by mean FSC) of clumps rise rapidly. Line of best fit with 95% CI band is a loess-regression line ignoring dependence by replicate.

Because preparation of single-cell suspensions is a basic requirement in many mycobacterial laboratory experiments, the effectiveness of a gold-standard method for single-cell preparation of mycobacteria was tested. This method, published by Saito *et al.*, uses low *g* centrifugation to purportedly pellet clumps leaving single-cells in supernatant.[489] Using FCM to quantify clumps and single-cells shows that, in fact, the ratio of clumps to singles is unaffected by this centrifuge processing (figure 12).

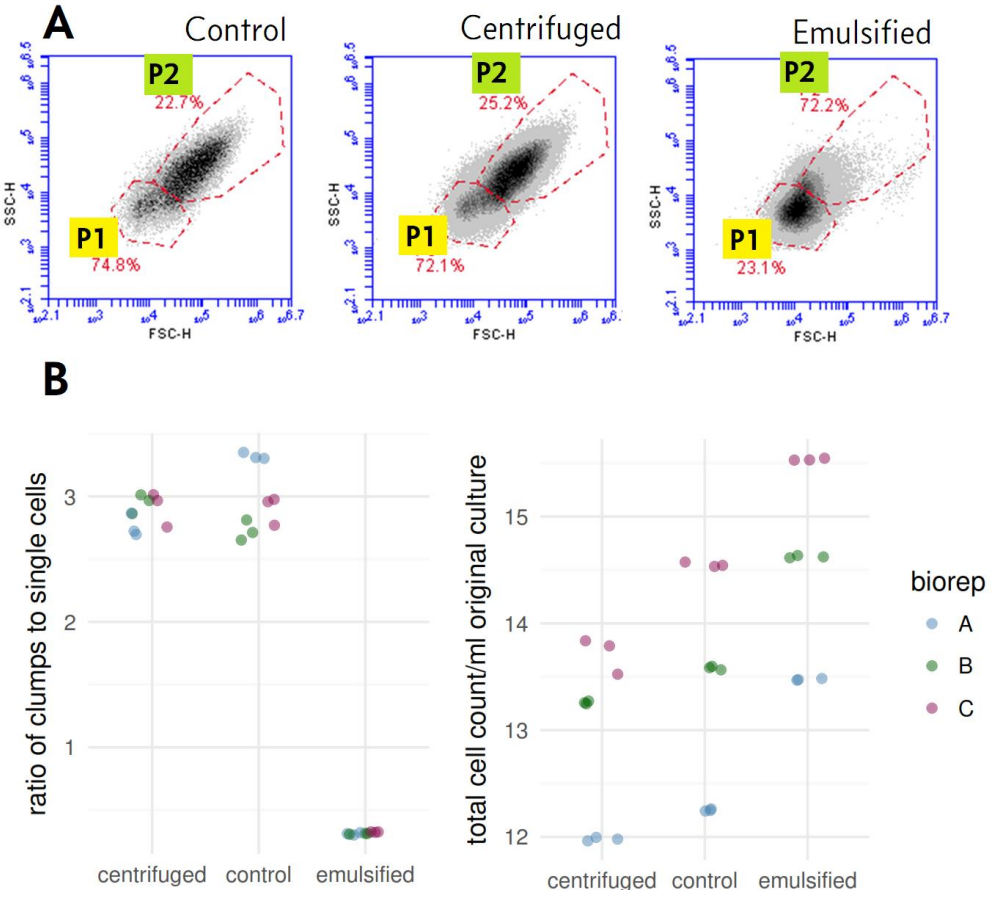

Figure 4-12. Testing Saito 'centrifuge' method for single-cell preparation

Three mid-log phase *M. smegmatis* cultures grown with 0.05% Tween80 (3 biological reps), processed three ways. **Control sample**: 10^-1 dilution in PBS/tween80 at 0.1%, no physical disruption. **Emulsified sample:** 10^-1 dilution in PBS/tween80 at 0.1% 12x needle emulsified. **Centrifuge sample:** 10ml + 5ml PBS/tween80 at 0.1%; spun in 15ml centrifuge tubes at 120 G for 8 min with no brake. Supernatant used for counts. (Saito et al. PNAS 2017 method). All samples heat-killed and stained with SYBR-gold as described previously, with thresholding on SSC and FL1. Three technical reps of each sample (x 3 biological reps x 3 sample prep conditions → 27 data points). **A**. Qualitatively, the FSC by SSc flow plots are similar for centrifuge method and control. B. The ratio of clumps to single cells is the same in the control and centrifuge preparations, but as expected much lower and with less variation across replicates with emulsification. Apparent cell counts are lower with centrifugation (due to loss of cells in pellet) and higher with emulsification (due to disruption of clumps).

4.10 CELL-SUBPOPULATION DYNAMICS DURING ANTIMICROBIAL FREE *IN VITRO* GROWTH OF MYCOBACTERIA

The method development and insights described above resulted in a final FCM experimental method which can be used to examine dynamics of mycobacterial cell sub-populations (figure 13). Before assessing antimicrobial killing, the dynamics of *in vitro* growth in the absence of antimicrobials was defined for *M. bovis* BCG.

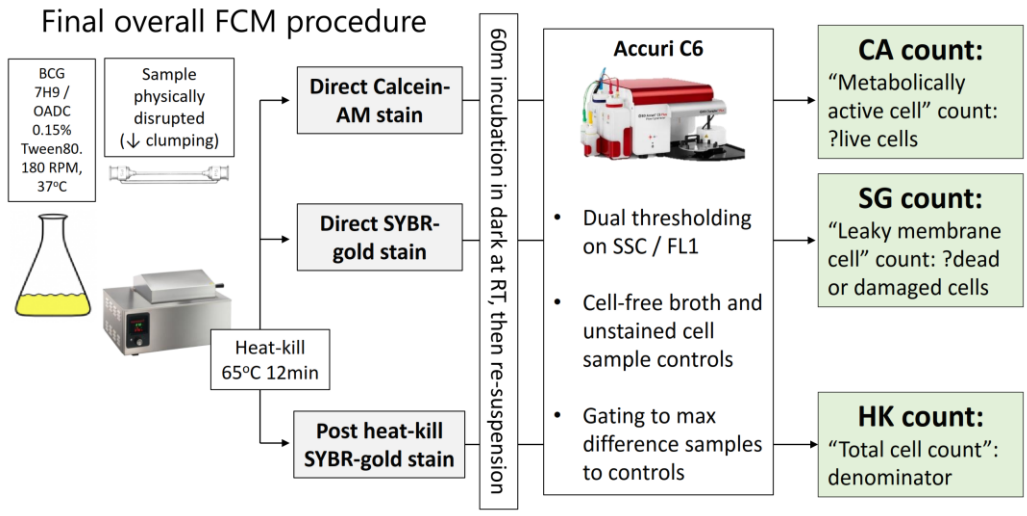

Figure 4-13. Schematic of final FCM method.

HK denominator counts were always the largest population. During log-phase CA+ and CFU counts were closely correlated and accounted for the majority of cells, with SG+ being a minority sub-population (figure 14). When entering stationary phase, both CA+ and CFU counts slowed more quickly than total cell count, then started to decline, with simultaneous rise in SG+ cells, in keeping with cell death (figure 14). Parallel rise in OD_{600} was more sigmoidal on a log scale (figure 15) with minimal detected change in OD until mid log-phase. Despite each of the four replicates being cultured in identical conditions, and subbed from the same original starter culture, differences in rate and maxima were apparent (figure 14 & 15).

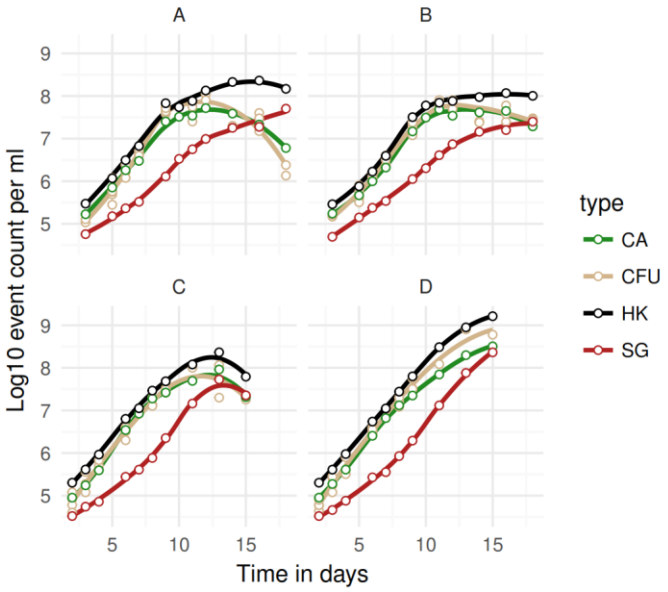

Figure 4-14. CFU and FCM defined *in vitro* growth curves of *M. bovis* BCG.

Four independent *M. bovis* BCG cultures in 50ml v/v 0.15% Tween 80 7H9 in 500ml tissue-culture flasks with 150 rpm agitation (A – D) serially quantified by CFU counts & FCM counts between 2 and 15 days after inoculation into warmed broth from log phase starter culture. FCM samples diluted 10-fold in v/v 0.15% Tween 80 PBS before data acquisition on Accuri C6, threshold SSC>1000 and FL1>1000, and gating to maximise difference from cell-free stained broth & unstained cell controls. All samples were needle-emulsified (12 passes through a double luer-lock ended, 25 Gauge, 4-inch, micro-emulsifying needle) prior to FCM and CFU count. Counts adjusted by dilution factor and volume processed to log10 count per ml of original broth.

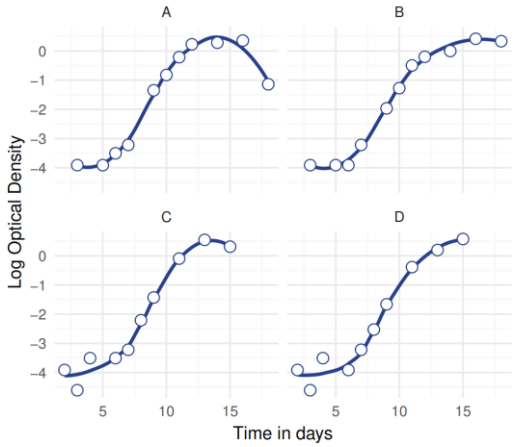

Figure 4-15. Optical density defined *in vitro* growth curves of *M. bovis* BCG.

Same four cultures (A-D) as shown in figure 14. Optical density measured on bench-top spectrometer at 600nm using undiluted samples and broth reference standard in 1ml cuvettes.

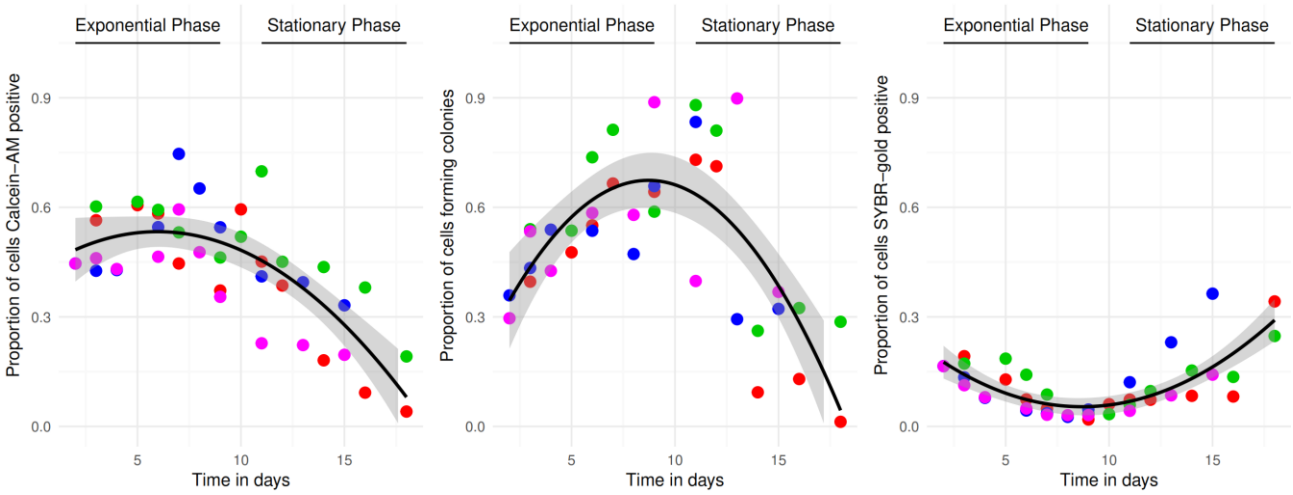

Figure 4-16. Sub-populations as a proportion of total cell count denominator.

Same four cultures (A-D) as shown in figure 14. Proportions of total cell count (HK denominator) which were CA+ (left) CFU forming (middle) or SG+ (right) shown. Each of the 4 replicates shown with different colour (A=red, B=green, C=blue, D=pink); line of best fit with 95% CI band is a loess-regression line ignoring dependence by replicate.

Some subtle differences between CA+ and CFU count are made visible by representing counts as proportion of total cell count (i.e. divided by the HK denominator count, figure18). Proportion of cells which are CFU forming increases to a maximum at end of log-phase / early stationary phase; at this point a significant proportion of CFUs must not be CA positive. CFU proportion has a greater dynamic range than CA+ cells.

Unlike proportion of cells which are CFU forming, proportion CA+ has significant correlation with the rate of growth of the whole population of cells, again suggesting that CFU forming behaviour is not simply a marker of metabolic activity (figure 19).

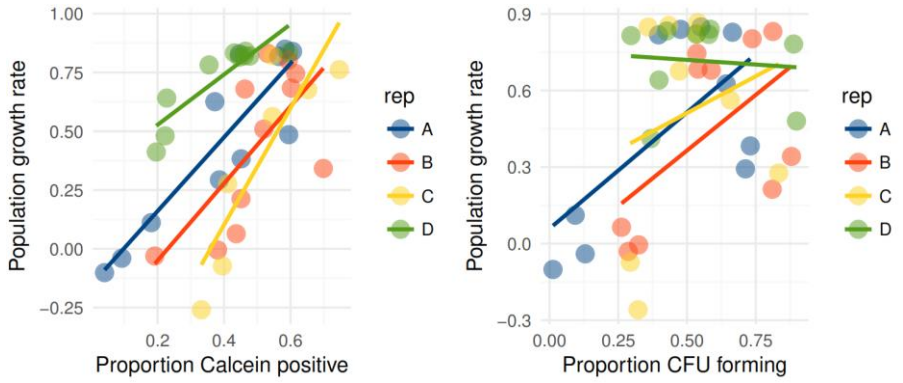

Figure 4-17. Rate of growth in broth culture correlates with proportion of cells CA+, but not proportion CFU positive.

Rate of population growth was defined as the instantaneous rate of change of the HK total cell count (i.e. the slope of the tangent to the curve at a given timepoint). This measure correlated with proportion CA+ at this time point (adjusted R^2 for model with different intercept by rep = 0.04; adjusted R2 for same model including proportion CA+ = 0.51; proportion CA+ explains 47% of variance in growth rate; p=4.7e-07). By contrast, the equivalent model for CFU proportion had R^2 0.12 (p=0.11).

Despite these differences, CA+ and CFU counts are highly correlated under *in vitro* broth growth conditions, such that CA+ FCM offers a reliable rapid surrogate of CFU count, with results in approximately 2 hours rather than 2-3 weeks for *M. bovis* BCG (figure 18).

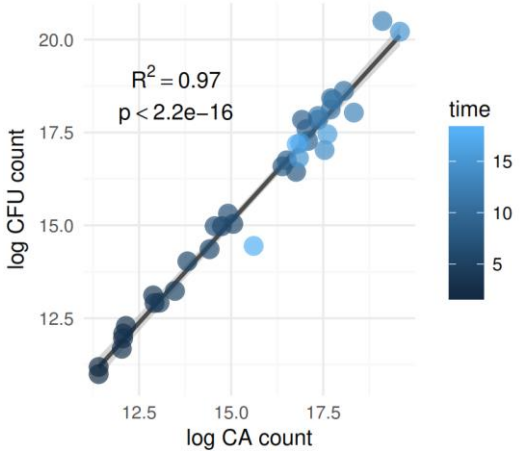

Figure 4-18. Correlation between CFU and CA+ counts under normal *in vitro* growth conditions.

Data from experiments shown in figure 14. Line of best fit with 95%CI shown. Greatest residual variance is found for late-stage cultures (time since inoculation indicated by colour), so correlation would be higher if only log-phase cultures were compared.

Optical density, which is often used as a rapid surrogate of CFU count, has only moderate linear correlation with CFU on a log-log scale (figure 19), and is instead strongly related to the summed FSC of all events in flow cytometry analysis (including debris and clumps etc.). Since the distribution of FSC for particles in a broth culture depends on the stage of culture (late cultures have more clumps for example), the relationship between CFU and OD is actually non-linear, with dependence on culture stage and conditions. An OD_{600} = 1 culture diluted to have OD_{600} = 0.6, will have a very different CFU and cell density to a culture which has just reached OD_{600} = 0.6.

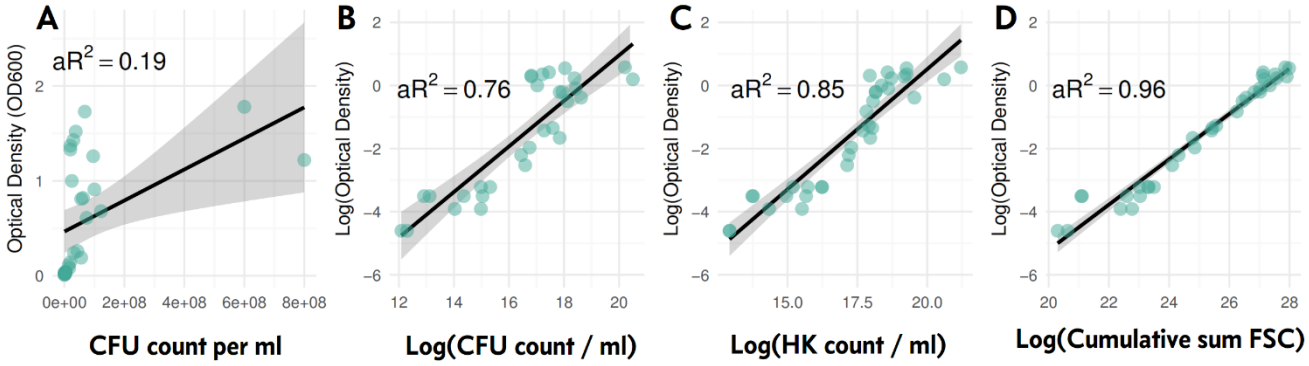

Figure 4-19. Optical density is determined by total biomass in culture, with condition dependent correlation with CFU count.

Data from figure 14 and 15 replotted to examine what determines optical density. OD_{600} shows some linear correlation with CFU count on a log-log plot (panel B), but is more closely correlated with total FCM cell count (HK denominator, panel C). When the HK count is weighted by FSC (i.e. rather than counting the HK cells, the FSC values of all events are summed – so that a 'larger' FSC event counts for more, and all events including debris are included, rather than just cells) gives the strongest correlation with OD (panel D).

4.11 *IN VITRO* PHARMACODYNAMICS OF MYCOBACTERIA BY FCM & CFU COUNTS

Having established growth dynamics of *in vitro* BCG cultures in the absence of antimicrobials, the FCM method was applied to pharmacodynamic time-kill analysis. *M. bovis* BCG grown in 500ml tissue culture flasks containing 0.15% v/v Tween 80 7H9 medium was grown. When these had reached 200000 CA+ cells per ml density, the stock was split into 20ml aliquots in 50ml conical flasks to which antimicrobials were added to a range of final concentrations chosen to be multiples of the minimum inhibitory concentration (MIC) for that antimicrobial. Samples were immediately drawn for CFU counting and FCM counting and the remaining aliquots incubated at 37°C in the dark under 180 rpm agitation. Further samples were drawn after 1, 2, 3, and 5 days incubation with antimicrobials, giving 5 timepoints to define time-kill curves.

As per the FCM methods established and validated previously, all samples were needle-emulsified prior to FCM and CFU counts. FCM samples were diluted 2-fold or 10-fold in v/v 0.15% PBS solution. Data acquisition was with FL1>1000 and SSC>1000 thresholding. Calcein-AM staining, SYBR-gold staining, and heat-killing followed by SYBR-gold staining was performed. CFU samples were diluted 2-fold in v/v 0.15% PBS solution and needle-emulsified, followed by washes to remove antimicrobials before serial dilution and plating. Sample processing method is summarised in figure 20.

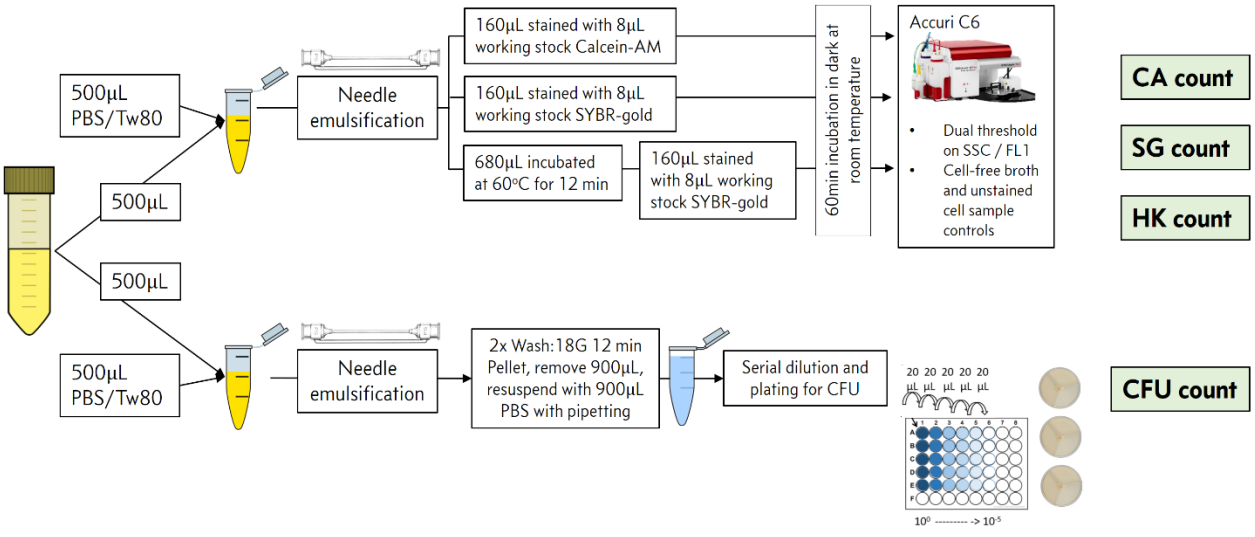

Figure 4-20. Sample processing for time-kill experiments.

4.11.1 Raw FCM data: qualitative FCM plots & clustering

Raw FCM data plots from a single replicate are shown for calcein-AM stained bacilli in figure 21. All plots show the same volume of sample processed, such that the density of events (dots) represents their density in the original sample, comparable across plots. All plots from day 0 are therefore nearly identical, but differences emerge in a time and concentration dependent manner. The kanamycin plots, for example, show that at the lowest concentration (0.5x MIC) a large CA+ population of cells grows over the 5-day time course (FL1 on x axes is capturing calcein-AM activity); while at higher concentrations of kanamycin, the CA+ population is progressively eliminated, with falling numbers and intensity of FL1 events. A similar, but more dramatic, pattern is seen for rifampicin plots. Isoniazid and ethambutol, by contrast, are qualitatively different. For both these drugs, at all concentrations greater than MIC, FL1 activity has increased on day 1, with shifting of the CA+ population to the right of the vertical dashed line, followed by a more sudden loss of CA+ cells from day 3. Similar to rifampicin versus kanamycin, isoniazid has effects at 0.5xMIc but ethambutol does not.

Raw FCM data plots from a single replicate are shown for heat-killed SYBR-gold stained bacilli in figure 22. These plots are capturing the total cell population in the samples, and only one drug concentration is shown (4x MIC) for each antimicrobial. The total cell count is seen to be less influenced by antimicrobial action, but there are some qualitative differences by antimicrobial class. Rifampicin, and to a lesser extent kanamycin, cause a tail of lower FL1 events to develop extending left from the main cell bright-FL1 population on the right of the plot.

All antimicrobials cause a rise in SG+ bacilli (cells with an abnormally permeant membrane) over time, but again there are qualitative differences by antimicrobial class (figure 23). Isoniazid and ethambutol result in a dense discrete region of SG+ cells, which may be disaggregating into two subpopulations, one with approximately double the FL1 intensity of the other (seen as two parallel, vertical ‘stripes’ of cells separated on the horizontal axis). This phenomenon is explored further in section 4.12.

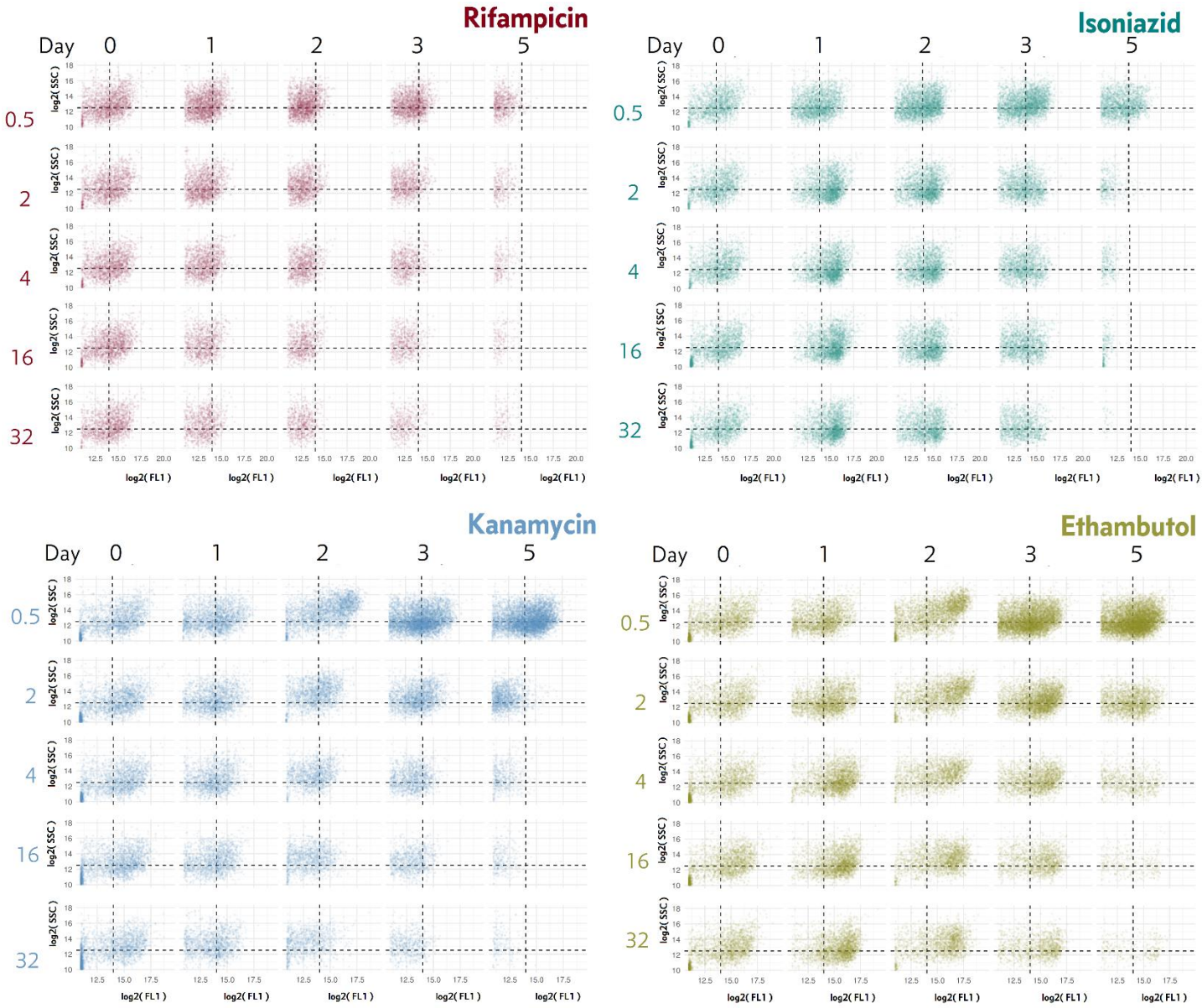

Figure 4-21. Raw data FCM plots for CA+ bacilli by time & antimicrobial condition

Five concentrations in multiples of MIC (0.5x, 2x, 4x, 16x, 32x) are shown for four antimicrobials (rifampicin, kanamycin, isoniazid, ethambutol) over 5 timepoints (day 0, 1, 2, 3 & 5) after addition of antimicrobials. Plots are log(SSC) by log(FL1); FL1 captures CA+ fluorescence.

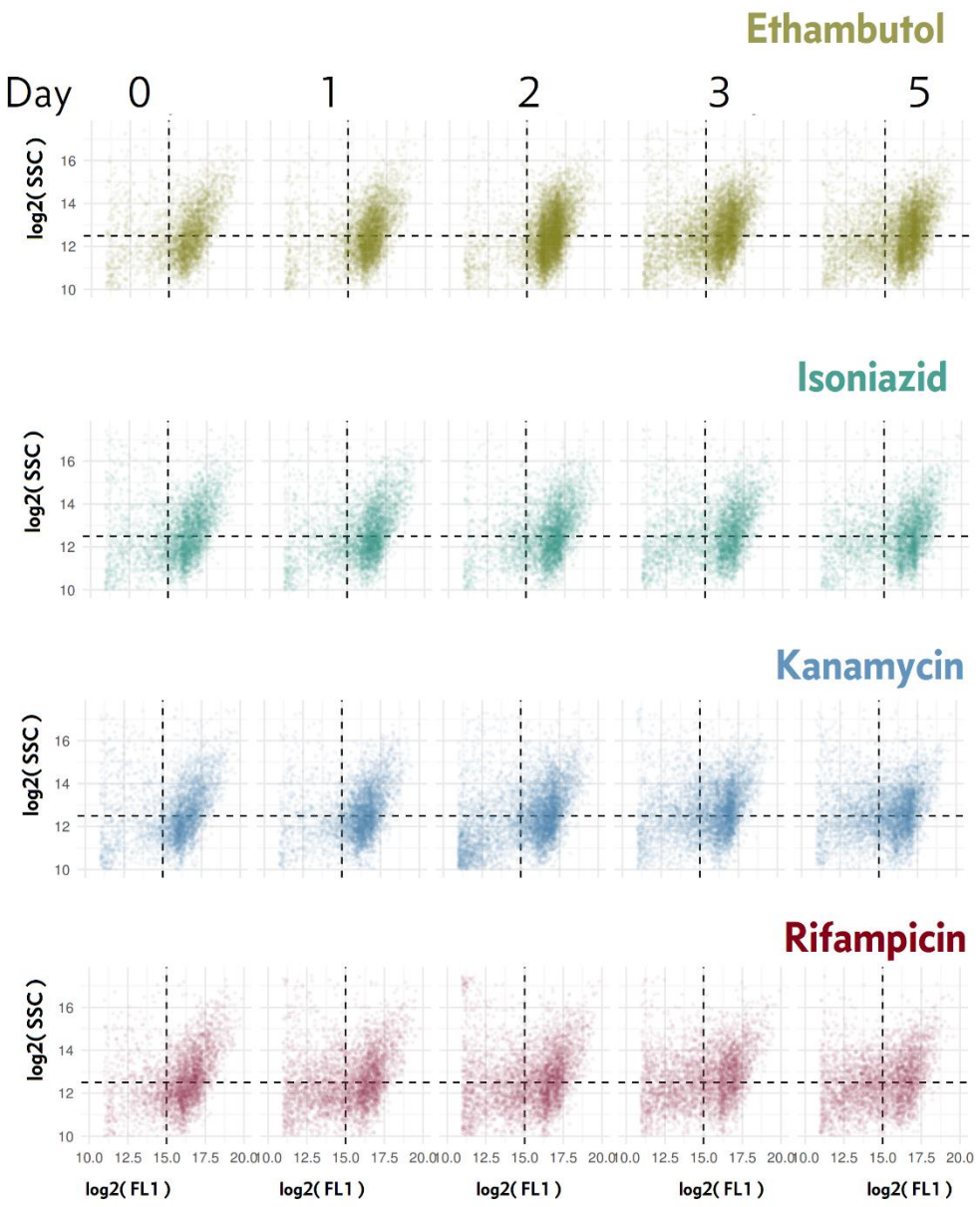

Figure 4-22. Raw data FCM plots for heat-killed SYBR-gold stained bacilli (HK total cell count data)

Only one concentration (corresponding to 4x MIC) for four antimicrobials is shown at 5 timepoints (day 0, 1, 2, 3 & 5) after addition of antimicrobials. Plots are log(SSC) by log(FL1); FL1 captures SYBR-gold fluorescence, which stains all heat-killed bacilli containing nucleic acid.

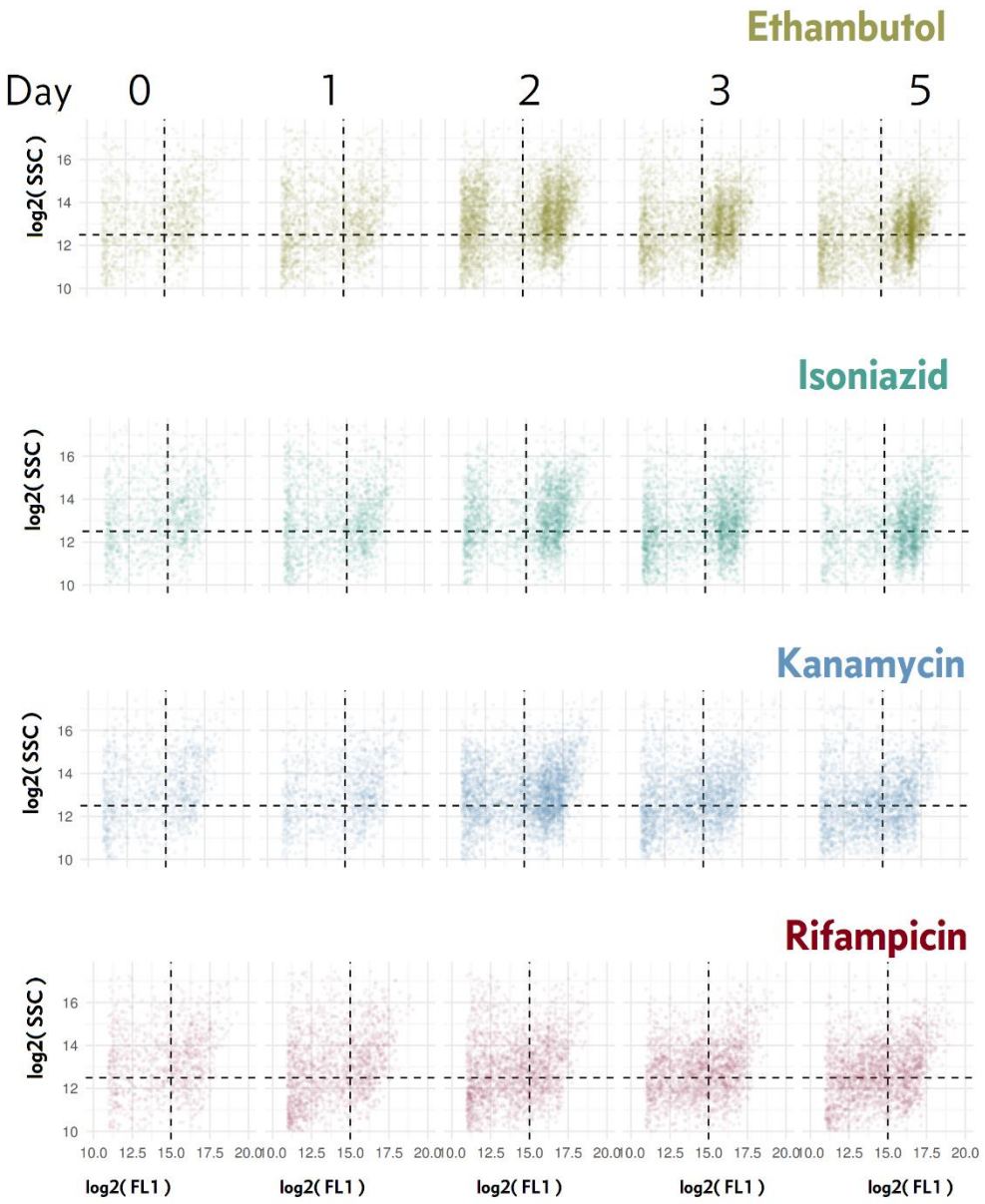

Figure 4-23. Raw data FCM plots for SYBR-gold stained bacilli (not heat-killed prior to staining)

Only one concentration (corresponding to 4x MIC) for four antimicrobials is shown at 5 timepoints (day 0, 1, 2, 3 & 5) after addition of antimicrobials. Plots are log(SSC) by log(FL1); FL1 captures SYBR-gold fluorescence, which is a probe of membrane integrity in these bacilli (which have not been heat-killed).

4.11.2 Classification of FCM events by clustering

In order to produce time-kill curves, events have to be classified as positive for counting.

This can be achieved by placing gates on two-dimensional flow plots using FCM

software. Alternatively, algorithmic clustering of the events by proximity on FCM measures can be used. This has the advantage of being able to use more than two dimensions to classify cells, and being more reproducible because it does not require user decisions on position of gates. A K-means clustering approach was used to classify all FCM events in the time-kill analysis (outlined in figure 24 & 25).

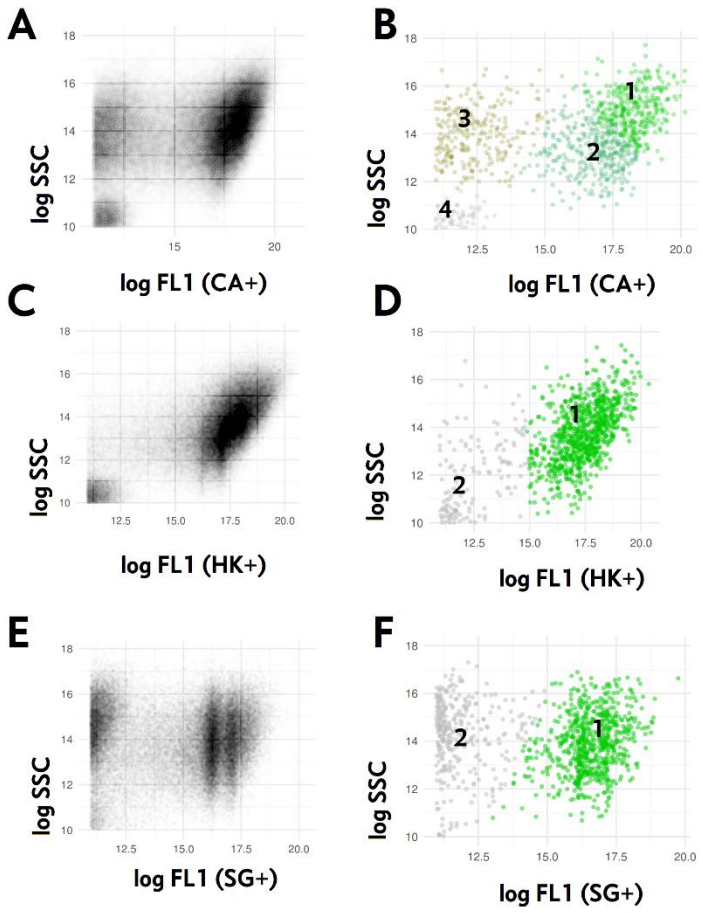

Figure 4-24. K-means clustering classification ("gating") of FCM events.

All FCM data from all antibiotic conditions were combined from one replicate of the time-kill experiments, which totalled millions of data points. These are plotted on a single combined plot for CA stained (A), HK cells (C) and SG cells (E). FCM measures for these data points – including FLI_H, FL1_A, SSC_H, FSC_H, and scaled ratio of FL1 to SSC – were used to define a multi-dimensional space in which events were clustered by their proximity in this space. For CA stained cells, 4 clusters were specified, and for SG and HK cells 2 clusters were specified. The result of this clustering is shown in panel B, D, F (only 1000 randomly selected events are shown to avoid over-plotting). This clustering was applied to the total dataset (all timepoints and replicates); for CA staining, events in cluster 1 or 2 were classified as CA+; for SG and HK, events in cluster 1 were classified as positive. This is equivalent to gating for event counting, but requires no user-dependent decisions about gate placement.

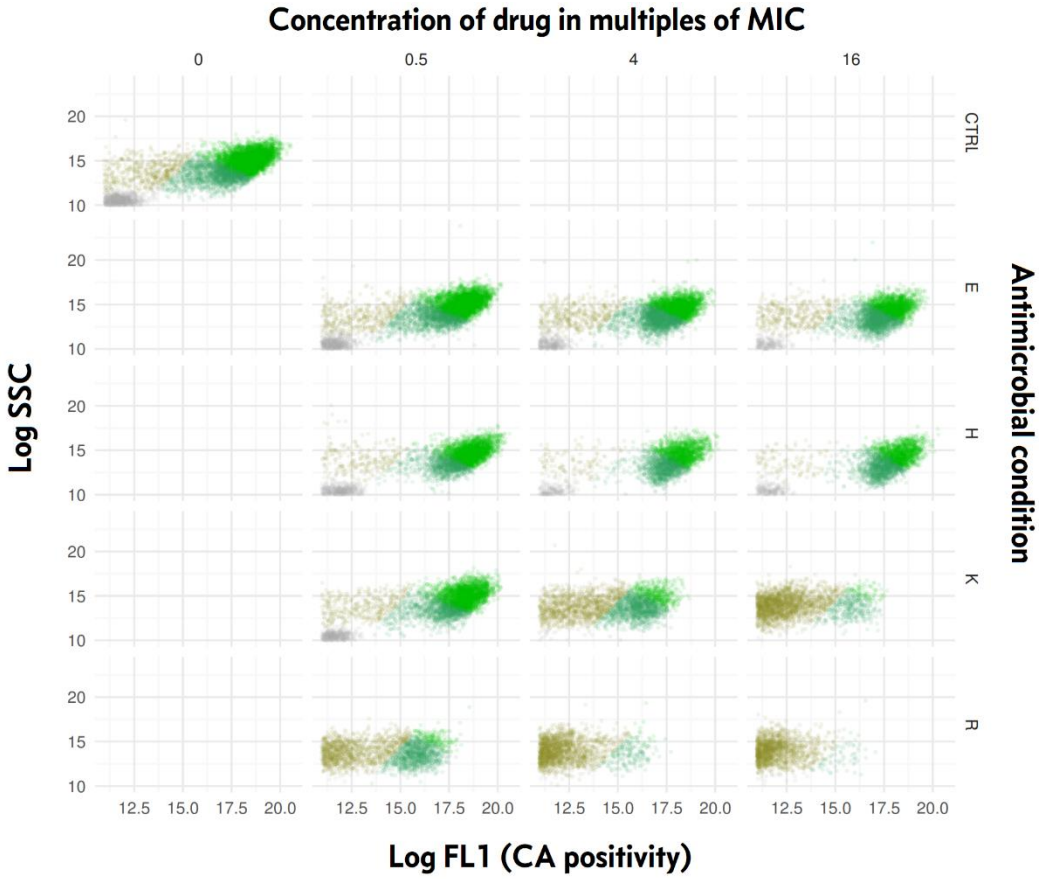

Figure 4-25. CA+ event clustering applied to new data

The clustering algorithm from previous figure applied to selected concentrations at day 2 timepoint from a different replicate of the time-kill experiment. CA+ events (cluster 1 and 2, light and dark green) are present in isoniazid (H), ethambutol (E) and no antibiotic control (CTRL) conditions, but substantially reduced by kanamycin and rifampicin in a concentration dependent manner. The clustering makes this easier to see compared to the raw FCM plots shown previously, and allows the CA+ events to be counted based on their clustering.

4.11.3 Time-kill curves

M. bovis BCG quantitative time-kill curves based on CFU count, CA+ count, SG+ count and total cell count (HK) are shown in figure 26. CFU, CA and SG as a proportion of total cell count are shown in figure 27.

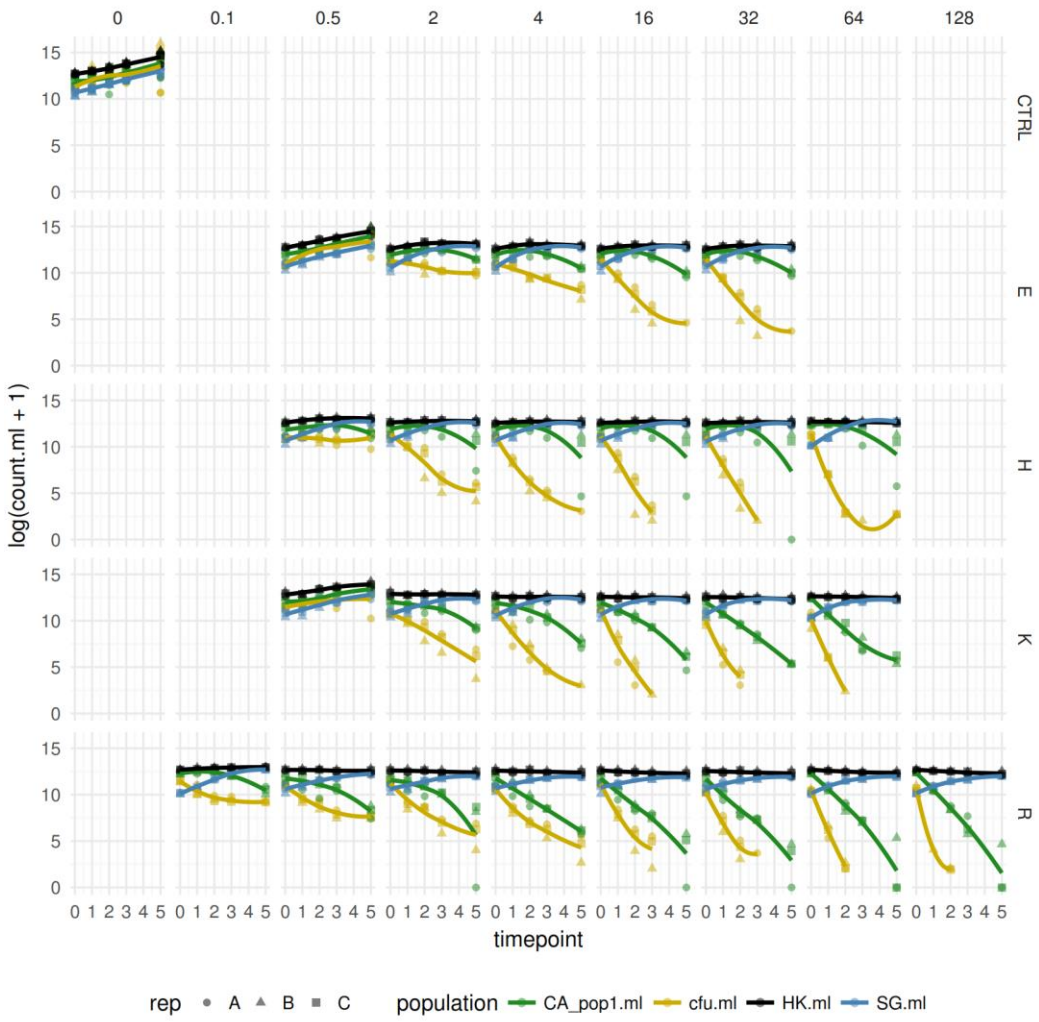

Figure 4-26. Time-kill curves for absolute counts.

Time-kill curves for ethambutol, isoniazid, kanamycin, and rifiampicin (E, H, K, R), and a no antimicrobial control growth curve are shown. All antimicrobials were tested at 0.5, 2, 4, 16, and 32x MIC; H and K were also tested at 64x MIC; R was also tested at 0.1, 64 and 128x MIC. The experiment was performed on three separate occasions with new *M. bovis* BCG cultures giving three replicates of each condition, except the no antimicrobial control which has six replicates. A loess regression line is fit to the data to show trend.

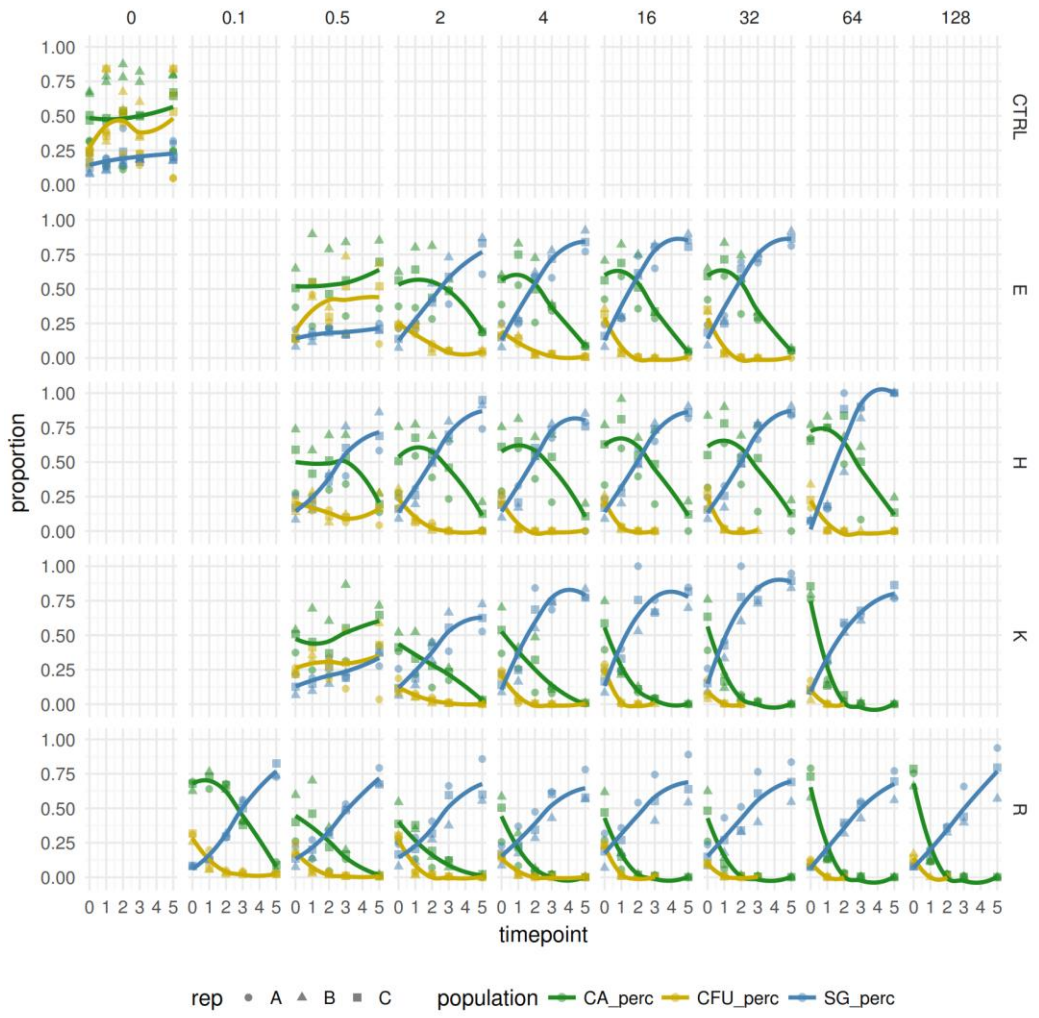

Figure 4-27. Time-kill curves based on proportions.

Same data as previous figure, but CA, CFU and SG counts are now represented as proportions of the HK total cell count denominator. A loess regression line is fit to the data to show trend.

The correlation between CA+ counts and CFU counts seen under nil antimicrobial growth conditions is lost when bacilli are exposed to antimicrobials. CFU counts decline more rapidly than CA+ counts under all antimicrobial conditions. CFU time-kill curves are linear or convex (on log scale) suggesting either mono or bi-exponential elimination; CA+ curves have a convex function for R and K, but a concave function for H and E where an initial increase in CA+ bacilli is seen around day 1. Overall, CFU forming behaviour is lost by many bacilli which are still intact and metabolically active according to FCM analysis.

SG+ counts rise under all antimicrobial conditions, but the rise is notably steeper and earlier for H & E compared to R & K.

4.11.4 Modelling FCM pharmacodynamics

Variation between replicates is notable on some plots, for example replicate A had overall lower proportion of CA+ events – including in drug free control – and a more profound collapse of CA+ counts by day 5, most clearly seen in the isoniazid conditions. There is also some variation in the starting inoculum between replicates in keeping with technical error.

To extract summary measures of PD effects as assessed by different population counts, the time-kill data was modelled using a linear mixed-effects model, with a fixed effect of intercept, and random slopes for antibiotic condition and replicate. The model form was:

$$\log cell\ count \sim intercept + (timepoint \mid condition) + (timepoint \mid rep)$$

where random effects are in parentheses. This captures the crossed design (as opposed to nested design) where-by each replicate was assessed under each antimicrobial condition. This allowed the effect of replicate to be estimated using data across all conditions, and the effect of condition to be estimated using data across all replicates (using Restricted Maximum Likelihood). The antibiotic condition effect, defined as slope gradient for the time-kill curve, was then extracted, independent of replicate effect, from the model as a summary PD measure. The R package *lme4* was used for this modelling.[312]

Figures 28 to 31 show CA+ count, CFU count, HK (total-cell) count, & SG+ proportion time kill curves respectively. In each, panel A shows the raw data, with a linear regression applied to each replicate within each condition. Panel B shows the output – predicted counts or proportions – after fitting a linear mixed-effects model. All models are for data from day 0 to day 5, except proportion SG+ (figure 31 B) which was modelled over day 0 to 3 because data appeared non-linear outside of this range.

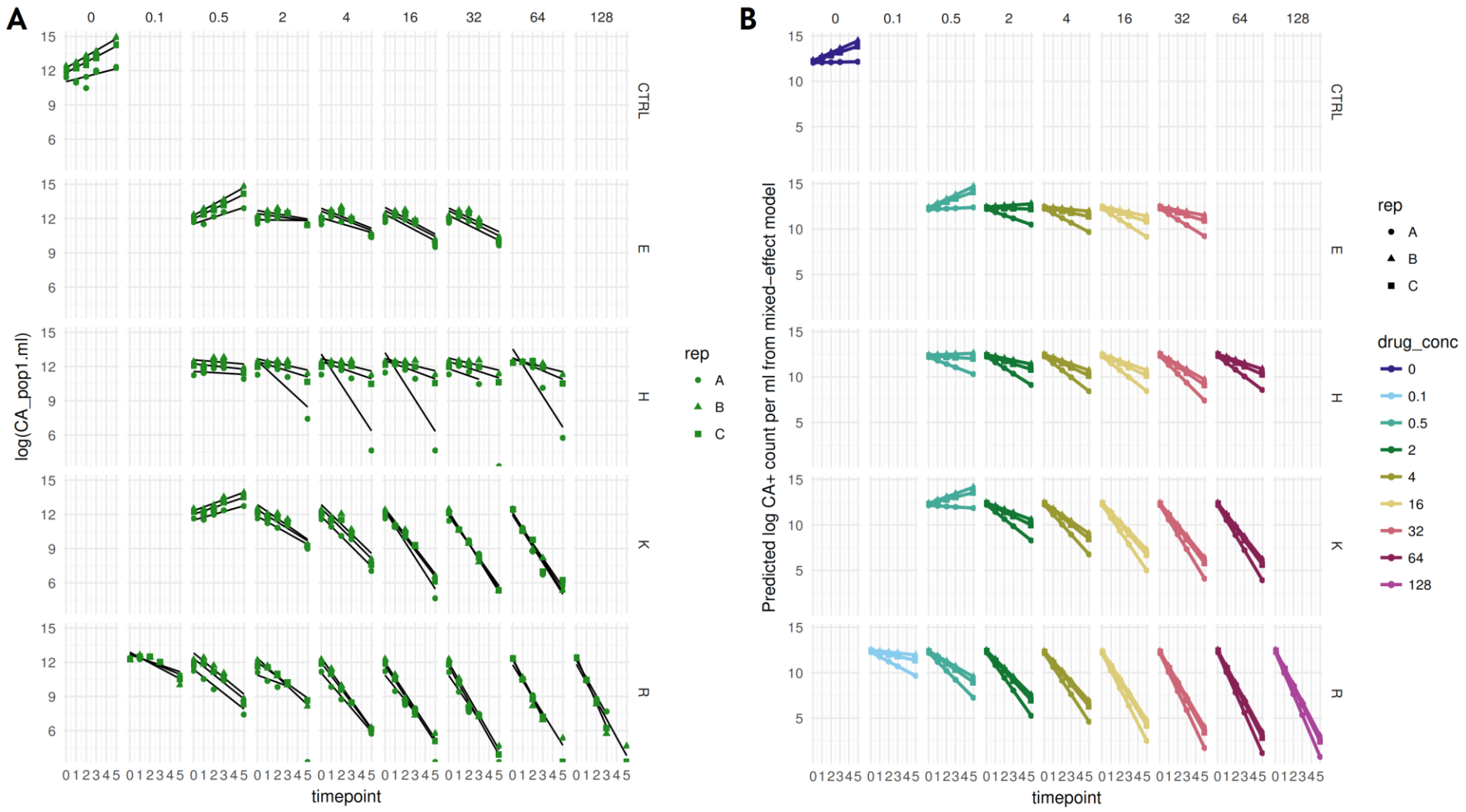

Figure 4-28. CA+ count time-kill data: raw (A) & modelled (B).

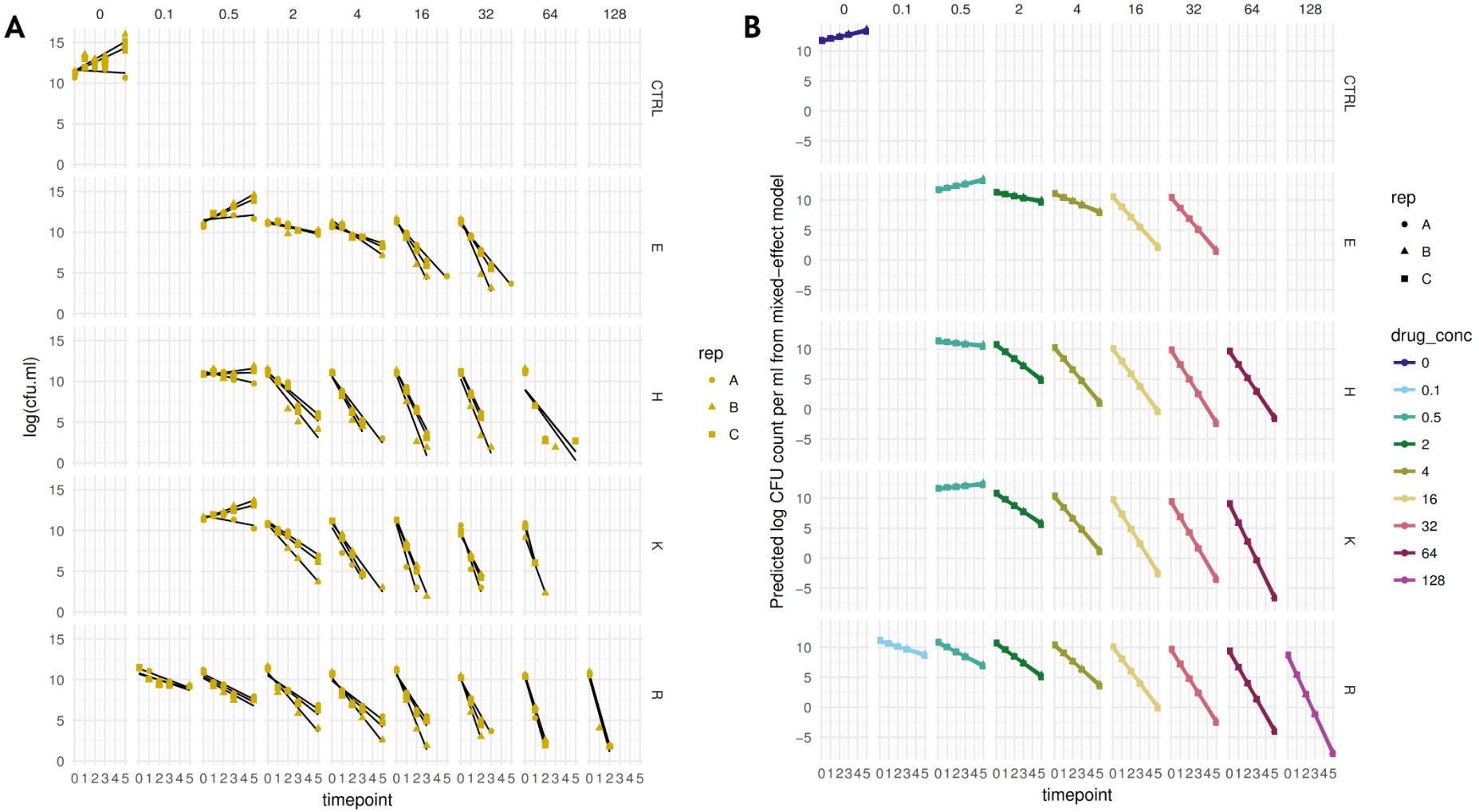

Figure 4-29. CFU count time-kill data: raw (A) & modelled (B).

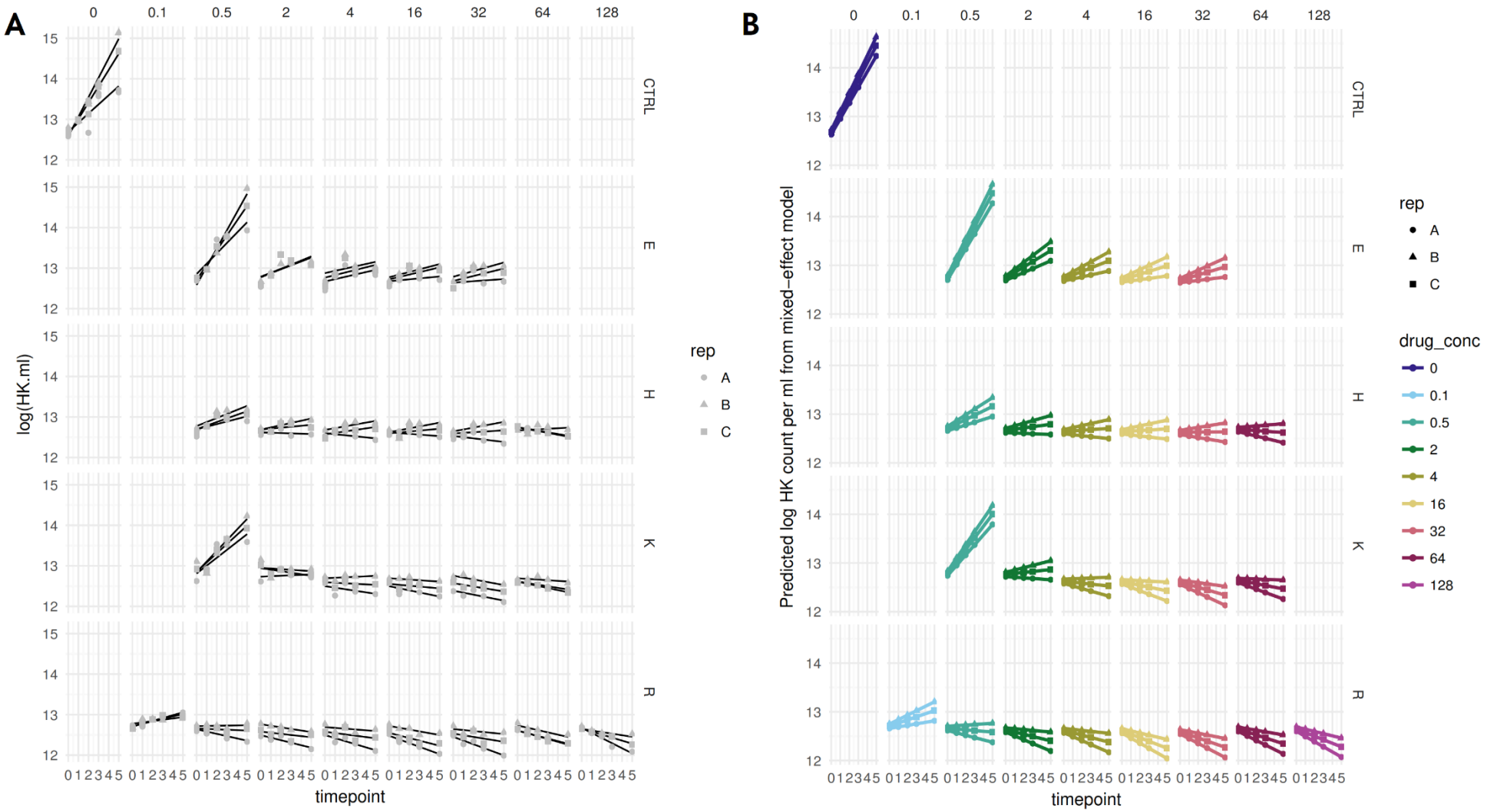

Figure 4-30. HK (total-cell) count time-kill data: raw (A) & modelled (B).

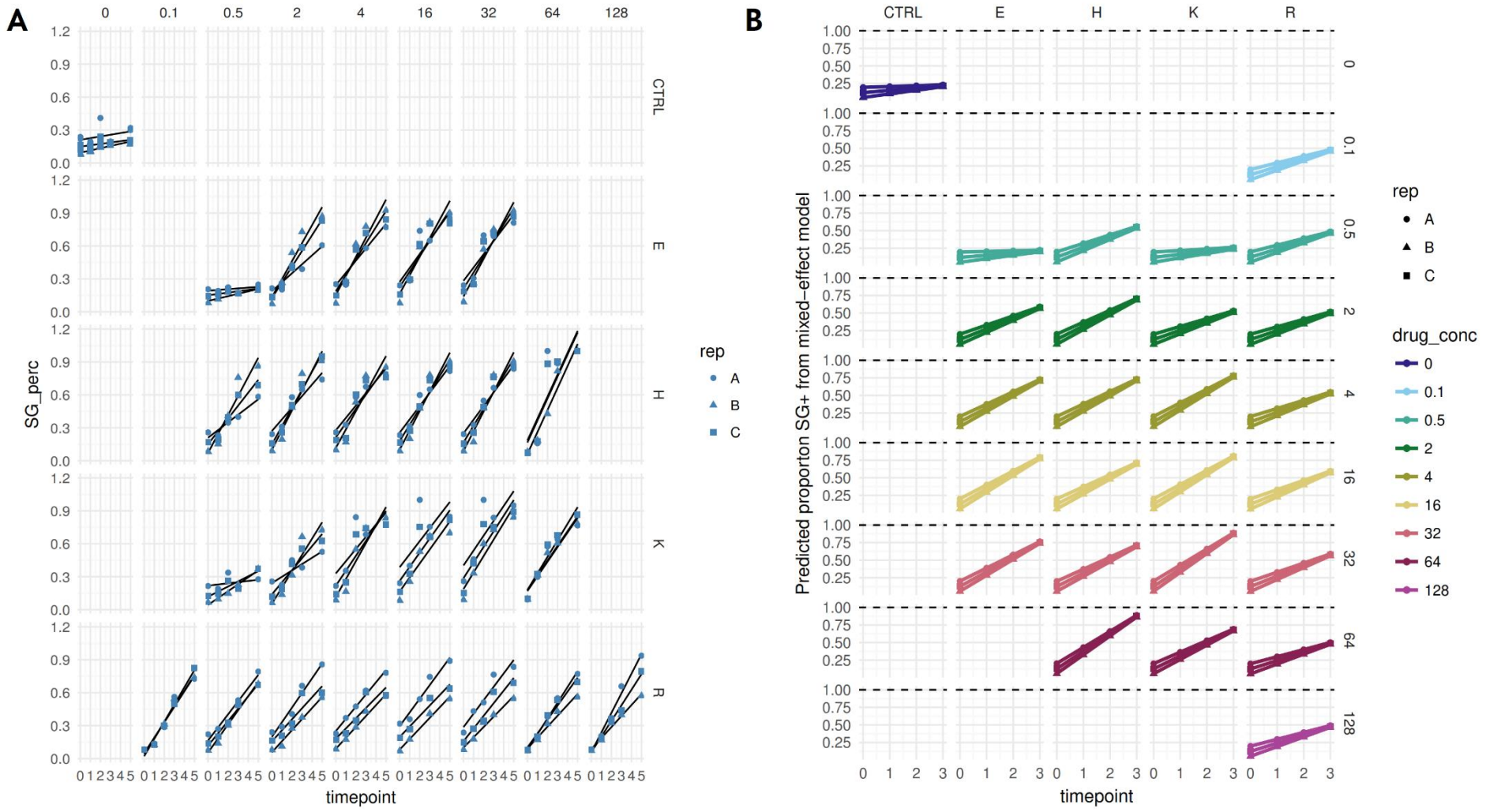

Figure 4-31. SG+ count time-kill data: raw (A) & modelled (B).

Antimicrobial effects extracted from these models were related to drug concentration for each antimicrobial using a standard sigmoid E_{max} PK/PD model, of form:

$$E = \frac{E_{max} \cdot C^n}{EC_{50}^n + C^n}$$

Where *E* is the PD effect (the slope gradient estimates by mixed-effects modelling above), *C* is the drug concentration (known from experimental condition), and the remaining parameters are estimated from the data: E_{max} (maximum achievable effect of antimicrobial), EC_{50} (the drug concentration where half of E_{max} is obtained), and *n* (a scaling parameter). These models summarise PKPD by antimicrobial and by cell population under study, i.e. allow comparison of antimicrobial killing effects when assessed by the different systems (CFU counting and FCM cell population counting).

Relative effects and rank order of antimicrobials differed depending on the cell population under study (figure 32). Rifampicin and kanamycin had higher estimated E_{max} for elimination of CA+ cells, while ethambutol and isoniazid had greater estimated E_{max} for rendering bacilli SG+. Indeed, effect of rifampicin and kanamycin on proportion SG% did not seem to follow a dose-response relationship (figure 32, bottom row). This is in keeping with their known mechanisms of action: intracellular acting rifampicin and kanamycin have more effect on intracellular metabolic activity, while cell-wall acting isoniazid and ethambutol, intuitively, would disrupt membrane integrity. For both CFU count and total cell count (HK population), rifampicin had the highest estimated E_{max} and lowest EC_{50}.

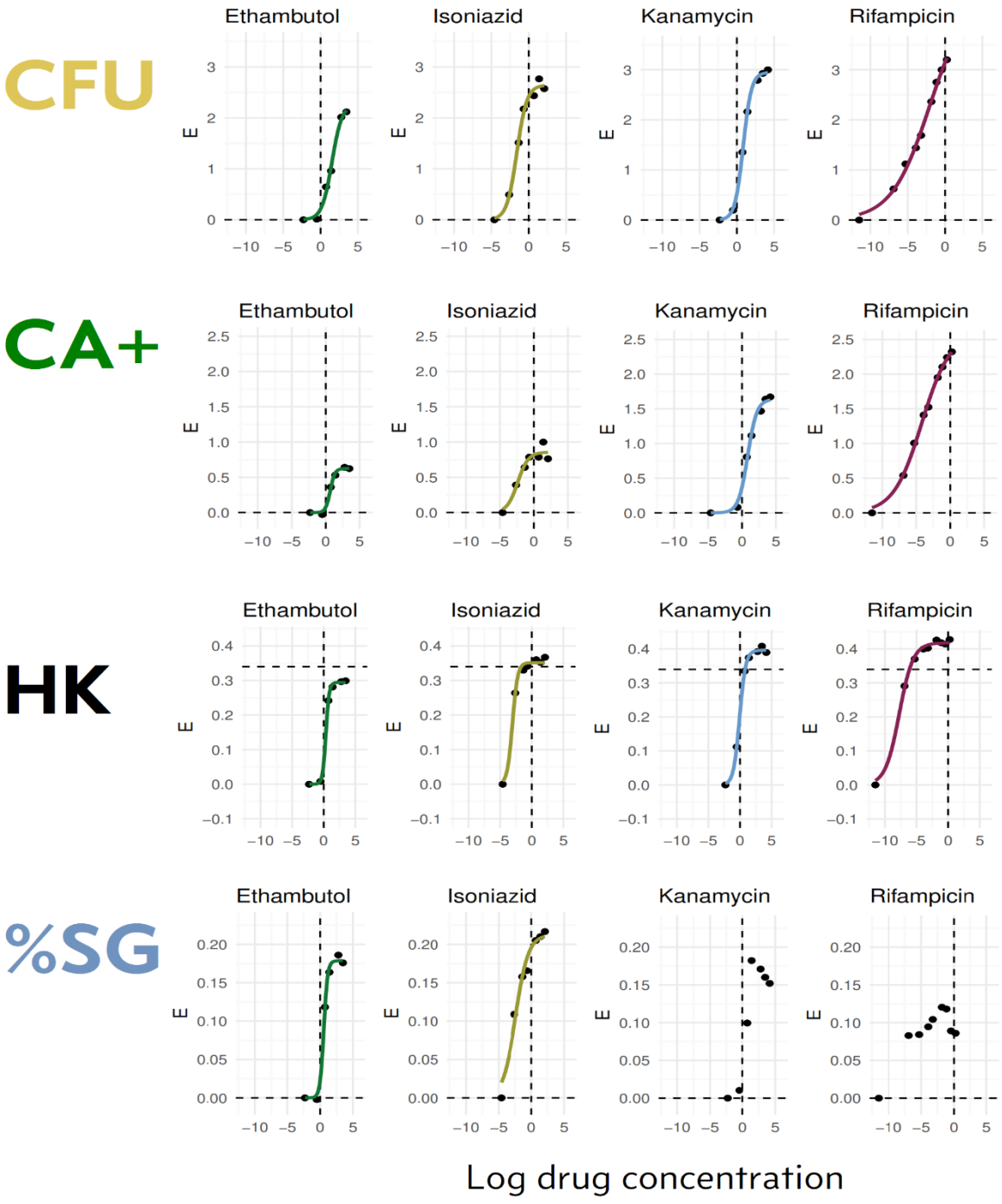

Figure 4-32. Sigmoid E_{max} models applied to CFU & FCM time-kill data.

Effects normalised against no antibiotic control and, in CFU, CA+ and HK counts, effects are all plotted on a positive scale, i.e. so that more effect = more cell death, & lower bounded at 0. The relationship between drug concentration and effect follows a sigmoid function in all cases, except the effect of rifampicin and kanamycin on proportion of cells SG+.

4.12 Dual SG+ population

As noted in figure 23, bacilli stained with SYBR-gold (without prior heat-killing) can be seen in some plots to have two populations separated by FL1, i.e. different SG+ brightness. This is most clearly seen for cultures treated with ethambutol or isoniazid. The brighter FL1 population has slightly higher SSC values, and approximately double fluorescence from SG staining of nucleic acid. This dual population is faintly visible in heat-killed SYBR-gold stained cells, but less clear perhaps due to disruption of nucleic acid structure by the action of heat. A detailed example is shown (figure 33).

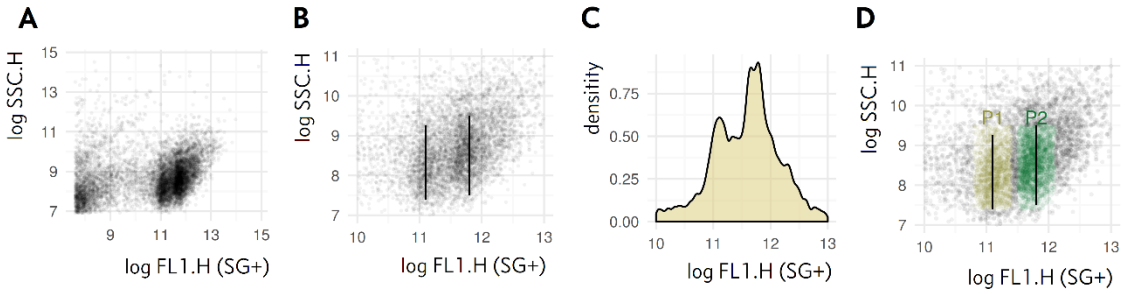

Figure 4-33. Example of dual SG staining population.

Example is from a BCG culture after 2 days exposure to ethambutol at concentration 16xMIC, with data acquisition o Accuri C6 with thresholding on FL1>2000 and SSC>2000 (**A**). Same data but 'zoomed-in' on dual population of interest, with horizontal bars on approximate median of the two populations (**B**). The dual FL1 fluorescence is most easily seen on a 1-dimension density plot of log FL1.H where 2 peaks are clearly seen (**C**). Gating by simple geometric region of the two populations (**D**).

Two possible explanations of this dual population were considered:

1. It exists in all cultures to the same extent, but is made more visible by increased cell permeance to SYBR-gold caused by cell wall active antimicrobials.
2. The dual population is a physiological response by bacilli, differentially induced by cell wall active versus intracellular acting antimicrobials.

To investigate these explanations further, it was thought necessary to develop a method to routinely permeabilise bacilli membranes to SYBR-gold, without heat-killing disruption of nucleic acid structure, and without causing significant cell destruction. This would allow observation of any differential effect of antimicrobials independent of their permeabilization of the cell membrane, and without the 'noise' created by nucleic acid damage from heat-killing.

4.12.1 Development of a membrane permeabilization method

Published methods for permeabilizing mycobacterial cell walls were reviewed; those with highest reported success and best description of validation[490,491] were taken forward for testing and adaptation. Some example iterations of the method development are shown in figures 34 & 35, all experiments were performed on early to mid-log phase *M. bovis* BCG cultures grown as per the time-kill experiments detailed above.

Without PFL and NH_4Cl fixation
No treatment control ("SG")
Heat killed control ("HK")
80% ethanol 60 min RT ("ET")
1M HCl 40min 37°C ("HCl")
40% ethanol + 1M HCl 40min 37°C ("AH")
Lysozyme (2mg ml^{-1} in H_2O) 37°C for 30 min ("LZ")
0.1% triton-X-100 30-60min RT ("TX")
Lysozyme as above + 0.1% triton-X-100 5min RT ("CM")

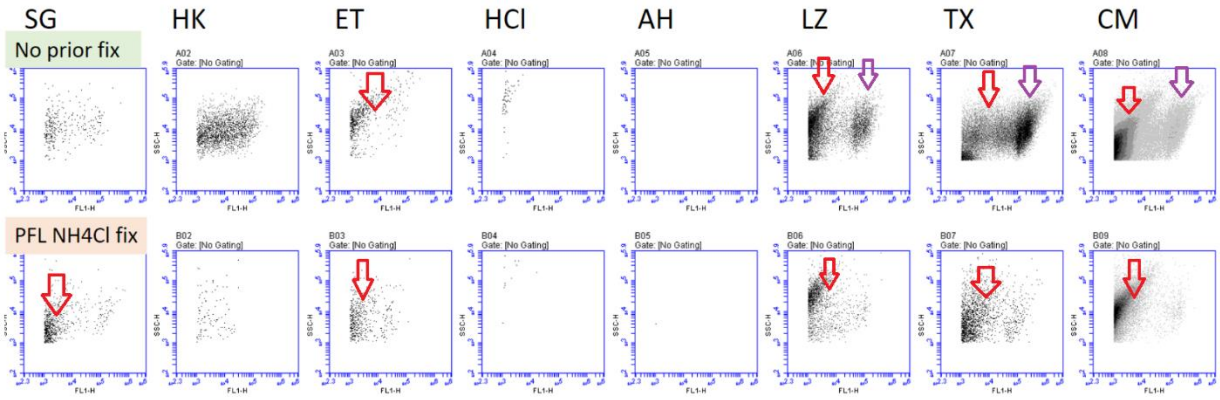

Figure 4-34. Permeabilization method development, experiment 3.4.

8 methods (summarised in table) were tested in this iteration, all with and without prior paraformaldehyde / ammonium chloride fixation (8 x 2 = 16 conditions), and with 2.5 hour SYBR-gold incubation or 16 hour SYBR-gold incubation (16 x 2 = 32 conditions). Only the 2.5hour incubation FCM plots are shown here as duration of SYBR-gold incubation had no observed effect. Ethanol and hydrochloric acid at the concentrations and incubations tested in this replicate caused near complete destruction of the cells. In this replicate, lysozyme and detergent conditions tested (LZ, TX, CM) were most able to reveal the dual SG stain population of interest (purple arrows); the addition of prior fixation with paraformaldehyde / ammonium chloride (PFL NH4CL, lower row) caused cell destruction. Note that heat fixing (HK) allowed SG to stain cells, but the dual population is not seen, possibly due to heat disruption of nucleic acid structures. Red arrows show poorly staining cells or possibly cell debris. In subsequent iterations, different concentrations and incubation times and temperatures were investigated for lysozyme and triton-X-100.

Condition	Initial wash step	Lysozyme		Triton-X-100		SG stain
		conc	incubation	conc	incubation	
A	4ml broth + 10ml PBS/tween, 4000G 15min	0mg/ml	20min 37oC	0%	5min RT	6 hours
B	4ml broth + 10ml PBS/tween, 4000G 15min	0.05mg/ml	20min 37oC	0%	5min RT	6 hours
C	4ml broth + 10ml PBS/tween, 4000G 15min	0.5mg/ml	20min 37oC	0%	5min RT	6 hours
D	4ml broth + 10ml PBS/tween, 4000G 15min	2mg/ml	20min 37oC	0%	5min RT	6 hours
E	4ml broth + 10ml PBS/tween, 4000G 15min	0mg/ml	20min 37oC	0.03%	5min RT	6 hours
F	4ml broth + 10ml PBS/tween, 4000G 15min	0.05mg/ml	20min 37oC	0.03%	5min RT	6 hours
G	4ml broth + 10ml PBS/tween, 4000G 15min	0.5mg/ml	20min 37oC	0.03%	5min RT	6 hours
H	4ml broth + 10ml PBS/tween, 4000G 15min	2mg/ml	20min 37oC	0.03%	5min RT	6 hours
I	4ml broth + 10ml PBS/tween, 4000G 15min	0mg/ml	20min 37oC	0.20%	5min RT	6 hours
J	4ml broth + 10ml PBS/tween, 4000G 15min	0.05mg/ml	20min 37oC	0.20%	5min RT	6 hours
K	4ml broth + 10ml PBS/tween, 4000G 15min	0.5mg/ml	20min 37oC	0.20%	5min RT	6 hours
L	4ml broth + 10ml PBS/tween, 4000G 15min	2mg/ml	20min 37oC	0.20%	5min RT	6 hours
M	None	0.1mg/ml	30min 37oC	0.20%	5min RT	4 hours
N	None	0.1mg/ml	30min 37oC	0.20%	5min RT	4 hours
O	None	0.1mg/ml	30min 37oC	0.20%	5min RT	4 hours
P	None	0.1mg/ml	45min 37oC	0%	5min RT	4 hours
Q	None	0.1mg/ml	45min 37oC	0%	5min RT	4 hours
R	None	0.1mg/ml	45min 37oC	0%	5min RT	4 hours
S	None	0.1mg/ml	60min 37oC	0.20%	5min RT	4 hours
T	None	0.1mg/ml	60min 37oC	0.20%	5min RT	4 hours
U	None	0.1mg/ml	60min 37oC	0.20%	5min RT	4 hours
V	None	0.1mg/ml	120min 37oC	0.20%	5min RT	4 hours
W	None	0.1mg/ml	120min 37oC	0.20%	5min RT	4 hours
X	None	0.1mg/ml	120min 37oC	0.20%	5min RT	4 hours

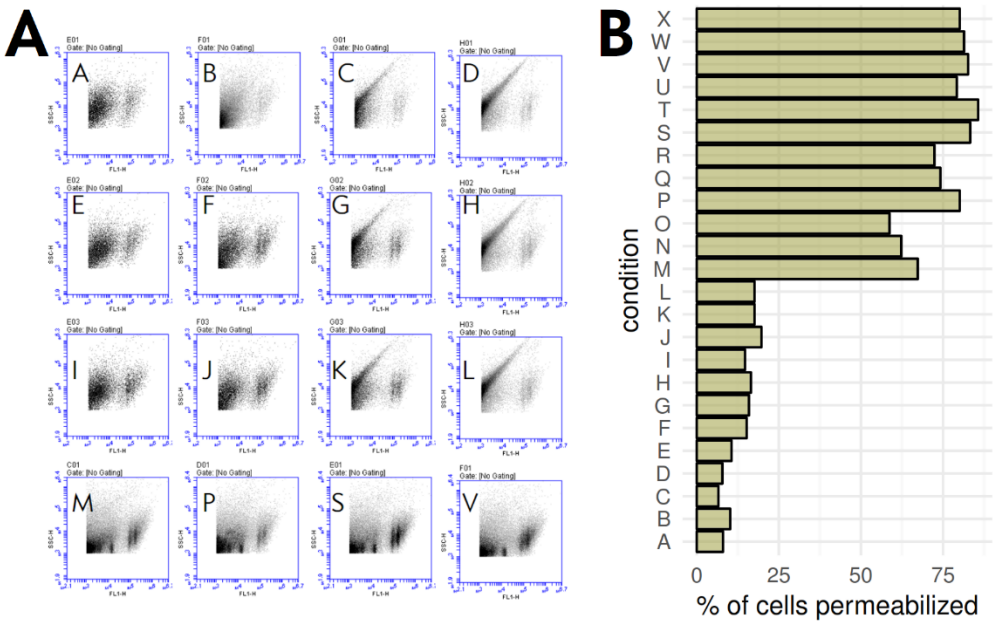

Figure 4-35. Permeabilization method development, experiment 5.0 & 5.1.

16 methods (A to L, and 3 reps of 4 conditions M to X)) tested using different wash, lysozyme and triton-X-100 concentrations and incubations. All resulted in a permeabilized cell population of interest with dual SG staining populations visible (**A**). Compared to a heat-killed control, which gives a reliable total cell count, methods with a lower lysozyme concentration but longer incubation times (e.g. method S and V), showed that up to 80% of cells could be permeabilized without cell destruction (**B**).

This led to a final method for reliable permeabilization of BCG bacilli without substantial cell loss, such that over 80% of bacilli could be SYBR-gold stained (compared to the heat-killed total cell count denominator gold standard). The final method used was:

1. 500µl broth culture sample diluted to 1ml with PBS v/v 0.15%Tween 80, but no wash step.
2. Needle emulsified (12 passes through a double luer-lock ended, 25 Gauge, 4-inch, micro-emulsifying needle).
3. 500µl lysozyme added to final conc 0.1mg/ml.
4. Incubated for 45 minutes at 37°C.
5. 500µl triton-X-100 added to final concentration v/v 0.2%.
6. Pelleted (16000 *g* , 5 min) and re-suspended in 500µl PBS-tween; 40µl working stock SYBR-gold added and incubated at room temperature for 2-4 hours.
7. FCM with thresholding on FL1 and SSC.

4.12.2 Differential dual SG staining population characteristics by antimicrobial action

To investigate the effect of antimicrobials on the development of dual SG staining populations, mid-log phase *M. bovis* BCG cultures were grown under the same conditions described for the time-kill experiments above. Independent cultures with different antimicrobial conditions were set up, sampled at timepoints 2, 3 and 5 days after addition of antimicrobials. Samples were processed as per the permeabilization method outlined in the previous section.

With standardised permeabilization of all bacilli (or about 80% of cells), all FCM plots demonstrated dual SG staining populations (figure 36).

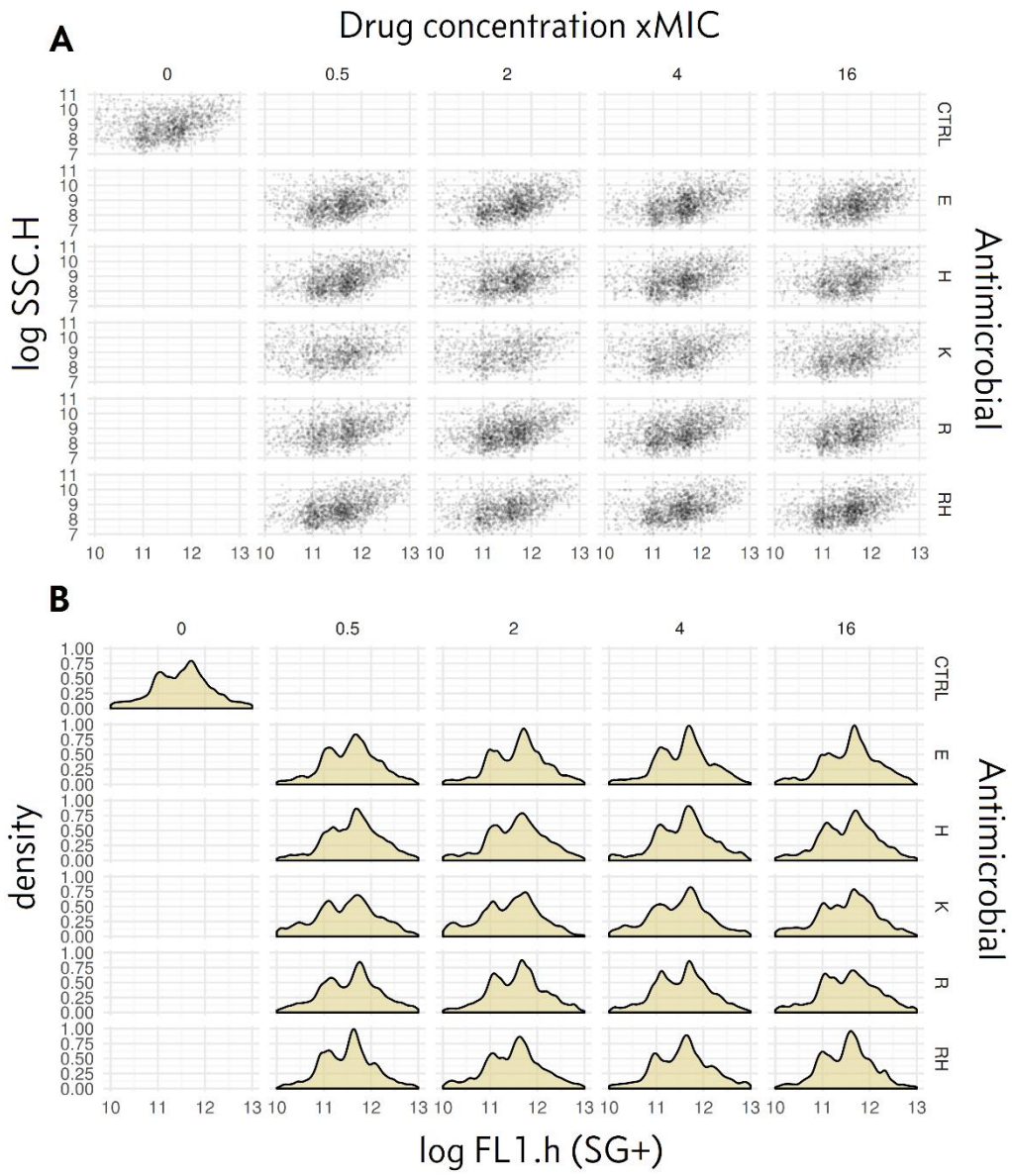

Figure 4-36. Permeabilized BCG cells show dual SG staining under all antimicrobial conditions tested.

Examples shown are from BCG cultures after 3 days exposure to 4 different antimicrobials (E=ethambutol, H=isoniazid, K=kanamycin, R=rifampicin) at concentrations 0.5, 2, 4, & 16 xMIC. RH is rifampicin at these concentrations, but with isoniazid added as a second agent at a constant 2 xMIC in all cases. A no antibiotic control is also shown (CTRL). Dual SG stained populations are visible in all conditions after permeabilization (**A**). The 1-D density plots (**B**) show two peaks, but the relative height of these twin peaks differs by antimicrobial.

Gating bacilli the SG stained bacilli into two populations (P1 and P2 as per figure 33) allows quantitative comparison of the populations. Across all the antimicrobial conditions and the three timepoints sampled, mean FL1 fluorescence of P1 and P2 was 11.1 and 11.8 respectively, meaning that on average P2 bacilli had almost exactly double the SG staining intensity of P1 bacilli [exp(11.8) / exp(11.1) = 2.01], in keeping with them containing twice the amount of nucleic acid, which SG stains.

The ratio of number of bacilli in P2 to number in P1 varied by antimicrobial. Bacilli treated with isoniazid or ethambutol increased the relative number of P2 bacilli compared to control and other antimicrobials (figure 37). Rifampicin, and to lesser extent, kanamycin, prevented the development of P2 bacilli (compared to control); bacilli treated with isoniazid also did not develop a larger P2 population when co-exposed to rifampicin (figure 37).

Some of the effects of antimicrobials on the dynamics of SG+ populations may have been partly time dependent (figure 38).

4.12.3 Imaging characteristics of the dual SG+ bacilli populations

To further explore the nature of the P1 and P2 cell populations, permeabilized SYBR-gold stained cells from day 3 after treatment with rifampicin, isoniazid, or ethambutol were cell-sorted based on their P1 and P2 gate for downstream fluorescent microscopy. The log SSC.H by FL1 plots were recreated for these samples on a FACS Vantage to permit sorting.[*******] Sorted populations were then examined by fluorescent microscopy.

P2 bacilli appeared to be longer, with more discrete SG positive regions; several P2 bacilli had a V shape similar to that seen in binary fission prior to cell division [492](figure 39).

[*******] With thanks to Mr Ronnie Dreyer from Division of Immunology University of Cape Town for access to and assistance with using the FACS Vantage for this experiment.

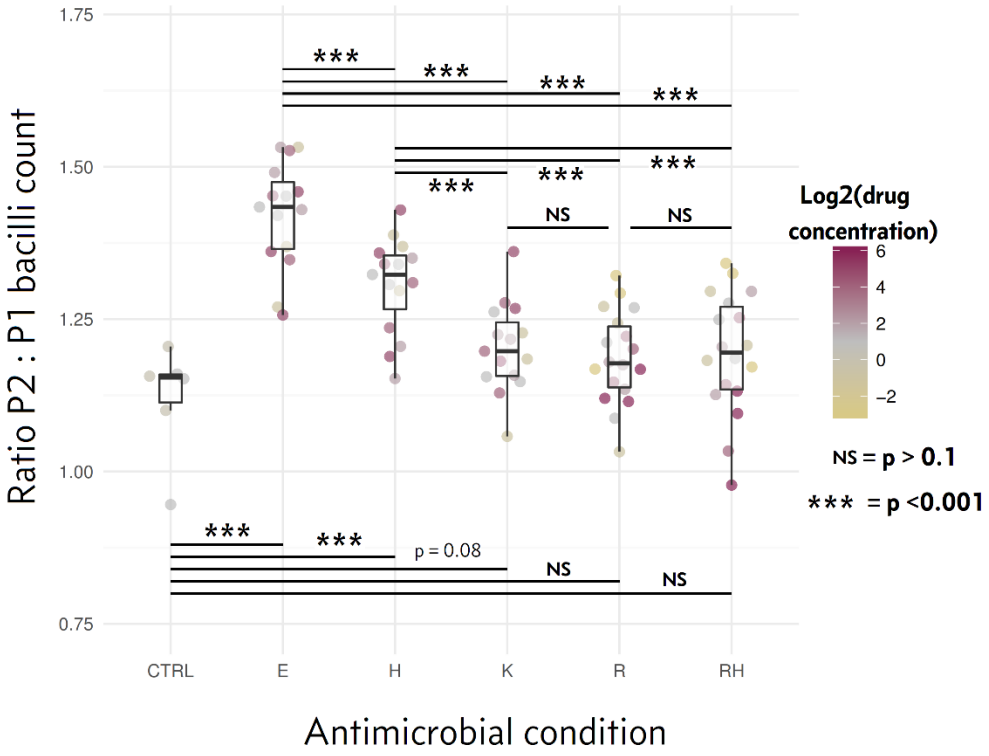

Figure 4-37. Ratio of P2 to P1 bacilli by antimicrobial condition.

Each antimicrobial condition (n= 27) is an independent culture; each was sampled at 3 timepoints (day 2, 3 &5 after addition of antimicrobials) giving 27*3 = 81 antimicrobial data points, plus two no antibiotic control cultures sampled at the three timepoints, giving 6 no antibiotic control (CTRL) data points. E=ethambutol, H=isoniazid, K=kanamycin, R=rifampicin at concentrations ranging from 0.1 to 64 xMIC. RH is rifampicin at range of concentrations, but with isoniazid added as a second agent at a constant 2 xMIC in all cases. Significance testing with pairwise t tests (all *** p-values remain <0.05 after Bonferroni correction for multiple comparison). Overlaid boxplots show median, IQR and range (bar, box, whiskers respectively).

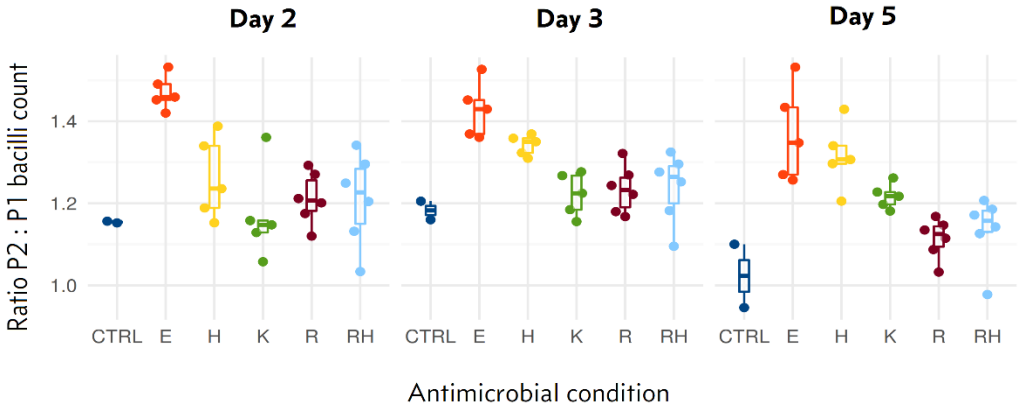

Figure 4-38. Ratio of P1 to P2 bacilli by antimicrobial and duration of exposure.

Same data as figure 35 disaggregated by timepoint of sample.

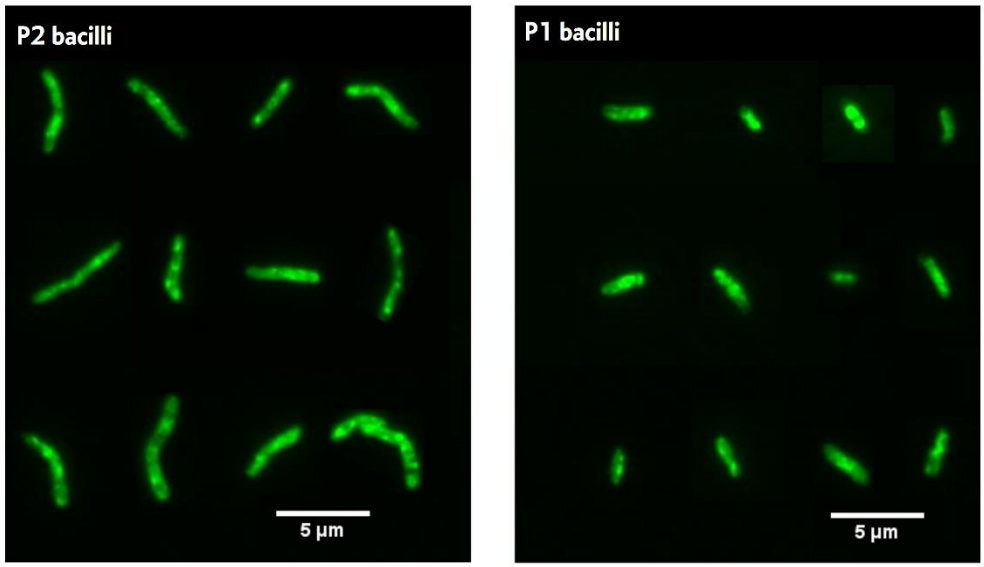

Figure 4-39. Images of bacilli stained with SYBR-gold and sorted by P1 & P2.

12 randomly selected images from microscopy of sorted P1 and P2 bacilli.

To quantify these differences, images of bacilli were analysed in Image J / FIJI.[493] An axis was drawn from one bacilli pole to another manually; the fluorescence intensity for each pixel on this axis, and its coordinates, were extracted as vectors (these vectors are plotted for each of 40 bacilli in figure 40). Local maxima (peaks) in fluorescence and the length of the bacilli were then derived from these vectors using custom written functions in R studio.

On average P2 bacilli were just under twice the length of P1 bacilli (mean 4.01 versus 2.45 µm; median 4.00 versus 2.52 µm respectively), and had almost exactly double the number of fluorescent peaks (mean 6.0 versus 3.2 peaks; median 5.5 versus 3.0 peaks respectively) (figure 40). Different degrees of smoothing altered the number of peaks, but the average ratio between P2 and P2 bacilli stayed approximately the same at ~2 (data not shown).

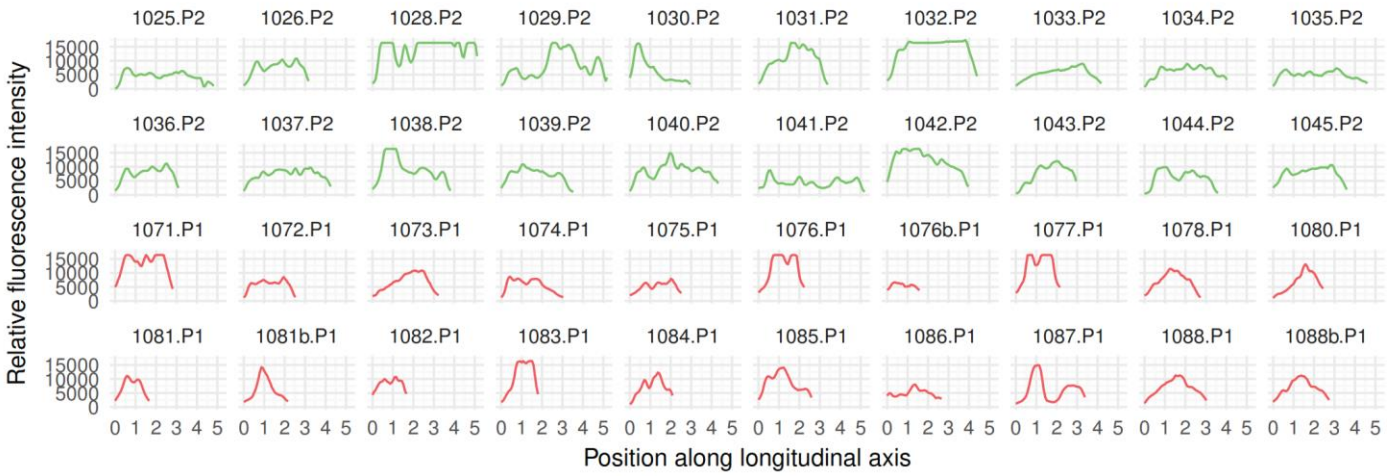

Figure 4-40. Fluorescence along longitudinal axis of P2 & P1 bacilli.

40 randomly selected bacilli images from antimicrobial treated (rifampicin, isoniazid or ethambutol), permeabilized, SG stained and sorted populations. Top rows (green) are bacilli from P2, bottom rows (red) are bacilli from P1. Images were analysed in Image J / FIJI to extract fluorescence intensity along the longitudinal axis. Each plot shows fluorescence intensity by distance (in uM) along bacilli axis.

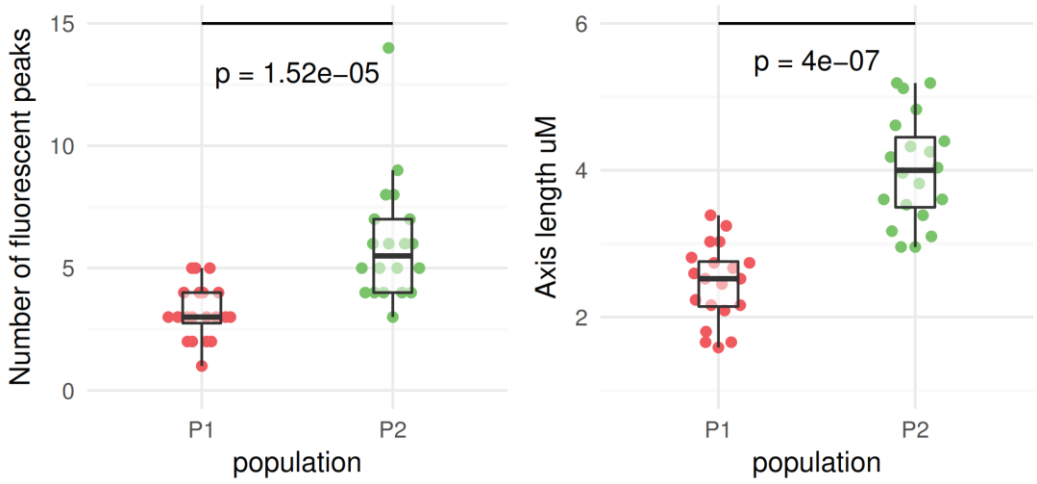

Figure 4-41. Number of fluorescent peaks and bacilli length by P1 & P2.

Number of peaks in the bacilli axis plots shown in figure 40 were counted using a custom written function in R studio. In brief, a loess regression line was applied to the fluorescence intensity by axis position data for each image to smooth out small peaks and local maxima along this regression line were counted. The number of fluorescent peaks differed significantly between P1 & P2 (left panel), as did bacilli length (right panel). P values are from Wilcox rank sum tests.

4.13 Discussion

This chapter describes development and validation of an absolute counting method for *in vitro* broth cultures of mycobacteria using flow cytometry. The most novel aspects of this method are the use of fluorescence signals based on SYBR-gold staining to define which FCM events are bacilli. The method showed a negligible false discovery rate, minimal coefficient of variation between replicates, and near perfect linearity of counts across serial dilutions. In addition, methods for measuring and minimising clumping in samples, and the major impact of clumping on apparent numbers of bacilli (e.g. CFU counts), were demonstrated.

Method development in laboratory science isn't generally met with enthusiasm by basic scientists who are more interested in mechanism discovery; it is worth explicating why the method developments in this chapter are important. The establishment of these methods is important for several reasons.

Firstly, much current work in research mycobacteriology is focussed on exploring phenotypic heterogeneity or sub-populations of bacilli with different physiological characteristics, such as the differentially culturable bacteria discussed at the start of this chapter. If the total cell count denominator is unknown in these experiments it makes the results harder to interpret. For example, showing that the most-probable number of bacteria in Rpf+ liquid culture is several-fold higher than CFU counts is interpreted as evidence of a predominant differentially culturable subpopulation.[406,407] But if the different processing and culture systems disrupt clumped bacilli to different degrees, this would make these findings spurious.

Similarly, if CFU-counts are regarded as equivalent to counts based on metabolic activity as assessed by fluorescent probes, comparisons between experimental conditions based on these two assays might be erroneous. For example, a recent study by Aljayyoussi *et al*. compared killing dynamics of first line TB drugs for extracellular versus intracellular GFP-expressing H37Rv *M. tuberculosis* bacilli.[494] Extracellular bacilli kill was assessed by decline in CFU count, while intracellular killing was assessed by decline in GFP+ bacilli; rifampicin had greatest effect on intracellular bacilli which

helped these *in vitro* results correlate with clinical trial findings. But is this evidence that rifampicin has better intracellular killing, or that it has greater effect on GFP expression than other drugs?

As a final example, consider *M. tuberculosis* multiples-of-infection (MOI) of immune cell models used by TB immunologists. These either rely on OD_{600} measurements of live cultures with dilution to required density, or on CFU counts of frozen aliquots.[495,496] Because the ratio of clumps to single-cells, and the ratio of CFU counts to total cell count, is uncontrolled and unobserved in these methods, MOI isn't actually known with accuracy and will not be comparable across studies. Also shown in the current work, the 'gold-standard' method for single-cell suspension preparation of bacilli using low *g* centrifugation does not work.

The work presented in this chapter shows how to prepare single-cell suspensions of bacilli (using early-log phase cultures and needle emulsifying), and how to accurately quantify bacilli for downstream experiments using flow cytometry. It is also shown that calcein positive bacilli counts can be used as a highly accurate and rapid surrogate of CFU count, available within hours rather than weeks for slowly growing mycobacteria. This has the potential to greatly simplify some *in vitro* mycobacteria experimental protocols.

Conversely, differences in CA+ and CFU counts – even in antibiotic-free cultures – were shown in this chapter. Proportion of cells which are CA+ correlates with instantaneous rate of growth of the whole population in a static culture (but CFU count does not). This compliments the findings of Hendon-Dunn et al. who showed that mean calcein fluorescence correlates with rate of growth in a continuous culture system.[443] This suggests that CFU formation is not simply a reflection of metabolic activity, but a more specific cell phenotype, possibly dependent on so far undefined factors rather than overall metabolic state.

Correlation of CFU counts with CA+ counts is unequivocally lost at early timepoints after exposure to antimicrobials. FCM defined populations appear to give different 'windows' on pharmacodynamic activity of anti-mycobacterial compounds. Intracellular acting antimicrobials (rifampicin, kanamycin) have more profound early effects on calcein activity, while cell-wall acting drugs (isoniazid, ethambutol) cause earlier marked

membrane damage assessed by SYBR-gold permeance. That FCM can distinguish antimicrobials by mechanism of action replicates the findings of Hendon-Dunn *et al.*,[443] but with the advance that proportions of cells are related to an absolute total cell count denominator. This is important, because differences were seen in the dynamics of this total cell count. Rifampicin appeared to cause greater complete cell destruction than other drugs; this effect would have been unobserved by the four cell populations defined by Hendon-Dunn *et al.*'s analysis.

In summary, FCM allows different pathways of cell death to be observed, giving some support to the hypothesised spectrum of cell vitality reviewed at the start of this chapter (figure 42).

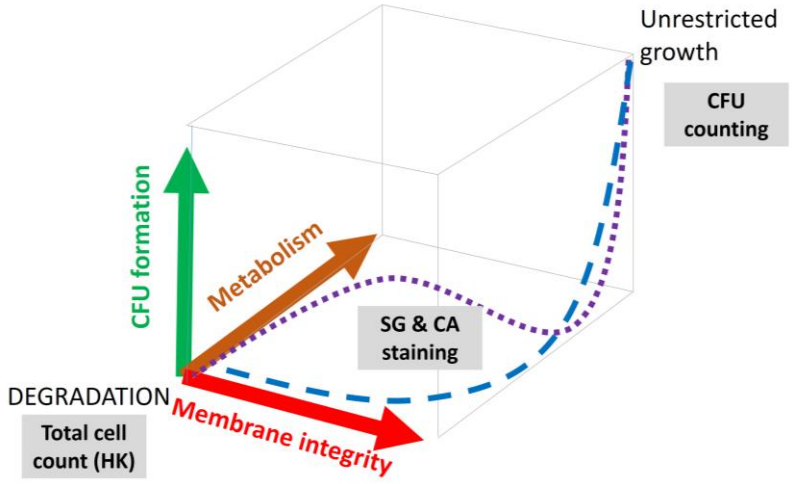

Figure 4-42. Continuous spectrum of live/dead cell states of bacilli, as observed by CFU & fluorescent probes in FCM.

Populations of cells defined by CFU and FCM are related to the schematic shown previously in figure 2. Loss of CFU formation is an early event in the pathway from unrestricted growth to irreversible cell death. Loss of metabolic activity (CA positivity) and membrane integrity (SG positivity) develop more slowly after exposure to antimicrobials, and differentially by antimicrobial mechanism of action (intracellular action drugs = dashed blue path; cell-wall activity drugs = dashed purple path). Eventual cell destruction can also be assessed by FCM analysis.

Perhaps the major question is which pharmacodynamic window is the most important? In other words, do dynamics of FCM defined populations give substantive information about antimicrobial activity? Unfortunately, the current analysis cannot answer this question. The point of irreversible cell death on these pathways, and markers of bacillary drug tolerance and persistence, remain poorly defined. The fact that different antibiotics have different effects on FCM defined subpopulations may be important, or may be an unhelpful complication.

Nonetheless, the methods developed in this chapter could be useful tools for exploring mycobacterial pharmacodynamics further. One approach would be to assess if there are greater differences in time-kill dynamics between different clinical isolates when assessed by FCM compared to CFU counting. One previous report has suggested that time-kill characteristics of clinical isolates *ex vivo* are predictive of clinical outcome, and independent of isolate MIC.[497] This could be further explored using the FCM methodology in this chapter. This would require overcoming a major technical difficulty of standardising growth *in vitro* for time-kill experiments. Cultures subbed from the same BCG starter culture – using identical broth, culture flasks and incubator – resulted in different growth curves when assessed with flow cytometry (for example random effects on %CA+ - figure 14). Rates of growth influence antimicrobial tolerance,[498-501] and this variation is a major weakness of the current analysis. Notably, use of a continuous culture chemostat (as per the Hendon-Dunn FCM study) can make growth conditions reproducible,[442] but is resource intensive and available in few labs.

Finally, a novel finding in the current analysis is that two populations of SYBR-gold staining bacilli are seen on FCM, one having double the fluorescence of the other. Drug exposure increased the relative abundance of the brighter SG+ population (P2), but with significant differences by antimicrobial. In particular, rifampicin demonstrated ability to suppress development of P2. Since SYBR-gold predominantly stains DNA it could be speculated that P2 bacilli have a higher complement of chromosome copies. This hypothesis is weakly supported by the fact the populations were discrete (and align to a log2 scale), and also by the results of imaging analysis, which suggested P2 bacilli were larger with more discrete SG+ regions, perhaps having arrested during binary fission prior to cleavage into two daughter cells.

Ploidy is harder to define for bacteria than eukaryotic cells, since bacteria are not consistently uni-nucleoid.[502] Decoupling of chromosome replication and cell division is, however, reported for mycobacteria. For example, bacilli in stress conditions are found to be diploid.[503] It is suspected that filamentous mycobacteria found in macrophages may be polyploid.[504] TB researchers have further noted that elongation without division results in polyploid cell phenotypes of *E. coli*, which are capable of persistence and drug-resistance mutation from a starting population of just 100 bacteria under some microenvironment conditions.[504] It could be speculated that the P2 population which developed under antimicrobial exposure in the current work represents a specific persister phenotype, and that if these cells contain multiple chromosome copies they would have increased propensity for developing drug resistance. In this interpretation, the fact that, in relative terms, isoniazid induces but rifampicin supresses P2 numbers is of interest. The FCM system developed in this chapter offers a potential high-throughput tool to investigate ploidy in mycobacterial pharmacodynamics.

In summary, the FCM method developed in this chapter facilitates mycobacterial lab work, and adds to the evidence that culturable mycobacteria give only one window on pharmacodynamics. Both these conclusions are exploited in the next chapter, which describes the development novel methods of counting mycobacteria in blood, and their use in a clinical pharmacodynamic study of MTBBSI.

5 Pharmacodynamics of MTBBSI: development of biomarkers & a clinical study

5.1 Introduction

5.1.1 Rationale for developing PD biomarkers of MTBBSI

MTBBSI is the mode of severe HIV-associated tuberculosis infection in adult inpatients. It is highly prevalent, and a strong, independent predictor of mortality. This is shown by the most detailed clinical study of severe HIV-associated TB to date (the KDHTB study, described in chapter 1), and by systematic review of all available unbiased TB blood culture data in previous publications (the individual patient data meta-analysis in chapter 2). Yet MTBBSI has not been the subject of any interventional study.

Surrogate biomarkers of clinical endpoints can facilitate interventional trials. Continuous biomarkers may have greater power to show difference between arms than a dichotomous outcome, increasing trial efficiency and accelerating development of therapeutic evidence-base.[505-507] A leading example is the use of HIV viral load dynamics in assessing anti-retroviral drugs: the meteoric development of highly-active antiretroviral therapy – based on phase-2 trials with less than 50 patients per arm – would have been impossible without this biomarker.[508,509] While HIV viral load is generally dichotomised in these trials (e.g. proportion with viral suppression by week 24), this is just a summary measure of a continuous variable. The justification for using HIV viral load as a biomarker was based on its kinetics as a continuous variable being able to predict clinical endpoints.[509] Early phase 2 trials of antiretroviral therapy used rate of change in viral load as the primary outcome measure,[510-515] and were not powered for detecting proportion with viral suppression by a

given time point. Regulatory approval based on surrogate biomarkers is well established for life-threatening diseases.[516]

Correlation of a biomarker with clinical outcome at the individual level is logically independent of correlation of that biomarker with outcome at group (or trial arm) level.[517,518] This phenomenon emerges depending on the causal structure which gave rise to the correlation between biomarker and outcome. If a biomarker does not lie on the (direct) causal pathway between treatment and outcome, it may turn out to be a misleading surrogate.

For example, cholesterol levels are linked to cardiovascular disease. Hormone replacement therapy and statins both reduce cholesterol. But, in RCTs, the former increases risk of cardiovascular disease, while the later reduces risk of cardiovascular disease.

In short, a biomarker should have a biologically plausible – preferably mechanistic – relationship to the clinical outcome.[519] In the search for sterilising cure of pulmonary tuberculosis, it is argued that *bacteriological* biomarkers (as opposed to host-response dynamics) – particularly those that might track persister organisms – are the most logical pharmacodynamic measure.[520,521]

Based on the work presented in this thesis, I would make a similar bacteriological case for severe HIV-associated tuberculosis. If we accept that MTBBSI is the mode of infection in severe HIV related TB, and is also a marker of total bacilli load, and directly linked to mortality, then serial quantification of MTBBSI is a promising basis for a pharmacodynamic biomarker capable of potentiating an urgent interventional research response to this neglected condition.

5.1.2 Chapter aims

1. Develop new methods, and optimise existing methods, for identifying and quantifying *M. tuberculosis* bacilli in patient blood samples.
2. Using these methods, report the pharmacodynamics of MTBBSI during the first 72-hours of standard anti-tuberculosis therapy.
3. Relate these MTBBSI pharmacodynamic measures to mortality and major clinical variables known to associate with mortality.

5.1.3 Chapter outline

Published methods for identifying mycobacteria in blood are reviewed for methodological insights. Previous attempts at quantifying *M. tuberculosis* in blood are rare, and no serial quantification has been described.

Novel method development is then described. This largely relied on optimisation of protocols using spiked blood samples, facilitated by the *in vitro* bacilli counting methods developed in chapter 4. Two pilot studies using clinical samples were also completed, recruiting patients using the predictive modelling described in chapter 3. The following methods and their development are described: optimised Myco/F lytic blood culture; a protocol for use of GeneXpert-ultra on blood; and fluorescent microscopy using a novel mycobacterial dye, 4-N,N-dimethylaminonaphthalimide-trehalose (DMN-Tre).

Finally, a sub-study nested within the KDHTB cohort study is described, in which blood bacilli burden was serially quantified at up to five timepoints after the start of anti-tuberculosis therapy, in 28 patients predicted to have high risk of MTBBSI.

5.2 Identifying & quantifying mycobacteria in blood: prior literature

5.2.1 Culture

The emergence of *M. avium – M. intracellulare* (MAI) as a significant opportunistic pathogen with the advent of AIDS in the early 1980s renewed interest in blood culture for mycobacteria. At that time no standard protocol for recovery of mycobacteria was established; over 20 different methods are described in the early case series of mycobacteraemia.[112,307,522-526] The subsequent development of mycobacterial blood culture methods can be summarised as follows:

- Initially, two main methods were in use: (1) lysis-centrifugation methods, in which a relatively large volume of blood (e.g. 5-10ml) is lysed and the pellet plated on solid media or inoculated into liquid culture; and (2) direct inoculation of radiometric

liquid culture systems, which had capacity for a smaller volume blood (e.g. 1-2ml). In head-to-head comparisons, lysis-centrifuge systems had best recovery of MAI, while direct inoculation had marginally lower recovery, but shorter time-to-detection (TTD).[526,527]

- Commercial systems which could culture larger volumes of blood for mycobacteria (e.g. 3-5ml) directly in liquid media without a lysis/concentration step were developed in the 1990s. Of these BACTEC Myco/F Lytic (MFL, BD Sparks, Md.) is the most common example still in production.

The major advantage of the MFL system is the ability to detect fungi, mycobacteria and other bacteria from a single sample, without processing steps and the use of multiple broths. In direct comparisons, MFL has shown better recovery of *M. tuberculosis* from blood than lysis-centrifuge systems when the lysate/concentrate was plated on solid media, and equivalent recovery to lysis-centrifuge systems when lysate/concentrate was inoculated into liquid media (table 1). This equivalence, and the convenience of MFL, has led to it being the most common system used in practice – 15 studies identified in the IPD meta-analysis in chapter 3 used MFL,[15,21,24,59,127,128,144,308,323,327-332] while only 2 older studies used lysis-centrifuge methods.[120,324]

In principle, lysis-centrifuge methods could be used to culture greater volumes of blood than the maximum 5ml for MFL, or used to pre-process blood prior to MFL culture. Such a strategy has not been tested. In general, work to optimise blood culture methods in medical mycobacteriology has stagnated. By contrast, veterinary microbiologists have performed extensive work to optimise culture of *Mycobacterium avium subspecies paratuberculosis* (MAP) from cattle and sheep blood, showing, for example, that presence of whole blood or just red blood cells inhibits mycobacterial growth, and that lysis and wash steps can increase recovery.[528,529] As shown in chapter 3 of this thesis, additional MFL cultures (even at same time point) increase detection of MTBBSI. In sum, a single MFL culture is convenient, but is unlikely to be optimal for identifying MTBBSI.

Also of note, no studies to date have performed serial cultures of blood during anti-tuberculosis treatment.

Table 5-1. Direct comparisons of MFL & alternative culture methods for recovery of M. tuberculosis from blood.

Ref	Comparator	Comparator blood volume	Positive by both method	MFL positive only	Comparator positive only
Martinez-Sanchez 2000 [306]	In house lysis-centrifuge method; concentrate inoculated to solid and liquid media.	Not clear	2	2	0
Crump 2011 [303]	BacT/Alert MB liquid culture system	4-6ml	12	8	2
Crump 2011 [303]	Isolator 10 lysis-centrifugation system with concentrate plated on 7H10 agar	4-6ml	9	7	0
Ref	**Comparator**	**Comparator blood volume**	**Positive by any method**	**MFL positive**	**Comparator positive**
Archibald 2000 [302]	Isolator 10 lysis-centrifugation system with concentrate inoculated in SC-AFB liquid culture system	5ml	33	27	25
Archibald 2000 [302]	Isolator 10 lysis-centrifugation system with concentrate plated on 7H11 agar	5ml	33	27	13

5.2.1.1 Quantification of MTBBSI with culture

While associated with poorer recovery of mycobacteria from blood, lysis-concentration and plating of the concentrate on solid media allows CFU counting. This was the basis of the only two published attempts at quantifying bacilli in blood in MTBBSI. Crump *et al*. found <1 to 150 (median 40) CFU per ml of blood in 9 patients with MTBBSI; CFU count correlated moderately with TTD in liquid culture (r=-0.49, p=0.262),[303] and CD4 count (Kendal τ = -0.33, p=0.45).[59] Munseri *et al*. showed a range of 1 to 23 (median 3) CFU/ml of blood, in 21 MTBBSI patients, although the majority of samples were processed more than 7 days after collection.[308]

5.2.2 Microscopy

The first account of *M. tuberculosis* visualised on microscopy of blood was from post mortems performed by Anton Weichselbaum[†††††††] in the 1880s.[530] A flurry of early 20th century reports that *M. tuberculosis* was visible on microscopy in a *majority* of TB patients' blood[531-533] [‡‡‡‡‡‡‡] were subsequently explained by the finding that acid-fast environmental bacilli were present in the distilled water used to prepare microscopy slides in these labs.[534]

Again, the emergence of MAI in the early AIDS epidemic renewed interest in identifying mycobacteraemia, including by microscopy. Eng *et al*. detected AFB by fluorescent microscopy of the buffy coats of 13/14 and 0/1 patients with MAI and *M. tuberculosis* blood culture positive disease respectively.[113] In 16 patients with MAI-positive blood cultures, Ruf *et al*. reported acid-fast bacilli in the buffy coat (13/16) and whole-blood lysed cell pellet (4/16), but 0/4 patients with *M. tuberculosis* blood culture had positive microscopy by either method.[307] Godwin *et al*. described acid-fast 'rod shaped inclusions' in monocytes and neutrophils of peripheral blood smear in 4/16 patients with bone marrow culture positive MAI infection.[535] Subsequent studies suggested 4% sensitivity of acid-fast microscopy of blood lysate, and 35% sensitivity of acid-fast microscopy of buffy coat compared to culture for MAI bacteraemia.[536,537] There is a single case report of detection of *M. tuberculosis* bacilli on blood microscopy from an HIV positive patient, using acid-fast staining of a whole blood lysate pellet.[538]

5.2.3 Nucleic acid amplification

A substantial number of attempts at *M. tuberculosis* PCR on blood, either specifically for patients suspected of having MTBBSI or in general TB populations, have been published, with wide variation in reported sensitivity (table 2). Unsurprisingly, studies which have focussed on PLWHIV at risk of MTBBSI have generally higher rates of PCR positivity in blood. Reported sensitivity of blood PCR in patients known to be TB blood culture positive have ranged from 5/25 (0.20, 95%CI 0.08 to 0.41)[539] up to 11/13 (0.85, 95%CI 0.54 to 0.97).[122] Notably, all studies have identified *M. tuberculosis* in blood of

[†††††††] Who is more famous for discovering *Neisseria meningitidis* when examining the cerebrospinal fluid of meningitis patients.
[‡‡‡‡‡‡‡] Including one from Dr Charles Forsyth, pathologist to Liverpool Hospital for Consumption and Diseases of the Chest.

patients who are blood culture *negative*, in keeping with potential limited sensitivity for both techniques. Estimates for the limit of detection from spiking blood *ex vivo* are around 5 CFU/ml;[540,541] as shown in chapter 4 of this thesis, the ratio of CFU to total cell count is highly dependent on growth conditions so these figures are methodologically flawed.

PCRs have generally been run on extracted PBMCs,[122,539,542] or on lysis-centrifuge concentrates,[15,543,544] or without pre-processing of blood prior to use in a commercial blood DNA extraction kit.[541,545] There is no clear pattern between studies to suggest which blood processing step is optimal (table 2), and no head-to-head comparisons of methods exist. The widespread belief that bacteraemic bacilli are intracellular and therefore concentrated in PBMC extractions is, to my knowledge, an assumption without direct evidence. Whole blood contains several known inhibitors of PCR, notably haem,[546] but also non-target (human) DNA and anticoagulants used in blood collection tubes.[547] It is surprising, then, that little attention has been given to optimisation of lysis and wash steps prior to PCR for *M. tuberculosis* in blood, which has been successful for blood PCR for other pathogens.[548]

Most of the studies have used labour intensive DNA elution and PCR SOPs, unfeasible in most high-MTBBSI burden settings. The exception is the attempt to test blood in the Xpert system after a single lysis-centrifugation step by Banada and colleagues.[540] Blood was mixed with a high-concentration red cell lysis buffer containing sucrose, magnesium chloride, Tris HCl and detergent. The ratio of blood to lysis buffer used was 85:15; the relatively low volume of lysis buffer being chosen to potentially lyse large volumes of blood in prefilled collection tubes. The authors reported no increase in the internal control C_T values with higher blood volumes, arguing this showed that PCR-inhibitors were not present. This seems unlikely, and no blood-free control data is presented. In a subsequent test on clinical samples, 27% of those tested had invalid results or errors; 4/9 were blood culture positive / Xpert negative, 4/9 were blood culture negative / Xpert positive, and 5 patients were positive by both tests.[15] This gives a sensitivity against culture of 0.44, but given blood culture is an imperfect reference, it could also be argued that the Xpert method may be as sensitive as blood culture (p=1 by McNemar's test for difference). In short, although these results are often described as showing poor

sensitivity of PCR and haven't been followed-up, I think they are actually promising, and with significant room for optimisation of centrifuge-lysis method.

Table 5-2. Selected blood PCR studies for TB diagnosis.

Reference	Study population	PCR method	Blood processing	PCR positive
Feasey 2013 [15]	104 HIV+ inpatients with suspected TB	Xpert	18ml blood underwent lysis-centrifuge concentration with pellet resuspended in 1ml PBS (based on Banada 2013) & added to Xpert with buffer.	10/104; 5/9 patients with positive MTB BC
Shenai 2013 [544]	24 HIV negative PTB patients	Xpert	10 ml blood concentrated into 2ml sample by RBC lysis centrifugation protocol (based on Banada 2013) & added to Xpert with buffer.	2/24
Rebollo 2006 [539]	57 patients diagnosed with TB (43 micro confirmed; 25 HIV+)	In house PCR based on IS6110 amplification.	PBMCs from 5ml blood, washed 2x in PBS, lysed in Tris-HCl and proteinase K, and DNA eluted.	18/57; 5/25 HIV+ patients with positive MTB BC
Bwanga 2015 [541]	31 HIV+ inpatients with suspected MTBBSI	FluoroType MTB commercial PCR based on IS6110 amplification	9ml blood underwent selective elution of MTB DNA using a commercial kit without prior blood processing.	6/31; 5/7 with positive MTB BC
Richter 1996 [122]	158 inpatients with EPTB (103 HIV+)	In house PCR based on IS986 amplification.	PBMCs from 2ml blood, lysed in Tris-HCl and proteinase K, and DNA eluted.	23/158; 11/13 HIV+ patients with positive MTB BC (buffy coat culture)
Folgueira 1996 [542]	32 inpatients with confirmed TB (11 HIV+)	In house PCR based on IS6110 amplification.	PBMCs from 5ml blood, washed 2x in PBS, lysed in Tris-HCl and proteinase K, and DNA eluted.	16/32; 9/11 HIV+
Crump 2012 [543]	25 patients with positive MTB BC (all HIV+)	In house PCR based on mycobacterial 16S rRNA gene amplification.	5ml blood concentrated to 0.3ml with lysis-centrifuge steps tube before DNA elution.	9/25
Hajiabdolbaghi 2014 [545]	190 inpatients with TB (45 HIV+)	In house PCR based on amplification of IS1081	3ml blood had total DNA eluted with QIAGEN commercial kit without any additional prior processing of blood.	78/190; 26/45 HIV+

MTB BC = *M. tuberculosis* blood culture (by MFL or other system)

5.3 Development of methods for identifying & quantifying bacilli in blood

In this chapter, I describe three methods that were developed or optimised for blood: microscopy, Xpert PCR, and MFL culture. The process of method development was iterative, including using data from both clinical pilots and the larger sub-study. The work is presented by method rather than chronologically. For convenience, the clinical pilots and sub-study design are summarised in figure 1 and referred to in subsequent text.

In pilot one, 16 patients were recruited who were predicted to have high risk of MTBBSI according to the machine learning models described in chapter 2. At each of four timepoints – 0h (prior to first dose of TB therapy), 4-12h, 24 h and 48 hours after first dose of TB therapy – two blood samples were taken at the same venesection. The first (5ml) was inoculated directly into a Myco/F Lytic (MFL) bottle. The second (5ml) was collected in a sterile sodium heparin tube, then centrifuged (3000G, 25min) to pellet cells and remove plasma, with inoculation of the cell pellet into an MFL bottle.

In pilot two, 15ml of blood was taken at a single timepoint immediately prior to start of TB therapy in sodium heparin tubes. This combined sample was centrifuged (1800G, 25min) to separate red cells, buffy coat, and plasma. Plasma and red cell pellet were inoculated separately into MFL bottles for culture. The buffy coat was split with ¼ being inoculated into MFL bottle; ¼ being inoculated into MFL with the addition of culture filtrate; ¼ stored at -20oC for downstream Xpert-ultra processing (described in section 5.3.3); and ¼ being processed for DMN-trehalose microscopy (described in section 5.3.1).

In the main sub-study 28 patients were recruited; the study design is described in detail in section 5.4. In brief, at each of the 5 timepoints shown, 4 blood samples in sodium heparin tubes (each ~4.5ml) were collected. One was processed to remove plasma with culture of the cell pellet in MFL system (as per pilot 1). The remaining three samples

underwent red cell lysis and water lysis / wash, before MFL culture, DMN-trehalose microscopy, and storage for downstream Xpert-ultra processing.

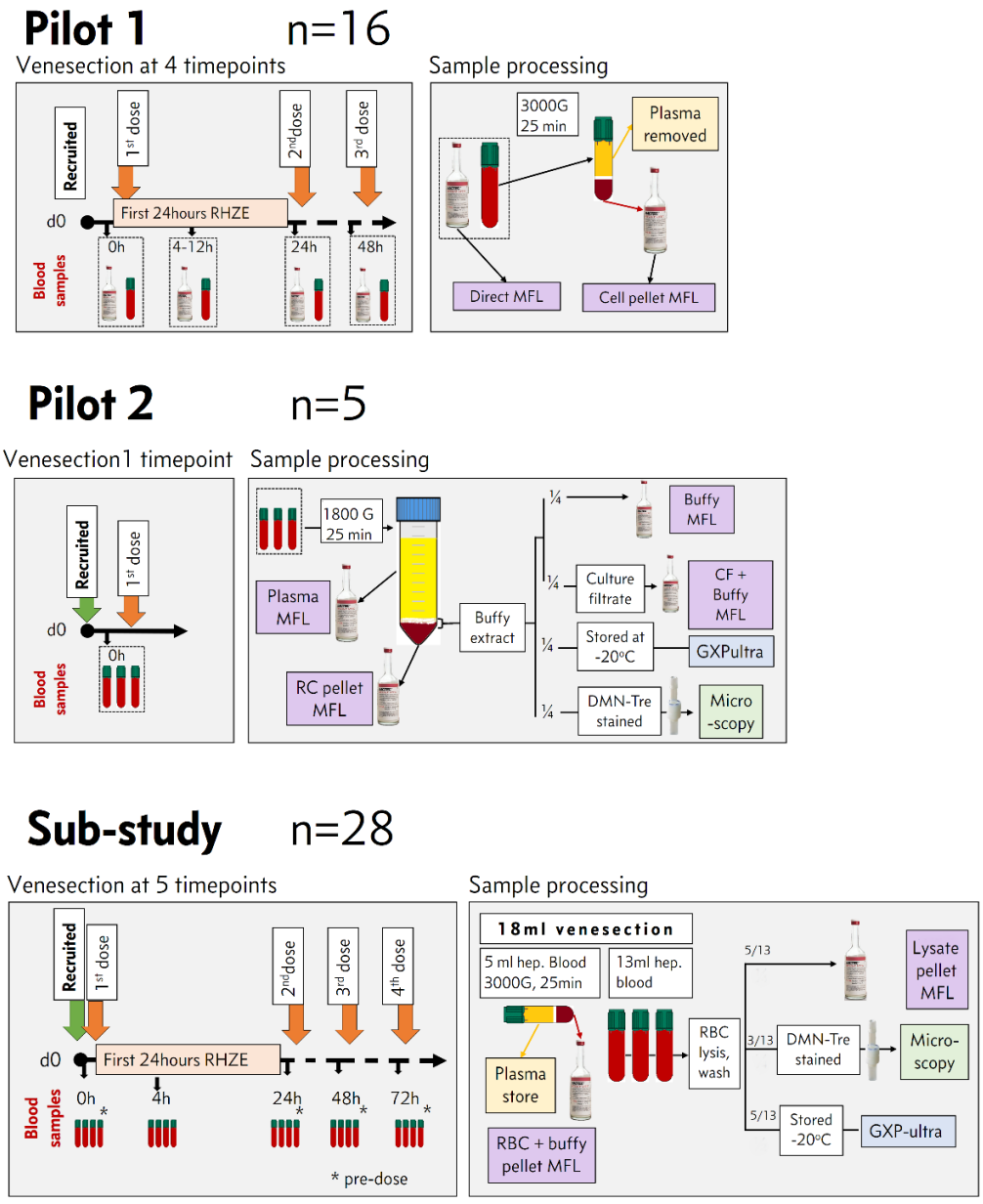

Figure 5-1. Two pilots & sub-study used to develop methods to identify &quantify MTBBSI.

5.3.1 Blood microscopy

5.3.1.1 Initial attempts demonstrate parameters for optimisation

The method for processing blood for microscopy was based on a publication by Sage & Neece[549] describing selective lysis and concentration of blood spiked with bacteria on a 0.6µM polycarbonate filter.§§§§§§§ Their lysis buffer contained tricine, Rhozyme 41 (a broad activity protease derived from *A. oryza* historically used by the food industry), NaOH, and Tween 20; this lysis buffer was developed to selectively lyse all human cells in blood, while not damaging bacteria.[550-552] Sage & Neece successfully concentrated up to 1ml of blood on a 3mm^2 polycarbonate membrane using vacuum suction.

Rhozyme 41 is no longer commercially available, so initial selective lysis and concentration attempts adopted the method described by Bower *et al*. for isolating MAP from cattle and sheep blood. Briefly, 9 ml of whole blood was collected from healthy volunteers in sodium heparin tubes, centrifuged at 1455 g for 20 min with slow brake, and buffy coat extracted by pipetting. This was then pelleted at 200g for 5min in 1.5ml Eppendorf, and resuspended in 400µl of PBS. To this was added 12ml erythrocyte lysis buffer (0.83% w/v NH4Cl, 0.1% w/v KHCO3, 0.01M EDTA pH 7.5) and the solution incubated at room temperature for 10 min to allow lysis of the erythrocytes. This was then pelleted at 300g for 10 minutes and resuspended in 1.5ml distilled water.

The Sage & Neece method for concentration of lysate on filter using air pressure risks aerosol formation so couldn't be used for pathogenic mycobacteria. Instead, a centrifuge ultrafiltration holder, which fits standard 30mm centrifuge tubes, was used, allowing up to 2ml of liquid to be filtered through a 13mm polycarbonate filter using centrifugal force with three levels of containment (UFREU1301, Sterlitech, Kent WA). This filter holder is reusable as it can be sterilised. 13mm, 0.6µm, black polycarbonate membrane filters designed to fit this holder were used (PCTB0613100, Sterlitech, Kent WA).******** Filters were mounted using 50% glycerol on 20mm glass bottom cell culture dishes (801001, Whitehead Scientific, Cape Town), which were sealed by attaching the

§§§§§§§ I acknowledge Dr Howard Shapiro for sending me this paper in response to a question on the Purdue Cytometry Discussion List.

******** I acknowledge Mr Kensen Hirohata of Sterlitech Corporation for his extensive expert advice on filter systems.

lid with cyanoacrylate (Superglue) before removal from the biosafety hood for microscopy.

The sealed cell culture dishes were further mounted in a custom made aluminium holder to allow attachment to the microscopy stage (figure 2).[††††††††] All microscopy was performed on a Zeiss Axio Observer 7 using the Plan-Apochromat 100x/1.4 Oil objective and 10x ocular lens giving 1000x magnification.

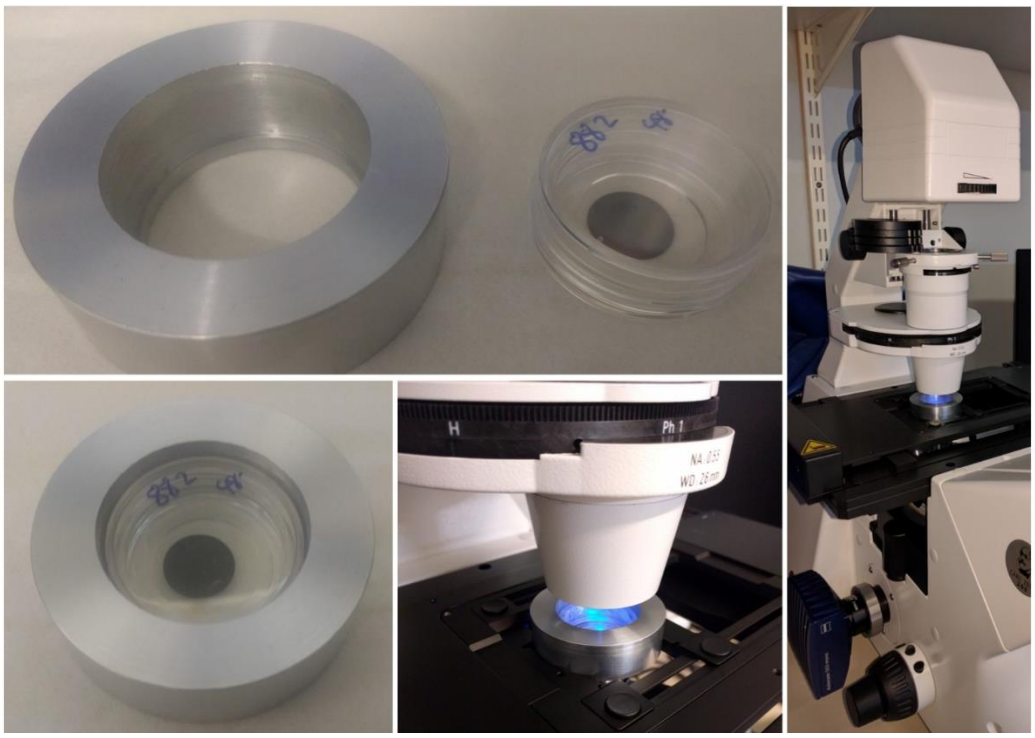

Figure 5-2. Visualisation of a 13mm filter membrane sealed in a 20mm tissue culture dish secured on microscope stage using custom machined aluminium holder.

[††††††††] I acknowledge Professor Robin Wood of University of Cape Town for machining this aluminium holder in his metal-workshop.

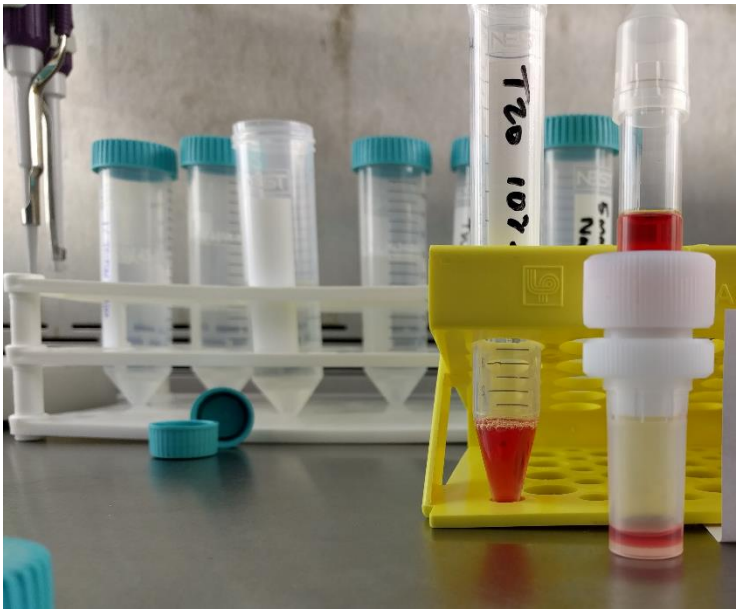

Figure 5-3. Centrifuge filter holder (right).

In this example, blood lysate (red) in the top compartment has incompletely filtered through the filter membrane into the lower chamber.

Initial attempts at microscopy were performed on volunteer blood spiked with 10^6/ml of *M. bovis* BCG (total cell count, using flow cytometry counting method described in chapter 4). Lysate was stained with SYBR-gold and heated at 65°C for 12 minutes before concentration on membrane filters. SYBR-gold has been shown to have higher sensitivity for mycobacteria in acid-fast staining than other more established dyes.[384] These were washed with 2 passes of acid-alcohol solution through the filter (0.5% HCl in 70% isopropanol).

Initial attempts were unsuccessful. Less than 5% of the lysate passed through the membrane after 30minutes centrifugation at 2000g (the maximum force supported by the filtration device). When filters were examined under microscope, they were found to be saturated with SYBR-gold stained cellular debris, with very few bacilli identified.

This identified factors that needed to be optimised:

1. Minimum centrifuge settings which result in complete pelleting of bacilli in solution.
2. Lysis buffer, to render lysate maximally filterable through 0.6µm membrane, without destruction of bacilli.
3. Staining procedure to maximise sensitivity and specificity of imaging.

5.3.1.2 Centrifuge parameters needed to reliably pellet mycobacteria

Mycobacteria are said to settle to the bottom of cultures under the action of gravity when left on the bench top.[553] Conversely, mycobacteria are said to have density less than water due to their lipid content, meaning they would not pellet in water under any g, and are even seen to accumulate on the surface of liquid cultures under no agitation.[554] Centrifuge methods described in the TB literature vary widely, ranging from 30 minutes at 1g, to 6000g for 15 minutes.[555] The WHO recommends 3000g for 15 minutes for sputum preparations without citing a source.[556] The limited published data are contradictory, suggesting 3000g for 15 minutes, 2000g for 20 minutes, or 3200g for 22 minutes are necessary to achieve effective sedimentation of mycobacteria.[557,558] This certainly implies that the typically low g methods for preparing buffy coat preparations may leave any free bacilli in the plasma fraction.

Centrifuge time and g were tested with BCG using the flow cytometry counting method described in chapter 4 (figure 4). Recovery of bacilli from resuspended sediment compared to a non-centrifuged control had a mono-exponential relationship to time and g, with increased centrifugation needed when bacilli were suspended in 50/50 plasma/PBS solution compared to PBS alone. For 5 minutes spin, >10000g was needed to recover >90% of bacilli, and >20minutes at 2000g.

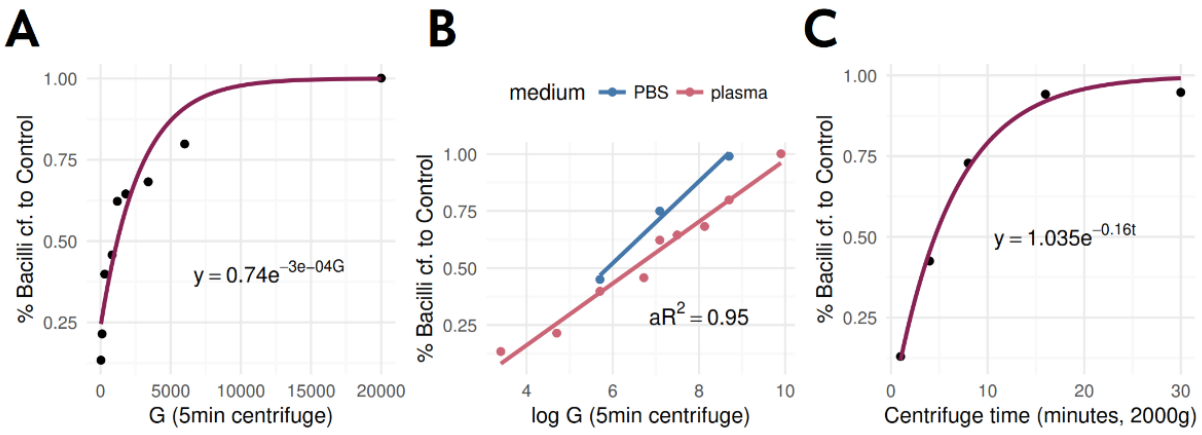

Figure 5-4. Centrifuge parameters to maximise recovery of bacilli in suspension.

A. 5-minute centrifuge of aliquots of the same suspension of BCG bacilli in 50/50 plasma/PBS solution. Each aliquot centrifuged under different g, with subsequent removal of 90% of

supernatant and resuspension to stated volume by pipetting. One aliquot was not centrifuged, and quantified directly, to give the control count. Counting was performed by flow cytometry using the heat-kill SYBR-gold stain method described in chapter 4. **B**. Same data as in A, but with 3 additional aliquots suspended in PBS (no plasma) – plasma increases centrifuge g needed to recover bacilli. **C**. Method as per A, but g held constant at 2000g, with centrifuge time varied.

5.3.1.3 Selective lysis methods

Based on several published selective lysis methods,[548-552] permutations of different detergent and enzyme-based lysis buffers were iteratively tested for ability to render healthy volunteer blood samples filterable through the 0.6µm polycarbonate membranes.

Initial lysis of buffy coat extract using erythrocyte lysis buffer in ratio >10:1, followed by 24 hour incubation in MFL buffer (which contains detergents), then a more aggressive lysis step with buffer containing v/v 1% triton-X-100 and 1% Tween 80 plus 1mg/ml proteinase-K incubated at 37°C for 25 minutes was found to result in >90% filtration of lysate through the filter membrane (figure 5 & 6).

To check if this lysis procedure caused significant loss or destruction of bacilli, pure *in vitro* cultures of BCG (not spiked in blood) were quantified by the flow cytometry method described in chapter 4, before and after being processed using the same buffers and incubations developed for blood samples. This showed that 85-90% of bacilli were recovered after processing using the selective lysis steps (data not shown).

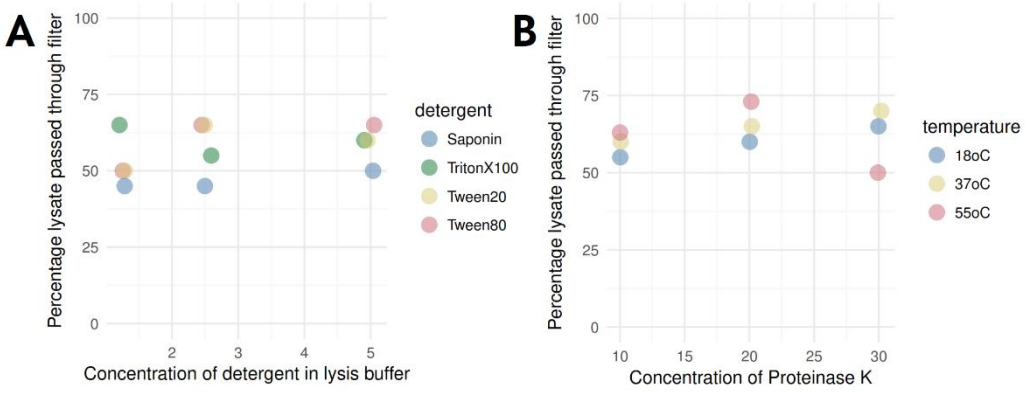

Figure 5-5. Example experiment testing different detergent & enzyme conditions of blood lysis buffer.

In these experiments 3.5ml of heparinised blood was collected from healthy volunteers, spun at 1800g for 10 minutes to separate cell layers, with the buffy coat extracted by pipetting. Extracted buffy coat (~0.5ml) was combined with 3ml of MFL broth and incubated in sodium heparin tubes for 24 hours at 37°C. These samples were then treated with 12ml of lysis buffer, the constituents of this lysis buffer being varied. In **A**, twelve conditions were tested: 4 different detergents at 3 concentrations (concentrations on x axis are v/v percentages); all contained 18mg of proteinase-K (for final concentration 1.2 mg/ml) and were incubated at room temperature for 20 minutes. In **B**, nine conditions were tested: 3 concentrations of proteinase K (amount on x axis is mg added to 15ml volume) incubated for 20 minutes at 3 different temperatures; all contained v/v 2.5% Tween 80. After lysis samples were pelleted at 4600g for 10 minutes and re-suspended in 1 ml of PBS before attempted filtration with the centrifuge-filtration system. The total volume which passed through the filter was measured to assess how effective the different lysis conditions had been.

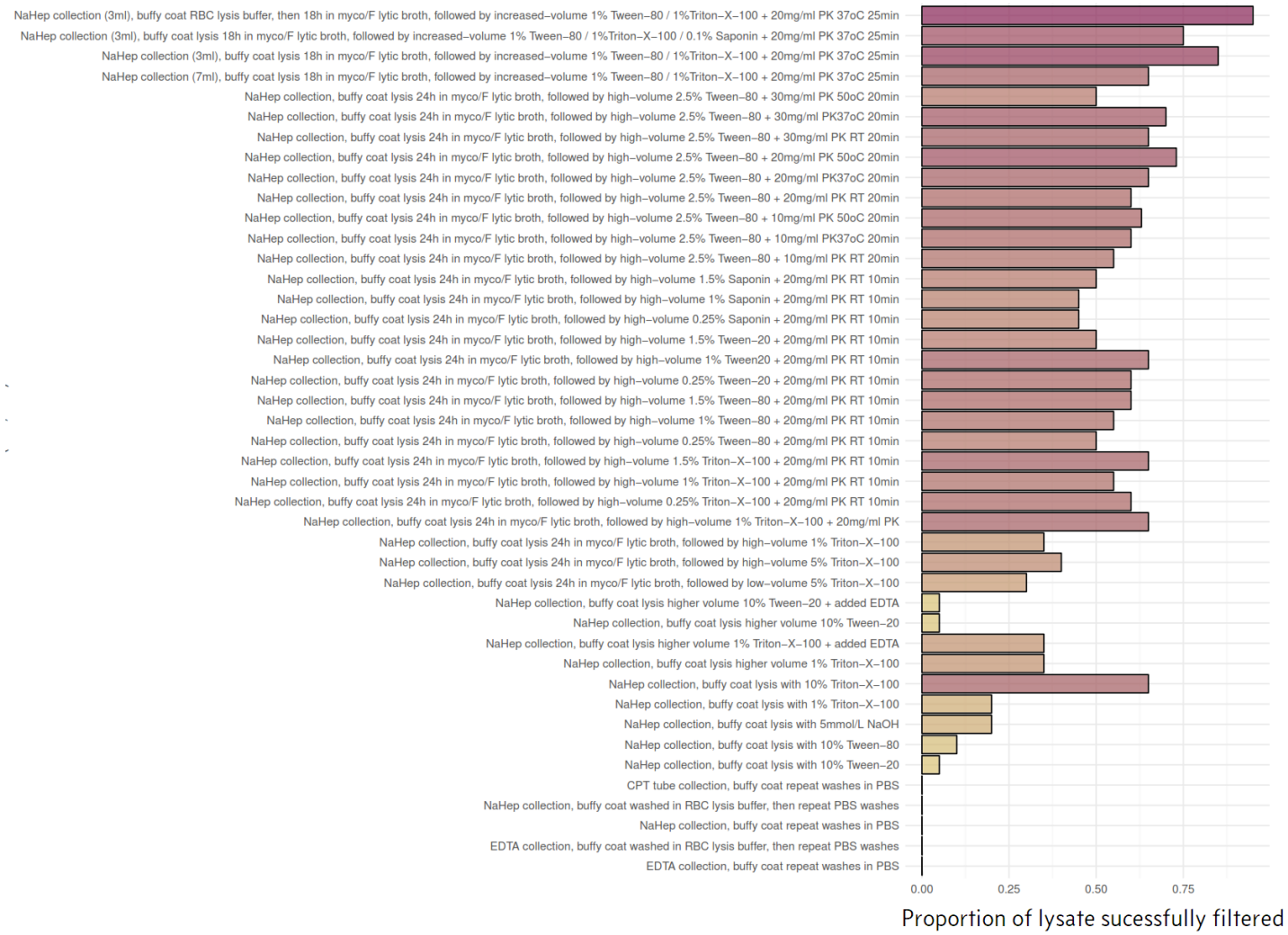

Figure 5-6. Summary of iterative development of selective lysis method.

Method development over time from earlier attempts (bottom) to later attempts (top). Factors that made major differences to filterability of blood lysate were use of a large volume for initial

lysis step, inclusion of proteinase-K in lysis buffer, and use of more than one detergent with different mechanisms of action (e.g. Triton-X-100 plus Tween 80).

5.3.1.4 Staining procedure & choice of dye

As described above, initial tests of blood microscopy with BCG-spiked blood used SYBR-gold staining, which was associated with sub-optimal results due to poor specificity of the dye with excessive staining of cell debris. Optimised acid-alcohol wash steps and counter staining procedures marginally improved the performance (data not shown), but the performance was radically improved by use of a novel dye, 4-*N,N*-dimethylamino-1,8-naphthalimide–conjugated trehalose (DMN-Tre), developed by the Bertozzi lab at Stanford.[559] This probe is metabolised by actinobacteria (including mycobacteria) to a trehalose mycolate and incorporated into the outer membrane of the bacilli, which specifically increases the molecule's fluorescence activity over 700-fold.[559] This means the dye has high specificity for mycobacteria (without staining typical gram-negative and gram-positive bacteria found in clinical samples), reports only metabolically active mycobacteria, and can be used without wash steps.[559] DMN-tre dye was gifted by the Bertozzi lab for the current work.‡‡‡‡‡‡‡‡ Initial tests of DMN-tre showed >100-fold improved detection of bacilli in spiked blood samples (figure 7).

‡‡‡‡‡‡‡‡ I acknowledge Professor Carolyn Bertozzi, and Dr. Mireille Kamariza who invented DMN-tre, and manually produced the aliquots of dye used in this research (DMN-tre is not currently commercially available; the current work would not have been possible without their generous assistance).

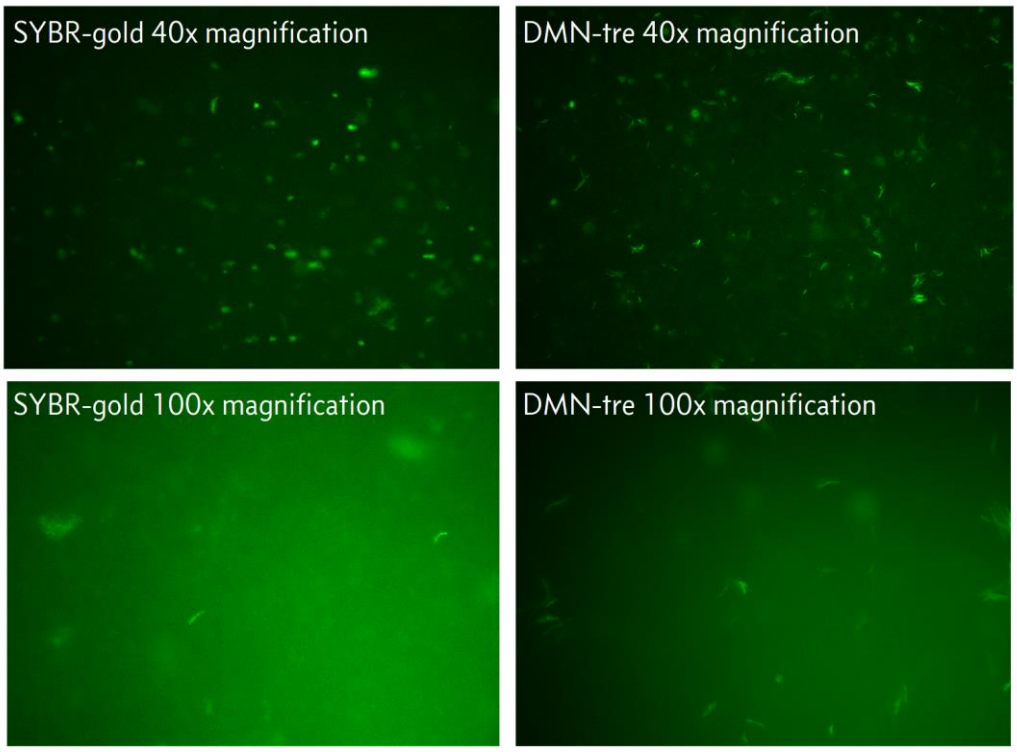

Figure 5-7. Initial test of DMN-tre staining of BCG spiked blood versus SYBR-gold staining.

Two 9 ml samples of whole blood collected from healthy volunteers in sodium heparin tubes, spiked with 3*10^5 BCG bacilli and incubated under agitation for 4 hours at 37°C. Centrifuged at 2000g for 25 min, buffy coat extracted by pipetting (~1.5ml). 12.5ml erythrocyte lysis buffer (0.83% w/v NH4Cl, 0.1% w/v KHCO3, 0.01M EDTA pH 7.5) added and incubated at room temperature for 30 min, then pelleted at 3000g for 25 minutes. Both samples resuspended in 5ml of MFL broth in sodium heparin tubes; one tube had 10µL of 100mM DMN-tre added (final concentration 167 µM), then both incubated under agitation for 18 hours at 37°C, then pelleted at 3000g for 25 minutes. Resuspended in 30ml distilled water for 30 minutes at room temperature, pelleted at 3000g for 25 minutes and resuspended in 1ml PBS. The second sample, not previously stained with DMN-tre, was stained with SYBR-gold (60µL of 10^-4 dilution working stock added to 1ml, then heated at 65°C for 12 minutes). 200µL of each sample concentrated on membrane filter using the Sterlitech centrifuge system (which should equate to ~500000 bacilli on membrane). In the SYBR-gold stained sample, occasional bacilli were visible at 100x magnification (two are visible in lower left panel, most fields of view contained no bacilli). In the DMN-tre sample, the number of visible bacilli were more than 100-fold more numerous (visible in most fields of view, lower right panel shows more than 40 bacilli).

5.3.1.5 Optimised microscopy method tested in spiked samples & clinical sample pilot

The optimised microscopy method is summarised below:

Consumables

- RBC lysis buffer [155mM NH_4Cl; 12mM $NaHCO_3$; 0.1 mM EDTA]
- Myco/F lytic broth [BD Bactec]
- Lysis buffer 2 [DI H2O with 0.5% Triton-X-100 and 1% Tween80]
- Proteinase K
- 13mm, 0.6micron black Polycarbonate (PCTE) membrane filters [Sterlitech PCTB0613100]
- Reusable centrifuge Ultrafiltration Holder, 13mm [Sterlitech UFREU1301]

Method

1. 5ml of blood collected in sterile sodium heparin tube. Centrifuged at 1800g for 20 minutes to separate cell layers from plasma; buffy coat extracted by pipetting.
2. Add 45ml RBC lysis buffer to buffy coat, incubate at room temperature for 30 minutes, inverting ~10 times during incubation to mix.
3. Pellet at 3000g for 25min, re-suspend pellet by reverse pipetting in 1-2ml of RBC lysis buffer.
4. Repeat this RBC lysis buffer lysis and wash (step 2 & 3).
5. Re-suspend pellet in 5ml of MFL broth.
6. Add 10µL of 100mM DMN-tre (final concentration 167 µM) and incubate under agitation for 18 hours at 37°C.
7. Add 25ml of lysis buffer 2 which has been pre-warmed to 37°C
8. Add 20mg of proteinase K to the sample / buffer solution.
9. Incubate at 37°C for 25 minutes, inverting to mix every ~5minutes.
10. Pellet at 3000g for 25min, re-suspend pellet by reverse pipetting in 2ml DIH_2O.
11. Spin sample through PCTE membrane in Ultrafiltration holder [1800G for 10min].

This was tested in volunteer blood samples (6ml) spiked with BCG bacilli at 100, 10, 1 and 0 bacilli per ml. Another lab user labelled these tubes so that the operator was blinded to sample identity. Samples were then processed as per the above optimised method. In three replicates, the 100 bacilli/ml sample was distinguished from the 0 bacilli control 3/3 times, the 10 bacilli/ml sample was distinguished from control 3/3 times, and the 1 bacilli/ml sample was distinguished from control correctly 1/3 times. Further *in vitro* validations were not performed to accurately determine the limit of detection due to limited availability of DMN-tre (which is currently not being commercially produced).

Instead, the method was next tested in clinical samples, in 5 patients from pilot 2 (figure 1). In this pilot, five patients were recruited based on high predicted probability of MTBBSI (using the machine learning modelling and bedside prediction app developed in chapter 2). Microscopy was performed on samples in the 24 hours after patient

recruitment, i.e. before blood culture or Xpert results were available, so with operator blinded to blood culture status (but not to patient identifiers).

Patients were classified as MTBBSI or not based on microscopy examination of blood. As with any microscopy, this is an operator dependent decision, as artefacts must be distinguished from bacilli based on morphology. Four out of five patients were judged to have bacilli on blood microscopy (figure 8); these same 4/5 patients were also subsequently blood culture positive and blood Xpert positive, meaning microscopy had full concordance with the other methods for identifying MTBBSI. Notably, one patient had more than 100,000 bacilli on the filter membrane, which would equate to >10^4 bacilli per ml of the original blood sample. This patient also had the lowest TTD in MFL and lowest C_T value on blood Xpert.

Results from this pilot, and from other investigations further detailed below, suggested that the assumption that maximum numbers of bacilli would be found in the buffy coat was invalid. Therefore, before the microscopy technique was taken forward to the larger sub-study, it was adapted so that the whole blood sample was lysed in RBC lysis buffer (step 2 in method above), with the previous step for extracting buffy coat being abandoned. Surprisingly, this increased the adequacy of filtration of the subsequent lysate to >95% (data not shown).

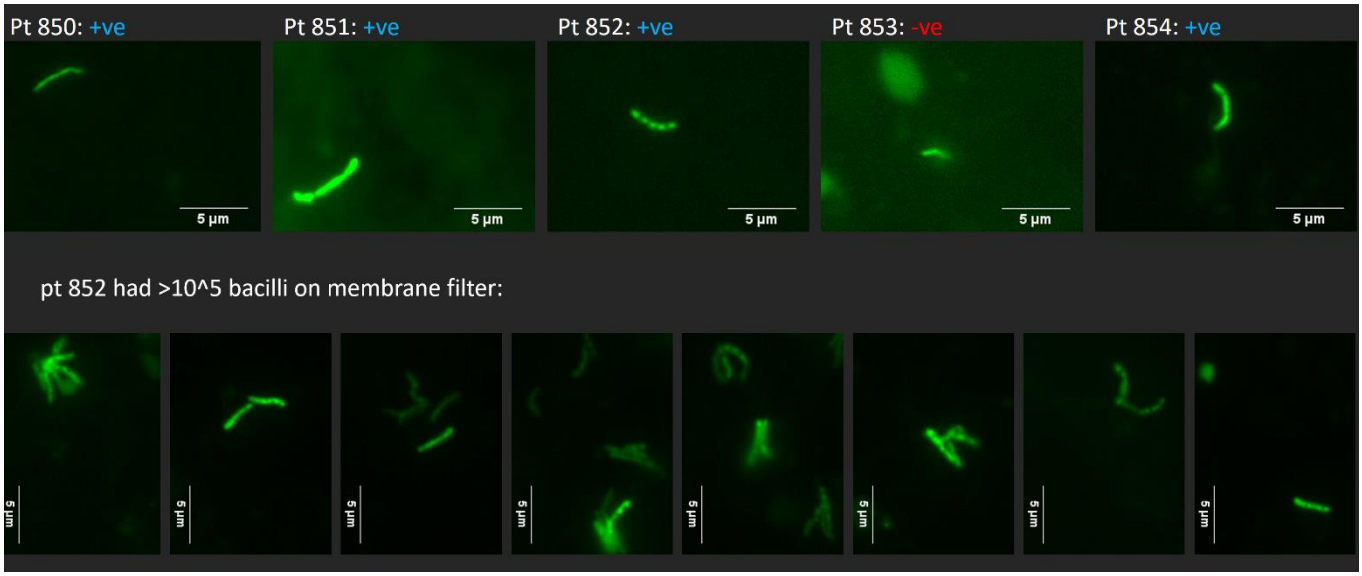

Figure 5-8. DMN-tre microscopy images from pilot 2.

Bacilli show variability in intensity of staining, variable lengths, and beaded appearance. Doublet cells and microcolonies are also seen, particularly in one patient (lower row) who had more than 100,000 bacilli on the filter membrane. One patient was classified as blood microscopy negative (Pt 853), an artefact which was closest to appearance of a bacilli is shown for this sample.

5.3.2 MFL blood culture

5.3.2.1 Pre-processing blood prior to MFL culture

Blood sampling for culture at serial time points after start of TB therapy inevitably results in antimicrobial carry-over from blood into the culture broth. Taking blood for culture only at pre-dose time points was not always possible for logistic (imperfect control over time doses were administered in real-hospital environment) and design (timepoints less than 24 hours after dose) reasons. In addition, although free drug in plasma may have predictably low trough levels, this may not be true of intra-cellular concentrations, or bound drug.

Therefore, methods for drug removal were investigated for patient blood samples in pilot 1 and the larger sub study (summarised in figure 1). In pilot 1, sixteen patients predicted to have high risk of MTBBSI underwent serial TB blood cultures over the first 48 hours of treatment. At each sampling timepoint, a direct inoculation of 5ml blood

into an MFL bottle was made, and a 5ml sample of blood collected in parallel in sterile sodium heparin tubes. This second sample was centrifuged (25 min at 3,000g), and the resulting cell pellet (red cells and buffy coat) inoculated into an MFL bottle.

This allowed comparison of direct inoculation to pellet inoculation. Pelleting before culture was associated with increased probability of positive culture, although the trend was not statistically significant (table 3). Conversely, pelleting was associated with an increase in time to detection in paired comparison (again not reaching statistical significance in this small sample) (figure 9).

Table 5-3. Direct versus pellet MFL blood culture results from pilot 1

Pairwise contingency by patient-timepoint, all timepoints

	Pellet positive	Pellet negative
Direct positive	11	2
Direct negative	7	31

McNemar's test p =0.182

Pairwise contingency by patient-timepoint, post-abx timepoints only

	Pellet positive	Pellet negative
Direct positive	3	2
Direct negative	5	28

McNemar's test p =0.4497

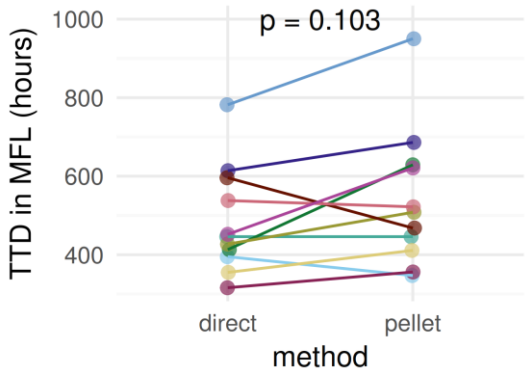

Figure 5-9. Time-to-detection in MFL for paired positive samples: direct versus cell pellet inoculation.

Eleven pairs of samples positive by both direct inoculation and cell pellet inoculation. In 7/11 samples pellet had longer TTD, in 3/11 direct had longer TTD and in 1/11 TTD was identical; mean difference 55 hours longer for pellet; p value from paired t-test.

In the larger sub-study direct inoculation was not used. Instead a pair of samples from each time point were processed two ways; the first (~4ml) by pelleting as described for pilot 1. For the second MFL culture from each timepoint, 14ml of blood collected in sodium heparin tubes was lysed with addition of 32ml RBC lysis buffer [155mM NH_4Cl; 12mM $NaHCO_3$; 0.1 mM EDTA], incubation at room temperature for 25 minutes, followed by centrifuging at 3000g for 25 minutes, resuspension of the pellet in 45ml of 0.22µm filtered deionized water for 25 minutes at room temperature, followed by centrifuging at 3000g for 25 minutes and resuspension to ~5ml in sterile PBS solution. One-quarter of this lysate was inoculated into a second MFL bottle (equating to 3.5ml of the original blood sample). This allowed comparison of pellet culture to lysate culture (table 4), showing that lysate resulted in better recovery of mycobacteria, with the effect restricted to samples taken after start of antimicrobials. Again, a converse pattern was seen for TTD in MFL, with the pellet method having shorter TTD despite lower sensitivity for recovery of mycobacteria (figure 10). This implies that manipulation of sample prior to culture changes the relationship between number of bacilli and TTD.

Table 5-4. Lysate versus pellet MFL blood culture results from sub-study

Pairwise contingency by patient-timepoint, all timepoints

	Pellet positive	Pellet negative
Lysate positive	18	23
Lysate negative	11	59

McNemar's test p =0.059

Pairwise contingency by patient-timepoint, post-abx timepoints only

	Pellet positive	Pellet negative
Lysate positive	9	18
Lysate negative	6	50

McNemar's test p =0.025

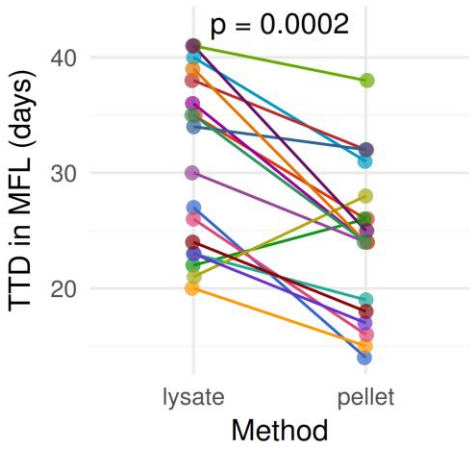

Figure 5-10. Time-to-detection in MFL for paired positive samples: blood lysate versus cell pellet inoculation.

Eighteen pairs of samples positive by both blood lysate inoculation and cell pellet inoculation. In 16/18 samples lysate had longer TTD, in 2/18 pellet had longer TTD; mean difference 6 days longer for lysate; p value from paired T-test.

5.3.2.2 Serial MFL results in pilot 1 study

Fourteen patients had at least 1 positive MFL blood culture, of these 13 had valid sample results from ≥24 hours after start of TB therapy, and 4/13 remained culture positive at one of these later timepoints (figure 11). All but 1 post 24-hour positive culture was from a pellet culture. TTD rose for all patients with positive cultures at more than one timepoint, except for two patients with MDR isolates (figure 12).

In sum, pre-processing blood before MFL culture demonstrated that culture positive MTBBSI was detectable after start of treatment and could therefore be used for an *in vivo* time kill study.

		0h	4-12h	24h	48h	
1	Direct	0	0	0	1	alive
MDR	Pellet	1	0	0	1	
2	Direct	1	0	0	NA	alive
	Pellet	1	0	1	0	
3	Direct	1	1	0	0	alive
	Pellet	1	0	0	0	
4	Direct	1	1	0	NA	alive
	Pellet	1	1	0	NA	
5	Direct	0	0	0	0	alive
	Pellet	0	0	0	0	
6	Direct	0	NA	NA	NA	died
	Pellet	1	NA	NA	NA	
7	Direct	1	0	0	0	died
	Pellet	1	1	0	0	
8	Direct	0	0	0	0	alive
	Pellet	NA	0	0	0	
9	Direct	1	0	0	NA	alive
	Pellet	1	0	1	NA	
10	Direct	1	1	0	0	died
MDR	Pellet	1	1	0	0	
11	Direct	0	0	0	0	alive
	Pellet	0	0	0	0	
12	Direct	1	0	0	0	alive
	Pellet	1	0	0	0	
13	Direct	0	0	0	0	alive
	Pellet	1	0	0	0	
14	Direct	1	0	0	NA	alive
	Pellet	NA	0	1	0	
15	Direct	1	0	NA	NA	died
	Pellet	1	1	NA	NA	
16	Direct	0	1	0	0	died
	Pellet	0	1	0	0	

0	No growth at 42 days
1	MTB
NA	No culture done

Figure 5-11. Serial MFL culture results from pilot 1.

Sixteen patients each had 2 cultures (rows) at timepoints relative to start of TB therapy (columns; prior to therapy=0h, and 4-12, 24, and 48h after first dose). Two patients had resistance to rifampicin (MDR) and were initially treated with standard therapy; five patients died by 12 weeks follow-up (last column).

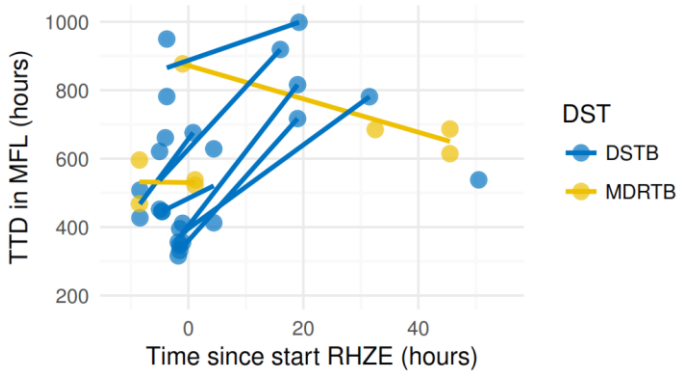

Figure 5-12. TTD from serial MFL culture results from pilot 1.

Patients with positive MFL from more than one timepoint are shown with a line of best fit applied to their observed TTDs by time. Two patients with MDR-TB isolates shown in yellow.

5.3.3 Xpert-ultra testing of processed blood

Xpert MTB/RIF (Xpert) is a nearly fully automated cartridge based hemi-nested PCR assay (products from the first PCR are used as the template in a second PCR, using different primers whose binding sites are 'nested' within the first set, thus increasing specificity) which amplifies five moieties on the *rpoB* gene of *M. tuberculosis* to detect the presence of bacilli and mutations responsible for the majority of rifampicin resistance. A next generation assay, Xpert MTB/RIF Ultra (Xpert-ultra) has been developed to have improved sensitivity. In addition to optimised cartridge fluids and chemistry, Xpert-ultra incorporates two extra amplification targets.[560] IS6110 and IS1081 are multicopy genes (copies vary between isolates, H37Rv for example has 16 copies of IS6110); Xpert-ultra labels both with the same fluorescent probe and measures combined signal to detect *M. tuberculosis*, while the five *rpoB* targets are probed separately to determine rifampicin resistance genotype.[560] Xpert-ultra has improved limit of detection by approximately 1-logarithm compared to Xpert.[338,560]

As discussed in chapter 4, Xpert *rpoB* probe C_T values are at least semi-quantitative for intact bacilli number. As with the previous system, Xpert-ultra also gives an ordinal read-out on quantity based on C_T values: high, medium, low, very low, & trace detection. The first 4 are bins of minimum *rpoB* C_T value across the 5 probes; the 5th "trace" is samples where *rpoB* PCR was negative, but IS6110-IS1081 signal was detected. Because these genes are multicopy, this could in theory complicate

interpretation of their C_T values as a read out of number of bacilli. Xpert-ultra cartridges, like their predecessors, also run an internal control PCR to assess PCR inhibition, but this value does not seem to be factored in when assigning ordinal category for bacilli quantity.§§§§§§§§

As discussed above, previous attempts to use Xpert to detect MTBBSI have had poor sensitivity, and probably had sub-optimal pre-processing of blood (focussing instead on low volume lysis buffer for practical reasons). In addition, the new generation Xpert-ultra has not been tested on blood. Therefore, Xpert-ultra testing of blood after more thorough lysis and washing was tested in the current analysis.

5.3.3.1 Xpert-ultra testing of spiked blood samples

A fully attenuated *M. tuberculosis* strain with auxotrophic mutations in leucine and pantothenate biosynthesis was grown and quantified in early-log phase growth using the calcein stained flow cytometry method described in chapter 4.********* Volumes of culture broth equating to range 60, 300, 600, 1200, and 4800 calcein positive (metabolically active) bacilli were inoculated into 6ml samples of volunteer blood collected in sodium heparin tubes (for final bacilli concentration 10, 50, 100, 200, 800 bacilli/ml). Samples were lysed in 40ml RBC lysis buffer for 30 minutes at room temperature then pelleted at 3000g for 25minues. The pellet was resuspended in 45ml of 0.22µm filtered deionised water for 30 minutes at room temperature and re-pelleted as before; this pellet was resuspended in 2ml of sterile PBS and stored at -20°C until time of Xpert-ultra testing. After thawing at room temperature, the 2ml sample was centrifuged at 16000g for 10 minutes, with removal of 1ml supernatant, and resuspension in remaining volume. This residual 1ml volume was mixed with 1ml of Xpert buffer, incubated at room temperature for 30 minutes, then pipetted into Xpert-ultra cartridges as per manufacturer instructions.

Three replicates of each bacilli concentration were performed; *M. tuberculosis* was detected in all samples except one replicate of 10 bacilli/ml (negative result) and one

§§§§§§§§ I can't find a citation for this, but have worked it out empirically from the raw data exports from Xpert-ultra machine.

********* The Δ*leuD*Δ*panCD* double auxotroph *M. tuberculosis* was kindly gifted by Professor Digby Warner of the Molecular Mycobacteriology Research Unit, University of Cape Town and was used here as it can be processed safely in biosafety level 2 laboratory.

replicate of 50 bacilli/ml (error result). Log transformed bacilli concentration correlated with Xpert-ultra C_T value (figure 13). This suggested that two high volume lysis step pre-processing of blood combined with Xpert-ultra testing was potentially highly sensitive for detecting MTBBSI.

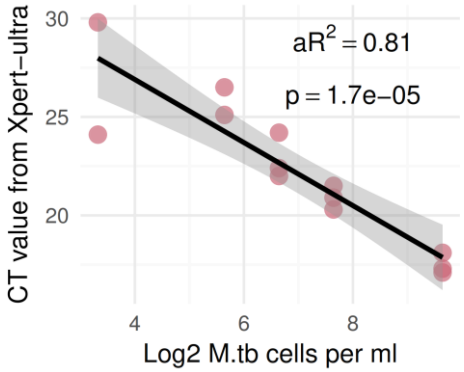

Figure 5-13. Xpert-ultra CT correlation with number of bacilli in spiked blood.

C_T values are for the combined IS6110-IS1081 probe. Internal control C_T values were all less than 28 providing evidence that PCR inhibition was not significant.

5.3.3.2 Pilot Xpert-ultra testing of patient blood samples

Next, the above cell lysis and Xpert-ultra method was tested on clinical samples from pilot studies.

Five samples were tested from pilot 2. Five patients were recruited based on high predicted probability of MTBBSI (using the machine learning modelling and bedside prediction app developed in chapter 2). Fifteen ml of blood was collected in sodium heparin tubes; buffy coat was extracted and lysed as described in steps 1-4 of method in section 5.3.1.5. One-quarter of the lysate (representing 3.75ml volume of original sample) was stored at -20°C until time of Xpert-ultra testing. After thawing at room temperature, lysate sample was made up to 15 ml volume with 0.22µm filtered deionised water, incubated for 30 minutes at room temperature, and pelleted at 3000g for 25 minutes. Fourteen ml of supernatant was removed, pellet resuspended in residual 1ml volume and mixed with 1ml of Xpert buffer, incubated at room temperature for 30 minutes, then pipetted into Xpert-ultra cartridges as per manufacturer instructions.

Four freezer stored whole blood samples (~5ml) from the KDHTB study were also processed using the same lysis steps (without buffy coat extraction, and without second freezing step after lysing).

From the total of 9 samples, 1 gave no result on Xpert-ultra testing (error message); of the eight with valid results, 6/8 were positive and 2/8 were negative. These results were in complete concordance with the MFL culture results performed on samples from the same venesection, and CT values correlated with TTD in MFL (figure 14).

Sample origin	Xpert-ultra	C_T	MFL	TTD
Pilot 2	very low detected	21.5	*M.tb*	22
Pilot 2	low detected	19.7	*M.tb*	25
Pilot 2	medium detected	16.2	*M.tb*	16
Pilot 2	negative	NA	negative	NA
Pilot 2	low detected	19.2	*M.tb*	24
Stored KDHTB	error	NA	*M.tb*	30
Stored KDHTB	low detected	20.2	*M.tb*	21
Stored KDHTB	negative	NA	*NA*	NA
Stored KDHTB	low detected	18.8	*M.tb*	18

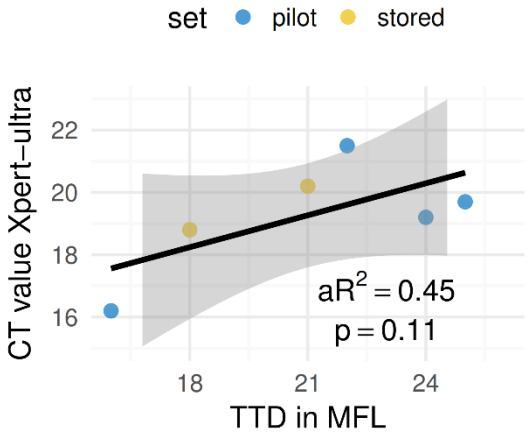

Figure 5-14. Blood Xpert-ultra versus MFL results from clinical pilot testing.

Xpert-ultra had 100% agreement with MFL results (left), and some evidence of correlation between CT value and TTD in MFL was also seen (right).

5.3.3.3 Imputing C_T values for trace detected blood samples

As discussed above, Xpert-ultra 'trace detected' results are given for samples which are negative for *rpoB* PCRs but positive for the combined IS6110-IS1081 probe. By definition, then, trace detected samples don't have a C_T value for *rpoB* moieties, but do have a C_T for the multicopy IS6110-IS1081 genes. To check if this C_T value can be used quantitatively, the correlation between minimum *rpoB* C_T and IS6110-IS1081 C_T was assessed for samples with both available from the serial sub-study. This revealed a reasonably strong relationship between the two (figure 15), which was then used to impute minimum *rpoB* C_T values for trace detected samples (hereafter referred to as Xpert-ultra C_T values for convenience).

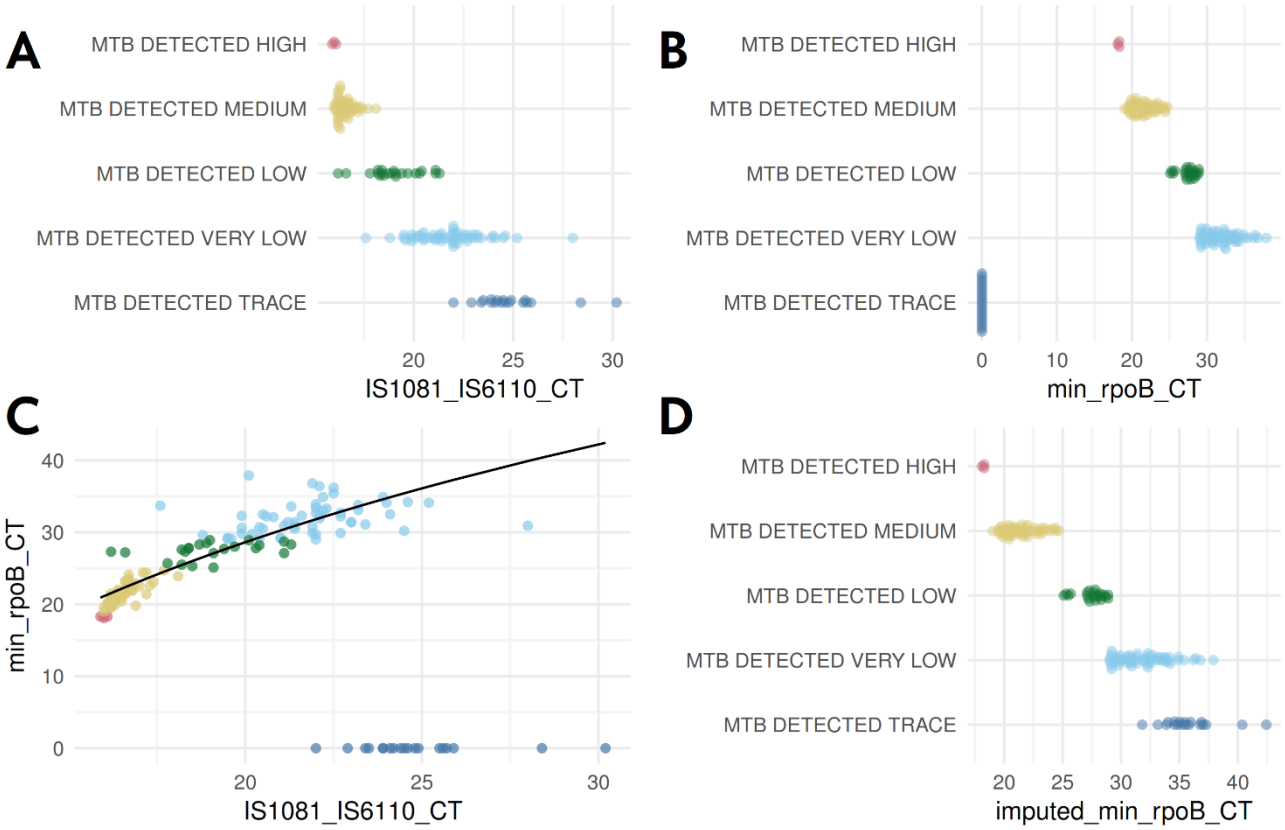

Figure 5-15. Comparing Xpert-ultra CT values based on rpoB & IS6110-IS1081 probes.

IS6110-IS1081 C_T values are available for all positive samples (**A**), but *rpoB* C_T values are not available for "trace detected" samples (**B**). IS6110-IS1081 C_T correlates with *rpoB* C_T for very-low to high detected samples, with a notably non-linear relationship (**C**, aR^2=0.80 for quadratic line of best fit shown). Trace-detected samples *rpoB* C_T imputed using this relationship (**D**).

5.3.4 Location of bacilli in MTBBSI

Cellular location of mycobacteria is of importance from an immunological and PKPD perspective.[103,494,561-564] As mentioned previously, many methods for identifying bacilli in MTBBSI use buffy coat / PBMC extraction, based on the assumption that most bacteraemic *M. tuberculosis* is intracellular. Also shown above was the finding that any free bacilli in plasma would not be expected to sediment in the buffy coat layer at the low g typically used for PBMC extraction methods. Therefore, whether bacilli in MTBBSI

are predominantly in white blood cells or extracellular is of fundamental and practical interest.

In pilot 2, plasma, buffy coat, and red cell pellet from 5 patients were separated and cultured in different MFL bottles. Of these, only 1/5 grew *M. tuberculosis* from the buffy coat, while 4/5 cultures of the red cell pellet were positive. These results contradict the assumption that most bacilli are within white cells in MTBBSI.

This finding was tested further with 10 samples from patients recruited to the sub-study. In each case, ~4ml of blood was syphoned for processing with Polymorphprep (Axis-Shield / Alere Technologies, Oslo). Polymorphprep is an osmotic density gradient designed to separate both PBMCs and polymorphonucleocytes from erythrocytes. This is important because: (1) in simple centrifuge preparations of the buffy coat, granulocytes may colocalise with red blood cells *below* the buffy coat,[565,566] and (2) neutrophils are the predominant phagocytic location of *M. tuberculosis* in at least some body compartments.[567] Polymorphprep was therefore used as a gold standard method of ensuring neutrophils were captured in buffy coat preparations for these ten samples. The procedure is illustrated in figure 16.

Extracted plasma, buffy coat preparation, and red cell pellet, were all processed with 3 lysis-wash steps (two with filtered deionised water prior to storage at -20°C, one after thawing) prior to Xpert-ultra testing, as previously described for whole blood samples. This allowed comparison of Xpert-ultra C_T values for the three blood compartments: red cell pellet; buffy coat preparation (which should contain >95% of all WBCs, but was generally contaminated with some RBCs); and plasma. The whole blood sample lysate processed in parallel for these samples is a further comparator, representing all 3 compartments combined.

Of these ten patient samples, most were positive from any compartment, with no statistically significant differences in recovery in any pairwise comparison (table 5). In particular, buffy coat layer did not have significantly higher recovery than plasma or red cell pellet. Cycle-threshold values, however, suggested that plasma had the lowest bacilli copy number (highest C_T), and that whole blood lysate had the greatest bacilli copy number (lowest C_T). Some patients had lower CT for buffy coat than red cell pellet,

while in others the reverse was seen; overall no significant difference between buffy and red cell pellet bacilli quantity was evident.

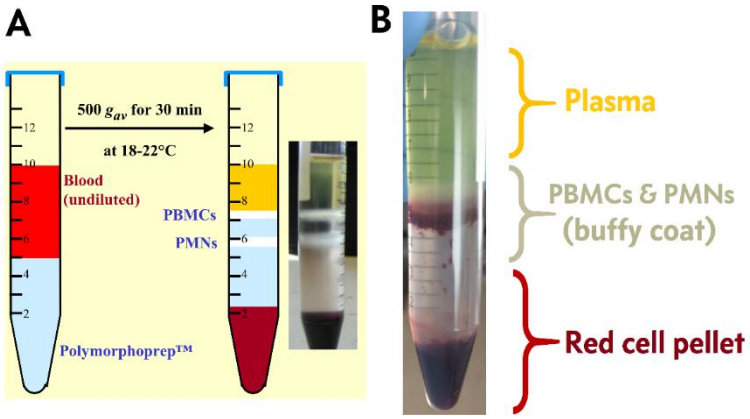

Figure 5-16. Polymorphprep SOP.

As shown in the manufacturer's schematic (**A**), blood is layered on top of an equal volume of polymorphprep, spun at a low g for 30 minutes without brake. This should result in two erythrocyte free WBC layers corresponding to PBMCs and granulocytes (PMNs). The manufacturer acknowledge that separation is less complete when not using health volunteer blood (example from MTBBSI patient from current analysis shows not all RBCs sediment to red cell pellet, **B**). The 1/3 of the processed sample containing PBMC/PMC buffy coat should, however, contain >95% of white cells, i.e. >95% of phagocytosed bacilli, despite some contamination with RBCs. In turn, the top and bottom 1/3 (plasma and red cell pellet respectively) should be largely free of white blood cells.

Table 5-5. Qualitative results Xpert-ultra for different blood compartments

sample	buffy	plasma	Rcp	WBlysate
1	*M.tb* detected	*M.tb* detected	*M.tb* detected	*M.tb* detected
2	**Negative**	*M.tb* detected	**Negative**	*M.tb* detected
3	*M.tb* detected	*M.tb* detected	*M.tb* detected	**Negative**
4	**Negative**	*M.tb* detected	**Negative**	**Negative**
5	*M.tb* detected	*M.tb* detected	*M.tb* detected	*M.tb* detected
6	*M.tb* detected	*M.tb* detected	*M.tb* detected	*M.tb* detected
7	*M.tb* detected	*M.tb* detected	*M.tb* detected	*M.tb* detected
8	*M.tb* detected	**Negative**	**Negative**	*M.tb* detected
9	*M.tb* detected	*M.tb* detected	*M.tb* detected	*M.tb* detected
10	*M.tb* detected	*M.tb* detected	*M.tb* detected	*M.tb* detected

*Plasma, buffy, rcp (red cel pellet) = the three polymorphprep separated blood compartments (see figure 16). WBlysate = whole blood lysate, a second same volume sample from the same patient-timepoint processed complete, without separation of the components.

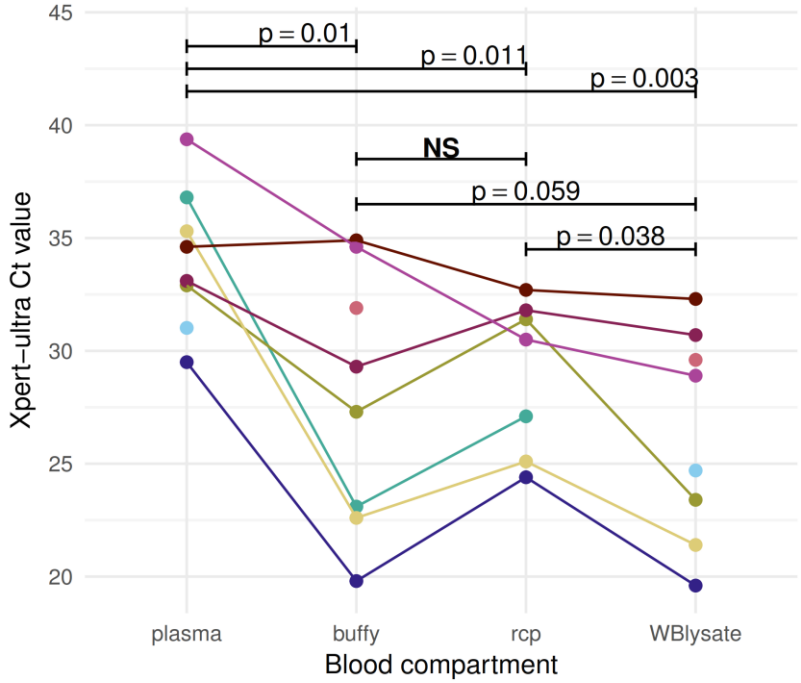

Figure 5-17. Comparison Xpert-ultra CT values for different blood compartments.

Each sample set (from the same patient timepoint, i.e. the same venesection) shown with individual colour. Line connect adjacent points only; if there is no CT value because the sample was negative, connecting line is interrupted. P-values are from paired t-tests from each pairwise comparison. Plasma, buffy, rcp (red cel pellet) = the three polymorphprep separated blood compartments (see figure 16). WBlysate = whole blood lysate, a second same volume sample from the same patient-timepoint processed complete, without separation of the components.

Taken together, these results are not in keeping with the majority of bacteraemic bacilli being intracellular in MTBBSI. Rather, *M. tuberculosis* appears to be spread across blood compartments, including association with red cells (it is unknown if this association results from similar density-centrifugation properties or if it is in some way mechanistic). In sum, it seems likely that extra-cellular bacilli are common in MTBBSI.

5.4 KDHTB sub-study to characterise clinical pharmacodynamics of MTBBSI

Having optimised existing methods and developed novel methods for identifying and quantifying MTBBSI, a cohort was recruited to

- report the dynamics of MTBBSI over the first 72 hours of anti-tuberculosis chemotherapy (ATC); and
- assess for association of MTBBSI pharmacodynamics with major clinical variables including mortality outcome.

This cohort was recruited as a sub-study within the KDHTB parent study.

5.4.1 Sub-study Methods

5.4.1.1 Patient recruitment, inclusion and exclusion

All patients in Khayelitsha Hospital emergency department, and patients admitted to medicine in the preceding 24-hours, were screened each morning Monday-Friday. All patients who were HIV positive and had at least one of thrombocytopenia, hyponatraemia < 130 mEp/L, haemoglobin < 10g/dL, raised creatinine, or CD4 count < 150 cells/mm3 were formally screened including collection of urine for urine-LAM testing on site. Patients who had already received a dose of ATC, and patients with a non-tuberculosis diagnosis already made, were excluded. An updated version of the MTBBSI prediction model using variables [presence adenopathy or splenic micro-abscesses, creatinine, sodium, white cell count, MCV, platelets, haemoglobin, CD4 count, urine-LAM lateral flow result (0 to +4)] was constructed.[†††††††††] Patients with predicted probability of MTBBI > 0.6, and who gave informed consent, were recruited. Because of the nature of the study, a further exclusion criterion was patients who did not start TB therapy, which was at the discretion of (non-study) hospital doctors. In practice, all patients with predicted probability of MTBBSI > 0.5 were started on TB

[†††††††††] https://davidadambarr.shinyapps.io/MTBBSI_v2/

therapy during admission, but sometimes this was delayed by more than 24 hours after initial study screening, meaning that recruitment was also delayed to this time.

5.4.1.2 Sample schedule & blood processing

Blood was collected at five timepoints: 0h (prior to first does ATC), and 4, 24, 48 & 72 hours after first does of ATC. At each time point 18ml of blood was collected in sterile sodium heparin tubes and transported to a laboratory at University of Cape Town. Five ml of blood was centrifuged at 3000g for 25 minutes to pellet all cells; this cell pellet was inoculated into a MFL bottle. The remaining blood (13ml) was split into 10ml and 3ml aliquots. Both were mixed with 30ml of 0.22µm filtered RBC lysis buffer [155mM NH_4Cl; 12mM $NaHCO_3$; 0.1 mM EDTA], incubated at room temperature for 30 minutes with regular inversions to mix, then pelleted at 3000g for 25min. Both pellets were then resuspended in 45ml 0.22µm filtered deionised water, incubated at room temperature for 30 minutes with regular inversions to mix, then pelleted again at 3000g for 25min. The pellet from the10ml blood aliquot was resuspended in 5ml sterile PBS and divided as follows:

- ½ (≡ 5ml of original blood sample) was inoculated into a second MFL bottle.
- ½ (≡ 3.5ml of original blood sample) was stored at -20°C for downstream Xpert-ultra testing.

The pellet from the 3ml blood aliquot was resuspended in 1ml sterile PBS and added to 5ml of MFL broth in a 50ml sterile, disposable conical flask. 10µL of 100mM DMN-tre (final concentration 154 µM) was added and the sample incubated in dark and under agitation for 18 hours at 37°C.

MFL cultures were transferred to the National Health Laboratory Service medical microbiology laboratory at Groote Schuur Hospital, and incubated within 24 hours of venesection.

5.4.1.3 DMN-tre microscopy

After incubation for 18 hours as above, samples were mixed with 30ml of detergent lysis buffer (0.22µm filtered deionised water with v/v 0.5% Triton-X-100 and 1% Tween80). 18mg of proteinase-K was added to this volume, before incubation in the dark at 37°C for 30 minutes, with mixing at 15 minutes by gentle inversion. This was then pelleted at 3000g for 25 minutes, and the pellet resuspended in 1.5ml 0.22µm filtered deionised

water by pipetting, before transfer to the centrifuge filtration device, with filtration at 1800g for 10 minutes. The black polycarbonate membrane was mounted for microscopy as previously described. Each membrane was examined for 1 hour at 100x magnification. If bacilli were identified, 500 random fields were examined at 100x magnification to quantify bacilli on membrane. The effective surface area of the membranes was measured to be 2850 fields of view (FOV), by experiments with fluorescent beads counted by flow cytometry – data not shown here, so the bacilli count per ml could be calculated as:

$$bacilli\ ml^{-1} = \frac{total\ microscopy\ count}{FOV\ examined} \times \frac{2850\ FOV}{3ml}$$

5.4.1.4 Xpert-ultra testing

Batches of thawed samples were made up to a volume of 10ml by addition of 0.22µm filtered deionised water, then centrifuged at 4200G for 25 minutes. Supernatant volume 9.3 ml was removed, leaving ~0.7ml sample, resuspended by pipetting. Xpert buffer (1.5ml) added for final volume ~2.2ml, and mixed by vigorous shaking 20 times, then incubated at room temperature for 10 minutes, followed by another 20 shakes and further 5-minute incubation, before adding to Xpert-ultra cartridges and processing as per manufacturer instructions.‡‡‡‡‡‡‡‡‡ Full results were outputted as .txt files and CT values extracted as described in section 5.3.3.3 using a custom R script.

5.4.1.5 Collection of demographic, clinical & follow-up data

All patients were examined by study clinicians at all sampling timepoints with clinical variables recorded on paper proformas. Blood and imaging results were extracted from electronic health records and the National Health Laboratory Service database, including all results recorded by routine care testing for 3 months after recruitment. Patients were formally followed-up by telephone call to ascertain 12-week survival by Mr M.K. Mpalali.

‡‡‡‡‡‡‡‡‡ I acknowledge Mr Avuyonke Balfour for assistance processing these samples, and to Professor Mark Nicol and Dr Slee Mbhele for access to Xpert machines.

5.4.2 Sub-study results

5.4.2.1 Recruitment & cohort description

Recruitment occurred Monday – Friday between 11/08/2017 and 21/11/2017, with serial blood sampling 7 days a week. Approximately 2500 patients underwent initial screening, 147 were formally screened (for a calculated predicted probability of MTBBSI > 0.56), and 28 met inclusion criteria.

Patient history, examination, imaging results, and baseline blood results are summarised in tables 6 to 9. Due to the enriched recruitment for MTBBSI, the cohort represented a markedly unwell population – all patients were tachycardic, tachyopnoeic, anaemic (median haemoglobin 6.5 g/dL), and profoundly immune-compromised (median CD4 count 33 cells/mm^3, 90% not currently taking anti-retrovirals). Functional impairment was nearly universal (26/28 ECOG score > 1). Within this severely unwell patient strata, variables associated with mortality included functional impairment, respiratory compromise (use of ancillary muscles of respiration, nasal flare, bilateral chest-X-ray disease, lower pulse oximetry saturation); renal compromise (higher creatinine & urea; lower bicarbonate & pH); lower haemoglobin, and higher AST. Patients who died had lower platelet counts, but this difference was not statistically significantly. By contrast, the fall in platelet count during admission (seen in nearly all patients) was significantly greater in those that died (table 10).

Table 5-6. Patient presenting histories, summary by 12-week outcome.

	n	alive (N=20)	died (N=8)	Total (N=28)	p value
sex male	28	6 (30.0%)	3 (37.5%)	9 (32.1%)	1
age	28				0.673
median		35.65	33.9	34.8	
IQR		29.87, 39.70	31.97, 41.98	29.87, 39.88	
ARV status	28				0.956
Naïve		12 (60.0%)	5 (62.5%)	17 (60.7%)	
Taking ARVs		2 (10.0%)	1 (12.5%)	3 (10.7%)	
Prior not current		6 (30.0%)	2 (25.0%)	8 (28.6%)	
Cough	28	13 (65.0%)	7 (87.5%)	20 (71.4%)	0.467
Fever	28	15 (75.0%)	5 (62.5%)	20 (71.4%)	0.843
Night sweats	28	15 (75.0%)	5 (62.5%)	20 (71.4%)	0.843
Weight loss	28	20 (100.0%)	8 (100.0%)	28 (100.0%)	1
ECOG level	28				**0.022***
1		2 (10.0%)	0 (0.0%)	2 (7.1%)	
2		5 (25.0%)	0 (0.0%)	5 (17.9%)	
3		7 (35.0%)	2 (25.0%)	9 (32.1%)	

4	6 (30.0%)	6 (75.0%)	12 (42.9%)	

n = number with complete observations. IQR = interquartile range. ECOG = Eastern Cooperative Oncology Group functional performance score. ARV = anti-retroviral.
P-value from Wilcox Rank Sum or Fisher exact test as appropriate; except * which is from Chi-squared test for a trend.

Table 5-7. Baseline examination findings, summary by 12-week outcome.

	n	alive (N=20)	died (N=8)	Total (N=28)	p value
Walks unaided	28	7 (35.0%)	2 (25.0%)	9 (32.1%)	0.949
Can self-feed	28	18 (90.0%)	5 (62.5%)	23 (82.1%)	0.242
GCS<15	28	5 (25.0%)	2 (25.0%)	7 (25.0%)	1
Wasting	28	12 (60.0%)	7 (87.5%)	19 (67.9%)	0.337
Candidiasis	28	9 (45.0%)	4 (50.0%)	13 (46.4%)	1
Oedema	28	5 (25.0%)	3 (37.5%)	8 (28.6%)	0.843
Peripheral adenopathy	28	7 (35.0%)	1 (12.5%)	8 (28.6%)	0.467
Flushed	28	8 (40.0%)	2 (25.0%)	10 (35.7%)	0.755
Sweating on exam	28	7 (35.0%)	3 (37.5%)	10 (35.7%)	1
Cool peripheries	28	6 (30.0%)	5 (62.5%)	11 (39.3%)	0.245
Capillary refill >2sec	28	7 (35.0%)	5 (62.5%)	12 (42.9%)	0.365
Doughy abdomen	28	3 (15.0%)	3 (37.5%)	6 (21.4%)	0.423
Tender abdomen	28	6 (30.0%)	4 (50.0%)	10 (35.7%)	0.575
Use ancillary muscles	28	5 (25.0%)	6 (75.0%)	11 (39.3%)	**0.043**
Nasal flare	28	6 (30.0%)	6 (75.0%)	12 (42.9%)	**0.08**
Full sentences	28	17 (85.0%)	6 (75.0%)	23 (82.1%)	0.938
Heart rate / min	28				0.989
median		121.5	121.5	121.5	
IQR		113.50, 128.00	117.50, 129.00	113.50, 128.00	
Systolic BP	28				0.697
median		113	108	111.5	
IQR		100.50, 128.25	95.50, 114.50	99.00, 127.25	
Diastolic BP	28				0.43
median		70	71	70	
IQR		63.50, 81.25	64.25, 82.25	63.50, 81.25	
Respiratory rate /min	28				0.553
median		30	32	31	
IQR		26.00, 38.00	29.00, 37.00	26.00, 38.00	
Pulse oxygenation	28				**0.008**
median		97	94.5	96	
IQR		95.75, 99.00	89.50, 96.50	95.00, 98.25	
Temperature ºC	28				0.59
median		38.25	37.9	37.95	
IQR		37.30, 39.25	37.17, 38.35	37.30, 38.75	

n = number with complete observations. IQR = interquartile range. BP = blood pressure. GCS = Glasgow Coma Scale.
P-value from Wilcox Rank Sum or Fisher exact test as appropriate

Table 5-8. Imaging, sputum & uLAM findings, summary by 12-week outcome.

	n	alive (N=20)	died (N=8)	Total (N=28)	p value
CXR pleural effusion	28				0.592
Bilateral		1 (5.0%)	1 (12.5%)	2 (7.1%)	
Unilateral		1 (5.0%)	1 (12.5%)	2 (7.1%)	
None		18 (90.0%)	6 (75.0%)	24 (85.7%)	
CXR miliary	28	2 (10.0%)	3 (37.5%)	5 (17.9%)	0.242
CXR bilateral infiltrate	28	10 (50.0%)	8 (100.0%)	18 (64.3%)	**0.04**
CXR symmetrical infiltrate	28	5 (25.0%)	5 (62.5%)	10 (35.7%)	0.151
CXR adenopathy	28	11 (55.0%)	5 (62.5%)	16 (57.1%)	1
USS hepatomegaly	22	3 (18.8%)	0 (0.0%)	3 (13.0%)	0.578
USS liver echogenic	22	8 (50.0%)	4 (57.1%)	12 (52.2%)	1
USS splenomegaly	22	2 (12.5%)	0 (0.0%)	2 (8.7%)	0.861
USS splenic micro-abscesses	22	13 (81.2%)	7 (100.0%)	20 (87.0%)	0.578
USS kidney echogenic	22				0.243
Very increased		0 (0.0%)	1 (14.3%)	1 (4.3%)	
Increased		11 (68.8%)	5 (71.4%)	16 (69.6%)	
Normal		5 (31.2%)	1 (14.3%)	6 (26.1%)	
USS kidney CMD loss	22	2 (12.5%)	1 (14.3%)	3 (13.0%)	1
USS frank ascities	22	1 (6.7%)	0 (0.0%)	1 (4.5%)	1
USS pleural effusion	22	3 (20.0%)	2 (28.6%)	5 (22.7%)	1
USS pericardial effusion >1cm	22	1 (6.7%)	1 (14.3%)	8 (36.4%)	1
USS adenopathy	22	11 (68.8%)	5 (71.4%)	16 (69.6%)	1
USS gall bladder oedema	22	3 (20.0%)	1 (14.3%)	4 (18.2%)	1
uLAM	28				0.691
0		1 (5.0%)	0 (0.0%)	1 (3.6%)	
1		5 (25.0%)	3 (37.5%)	8 (28.6%)	
2		5 (25.0%)	1 (12.5%)	6 (21.4%)	
3		5 (25.0%)	1 (12.5%)	6 (21.4%)	
4		4 (20.0%)	3 (37.5%)	7 (25.0%)	
Sputum Xpert	28				0.684
MTB		5 (25.0%)	3 (37.5%)	8 (28.6%)	
Negative		1 (5.0%)	0 (0.0%)	1 (3.6%)	
No sputum obtained		14 (70.0%)	5 (62.5%)	19 (67.9%)	

n = number with complete observations. CXR = chest x-ray. USS = ultrasound scan of abdomen. Both performed as part of routine care, USS were all reported using a standardised template, CXRs all interpreted by the author. Small effusions were common but all were sub-clinical. P-vales from Fisher exact test.

Table 5-9. Baseline blood results, summary by 12-week outcome.

	n	alive (N=20)	died (N=8)	Total (N=28)	p value
log CD4 count	28	3.63 (0.83)	2.72 (1.67)	3.37 (1.17)	**0.063**
pH	28	7.44 (0.08)	7.36 (0.11)	7.42 (0.10)	**0.032**
HCO3	28	23.04 (5.72)	18.01 (5.86)	21.60 (6.11)	**0.047**
Base Excess	28	-2.08 (6.75)	-7.46 (7.86)	-3.62 (7.36)	**0.08**
log venous lactate	28	1.02 (0.51)	1.32 (0.51)	1.10 (0.52)	0.162
pCO2 (venous)	28	4.10 (1.06)	3.90 (0.87)	4.05 (1.00)	0.632
log glucose	28	1.94 (0.28)	1.92 (0.19)	1.93 (0.25)	0.854
Haemoglobin*	28	7.53 (1.51)	5.47 (0.54)	6.94 (1.61)	**< 0.001**
MCV	28	80.69 (8.53)	77.01 (8.77)	79.64 (8.60)	0.316
log platelet count	28	5.37 (0.57)	5.20 (0.41)	5.32 (0.52)	0.445
log white cell count	28	1.97 (0.59)	1.69 (0.55)	1.89 (0.58)	0.256
log sodium	27	4.85 (0.05)	4.84 (0.06)	4.84 (0.05)	0.674
Potassium	27	4.26 (0.77)	4.15 (0.68)	4.23 (0.73)	0.722
log urea	27	1.85 (0.78)	3.03 (0.75)	2.20 (0.94)	**0.001**
log creatinine	28	4.54 (0.78)	5.34 (0.71)	4.77 (0.83)	**0.018**
log albumin	14	2.89 (0.17)	2.88 (0.19)	2.88 (0.17)	0.898
Alkaline phosphatase	12	160.17 (74.42)	187.00 (104.91)	173.58 (87.84)	0.62
log ALT	21	3.53 (1.08)	3.71 (0.78)	3.60 (0.96)	0.685
log AST	19	4.51 (1.02)	5.27 (0.78)	4.83 (0.98)	**0.093**
log conjugated bilirubin	10	1.88 (0.31)	1.93 (0.91)	1.91 (0.64)	0.903
Ferritin	8	1378.75 (242.50)	1304.25 (391.50)	1341.50 (304.10)	0.757

n = number with complete observations. Mean (standard deviation) shown. Gas results are venous. Variables have been transformed to approximate normal distributions. P-value from t-tests. Baseline values are defined as closest result to day of admission within a 7-day range. * Rather than baseline, haemoglobin results are the nadir haemoglobin during admission, because admission full blood counts overestimated haemoglobin due to haemoconcentration secondary to low extra-cellular fluid volumes.

Table 5-10. Daily rate of change in platelet count, haemoglobin, & log creatinine during admission period.

	n	alive (N=20)	died (N=8)	Total (N=28)	p value
Platelet count change, cells/µL/day	21				**0.008**
Median		-2.64	-11.88	-4.1	
IQR		-7.56, 3.67	-24.33, -6.82	-12.00, -0.08	
Haemoglobin change, g/dL/day	21				0.404
Median		-0.06	0.04	0.03	
IQR		-0.20, 0.07	-0.11, 0.14	-0.22, 0.11	
Creatinine change, log µmol/L/day	24				0.417
Median		-0.08	-0.06	-0.08	
IQR		-0.09, -0.06	-0.12, 0.04	-0.10, -0.02	

n = number with complete observations. IQR = interquartile range.
P-value from Wilcox Rank Sum. Rate of change for each variable was calculated from slope of a line of best fit applied to data points from up to 14-days after admission. Residual variation in haemoglobin was marked due to the effects of haemodilution (all patients received IV fluids on

admission), blood transfusion (3 patients), and blood loss after blood anticoagulation due to venous thrombo-embolism (2 patients)

5.4.2.2 Overall MTBBSI detection by method at all patient-timepoints

28 patients by 5 timepoints is 140 sample time points. This gave a potential 140 DMN-tre microscopy and blood Xpert-ultra samples, and 280 MFL culture samples (two at each patient-timepoint). Samples were not collected at 25 patient timepoints (10 discharges or patient transfers where patient could not be located or brought back; 7 declined samples; 5 missed due to time constraint; 3 because patient died before timepoint).

Blood Xpert-ultra and DMN-microscopy had substantially higher detection rates (83/114 & 73/101 positive tests in valid samples, 72% for both) compared to MFL culture (71/226 valid results, 31%) (table 11 & 12).

Overall agreement of tests across all patient-timepoints was moderate:

- MFL ~ DMN-tre: kappa = 0.37; p = 1.7e-05
- MFL ~ blood Xpert-ultra: kappa = 0.27; p = 1.0e-03
- Blood Xpert-ultra ~ DMN-tre: kappa = 0.34; p = 9.2e-05

For comparison, no agreement with urine-Xpert-ultra result beyond chance was found for any of the three TB blood tests (95% confidence intervals for kappa all cross zero).

Table 5-11. Available samples by method.

method	samples processed	Potential	technical failures*	valid results	M.tb detected	negative	M.tb quantified
MFL blood culture	229	280	5	226	71	155	69
DMN-tre microscopy	115	140	14	101	73	28	73
Blood Xpert-ultra	115	140	1	114	83	31	83

*Technical failures for MFL = 2 contamination, 1 lost viability, 1 lost by lab, 1 discarded by accident. Technical failures for DMN = 2 contamination, 2 lost sample (filter caught in hood airflow), 1 discarded by accident, 9 had debris or some other fluorescence obscuring the fields of view. Technical failures for Xpert = 1 discarded by accident.

Table 5-12. Pairwise comparison of method for detecting MTBBSI across all patient timepoints.

All patient-timepoints:									
	DMN-tre positive	DMN-tre negative		Blood -Xpert-ultra positive	Blood -Xpert-ultra negative		DMN-tre positive	DMN-tre negative
MFL positive	42	3	MFL positive	46	6	Blood -Xpert-ultra positive	61	13
MFL negative	30	25	MFL negative	36	23	Blood -Xpert-ultra negative	11	12
		p=6.0e-06			p=7.6e-06			p=0.838
Timepoint 0hours only (pre-antimicrobials):									
	DMN-tre positive	DMN-tre negative		Blood -Xpert-ultra positive	Blood -Xpert-ultra negative		DMN-tre positive	DMN-tre negative
MFL positive	16	0	MFL positive	16	3	Blood -Xpert-ultra positive	16	2
MFL negative	4	5	MFL negative	4	4	Blood -Xpert-ultra negative	4	2
		p=0.134			p=1			p=0.838

DMN-tre microscopy and blood Xpert had higher detection rates across all patient timepoints (top row of tables); and were similar to MFL culture when analysis was restricted to 0h timepoint, i.e. samples taken before anti-tuberculosis therapy was started. P-values from McNemar's Chi-squared test for count data.

5.4.2.3 MTBBSI detection by patient

In total, 20/28 (71%) patients had at least one positive MFL blood culture; 22/28 (79%) had at least one positive DMN-tre microscopy sample; and 26/28 (93%) had at least one positive blood Xpert-ultra. Eighteen patients were positive by all three tests; 5 by two tests, 4 by one test, and 1 patient was negative on all tests at all time points.

This aggregate (test positive on at least one timepoint = MTBBSI detected by that diagnostic), was used to calculate diagnostic performance. Compared to MFL blood culture as gold standard, blood Xpert-ultra had sensitivity 0.95 (95%CI 0.75 to 1.00) and specificity 0.12 (95%CI 0.00 to 0.53), and DMN-tre microscopy had sensitivity 0.95 (95%CI 0.75 to 1.00) and specificity 0.62 (95%CI 0.24 to 0.91).

If the gold standard was defined as MTBBSI detected by two or more diagnostics (at any timepoint), sensitivity was 0.87, 0.96, and 0.96, and specificity was 1.00, 1.00, and 0.20, for MFL, DMN-tre microscopy, and blood Xpert-ultra respectively (table 13).

Table 5-13. Sensitivity & specificity of MTBBSI detection in patient for each diagnostic.

Gold standard = MTBBSI detected by ≥ 2 diagnostics (n=23)		
	Sensitivity (95%CI)	Specificity (95%CI)
MFL blood culture	0.87 (0.66 to 0.97)	1.00 (0.48 to 1.00)
DMN-tre microscopy	0.96 (0.78 to 1.00)	1.00 (0.48 to 1.00)
Blood Xpert-ultra	0.96 (0.78 to 1.00)	0.20 (0.01 to 0.72)
Gold standard = MTBBSI detected by ≥ 1 diagnostics (n=27)		
	Sensitivity (95%CI)	**Specificity* (95%CI)**
MFL blood culture	0.74 (0.54 to 0.89)	1.00 (0.02 to 1.00)
DMN-tre microscopy	0.81 (0.62 to 0.94)	1.00 (0.02 to 1.00)
Blood Xpert-ultra	0.96 (0.81 to 1.00)	1.00 (0.02 to 1.00)

* Specificity under this gold-standard is, by definition, equal to 1.00 (as if any diagnostic was positive patients are defined as having MTBBSI, so false positives are impossible) so is not meaningful.

5.4.2.4 MTBBSI detection by timepoint

Detection of MTBBSI by method over time and patient is shown in figure 18, and summarised across patients in figure 19. A marked decline in MFL culture positivity was seen by 4 hours after receipt of anti-tuberculosis chemotherapy, with continued decline out to 72 hours. In contrast, detection of TB in blood by DMN-tre microscopy and Xpert-ultra persisted to 72 hours, the last observed timepoint.

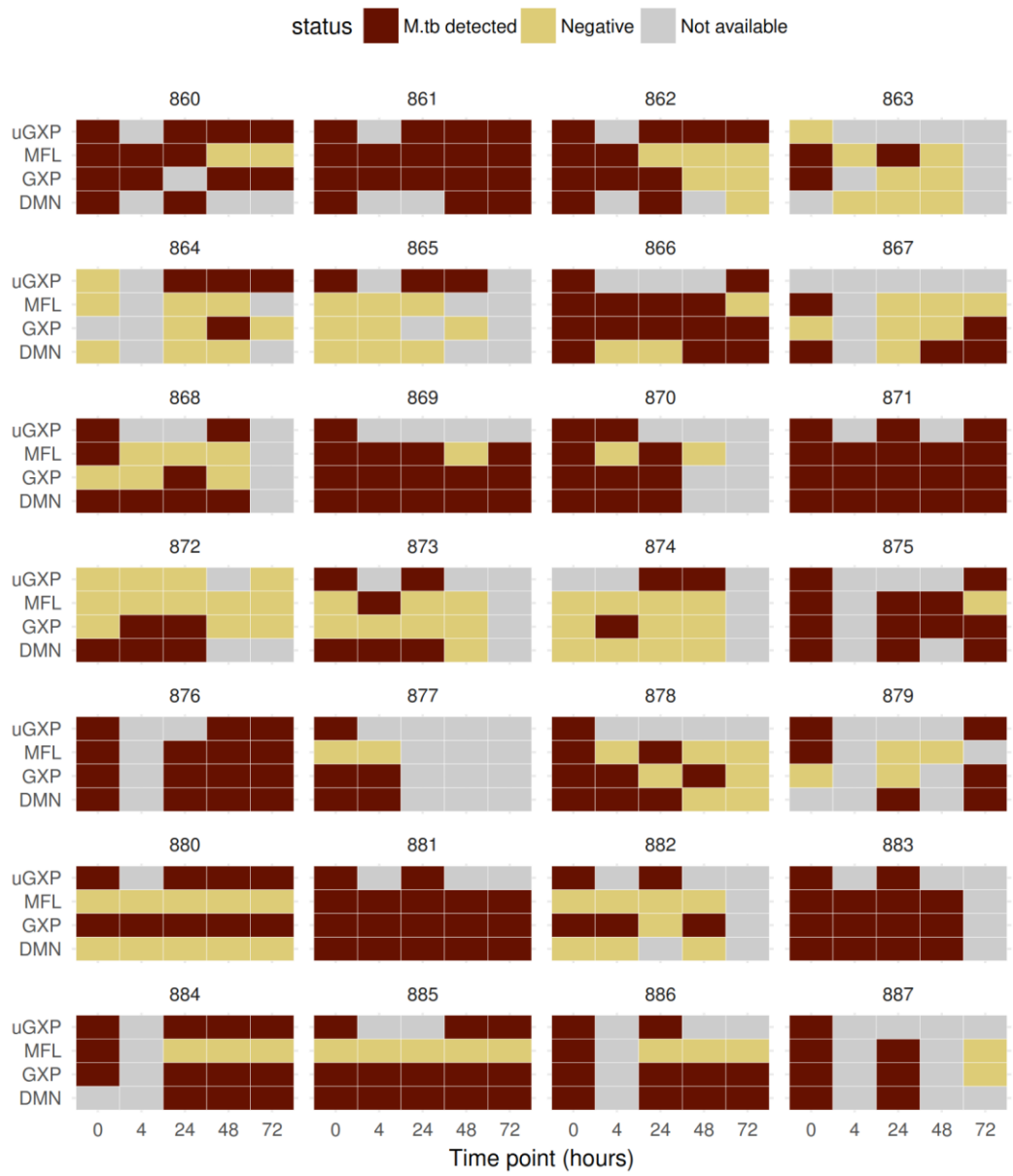

Figure 5-18. MTBBSI detection by method, patient & timepoint.

uGXP = urine Xpert-ultra; MFL = MFL blood culture; GXP = blood Xpert-ultra; DMN = DMN-tre microscopy. Each 4x5 block represents a different patient (n=28).

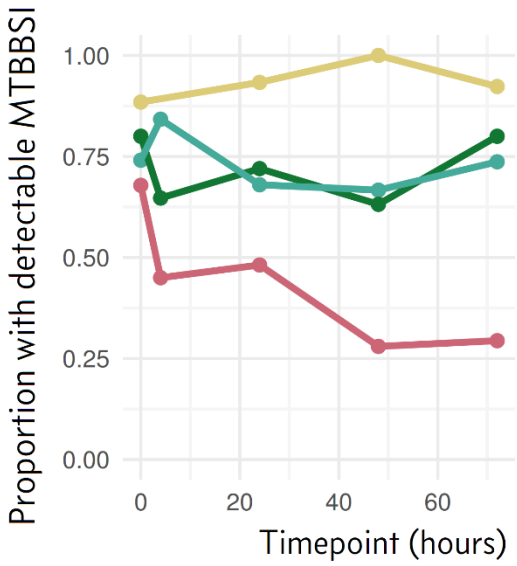

Numbers "at risk" (valid tests)

	0h	4h	24h	48h	72h
DMN-tre micrscopy	25	17	25	19	15
Blood Xpert-ultra	27	19	25	24	19
MFL culture	28	20	27	25	17
urine Xpert-ultra	26	0	15	11	13

Figure 5-19. MTBBSI detection across patients by method & timepoint.

5.4.2.5 Quantification of MTBBSI: univariate & bivariate distributions

Distributions are shown for the three methods of quantifying MTBBSI, along with urine Xpert-ultra C_T, in figure 20. These show patients' DMN-tre bacilli count per ml has a positively skewed distribution, with a long tail extending into thousands of bacilli per ml. This long-tail of very high bacilli burden is not obvious from the TTD and C_T distributions.

Moderate to strong pairwise correlation between the three measures of bacilli burden were apparent, and were more pronounced than correlation of blood measures with urine Xpert-ultra C_T value (figure 21).

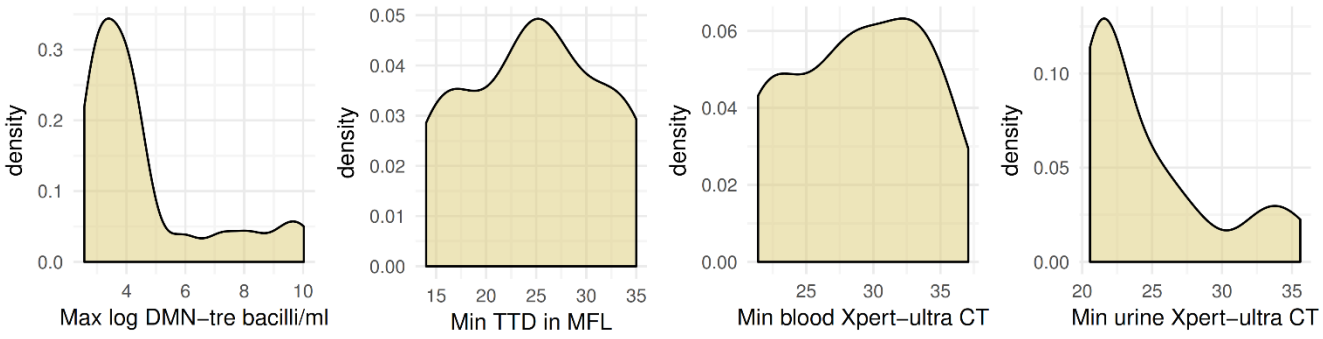

Figure 5-20. MTBBSI quantification: distribution of maximum values by method.

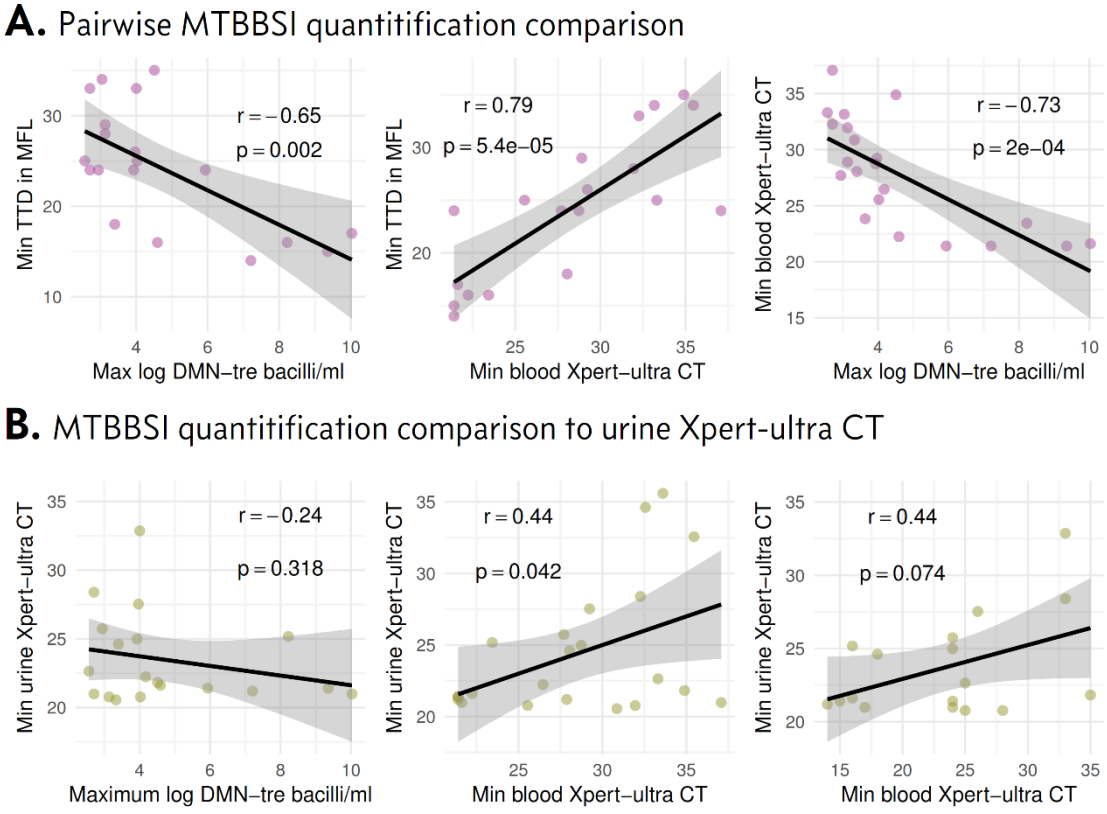

Figure 5-21. Pairwise correlations for MTBBSI quantification methods, & urine Xpert-ultra CT.

In general patients have more than one measure on each method of quantification, so the maximum (DMN-tre count) or minimum (TTD and C_T values) value by patient was extracted to summarise. Min = minimum; Max = maximum.

5.4.2.6 Time-kill curves for MTBBSI by method of quantification

Quantitative values for MFL culture (time to detection, TTD), DMN-tre microscopy (log bacilli per ml blood), blood Xpert-ultra (C_T value), and urine Xpert-ultra (C_T value) over time by patient are shown from 0 to 72 hours in figures 22 to 25. In the majority, a line can be fit to available data by patient, and in most of these TTD and blood C_T values increase, while DMN-tre bacilli per ml decrease. There is, however, marked variation in the intercept (which is generally the maximum or minimum value for each patient) and the slope of the fitted lines.

In contrast to the blood time-kill curves, urine Xpert-ultra C_T values were in most cases flat over the time course (figure 25).

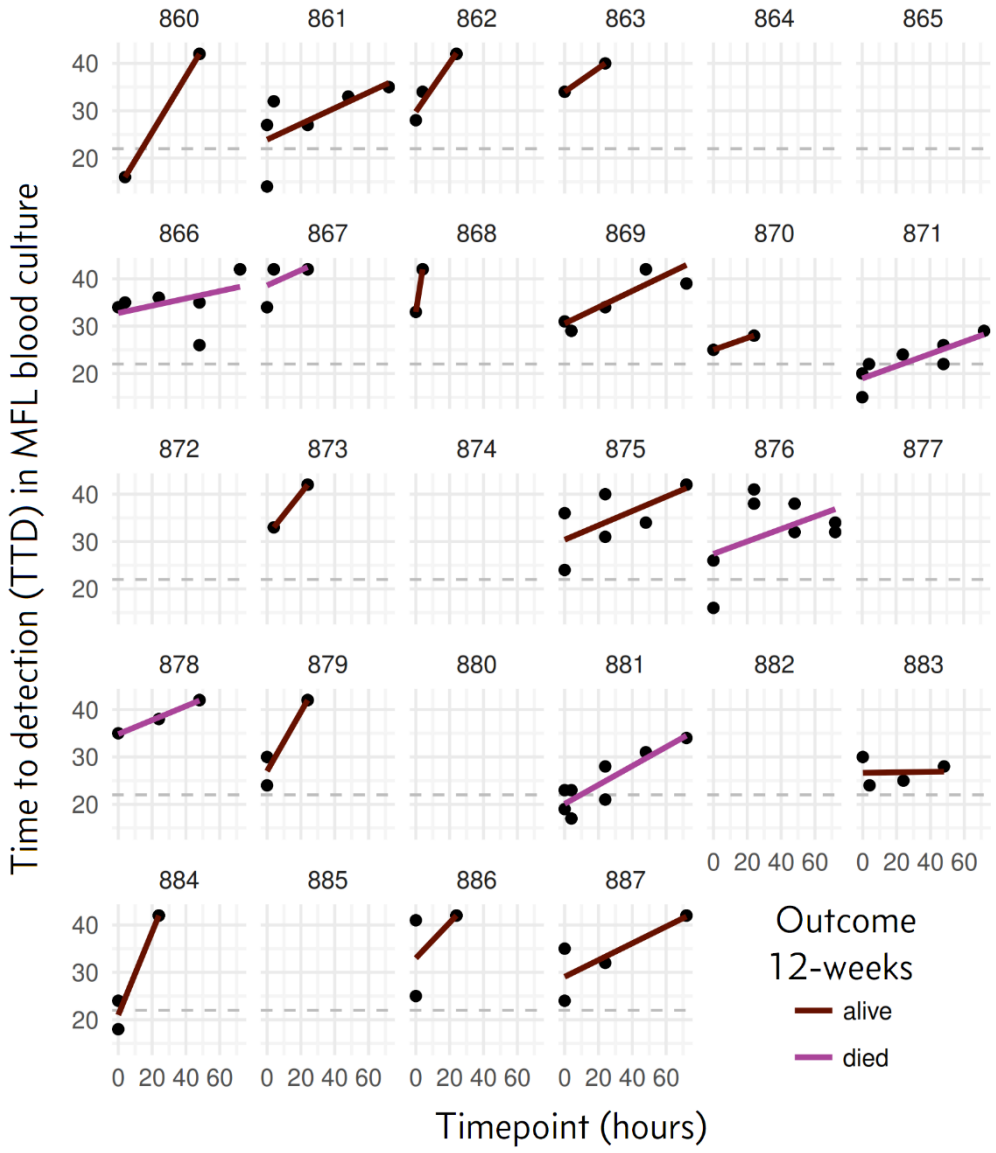

Figure 5-22. TTD in MFL MTBBSI time-kill curve.

Each patient is shown in different panel. In cases where cultures became negative (an initial positive test was followed by one or more negative tests, not including missing/invalid results), the first negative test was imputed at the limit of detection value (TTD = 42 days). Curves are modelled with a line of best fit on TTD scale.

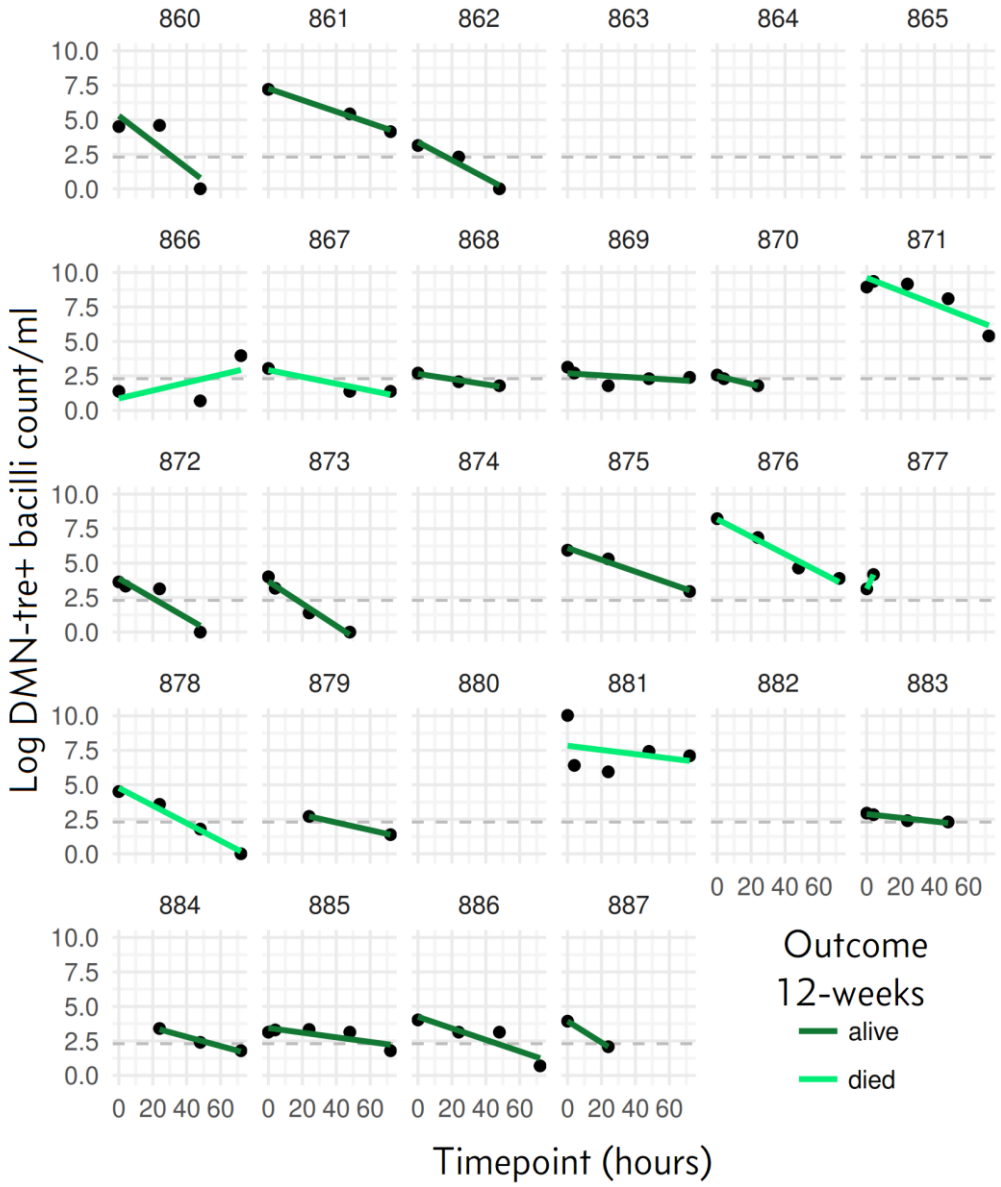

Figure 5-23. Log DMN-tre+ bacilli per ml MTBBSI time-kill curve.

Each patient is shown in different panel. In cases where DMN-tre microscopy became negative (an initial positive test was followed by one or more negative tests, not including missing/invalid results), the first negative test was imputed at the limit of detection value (= 1 bacilli per ml, rounded to nearest whole number). Curves are modelled with a line of best fit on log scale, representing a mono-exponential decline.

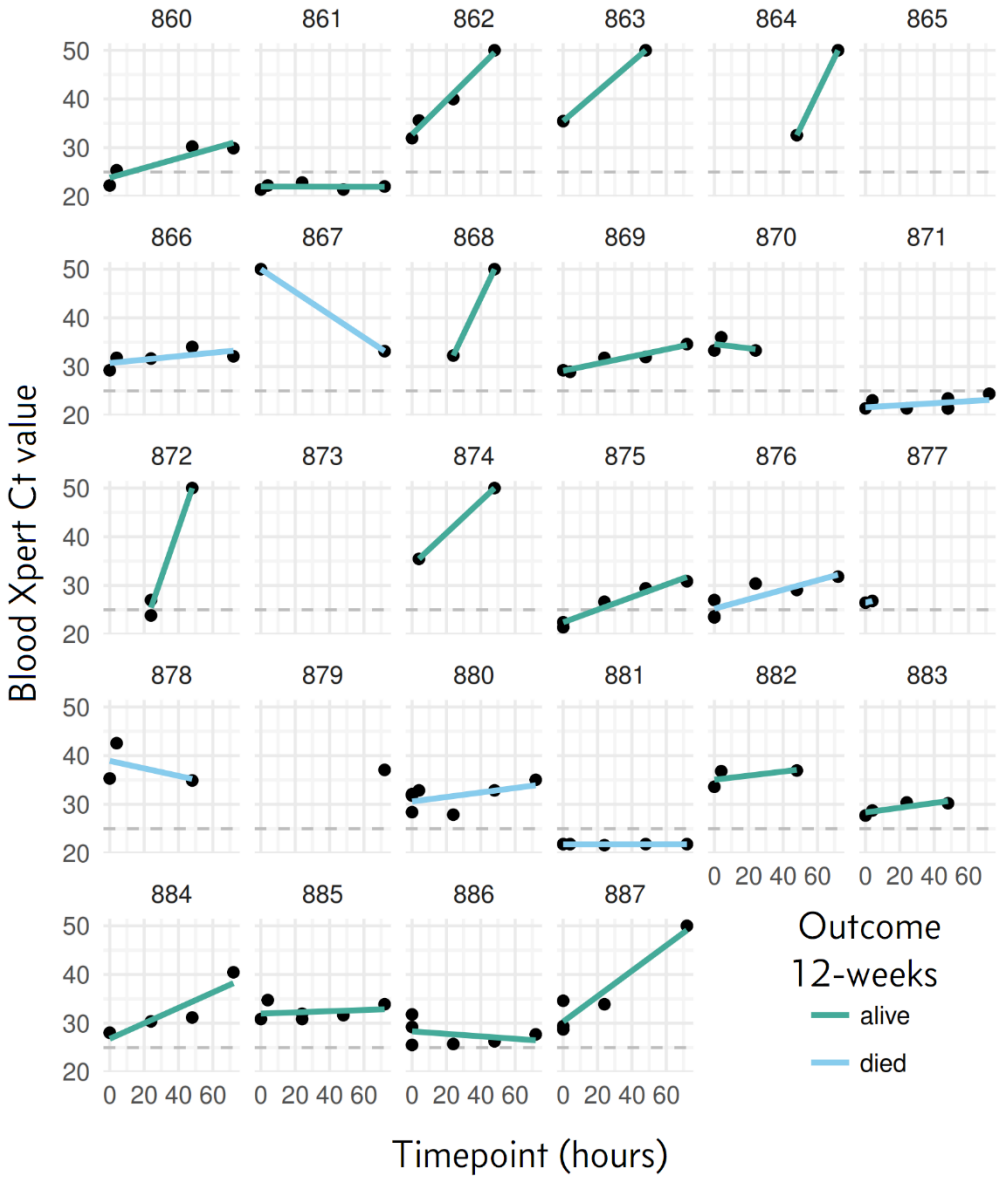

Figure 5-24.Blood Xpert-ultra CT value MTBBSI time-kill curve.

Each patient is shown in different panel. In cases where blood Xpert-ultra became negative (an initial positive test was followed by one or more negative tests, not including missing/invalid results), the first negative test was imputed at the limit of detection value (C_T = 50). Curves are modelled with a line of best fit on C_T scale, which approximates a log2 scale (doubling cycle threshold), thus likely represents a mono-exponential decline.

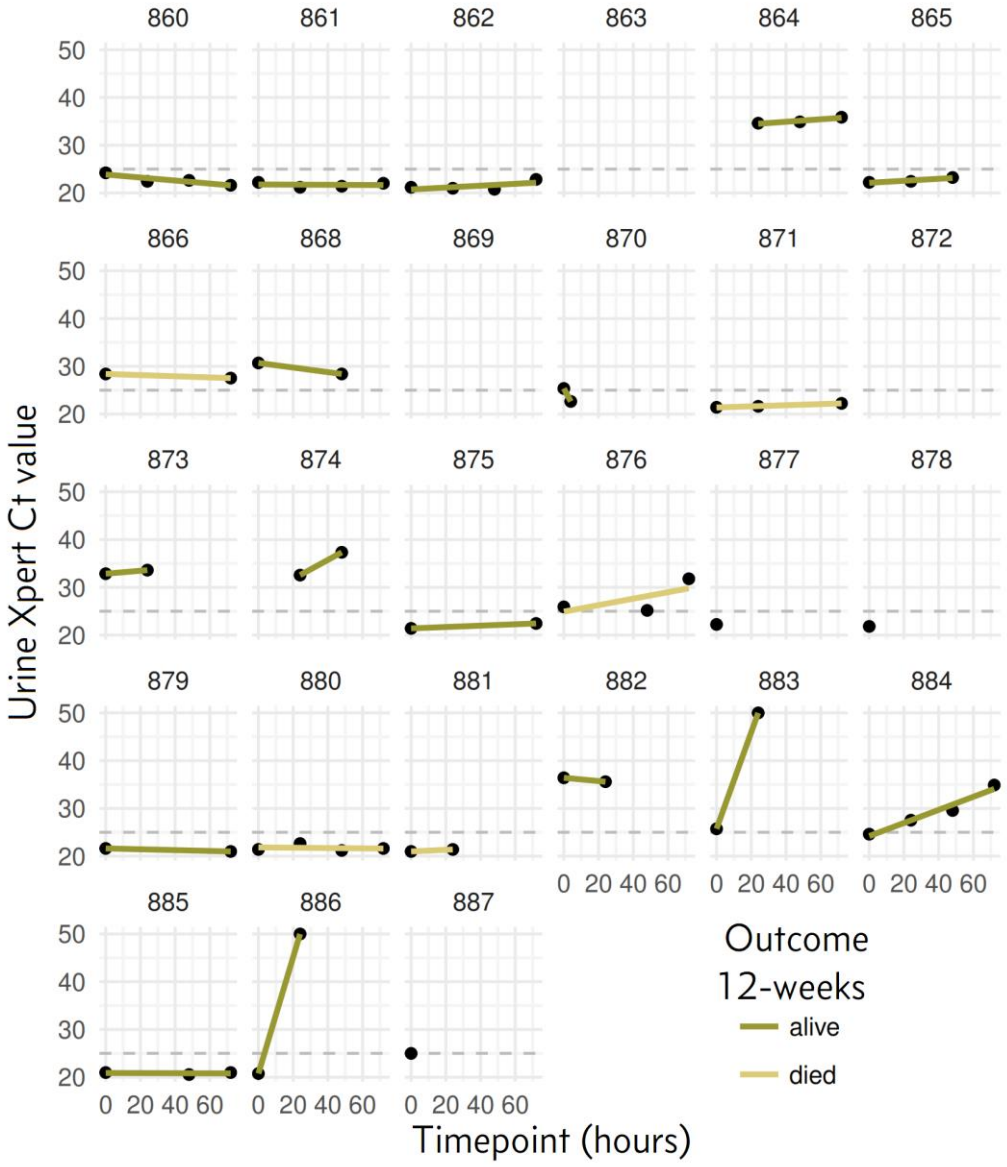

Figure 5-25. Urine Xpert-ultra CT value MTBBSI time-kill curve.

Each patient is shown in different panel. In cases where urine Xpert-ultra became negative (an initial positive test was followed by one or more negative tests, not including missing/invalid results), the first negative test was imputed at the limit of detection value (C_T = 50). Curves are modelled with a line of best fit on C_T scale, which approximates a log2 scale (doubling cycle threshold), thus likely represents a mono-exponential decline.

5.4.2.7 Pharmacodynamic summary measures extracted from time-kill curves

To allow assessment for associations between MTBBSI pharmacodynamics and clinical outcomes, three summary measures of the time-kill curves were extracted.

1. The minimum (C_T and TTD) or maximum (DMN-tre bacilli count) observed value for each patient.
2. The slope of the fitted line, extracted as the gradient parameter from an lmList() object generated using *lme4* package in R.
3. The area under the time-kill curve (AUC), representing overall exposure to the bacillaemia during the 72-hour period of observation. This was extracted using the trapezoid method from *DescTools* package in R. For this analysis, missing values due to negative tests were imputed with the limit of detection value; missing values due to invalid or missing test result were dropped. In the case of the patient who died before 72-hours follow-up, the 72-hour AUC was estimated by extrapolating the line of best fit to 72-hours. AUCs were calculated relative to the limit of detection value, e.g. for Xpert AUC was calculated between the curve and a constant C_T value of 50 (method illustrated in figure 26)

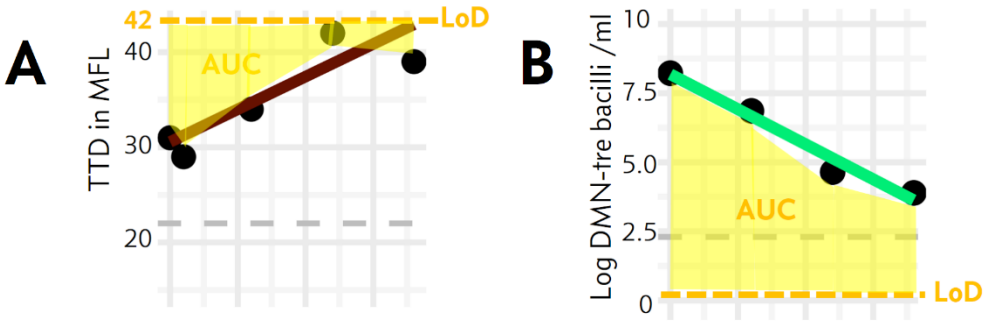

Figure 5-26. Deriving AUC PD summary for time-kill curves

Shaded yellow area shows area between line connecting all points (not line of best fit) and limit of detection (LoD – dashed yellow line), and was calculated using trapezoid rule. This is actually area 'above the curve' where lower bacilli numbers result in higher measurement values (e.g. TTD, **A**). It represents the total exposure to bacillaemia over the time period, for example, in DMN-tre bacilli counts per ml (**B**), the units would be $log(bacill) \bullet ml^{-1} \bullet hour^{-1}$.

In addition, a mixed-effects model, with random intercept and slope permitted by patient, was fitted with a fixed effect for *timepoint*, *outcome*, and the interaction *time*outcome*. The outcome term allows for a fixed (average) difference in time-kill curve

intercept by outcome, and the interaction term allows the slope to differ by outcome. The same model was also fitted but without outcome covariates, and the two models then compared using likelihood ratio tests. This tests the hypothesis that time-kill curves differed on average (in intercept and /or slope) between patients who survived and those that died (i.e. were residual sums of squares less when patient outcome was included as a covariate). This gives a single global test of time-kill curve function association with death.

The results of PD summary measures and mixed-effects modelling are presented in table 14 giving comparisons of patients who died to those that survived. In all cases, PD summary measures were more adverse in those that died, and several were statistically associated with death at alpha<0.05 or alpha<0.1, including MFL TTD slope, DMN-tre log bacilli/ml maximum and AUC, blood Xpert-ultra slope and AUC. Inclusion of outcome as a covariate in mixed-effects modelling of time-kill dynamics improved model fit for DMN-tre and blood Xpert-ultra data (at p = 0.059 and p=0.071 respectively). By comparison, none of the urine Xpert summary PD measures were statistically associated with mortality.

In general, PD summary measures also correlated with important clinical variables. For example, AUC for log DMN-tre bacilli count per ml was associated with functional status, lactate, AST, renal function, extent of infiltrates on chest-x-ray, respiratory rate, pulse oximetry O_2 saturation, platelet count (and possibly rate of platelet decline during admission), total white cell count and CD4 cell count (figure 27 & 28).

Table 5-14. Pharmacodynamic summary measures association with outcome.

MFL TTD

PD summary measures	Died, median (range)	Survived, Median (range)	P-value
Minimum TTD value	21.5 (15 to 35)	24.5 (14 to 34)	0.9669
Fitted gradient over 72hours	0.005 (0.002 to 0.008)	0.009 (0.000 to 0.060)	**0.0758**
AUC, TTD value per hour over 27 hours	262 (0.5 to 899)	67.8 (2.4 to 559)	0.3200
Mixed-effects model	**Intercept**	**Slope**	
Estimated fixed effect association of death	-3.6	-0.08	0.1560

log DMN-tre bacilli/ml

PD summary measures	Died, median (range)	Survived, Median (range)	P-value
Maximum log bacilli/ml observed	4.5 (3.0 to 10.0)	3.4 (2.6 to 7.2)	**0.0344**
Fitted gradient over 72hours	-0.02 (-0.06 to 0.26)	-0.04 (-0.09 to -0.01)	0.2571
AUC, log bacilli/ml per hour over 27 hours	241 (0 to 591)	102 (0 to 418)	**0.0989**
Mixed-effects model	**Intercept**	**Slope**	
Estimated fixed effect association of death	1.85	0.01	**0.0594**

Blood Xpert

PD summary measures	Died, median (range)	Survived, Median (range)	P-value
Minimum CT value	27.2 (21.4 to 34.9)	29.9 (21.4 to 37.1)	0.3305
Fitted gradient over 72hours	0.03 (-0.23 to 0.09)	0.13 (-0.04 to 1.02)	**0.0266**
AUC, CT value per hour over 27 hours	1401 (209 to 2040)	430 (5 to 2017)	**0.0502**
Mixed-effects model	**Intercept**	**Slope**	
Estimated fixed effect association of death	-2.54	-0.23	**0.0712**

Urine Xpert

PD summary measures	Died, median (range)	Survived, Median (range)	P-value
Minimum CT value	21.8 (21.0 to 27.5)	22.6 (20.6 to 35.6)	0.6110
Fitted gradient over 72hours	0.01 (-0.01 to 0.07)	0.02 (-0.68 to 1.22)	0.7798
AUC, CT value per hour over 27 hours	1697 (0 to 2039)	657 (0 to 2112)	0.3753
Mixed-effects model	**Intercept**	**Slope**	
Estimated fixed effect association of death	-6.3	-0.13	0.3005

P-values for PD summary measure comparisons from Wilcox rank sum, comparing those that survived to those that died. P-values for mixed effects models compare a baseline model of form *bacilli burden ~ timepoint + (timepoint | patient)* to model of form *bacilli burden ~ timepoint + outcome + timepoint*outcome + (timepoint | patient)*, where random effect is shown in parentheses, and bacilli burden is TTD, CT value or log DMN-tre bacilli count per ml, by likelihood ratio test.

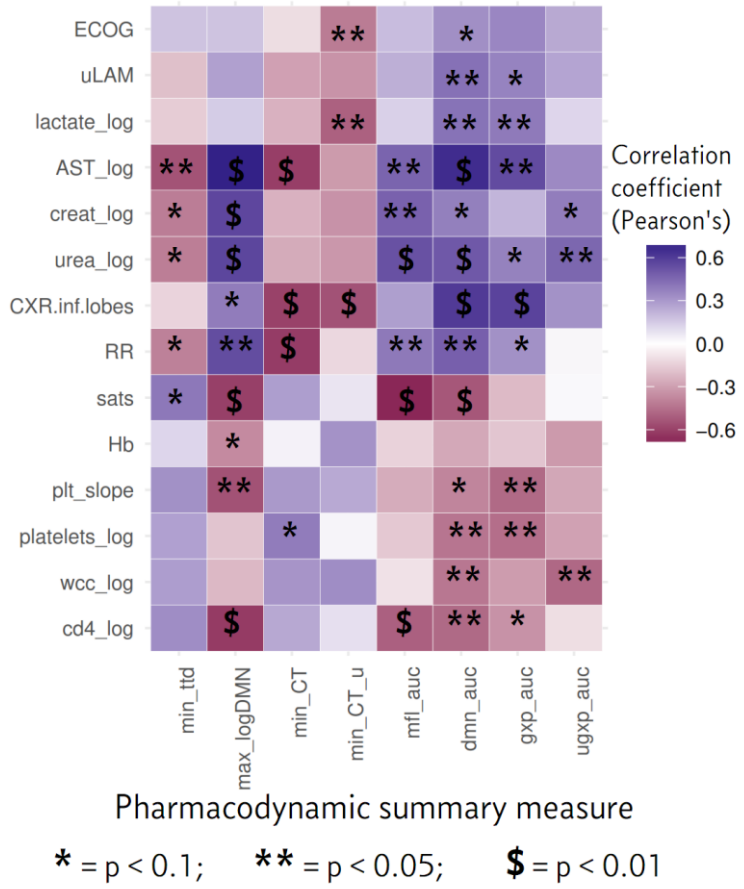

Figure 5-27. Correlation of clinical variables with PD summary measures.

Correlation of eight PD summary measures (columns; values by patient for maximum log DMN-tre bacilli per ml, minimum blood Xpert-ultra C_T, minimum urine Xpert-ultra C_T, minimum TTD in MFL, and AUCs for these detection methods as described in text and figure 26) with clinical variables (rows) selected because of their suggested association with mortality (both in this sub-study or in the wider KDHTB cohort). These variables were transformed to approximate normal distributions (assessed by histograms and QQ plots) where appropriate, and correlations were by Pearson's r (magnitude and direction indicated by colour in matrix plot). P-values for the Pearson's r test are indexed as shown.

ECOG = Eastern Cooperative Oncology Group functional performance score; lactate_log = log venous lactate level; AST_log = log serum aspartate transaminase; creat_log = log serum creatinine; urea_log = log serum urea; CXR.inf.lobes = number of lobes with infiltrate seen on chest-x-ray; RR = respiratory rate per minute; sats = oxygen saturation on pulse oximeter; Hb = haemoglobin nadir during admission; plt_slope = Platelet count change, cells/µL/day during admission (see table 10); platelets_log = log platelet count; wcc_log = log white cell count; cd4_log = log CD4 cell count.

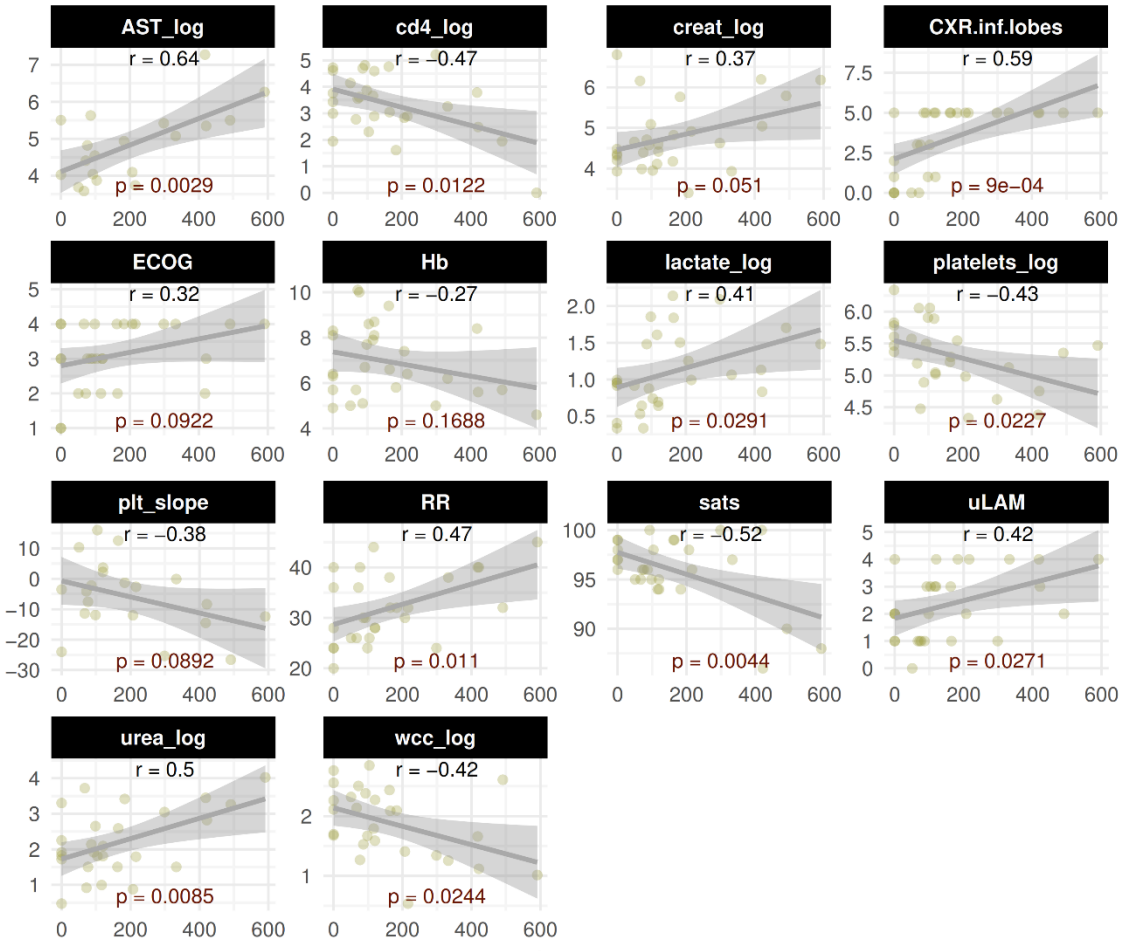

Figure 5-28. Correlation of clinical variables with AUC72h log DMN-tre bacilli per ml.

These are the raw data for the correlations shown for DMN-tre AUC in the previous figure. Line of best fit with 95% confidence interval in shaded area, Pearson's r and associated p value shown.

ECOG = Eastern Cooperative Oncology Group functional performance score; lactate_log = log venous lactate level; AST_log = log serum aspartate transaminase; creat_log = log serum creatinine; urea_log = log serum urea; CXR.inf.lobes = number of lobes with infiltrate seen on chest-x-ray; RR = respiratory rate per minute; sats = oxygen saturation on pulse oximeter; Hb = haemoglobin nadir during admission; plt_slope = Platelet count change, cells/µL/day during admission (see table 10); platelets_log = log platelet count; wcc_log = log white cell count; cd4_log = log CD4 cell count.

5.4.2.8 DMN-tre microscopy bacilli morphology

The majority of TB bacteria seen on microscopy of blood were single bacilli of length 2 – 4 μm; most, but not all, had a beaded appearance or discontinuous DMN-tre staining (figure 29). Doublets, with v-shape arrangement at variable angle, were also common in higher bacilli burden patients, more commonly at early timepoints (figure 30). Bacilli of length greater than 4μm were not infrequent, sometimes up to 8-10μm, and sometimes with the appearance of budding or branching (figure 31, lower row), although these features are hard to distinguish from overlaying of more than one bacilli. Longer bacilli were more likely to be seen at later timepoints after starting anti-tuberculosis therapy (figure 33). Microcolonies of bacilli – clumps of more than 5 bacilli – were also seen (figure 32). Three patients had extensive microcolonies on baseline sample (more than one per field of view), all three of these patients died.

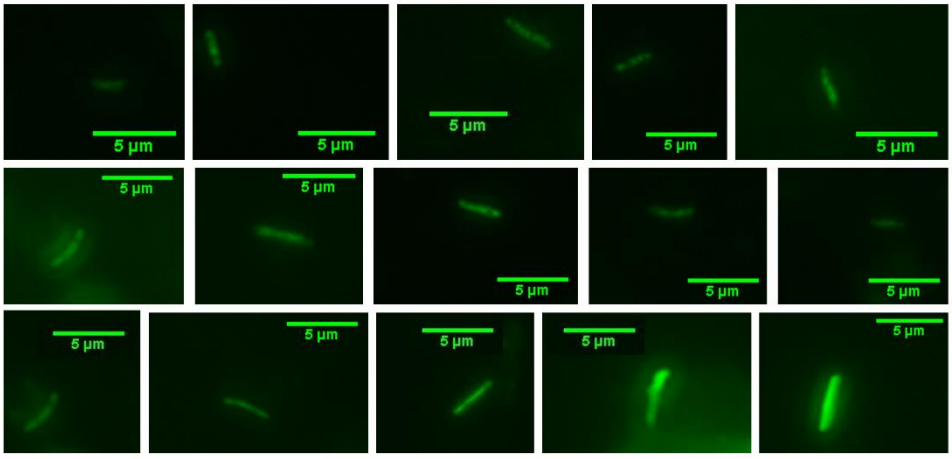

Figure 5-29. DMN-tre microscopy of MTBBSI: single bacilli 2-4μm.

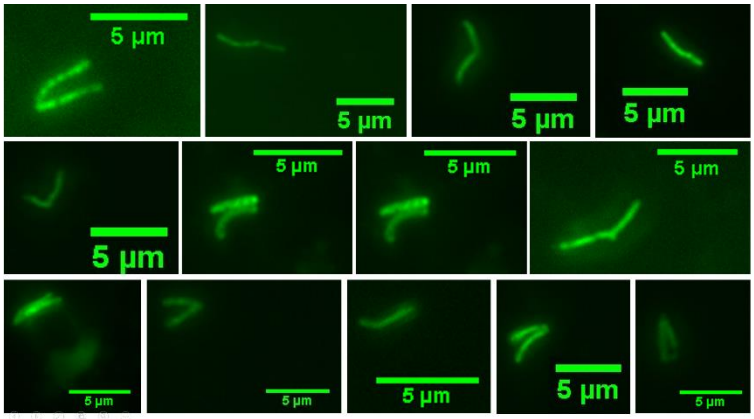

Figure 5-30. DMN-tre microscopy of MTBBSI: doublet bacilli

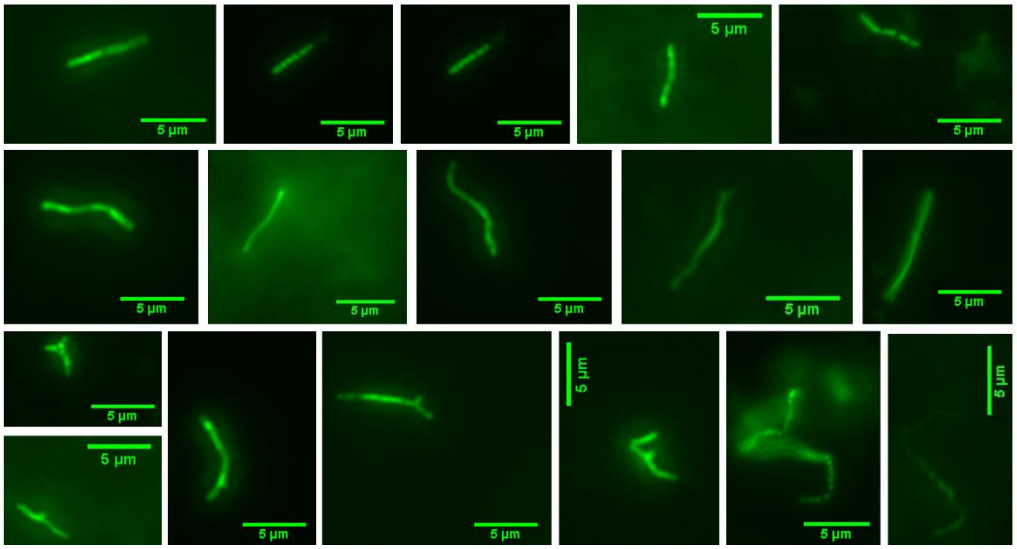

Figure 5-31. DMN-tre microscopy of MTBBSI: single bacilli 4-10µm

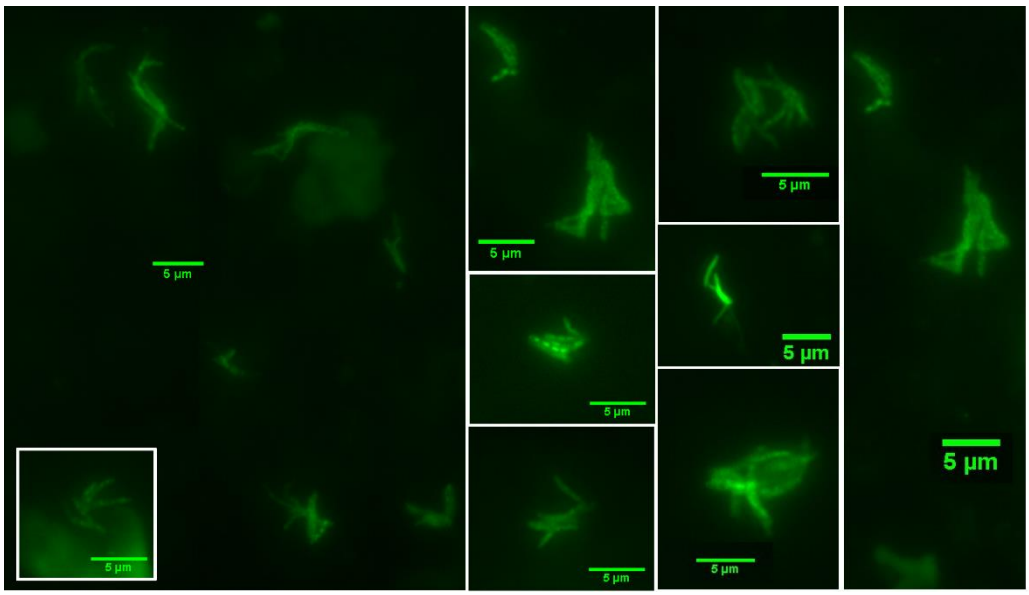

Figure 5-32. DMN-tre microscopy of MTBBSI: microcolonies.

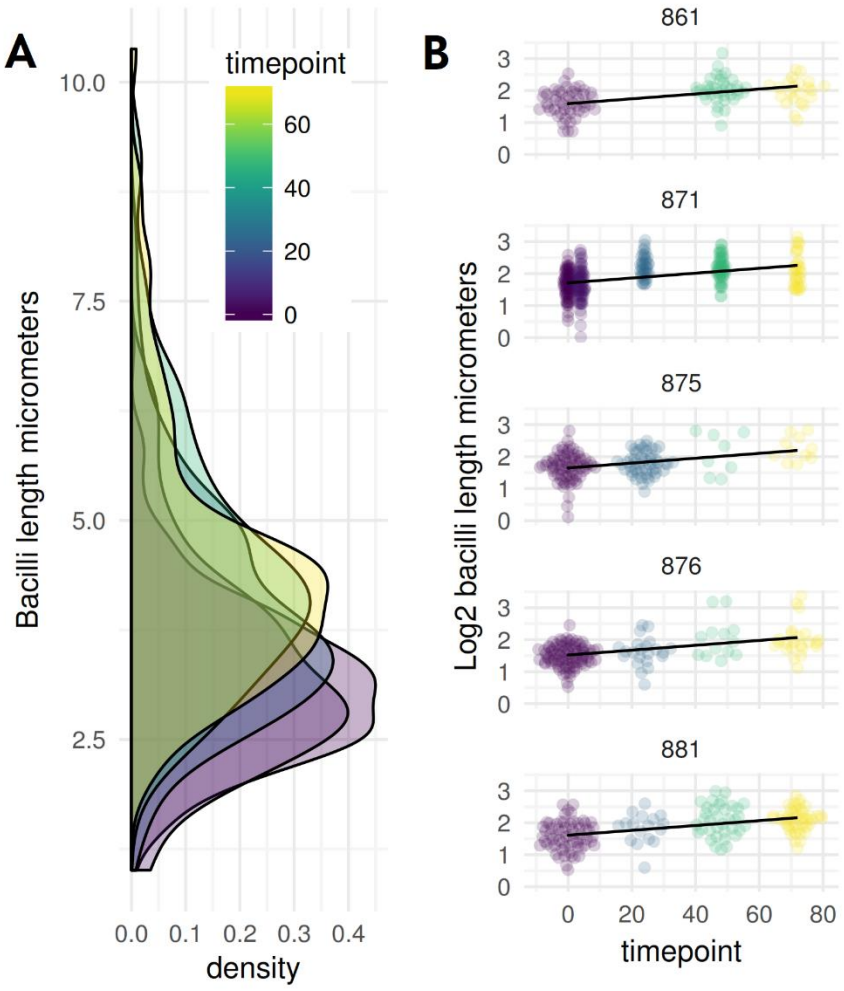

Figure 5-33. Bacilli length on DMN-tre microscopy by sample timepoint

Stored microscopy images from five patients with high bacilli burden in blood were processed in FIJI/Image-J software. Bacilli length was measured manually along the longest axis using a segmented line. 850 bacilli were measured. The distribution of bacilli length shifts so that more bacilli from later timepoint samples were >4µm long (**A**). A mixed-effects model with random intercept by patient suggested a significant fixed effect of time on mean log2 bacilli length (estimated fixed-effect of time shown with black line, **B**) – comparing model with bacilli length allowed to vary by timepoint to a null model containing only random intercept by patient gives $p < 2.2e\text{-}16$ for the effect of time of bacilli length.

5.5 Discussion

This chapter described the development of novel methods for identifying and quantifying blood bacilli, and provides evidence that these methods may provide a basis for a pharmacodynamic biomarker of treatment response in MTBBSI. Bacilli burden and rate of sterilisation of blood varied between patients, and there was evidence that summary measures of bacillaemia during the first 72-hours of anti-tuberculosis treatment (ATT) correlated with important clinical variables and mortality outcomes. The patient sample size was small and the significance tests relating the presented MTBBSI PD summary measures to outcome are borderline – none would remain significant at alpha <0.05 if corrected for multiple comparison, for example. Nevertheless, taken together, the results support the idea that blood bacilli load measured with these methods is likely to be causally related to outcome, and therefore a promising pharmacodynamic biomarker. Development of these methods could facilitate future interventional trials.

Although the analysis was not designed to validate DMN-tre microscopy and optimised blood Xpert-ultra as diagnostics, both performed well against blood culture (both 95% sensitive for diagnosing culture positive MTBBSI in a given patient, and significantly outperforming MFL blood culture on a paired sample basis across patient-timepoints). The fact that most samples were taken after start of ATT may have underestimated blood culture sensitivity – carry over of antimicrobial bound to cellular receptors is possible despite the processing of blood to remove free antimicrobial. This is suggested by the marked drop in MFL positivity even by the 4-hour time point. However, in counterpoise, it should also be noted that, at each patient-timepoint, approximately double the volume of blood was allocated to MFL culture (2 x 5ml) as to Xpert-ultra (1 x 5ml) or DMN-microscopy (1 x 3ml), which would have acted to overestimate relative MFL culture sensitivity. The blood Xpert-ultra method is particularly feasible as a diagnostic test in low resource settings which already have access to Xpert testing facilities. Additional processing time compared to sputum is less than 2 hours, with

negligible consumable costs. Blood is more easily and rapidly obtained than other patient samples for unwell patients in secondary care settings. Hypothetically, a blood-based diagnostic could shorten time to diagnosis even more than urine-based diagnostics. In the current analysis, blood Xpert-ultra had low specificity (0.20) compared to a composite gold-standard. This was because 4 patients had MTBBSI detected by Xpert-ultra who were culture and DMN-tre microscopy negative on all samples (patients 864, 874, 880, & 882 in figure 18). All these 4 patients were urine-LAM and urine-Xpert-ultra positive for *M. tuberculosis*, so I would argue they were true positive blood-Xpert results for disseminated tuberculosis. The overall diagnostic utility of blood Xpert-ultra using the method developed in this thesis is currently being tested on stored whole blood from the full KDHTB cohort.

In the current form, DMN-tre microscopy of blood is too labour intensive to be a practical diagnostic – requiring extensive (and relatively expensive) processing of blood. The technique is, however, a substantive innovation for understanding MTBBSI. The results presented in this chapter expand the estimates of bacilli burden in MTBBSI and show for the first time that some patients harbour sustained bacteraemia with 10^5 bacilli per ml. This adds further credence to the idea that bacterial burden is likely to be mechanistically related to disease phenotype and outcome in severe HIV-associated TB. DMN-tre microscopy count on blood showed a different distribution to MFL TTD, correlated more closely with a range of clinical markers of disease severity, and was significantly associated with mortality. Bacteraemias in the range 10^5 cells/ml have not been described for most pathogens,[568-573] but are seen in MAC disease.[574]

DMN-tre microscopy also allowed characterisation of bacilli morphology in blood. *In vitro*, mycobacteria length is relatively heterogeneous in log phase, and on average shorter and more homogeneous in stationary phase.[492] V-forms likely represent active growth and 'snapping division'.[492] Eum *et al*. measured TB bacilli length in cavity caseum, sputum, and bronco-alveolar lavage (BAL) fluid, finding bacilli were shortest in the former (mean 1.9, range 0.5 to 9μm) and longest in the later (mean 3.6, range 0.5 to 9μm).[567] They concluded that this showed intra-cavity bacilli were in stationary phase, while BAL/sputum bacilli were in log growth. The data presented here are the first measurement of bacilli length from blood (i.e. bacilli not destined to be expectorated),

and to my knowledge the first serial measure of bacilli length at different timepoints into ATT. The morphological features were in keeping with unrestricted, log-growth of bacilli. The shift to longer bacilli morphology with exposure to antibiotics is in keeping with a phenotypic response to ATT mediated through changes in the cell-cycle. This in turn echoes the flow cytometry data on cell length from *in vitro* time-kill curves presented in chapter 4. There are, however, limitations to this analysis. Only five patients had enough bacilli imaged to allow distribution of cell sizes to be estimated at each timepoint, and the number of bacilli measured was uneven with fewer bacilli recorded at later timepoints. It is not always clear if an image shows one long bacilli or two short bacilli end-to-end. Finally, although the 18-hour incubation period with DMN-tre dye is less than a generation time for mycobacteria, some growth presumably has occurred *ex vivo* in these conditions. Despite this, the results show that MTBBSI provides an important window on bacilli phenotypes beyond the airway compartment, and supports further investigation of cell-cycle dynamics in relation to drug tolerance.[504]

The blood microscopy technique requires complete lysis of human blood cells during processing. This unfortunately means the cellular location of bacilli was not visualised. However, detection of *M. tuberculosis* by Xpert-ultra was not significantly higher in granulocyte enriched buffy coat preparations compared to red cell pellets – a result not in keeping with most bacilli being intracellular. Indeed, the colocalization with red cells is surprising and doesn't seem to occur in spiked samples (data not shown here). Despite substantial evidence that *M. tuberculosis* routinely accesses the blood stream to infect distal sites (discussed in chapter 1), little is known about how this occurs.[103] Cellular location of bacilli has implications for understanding the immune response in MTBBSI, not least in whole-blood host transcriptome analysis.[575] Development of the DMN-tre blood microscopy method to preserve white blood cell integrity would be worthwhile.

In conclusion, this chapter has demonstrated novel or optimised methods for identifying MTBBSI. These methods can be used to give unprecedented characterisation of MTBBSI and are promising biomarkers of treatment response.

6 Conclusion

6.1 Main findings & call for interventional trials in MTBBSI

Interventions with enhanced anti-tuberculosis bactericidal activity should be tested in patients with severe HIV-associated TB, and, specifically in patients with *M. tuberculosis* blood stream infection (MTBBSI). That is the central message of this thesis, combining several lines of evidence.

The extent and magnitude of *M. tuberculosis* blood stream dissemination can explain a substantial proportion of variance in major clinical variables and risk of death. In chapter 1, data from the KDHTB cohort study was analysed with respect to MTBBSI. This cohort study is the most detailed description of severe HIV-associated tuberculosis carried out to date. It was argued that TB blood culture, urine-LAM and urine-Xpert results – which strongly covary – all report on blood stream dissemination, and can be combined to deal with measurement error in all three tests. Aggregated results of these three tests – a "disseminated TB score" – was strongly related to all reduced-dimension representations of clinical variables, and to mortality, placing extent and magnitude of blood stream infection at the centre of structural models relating clinical phenotype to mortality in severe HIV-associated tuberculosis.

This finding is supported by other work in the thesis. On systematic review of all previous studies performing unselected TB blood cultures in people living with HIV (IPD meta-analysis in chapter 3), positive TB blood culture had double the hazard ratio for death compared to blood culture negative HIV-TB patients, after adjustment for major confounders like CD4 count.

In addition, the smaller sub-study presented in chapter 5 of novel methods for quantifying MTBBSI showed that several measures of bacilli burden exposure were associated with death, demonstrating a 'dose-response' relationship even in this stratum

of patients with most severe disease. In addition, this study gives direct evidence that the dynamics of bacterial load during initial antimicrobial treatment is a determinant of outcome.

Each of these lines of evidence has limitations. Substantial variance in clinical observations and mortality is unexplained by disseminated TB score or MTBBSI; this could be due to noise (i.e. measurement error) or to differences in host response at a given bacterial load. The IPD meta-analysis successfully reduced apparent heterogeneity between studies, but substantial unexplained differences in MTBBSI-associated risk of death remained between studies. This is likely related to the marked differences in inclusion criteria and study populations across settings, and the included studies may not accurately reflect non-study hospital populations as a whole. The major weakness of the chapter 5 sub-study is that it is underpowered, particularly because multiple comparisons could not be adjusted for with the small sample size.

Nonetheless, such a systematic and accurate measurement of systemic bacilli burden in tuberculosis has not previously been reported, and taken together, these results substantiate the long-held belief that bacilli numbers are a major axis of variation underlying tuberculosis pathophysiology.[45-47] Just as latent tuberculosis is not a homogenous category, but probably a spectrum characterised by bacterial load,[576,577] so too is severe HIV-associated disease at the other end of the tuberculosis gamut, where blood stream dissemination is the mode of infection. If bacilli burden and MTBBSI drives pathophysiology, more rapid clearance of MTB from blood is a rational interventional target.

One objection to the above reasoning could be that MTBBSI is too rare an event to be the mode of infection in HIV-associated tuberculosis. In chapter 2 it was shown that a single TB blood culture under-estimates the point prevalence of blood culture positive disease by around one-third compared to multiple blood cultures. Since almost all studies have relied on a single blood culture, the previous estimates of MTBBSI prevalence are flawed. In chapter 3, all available individual patient data from studies performing unselected TB blood cultures were reanalysed with model-based adjustment for this, and other technical factors such as timing of antimicrobials. This showed that TB was more commonly cultured than not from the bloodstream of critically unwell

(WHO danger-sign positive) inpatients with HIV-associated tuberculosis and a CD4 count less than 100 cells/mm^3.§§§§§§§§§ This hypothesised patient population probably encompasses a majority of patients who die in hospital of HIV-associated tuberculosis.[19,217] Notably, blood culture, the gold-standard diagnostic, may have poor sensitivity for MTBBSI. The *in vitro* work described in chapter 4 adds to the growing evidence that mycobacteria are often non-culturable under standard conditions yet are intact and metabolically active by other measures.[403,404,407] Although not designed to assess diagnostic performance, the sub-study described in chapter 5 suggests the novel blood-processing method combined with Xpert-ultra testing has greater sensitivity for detecting MTBBSI than culture. This may be because of antimicrobial carry-over in blood culture despite plasma removal or lysis/wash prior to inoculation, but is currently being investigated in the wider KDHTB cohort using stored whole blood samples.

As it stands, the evidence outlined suggests that bacillaemia has been under-ascertained due to simple technical reasons, and MTBBSI is highly prevalent in HIV-infected patients at highest risk of death. Patients with detectable TB in blood are a rational population in which to assess current and novel management strategies aimed at reducing persistently high inpatient HIV-associated mortality.

This can be illustrated with the issue of empirical TB therapy in patients with advanced HIV infection. Evidence from the IPD meta-analysis suggested that delay of empirical treatment in HIV-associated TB by four days or more (a cut-off chosen to reflect the WHO algorithm for seriously unwell patients with suspected TB and non-diagnostic initial tests) was associated with greater mortality after adjustment for disease severity. Importantly, this effect was evident only for patients with MTBBSI, with a significant interaction between treatment delay and positive blood culture. This was also seen in the STAMP trial, which established that availability of urine-based rapid diagnostics decreased time to TB diagnosis amongst HIV-infected inpatients, and this resulted in a 7-9% absolute mortality reduction in patients with CD4 count < 100/mm^3 or haemoglobin <8d/dL.[22] By contrast, the negative findings reported from trials of

§§§§§§§§§ Assumes two blood cultures are taken prior to start of antimicrobial therapy, and that the population in question has a uniform CD4 count distribution between 0 and 100.

presumptive TB therapy in people living with HIV[349-351] can be understood by the exclusion of patients most likely to have had MTBBSI.

As well as making a case for interventional trials focussed on MTBBSI, this thesis has developed tools to facilitate such studies. Presence of MTBBSI can be reliably predicted using the modelling approaches outlined and validated in chapter 2. DMN-trehalose microscopy of blood, and optimised blood processing methods combined with culture and Xpert-ultra testing, demonstrate potential as pharmacodynamic biomarkers which could maximise power.

6.2 Secondary findings & future directions

The ability of a novel flow cytometry to probe *in vitro* pharmacodynamics of mycobacteria was shown in chapter 4. The potential for high-throughput characterisation of phenotypic sub-populations would be a major advance if this method could be combined with DMN-trehalose staining in clinical samples. Differences in bacilli morphology (length and nucleic acid staining with SYBR-gold) were shown to define discrete sub-populations in an antimicrobial dependent manner in *in-vitro* cultures of *M. bovis* BCG. Distribution of bacilli length in blood samples appears to increase with antimicrobial exposure in clinical samples, as shown with manual measurement of DMN-trehalose microscopy images. As noted by leading molecular mycobacteriologists,[504] morphology phenotype has been related to cell-cycle dynamics, drug-tolerance, and propensity to develop drug-resistance in other bacteria, and could be an important mechanism of poor treatment response in tuberculosis. The ability to label, cell-sort, and investigate *ex vivo*, bacilli with different morphological phenotypes from clinical samples could support basic science investigations in this area. Further, cytometry-based time-kill curves could better characterise drug tolerance between clinical isolates *ex vivo*. While minimum inhibitory concentration of (wild-type) TB isolates to first-line drugs may not be variable enough to be a major determinant of outcome,[578] measures of bacteriocidal activity could be independent of bacteriostatic activity,[497] and remain to be investigated in detail. Such an approach would be possible using the flow method, if technical difficulties about standardising *in vitro* culture can be overcome.

The systematic phenotyping of patients using the 'disseminated TB score' facilitates a rational approach to characterising host-response. Previously, immunological investigations of advance HIV-associated tuberculosis have attempted to adjust for bacteriological variation by crude stratification, such as pulmonary versus extra-pulmonary disease. By contrast, systematic quantification of blood stream dissemination has better resolution of patients on a continuous scale, avoids ascertainment bias (diagnosis of extra-pulmonary disease in pulmonary TB patients is largely a function of how hard you look for extra-pulmonary disease), and other category errors (extra-pulmonary disease can be paucibacillary and localised, or multibacillary and disseminated; merging all makes little sense clinically). In a planned analysis of KDHTB whole blood RNA, transcriptome data will be related to burden of MTBBSI using the disseminated TB score.

Finally, it has been argued here that MTBBSI is the elephant in the room for severe HIV-associated TB, but that elephant is also increasingly spotted by researchers working on sepsis more generally. The finding that TB bacteraemia is the foremost microbiological diagnosis in patients with severe sepsis in cohorts[127,332] and RCTs[268,289] from high HIV-burden settings, has led to calls to include TB in the sepsis research agenda.[353] The analysis in this thesis supports the idea that MTBBSI is an informative model of sepsis. In support of recent developments in the understanding of sepsis pathophysiology,[247,248,251] blood lactate is more closely related to inflammation (and bacilli load) than markers of macro-haemodynamic compromise in MTBBSI. If elevated lactate is caused by upregulated aerobic glycolysis from tuberculosis-induced inflammation,[252,253] this finding could be corroborated by correlating 24-hour lactate production with extent of F-fluorodeoxyglucose uptake as measured by positron emission tomography (FDG-PET-CT) scanning in patients with HIV-associated TB and sepsis. Similarly, there is little evidence that the substantial proportion of MTBBSI patients with acute kidney injury (AKI) is the result of hypotension. Rather, a complex (and probably sub-acute) pathophysiology involving both depletion of extra-cellular fluid circulating volume from profound sodium and water depletion, and abnormalities of ADH regulation well established in tuberculosis, is suggested. The mortality-effect of highly-aggressive fluid resuscitation protocols in sepsis patients who predominantly have MTBBSI is understandable considering these findings.[268,289] A next step could be

to establish how much AKI is attributed to functional, adaptive host-responses, and how much is related to direct pathological 'hits' capable of decompensating this response. It would be surprising if filtering blood volumes per day corresponding to tens of millions of TB bacilli did not have direct pathological sequalae on the kidney. This could be investigated with urine and blood biomarkers reporting renal cytotoxicity and ischaemia in MTBBSI patients,[178] which could in turn be an important host-biomarker of treatment response in intervention trials.

6.3 Conclusion

In summary, MTBBSI is a common and specific form of HIV-associated tuberculosis seen in high-burden settings. It is patho-physiologically distinct from 'classic' pulmonary forms of tuberculosis and is responsible for disproportionate mortality. Despite this no interventional evidence-base exists for its management. The data and tools to remedy this neglect are now available.

7 References

1. UNAIDS. Global AIDS update 2016. Geneva, Switzerland: Joint United Nations Programme on HIV/AIDS, 2016.
2. Johnson LF, May MT, Dorrington RE, et al. Estimating the impact of antiretroviral treatment on adult mortality trends in South Africa: A mathematical modelling study. *PLoS Med* 2017; **14**(12): e1002468.
3. Wandeler G, Johnson LF, Egger M. Trends in life expectancy of HIV-positive adults on antiretroviral therapy across the globe: comparisons with general population. *Curr Opin HIV AIDS* 2016; **11**(5): 492-500.
4. Exchange TGHD. Global burden of Disease 2016. In: Evaluation IfHMa, editor. Seattle, WA.; 2017.
5. Carmona S, Bor J, Nattey C, et al. Persistent High Burden of Advanced HIV Disease Among Patients Seeking Care in South Africa's National HIV Program: Data From a Nationwide Laboratory Cohort. *Clin Infect Dis* 2018; **66**(suppl_2): S111-S7.
6. IeDea, Collaborations CC. Global Trends in CD4 Cell Count at the Start of Antiretroviral Therapy: Collaborative Study of Treatment Programs. *Clin Infect Dis* 2018; **66**(6): 893-903.
7. Osler M, Hilderbrand K, Goemaere E, et al. The Continuing Burden of Advanced HIV Disease Over 10 Years of Increasing Antiretroviral Therapy Coverage in South Africa. *Clin Infect Dis* 2018; **66**(suppl_2): S118-S25.
8. Ousley J, Niyibizi AA, Wanjala S, et al. High Proportions of Patients With Advanced HIV Are Antiretroviral Therapy Experienced: Hospitalization Outcomes From 2 Sub-Saharan African Sites. *Clin Infect Dis* 2018; **66**(suppl_2): S126-S31.
9. Siika A, McCabe L, Bwakura-Dangarembizi M, et al. Late Presentation With HIV in Africa: Phenotypes, Risk, and Risk Stratification in the REALITY Trial. *Clin Infect Dis* 2018; **66**(suppl_2): S140-S6.
10. Ford N, Shubber Z, Meintjes G, et al. Causes of hospital admission among people living with HIV worldwide: a systematic review and meta-analysis. *The Lancet HIV* 2015; **2**(10): e438-e44.
11. Meintjes G, Kerkhoff AD, Burton R, et al. HIV-Related Medical Admissions to a South African District Hospital Remain Frequent Despite Effective Antiretroviral Therapy Scale-Up. *Medicine (Baltimore)* 2015; **94**(50): e2269.
12. Ford N, Matteelli A, Shubber Z, et al. TB as a cause of hospitalization and in-hospital mortality among people living with HIV worldwide: a systematic review and meta-analysis. *J Int AIDS Soc* 2016; **19**(1): 20714.
13. Gupta RK, Lucas SB, Fielding KL, Lawn SD. Prevalence of tuberculosis in post-mortem studies of HIV-infected adults and children in resource-limited settings: a systematic review and meta-analysis. *AIDS* 2015; **29**(15): 1987-2002.
14. Bigna JJ, Noubiap JJ, Agbor AA, et al. Early Mortality during Initial Treatment of Tuberculosis in Patients Co-Infected with HIV at the Yaounde Central Hospital,

Cameroon: An 8-Year Retrospective Cohort Study (2006-2013). *PLoS One* 2015; **10**(7): e0132394.
15. Feasey NA, Banada PP, Howson W, et al. Evaluation of Xpert MTB/RIF for detection of tuberculosis from blood samples of HIV-infected adults confirms Mycobacterium tuberculosis bacteremia as an indicator of poor prognosis. *J Clin Microbiol* 2013; **51**(7): 2311-6.
16. Kerkhoff AD, Lawn SD, Schutz C, et al. Anemia, Blood Transfusion Requirements and Mortality Risk in Human Immunodeficiency Virus-Infected Adults Requiring Acute Medical Admission to Hospital in South Africa. *Open Forum Infect Dis* 2015; **2**(4): ofv173.
17. Pecego AC, Amancio RT, Ribeiro C, et al. Six-month survival of critically ill patients with HIV-related disease and tuberculosis: a retrospective study. *BMC Infect Dis* 2016; **16**: 270.
18. Subbarao S, Wilkinson KA, Van Halsema CL, et al. Raised venous lactate and markers of intestinal translocation are associated with mortality amongst in-patients with HIV-associated TB in rural South Africa. *J Acquir Immune Defic Syndr* 2015.
19. Sileshi B, Deyessa N, Girma B, Melese M, Suarez P. Predictors of mortality among TB-HIV Co-infected patients being treated for tuberculosis in Northwest Ethiopia: a retrospective cohort study. *BMC Infect Dis* 2013; **13**: 297.
20. Getahun H, Kittikraisak W, Heilig CM, et al. Development of a standardized screening rule for tuberculosis in people living with HIV in resource-constrained settings: individual participant data meta-analysis of observational studies. *PLoS Med* 2011; **8**(1): e1000391.
21. Griesel R, Stewart A, van der Plas H, et al. Optimizing Tuberculosis Diagnosis in HIV-Infected Inpatients Meeting the Criteria of Seriously Ill in the WHO Algorithm. *Clin Infect Dis* 2017.
22. Gupta-Wright AC, E.L.; van Oosterhout,J.J.;Wilson,D.; Grint, D.; Alufandiki,M.; Peters, J.A; Chiume,L.; Lawn,S.D.;Fielding,K. Rapid urine-based screening for TB to reduce AIDS-realted mortality in hospitalized patients in Africa (STAMP) trial. 25th CROI. Bostin, Massachusettes: CROI; 2018.
23. Keiper MD, Beumont M, Elshami A, Langlotz CP, Miller WT, Jr. CD4 T lymphocyte count and the radiographic presentation of pulmonary tuberculosis. A study of the relationship between these factors in patients with human immunodeficiency virus infection. *Chest* 1995; **107**(1): 74-80.
24. Lawn SD, Kerkhoff AD, Burton R, et al. Rapid microbiological screening for tuberculosis in HIV-positive patients on the first day of acute hospital admission by systematic testing of urine samples using Xpert MTB/RIF: a prospective cohort in South Africa. *BMC Med* 2015; **13**: 192.
25. Lawn SD, Kerkhoff AD, Vogt M, Wood R. HIV-associated tuberculosis: relationship between disease severity and the sensitivity of new sputum-based and urine-based diagnostic assays. *BMC Med* 2013; **11**: 231.
26. Connolly C, Davies GR, Wilkinson D. Impact of the human immunodeficiency virus epidemic on mortality among adults with tuberculosis in rural South Africa, 1991-1995. *Int J Tuberc Lung Dis* 1998; **2**(11): 919-25.
27. Hargreaves NJ, Kadzakumanja O, Whitty CJ, Salaniponi FM, Harries AD, Squire SB. 'Smear-negative' pulmonary tuberculosis in a DOTS programme: poor outcomes in an area of high HIV seroprevalence. *Int J Tuberc Lung Dis* 2001; **5**(9): 847-54.

28. Harries AD, Nyangulu DS, Kang'ombe C, et al. Treatment outcome of an unselected cohort of tuberculosis patients in relation to human immunodeficiency virus serostatus in Zomba Hospital, Malawi. *Trans R Soc Trop Med Hyg* 1998; **92**(3): 343-7.
29. Kang'ombe C, Harries AD, Banda H, et al. High mortality rates in tuberculosis patients in Zomba Hospital, Malawi, during 32 months of follow-up. *Trans R Soc Trop Med Hyg* 2000; **94**(3): 305-9.
30. Elliott AM, Halwiindi B, Hayes RJ, et al. The impact of human immunodeficiency virus on presentation and diagnosis of tuberculosis in a cohort study in Zambia. *J Trop Med Hyg* 1993; **96**(1): 1-11.
31. Gupta RK, Lawn SD, Bekker LG, Caldwell J, Kaplan R, Wood R. Impact of human immunodeficiency virus and CD4 count on tuberculosis diagnosis: analysis of city-wide data from Cape Town, South Africa. *Int J Tuberc Lung Dis* 2013; **17**(8): 1014-22.
32. Organization WH. Guidelines for treatment of drug-susceptible tuberculosis and patient care, 2017 update. Geneva: WHO, 2017.
33. Khan FA, Minion J, Pai M, et al. Treatment of active tuberculosis in HIV-coinfected patients: a systematic review and meta-analysis. *Clin Infect Dis* 2010; **50**(9): 1288-99.
34. Barnett T, Whiteside A. AIDS in the Twenty-First Century: Disease and Globalization: Palgrave Macmillan UK; 2002.
35. Burkey MD, Weiser SD, Fehmie D, et al. Socioeconomic determinants of mortality in HIV: evidence from a clinical cohort in Uganda. *J Acquir Immune Defic Syndr* 2014; **66**(1): 41-7.
36. Kabudula CW, Houle B, Collinson MA, et al. Socioeconomic differences in mortality in the antiretroviral therapy era in Agincourt, rural South Africa, 2001-13: a population surveillance analysis. *Lancet Glob Health* 2017; **5**(9): e924-e35.
37. Probst C, Parry CD, Rehm J. Socio-economic differences in HIV/AIDS mortality in South Africa. *Trop Med Int Health* 2016; **21**(7): 846-55.
38. de Waal A. AIDS and Power: Why There Is No Political Crisis Yet: Zed Books; 2013.
39. Ansari NA, Kombe AH, Kenyon TA, et al. Pathology and causes of death in a group of 128 predominantly HIV-positive patients in Botswana, 1997-1998. *Int J Tuberc Lung Dis* 2002; **6**(1): 55-63.
40. Rana FS, Hawken MP, Mwachari C, et al. Autopsy study of HIV-1-positive and HIV-1-negative adult medical patients in Nairobi, Kenya. *J Acquir Immune Defic Syndr* 2000; **24**(1): 23-9.
41. Wong EB, Omar T, Setlhako GJ, et al. Causes of death on antiretroviral therapy: a post-mortem study from South Africa. *PLoS One* 2012; **7**(10): e47542.
42. Cohen T, Murray M, Wallengren K, Alvarez GG, Samuel EY, Wilson D. The prevalence and drug sensitivity of tuberculosis among patients dying in hospital in KwaZulu-Natal, South Africa: a postmortem study. *PLoS Med* 2010; **7**(6): e1000296.
43. Hudson CP, Maartens G, Wood R, et al. Unrecognised mycobacterium tuberculosis (multiple letters). *Lancet* 2000; **355**(9198): 141-3.
44. Esmail H, Lai RP, Lesosky M, et al. Characterization of progressive HIV-associated tuberculosis using 2-deoxy-2-[(18)F]fluoro-D-glucose positron emission and computed tomography. *Nat Med* 2016; **22**(10): 1090-3.
45. Kayne GGP, W.; O'Shaghnessey, L. . Pulmonary Tuberculosis: Pathology, diagnosis, managemnet and prevention. Oxford: Oxford University Press; 1939.

46. Krause AK. The spread of tuberculous infection in the body. *Amer Rev Tuberculosis* 1924; **9**: 83–96.
47. Koch R, Carter KC. Essays of Robert Koch: Greenwood Publishing Group, Incorporated; 1987.
48. WHO. Consolidated guidelines on the use of antiretroviral drugs for treating and preventing HIV infection: recommendations for a public health approach. Geneva: World Health Organisation, 2016.
49. (SDI&GIS) SDIaGD. City of Cape Town 2011 Census - Khayelitsha Health District., 2013.
50. Health. NDo. The 2012 National Antenatal Sentinel HIV & Herpes Simplex Type-2 Prevalence Survey in South Africa Pretoria, South Africa: National Department of Health.; 2014.
51. Cox HS, Daniels JF, Muller O, et al. Impact of Decentralized Care and the Xpert MTB/RIF Test on Rifampicin-Resistant Tuberculosis Treatment Initiation in Khayelitsha, South Africa. *Open Forum Infect Dis* 2015; **2**(1): ofv014.
52. Organisation WH. International Statistical Classification of Diseases and Related Health Problems 10th Revision. 2016 2016. http://apps.who.int/classifications/icd10/browse/2016/en (accessed 10/04/2018 2018).
53. WHO. Improving the diagnosis and treatmnet of smear-negative pulmonary and extrapulmonary tuberculosis among adults and adolescents. Recommendations for HIV-prevalent and resource-constrained settings. Geneva: World Health Organisation, 2006.
54. Archibald LK, McDonald LC, Nwanyanwu O, et al. A hospital-based prevalence survey of bloodstream infections in febrile patients in Malawi: implications for diagnosis and therapy. *J Infect Dis* 2000; **181**(4): 1414-20.
55. Archibald LK, McDonald LC, Rheanpumikankit S, et al. Fever and human immunodeficiency virus infection as sentinels for emerging mycobacterial and fungal bloodstream infections in hospitalized patients >/=15 years old, Bangkok. *J Infect Dis* 1999; **180**(1): 87-92.
56. Bell M, Archibald LK, Nwanyanwu O, et al. Seasonal variation in the etiology of bloodstream infections in a febrile inpatient population in a developing country. *Int J Infect Dis* 2001; **5**(2): 63-9.
57. Lewis DK, Peters RP, Schijffelen MJ, et al. Clinical indicators of mycobacteraemia in adults admitted to hospital in Blantyre, Malawi. *Int J Tuberc Lung Dis* 2002; **6**(12): 1067-74.
58. McDonald LC, Archibald LK, Rheanpumikankit S, et al. Unrecognised Mycobacterium tuberculosis bacteraemia among hospital inpatients in less developed countries. *Lancet* 1999; **354**(9185): 1159-63.
59. Crump JA, Ramadhani HO, Morrissey AB, et al. Bacteremic disseminated tuberculosis in sub-saharan Africa: a prospective cohort study. *Clin Infect Dis* 2012; **55**(2): 242-50.
60. Crump JA, Reller LB. Two decades of disseminated tuberculosis at a university medical center: the expanding role of mycobacterial blood culture. *Clin Infect Dis* 2003; **37**(8): 1037-43.
61. Mert A, Ozaras R. A terminological controversy: do disseminated and miliary tuberculosis mean the same? *Respiration* 2005; **72**(1): 113.

62. Hopewell PCK-M, M.; Ernst, J.D. Murray and Nadel's Textbook of Respiratory Medicine. In: Broaddus VCM, R.J.; Ersnt,J.D.; Gotaway, M.B., ed. Murray and Nadel's Textbook of Respiratory Medicine. 6th ed. Philadelphia: W.B. Saunders; 2016: 593-628.
63. Van Crevel RH, P.C. Tuberculosis. In: Cohen JP, W.G.; Opal, S.M., ed. Infectious Diseases. London: Elsevier; 2017: 271-84.
64. Auerbach O. Acute Generalized Miliary Tuberculosis. *Am J Pathol* 1944; **20**(1): 121-36.
65. Chapman CB, Whorton CM. Acute generalized miliary tuberculosis in adults. *N Engl J Med* 1946; **235**: 239-48.
66. Lewison MF, E.B.; Ragins,O.B. Correlation of clinical diagnosis and pathological diagnosis with special reference to tuberculosis: analysis of autopsy findings in 893 cases. *Am Rev Tuberc* 1931; **24**: 152-71.
67. O'Brien JR. Non-reactive tuberculosis. *J Clin Pathol* 1954; **7**(3): 216-25.
68. Ball K, Joules H, Pagel W. Acute tuberculous septicaemia with leucopenia. *Br Med J* 1951; **2**(4736): 869-73.
69. Cameron SJ. Tuberculosis and the blood--a special relationship? *Tubercle* 1974; **55**(1): 55-72.
70. Patel MP. Acute tuberculous septicaemia. *Br Med J* 1963; **1**(5344): 1525-6.
71. Osler WM, T. The principles and practice of medicine. 9th ed. New York, London.: D. Appleton and company; 1920.
72. Nodstrom G. CHAPTER IV: The Yersin Type of Avian Tuberculosis in Rabbits. *Acta Medica Scandinavica* 1941; **109**(S124): 47-55.
73. Ahuja SS, Ahuja SK, Phelps KR, Thelmo W, Hill AR. Hemodynamic confirmation of septic shock in disseminated tuberculosis. *Crit Care Med* 1992; **20**(6): 901-3.
74. Arends A. Blood disease and the so-called generalized non-reactive tuberculosis; typhobacillosis of Landouzy, sepsis tuberculosa acutissima. *Acta Med Scand* 1950; **136**(6): 417-29.
75. Geiss HK, Feldhues R, Niemann S, Nolte O, Rieker R. Landouzy septicemia (sepsis tuberculosa acutissima) due to Mycobacterium microti in an immunocompetent man. *Infection* 2005; **33**(5-6): 393-6.
76. George S, Papa L, Sheils L, Magnussen CR. Septic shock due to disseminated tuberculosis. *Clin Infect Dis* 1996; **22**(1): 188-9.
77. Vaizey JM. Chronic Miliary Tuberculosis: (Section of Medicine). *Proc R Soc Med* 1937; **30**(10): 1208-10.
78. Hoyle CV, M. Chronic miliary tuberculosis. London: Oxford University Press; 1937.
79. Rogers WN. Chronic miliary tuberculosis. *Br J Tuberc Dis Chest* 1947; **41**(4): 79-84.
80. Pagel W. Chronic disseminated tuberculosis. *BMJ* 1937: 555-6.
81. Auerbach O. The natural history of the tuberculous pulmonary lesion. *Med Clin North Am* 1959; **43**(1): 239-51.
82. Slavin RE, Walsh TJ, Pollack AD. Late generalized tuberculosis: a clinical pathologic analysis and comparison of 100 cases in the preantibiotic and antibiotic eras. *Medicine (Baltimore)* 1980; **59**(5): 352-66.
83. Jacques J, Sloan JM. The changing pattern of miliary tuberculosis. *Thorax* 1970; **25**(2): 237-40.
84. Proudfoot AT, Akhtar AJ, Douglas AC, Horne NW. Miliary tuberculosis in adults. *Br Med J* 1969; **2**(5652): 273-6.

85. Sahn SA, Neff TA. Miliary tuberculosis. *Am J Med* 1974; **56**(4): 494-505.
86. Bottiger LE, Nordenstam HH, Wester PO. Disseminated tuberculosis as a cause of fever of obscure origin. *Lancet* 1962; **1**(7219): 19-20.
87. Saldanha PS, J. Eponyms in Tuberculosis. *Arch Med Health Sci* 2016; **4**: 287-9.
88. May O. The Relation between Trauma and Tuberculosis: From the Point of View of Accident, Insurance. *Br Med J* 1928; **2**(3545): 1090-1.
89. Anyanwu CH, Nassau E, Yacoub M. Miliary tuberculosis following homograft valve replacement. *Thorax* 1976; **31**(1): 101-6.
90. Montes Ruiz-Cabello M, Guirao Arrabal E, Aisa Denaroso LM. Simultaneous Miliary and Genital Tuberculosis. *Arch Bronconeumol* 2017; **53**(7): 397.
91. Morano Amado LE, Amador Barciela L, Rodriguez Fernandez A, Martinez-Sapina Llamas I, Vazquez Alvarez O, Fernandez Martin J. Extracorporeal shock wave lithotripsy complicated with miliary tuberculosis. *J Urol* 1993; **149**(6): 1532-4.
92. Salem B. Disseminated tuberculosis following the placement of ureteral stents: a case repot. *Cases J* 2008; **1**(1): 383.
93. Yekanath H, Gross PA, Vitenson JH. Miliary tuberculosis following ureteral catheterization. *Urology* 1980; **16**(2): 197-8.
94. Behr MA, Waters WR. Is tuberculosis a lymphatic disease with a pulmonary portal? *Lancet Infect Dis* 2014; **14**(3): 250-5.
95. Key to Current Medical Literature. *Br Med J* 1938; **2**(4048): E41-8.
96. Gupta UD, Katoch VM. Animal models of tuberculosis. *Tuberculosis (Edinb)* 2005; **85**(5-6): 277-93.
97. Smith DW, Balasubramanian V, Wiegeshaus E. A guinea pig model of experimental airborne tuberculosis for evaluation of the response to chemotherapy: the effect on bacilli in the initial phase of treatment. *Tubercle* 1991; **72**(3): 223-31.
98. Willis HS. Studies on tuberculosis infection. *Amer Rev Tuberc* 1925; **11**: 427-39.
99. Calmette AH-S, G.; Soper,W.B. Tubercle Bacillus Infection and Tuberculosis in Man and Animals, Processes of Infection and Resistance. Philadelphia: Williams & Wilkins company; 1923.
100. Wilkinson MC. Pathogenesis of Non-pulmonary Tuberculosis. *Br Med J* 1940; **2**(4167): 660-1.
101. Barr DA, Whittington AM, White B, Patterson B, Davidson RN. Extra-pulmonary tuberculosis developing at sites of previous trauma. *J Infect* 2013; **66**(4): 313-9.
102. Stead WW, Bates JH. Evidence of a "silent" bacillemia in primary tuberculosis. *Ann Intern Med* 1971; **74**(4): 559-61.
103. Laal S. How does Mycobacterium tuberculosis establish infection? *J Infect Dis* 2012; **206**(8): 1157-9.
104. Barrios-Payan J, Saqui-Salces M, Jeyanathan M, et al. Extrapulmonary locations of mycobacterium tuberculosis DNA during latent infection. *J Infect Dis* 2012; **206**(8): 1194-205.
105. Lieberman TD, Wilson D, Misra R, et al. Genomic diversity in autopsy samples reveals within-host dissemination of HIV-associated Mycobacterium tuberculosis. *Nat Med* 2016; **22**(12): 1470-4.
106. Pagel W. Pulmonary tuberculosis. London: Oxford University Press; 1964.
107. Pagel W. An outline of the principal forms of tuberculosis in man; primary, disseminated and bronchogenic tuberculosis. *Postgrad Med J* 1952; **28**(326): 606.

108. Barber TW, Craven DE, McCabe WR. Bacteremia due to Mycobacterium tuberculosis in patients with human immunodeficiency virus infection. A report of 9 cases and a review of the literature. *Medicine (Baltimore)* 1990; **69**(6): 375-83.
109. Barnes PF, Arevalo C. Six cases of Mycobacterium tuberculosis bacteremia. *J Infect Dis* 1987; **156**(2): 377-9.
110. Bouza E, Martin-Scapa C, Bernaldo de Quiros JC, et al. High prevalence of tuberculosis in AIDS patients in Spain. *Eur J Clin Microbiol Infect Dis* 1988; **7**(6): 785-8.
111. Brisson-Noel A, Gicquel B, Lecossier D, Levy-Frebault V, Nassif X, Hance AJ. Rapid diagnosis of tuberculosis by amplification of mycobacterial DNA in clinical samples. *Lancet* 1989; **2**(8671): 1069-71.
112. Damsker B, Bottone EJ. Mycobacteria and cryptococci cultured from the buffy coat of AIDS patients prior to symptomatology: a rationale for early therapy. *AIDS Res* 1986; **2**(4): 343-8.
113. Eng RH, Bishburg E, Smith SM, Mangia A. Diagnosis of Mycobacterium bacteremia in patients with acquired immunodeficiency syndrome by direct examination of blood films. *J Clin Microbiol* 1989; **27**(4): 768-9.
114. Handwerger S, Mildvan D, Senie R, McKinley FW. Tuberculosis and the acquired immunodeficiency syndrome at a New York City hospital: 1978-1985. *Chest* 1987; **91**(2): 176-80.
115. Prego V, Glatt AE, Roy V, Thelmo W, Dincsoy H, Raufman JP. Comparative yield of blood culture for fungi and mycobacteria, liver biopsy, and bone marrow biopsy in the diagnosis of fever of undetermined origin in human immunodeficiency virus-infected patients. *Arch Intern Med* 1990; **150**(2): 333-6.
116. Saltzman BR, Motyl MR, Friedland GH, McKitrick JC, Klein RS. Mycobacterium tuberculosis bacteremia in the acquired immunodeficiency syndrome. *JAMA* 1986; **256**(3): 390-1.
117. Shafer RW, Goldberg R, Sierra M, Glatt AE. Frequency of Mycobacterium tuberculosis bacteremia in patients with tuberculosis in an area endemic for AIDS. *Am Rev Respir Dis* 1989; **140**(6): 1611-3.
118. Witebsky FG, Keiser JF, Conville PS, et al. Comparison of BACTEC 13A medium and Du Pont isolator for detection of mycobacteremia. *J Clin Microbiol* 1988; **26**(8): 1501-5.
119. Archibald LK, den Dulk MO, Pallangyo KJ, Reller LB. Fatal Mycobacterium tuberculosis bloodstream infections in febrile hospitalized adults in Dar es Salaam, Tanzania. *Clin Infect Dis* 1998; **26**(2): 290-6.
120. Gilks CF, Brindle RJ, Mwachari C, et al. Disseminated Mycobacterium avium infection among HIV-infected patients in Kenya. *J Acquir Immune Defic Syndr Hum Retrovirol* 1995; **8**(2): 195-8.
121. Gilks CF, Brindle RJ, Otieno LS, et al. Extrapulmonary and disseminated tuberculosis in HIV-1-seropositive patients presenting to the acute medical services in Nairobi. *AIDS* 1990; **4**(10): 981-5.
122. Richter C, Kox LF, Van Leeuwen JV, Mtoni I, Kolk AH. PCR detection of mycobacteraemia in tanzanian patients with extrapulmonary tuberculosis. *Eur J Clin Microbiol Infect Dis* 1996; **15**(10): 813-7.
123. Ssali FN, Kamya MR, Wabwire-Mangen F, et al. A prospective study of community-acquired bloodstream infections among febrile adults admitted to Mulago Hospital in Kampala, Uganda. *J Acquir Immune Defic Syndr Hum Retrovirol* 1998; **19**(5): 484-9.

124. Muchemwa L, Shabir L, Andrews B, Bwalya M. High prevalence of Mycobacterium tuberculosis bacteraemia among a cohort of HIV-infected patients with severe sepsis in Lusaka, Zambia. *Int J STD AIDS* 2017; **28**(6): 584-93.
125. Nakiyingi L, Ssengooba W, Nakanjako D, et al. Predictors and outcomes of mycobacteremia among HIV-infected smear- negative presumptive tuberculosis patients in Uganda. *BMC Infect Dis* 2015; **15**: 62.
126. Crump JA, Wu X, Kendall MA, et al. Predictors and outcomes of Mycobacterium tuberculosis bacteremia among patients with HIV and tuberculosis co-infection enrolled in the ACTG A5221 STRIDE study. *BMC Infect Dis* 2015; **15**(1): 12.
127. Jacob ST, Pavlinac PB, Nakiyingi L, et al. Mycobacterium tuberculosis bacteremia in a cohort of hiv-infected patients hospitalized with severe sepsis in uganda-high frequency, low clinical suspicion [corrected] and derivation of a clinical prediction score. *PLoS One* 2013; **8**(8): e70305.
128. Varma JK, McCarthy KD, Tasaneeyapan T, et al. Bloodstream infections among HIV-infected outpatients, Southeast Asia. *Emerg Infect Dis* 2010; **16**(10): 1569-75.
129. von Gottberg A, Sacks L, Machala S, Blumberg L. Utility of blood cultures and incidence of mycobacteremia in patients with suspected tuberculosis in a South African infectious disease referral hospital. *Int J Tuberc Lung Dis* 2001; **5**(1): 80-6.
130. Chipman J, Braun D. Simpson's paradox in the integrated discrimination improvement. *Stat Med* 2017; **36**(28): 4468-81.
131. Arah OA. The role of causal reasoning in understanding Simpson's paradox, Lord's paradox, and the suppression effect: covariate selection in the analysis of observational studies. *Emerg Themes Epidemiol* 2008; **5**: 5.
132. Hofler M, Venz J, Trautmann S, Miller R. Writing a discussion section: how to integrate substantive and statistical expertise. *BMC Med Res Methodol* 2018; **18**(1): 34.
133. Norman G. Research in clinical reasoning: past history and current trends. *Med Educ* 2005; **39**(4): 418-27.
134. Weiss G, Goodnough LT. Anemia of chronic disease. *N Engl J Med* 2005; **352**(10): 1011-23.
135. Drakesmith H, Prentice AM. Hepcidin and the iron-infection axis. *Science* 2012; **338**(6108): 768-72.
136. Kerkhoff AD, Meintjes G, Opie J, et al. Anaemia in patients with HIV-associated TB: relative contributions of anaemia of chronic disease and iron deficiency. *Int J Tuberc Lung Dis* 2016; **20**(2): 193-201.
137. Wisaksana R, de Mast Q, Alisjahbana B, et al. Inverse relationship of serum hepcidin levels with CD4 cell counts in HIV-infected patients selected from an Indonesian prospective cohort study. *PLoS One* 2013; **8**(11): e79904.
138. Lee SW, Kang YA, Yoon YS, et al. The prevalence and evolution of anemia associated with tuberculosis. *J Korean Med Sci* 2006; **21**(6): 1028-32.
139. Minchella PA, Donkor S, Owolabi O, Sutherland JS, McDermid JM. Complex anemia in tuberculosis: the need to consider causes and timing when designing interventions. *Clin Infect Dis* 2015; **60**(5): 764-72.
140. Kerkhoff AD, Meintjes G, Burton R, Vogt M, Wood R, Lawn SD. Relationship Between Blood Concentrations of Hepcidin and Anemia Severity, Mycobacterial Burden, and Mortality Among Patients With HIV-Associated Tuberculosis. *J Infect Dis* 2016; **213**(1): 61-70.

141. Janssen S, Schutz C, Ward AM, et al. Hemostatic Changes Associated With Increased Mortality Rates in Hospitalized Patients With HIV-Associated Tuberculosis: A Prospective Cohort Study. *J Infect Dis* 2017; **215**(2): 247-58.
142. Janssen S, Schutz C, Ward A, et al. Mortality in Severe Human Immunodeficiency Virus-Tuberculosis Associates With Innate Immune Activation and Dysfunction of Monocytes. *Clin Infect Dis* 2017; **65**(1): 73-82.
143. Brakenhoff TB, Mitroiu M, Keogh RH, Moons KGM, Groenwold RHH, van Smeden M. Measurement error is often neglected in medical literature: a systematic review. *J Clin Epidemiol* 2018.
144. Shah M, Variava E, Holmes CB, et al. Diagnostic accuracy of a urine lipoarabinomannan test for tuberculosis in hospitalized patients in a High HIV prevalence setting. *J Acquir Immune Defic Syndr* 2009; **52**(2): 145-51.
145. Gupta-Wright A, Peters JA, Flach C, Lawn SD. Detection of lipoarabinomannan (LAM) in urine is an independent predictor of mortality risk in patients receiving treatment for HIV-associated tuberculosis in sub-Saharan Africa: a systematic review and meta-analysis. *BMC Med* 2016; **14**: 53.
146. Tessema TA, Bjune G, Hamasur B, Svenson S, Syre H, Bjorvatn B. Circulating antibodies to lipoarabinomannan in relation to sputum microscopy, clinical features and urinary anti-lipoarabinomannan detection in pulmonary tuberculosis. *Scand J Infect Dis* 2002; **34**(2): 97-103.
147. Sakamuri RM, Price DN, Lee M, et al. Association of lipoarabinomannan with high density lipoprotein in blood: implications for diagnostics. *Tuberculosis (Edinb)* 2013; **93**(3): 301-7.
148. Wood R, Racow K, Bekker LG, et al. Lipoarabinomannan in urine during tuberculosis treatment: association with host and pathogen factors and mycobacteriuria. *BMC Infect Dis* 2012; **12**: 47.
149. Cox JA, Lukande RL, Kalungi S, et al. Is Urinary Lipoarabinomannan the Result of Renal Tuberculosis? Assessment of the Renal Histology in an Autopsy Cohort of Ugandan HIV-Infected Adults. *PLoS One* 2015; **10**(4): e0123323.
150. De P, Amin AG, Valli E, Perkins MD, McNeil M, Chatterjee D. Estimation of D-Arabinose by Gas Chromatography/Mass Spectrometry as Surrogate for Mycobacterial Lipoarabinomannan in Human Urine. *PLoS One* 2015; **10**(12): e0144088.
151. Paris L, Magni R, Zaidi F, et al. Urine lipoarabinomannan glycan in HIV-negative patients with pulmonary tuberculosis correlates with disease severity. *Sci Transl Med* 2017; **9**(420).
152. Fox JW, S. An R Companion to Applied Regression. 2nd ed. Thousand Oaks, CA: Sage; 2011.
153. Pearl J, Glymour M, Jewell NP. Causal Inference in Statistics: A Primer: Wiley; 2016.
154. Wolpin KI, Haile P. The Limits of Inference without Theory: MIT Press; 2013.
155. Husson F, Lê S, Pags J. Exploratory Multivariate Analysis by Example Using R: CRC Press LLC; 2017.
156. Charrad MG, N. NbClust: An R Package for Determining the Relevant Number of Clusters in a Data Set. *Journal of statistical software* 2014; **61**(6): 1-36.
157. Gaw A. Clinical Biochemistry: An Illustrated Colour Text: Churchill Livingstone; 1999.
158. Lippi G, Salvagno GL, Montagnana M, Brocco G, Guidi GC. Influence of hemolysis on routine clinical chemistry testing. *Clin Chem Lab Med* 2006; **44**(3): 311-6.

159. Machowicz R, Boguradzki P, Drozd-Sokolowska J, et al. Hemophagocytic Lymphohistiocytosis (HLH) in 44 Adults: Results from the Retrospective Polish Registry. Am Soc Hematology; 2015.
160. Nathwani RA, Pais S, Reynolds TB, Kaplowitz N. Serum alanine aminotransferase in skeletal muscle diseases. *Hepatology* 2005; **41**(2): 380-2.
161. Rief P, Pichler M, Raggam R, et al. The AST/ALT (De-Ritis) ratio: A novel marker for critical limb ischemia in peripheral arterial occlusive disease patients. *Medicine (Baltimore)* 2016; **95**(24): e3843.
162. Weibrecht K, Dayno M, Darling C, Bird SB. Liver aminotransferases are elevated with rhabdomyolysis in the absence of significant liver injury. *J Med Toxicol* 2010; **6**(3): 294-300.
163. Beeching NJ, Fenech M, Houlihan CF. Ebola virus disease. *BMJ* 2014; **349**: g7348.
164. Chang ML, Yang CW, Chen JC, et al. Disproportional exaggerated aspartate transaminase is a useful prognostic parameter in late leptospirosis. *World J Gastroenterol* 2005; **11**(35): 5553-6.
165. Cohen J, Powderly WG, Opal SM. Infectious Diseases E-Book: Elsevier Health Sciences; 2016.
166. Miyashima Y, Iwamuro M, Shibata M, et al. Prediction of Disseminated Intravascular Coagulation by Liver Function Tests in Patients with Japanese Spotted Fever. *Intern Med* 2018; **57**(2): 197-202.
167. Spec A, Barrios CR, Ahmad U, Proia LA. AST to ALT Ratio is elevated in disseminated histoplasmosis as compared to localized pulmonary disease and other endemic mycoses. *Med Mycol* 2017; **55**(5): 541-5.
168. Nalpas B, Vassault A, Guillou AL, et al. Serum activity of mitochondrial aspartate aminotransferase: a sensitive marker of alcoholism with or without alcoholic hepatitis. *Hepatology* 1984; **4**(5): 893-6.
169. Hickey AJ, Gounder L, Moosa MY, Drain PK. A systematic review of hepatic tuberculosis with considerations in human immunodeficiency virus co-infection. *BMC Infect Dis* 2015; **15**: 209.
170. Gounder L, Moodley P, Drain PK, Hickey AJ, Moosa MS. Hepatic tuberculosis in human immunodeficiency virus co-infected adults: a case series of South African adults. *BMC Infect Dis* 2017; **17**(1): 115.
171. Badr KF. Sepsis-associated renal vasoconstriction: potential targets for future therapy. *Am J Kidney Dis* 1992; **20**(3): 207-13.
172. Schrier RW, Wang W. Acute renal failure and sepsis. *N Engl J Med* 2004; **351**(2): 159-69.
173. Murugan R, Karajala-Subramanyam V, Lee M, et al. Acute kidney injury in non-severe pneumonia is associated with an increased immune response and lower survival. *Kidney Int* 2010; **77**(6): 527-35.
174. Langenberg C, Bellomo R, May C, Wan L, Egi M, Morgera S. Renal blood flow in sepsis. *Crit Care* 2005; **9**(4): R363-74.
175. Umbro I, Gentile G, Tinti F, Muiesan P, Mitterhofer AP. Recent advances in pathophysiology and biomarkers of sepsis-induced acute kidney injury. *J Infect* 2016; **72**(2): 131-42.
176. Devarajan P. Acute kidney injury: Acute kidney injury: still misunderstood and misdiagnosed. *Nat Rev Nephrol* 2017; **13**(3): 137-8.

177. Xu K, Rosenstiel P, Paragas N, et al. Unique Transcriptional Programs Identify Subtypes of AKI. *J Am Soc Nephrol* 2017; **28**(6): 1729-40.
178. Zhang A, Cai Y, Wang PF, et al. Diagnosis and prognosis of neutrophil gelatinase-associated lipocalin for acute kidney injury with sepsis: a systematic review and meta-analysis. *Crit Care* 2016; **20**: 41.
179. Afzal Z, Kallumadanda S, Wang F, Hemmige V, Musher D. Acute Febrile Illness and Complications Due to Murine Typhus, Texas, USA1,2. *Emerg Infect Dis* 2017; **23**(8): 1268-73.
180. Dixon BS, Anderson RJ. Pneumonia and the syndrome of inappropriate antidiuretic hormone secretion: don't pour water on the fire. *Am Rev Respir Dis* 1988; **138**(3): 512-3.
181. Gottlieb M, Long B, Koyfman A. The Evaluation and Management of Rocky Mountain Spotted Fever in the Emergency Department: a Review of the Literature. *J Emerg Med* 2018.
182. Kashef Hamadani BH, Franco-Paredes C, McCollister B, Shapiro L, Beckham JD, Henao-Martinez AF. Cryptococcosis and cryptococcal meningitis: New predictors and clinical outcomes at a United States academic medical centre. *Mycoses* 2018; **61**(5): 314-20.
183. Miller AC. Hyponatraemia in Legionnaires' disease. *Br Med J (Clin Res Ed)* 1982; **284**(6315): 558-9.
184. Miller LH, Makaranond P, Sitprija V, Suebsanguan C, Canfield CJ. Hyponatraemia in malaria. *Ann Trop Med Parasitol* 1967; **61**(3): 265-79.
185. Sitprija V. Altered fluid, electrolyte and mineral status in tropical disease, with an emphasis on malaria and leptospirosis. *Nat Clin Pract Nephrol* 2008; **4**(2): 91-101.
186. Liamis G, Milionis HJ, Elisaf M. Hyponatremia in patients with infectious diseases. *J Infect* 2011; **63**(5): 327-35.
187. Braconnier P, Delforge M, Garjau M, Wissing KM, De Wit S. Hyponatremia is a marker of disease severity in HIV-infected patients: a retrospective cohort study. *BMC Infect Dis* 2017; **17**(1): 98.
188. Cusano AJ, Thies HL, Siegal FP, Dreisbach AW, Maesaka JK. Hyponatremia in patients with acquired immune deficiency syndrome. *J Acquir Immune Defic Syndr* 1990; **3**(10): 949-53.
189. Dao CN, Peters PJ, Kiarie JN, et al. Hyponatremia, hypochloremia, and hypoalbuminemia predict an increased risk of mortality during the first year of antiretroviral therapy among HIV-infected Zambian and Kenyan women. *AIDS Res Hum Retroviruses* 2011; **27**(11): 1149-55.
190. Shu Z, Tian Z, Chen J, et al. HIV/AIDS-related hyponatremia: an old but still serious problem. *Ren Fail* 2018; **40**(1): 68-74.
191. Xu L, Ye H, Huang F, et al. Moderate/Severe hyponatremia increases the risk of death among hospitalized Chinese human immunodeficiency virus/acquired immunodeficiency syndrome patients. *PLoS One* 2014; **9**(10): e111077.
192. Glassock RJ, Cohen AH, Danovitch G, Parsa KP. Human immunodeficiency virus (HIV) infection and the kidney. *Ann Intern Med* 1990; **112**(1): 35-49.
193. Tang WW, Kaptein EM, Feinstein EI, Massry SG. Hyponatremia in hospitalized patients with the acquired immunodeficiency syndrome (AIDS) and the AIDS-related complex. *Am J Med* 1993; **94**(2): 169-74.

194. Vitting KE, Gardenswartz MH, Zabetakis PM, et al. Frequency of hyponatremia and nonosmolar vasopressin release in the acquired immunodeficiency syndrome. *JAMA* 1990; **263**(7): 973-8.
195. Bennett JE, Dolin R, Blaser MJ. Principles and Practice of Infectious Diseases: Elsevier - Health Sciences Division; 2014.
196. Hill AR, Uribarri J, Mann J, Berl T. Altered water metabolism in tuberculosis: role of vasopressin. *Am J Med* 1990; **88**(4): 357-64.
197. Francois Venter WD, Panz VR, Feldman C, Joffe BI. Adrenocortical function in hospitalised patients with active pulmonary tuberculosis receiving a rifampicin-based regimen -- a pilot study. *S Afr Med J* 2006; **96**(1): 62-6.
198. Kaplan FJ, Levitt NS, Soule SG. Primary hypoadrenalism assessed by the 1 microg ACTH test in hospitalized patients with active pulmonary tuberculosis. *QJM* 2000; **93**(9): 603-9.
199. Diringer M. Chapter 38 - Neurologic manifestations of major electrolyte abnormalities. In: Wijdicks EFM, Kramer AH, eds. Handbook of Clinical Neurology: Elsevier; 2017: 705-13.
200. Bowen DL, Lane HC, Fauci AS. Immunopathogenesis of the acquired immunodeficiency syndrome. *Ann Intern Med* 1985; **103**(5): 704-9.
201. Lucey DR, Hensley RE, Ward WW, Butzin CA, Boswell RN. CD4+ monocyte counts in persons with HIV-1 infection: an early increase is followed by a progressive decline. *J Acquir Immune Defic Syndr* 1991; **4**(1): 24-30.
202. De Santis GC, Brunetta DM, Vilar FC, et al. Hematological abnormalities in HIV-infected patients. *Int J Infect Dis* 2011; **15**(12): e808-11.
203. Levine AM, Karim R, Mack W, et al. Neutropenia in human immunodeficiency virus infection: data from the women's interagency HIV study. *Arch Intern Med* 2006; **166**(4): 405-10.
204. Castelino DJ, McNair P, Kay TW. Lymphocytopenia in a hospital population--what does it signify? *Aust N Z J Med* 1997; **27**(2): 170-4.
205. Brass D, McKay P, Scott F. Investigating an incidental finding of lymphopenia. *BMJ* 2014; **348**: g1721.
206. Sulkowski MS, Chaisson RE, Karp CL, Moore RD, Margolick JB, Quinn TC. The effect of acute infectious illnesses on plasma human immunodeficiency virus (HIV) type 1 load and the expression of serologic markers of immune activation among HIV-infected adults. *J Infect Dis* 1998; **178**(6): 1642-8.
207. Bentler PM, Yuan KH. Test of linear trend in eigenvalues of a covariance matrix with application to data analysis. *Br J Math Stat Psychol* 1996; **49 (Pt 2)**: 299-312.
208. Lyadova IV. Neutrophils in Tuberculosis: Heterogeneity Shapes the Way? *Mediators Inflamm* 2017; **2017**: 8619307.
209. Martineau AR, Newton SM, Wilkinson KA, et al. Neutrophil-mediated innate immune resistance to mycobacteria. *J Clin Invest* 2007; **117**(7): 1988-94.
210. Lowe DM, Redford PS, Wilkinson RJ, O'Garra A, Martineau AR. Neutrophils in tuberculosis: friend or foe? *Trends Immunol* 2012; **33**(1): 14-25.
211. Brahmbhatt S, Black GF, Carroll NM, et al. Immune markers measured before treatment predict outcome of intensive phase tuberculosis therapy. *Clin Exp Immunol* 2006; **146**(2): 243-52.
212. Martineau AR, Timms PM, Bothamley GH, et al. High-dose vitamin D(3) during intensive-phase antimicrobial treatment of pulmonary tuberculosis: a double-blind randomised controlled trial. *Lancet* 2011; **377**(9761): 242-50.

213. Fan YM, Ding SP, Bao ZJ, et al. Prognostic factors for treatment success in patients with multidrug-resistant tuberculosis in China. *Int J Tuberc Lung Dis* 2018; **22**(3): 300-5.
214. Barnes PF, Leedom JM, Chan LS, et al. Predictors of short-term prognosis in patients with pulmonary tuberculosis. *J Infect Dis* 1988; **158**(2): 366-71.
215. Han Y, Kim SJ, Lee SH, et al. High blood neutrophil-lymphocyte ratio associated with poor outcomes in miliary tuberculosis. *J Thorac Dis* 2018; **10**(1): 339-46.
216. Lowe DM, Bandara AK, Packe GE, et al. Neutrophilia independently predicts death in tuberculosis. *Eur Respir J* 2013; **42**(6): 1752-7.
217. Bisson GP, Ramchandani R, Miyahara S, et al. Risk factors for early mortality on antiretroviral therapy in advanced HIV-infected adults. *AIDS* 2017; **31**(16): 2217-25.
218. Underwood J, Cresswell F, Salam AP, et al. Complications of miliary tuberculosis: low mortality and predictive biomarkers from a UK cohort. *BMC Infect Dis* 2017; **17**(1): 295.
219. Singanayagam A, Manalan K, Connell DW, et al. Evaluation of serum inflammatory biomarkers as predictors of treatment outcome in pulmonary tuberculosis. *Int J Tuberc Lung Dis* 2016; **20**(12): 1653-60.
220. Kerkhoff AD, Wood R, Lowe DM, Vogt M, Lawn SD. Blood neutrophil counts in HIV-infected patients with pulmonary tuberculosis: association with sputum mycobacterial load. *PLoS One* 2013; **8**(7): e67956.
221. Houghton LE. Blood Examinations in the Prognosis and Treatment of Pulmonary Tuberculosis. *Br Med J* 1936; **2**(3963): 1246-51.
222. Panteleev AV, Nikitina IY, Burmistrova IA, et al. Severe Tuberculosis in Humans Correlates Best with Neutrophil Abundance and Lymphocyte Deficiency and Does Not Correlate with Antigen-Specific CD4 T-Cell Response. *Front Immunol* 2017; **8**: 963.
223. Worodria W, Menten J, Massinga-Loembe M, et al. Clinical spectrum, risk factors and outcome of immune reconstitution inflammatory syndrome in patients with tuberculosis-HIV coinfection. *Antivir Ther* 2012; **17**(5): 841-8.
224. Nakiwala JK, Walker NF, Diedrich CR, et al. Neutrophil Activation and Enhanced Release of Granule Products in HIV-TB Immune Reconstitution Inflammatory Syndrome. *J Acquir Immune Defic Syndr* 2018; **77**(2): 221-9.
225. Freigang B, Boyd RP, Elliott GB. Serum protein electrophoresis in tuberculosis. *Can Med Assoc J* 1963; **88**: 240-2.
226. Gilliland IC, Johnston RN, Stradling P, Abdel-Wahab EM. Serum proteins in pulmonary tuberculosis. *Br Med J* 1956; **1**(4981): 1460-4.
227. Leggat PO. Serial serum protein changes in pulmonary tuberculosis. *Br J Tuberc Dis Chest* 1957; **51**(2): 139-45.
228. Juraschek SP, Moliterno AR, Checkley W, Miller ER, 3rd. The Gamma Gap and All-Cause Mortality. *PLoS One* 2015; **10**(12): e0143494.
229. Fulks M, Stout RL, Dolan VF. Serum globulin predicts all-cause mortality for life insurance applicants. *J Insur Med* 2014; **44**(2): 93-8.
230. Dey SK, Ghosh I, Bhattacharjee D, et al. Liver Function Profile Anomalies in HIV Seropositive Tuberculosis. *J Clin Diagn Res* 2013; **7**(6): 1068-72.
231. de Beer FC, Nel AE, Gie RP, Donald PR, Strachan AF. Serum amyloid A protein and C-reactive protein levels in pulmonary tuberculosis: relationship to amyloidosis. *Thorax* 1984; **39**(3): 196-200.
232. Boelaert JR, Vandecasteele SJ, Appelberg R, Gordeuk VR. The effect of the host's iron status on tuberculosis. *J Infect Dis* 2007; **195**(12): 1745-53.

233. Quaye IK. Haptoglobin, inflammation and disease. *Trans R Soc Trop Med Hyg* 2008; **102**(8): 735-42.
234. Roe JK, Thomas N, Gil E, et al. Blood transcriptomic diagnosis of pulmonary and extrapulmonary tuberculosis. *JCI Insight* 2016; **1**(16): e87238.
235. Wang C, Li YY, Li X, et al. Serum complement C4b, fibronectin, and prolidase are associated with the pathological changes of pulmonary tuberculosis. *BMC Infect Dis* 2014; **14**: 52.
236. Ashenafi S, Aderaye G, Zewdie M, et al. BCG-specific IgG-secreting peripheral plasmablasts as a potential biomarker of active tuberculosis in HIV negative and HIV positive patients. *Thorax* 2013; **68**(3): 269-76.
237. Welch RJ, Lawless KM, Litwin CM. Antituberculosis IgG antibodies as a marker of active Mycobacterium tuberculosis disease. *Clin Vaccine Immunol* 2012; **19**(4): 522-6.
238. Gilliland IC, Stradling P, Abdelwahab EM. Serum protein changes following B. C. G. vaccination. *Br Med J* 1958; **1**(5062): 87-8.
239. Lawn SD, Obeng J, Acheampong JW, Griffin GE. Resolution of the acute-phase response in West African patients receiving treatment for pulmonary tuberculosis. *Int J Tuberc Lung Dis* 2000; **4**(4): 340-4.
240. Mesquita ED, Gil-Santana L, Ramalho D, et al. Associations between systemic inflammation, mycobacterial loads in sputum and radiological improvement after treatment initiation in pulmonary TB patients from Brazil: a prospective cohort study. *BMC Infect Dis* 2016; **16**: 368.
241. Bone RC, Balk RA, Cerra FB, et al. Definitions for sepsis and organ failure and guidelines for the use of innovative therapies in sepsis. The ACCP/SCCM Consensus Conference Committee. American College of Chest Physicians/Society of Critical Care Medicine. *Chest* 1992; **101**(6): 1644-55.
242. Seymour CW, Liu VX, Iwashyna TJ, et al. Assessment of Clinical Criteria for Sepsis: For the Third International Consensus Definitions for Sepsis and Septic Shock (Sepsis-3). *JAMA* 2016; **315**(8): 762-74.
243. Singer M, Deutschman CS, Seymour CW, et al. The Third International Consensus Definitions for Sepsis and Septic Shock (Sepsis-3). *JAMA* 2016; **315**(8): 801-10.
244. Michaeli B, Martinez A, Revelly JP, et al. Effects of endotoxin on lactate metabolism in humans. *Crit Care* 2012; **16**(4): R139.
245. Boekstegers P, Weidenhofer S, Kapsner T, Werdan K. Skeletal muscle partial pressure of oxygen in patients with sepsis. *Crit Care Med* 1994; **22**(4): 640-50.
246. Sair M, Etherington PJ, Peter Winlove C, Evans TW. Tissue oxygenation and perfusion in patients with systemic sepsis. *Crit Care Med* 2001; **29**(7): 1343-9.
247. Garcia-Alvarez M, Marik P, Bellomo R. Sepsis-associated hyperlactatemia. *Crit Care* 2014; **18**(5): 503.
248. Zhu L, Zhao Q, Yang T, Ding W, Zhao Y. Cellular metabolism and macrophage functional polarization. *Int Rev Immunol* 2015; **34**(1): 82-100.
249. Srivastava A, Mannam P. Warburg revisited: lessons for innate immunity and sepsis. *Front Physiol* 2015; **6**: 70.
250. Taylor DJ, Faragher EB, Evanson JM. Inflammatory cytokines stimulate glucose uptake and glycolysis but reduce glucose oxidation in human dermal fibroblasts in vitro. *Circ Shock* 1992; **37**(2): 105-10.
251. Kraut JA, Madias NE. Lactic acidosis. *N Engl J Med* 2014; **371**(24): 2309-19.

252. Gleeson LE, Sheedy FJ, Palsson-McDermott EM, et al. Cutting Edge: Mycobacterium tuberculosis Induces Aerobic Glycolysis in Human Alveolar Macrophages That Is Required for Control of Intracellular Bacillary Replication. *J Immunol* 2016; **196**(6): 2444-9.
253. Lachmandas E, Rios-Miguel AB, Koeken V, et al. Tissue metabolic changes drive cytokine responses to Mycobacterium tuberculosis. *J Infect Dis* 2018.
254. Ingels C, Vanhorebeek I, Van den Berghe G. Glucose homeostasis, nutrition and infections during critical illness. *Clin Microbiol Infect* 2018; **24**(1): 10-5.
255. Selye H. What is stress? *Metabolism* 1956; **5**(5): 525-30.
256. Shimokata H, Muller DC, Fleg JL, Sorkin J, Ziemba AW, Andres R. Age as independent determinant of glucose tolerance. *Diabetes* 1991; **40**(1): 44-51.
257. Short KR, Vittone JL, Bigelow ML, et al. Impact of aerobic exercise training on age-related changes in insulin sensitivity and muscle oxidative capacity. *Diabetes* 2003; **52**(8): 1888-96.
258. Passos AM, Treitinger A, Spada C. An overview of the mechanisms of HIV-related thrombocytopenia. *Acta Haematol* 2010; **124**(1): 13-8.
259. Vaughan J, Wiggill T, Munster M. Immature platelet fraction levels in a variety of bone marrow pathologies in South African HIV-positive patients with thrombocytopenia. *Hematology* 2014; **19**(7): 417-23.
260. Baynes RD, Bothwell TH, Flax H, et al. Reactive thrombocytosis in pulmonary tuberculosis. *J Clin Pathol* 1987; **40**(6): 676-9.
261. Morris CD, Bird AR, Nell H. The haematological and biochemical changes in severe pulmonary tuberculosis. *Q J Med* 1989; **73**(272): 1151-9.
262. Renshaw AA, Gould EW. Thrombocytosis is associated with Mycobacterium tuberculosis infection and positive acid-fast stains in granulomas. *Am J Clin Pathol* 2013; **139**(5): 584-6.
263. Ghobrial MW, Albornoz MA. Immune thrombocytopenia: a rare presenting manifestation of tuberculosis. *Am J Hematol* 2001; **67**(2): 139-43.
264. Brackers de Hugo L, Ffrench M, Broussolle C, Seve P. Granulomatous lesions in bone marrow: clinicopathologic findings and significance in a study of 48 cases. *Eur J Intern Med* 2013; **24**(5): 468-73.
265. Cameron SJ. Rifampicin and thrombocytopenia. *Lancet* 1971; **2**(7716): 167.
266. Fujita M, Kunitake R, Nagano Y, Maeda F. Disseminated intravascular coagulation associated with pulmonary tuberculosis. *Intern Med* 1997; **36**(3): 218-20.
267. Mayne ES, Mayne ALH, Louw SJ. Pathogenic factors associated with development of disseminated intravascular coagulopathy (DIC) in a tertiary academic hospital in South Africa. *PLoS One* 2018; **13**(4): e0195793.
268. Andrews B, Semler MW, Muchemwa L, et al. Effect of an Early Resuscitation Protocol on In-hospital Mortality Among Adults With Sepsis and Hypotension: A Randomized Clinical Trial. *JAMA* 2017; **318**(13): 1233-40.
269. Douglas H, xa, E. Reintroducing Prediction to Explanation. *Philosophy of Science* 2009; **76**(4): 444-63.
270. Toll DB, Janssen KJ, Vergouwe Y, Moons KG. Validation, updating and impact of clinical prediction rules: a review. *J Clin Epidemiol* 2008; **61**(11): 1085-94.
271. American College of Chest Physicians/Society of Critical Care Medicine Consensus Conference: definitions for sepsis and organ failure and guidelines for the use of innovative therapies in sepsis. *Crit Care Med* 1992; **20**(6): 864-74.

272. Teasdale G, Jennett B. Assessment of coma and impaired consciousness. A practical scale. *Lancet* 1974; **2**(7872): 81-4.
273. Knaus WA, Draper EA, Wagner DP, Zimmerman JE. APACHE II: a severity of disease classification system. *Crit Care Med* 1985; **13**(10): 818-29.
274. Corfield AP, Cooper MJ, Williamson RC, et al. Prediction of severity in acute pancreatitis: prospective comparison of three prognostic indices. *Lancet* 1985; **2**(8452): 403-7.
275. Wilson PW, D'Agostino RB, Levy D, Belanger AM, Silbershatz H, Kannel WB. Prediction of coronary heart disease using risk factor categories. *Circulation* 1998; **97**(18): 1837-47.
276. Lim WS, van der Eerden MM, Laing R, et al. Defining community acquired pneumonia severity on presentation to hospital: an international derivation and validation study. *Thorax* 2003; **58**(5): 377-82.
277. Kanis JA, Johnell O, Oden A, Johansson H, McCloskey E. FRAX and the assessment of fracture probability in men and women from the UK. *Osteoporos Int* 2008; **19**(4): 385-97.
278. Malinchoc M, Kamath PS, Gordon FD, Peine CJ, Rank J, ter Borg PC. A model to predict poor survival in patients undergoing transjugular intrahepatic portosystemic shunts. *Hepatology* 2000; **31**(4): 864-71.
279. Sullivan LM, Massaro JM, D'Agostino RB, Sr. Presentation of multivariate data for clinical use: The Framingham Study risk score functions. *Stat Med* 2004; **23**(10): 1631-60.
280. Chen JH, Asch SM. Machine Learning and Prediction in Medicine - Beyond the Peak of Inflated Expectations. *N Engl J Med* 2017; **376**(26): 2507-9.
281. Darcy AM, Louie AK, Roberts LW. Machine Learning and the Profession of Medicine. *JAMA* 2016; **315**(6): 551-2.
282. Adams ST, Leveson SH. Clinical prediction rules. *BMJ* 2012; **344**: d8312.
283. Hastie T, Tibshirani R, Friedman J. The Elements of Statistical Learning: Data Mining, Inference, and Prediction: Springer New York; 2013.
284. Bilogur A. Bias-variance tradeoff. 2017. https://www.kaggle.com/residentmario/bias-variance-tradeoff (accessed 24/05/2018 2018).
285. Leek JP, R.D.;Caffo,B. Practical machine learning.: Coursera, 2016.
286. James G, Witten D, Hastie T, Tibshirani R. An Introduction to Statistical Learning: with Applications in R: Springer New York; 2013.
287. Hyndman RJ. Why every statistician should know about cross-validation. 2010. https://robjhyndman.com/hyndsight/crossvalidation/ (accessed 24/05/2018 2018).
288. Kuhn M, Johnson K. Applied Predictive Modeling: Springer New York; 2013.
289. Andrews B, Muchemwa L, Kelly P, Lakhi S, Heimburger DC, Bernard GR. Simplified severe sepsis protocol: a randomized controlled trial of modified early goal-directed therapy in Zambia. *Crit Care Med* 2014; **42**(11): 2315-24.
290. Hira ZM, Gillies DF. A Review of Feature Selection and Feature Extraction Methods Applied on Microarray Data. *Adv Bioinformatics* 2015; **2015**: 198363.
291. Michiels S, Kramar A, Koscielny S. Multidimensionality of microarrays: statistical challenges and (im)possible solutions. *Mol Oncol* 2011; **5**(2): 190-6.
292. Guyon IE, A. An Introduction to Variable and Feature Selection. *Journal of Machine Learning Research* 2003; **3**: 1157-82.

293. Thwaites GE, Scarborough M, Szubert A, et al. Adjunctive rifampicin for Staphylococcus aureus bacteraemia (ARREST): a multicentre, randomised, double-blind, placebo-controlled trial. *Lancet* 2018; **391**(10121): 668-78.
294. De Pauw BE, Deresinski SC, Feld R, Lane-Allman EF, Donnelly JP. Ceftazidime compared with piperacillin and tobramycin for the empiric treatment of fever in neutropenic patients with cancer. A multicenter randomized trial. The Intercontinental Antimicrobial Study Group. *Ann Intern Med* 1994; **120**(10): 834-44.
295. Piccart M, Klastersky J, Meunier F, Lagast H, Van Laethem Y, Weerts D. Single-drug versus combination empirical therapy for gram-negative bacillary infections in febrile cancer patients with and without granulocytopenia. *Antimicrob Agents Chemother* 1984; **26**(6): 870-5.
296. Theron G, Peter J, Dowdy D, Langley I, Squire SB, Dheda K. Do high rates of empirical treatment undermine the potential effect of new diagnostic tests for tuberculosis in high-burden settings? *Lancet Infect Dis* 2014; **14**(6): 527-32.
297. Nakiyingi L, Bwanika JM, Kirenga B, et al. Clinical predictors and accuracy of empiric tuberculosis treatment among sputum smear-negative HIV-infected adult TB suspects in Uganda. *PLoS One* 2013; **8**(9): e74023.
298. Djulbegovic B, Elqayam S, Reljic T, et al. How do physicians decide to treat: an empirical evaluation of the threshold model. *BMC Med Inform Decis Mak* 2014; **14**: 47.
299. Willis BH. Empirical evidence that disease prevalence may affect the performance of diagnostic tests with an implicit threshold: a cross-sectional study. *BMJ Open* 2012; **2**(1): e000746.
300. Mamede SS, H.G. The twin traps of overtreatmnet and therapeutic nihilism in clinical practice. *Med Educ* 2014; **48**(1): 34-43.
301. Hollander N, Sauerbrei W, Schumacher M. Confidence intervals for the effect of a prognostic factor after selection of an 'optimal' cutpoint. *Stat Med* 2004; **23**(11): 1701-13.
302. Archibald LK, McDonald LC, Addison RM, et al. Comparison of BACTEC MYCO/F LYTIC and WAMPOLE ISOLATOR 10 (lysis-centrifugation) systems for detection of bacteremia, mycobacteremia, and fungemia in a developing country. *J Clin Microbiol* 2000; **38**(8): 2994-7.
303. Crump JA, Morrissey AB, Ramadhani HO, Njau BN, Maro VP, Reller LB. Controlled comparison of BacT/Alert MB system, manual Myco/F lytic procedure, and isolator 10 system for diagnosis of Mycobacterium tuberculosis Bacteremia. *J Clin Microbiol* 2011; **49**(8): 3054-7.
304. Fandinho FC, Grinsztejn B, Veloso VG, et al. Diagnosis of disseminated mycobacterial infection: testing a simple and inexpensive method for use in developing countries. *Bull World Health Organ* 1997; **75**(4): 361-6.
305. Gill VJ, Park CH, Stock F, Gosey LL, Witebsky FG, Masur H. Use of lysis-centrifugation (isolator) and radiometric (BACTEC) blood culture systems for the detection of mycobacteremia. *J Clin Microbiol* 1985; **22**(4): 543-6.
306. Martinez-Sanchez L, Ruiz-Serrano J, Bouza E, et al. Utility of the BACTEC Myco/F lytic medium for the detection of mycobacteria in blood. *Diagn Microbiol Infect Dis* 2000; **38**(4): 223-6.
307. Ruf B, Schurmann D, Brehmer W, Mauch H, Pohle HD. Mycobacteremia in AIDS patients. Results of a prospective study. *Klin Wochenschr* 1989; **67**(14): 717-22.

308. Munseri PJ, Talbot EA, Bakari M, Matee M, Teixeira JP, von Reyn CF. The bacteraemia of disseminated tuberculosis among HIV-infected patients with prolonged fever in Tanzania. *Scand J Infect Dis* 2011; **43**(9): 696-701.
309. CLSI. Clinical and Laboratory Standards Institute Principles and Procedures for Blood Cultures; Approved Guideline. Document M47-A. . Wayne, PA: Clinical and Laboratory Standards Institute, 2007.
310. Lee A, Mirrett S, Reller LB, Weinstein MP. Detection of bloodstream infections in adults: how many blood cultures are needed? *J Clin Microbiol* 2007; **45**(11): 3546-8.
311. Pavlinac PB, Lokken EM, Walson JL, Richardson BA, Crump JA, John-Stewart GC. Mycobacterium tuberculosis bacteremia in adults and children: a systematic review and meta-analysis. *Int J Tuberc Lung Dis* 2016; **20**(7): 895-902.
312. Bates DM, M.; Bolker, B.; Walker, S. Fitting Linear Mixed-Effects Models Using lme4. *Journal of Statistical Software* 2015; **67**(1): 1-48.
313. Austin PC, Merlo J. Intermediate and advanced topics in multilevel logistic regression analysis. *Stat Med* 2017; **36**(20): 3257-77.
314. Snijders TABB, R.J. Multilevel analysis: An introduction to basic and advanced multilevel modelling. 2nd ed. London: Sage; 2012.
315. Weinmayr G, Dreyhaupt J, Jaensch A, Forastiere F, Strachan DP. Multilevel regression modelling to investigate variation in disease prevalence across locations. *Int J Epidemiol* 2017; **46**(1): 336-47.
316. Barton K. MuMIn: Multi-Model Inference. R package. 1.40.0. ed; 2017.
317. Johnson PC. Extension of Nakagawa & Schielzeth's R(2)GLMM to random slopes models. *Methods Ecol Evol* 2014; **5**(9): 944-6.
318. Nakagawa S, Johnson PCD, Schielzeth H. The coefficient of determination R(2) and intra-class correlation coefficient from generalized linear mixed-effects models revisited and expanded. *J R Soc Interface* 2017; **14**(134).
319. Nakagawa S, Schielzeth H. A general and simple method for obtaining R2 from generalized linear mixed-effects models. *Methods in Ecology and Evolution* 2013; **4**(2): 133-42.
320. Bolker B. Confidence and prediction intervals for unobserved levels: Comment on “simulate new random effects/conditional modes conditional on observed data #388”. 2016. https://github.com/lme4/lme4/issues/388#issuecomment-231398937 (accessed 18 August 2017 2017).
321. Canty AR, B. . R package boot: Bootstrap R (S-Plus) Functions. 1.3-20. ed; 2017.
322. Lawn SD, Kerkhoff AD, Burton R, et al. Diagnostic accuracy, incremental yield and prognostic value of Determine TB-LAM for routine diagnostic testing for tuberculosis in HIV-infected patients requiring acute hospital admission in South Africa: a prospective cohort. *BMC Med* 2017; **15**(1): 67.
323. Bacha HA, Cimerman S, de Souza SA, Hadad DJ, Mendes CM. Prevalence of mycobacteremia in patients with AIDS and persistant fever. *Braz J Infect Dis* 2004; **8**(4): 290-5.
324. Grinsztejn B, Fandinho FC, Veloso VG, et al. Mycobacteremia in patients with the acquired immunodeficiency syndrome. *Arch Intern Med* 1997; **157**(20): 2359-63.
325. Gopinath K, Kumar S, Singh S. Prevalence of mycobacteremia in Indian HIV-infected patients detected by the MB/BacT automated culture system. *Eur J Clin Microbiol Infect Dis* 2008; **27**(6): 423-31.

326. Vugia DJ, Kiehlbauch JA, Yeboue K, et al. Pathogens and predictors of fatal septicemia associated with human immunodeficiency virus infection in Ivory Coast, west Africa. *J Infect Dis* 1993; **168**(3): 564-70.
327. Bedell RA, Anderson ST, van Lettow M, et al. High prevalence of tuberculosis and serious bloodstream infections in ambulatory individuals presenting for antiretroviral therapy in Malawi. *PLoS One* 2012; **7**(6): e39347.
328. Shutz CM, G. et al. KDHTB study. 2018.
329. Wilson D, Nachega J, Morroni C, Chaisson R, Maartens G. Diagnosing smear-negative tuberculosis using case definitions and treatment response in HIV-infected adults. *Int J Tuberc Lung Dis* 2006; **10**(1): 31-8.
330. Nakiyingi L, Moodley VM, Manabe YC, et al. Diagnostic accuracy of a rapid urine lipoarabinomannan test for tuberculosis in HIV-infected adults. *J Acquir Immune Defic Syndr* 2014; **66**(3): 270-9.
331. Louie JK, Chi NH, Thao le TT, et al. Opportunistic infections in hospitalized HIV-infected adults in Ho Chi Minh City, Vietnam: a cross-sectional study. *Int J STD AIDS* 2004; **15**(11): 758-61.
332. Jacob ST, Moore CC, Banura P, et al. Severe sepsis in two Ugandan hospitals: a prospective observational study of management and outcomes in a predominantly HIV-1 infected population. *PLoS One* 2009; **4**(11): e7782.
333. Gonzalez-Angulo Y, Wiysonge CS, Geldenhuys H, et al. Sputum induction for the diagnosis of pulmonary tuberculosis: a systematic review and meta-analysis. *Eur J Clin Microbiol Infect Dis* 2012; **31**(7): 1619-30.
334. Li S, Liu B, Peng M, et al. Diagnostic accuracy of Xpert MTB/RIF for tuberculosis detection in different regions with different endemic burden: A systematic review and meta-analysis. *PLoS One* 2017; **12**(7): e0180725.
335. Steingart KR, Schiller I, Horne DJ, Pai M, Boehme CC, Dendukuri N. Xpert(R) MTB/RIF assay for pulmonary tuberculosis and rifampicin resistance in adults. *Cochrane Database Syst Rev* 2014; (1): CD009593.
336. Walusimbi S, Bwanga F, De Costa A, Haile M, Joloba M, Hoffner S. Meta-analysis to compare the accuracy of GeneXpert, MODS and the WHO 2007 algorithm for diagnosis of smear-negative pulmonary tuberculosis. *BMC Infect Dis* 2013; **13**: 507.
337. Dinnes J, Deeks J, Kirby J, Roderick P. A methodological review of how heterogeneity has been examined in systematic reviews of diagnostic test accuracy. *Health Technol Assess* 2005; **9**(12): 1-113, iii.
338. Dorman SE, Schumacher SG, Alland D, et al. Xpert MTB/RIF Ultra for detection of Mycobacterium tuberculosis and rifampicin resistance: a prospective multicentre diagnostic accuracy study. *Lancet Infect Dis* 2018; **18**(1): 76-84.
339. Rhodes A, Evans LE, Alhazzani W, et al. Surviving Sepsis Campaign: International Guidelines for Management of Sepsis and Septic Shock: 2016. *Crit Care Med* 2017; **45**(3): 486-552.
340. Mandell LA, Wunderink RG, Anzueto A, et al. Infectious Diseases Society of America/American Thoracic Society consensus guidelines on the management of community-acquired pneumonia in adults. *Clin Infect Dis* 2007; **44 Suppl 2**: S27-72.
341. Sartelli M, Catena F, Abu-Zidan FM, et al. Management of intra-abdominal infections: recommendations by the WSES 2016 consensus conference. *World J Emerg Surg* 2017; **12**: 22.

342. Houck PM, Bratzler DW, Nsa W, Ma A, Bartlett JG. Timing of antibiotic administration and outcomes for Medicare patients hospitalized with community-acquired pneumonia. *Arch Intern Med* 2004; **164**(6): 637-44.
343. Ferrer R, Martin-Loeches I, Phillips G, et al. Empiric antibiotic treatment reduces mortality in severe sepsis and septic shock from the first hour: results from a guideline-based performance improvement program. *Crit Care Med* 2014; **42**(8): 1749-55.
344. Meehan TP, Fine MJ, Krumholz HM, et al. Quality of care, process, and outcomes in elderly patients with pneumonia. *JAMA* 1997; **278**(23): 2080-4.
345. Seymour CW, Gesten F, Prescott HC, et al. Time to Treatment and Mortality during Mandated Emergency Care for Sepsis. *N Engl J Med* 2017; **376**(23): 2235-44.
346. Liu VX, Fielding-Singh V, Greene JD, et al. The Timing of Early Antibiotics and Hospital Mortality in Sepsis. *Am J Respir Crit Care Med* 2017; **196**(7): 856-63.
347. Peter JG, Zijenah LS, Chanda D, et al. Effect on mortality of point-of-care, urine-based lipoarabinomannan testing to guide tuberculosis treatment initiation in HIV-positive hospital inpatients: a pragmatic, parallel-group, multicountry, open-label, randomised controlled trial. *Lancet* 2016; **387**(10024): 1187-97.
348. Manabe YC, Worodria W, van Leth F, et al. Prevention of Early Mortality by Presumptive Tuberculosis Therapy Study: An Open Label, Randomized Controlled Trial. *Am J Trop Med Hyg* 2016; **95**(6): 1265-71.
349. Hosseinipour MC, Bisson GP, Miyahara S, et al. Empirical tuberculosis therapy versus isoniazid in adult outpatients with advanced HIV initiating antiretroviral therapy (REMEMBER): a multicountry open-label randomised controlled trial. *Lancet* 2016; **387**(10024): 1198-209.
350. Grant AC, S.; Tlali, M.; Johnson, S.; Dorman, S.; Hoffmann, C.; Karat, A.; Vassall, A.; Churchyard, G.; Fielding, K.L. Empirical TB Treatment in Advanced HIV Disease: Results of the TB Fast Track Trial. 23rd CROI. Boston, Massachusetts: IAS-USA; 2016.
351. Blanc FXB, A.; Bonnet, M.; Gabillard, D.; Messou, E.; Muzoora, C.; Samreth, S.; Nguyen, D. B.; Borand, L.; Domergue, A.; Natukunda, N.; Eholie, S.; Domoua, S.; Anglaret, X.; Laureillard, D. Systematic versus test-guided tuberculosis treatmnet: data of the STATIS randomised trial. 25th CROI. Boston, MA: IAS-USA; 2018.
352. Currier JS, Havlir DV. CROI 2018: Complications of HIV Infection and Antiretroviral Therapy. *Top Antivir Med* 2018; **26**(1): 22-9.
353. Cummings MJ, O'Donnell MR. Inverting the pyramid: increasing awareness of mycobacterial sepsis in sub-Saharan Africa. *Int J Tuberc Lung Dis* 2015; **19**(10): 1128-34.
354. Bergmann JS, Fish G, Woods GL. Evaluation of the BBL MGIT (Mycobacterial growth indicator tube) AST SIRE system for antimycobacterial susceptibility testing of Mycobacterium tuberculosis to 4 primary antituberculous drugs. *Arch Pathol Lab Med* 2000; **124**(1): 82-6.
355. Leonard B, Coronel J, Siedner M, et al. Inter- and intra-assay reproducibility of microplate Alamar blue assay results for isoniazid, rifampicin, ethambutol, streptomycin, ciprofloxacin, and capreomycin drug susceptibility testing of Mycobacterium tuberculosis. *J Clin Microbiol* 2008; **46**(10): 3526-9.
356. Bollela VR, Sato DN, Fonseca BA. McFarland nephelometer as a simple method to estimate the sensitivity of the polymerase chain reaction using Mycobacterium tuberculosis as a research tool. *Braz J Med Biol Res* 1999; **32**(9): 1073-6.

357. Elbir H, Abdel-Muhsin AM, Babiker A. A one-step DNA PCR-based method for the detection of Mycobacterium tuberculosis complex grown on Lowenstein-Jensen media. *Am J Trop Med Hyg* 2008; **78**(2): 316-7.
358. Syre H, Phyu S, Sandven P, Bjorvatn B, Grewal HM. Rapid colorimetric method for testing susceptibility of Mycobacterium tuberculosis to isoniazid and rifampin in liquid cultures. *J Clin Microbiol* 2003; **41**(11): 5173-7.
359. Penuelas-Urquides K, Villarreal-Trevino L, Silva-Ramirez B, Rivadeneyra-Espinoza L, Said-Fernandez S, de Leon MB. Measuring of Mycobacterium tuberculosis growth. A correlation of the optical measurements with colony forming units. *Braz J Microbiol* 2013; **44**(1): 287-9.
360. Iona E, Giannoni F, Pardini M, Brunori L, Orefici G, Fattorini L. Metronidazole plus rifampin sterilizes long-term dormant Mycobacterium tuberculosis. *Antimicrob Agents Chemother* 2007; **51**(4): 1537-40.
361. Martin-Casabona N, Xairo Mimo D, Gonzalez T, Rossello J, Arcalis L. Rapid method for testing susceptibility of Mycobacterium tuberculosis by using DNA probes. *J Clin Microbiol* 1997; **35**(10): 2521-5.
362. Janagama HK, Jeong K, Kapur V, Coussens P, Sreevatsan S. Cytokine responses of bovine macrophages to diverse clinical Mycobacterium avium subspecies paratuberculosis strains. *BMC Microbiol* 2006; **6**: 10.
363. Bogli-Stuber K, Kohler C, Seitert G, et al. Detection of Mycobacterium avium subspecies paratuberculosis in Swiss dairy cattle by real-time PCR and culture: a comparison of the two assays. *J Appl Microbiol* 2005; **99**(3): 587-97.
364. Chui LW, King R, Lu P, Manninen K, Sim J. Evaluation of four DNA extraction methods for the detection of Mycobacterium avium subsp. paratuberculosis by polymerase chain reaction. *Diagn Microbiol Infect Dis* 2004; **48**(1): 39-45.
365. Castilho AL, Caleffi-Ferracioli KR, Canezin PH, Dias Siqueira VL, de Lima Scodro RB, Cardoso RF. Detection of drug susceptibility in rapidly growing mycobacteria by resazurin broth microdilution assay. *J Microbiol Methods* 2015; **111**: 119-21.
366. von Groll A, Martin A, Portaels F, da Silva PE, Palomino JC. Growth kinetics of Mycobacterium tuberculosis measured by quantitative resazurin reduction assay: a tool for fitness studies. *Braz J Microbiol* 2010; **41**(2): 300-3.
367. Affolabi D, Sanoussi N, Odoun M, et al. Rapid detection of multidrug-resistant Mycobacterium tuberculosis in Cotonou (Benin) using two low-cost colorimetric methods: resazurin and nitrate reductase assays. *J Med Microbiol* 2008; **57**(Pt 8): 1024-7.
368. Martin A, Palomino JC, Portaels F. Rapid detection of ofloxacin resistance in Mycobacterium tuberculosis by two low-cost colorimetric methods: resazurin and nitrate reductase assays. *J Clin Microbiol* 2005; **43**(4): 1612-6.
369. Martin A, Camacho M, Portaels F, Palomino JC. Resazurin microtiter assay plate testing of Mycobacterium tuberculosis susceptibilities to second-line drugs: rapid, simple, and inexpensive method. *Antimicrob Agents Chemother* 2003; **47**(11): 3616-9.
370. Palomino JC, Martin A, Camacho M, Guerra H, Swings J, Portaels F. Resazurin microtiter assay plate: simple and inexpensive method for detection of drug resistance in Mycobacterium tuberculosis. *Antimicrob Agents Chemother* 2002; **46**(8): 2720-2.
371. Taneja NK, Tyagi JS. Resazurin reduction assays for screening of anti-tubercular compounds against dormant and actively growing Mycobacterium tuberculosis,

Mycobacterium bovis BCG and Mycobacterium smegmatis. *J Antimicrob Chemother* 2007; **60**(2): 288-93.
372. Patil SS, Mohite ST, Kulkarni SA, Udgaonkar US. Resazurin tube method: rapid, simple, and inexpensive method for detection of drug resistance in the clinical isolates of mycobacterium tuberculosis. *J Glob Infect Dis* 2014; **6**(4): 151-6.
373. Gold B, Roberts J, Ling Y, et al. Visualization of the Charcoal Agar Resazurin Assay for Semi-quantitative, Medium-throughput Enumeration of Mycobacteria. *J Vis Exp* 2016; (118).
374. Disease IUATaL. Technical Guide: Sputum Examination for Tuberculosis by Direct Microscopy in Low-Income Countries. Geneva: IUATLD, 2000.
375. Parsons LM, Somoskovi A, Gutierrez C, et al. Laboratory diagnosis of tuberculosis in resource-poor countries: challenges and opportunities. *Clin Microbiol Rev* 2011; **24**(2): 314-50.
376. Castan P, de Pablo A, Fernandez-Romero N, et al. Point-of-care system for detection of Mycobacterium tuberculosis and rifampin resistance in sputum samples. *J Clin Microbiol* 2014; **52**(2): 502-7.
377. Kent PTK, G.P. . Public Health Mycobacteriology: A Guide for the Level III Laboratory. Atlanta, Ga, USA: Department of Health and Human Services; 2011.
378. Farrar JH, P.; Junghanss, T.; Kang,G.; Lalloo,D.G.; White,N.J. Manson's Tropical Infectious Diseases. 23rd ed. London: Elsevier; 2015.
379. Cruickshank DB. Bacteriology of tuberculosis. Modern practice of tuberculosis. London: Butterworth; 1952: 53.
380. Yeager H, Jr., Lacy J, Smith LR, LeMaistre CA. Quantitative studies of mycobacterial populations in sputum and saliva. *Am Rev Respir Dis* 1967; **95**(6): 998-1004.
381. Hobby GL, Holman AP, Iseman MD, Jones JM. Enumeration of tubercle bacilli in sputum of patients with pulmonary tuberculosis. *Antimicrob Agents Chemother* 1973; **4**(2): 94-104.
382. Steingart KR, Henry M, Ng V, et al. Fluorescence versus conventional sputum smear microscopy for tuberculosis: a systematic review. *Lancet Infect Dis* 2006; **6**(9): 570-81.
383. Treuer R, Haydel SE. Acid-fast staining and Petroff-Hausser chamber counting of mycobacterial cells in liquid suspension. *Curr Protoc Microbiol* 2011; **Chapter 10**: Unit 10A 6.
384. Ryan GJ, Shapiro HM, Lenaerts AJ. Improving acid-fast fluorescent staining for the detection of mycobacteria using a new nucleic acid staining approach. *Tuberculosis (Edinb)* 2014; **94**(5): 511-8.
385. Bhatt A, Fujiwara N, Bhatt K, et al. Deletion of kasB in Mycobacterium tuberculosis causes loss of acid-fastness and subclinical latent tuberculosis in immunocompetent mice. *Proc Natl Acad Sci U S A* 2007; **104**(12): 5157-62.
386. Deb C, Lee CM, Dubey VS, et al. A novel in vitro multiple-stress dormancy model for Mycobacterium tuberculosis generates a lipid-loaded, drug-tolerant, dormant pathogen. *PLoS One* 2009; **4**(6): e6077.
387. Ryan GJ, Hoff DR, Driver ER, et al. Multiple M. tuberculosis phenotypes in mouse and guinea pig lung tissue revealed by a dual-staining approach. *PLoS One* 2010; **5**(6): e11108.
388. Seiler P, Ulrichs T, Bandermann S, et al. Cell-wall alterations as an attribute of Mycobacterium tuberculosis in latent infection. *J Infect Dis* 2003; **188**(9): 1326-31.

389. Ulrichs T, Lefmann M, Reich M, et al. Modified immunohistological staining allows detection of Ziehl-Neelsen-negative Mycobacterium tuberculosis organisms and their precise localization in human tissue. *J Pathol* 2005; **205**(5): 633-40.
390. Yuan Y, Zhu Y, Crane DD, Barry CE, 3rd. The effect of oxygenated mycolic acid composition on cell wall function and macrophage growth in Mycobacterium tuberculosis. *Mol Microbiol* 1998; **29**(6): 1449-58.
391. Sutton S. Accuracy of plate counting. *Journal of validation technology* 2011; (Summer 2011): 42-6.
392. Hafner R, Cohn JA, Wright DJ, et al. Early bactericidal activity of isoniazid in pulmonary tuberculosis. Optimization of methodology. The DATRI 008 Study Group. *Am J Respir Crit Care Med* 1997; **156**(3 Pt 1): 918-23.
393. Sirgel F, Venter A, Mitchison D. Sources of variation in studies of the early bactericidal activity of antituberculosis drugs. *J Antimicrob Chemother* 2001; **47**(2): 177-82.
394. Muyoyeta M, Schaap JA, De Haas P, et al. Comparison of four culture systems for Mycobacterium tuberculosis in the Zambian National Reference Laboratory. *Int J Tuberc Lung Dis* 2009; **13**(4): 460-5.
395. Lee JJ, Suo J, Lin CB, Wang JD, Lin TY, Tsai YC. Comparative evaluation of the BACTEC MGIT 960 system with solid medium for isolation of mycobacteria. *Int J Tuberc Lung Dis* 2003; **7**(6): 569-74.
396. Chien HP, Yu MC, Wu MH, Lin TP, Luh KT. Comparison of the BACTEC MGIT 960 with Lowenstein-Jensen medium for recovery of mycobacteria from clinical specimens. *Int J Tuberc Lung Dis* 2000; **4**(9): 866-70.
397. Dhillon J, Fourie PB, Mitchison DA. Persister populations of Mycobacterium tuberculosis in sputum that grow in liquid but not on solid culture media. *J Antimicrob Chemother* 2014; **69**(2): 437-40.
398. Kana BD, Mizrahi V. Resuscitation-promoting factors as lytic enzymes for bacterial growth and signaling. *FEMS Immunol Med Microbiol* 2010; **58**(1): 39-50.
399. Mukamolova GV, Turapov OA, Young DI, Kaprelyants AS, Kell DB, Young M. A family of autocrine growth factors in Mycobacterium tuberculosis. *Mol Microbiol* 2002; **46**(3): 623-35.
400. Rosser A, Stover C, Pareek M, Mukamolova GV. Resuscitation-promoting factors are important determinants of the pathophysiology in Mycobacterium tuberculosis infection. *Crit Rev Microbiol* 2017: 1-10.
401. Turapov O, Glenn S, Kana B, Makarov V, Andrew PW, Mukamolova GV. The in vivo environment accelerates generation of resuscitation-promoting factor-dependent mycobacteria. *Am J Respir Crit Care Med* 2014; **190**(12): 1455-7.
402. Shleeva MO, Bagramyan K, Telkov MV, et al. Formation and resuscitation of "non-culturable" cells of Rhodococcus rhodochrous and Mycobacterium tuberculosis in prolonged stationary phase. *Microbiology* 2002; **148**(Pt 5): 1581-91.
403. Biketov S, Mukamolova GV, Potapov V, et al. Culturability of Mycobacterium tuberculosis cells isolated from murine macrophages: a bacterial growth factor promotes recovery. *FEMS Immunol Med Microbiol* 2000; **29**(4): 233-40.
404. Kana BD, Gordhan BG, Downing KJ, et al. The resuscitation-promoting factors of Mycobacterium tuberculosis are required for virulence and resuscitation from dormancy but are collectively dispensable for growth in vitro. *Mol Microbiol* 2008; **67**(3): 672-84.

405. Hu Y, Liu A, Ortega-Muro F, Alameda-Martin L, Mitchison D, Coates A. High-dose rifampicin kills persisters, shortens treatment duration, and reduces relapse rate in vitro and in vivo. *Front Microbiol* 2015; **6**: 641.
406. Mukamolova GV, Turapov O, Malkin J, Woltmann G, Barer MR. Resuscitation-promoting factors reveal an occult population of tubercle Bacilli in Sputum. *Am J Respir Crit Care Med* 2010; **181**(2): 174-80.
407. Chengalroyen MD, Beukes GM, Gordhan BG, et al. Detection and Quantification of Differentially Culturable Tubercle Bacteria in Sputum from Patients with Tuberculosis. *Am J Respir Crit Care Med* 2016; **194**(12): 1532-40.
408. Lambrecht RS, Carriere JF, Collins MT. A model for analyzing growth kinetics of a slowly growing Mycobacterium sp. *Appl Environ Microbiol* 1988; **54**(4): 910-6.
409. Barr DA, Kamdolozi M, Nishihara Y, et al. Serial image analysis of Mycobacterium tuberculosis colony growth reveals a persistent subpopulation in sputum during treatment of pulmonary TB. *Tuberculosis (Edinb)* 2016; **98**: 110-5.
410. Bowness R, Boeree MJ, Aarnoutse R, et al. The relationship between Mycobacterium tuberculosis MGIT time to positivity and cfu in sputum samples demonstrates changing bacterial phenotypes potentially reflecting the impact of chemotherapy on critical sub-populations. *J Antimicrob Chemother* 2015; **70**(2): 448-55.
411. Diacon AH, Maritz JS, Venter A, van Helden PD, Dawson R, Donald PR. Time to liquid culture positivity can substitute for colony counting on agar plates in early bactericidal activity studies of antituberculosis agents. *Clin Microbiol Infect* 2012; **18**(7): 711-7.
412. Sloan DJ, Mwandumba HC, Garton NJ, et al. Pharmacodynamic modelling of bacillary elimination rates and detection of bacterial lipid bodies in sputum to predict and understand outcomes in treatment of pulmonary tuberculosis. *Clin Infect Dis* 2015.
413. Diacon AH, van der Merwe L, Demers AM, von Groote-Bidlingmaier F, Venter A, Donald PR. Time to positivity in liquid culture predicts colony forming unit counts of Mycobacterium tuberculosis in sputum specimens. *Tuberculosis (Edinb)* 2014; **94**(2): 148-51.
414. Bark CM, Okwera A, Joloba ML, et al. Time to detection of Mycobacterium tuberculosis as an alternative to quantitative cultures. *Tuberculosis (Edinb)* 2011; **91**(3): 257-9.
415. Diacon AH, Maritz JS, Venter A, et al. Time to detection of the growth of Mycobacterium tuberculosis in MGIT 960 for determining the early bactericidal activity of antituberculosis agents. *Eur J Clin Microbiol Infect Dis* 2010; **29**(12): 1561-5.
416. Kolibab K, Yang A, Parra M, Derrick SC, Morris SL. Time to detection of Mycobacterium tuberculosis using the MGIT 320 system correlates with colony counting in preclinical testing of new vaccines. *Clin Vaccine Immunol* 2014; **21**(3): 453-5.
417. Pheiffer C, Carroll NM, Beyers N, et al. Time to detection of Mycobacterium tuberculosis in BACTEC systems as a viable alternative to colony counting. *Int J Tuberc Lung Dis* 2008; **12**(7): 792-8.
418. Blodgett R. BAM Appendix 2: Most Probable Number from Serial Dilutions. 2010. https://www.fda.gov/Food/FoodScienceResearch/LaboratoryMethods/ucm109656.htm (accessed 06/06/2018 2018).

419. Blakemore R, Story E, Helb D, et al. Evaluation of the analytical performance of the Xpert MTB/RIF assay. *J Clin Microbiol* 2010; **48**(7): 2495-501.
420. van Zyl-Smit RN, Binder A, Meldau R, et al. Comparison of quantitative techniques including Xpert MTB/RIF to evaluate mycobacterial burden. *PLoS One* 2011; **6**(12): e28815.
421. Blakemore R, Nabeta P, Davidow AL, et al. A multisite assessment of the quantitative capabilities of the Xpert MTB/RIF assay. *Am J Respir Crit Care Med* 2011; **184**(9): 1076-84.
422. Kayigire XA, Friedrich SO, Venter A, et al. Direct comparison of Xpert MTB/RIF assay with liquid and solid mycobacterial culture for quantification of early bactericidal activity. *J Clin Microbiol* 2013; **51**(6): 1894-8.
423. Pathak S, Awuh JA, Leversen NA, Flo TH, Asjo B. Counting mycobacteria in infected human cells and mouse tissue: a comparison between qPCR and CFU. *PLoS One* 2012; **7**(4): e34931.
424. Honeyborne I, McHugh TD, Phillips PP, et al. Molecular bacterial load assay, a culture-free biomarker for rapid and accurate quantification of sputum Mycobacterium tuberculosis bacillary load during treatment. *J Clin Microbiol* 2011; **49**(11): 3905-11.
425. Honeyborne I, Mtafya B, Phillips PP, et al. The molecular bacterial load assay replaces solid culture for measuring early bactericidal response to antituberculosis treatment. *J Clin Microbiol* 2014; **52**(8): 3064-7.
426. de Knegt GJ, Dickinson L, Pertinez H, et al. Assessment of treatment response by colony forming units, time to culture positivity and the molecular bacterial load assay compared in a mouse tuberculosis model. *Tuberculosis (Edinb)* 2017; **105**: 113-8.
427. Malherbe ST, Shenai S, Ronacher K, et al. Persisting positron emission tomography lesion activity and Mycobacterium tuberculosis mRNA after tuberculosis cure. *Nat Med* 2016; **22**(10): 1094-100.
428. Devonshire AS, O'Sullivan DM, Honeyborne I, et al. The use of digital PCR to improve the application of quantitative molecular diagnostic methods for tuberculosis. *BMC Infect Dis* 2016; **16**: 366.
429. Aldous WK, Pounder JI, Cloud JL, Woods GL. Comparison of six methods of extracting Mycobacterium tuberculosis DNA from processed sputum for testing by quantitative real-time PCR. *J Clin Microbiol* 2005; **43**(5): 2471-3.
430. Amaro A, Duarte E, Amado A, Ferronha H, Botelho A. Comparison of three DNA extraction methods for Mycobacterium bovis, Mycobacterium tuberculosis and Mycobacterium avium subsp. avium. *Lett Appl Microbiol* 2008; **47**(1): 8-11.
431. Pan S, Gu B, Wang H, et al. Comparison of four DNA extraction methods for detecting Mycobacterium tuberculosis by real-time PCR and its clinical application in pulmonary tuberculosis. *J Thorac Dis* 2013; **5**(3): 251-7.
432. Radomski N, Kreitmann L, McIntosh F, Behr MA. The critical role of DNA extraction for detection of mycobacteria in tissues. *PLoS One* 2013; **8**(10): e78749.
433. Thakur R, Sarma S, Goyal R. Comparison of DNA Extraction Protocols for Mycobacterium Tuberculosis in Diagnosis of Tuberculous Meningitis by Real-time Polymerase Chain Reaction. *J Glob Infect Dis* 2011; **3**(4): 353-6.
434. Palomo FS, Rivero MGC, Quiles MG, Pinto FP, Machado AMO, Carlos Campos Pignatari A. Comparison of DNA Extraction Protocols and Molecular Targets to Diagnose Tuberculous Meningitis. *Tuberc Res Treat* 2017; **2017**: 5089046.
435. Steen HB. Flow cytometry of bacteria: glimpses from the past with a view to the future. *J Microbiol Methods* 2000; **42**(1): 65-74.

436. Muller S, Nebe-von-Caron G. Functional single-cell analyses: flow cytometry and cell sorting of microbial populations and communities. *FEMS Microbiol Rev* 2010; **34**(4): 554-87.
437. Shapiro HM. Practical flow cytometry. 4th ed. New Jersey: Wiley; 2003.
438. Biosciences B. Threshold and analysis of small particles on the BD Accuri(TM) C6 cytometer. In: Biosciences B, editor. San Jose, CA.: BD Biosciences; 2012.
439. Longobardi-Givan A. Folw cytometry: first principles. New York: Wiley-Liss; 2001.
440. Biosciences B. A guide to absolute counting using the BD Accuri(TM) C6 flow cytometer. In: Biosciences B, editor. San Jose, CA.: BD Biosciences.; 2012.
441. Costerton JW, Lewandowski Z, Caldwell DE, Korber DR, Lappin-Scott HM. Microbial biofilms. *Annu Rev Microbiol* 1995; **49**: 711-45.
442. James BW, Williams A, Marsh PD. The physiology and pathogenicity of Mycobacterium tuberculosis grown under controlled conditions in a defined medium. *J Appl Microbiol* 2000; **88**(4): 669-77.
443. Hendon-Dunn CL, Doris KS, Thomas SR, et al. A flow cytometry method for rapidly assessing M. tuberculosis responses to antibiotics with different modes of action. *Antimicrob Agents Chemother* 2016.
444. Scott LE, Gous N, Cunningham BE, et al. Dried culture spots for Xpert MTB/RIF external quality assessment: results of a phase 1 pilot study in South Africa. *J Clin Microbiol* 2011; **49**(12): 4356-60.
445. Pina-Vaz C, Costa-de-Oliveira S, Rodrigues AG. Safe susceptibility testing of Mycobacterium tuberculosis by flow cytometry with the fluorescent nucleic acid stain SYTO 16. *J Med Microbiol* 2005; **54**(Pt 1): 77-81.
446. Gollnick NS, Mitchell RM, Baumgart M, Janagama HK, Sreevatsan S, Schukken YH. Survival of Mycobacterium avium subsp. paratuberculosis in bovine monocyte-derived macrophages is not affected by host infection status but depends on the infecting bacterial genotype. *Vet Immunol Immunopathol* 2007; **120**(3-4): 93-105.
447. Akselband Y, Cabral C, Shapiro DS, McGrath P. Rapid mycobacteria drug susceptibility testing using Gel Microdrop (GMD) Growth Assay and flow cytometry. *J Microbiol Methods* 2005; **62**(2): 181-97.
448. Walberg M, Gaustad P, Steen HB. Uptake kinetics of nucleic acid targeting dyes in S. aureus, E. faecalis and B. cereus: a flow cytometric study. *J Microbiol Methods* 1999; **35**(2): 167-76.
449. Shi L, Gunther S, Hubschmann T, Wick LY, Harms H, Muller S. Limits of propidium iodide as a cell viability indicator for environmental bacteria. *Cytometry A* 2007; **71**(8): 592-8.
450. Biosciences B. BD Cell Viability Kit. In: Biosciences B, editor. Product insert. San Jose: BD Biosciences; 2011.
451. Probes M. LIVE/DEAD BacLight Bacterial Viability Kits2004, 2004. (accessed 3rd March 2016).
452. Nebe-von-Caron G. Standardization in microbial cytometry. *Cytometry A* 2009; **75**(2): 86-9.
453. Votyakova TV, Kaprelyants AS, Kell DB. Influence of Viable Cells on the Resuscitation of Dormant Cells in Micrococcus luteus Cultures Held in an Extended Stationary Phase: the Population Effect. *Appl Environ Microbiol* 1994; **60**(9): 3284-91.

454. Bosshard F, Berney M, Scheifele M, Weilenmann HU, Egli T. Solar disinfection (SODIS) and subsequent dark storage of Salmonella typhimurium and Shigella flexneri monitored by flow cytometry. *Microbiology* 2009; **155**(Pt 4): 1310-7.
455. Joux F, Lebaron P. Use of fluorescent probes to assess physiological functions of bacteria at single-cell level. *Microbes Infect* 2000; **2**(12): 1523-35.
456. Lebaron P, Catala P, Parthuisot N. Effectiveness of SYTOX Green stain for bacterial viability assessment. *Appl Environ Microbiol* 1998; **64**(7): 2697-700.
457. Langsrud S, Sundheim G. Flow cytometry for rapid assessment of viability after exposure to a quaternary ammonium compound. *J Appl Bacteriol* 1996; **81**(4): 411-8.
458. Caron GN, Stephens P, Badley RA. Assessment of bacterial viability status by flow cytometry and single cell sorting. *J Appl Microbiol* 1998; **84**(6): 988-98.
459. Müller S, Bley T. High Resolution Microbial Single Cell Analytics: Springer Berlin Heidelberg; 2011.
460. Bornscheuer UT. Microbial carboxyl esterases: classification, properties and application in biocatalysis. *FEMS Microbiol Rev* 2002; **26**(1): 73-81.
461. Berney M, Vital M, Hulshoff I, Weilenmann HU, Egli T, Hammes F. Rapid, cultivation-independent assessment of microbial viability in drinking water. *Water Res* 2008; **42**(14): 4010-8.
462. Nebe-von-Caron G, Stephens PJ, Hewitt CJ, Powell JR, Badley RA. Analysis of bacterial function by multi-colour fluorescence flow cytometry and single cell sorting. *J Microbiol Methods* 2000; **42**(1): 97-114.
463. Breeuwer P, Abee T. Assessment of viability of microorganisms employing fluorescence techniques. *Int J Food Microbiol* 2000; **55**(1-3): 193-200.
464. Hammes F, Berney M, Egli T. Cultivation-independent assessment of bacterial viability. *Adv Biochem Eng Biotechnol* 2011; **124**: 123-50.
465. Novo D, Perlmutter NG, Hunt RH, Shapiro HM. Accurate flow cytometric membrane potential measurement in bacteria using diethyloxacarbocyanine and a ratiometric technique. *Cytometry* 1999; **35**(1): 55-63.
466. Davies GR. Discussion document on operational definitions of cell states. University of Liverpool: PreDiCT-TB; 2015.
467. Davey HM. Life, death, and in-between: meanings and methods in microbiology. *Appl Environ Microbiol* 2011; **77**(16): 5571-6.
468. Pina-Vaz C, Costa-Oliveira S, Rodrigues AG, Salvador A. Novel Method Using a Laser Scanning Cytometer for Detection of Mycobacteria in Clinical Samples. *Journal of Clinical Microbiology* 2004; **42**(2): 906-8.
469. Soejima T, Iida K, Qin T, Taniai H, Yoshida S. Discrimination of live, anti-tuberculosis agent-injured, and dead Mycobacterium tuberculosis using flow cytometry. *FEMS Microbiol Lett* 2009; **294**(1): 74-81.
470. Hammond RJ, Baron VO, Oravcova K, Lipworth S, Gillespie SH. Phenotypic resistance in mycobacteria: is it because I am old or fat that I resist you? *J Antimicrob Chemother* 2015; **70**(10): 2823-7.
471. Gonzalez YMJA, Zaragoza-Contreras R, Guadarrama-Medina R, et al. Evaluation of the cell growth of mycobacteria using Mycobacterium smegmatis mc2 155 as a representative species. *J Microbiol* 2012; **50**(3): 419-25.
472. Qin D, He X, Wang K, Tan W. Using fluorescent nanoparticles and SYBR Green I based two-color flow cytometry to determine Mycobacterium tuberculosis avoiding false positives. *Biosens Bioelectron* 2008; **24**(4): 626-31.

473. Shapiro HM. Flow cytometry of bacterial membrane potential and permeability. *Methods Mol Med* 2008; **142**: 175-86.
474. Fredricks BA, DeCoster DJ, Kim Y, Sparks N, Callister SM, Schell RF. Rapid pyrazinamide susceptibility testing of Mycobacterium tuberculosis by flow cytometry. *Journal of Microbiological Methods* 2006; **67**(2): 266-72.
475. DeCoster DJ, Vena RM, Callister SM, Schell RF. Susceptibility testing of Mycobacterium tuberculosis: comparison of the BACTEC TB-460 method and flow cytometric assay with the proportion method. *Clin Microbiol Infect* 2005; **11**(5): 372-8.
476. Reis RS, Neves I, Lourenco SLS, Fonseca LS, Lourenco MCS. Comparison of Flow Cytometric and Alamar Blue Tests with the Proportional Method for Testing Susceptibility of Mycobacterium tuberculosis to Rifampin and Isoniazid. *Journal of Clinical Microbiology* 2004; **42**(5): 2247-8.
477. Govender SdP, S.J.; van de Venter, M.; Hayes, C. Antibiotic susptibility of multi-drug resistant Mycobacterium tuberculosis using flow cytometry. *Medical Technology SA* 2010; **24**(2): 25-8.
478. Burdz TVN, Wolfe J, Kabani A. Evaluation of sputum decontamination methods for Mycobacterium tuberculosis using viable colony counts and flow cytometry. *Diagnostic Microbiology and Infectious Disease* 2003; **47**(3): 503-9.
479. Piuri M, Jacobs WR, Jr., Hatfull GF. Fluoromycobacteriophages for rapid, specific, and sensitive antibiotic susceptibility testing of Mycobacterium tuberculosis. *PLoS One* 2009; **4**(3): e4870.
480. Norden MA, Kurzynski TA, Bownds SE, Callister SM, Schell RF. Rapid susceptibility testing of Mycobacterium tuberculosis (H37Ra) by flow cytometry. *J Clin Microbiol* 1995; **33**(5): 1231-7.
481. Bownds SE, Kurzynski TA, Norden MA, Dufek JL, Schell RF. Rapid susceptibility testing for nontuberculosis mycobacteria using flow cytometry. *J Clin Microbiol* 1996; **34**(6): 1386-90.
482. Kirk SM, Schell RF, Moore AV, Callister SM, Mazurek GH. Flow cytometric testing of susceptibilities of Mycobacterium tuberculosis isolates to ethambutol, isoniazid, and rifampin in 24 hours. *J Clin Microbiol* 1998; **36**(6): 1568-73.
483. Moore AV, Kirk SM, Callister SM, Mazurek GH, Schell RF. Safe determination of susceptibility of Mycobacterium tuberculosis to antimycobacterial agents by flow cytometry. *J Clin Microbiol* 1999; **37**(3): 479-83.
484. Vena RM, Munson EL, DeCoster DJ, et al. Flow cytometric testing of susceptibilities of Mycobacterium avium to amikacin, ciprofloxacin, clarithromycin and rifabutin in 24 hours. *Clin Microbiol Infect* 2000; **6**(7): 368-75.
485. Ibrahim P, Whiteley AS, Barer MR. SYTO16 labelling and flow cytometry of Mycobacterium avium. *Lett Appl Microbiol* 1997; **25**(6): 437-41.
486. Ryan C, Nguyen BT, Sullivan SJ. Rapid assay for mycobacterial growth and antibiotic susceptibility using gel microdrop encapsulation. *J Clin Microbiol* 1995; **33**(7): 1720-6.
487. Yi WC, Hsiao S, Liu JH, et al. Use of fluorescein labelled antibody and fluorescence activated cell sorter for rapid identification of Mycobacterium species. *Biochem Biophys Res Commun* 1998; **250**(2): 403-8.
488. Resnick MS, S.; Bercovier,H. Bacterial membrane potential analysed by spectrofluorocytometry. *Current Microbiology* 1985; **12**: 183-6.

489. Saito K, Warrier T, Somersan-Karakaya S, et al. Rifamycin action on RNA polymerase in antibiotic-tolerant Mycobacterium tuberculosis results in differentially detectable populations. *Proc Natl Acad Sci U S A* 2017; **114**(24): E4832-E40.
490. Carr EL, Eales K, Soddell J, Seviour RJ. Improved permeabilization protocols for fluorescence in situ hybridization (FISH) of mycolic-acid-containing bacteria found in foams. *J Microbiol Methods* 2005; **61**(1): 47-54.
491. Cimino M, Alamo L, Salazar L. Permeabilization of the mycobacterial envelope for protein cytolocalization studies by immunofluorescence microscopy. *BMC Microbiol* 2006; **6**: 35.
492. Thanky NR, Young DB, Robertson BD. Unusual features of the cell cycle in mycobacteria: polar-restricted growth and the snapping-model of cell division. *Tuberculosis (Edinb)* 2007; **87**(3): 231-6.
493. Schindelin J, Arganda-Carreras I, Frise E, et al. Fiji: an open-source platform for biological-image analysis. *Nat Methods* 2012; **9**(7): 676-82.
494. Aljayyoussi G, Jenkins VA, Sharma R, et al. Pharmacokinetic-Pharmacodynamic modelling of intracellular Mycobacterium tuberculosis growth and kill rates is predictive of clinical treatment duration. *Sci Rep* 2017; **7**(1): 502.
495. Johnson BK, Abramovitch RB. Macrophage infection models for Mycobacterium tuberculosis. *Methods Mol Biol* 2015; **1285**: 329-41.
496. Portevin D, Gagneux S, Comas I, Young D. Human macrophage responses to clinical isolates from the Mycobacterium tuberculosis complex discriminate between ancient and modern lineages. *PLoS Pathog* 2011; **7**(3): e1001307.
497. Wallis RS, Patil S, Cheon SH, et al. Drug tolerance in Mycobacterium tuberculosis. *Antimicrob Agents Chemother* 1999; **43**(11): 2600-6.
498. Gomez JE, McKinney JD. M. tuberculosis persistence, latency, and drug tolerance. *Tuberculosis (Edinb)* 2004; **84**(1-2): 29-44.
499. Kester JC, Fortune SM. Persisters and beyond: mechanisms of phenotypic drug resistance and drug tolerance in bacteria. *Crit Rev Biochem Mol Biol* 2014; **49**(2): 91-101.
500. Lewis K. Persister cells, dormancy and infectious disease. *Nat Rev Microbiol* 2007; **5**(1): 48-56.
501. Wu Y, Vulic M, Keren I, Lewis K. Role of oxidative stress in persister tolerance. *Antimicrob Agents Chemother* 2012; **56**(9): 4922-6.
502. Schaechter M. Of Terms in Biology: Bacterial Ploidy. In: Schaechter MK, R., editor. Small things considered: Of Terms in Biology: Bacterial Ploidy: American Society of Microbiology; 2010.
503. Warner DF, Evans JC, Mizrahi V. Nucleotide Metabolism and DNA Replication. *Microbiol Spectr* 2014; **2**(5).
504. Ditse Z, Lamers MH, Warner DF. DNA Replication in Mycobacterium tuberculosis. *Microbiol Spectr* 2017; **5**(2).
505. Biomarkers Definitions Working G. Biomarkers and surrogate endpoints: preferred definitions and conceptual framework. *Clin Pharmacol Ther* 2001; **69**(3): 89-95.
506. Boissel JP, Collet JP, Moleur P, Haugh M. Surrogate endpoints: a basis for a rational approach. *Eur J Clin Pharmacol* 1992; **43**(3): 235-44.
507. De Gruttola VG, Clax P, DeMets DL, et al. Considerations in the evaluation of surrogate endpoints in clinical trials. summary of a National Institutes of Health workshop. *Control Clin Trials* 2001; **22**(5): 485-502.

508. (CDER) USDoHaHSFaDACfDEaR. Antiretroviral Drugs Using Plasma HIV RNA Measurements - Clinical Considerations for Accelerated and Traditional Approval: FDA, 2002.
509. Murray JS, Elashoff MR, Iacono-Connors LC, Cvetkovich TA, Struble KA. The use of plasma HIV RNA as a study endpoint in efficacy trials of antiretroviral drugs. *AIDS* 1999; **13**(7): 797-804.
510. Grinsztejn B, Nguyen BY, Katlama C, et al. Safety and efficacy of the HIV-1 integrase inhibitor raltegravir (MK-0518) in treatment-experienced patients with multidrug-resistant virus: a phase II randomised controlled trial. *Lancet* 2007; **369**(9569): 1261-9.
511. Gulick RM, Su Z, Flexner C, et al. Phase 2 study of the safety and efficacy of vicriviroc, a CCR5 inhibitor, in HIV-1-Infected, treatment-experienced patients: AIDS clinical trials group 5211. *J Infect Dis* 2007; **196**(2): 304-12.
512. Landovitz RJ, Angel JB, Hoffmann C, et al. Phase II study of vicriviroc versus efavirenz (both with zidovudine/lamivudine) in treatment-naive subjects with HIV-1 infection. *J Infect Dis* 2008; **198**(8): 1113-22.
513. Saag MS, Sonnerborg A, Torres RA, et al. Antiretroviral effect and safety of abacavir alone and in combination with zidovudine in HIV-infected adults. Abacavir Phase 2 Clinical Team. *AIDS* 1998; **12**(16): F203-9.
514. Schooley RT, Ruane P, Myers RA, et al. Tenofovir DF in antiretroviral-experienced patients: results from a 48-week, randomized, double-blind study. *AIDS* 2002; **16**(9): 1257-63.
515. Zolopa AR, Berger DS, Lampiris H, et al. Activity of elvitegravir, a once-daily integrase inhibitor, against resistant HIV Type 1: results of a phase 2, randomized, controlled, dose-ranging clinical trial. *J Infect Dis* 2010; **201**(6): 814-22.
516. (CDER) USDoHaHSFaDACfDEaR. Fast Track Drug Development Programs-Designation, Development, And Application Review.: US Food and Drug Administration, 2004.
517. Baker SG, Kramer BS. A perfect correlate does not a surrogate make. *BMC Med Res Methodol* 2003; **3**: 16.
518. Fleming TR, DeMets DL. Surrogate end points in clinical trials: are we being misled? *Ann Intern Med* 1996; **125**(7): 605-13.
519. Davies GR. Early clinical development of anti-tuberculosis drugs: science, statistics and sterilizing activity. *Tuberculosis (Edinb)* 2010; **90**(3): 171-6.
520. Davies GR, Phillips PP, Nunn AJ. Biomarkers and surrogate end points in clinical trials of tuberculosis treatment. *J Infect Dis* 2007; **196**(4): 648-9; author reply 9-50.
521. Phillips PP, Davies GR, Mitchison DA. Biomarkers for tuberculosis disease activity, cure, and relapse. *Lancet Infect Dis* 2010; **10**(2): 69-70; author reply -1.
522. Berlin OG, Zakowski P, Bruckner DA, Johnson BL, Jr. New biphasic culture system for isolation of mycobacteria from blood of patients with acquired immune deficiency syndrome. *J Clin Microbiol* 1984; **20**(3): 572-4.
523. Elliott JL, Hoppes WL, Platt MS, Thomas JG, Patel IP, Gansar A. The acquired immunodeficiency syndrome and Mycobacterium avium-intracellulare bacteremia in a patient with hemophilia. *Ann Intern Med* 1983; **98**(3): 290-3.
524. Landau W, Feczko J, Kaplan RL. Radiometric detection of mycobacteria in routine blood cultures. *J Clin Microbiol* 1980; **12**(3): 477-8.

525. Macher AM, Kovacs JA, Gill V, et al. Bacteremia due to Mycobacterium avium-intracellulare in the acquired immunodeficiency syndrome. *Ann Intern Med* 1983; **99**(6): 782-5.
526. Pierce PF, DeYoung DR, Roberts GD. Mycobacteremia and the new blood culture systems. *Ann Intern Med* 1983; **99**(6): 786-9.
527. Salfinger M, Stool EW, Piot D, Heifets L. Comparison of three methods for recovery of Mycobacterium avium complex from blood specimens. *J Clin Microbiol* 1988; **26**(6): 1225-6.
528. Bower K, Begg DJ, Whittington RJ. Optimisation of culture of Mycobacterium avium subspecies paratuberculosis from blood samples. *J Microbiol Methods* 2010; **80**(1): 93-9.
529. Bower KL, Begg DJ, Whittington RJ. Culture of Mycobacterium avium subspecies paratuberculosis (MAP) from blood and extra-intestinal tissues in experimentally infected sheep. *Vet Microbiol* 2011; **147**(1-2): 127-32.
530. Weichselbaum A. The Elements of Pathological Histology: With Special Reference to Practical Methods (Classic Reprint): Fb&c Limited; 2015.
531. Forsyth CE. The Occurrence of Tubercle Bacilli in the Blood in Tuberculosis. *Br Med J* 1909; **1**(2521): 1001-2.
532. Petty OHM, A.M. Tubercle bacilli in the blood. *JAMA* 1909; **liii**: 867.
533. Rosenberger RC. The presence of tubercle bacilli in the circulating blood in tuberculosis. *Am J Med Sci* 1909; **cxxxvii**: 267.
534. Brem WV. Investigation of blood for tubercle bacilli. *JAMA* 1909: 909.
535. Godwin JH, Stopeck A, Chang VT, Godwin TA. Mycobacteremia in acquired immune deficiency syndrome. Rapid diagnosis based on inclusions in the peripheral blood smear. *Am J Clin Pathol* 1991; **95**(3): 369-75.
536. Nussbaum JM, Dealist C, Lewis W, Heseltine PN. Rapid diagnosis by buffy coat smear of disseminated Mycobacterium avium complex infection in patients with acquired immunodeficiency syndrome. *J Clin Microbiol* 1990; **28**(3): 631-2.
537. Stone BL, Cohn DL, Kane MS, Hildred MV, Wilson ML, Reves RR. Utility of paired blood cultures and smears in diagnosis of disseminated Mycobacterium avium complex infections in AIDS patients. *J Clin Microbiol* 1994; **32**(3): 841-2.
538. Biron F, Reveil JC, Penalba C, Boibieux A, Bertrand JL, Peyramond D. Direct visualization of Mycobacterium tuberculosis in a blood sample from an AIDS patient. *AIDS* 1990; **4**(3): 259.
539. Rebollo MJ, San Juan Garrido R, Folgueira D, et al. Blood and urine samples as useful sources for the direct detection of tuberculosis by polymerase chain reaction. *Diagn Microbiol Infect Dis* 2006; **56**(2): 141-6.
540. Banada PP, Koshy R, Alland D. Detection of Mycobacterium tuberculosis in blood by use of the Xpert MTB/RIF assay. *J Clin Microbiol* 2013; **51**(7): 2317-22.
541. Bwanga F, Disque C, Lorenz MG, et al. Higher blood volumes improve the sensitivity of direct PCR diagnosis of blood stream tuberculosis among HIV-positive patients: an observation study. *BMC Infect Dis* 2015; **15**: 48.
542. Folgueira L, Delgado R, Palenque E, Aguado JM, Noriega AR. Rapid diagnosis of Mycobacterium tuberculosis bacteremia by PCR. *J Clin Microbiol* 1996; **34**(3): 512-5.
543. Crump JA, Tuohy MJ, Morrissey AB, et al. Performance of nucleic acid amplification following extraction of 5 milliliters of whole blood for diagnosis of Mycobacterium tuberculosis bacteremia. *J Clin Microbiol* 2012; **50**(1): 138-41.

544. Shenai S, Amisano D, Ronacher K, et al. Exploring alternative biomaterials for diagnosis of pulmonary tuberculosis in HIV-negative patients by use of the GeneXpert MTB/RIF assay. *J Clin Microbiol* 2013; **51**(12): 4161-6.
545. Hajiabdolbaghi M, Rasoulinejad M, Davoudi AR, Alikhani A, Najafi N. Application of peripheral blood Mycobacterium tuberculosis PCR for diagnosis of tuberculosis patients. *Eur Rev Med Pharmacol Sci* 2014; **18**(2): 185-9.
546. Akane A, Matsubara K, Nakamura H, Takahashi S, Kimura K. Identification of the heme compound copurified with deoxyribonucleic acid (DNA) from bloodstains, a major inhibitor of polymerase chain reaction (PCR) amplification. *J Forensic Sci* 1994; **39**(2): 362-72.
547. Schrader C, Schielke A, Ellerbroek L, Johne R. PCR inhibitors - occurrence, properties and removal. *J Appl Microbiol* 2012; **113**(5): 1014-26.
548. Boyd MA, Tennant SM, Melendez JH, et al. Adaptation of red blood cell lysis represents a fundamental breakthrough that improves the sensitivity of Salmonella detection in blood. *J Appl Microbiol* 2015; **118**(5): 1199-209.
549. Sage BH, Jr., Neece VR. Rapid visual detection of microorganisms in blood culture. *J Clin Microbiol* 1984; **20**(1): 5-8.
550. Mansour JD, Robson JA, Arndt CW, Schulte TH. Detection of Escherichia coli in blood using flow cytometry. *Cytometry* 1985; **6**(3): 186-90.
551. Zierdt CH. Blood-lysing solution nontoxic to pathogenic bacteria. *J Clin Microbiol* 1982; **15**(1): 172-4.
552. Zierdt CH, Peterson DL, Swan JC, MacLowry JD. Lysis-filtration blood culture versus conventional blood culture in a bacteremic rabbit model. *J Clin Microbiol* 1982; **15**(1): 74-7.
553. Control ECfDPa. Handbook on TB laboratory diagnostic methods for the European Union. Stockholm: ECDC, 2016.
554. Thornton CG, MacLellan KM, Brink TL, Jr., et al. Novel method for processing respiratory specimens for detection of mycobacteria by using C18-carboxypropylbetaine: blinded study. *J Clin Microbiol* 1998; **36**(7): 1996-2003.
555. Steingart KR, Ng V, Henry M, et al. Sputum processing methods to improve the sensitivity of smear microscopy for tuberculosis: a systematic review. *Lancet Infect Dis* 2006; **6**(10): 664-74.
556. diagnostics GLIfaT. Mycobacteriology Laboratory Manual. Geneva: WHO, 2014.
557. den Hertog AL, Klatser PR, Anthony RM. Buoyant density of Mycobacterium tuberculosis: implications for sputum processing. *Int J Tuberc Lung Dis* 2009; **13**(4): 466-71.
558. Ratnam S, March SB. Effect of relative centrifugal force and centrifugation time on sedimentation of mycobacteria in clinical specimens. *J Clin Microbiol* 1986; **23**(3): 582-5.
559. Kamariza M, Shieh P, Ealand CS, et al. Rapid detection of Mycobacterium tuberculosis in sputum with a solvatochromic trehalose probe. *Sci Transl Med* 2018; **10**(430).
560. Chakravorty S, Simmons AM, Rowneki M, et al. The New Xpert MTB/RIF Ultra: Improving Detection of Mycobacterium tuberculosis and Resistance to Rifampin in an Assay Suitable for Point-of-Care Testing. *MBio* 2017; **8**(4).
561. Grosset J. Mycobacterium tuberculosis in the extracellular compartment: an underestimated adversary. *Antimicrob Agents Chemother* 2003; **47**(3): 833-6.

562. Hoff DR, Ryan GJ, Driver ER, et al. Location of intra- and extracellular M. tuberculosis populations in lungs of mice and guinea pigs during disease progression and after drug treatment. *PLoS One* 2011; **6**(3): e17550.
563. Lenaerts A, Barry CE, 3rd, Dartois V. Heterogeneity in tuberculosis pathology, microenvironments and therapeutic responses. *Immunol Rev* 2015; **264**(1): 288-307.
564. Lerner TR, de Souza Carvalho-Wodarz C, Repnik U, et al. Lymphatic endothelial cells are a replicative niche for Mycobacterium tuberculosis. *J Clin Invest* 2016; **126**(3): 1093-108.
565. Sutton DW, Chen PC, Schmid-Schonbein GW. Cell separation in the buffy coat. *Biorheology* 1988; **25**(4): 663-73.
566. Teetson W, Cartwright C, Dreiling BJ, Steinberg MH. The leukocyte composition of peripheral blood buffy coat. *Am J Clin Pathol* 1983; **79**(4): 500-1.
567. Eum SY, Kong JH, Hong MS, et al. Neutrophils are the predominant infected phagocytic cells in the airways of patients with active pulmonary TB. *Chest* 2010; **137**(1): 122-8.
568. DuPont HL, Spink WW. Infections due to gram-negative organisms: an analysis of 860 patients with bacteremia at the University of Minnesota Medical Center, 1958-1966. *Medicine (Baltimore)* 1969; **48**(4): 307-32.
569. Henry NK, McLimans CA, Wright AJ, Thompson RL, Wilson WR, Washington JA, 2nd. Microbiological and clinical evaluation of the isolator lysis-centrifugation blood culture tube. *J Clin Microbiol* 1983; **17**(5): 864-9.
570. Kreger BE, Craven DE, Carling PC, McCabe WR. Gram-negative bacteremia. III. Reassessment of etiology, epidemiology and ecology in 612 patients. *Am J Med* 1980; **68**(3): 332-43.
571. Yagupsky P, Nolte FS. Quantitative aspects of septicemia. *Clin Microbiol Rev* 1990; **3**(3): 269-79.
572. Kellogg JA, Manzella JP, Shaffer SN, Schwartz BB. Clinical relevance of culture versus screens for the detection of microbial pathogens in urine specimens. *Am J Med* 1987; **83**(4): 739-45.
573. Wain J, Diep TS, Ho VA, et al. Quantitation of bacteria in blood of typhoid fever patients and relationship between counts and clinical features, transmissibility, and antibiotic resistance. *J Clin Microbiol* 1998; **36**(6): 1683-7.
574. Havlir D, Kemper CA, Deresinski SC. Reproducibility of lysis-centrifugation cultures for quantification of Mycobacterium avium complex bacteremia. *J Clin Microbiol* 1993; **31**(7): 1794-8.
575. Cliff JM, Kaufmann SH, McShane H, van Helden P, O'Garra A. The human immune response to tuberculosis and its treatment: a view from the blood. *Immunol Rev* 2015; **264**(1): 88-102.
576. Barry CE, 3rd, Boshoff HI, Dartois V, et al. The spectrum of latent tuberculosis: rethinking the biology and intervention strategies. *Nat Rev Microbiol* 2009; **7**(12): 845-55.
577. Esmail H, Barry CE, 3rd, Wilkinson RJ. Understanding latent tuberculosis: the key to improved diagnostic and novel treatment strategies. *Drug Discov Today* 2012; **17**(9-10): 514-21.
578. Rockwood N, Pasipanodya JG, Denti P, et al. Concentration-Dependent Antagonism and Culture Conversion in Pulmonary Tuberculosis. *Clin Infect Dis* 2017; **64**(10): 1350-9.

8 Appendix

8.1 Ethics approvals

The sub-study described in chapter 5 was completed under an amendment to the KDHTB ethics approval by the Human Research Ethics Committee (HREC), University of Cape Town. The HREC submission protocol and approval documentation are attached below.

Form FHS006: Protocol Amendment

HREC office use only (FWA00001637; IRB00001938)			
☐ Approved	☐ Type of review: Expedited	☐ Full committee	
This serves as notification that all changes and documentation described below are approved.			
Signature Chairperson of the HREC		Date	

Note: All major amendments must include a local **PI Synopsis** justifying the changes for the amendment. Please note that incomplete amendment submissions will not be reviewed.

Comments from the HREC to the Principal Investigator:
Note: The approval of this protocol amendment does not grant annual approval. Please complete the FHS016 / FHS017 form for annual approval at least one month before study expiration.

Principal Investigator to complete the following:

1. Protocol information

Date (when submitting this form)	11 July 2017	
HREC REF Number	057/2013	
Protocol title	Defining interventions to reduce mortality in severe HIV-associated tuberculosis (Short title: KDH-TB study)	
Protocol number (if applicable)	NA	
Principal Investigator	Graeme Meintjes	
Department / Office Internal Mail Address	CIDRI office, 1st floor, Wolfson Pavilion, IDM, FHS	
1.1 Is this a major or a minor amendment? (see FHS006hlp) Major (tick box) Minor (tick box)	☐ Major	✓ Minor

1.2 Does this protocol receive US Federal funding?	☐ Yes	✓ No
1.3 If the amendment is a major amendment and receives US Federal Funding, does the amendment require full committee approval?	☐ Yes	☐ No

2. List of Proposed Amendments with Revised Version Numbers and Dates

Please itemise on the page below, all amendments with revised version numbers and dates, which need approval. This page will be detached, signed and returned to the PI as notification of approval. Please add extra pages if necessary.
Revised consent form "KDHTB_MTBBSI_serial_quantification.ICF_English.V3.0_12Jul2017" See section 4.1

3. Protocol status (tick ✓)

✓	Open to enrolment
☐	No participants have been enrolled
☐ ☐ ☐ ☐	Closed to enrolment (tick ✓) Research-related activities are ongoing Research-related activities are complete, long-term follow-up only Research-related activities are complete, data analysis only

4. Proposed changes will affect: (tick ✓ all the categories that apply)

	Protocol
☐	Study objectives, design (including investigator's brochure, clinical activities, study length)

☐	Study instruments, questionnaires, interview schedules
✓	Sample size
☐	Recruitment methods
✓	Eligibility criteria (inclusion and exclusion criteria)
☐	Drug/device (composition, amount, schedule, route of administration, combination with other drugs/devices, safety information)
☐	Data collection/ analysis
☐	Principal Investigator. (Please attach revised conflict of interest and PI declaration statements. Refer: sections 7 and 8.4 in the New Protocol Application Form FHS013)
✓	Consent form and information sheet
☐	Recruitment materials (e.g. advertisements)
☐	Administrative (e.g. change in sponsor's name, change in contact information)
✓	Other. Please specify: • We want to take a higher volume of blood during scheduled venesections, for additional/novel detection of *M. tuberculosis* blood stream infection.

4.1 In your opinion, will there be any **increase** in risk, discomfort or inconvenience to participants?	✓ Yes	☐ No
If yes, please provide a detailed justification/explanation:		

Explanation

The proposed amendment is to take a **larger total volume of blood from individual patients**.

We previously received HREC permission to collect blood at additional time points (6, 24, 48 and 72 hours after recruitment) [057/2013 amendment date 24/04/2016], and also to trial novel techniques to identify *M. tuberculosis* blood stream infection at a single time point [057/2013 amendment date 07/04/2017].

We now want to use the novel techniques (microscopy, polymerase-chain reaction (PCR) and modified culture protocol) in serial time point samples. However, this involves a higher total volume of blood being taken from patients.

To off-set this we will not take the baseline blood samples specified in the original KDH-TB study protocol (~55ml of blood at baseline, 0 hours). Instead we propose taking 18ml of blood at 5 time points (0, 4, 24, 48, 72 hours), totaling 90ml at 72 hours.

Comparison of blood volumes in original protocol, 2016 amendment, and current proposed amendment:

Protocol	**Amendment**	**Volume blood first 24h**	**Total volume blood over 72h**
KDH-TB 057/2013	N/A (original protocol)	55ml	55ml
KDH-TB 057/2013	24/04/2016	60ml	75ml
KDH-TB 057/2013	Current proposal	36ml	90ml

Justification and mitigation of risk, inconvenience, and discomfort

- Repeated blood culture to determine sterilization of the blood compartment is a standard of care in other bacteraemic conditions such as infective endocarditis, and daily venesection is not uncommon among unwell inpatients.
- Although from a different patient population, it has been shown that 100ml of blood venesectioned at a single time point is associated with a mean 0.7g/dL (SE for mean 0.1g/dL) haemoglobin drop in inpatients (Thavendiranathan et al 2005). This mean drop was smaller in patients with lower haemoglobin levels on admission, presumably because patients with higher haemoglobin levels lost more per ml venesected. Based on prior literature, Thavendiranathan et al. considered a clinically significant change in haemoglobin to be greater than 0.7-1.0 g/dL.
- Therefore, we propose that patients with haemoglobin levels less than 5g/dL, or symptomatic anaemia in the range 5-8g/dL, will be excluded from this additional venesection, thus reducing risk of contribution to significant anaemia. Patients with clinical evidence of hypovolaemic shock will also be excluded.
- To reduce inconvenience for participants we would coordinate this venesection to coincide with blood sampling for clinical indications (as directed by hospital doctors responsible for patient care).

- An additional meal with high dietary iron content would be provided each day to participants undergoing additional venesection, to offset any contribution to iron deficiency.

Thavendiranathan, P., et al., *Do blood tests cause anemia in hospitalized patients? The effect of diagnostic phlebotomy on hemoglobin and hematocrit levels.* Journal of general internal medicine, 2005. **20**(6): p. 520-4.

4.2 What follow-up action do you propose for participants who are already enrolled in the study?	
☐	Inform current participants as soon as possible
☐	Re-consent current participants with revised consent/assent forms (append)
✓	No action required
☐	Other. Please describe:

5. Detailed description of the change(s)

Please attach, for each amendment, a summary of all changes which clearly indicates:

i. Old wording (e.g. ~~strikethrough~~ text, CHANGED FROM and CHANGED TO)
ii. New wording (e.g. *italicized*, **bold**, tracked)
iii. Detailed rationale/ justification/ explanation for each change

UNIVERSITY OF CAPE TOWN
IYUNIVESITHI YASEKAPA • UNIVERSITEIT VAN KAAPSTAD

FACULTY OF HEALTH SCIENCES
Human Research Ethics Committee

HUMAN RESEARCH ETHICS COMMITTEE
14 JUL 2017
HEALTH SCIENCES FACULTY
UNIVERSITY OF CAPE TOWN

Form FHS006: Protocol Amendment

HREC office use only (FWA00001637; IRB00001938)			
☑ Approved	☐ Type of review: Expedited	☐ Full committee	
This serves as notification that all changes and documentation described below are approved.			
Signature Chairperson of the HREC		Date	17/7/2017

Note: All major amendments must include a local **PI Synopsis** justifying the changes for the amendment. Please note that incomplete amendment submissions will not be reviewed.

Comments from the HREC to the Principal Investigator:
Note: The approval of this protocol amendment does not grant annual approval. Please complete the FHS016 / FHS017 form for annual approval at least one month before study expiration.

Principal Investigator to complete the following:

1. Protocol information

Date (when submitting this form)	11 July 2017		
HREC REF Number	057/2013		
Protocol title	Defining interventions to reduce mortality in severe HIV-associated tuberculosis (Short title: KDH-TB study)		
Protocol number (if applicable)	NA		
Principal Investigator	Graeme Meintjes		
Department / Office Internal Mail Address	CIDRI office, 1st floor, Wolfson Pavilion, IDM, FHS		
1.1 Is this a major or a minor amendment? (see FHS006hlp) Major (tick box) Minor (tick box)		☐ Major	✓ Minor
1.2 Does this protocol receive US Federal funding?		☐ Yes	✓ No
1.3 If the amendment is a major amendment and receives US Federal Funding, does the amendment require full committee approval?		☐ Yes	☐ No

2. List of Proposed Amendments with Revised Version Numbers and Dates

Please itemise on the page below, all amendments with revised version numbers and dates, which need approval. This page will be detached, signed and returned to the PI as notification of approval. Please add extra pages if necessary.
Revised consent form "KDHTB_MTBBSI_serial_quantification.ICF_English.V3.0_12Jul2017" See section 4.1

3. Protocol status (tick ✓)

✓	Open to enrolment
☐	No participants have been enrolled
☐	Closed to enrolment (tick ✓)
☐	Research-related activities are ongoing
☐	Research-related activities are complete, long-term follow-up only
☐	Research-related activities are complete, data analysis only

4. Proposed changes will affect: (tick ✓ all the categories that apply)

	Protocol
☐	Study objectives, design (including investigator's brochure, clinical activities, study length)
☐	Study instruments, questionnaires, interview schedules
✓	Sample size
☐	Recruitment methods
✓	Eligibility criteria (inclusion and exclusion criteria)
☐	Drug/device (composition, amount, schedule, route of administration, combination with other drugs/devices, safety information)
☐	Data collection/ analysis
☐	Principal Investigator. (Please attach revised conflict of interest and PI declaration statements. Refer: sections 7 and 8.4 in the New Protocol Application Form FHS013)
✓	Consent form and information sheet
☐	Recruitment materials (e.g. advertisements)
☐	Administrative (e.g. change in sponsor's name, change in contact information)
✓	Other. Please specify: • We want to take a higher volume of blood during scheduled venesections, for additional/novel detection of *M. tuberculosis* blood stream infection.

4.1 In your opinion, will there be any **increase** in risk, discomfort or inconvenience to participants?	✓ Yes	☐ No
If yes, please provide a detailed justification/explanation:		

Explanation
The proposed amendment is to take a **larger total volume of blood from individual patients**.

We previously received HREC permission to collect blood at additional time points (6, 24, 48 and 72 hours after recruitment) [057/2013 amendment date 24/04/2016], and also to trial novel techniques to identify *M. tuberculosis* blood stream infection at a single time point [057/2013 amendment date 07/04/2017].

We now want to use the novel techniques (microscopy, polymerase-chain reaction (PCR) and modified culture protocol) in serial time point samples. However, this involves a higher total volume of blood being taken from patients.

To off-set this we will not take the baseline blood samples specified in the original KDH-TB study protocol (~55ml of blood at baseline, 0 hours). Instead we propose taking 18ml of blood at 5 time points (0, 4, 24, 48, 72 hours), totaling 90ml at 72 hours.

Comparison of blood volumes in original protocol, 2016 amendment, and current proposed amendment:

Protocol	Amendment	Volume blood first 24h	Total volume blood over 72h
KDH-TB 057/2013	N/A (original protocol)	55ml	55ml
KDH-TB 057/2013	24/04/2016	60ml	75ml
KDH-TB 057/2013	Current proposal	36ml	90ml

Justification and mitigation of risk, inconvenience, and discomfort

- Repeated blood culture to determine sterilization of the blood compartment is a standard of care in other bacteraemic conditions such as infective endocarditis, and daily venesection is not uncommon among unwell inpatients.
- Although from a different patient population, it has been shown that 100ml of blood venesectioned at a single time point is associated with a mean 0.7g/dL (SE for mean 0.1g/dL) haemoglobin drop in inpatients (Thavendiranathan et al 2005). This mean drop was smaller in patients with lower haemoglobin levels on admission, presumably because patients with higher haemoglobin levels lost more per ml venesected. Based on prior literature, Thavendiranathan et al. considered a clinically significant change in haemoglobin to be greater than 0.7-1.0 g/dL.
- Therefore, we propose that patients with haemoglobin levels less than 5g/dL, or symptomatic anaemia in the range 5-8g/dL, will be excluded from this additional venesection, thus reducing risk of contribution to significant anaemia. Patients with clinical evidence of hypovolaemic shock will also be excluded.
- To reduce inconvenience for participants we would coordinate this venesection to coincide with blood sampling for clinical indications (as directed by hospital doctors responsible for patient care).
- An additional meal with high dietary iron content would be provided each day to participants undergoing additional venesection, to offset any contribution to iron deficiency.

Thavendiranathan, P., et al., *Do blood tests cause anemia in hospitalized patients? The effect of diagnostic phlebotomy on hemoglobin and hematocrit levels.* Journal of general internal medicine, 2005. **20**(6): p. 520-4.

4.2 What follow-up action do you propose for participants who are already enrolled in the study?	
☐	Inform current participants as soon as possible
☐	Re-consent current participants with revised consent/assent forms (append)

✓	No action required
☐	Other. Please describe:

5. Detailed description of the change(s)

Please attach, for each amendment, a summary of all changes which clearly indicates:

i. Old wording (e.g. ~~strikethrough~~ text, CHANGED FROM and CHANGED TO)

ii. New wording (e.g. *italicized*, **bold**, tracked)

iii. Detailed rationale/ justification/ explanation for each change

6. Ethics Review Levy – cost including vat

Cost for Major Amendments - R3 659.10

(Protocols funded by UCT (e.g. departmental funding / student research) and by certain grant funding organizations (e.g. MRC, NRF, CANSA,) are exempt from charges)

For invoicing purposes, please provide:

Sponsor's name	
Contact person	
Address	
Telephone number	
Email Address	

7. Signature

My signature certifies that I will maintain the anonymity and/ or confidentiality of information collected in this research. If at any time I want to share or re-use the information for purposes other than those disclosed in the original approval, I will seek further approval from the HREC.

Signature of PI	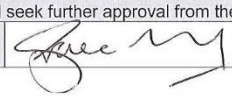	Date	14/7/2017